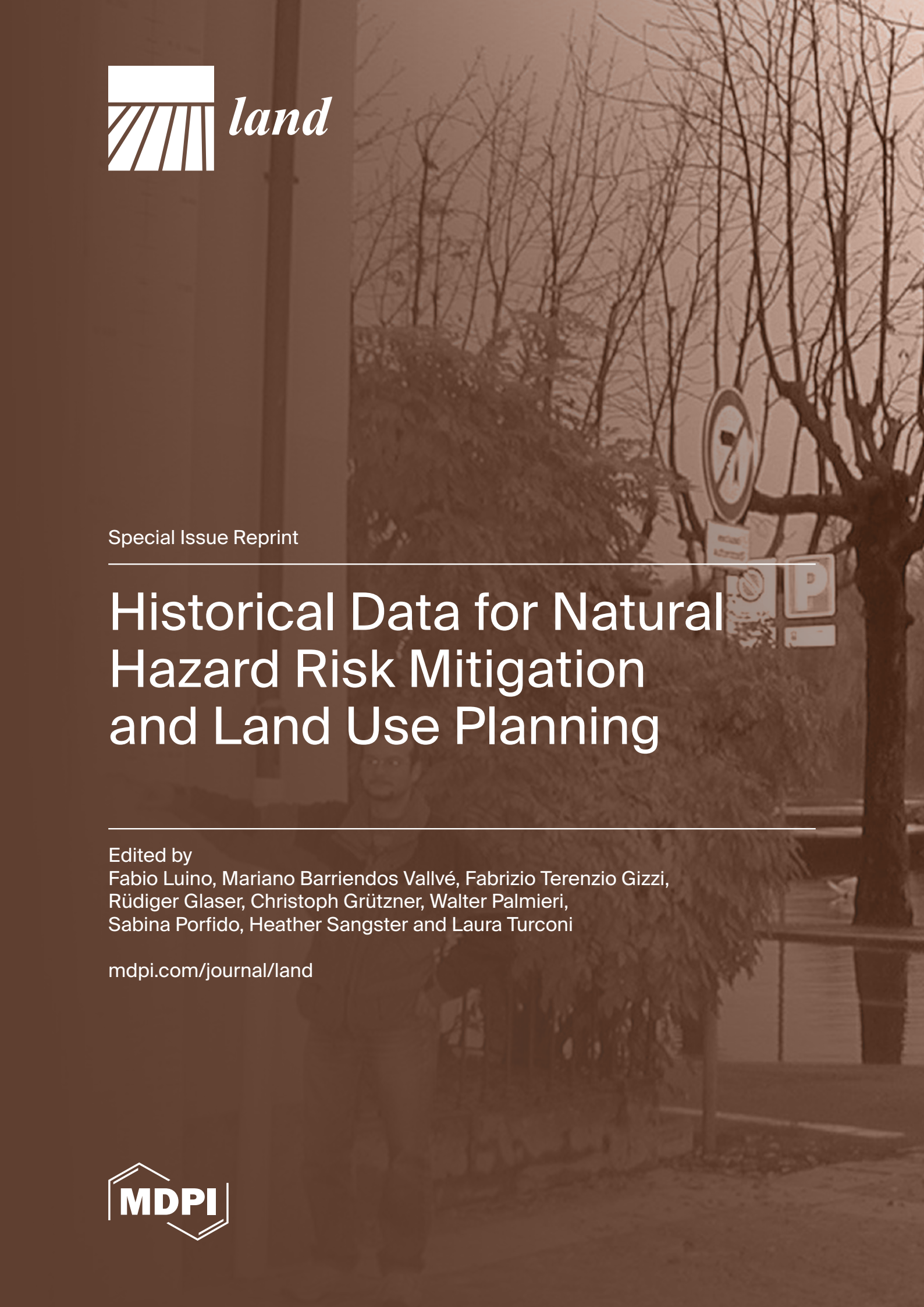


land

Special Issue Reprint

# Historical Data for Natural Hazard Risk Mitigation and Land Use Planning

Edited by
Fabio Luino, Mariano Barriendos Vallvé, Fabrizio Terenzio Gizzi,
Rüdiger Glaser, Christoph Grützner, Walter Palmieri,
Sabina Porfido, Heather Sangster and Laura Turconi

mdpi.com/journal/land

MDPI

# Historical Data for Natural Hazard Risk Mitigation and Land Use Planning

# Historical Data for Natural Hazard Risk Mitigation and Land Use Planning

Guest Editors

**Fabio Luino**
**Mariano Barriendos Vallvé**
**Fabrizio Terenzio Gizzi**
**Rüdiger Glaser**
**Christoph Grützner**
**Walter Palmieri**
**Sabina Porfido**
**Heather Sangster**
**Laura Turconi**

MDPI

Basel • Beijing • Wuhan • Barcelona • Belgrade • Novi Sad • Cluj • Manchester

*Editors*

Fabio Luino
Research Institute for Geo-Hydrological Protection
Italian National Research Council (IRPI-CNR)
Torino
Italy

Mariano Barriendos Vallvé
Department of History and Archaeology
University of Barcelona
Barcelona
Spain

Fabrizio Terenzio Gizzi
Institute of Heritage Science
Italian National Research Council (ISPC-CNR)
Potenza
Italy

Rüdiger Glaser
Department of Physical Geography
University of Freiburg
Freiburg
Germany

Christoph Grützner
Institute of Geological Sciences
Friedrich Schiller University Jena
Jena
Germany

Walter Palmieri
Research Institute of Studies on Mediterranean Sea
Italian National Research Council (ISMED-CNR)
Napoli
Italy

Sabina Porfido
Istituto Nazionale di Geofisica e Vulcanologia
Sezione di Napoli
Osservatorio Vesuviano
Napoli
Italy

Heather Sangster
Department of Geography and Planning
The University of Liverpool
Liverpool
UK

Laura Turconi
Research Institute for Geo-Hydrological Protection
Italian National Research Council (IRPI-CNR)
Torino
Italy

*Editorial Office*
MDPI AG
Grosspeteranlage 5
4052 Basel, Switzerland

This is a reprint of the Special Issue, published open access by the journal *Land* (ISSN 2073-445X), freely accessible at: https://www.mdpi.com/journal/land/special_issues/historical_data_natural_hazard_risk_mitigation_land_use_planning.

For citation purposes, cite each article independently as indicated on the article page online and as indicated below:

Lastname, A.A.; Lastname, B.B. Article Title. *Journal Name* **Year**, *Volume Number*, Page Range.

**ISBN 978-3-7258-3985-8 (Hbk)**
**ISBN 978-3-7258-3986-5 (PDF)**
**https://doi.org/10.3390/books978-3-7258-3986-5**
Cover image courtesy of Fabio Luino

© 2025 by the authors. Articles in this book are Open Access and distributed under the Creative Commons Attribution (CC BY) license. The book as a whole is distributed by MDPI under the terms and conditions of the Creative Commons Attribution-NonCommercial-NoDerivs (CC BY-NC-ND) license (https://creativecommons.org/licenses/by-nc-nd/4.0/).

# Contents

**About the Editors** . . . . . **vii**

**Fabio Luino, Mariano Barriendos, Fabrizio Terenzio Gizzi, Ruediger Glaser, Christoph Gruetzner, Walter Palmieri, et al.**
Historical Data for Natural Hazard Risk Mitigation and Land Use Planning
Reprinted from: *Land* **2023**, *12*, 1777, https://doi.org/10.3390/land12091777 . . . . . **1**

**Michael Kempf**
Documentary Evidence of 17th Century Landcover and Climate Change in Northern China and Mongolia Compared to Modern Spectral Greening Trends
Reprinted from: *Land* **2022**, *11*, 100, https://doi.org/10.3390/land11010100 . . . . . **22**

**Mario Bentivenga, Fabrizio Terenzio Gizzi, Giuseppe Palladino, Marco Piccarreta, Maria Rosaria Potenza, Angela Perrone, et al.**
Multisource and Multilevel Investigations on a Historical Landslide: The 1907 Servigliano Earth Flow in Montemurro (Basilicata, Southern Italy)
Reprinted from: *Land* **2022**, *11*, 408, https://doi.org/10.3390/land11030408 . . . . . **41**

**Laura Turconi, Domenico Tropeano, Gabriele Savio, Barbara Bono, Sunil Kumar De, Marco Frasca and Fabio Luino**
Torrential Hazard Prevention in Alpine Small Basin through Historical, Empirical and Geomorphological Cross Analysis in NW Italy
Reprinted from: *Land* **2022**, *11*, 699, https://doi.org/10.3390/land11050699 . . . . . **65**

**Gianni Petino, Maria Donata Napoli and Mario Mattia**
Landscape, Memory, and Adverse Shocks: The 1968 Earthquake in Belìce Valley (Sicily, Italy): A Case Study
Reprinted from: *Land* **2022**, *11*, 754, https://doi.org/10.3390/land11050754 . . . . . **89**

**Mustapha Ikirri, Farid Faik, Fatima Zahra Echogdali, Isabel Margarida Horta Ribeiro Antunes, Mohamed Abioui, Kamal Abdelrahman, et al.**
Flood Hazard Index Application in Arid Catchments: Case of the Taguenit Wadi Watershed, Lakhssas, Morocco
Reprinted from: *Land* **2022**, *11*, 1178, https://doi.org/10.3390/land11081178 . . . . . **112**

**Davide Notti, Diego Guenzi, Rosa Lasaponara and Daniele Giordan**
Merging Historical Archives with Remote Sensing Data: A Methodology to Improve Rockfall Mitigation Strategy for Small Communities
Reprinted from: *Land* **2022**, *11*, 1951, https://doi.org/10.3390/land11111951 . . . . . **132**

**Jordi Tuset, Mariano Barriendos and Josep Barriendos**
Historical Floods on the Spanish Mediterranean Basin: A Methodological Proposal for the Classification of Information at High Spatio–Temporal Resolution—AMICME Database (CE 1035–2022)
Reprinted from: *Land* **2022**, *11*, 2311, https://doi.org/10.3390/land11122311 . . . . . **150**

**Philipp Marr, Yenny Alejandra Jiménez Donato, Edoardo Carraro, Robert Kanta and Thomas Glade**
The Role of Historical Data to Investigate Slow-Moving Landslides by Long-Term Monitoring Systems in Lower Austria
Reprinted from: *Land* **2023**, *12*, 659, https://doi.org/10.3390/land12030659 . . . . . **167**

**Fabio Luino, Fabrizio Terenzio Gizzi, Walter Palmieri, Sabina Porfido and Laura Turconi**
Historical Memory as an Effective and Useful Tool for Proper Land Use Planning: Lessons Learnt from Some Italian Cases
Reprinted from: *Land* **2023**, *12*, 1751, https://doi.org/10.3390/land12091751 . . . . . **189**

**Antonio Oliva and Jorge Olcina**
Historical Floods and Territorial Planning: Lessons Learned and Opportunities Lost after the Santa Teresa Flood (1879) in the Segura Basin (Spain)
Reprinted from: *Land* **2024**, *13*, 28, https://doi.org/10.3390/land13010028 . . . . . **228**

**Asia Bernardi, Michele Licata, Francesco Seitone and Giandomenico Fubelli**
MAGUS (Model for the Analysis of Geomorphological Urban Systems): From Conception to Validation on the Historic City Center of Turin (Italy)
Reprinted from: *Land* **2024**, *13*, 1851, https://doi.org/10.3390/land13111851 . . . . . **257**

**Violet Kanyiginya, Ronald Twongyirwe, David Mubiru, Caroline Michellier, Mercy Gloria Ashepet, Grace Kagoro-Rugunda, et al.**
Historicizing Natural Hazards and Human-Induced Landscape Transformation in a Tropical Mountainous Environment in Africa: Narratives from Elderly Citizens
Reprinted from: *Land* **2025**, *14*, 346, https://doi.org/10.3390/land14020346 . . . . . **277**

# About the Editors

**Fabio Luino**

With a degree in Geological Science at Turin University, he is currently a senior researcher of the Italian National Research Council, Institute for Geo-Hydrological Protection and Prevention in Turin. His research concerns floods, mud-debris flows, and landslides: he studies these processes from a geomorphological and historical point of view, analysing their interferences in town-and-country planning. Since 1994, he has been an expert of the National Department of Civil Protection of Rome. During emergencies, he is consulted for evaluating the geo-hydrological risk in urbanised areas. He has been a scientific leader for many different administration bodies for research on the management of geo-hydrological risks along the river, offering courses oriented at Civil Defence Plans. For the Regione Lombardia Administration, he was scientific leader in the UE Project DAMAGE (2004–2006) for determining a methodology to carry out a real time assessment of potential direct economic loss due to a catastrophe. In recent years, he has tackled the problem of flood insurance, analysing criteria for a new methodological approach. In the period 2018–2024, he was responsible for the CNR IRPI of the RECONECT Horizon 2020 project. The RECONECT project involves the design, implementation, and evaluation of a series of "tailor-made" solutions for geo-hydrological risk mitigation in the Portofino Park (Ligurian coast, Italy). Before this Special Issue, Luino was an editor of the Proceedings for the International Conference (1996) "Prevention of Hydrogeological Hazards: the role of scientific research" and an editor for the Scientific Journal NHESS (2012) of the Special Issue "Geo-hydrological risk and town and country planning". He is the author of some 200 papers and 10 books, with 70 of them in international journals.

**Mariano Barriendos Vallvé**

Mariano is an environmental consultant, as well as a visiting researcher on IDAEA-CSIC (Institute of Environmental Assessment and Water Research, Spanish Scientific Research Council). Mariano's research activity is focused on historical climatology and the identification, collection, and analysis of proxy-data for climatic reconstruction. Their work focuses on the Iberian Peninsula over the past 500 years. Their original information involves extreme climatic event descriptions in historical documentary sources and rogation ceremonies by environmental factors recorded in ecclesiastical and municipal documentary sources. Their research results are published in more than 250 publications, 81 of them in SCI journals, participating in more than 20 projects, 5 of which are European projects.

**Fabrizio Terenzio Gizzi**

Fabrizio Terenzio Gizzi is a senior researcher at the Institute of Heritage Science of the Italian National Research Council (ISPC-CNR). His research interests span across the study of the relationship between natural hazards and built heritage, aiming to determine strategies for risk knowledge and risk mitigation. His research draws on the analytical study of historical sources to investigate the consequences caused by earthquakes, landslides, and floods in the past, picking up valuable lessons for the future and for territorial planning. The focus of his research centres on both the physical damage to the urban areas and historical centres and the socio-economic effects in the short, medium, and long term, with specific regard to the phenomenon of settlement abandonment, in a diachronic perspective. Moreover, he is engaged in tapping into big data and innovative methodologies of digital social research to come up with risk management strategies, bringing in a bottom–up approach. On these topics, he has published over 160 articles in indexed journals and international and national conference proceedings, as

well as monographic studies, and has managed or taken part in several research projects. He also serves on the editorial board of some renowned international journals.

**Rüdiger Glaser**

Rüdiger's areas of interest are climatology, in particular, historical climatology and historical environmental research, climate change adaptation, regional studies, sustainability, and global change. One of his areas of focus is the virtual research environment "tambora.org", in which data, projects and information can be stored, shared, analysed, and published. His ongoing projects include the Clim'AbilityCARE and RiverDiv deal with risk assessment, climate change adaptation, and implementation measures. In more recent contexts, the team deals with questions of artificial intelligence in the field of text-based analysis. Many of his works on historical climate and environmental research and e-learning have received awards. Rüdiger Glaser has co-authored several textbooks and written a number of fundamental works in his field of research.

**Christoph Grützner**

Christoph Grützner is a researcher at the Friedrich Schiller University Jena, Germany. He is mainly interested in active tectonics, tectonic geomorphology, and paleoseismology. His specialty is to identify evidence for past large earthquakes in the geological record, and to investigate how seismic activity is preserved in the landscape. Currently, he is working on the North American–Caribbean plate boundary in Guatemala, the European Alps, and Central Asia. Earlier projects took him mainly to the Mediterranean region.

**Walter Palmieri**

Walter Palmieri is a senior researcher of the Istituto di Studi sul Mediterraneo of CNR. He has published essays in several anthologies and on several historical journals like "Meridiana. Rivista di Storia e Scienze Sociali", "Storia Urbana", "Società e Storia", and "Archivio Storico per la Calabria e la Lucania". He is also currently a member of the review board for "Global Environment. The Journal of Transdisciplinary History". His research focuses on Southern Italy before unification with an emphasis on territory and deforestation. His current project is the development of a database on landslides and floods in Southern Italy during previous centuries and their historical significance.

**Sabina Porfido**

Sabina is a former senior researcher at the CNR-ISA (Avellino, Italy), now retired, and is a researcher at the INGV-Vesuviano Observatory in Naples (Italy). She is a geologist with multidisciplinary experience in active tectonics, natural hazards, seismic hazard, paleoseismology, floods, historical floods, cultural heritage, and the study of historic and recent earthquakes and their induced effects on the ground. She is a co-author of the new Esi 2007 macroseismic scale approved by INQUA. She is also the author of many international papers, books, and chapters and a reviewer for a large number of journals. Currently, they are involved in several projects investigating active faults and the use of ESI scales in different geological contexts around the world (Mexico, Korea, India, Tibet, etc.). She is an editor of two MDPI Special Issues: · New Perspectives in the Definition/Evaluation of Seismic Hazard through Analysis of the Environmental Effects Induced by Earthquakes. · The November 23rd, 1980 Irpinia-Lucania, Southern Italy Earthquake: Insights and Reviews 40 Years Later. Concerning the 1930 earthquake in Irpinia and the reconstruction post the 1980 Campania-Lucania earthquake, she has published several books of photographs.

**Heather Sangster**

She is a senior lecturer in Physical Geography at The University of Liverpool. Her research is inter-disciplinary in nature and engages with a series of core components and epistemologies in the field of natural hazards. She uses methods and ideas from across the physical, earth, and social sciences to unravel the ways in which societies have reacted historically to extreme events (e.g., geophysical, hydrological, and meteorological), and how such responses influence current policies and practices of disaster risk reduction and mitigation through cumulative disaster knowledges. She considers how societies relate to, understand and record past natural hazard risks, the management of environmental uncertainties, and the integration of different forms of knowledge into policies in natural hazard management and mitigation for risk assessment planning.

**Laura Turconi**

Laura's main area of interest is applied geomorphology, focusing on preventive studies of slope instability and stream floods, with special attention to torrential risk during extreme rainfall events. This activity has been carried out with the aim of developing event scenarios related to natural and/or human-induced instability processes, their sequential development, expected effects, possible magnitude, and mean recurrence interval, also based on historical research. Her work includes on-site technical surveys, particularly during and after several geo-hydrological emergencies. She has also participated in monitoring activities related to landslide processes, rainfall runoff, and water–sediment discharge experiments, as well as debris flow monitoring at test sites in the Western Italian Alps. Additionally, she has contributed to the development of an empirical formula for debris flow magnitude. Laura has been the project manager of experimental research in a mountain basin on debris flows and torrential processes since 1998. She is also co-responsible for several projects, including EU Horizon, PRIN 2020–2022, Risknat Alcotra 2007–2013, POR FESR 2007–2013 IoD, and various agreements with Italian regions, provinces, mountain communities, and the Italian Civil Protection Department.

land

*Editorial*

# Historical Data for Natural Hazard Risk Mitigation and Land Use Planning

**Fabio Luino [1,*], Mariano Barriendos [2], Fabrizio Terenzio Gizzi [3], Ruediger Glaser [4], Christoph Gruetzner [5], Walter Palmieri [6], Sabina Porfido [7,8], Heather Sangster [9] and Laura Turconi [1]**

1 Istituto di Ricerca per la Protezione Idrogeologica, Consiglio Nazionale delle Ricerche, Strada della Cacce 73, 10135 Torino, Italy; laura.turconi@irpi.cnr.it
2 Institute of Environmental Assessment and Water Research (IDAEA-CSIC), 08034 Barcelona, Spain; mariano.barriendos@idaea.csic.es
3 Istituto di Scienze del Patrimonio Culturale, Consiglio Nazionale delle Ricerche, C. da S. Loja, 85050 Potenza, Italy; fabrizioterenzio.gizzi@cnr.it
4 Department of Physical Geography, Institute of Environmental Social Science and Geography, University of Freiburg, 79110 Freiburg, Germany; ruediger.glaser@geographie.uni-freiburg.de
5 Institute of Geological Sciences, Friedrich Schiller University Jena, 07749 Jena, Germany; christoph.gruetzner@uni-jena.de
6 Istituto di Studi sul Mediterraneo, Consiglio Nazionale delle Ricerche, Via Guglielmo Sanfelice, 8, 80134 Napoli, Italy; palmieri@ismed.cnr.it
7 Istituto di Scienze dell'Alimentazione, Consiglio Nazionale delle Ricerche, Via Roma 64, 83100 Avellino, Italy; sabina.porfido@cnr.it
8 INGV, Osservatorio Vesuviano, Via Diocleziano 328, 80124 Napoli, Italy
9 Department of Geography and Planning, School of Environmental Sciences, The University of Liverpool, Liverpool L69 7ZT, UK; heather.sangster@liverpool.ac.uk
* Correspondence: fabio.luino@irpi.cnr.it

**Abstract:** This paper demonstrates how historical research is a valuable tool for identifying past geological, geomorphological and climatic hazards and therefore critical for mitigating and reducing future risk. The authors describe the potential of a scientific field that straddles that of the geologist, geographer, historian and archivist. Historical records include a range of materials and sources of information, which can be very diverse; from written documents to cartographies, and from drawings to marble tombstones. They are all useful and convey important data, on the date of the event, the size of the phenomena, sometimes on ground effects, damage or magnitude. The authors discuss how to conduct historical research by providing a list of locations and how important historical documents can be found. Works that mention geological phenomena are listed, starting with the first occasional descriptions by individuals in letters, up to very specific publications in individual fields of interest. With this introduction, the editors of the Special Issue wish to draw attention to the importance of historical documentation, which is too often ignored or considered of low priority by the scientific community, but can contain key information on events, their impacts and social and cultural adaptations.

**Keywords:** geological and geo-hydrological processes; historical research; old documents; land-use planning; natural hazards; risk mitigation; Europe

**Citation:** Luino, F.; Barriendos, M.; Gizzi, F.T.; Glaser, R.; Gruetzner, C.; Palmieri, W.; Porfido, S.; Sangster, H.; Turconi, L. Historical Data for Natural Hazard Risk Mitigation and Land Use Planning. *Land* **2023**, *12*, 1777. https://doi.org/10.3390/land12091777

Received: 3 July 2023
Accepted: 5 September 2023
Published: 13 September 2023

**Copyright:** © 2023 by the authors. Licensee MDPI, Basel, Switzerland. This article is an open access article distributed under the terms and conditions of the Creative Commons Attribution (CC BY) license (https://creativecommons.org/licenses/by/4.0/).

## 1. Introduction

Every year, many areas of the world are affected by natural phenomena. Endogenous and exogenous processes threaten human life by posing a persistent danger that can become a disaster when they affect inhabited areas. The effects of the disaster may be immediate and localised, but are often widespread and may last for a long period of time. The effects may test or exceed the ability of a community or society to cope with its own resources, and therefore may require assistance from external sources, including neighbouring jurisdictions or those at the national or international level [1].

In the last century, over 15,000 disasters occurred worldwide, causing damage to human activities (EM-DAT, CRED, www.emdat.be) [2] with a global increase of disaster frequency and severity over time (WMO, 2021) [3]. This increase results from the growth of the global population and the increased occupation of areas exposed to risks such as flood plains and coastal areas; other factors responsible for the increase in the frequency of disasters are related to the vulnerability of structures and infrastructures, the ineffectiveness of mitigation actions and possibly climate change [4,5].

The global population has increased from 1 billion in 1800 to the current 7.7 billion [6], and as such has placed greater pressure on resources and increased community exposure to hazards. As the pressure on spaces and resources increases, the growing population expands into areas that have not yet been occupied due to being deemed suboptimal for a variety of reasons, including poor/difficult accessibility or their exposure to hazards. In Italy, for example, the paradox emerges of having a low population growth rate but the highest land consumption rate in Europe [7], with illegal buildings being particularly widespread [8]. The coexistence of humans with natural hazards is challenging and is likely to increase over time as a result of diminishing new spaces.

## 2. Historical Research as a Tool to Mitigate and Reduce Geological, Geomorphological and Climatic Risks

Natural instability phenomena and their manifestations have long threatened human life [9–14]. Volcanic eruptions, earthquakes, landslides and floods and other natural processes are capable of causing casualties and serious economic losses.

Research on natural hazards has two main challenges. The first is directed towards the future projection of extreme events and their modelling; the primary concern in this dimension is the great uncertainty caused by human-induced climate change. The second challenge is the past and how we identify and analyse events of low frequency, which are therefore by definition rare and whose presence in the modern instrumental period is often infrequent or non-existent. To address this, we can use historic or palaeodata of different origins to reconstruct the characteristics and frequency patterns of past events.

Recent technological developments have facilitated new ways of observing the Earth and monitoring different processes; for example, surveys undertaken with laser scanners, both terrestrial and aerial, can filter vegetation or avoid obstacles that enable three-dimensional maps with errors of less than a centimetre or a few millimetres [15,16]. With satellite techniques and the numerous UAV (unmanned aerial vehicle) techniques [17], it is possible to cover much larger areas with a high resolution [18,19] and in an infinitely shorter time compared to surveys performed exclusively through direct observations in the field [20].

A considerable contribution comes from Information and Communication Technology (ICT), which has made progress in the field of cartographic representation [21].The data are managed by geo-information services [22] which document and provide updated cartography, enabling the evolution of the Earth's surface and therefore allowing the dynamics of the soil morphology, elements of geo-hydrological instability and change, vegetation cover change, introduction of infrastructures and distribution of waters to be analysed. The scientific community uses the most sophisticated technologies to predict and prevent endogenous and exogenous processes [23,24]; in the future, projections will certainly achieve better management of the territory and therefore a reduction of the harmful consequences. This will make it possible to direct resources to where they are most needed.

Analysis of historical sources to improve understanding of past frequency, magnitudes and/or intensities and their consequences on humans has recently seen an increased recognition of the value of historical (non-continuous) information. Historical sources can provide important insights into the frequency of events, in particular for rare events; these sporadic cases offer considerable opportunities to improve our understanding of low-frequency and

high-magnitude events, enabling improved knowledge for the prediction, management and/or prevention of geophysical, meteorological or geo-hydrological processes.

Sources of information can be primary and secondary. Primary sources are preferred; they consist of direct and coeval traces of a human presence or activity related to the subject of the study (hazards in our case). On the other hand, secondary sources are those works compiled by subsequent works, either compiling previously recorded materials, or accounts that document events sometime after, often by individuals that did not witness the event directly.

The documents of our predecessors can be found in many different forms, including paper documents, books (Figure 1), newspaper articles, cartographies, photographs and many more [25–39]. Some sources are specific to particular types of hazards, such as weather diaries being specific to meteorological hazards [40].

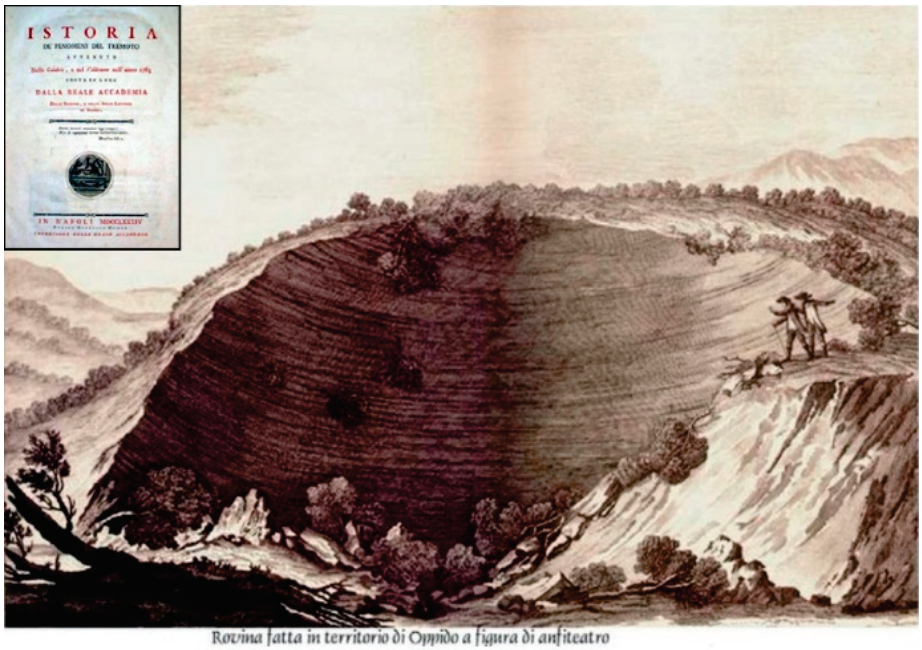



**Figure 1.** This book by Michele Sarconi (1784) was one of the first published in Italy to deal with landslides due to the terrible sequence of earthquakes that occurred in southern Italy in 1783 [41].

Paper documents are clearly the most numerous; geological and geomorphological phenomena have always stimulated the curiosity of scientists who have tried to describe what they witnessed or to transcribe the testimonies of those who had experienced the phenomena. Newspaper articles are of great help as they are often written shortly after the event and can provide high levels of information; they are often not too technical, but very importantly can record the hazard's development over time, the manner of the processes, the damage and human responses.

For example, the first land registers of the eighteenth century in northern Italy, of a geometric parcel type, constituted a real fiscal instrument which recorded the cognitive characteristics of the State territory from an administrative, political–economic and military point of view. In France, the first general maps of the territory using a measuring apparatus were made by the Cassini family during the 18th century at 1:86,400 scale [42]. These maps were a technical innovation because they were the first maps based on geodetic triangulation. It took more than 50 years to complete them. The 19th century was the century of systematic topographic surveys (Figure 2). This intense activity was mainly due to the need for the so-called "military revolution", which increased the need for information as the scale of wars widened. Several National Geographic Institutes arose in France, England, Prussia, the United States of America and Austria. For example,

reliable maps (75% of them in colour) were carefully produced by cartographers following Napoleon Bonaparte's army in the early decades of the 19th century [43].




**Figure 2.** Po River. Table X, called Mortizza (Piacenza province). Map of the River Po, from Ticino to the sea (from direct surveys carried out in 1821 and updated in 1853), at a scale of 1:15,000 by Corpo Reale del Genio Civile. Archive CNR IRPI Turin.

With the passage of time, maps have become more precise and feature increasingly detailed scales, up to the present day, where anyone can access Google Earth or other geographic databases from their personal computer to admire the small details of any place on Earth, or even other planets (https://www.google.com/mars/, last accessed on 30 June 2023).

Cartography is often helpful when indicating toponyms of areas that were affected by natural instability processes in the past. This is how we include places such as "Alluvioni Cambiò" namely "Changed by Floods" (Piedmont-Italy) or the place "Landslide Lake" (Comox-Strathcona D., British Columbia, Canada) or the town of "Floodwood" (Minnesota, USA) [44,45].

Another great contribution of historical sources is photographic heritage. In the course of history, photography has proved to be an indispensable tool in the documentation of territory and in the study of its transformations [46]. Landscape photography was delivering something that only painting was capable of doing until that time—rendering reality in a two-dimensional format. For photographic heritage, we must not only consider those consisting of images taken on the countryside level [47], which started from around 1830–1840, but also aerial photographs. The first images taken with the aim of representing the Earth's surface were made by hot air balloons in the mid-nineteenth century [48], and then from planes in later years, with increasingly sophisticated instruments that allowed faithful reproduction of the territory [49].

But historical information is not just paper or digital: it can also be traced on the ground. Sometimes, in fact, catastrophic events that caused casualties or damages are remembered through paintings or the billsticking of marble plaques or tombstones, or via the construction of votive chapels or marble memorial stones [50]. Plaques, tombstones, epigraphs and monuments constitute a great heritage of "historical memory" for a community (Figures 3 and 4): they help not to forget tragedies and can foster better land-use planning.




(**a**) (**b**)

(**c**) (**d**)

**Figure 3.** (**a**) Passau (Germany): Danube flood levels on the old Town Hall (courtesy of Luke M McLean); (**b**) Florence: entrance to the "Cappella dei Pazzi" with three marble plaques indicating the heights reached by the waters during three major floods of the Arno River (photo F. Luino); (**c**) Darfo Boario Terme (Brescia-Italy): On the perimeter wall of the apse of the Montecchio church this plaque is visible, with a Latin inscription, concerning the 'ruin' that struck Montecchio in 1475. It was not a flood of the River Oglio, but a torrential debris flow of the T. Rovinazza, a dangerous left-hand tributary (photo F. Luino); (**d**) The site of one of the largest landslides in Canadian history. On the morning of 9 January 1965, a minor earthquake caused this landslide, which displaced Outram Lake and destroyed three kilometres of the Hope-Princeton Highway. The landslide consisted of more than 46 million $m^3$ from the side of Johnson Peak. The rubble is 70 m deep in some places. The new highway is about 55 m above the original ground level and somewhat south of its original path. Four people were killed, but only two bodies were ever found. Source: https://www.komoot.com/it-it/highlight/912190 (accessed on 30 May 2023).




**Figure 4.** Sesto Calende (Varese-Italy). Image of the famous marble plaque, located in Piazza De Cristoforis, on which are indicated the maximum heights reached by the waters of Lake Maggiore from 1705 until 1981. More recently, the levels reached by the great floods of 1993 and 2000 have been added, but they are not engraved in the marble like the previous ones, but only written with a felt-tip pen.

These "stones" are and remain testimonies of mournful dates and severe events for a community, educating and reminding future generations. They can be found across all continents except Antarctica. Some of them, unfortunately, have been lost, while others now worn out by time are seriously ruined or have become illegible. The first great difficulty is perhaps in knowing where they can be found, with few being documented centrally. As such, they need to be found or located, often through visiting sites or talking to those familiar with local histories.

The exceptional heritage that experts of the past have handed down to us, therefore, is always of great importance: it constitutes "zero time" and therefore allows comparisons that otherwise could not be made. The historical data, therefore, prove to be of great help to better understand the evolution of a particular territory and therefore for a mitigation of geological, geomorphological and hydrological risk. Many inhabited centres all over the world, repeatedly involved in endogenous and exogenous processes in the past, have continued to expand, often in the same areas where there have been serious events that have caused damage and victims, without taking due account of previous teachings [51]. This occurred mainly because of the loss of "historical memory", which in turn favoured a lack of adequate territorial planning for decades; therefore, urban expansion took place, which has often resulted in an inevitable proliferation of risk.

The growth in the use of historical materials across disciplines and cross-disciplinary studies [38] has been fostered by a greater appreciation of the value that such sources offer. Interpretation of historical sources sometimes makes it possible to translate information in qualitative and quantitative terms, both the physical process of the natural hazard and the directly associated risks [29].

But a focus on the event in terms of temporal evolution of the phenomenon, evaluation of recurrence times, effects on the environment and epidemiological studies on the population (dead and injured) can also be considered without forgetting the damage suffered by the urban fabric (from residential buildings to cultural heritage) and infrastructure. Such

information is valuable in understanding short-, medium- and long-term risk, and it can provide valuable knowledge for risk mitigation and for prevention in affected areas [52–58].

The use of historically rooted information does not mean to underestimate the importance of other types of investigations, of a more distinctly methodological or applicative nature, in the vast field of disciplines concerning protection from natural hazards. However it is suitable to underline the usefulness of scholars' systematic collection of published and unpublished sources, which are still largely scattered in many places and often poorly preserved.

In addition to the conscious need to hand down written memory of such information in an appropriately elaborated form, the cardinal concept that guides scholars who consider historical data as valuable sources of information is the awareness that exogenous and endogenous phenomena are likely to repeat in space (very often in the same places) and time (according to extremely variable intervals of recurrence), with phenomenological features similar to those that occurred in the past.

The criteria for cataloguing past sources are almost exclusively designed according to questions that are very different from those a geologist/hydrologist/geomorphologist or risk assessor would usually ask. However, despite the initial difficulties, once one has acquired a basic knowledge, it is possible to become familiar with the investigation method also in relationship with the research questions about the natural phenomenon ("where, when, how and what").

There are many countries in the world with an extensive historical record. The nature and evolution of historical document use varies in and across countries and continents, dependent on the range of written sources available. While some specific types of source materials are typical to a region or country, others are more ubiquitous and widely recorded, e.g., tax returns, epigraphic flood marks and so-called "Hunger stones" (Figure 5) [59].

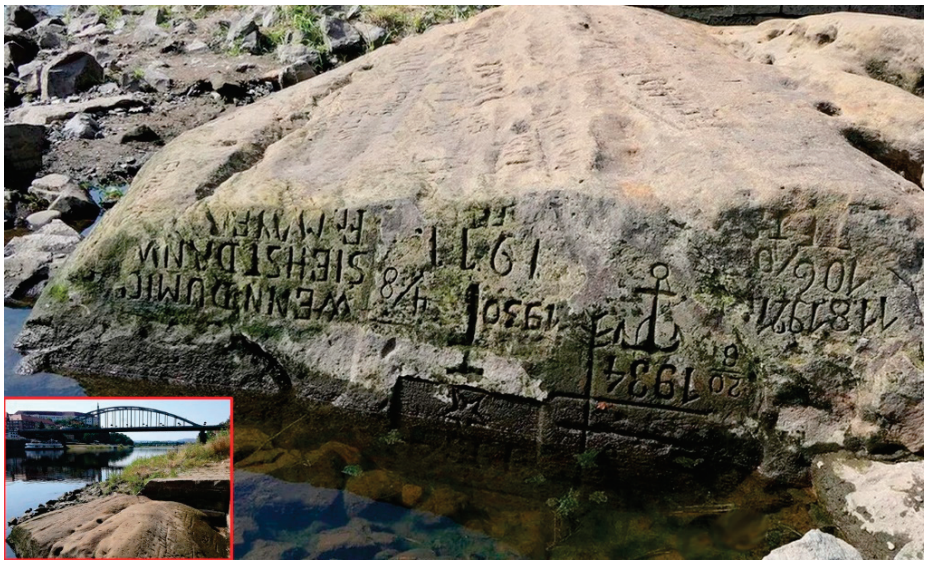


**Figure 5.** "Hunger stone" with several inscriptions discovered on one of the banks of the Elbe River in Decin, northern Czech Republic, photographed in August 2018. Between the 15th and 19th century, the extremely low water levels of the river were engraved, along with some warnings about the consequences of drought. One engraving reads "Wenn Du michsiehst, dannweine" ("'If you see me, weep").

The possibility of extending one's research over time, sometimes for centuries, depends on many factors, including the period when the recording of documents began, the way in which archival material is preserved and, of course, the possibilities for scholars to use it.

The following sections provide a brief review of source materials in different countries and how these have been considered and used in understanding, forecasting and preventing risks.

## 3. Italy

The first documentary archives that are usually consulted in Italy are the State Archives. These are present in each provincial capital city (and not only these), with a total of about 100 offices located throughout the country. State Archives perform the functions of protection and valorisation of archival assets, ensuring their public use, as well as the role of protecting the archives, including current and past State materials [60]. They contain an exceptional range of documentary heritage, i.e., the archives of the central and peripheral administrations of the pre-unification states and the archives of the peripheral administrations of the unitary state, converge (or should converge) once 30 years have elapsed since recording. Leafing through the thick folds containing interesting documents, one can find manuscripts, sometimes difficult to understand (the presence of an archivist with knowledge of palaeography can certainly help), technical reports, chronicles of natural phenomena and related events, sometimes accompanied by cartographies (Figure 6).

Technical reports were compiled by different figures: surveyors of the time, but also architects or engineers, who went to affected areas, described the events, produced maps and drawings, undertook measurements and sometimes described the countermeasures to be taken. When considering floods, for example, land surveyors measured the surface of the flooded lands that had become unproductive, sometimes also giving indications on the thickness of the deposited material, changes to the riverbed or damages suffered in the territory.

Another precious and widely used original source are those preserved at the Central State Archives in Rome, which constitute the archival institution gathering the documentary memory of the unitary State (1861). The Ministry of Cultural Heritage is responsible for these heritage activities and for tourism. In particular, the Central State Archive preserves archives and documents, on different typologies, of the central organs of the unitary State and of public bodies of national importance and of private individuals that the State has in property. The Institute makes use of an IT platform that allows targeted searches to be made, through proper keywords, following the traditional hierarchical path of exploration of archival funds (https://acs.cultura.gov.it/ (accessed on 30 May 2023)) [61].

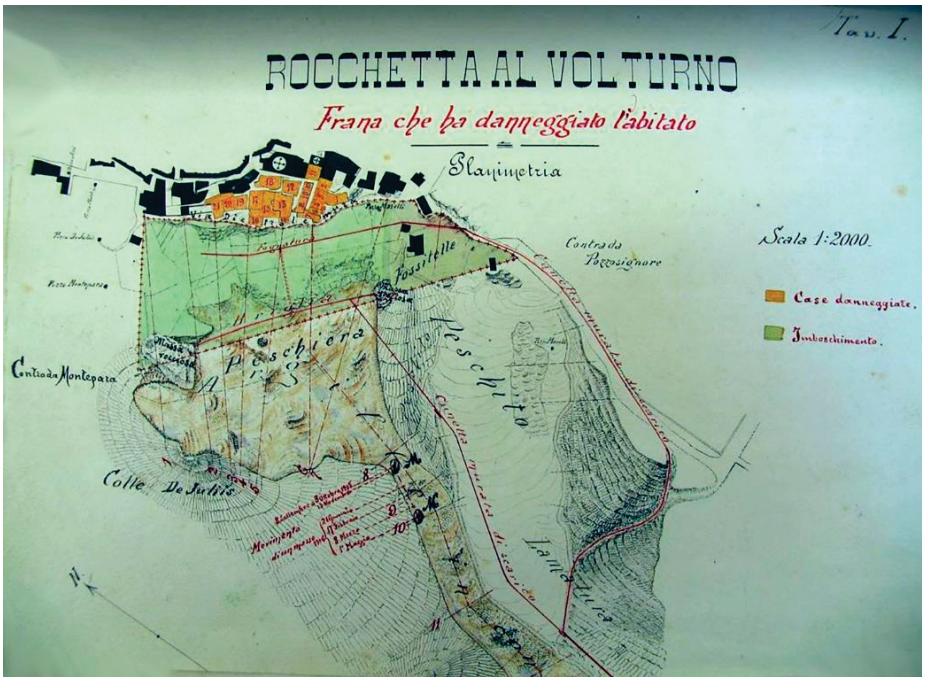



**Figure 6.** State Archive of Campobasso: document drawn in 1906 concerning a landslide that occurred in Rocchetta al Volturno (ASCb, Genio Civile, II, b. 816) [62]. Above the painting, the inscription reads "landslide that damaged the village" (translated from Italian). In orange are the damaged houses; in green, the wooded area [63].

Municipal historical archives offer another possible rich and capillary collection of information; in some cases, they are well preserved (Figure 7a), but others, unfortunately, are in a poor state (Figure 7b). Often, the material does not have an inventory and can therefore not be easily consulted. This usually requires a great expense of time.



(**a**)



(**b**)

**Figure 7.** (**a**) Municipal archive of Alba (Cuneo province). A very rich, well-organised archive with the opportunity to find documents by database. The re-organisation took place in recent years with the help of a professional archivist (photo F. Luino); (**b**) municipal archive of Cividate Camuno (Brescia province). The documents are stored in an attic and contained in folders; the microclimatic conditions, freezing cold in winter, high relative humidity in rainy periods and torrid in summer, contrast with the requirements for proper conservation of documentation (photo F. Luino).

In Italy, the archiving of documents in the nineteenth century took place through subdivision by subjects and criteria that varied from state to state. Archival cataloguing often took place for subjects that were not unambiguously identified. After the unification of Italy in 1861, a revision began that led to a circular of the Ministry of the Interior in 1897. The "legislative criterion" was introduced which standardized the methodology followed for archiving documents produced by municipalities [64]. It included 15 categories divided into classes defined by topic. The focus of research relating to natural hazards is usually concentrated in the two categories X and XV, "Public Works" and "Public Safety", respectively.

It is also advisable to devote some time to the parish archives, especially if the town has in the past been affected by an event that resulted in casualties; in particular, earthquakes, landslides or debris flows, as occurred in Gromo (Bergamo province) in 1666 [65]. The documentation kept in the parish archives is an almost unique and exclusive source for the history of the church itself, but also for the knowledge of the history of small urban and rural agglomerations spread throughout the country and their populations. Finally, we should not underestimate the possibility of also collecting information from private archives of individuals, families, associations, bodies or private companies. A particularly catastrophic event, precisely for the consequences it entails, leaves numerous traces among all the subjects that lived it.

Civic libraries are another particularly rich repository for finding local materials, especially those of the great cities, specifically those materials recording local history. These include books, journals and articles that describe the town and its territory from a geographical and historical point of view, sometimes also from an architectural and/or urbanistic standpoint. However, they take on great importance when they contain information concerning past calamities that occurred in the municipal area (floods, landslides, earthquakes, volcanic eruptions, fires, famines, plague, etc.). In civic libraries, one can also find rich newspaper libraries (in paper or microfilm) and precious collections of historical photographs

(sometimes already scanned) which can assist the researcher in locating the occurrence of a natural hazard both in space and time.

## 4. Germany

The situation in Germany is similar to that described in Italy. The official state and regional archives and libraries are the first port of call in historical analysis due to the strong role of the "Bundesländer" and historical territorial fragmentation, with over 50 state and provincial archives. Since the beginning of the 19th century, the MGH (Monumenta Germaniae Historiae) [66] editions have been a central source of medieval history, containing numerous references to earthquakes, volcanic eruptions, climatic extremes, etc., which, contrary to what the name suggests, also covers Western and parts of Southern Europe.

The digitised holdings of the Monumenta Germaniae Historica MGH (www.dmgh.de (accessed on 30 May 2023)) [66] are an example of new forms of access, or those of the Freiburger Zeitung (https://www.ub.uni-freiburg.de/recherche/digitale-bibliothek/freiburger-historische-bestaende/freiburger-zeitung (accessed on 30 May 2023)) [67]. Comprehensive image galleries of flood marks and many other digitised materials are also available online. In addition to these digitization projects, there are new forms of digital portals and virtual research environments such as https://tambora.org (accessed on 30 May 2023) [68], in which environmental and climate-related information is held, evaluated, coded and indexed, with information and sources published using the DOI standard. In this way, the processing of sources can be comprehensively mapped, while complying with international standards such as copyrights [69]. With regard to landslides, Damm and Klose [70] present their concept of a national landslide database for Germany, which mainly includes events of the last 200 years, though the oldest of the 4200 catalogued landslides dates back to the 12th century. The authors conclude that historical archives make up only 10% of the data and that the quality of these reports allows an estimation of the location and date of events. They further state that "the level of accuracy required in data analysis usually became available since the mid-19th century". Although landslides are frequent in Germany and sinkholes occur in geologically favourable areas as well, they are not the major concern when it comes to loss of lives and costs due to natural hazards [71].

Floods constitute the main environmental hazard in Germany. The deadliest events were storm surges at the North Sea, records of which date back to the 13th century. In 1219, tens of thousands of people died in the "Grote Mandranke" or "Erste Marcellusflut", which was witnessed by the Frisian abbot and chronicler Emo von Wittewierum. Other extremely deadly storm surges happened in the 14th and 17th centuries. Dramatic changes to the coastal environment are not only proven by historical sources [72], but also by environmental and sedimentological data [73,74]. Rivers are the second-largest source of flooding hazards in Germany. Historical reports on the River Rhine date back to ~800 AD, with the impact of floods on cities and their populations well documented in archives [75,76], and have enabled the reconstruction of environmental parameters [77–80].

With regard to earthquakes, although its intraplate setting spares Germany from very strong earthquakes, the country has been repeatedly hit by damaging events. Understandably, earthquakes caught the attention of people throughout the centuries and reports on events regularly made it into the newspapers. The first earthquake catalogues for Germany were compiled as early as in the 16th century. Grünthal [81] summarizes "The history of historical earthquake research in Germany" in his study of the same title; he notes that the catalogue of Lycosthène [82] dating back to 1557 (Figure 8) was "one of the most popular of those compilations" and contained close to 200 events. In the 19th century, von Hoff [83,84] published important catalogues of worldwide earthquake data. Perhaps the most famous catalogues are those produced by Sieberg [85] and Sponheuer [86], who "both rely to a certain extent on the monumental work by Lersch" [81,87].

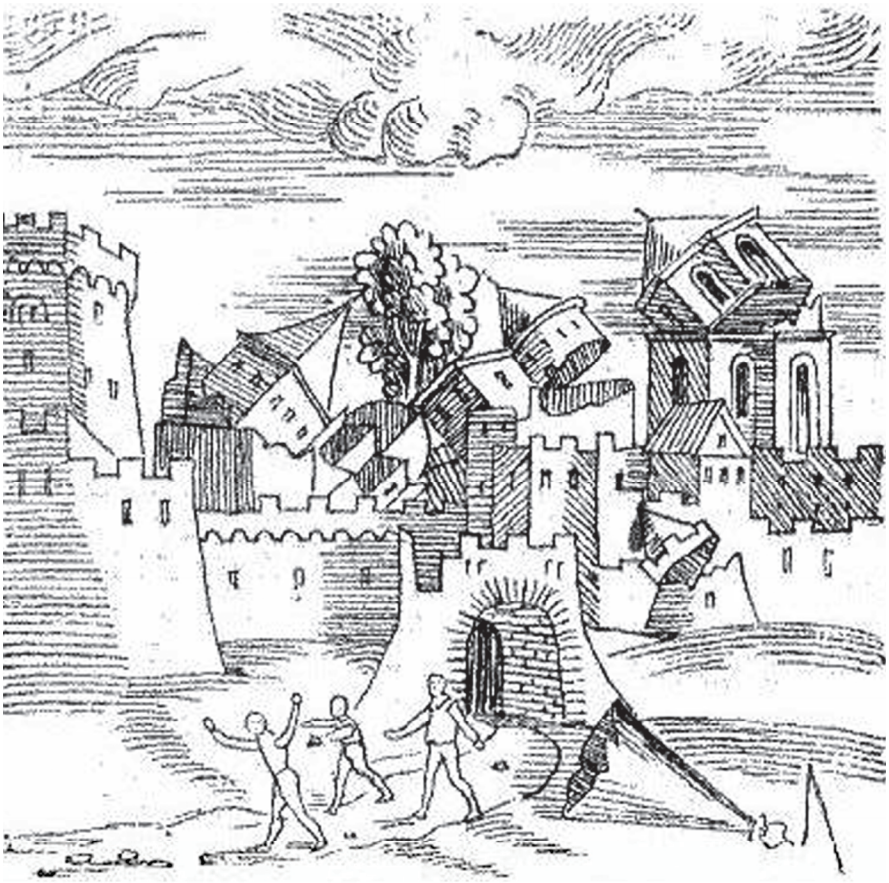



**Figure 8.** Nineteenth century reproduction from "Prodigiorum ac ostentorum chronicon" (1557) by Conrad Lycosthène. https://commons.wikimedia.org/w/index.php?curid=2119198 (accessed on 30 May 2023).

## 5. The United Kingdom

A long history of using historical source material to improve and aid in understanding hazards is present in the UK [38]. This rich legacy continues today, with recent studies exploring and reconstructing a wealth of information to better understand a range of hazards, including flood reconstructions [88]; coastal flooding [89] landslides/landslips [90]; historic droughts [91]; storm and weather reconstructions [92]; and earthquakes [93]. In recent years, focus has turned to better understanding the social and cultural impacts of such events, whilst recognizing that the impacts are felt differently across society, reflecting socio-cultural characteristics. There has also been a move to understand not just the large events, but also how changes during quiescent or mundane phases of time can influence events when they happen. Analysis of archives continues to identify new sources; whilst commonly analysed materials, as previously discussed, are still widely used, a recent example of a new source is the use of school log-books in the Outer Hebrides for reconstructing storm impacts on communities, where few other source materials are available [94]. Historical sources and archives play an important role in helping communities understand the risks presented to them; it can help them envisage complex concepts such as extreme flood magnitudes and impacts, can help build awareness and importantly facilitate better preparedness in communities, reminding them that whilst such events may be rare, they do happen, and likely will again in the future.

The long history of using historical records in the UK has resulted in an expectation that such materials will be considered when looking at high-magnitude, low-frequency

events; as noted by Kjeldsen et al. [95], the UK and Spain are the only countries in which consideration of historical materials is part of the planning consent process. This, in part, is a reflection of the wealth of digitized materials and increasing use of online search tools (see Table 1). However, it is notable that the majority of these databases focus on the physical event rather than the impacts experienced. The result is that few databases have sought to capture the human element of the hazard impacts, nor have they been designed to provide full archival details; a rare exception to this is the TEMPEST database [96].

**Table 1.** Digital databases relating to different hazards in the UK; an example subset.

| Hazard | Digital Search Engine/Tool |
|---|---|
| Weather | National Meteorological Archive |
| Earthquakes | BGS Earthquake database |
| Flooding/Drought | BHS Chronology of British Hydrological Events |
| Landslides | BGS National Landslide Database |
| Coastal flooding | Surgewatch |
| Avalanche | Scottish Avalanche Information Service |

## 6. The Iberian Peninsula

The Iberian Peninsula in general offers an excellent potential for documentary sources for this type of research, both in its cities and in its institutions, thanks to its long history. The types of documentary sources are different from those known in Central Europe or Northern Europe: In the western Mediterranean area, private or personal documentary sources are not common. However, there is a huge public, reliable and homogeneous documentary heritage: the administrative documentation of local authorities, both civil and ecclesiastical. This is documentation ranging from the 14th century to the present. The source materials are of great magnitude and continuity, they are well preserved and their access conditions are optimal (Figure 9).

The administrative sources are objective and reliable due to their origin and the official purposes that define them. Perhaps the main drawback is the low density of information that the sources contain in relation to natural hazards. Its content is routine: it contains bureaucratic procedures that have changed little in recent centuries in the kingdoms of the Hispanic Monarchy; however, phenomena that cause an alteration in these routines with some impact on the daily life of local communities are meticulously documented. Any event that requires a response from public institutions leaves detailed records in administrative sources. This administrative structure and its documentary sources and contents can be found beyond the Iberian Peninsula. Its scope can be defined as that of the group of former kingdoms of the Hispanic Monarchy in the 15th–19th centuries, which includes the states of Spain and Portugal, some regions of Italy and France, and the current Central and South American republics. In these territories, the cities with a minimum capacity for their authorities to generate, store and preserve documentary records, are likely to have useful documentary collections.

Information obtained on natural hazards has important applications for the challenges posed by climate change. It can inform urban planning and support the design and location of public infrastructures so as to reduce risk. Historical information can improve the management of water resources, both in excess (torrential rains, pluvial floods) and deficit situations (droughts). In addition to knowing in detail the behaviour of these natural events, the historical records can be used to supplement long time series based on event severity, duration, extension and frequency, at a range of timescales from daily to annual resolutions. In situations detailing water stress, the documentary records also preserve details of the economic and social impacts, with additional information documenting the decisions adopted at the private and institutional levels in response to these situations. Consequently,

it is also possible to analyse the human dimension of natural hazards using the same sources, assessing the results of the different mitigation or adaptation measures applied.

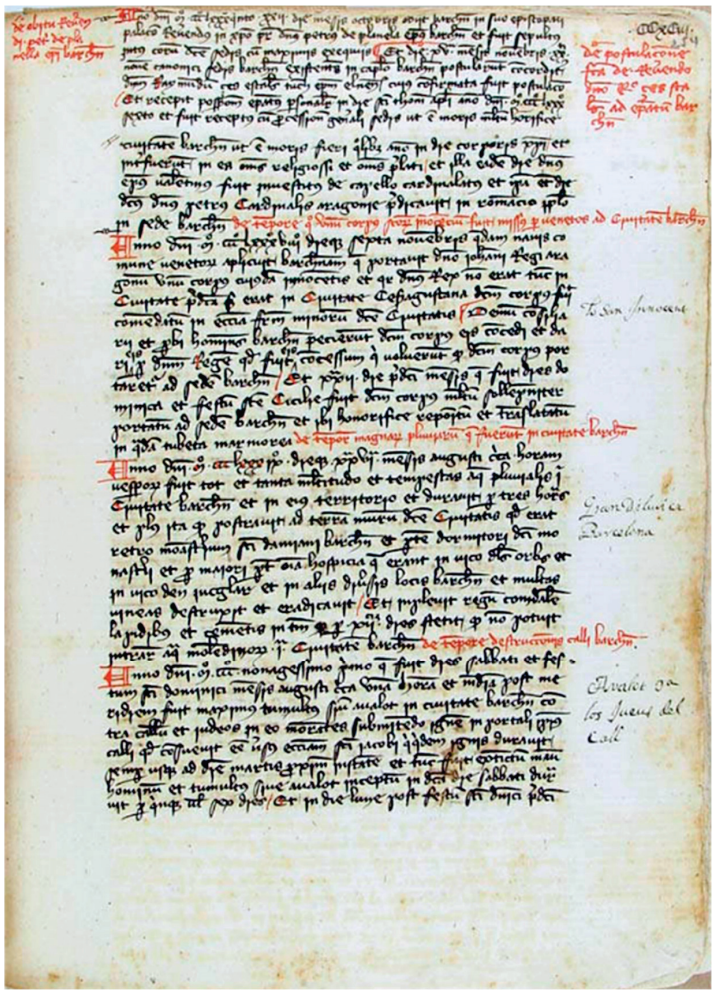


**Figure 9.** Original manuscript describing the first catastrophic flood event in Barcelona city that occurred on 27August 1389. This event, caused by short and torrential rainfall, produced floods that caused the collapse of several buildings and the destruction of crops. Most water mills were closed for two weeks.

Transcription:

"Anno domini m ccc lxxx ix dies xxvii mensis augusti circa horam vespro fuit tot et tanta multitudo et tempestas aquas pluvialis in civitate barchinona et in eio territorio et duravit per tres horas et plo ita qui postravit ad terram murum ditem Civitatis quod erat retro monasterius sancti damiani barchinone et pte dormitori dicti monasteri et per maiori pt ora hospitia q erant in vico dls Orbs et in vico den Jucglar et in alys diversis locus barchinona et multas vineas destruxit et eraditavit/Et inplevit regum comdale lapidibus et cementis in tum qp per xii dies stetit qp no potuit intrar aquam moledinos in civitate barchn."

Reference: Biblioteca de Catalunya, Ms. 485, Bartolomé de Monfar, "Cronicó de Guillem Mascaró", fol. 293. Source for graphic file: Biblioteca de Catalunya [97].

Web site: https://mdc.csuc.cat/digital/collection/manuscritBC/id/28989/rec/1 (accessed on 30 May 2023).

Download date: 7 May 2023

Rights: http://creativecommons.org/publicdomain/mark/1.0/ (accessed on 30 May 2023).

Some examples of this research include the analysis of flood episodes, with more than 5000 episodes catalogued in the Spanish Mediterranean Basin. Some episodes show unprecedented magnitudes compared to the instrumental period, such as that of November 1617, with descriptions of flood levels that exceed the absolute records of current instrumental series in different rivers, and with the documented destruction of 450 structures [98,99]. The administrative sources contain descriptive records of droughts on a daily and systematic basis; they do not contain instrumental records, but document the religious responses that the local authorities, civil and ecclesiastical structures launched in response to reports from the farmer's guilds on the impact of the rainfall deficit on crops. Cultural proxydata such as the "pro pluvia" prayer ceremonies provide a degree of objectivity and independence from institutional structures, providing an opportunity for the quantification in event severity following the different formats of ceremonies that were performed, from simple prayers within the parish churches to processions through the streets of each town, or large pilgrimages to sanctuaries on a regional scale [100,101]. After a systematic compilation in different local archives, it is possible to map the behaviour of severe droughts on a daily basis, such as the droughts detected during the Little Ice Age in the Catalonia region [102] or the mega-drought identified during the Dalton Solar Minimum (1812–1824) in Spain [103].

The potential of historical sources of information is considerable when recognising their homogeneity and availability in hundreds of cities that have preserved documentary collections in local and departmental historical archives. Perhaps the only critical difficulty in this research is the sheer size of the enormous documentary heritage potentially available, with limited capacity for applying technological or computer resources to collect large amounts of information automatically. For example, collections from two main cities in Spain include 2000 linear kilometres of shelves with unexplored handwritten documents; of these, only 3–4% have been systematically consulted. Research opportunities are numerous and diverse, and unexplored materials can provide highly relevant insights into past natural hazards.

## 7. A Global Picture: The Help of the Web

In addition to the aforementioned national sources, there is an increasing range of web-based resources; these can be specific to a region (e.g., Vesuvio Observatory), country/national-level (e.g., British Hydrological Societies—Chronology of British Hydrological Events), continental (e.g., European Catalogue of Volcanoes) or global (e.g., Copernicus—ACRE) [104]. Although the number of such collections has grown in recent decades, they are often planned with a specific focus and/or objective and as such may be of limited utility if analysed from a different perspective. In recent years, there has been an increase in scanning and digitization programmes covering older materials, some undertaken by local/national archives to facilitate the increased availability of rare sources, whilst others have focused on widescale programs of scanning, such as "Google Books", the tool developed by Google to search the text of digitized historical books. "Europeana" (https://www.europeana.eu/it (accessed on 30 May 2023)) [105], on the other hand, is the European digital library that brings together contributions already digitized by various institutions of the European Union; its resources include books, films, paintings, newspapers, sound archives, maps, manuscripts and archives.

Among the other web resources useful for the analysis of natural events is eBay is [106], while elsewhere social networks have facilitated sharing news, old documents, comments and photographs of great historical importance (see, for example, the Italian Facebook group called "Memoria storica dei processi geo-idrologici", that is "Historical memory of geo-hydrological processes"). Sometimes, even small municipalities publish 'misfortunes' of the past that have severely affected the village on their webpage or as blogs. Developing a detailed knowledge of past event magnitude, frequency and impacts presents an opportunity to better understand future risks [56], and also explore our climate futures.

Numerous studies, institutions and procedures exist in the field of historical climatology, especially in Europe, which underline the value of historical documents in the analysis

of climate change and climate extremes. In addition to temperature and precipitation trends over the last 1000 years, long-term reconstructions of climatic extremes are available, which often refer to modern risk assessment: LeRoy Ladurie 1983 [107] mainly for France, Alexandre 1987 [108] for Belgium and western and central Europe, van Engelen et al. 2001 [109] for the Netherlands, Jakubowski-Thiessen [110] for storm surges along the North Sea coastline, Büntgen et al. 2011 and 2021 [111,112] for the whole of Europe and Wanner 2016 for Central Europe [113]. In particular, questions on the frequency and intensity of floods, droughts, storm surges and storms, as well as their long-term changes and relations to climate change, are numerous [75,76,112–115]. In addition to reconstructions of long-term development, there are also elaborations on particularly striking phases such as the Spörer Minimum 1430–1445 [116]. Historical extreme events, such as the 1824 flood in the Neckar, have been used to improve current risk assessments [69,117].

Compilations, which also have a long tradition, form a genre of their own. They are often not written according to modern standards of source criticism, but they offer starting points for further research; for example, Weikinn [118] on weather history, Pfaff [119] on severe winters, or Pötzsch [120] on hydrological extremes along the transnational Elbe/Labe River.

There are numerous institutions and portals on selected topics, both at the national and European levels, which are based on sources such as the information platform "Undine" (https://undine.bafg.de/index.html (accessed on 30 May 2023)) [121]. "Undine" offers descriptions of current and historical high and low water levels for the Elbe, Oder, Rhine, Weser, Ems and Danube rivers, as well as current measured values and historical comparative values.

For technically relevant analyses, a number of impressive databases are now available online. These include PREDIFLOOD [122] in Spain, ORRION in France [123], ICOADS [124], CLIWOC [125], euroclimhist.ch [126] and REACHES [127]. In addition, there are specialised databases, such as those on droughts, including EDII [128], or on marine and early instrumental data [129,130]; further access can be found at https://www.ncdc.noaa.gov/dataaccess/paleoclimatologydata/datasets/historical (accessed on 30 May 2023) [131]. In the nationally funded digitisation projects KLIDADIGI [132] and the manifold historical records of the DWD [129], corresponding collections from German archive holdings have been integrated. In the context of these efforts, questions of data standardisation are also increasingly emerging. At PAGES (https://pastglobalchanges.org/ (accessed on 30 May 2023)) [133], for example, various palaeo data are merged in a common data format (LiPD) according to the FAIR (Findable Accessible Interoperable and Reusable) principles. This opens up new possibilities for Big Data analysis as well as reanalysis [134–136]. Likewise, citizen science activities are contributing to the indexing and analysis of historical datasets. Transcriptions from countless ship diaries, such as those in the https://oldweather.org/ (accessed on 30 May 2023) [137] project, are particularly advanced. These are connected to the International Comprehensive Ocean-Atmosphere Data Set (ICOADS) [138]. Here, the handwritten records of ship diaries, which are therefore difficult to analyse automatically, are transcribed by citizen scientists and thus made accessible for further analysis. Supported by the public media, the weather detectives (www.weatheraustria.net/ (accessed on 30 May 2023)) [139] were able to transcribe more than 400,000 entries from 11,000 citizen scientists by October 2015.

As a further step towards coping with and using the increased amounts of data, automation procedures and their analysis by means of statistics and artificial intelligence are increasingly being applied. In this context, the "digital humanities" are concerned with researching text-based questions in the humanities using digital methods. One methodological basis of these approaches is hermeneutic interpretation [140]. Texts that a few years ago were difficult to read can now be made accessible in a fraction of a second by means of automatic text recognition (Optical Character Recognition—OCR). Many approaches aim to go beyond qualitative analysis to quantification by means of word decomposition (tokenising). In order to go beyond word boundaries and to recognise grammatical connections, methods from the field of artificial intelligence and machine learning are increasingly

being used. Common methods include text mining [141], natural language processing (NLP), reinforcement learning and classification. Their application to newspaper archives and information in the context of climatic issues is demonstrated by Yzaguirre, Smit and Warren [142] with their impressive analysis of over two million articles, and Kang and Park [143] using Korean newspapers.

Historical documents are also the basis for comprehensive catalogues; for example, of earthquakes in Central Europe from the years 800 to2008 compiled by Leydecker [144], as maintained by official bodies [145].

In conclusion, there is a wide range of historical sources from which anyone can learn about the past; finding them is not easy amidst the flood of existing data in the world. Once found, however, it is clear that each individual account requires an assessment of its veracity, such as by comparing it with other sources before putting it into the public domain. This should be taken as warm advice; for example, the landslide generated by the very strong earthquake that occurred in 1857 in Montemurro, Basilicata, Southern Italy [146]. Many Italian geologists and experts in later years reported that the landslide caused 5000 casualties (it would have been one of the most catastrophic historical landslides in Europe), but an analysis in the different archives (conducted also by the present authors) has never made it possible to ascertain a certain and verified figure. Perhaps it was a misunderstanding (probably generated by an error in Almagià's 1907 book [147] that first reported this news): the earthquake caused the victims, while the landslide triggered by the earthquake probably did not cause loss of human life.

**Author Contributions:** Conceptualization and methodology, F.L., L.T., M.B., F.T.G., R.G., C.G., W.P., S.P. and H.S.; validation, investigation and data curation, F.L., L.T., M.B., F.T.G., R.G., C.G., W.P., S.P. and H.S.; proposal for the formation of the Special Issue, F.L.; search and contact for contributions from colleagues, F.L. and S.P.; writing—original draft preparation, F.L., L.T., M.B., F.T.G., R.G., C.G., W.P., S.P. and H.S.; writing—review and editing, F.L., L.T., M.B., F.T.G., R.G., C.G., W.P., S.P. and H.S.; grammatical correction of the text, H.S.; supervision, F.L. All authors have read and agreed to the published version of the manuscript.

**Funding:** This research was funded by: (i) FONTES PRIN Project (Italian National Research Project "Fonti geostoriche e sistemi informativi per la conoscenza del territorio e la gestione dei rischi ambientali e culturali") (https://fontes.univr.it/ (accessed on 30 May 2023)), supported by Government Funding (Project CNR Number DTA.AD003.737). The research activity was also sustained by: (ii) the BEGIN project (DUS.AD017.190, CUP C39J20001760002), financed by Basilicata ERDF-ROP 2014-2020. This research was also funded by: (iii) "Project PID2021-126411OB-I00 (DENDROHIST), Ministerio de Ciencia e Innovación, Spain".

**Data Availability Statement:** Data sharing does not apply to this paper.

**Conflicts of Interest:** The authors declare no conflict of interest.

## References

1. UNDRR. Available online: https://www.undrr.org/terminology/disaster (accessed on 28 June 2023).
2. EM-DAT. The International Disaster Database. Available online: www.emdat.be (accessed on 28 June 2023).
3. WMO. 2021. Available online: https://public.wmo.int/en/media/press-release/weather-related-disasters-increase-over-past-50-years-causing-more-damage-fewer (accessed on 28 June 2023).
4. Barredo, J.I. Major Flood Disasters in Europe: 1950–2005. *Nat. Hazards* **2007**, *42*, 125–148. [CrossRef]
5. Neumayer, E.; Barthel, F. Normalizing economic loss from natural disasters: A global analysis. *Glob. Environ. Chang.* **2011**, *21*, 13–24. [CrossRef]
6. Roser, M.; Ritchie, H.; Ortiz-Ospina, E. World Population Growth. 2020. Available online: https://ourworldindata.org/world-population-growth (accessed on 15 June 2023).
7. Settis, S. *Paesaggio Costituzione Cemento. La Battaglia per L'ambiente Contro Il Degrado Civile*; Einaudi Ed: Rome, Italy, 2010; p. 328, ISBN 9788806198718.
8. Gizzi, F.T.; Porrini, D.; De Masi, F. Building a Natural Hazard Insurance System (NHIS): The Long-lasting Italian Case. *Sustainability* **2021**, *13*, 12269. [CrossRef]
9. Butler, J.E. *Natural Disasters*; Heinemann Educational: Richmond, Australia, 1976; 138p.

10. Alexander, D.E. *Natural Disasters*; University College London Press: London, UK; Kluwer Academic Publishers: Boston, MA, USA, 1993; 632p.
11. Jonkman, S.N. Global Perspectives on Loss of Human Life Caused by Floods. *Nat. Hazards* **2005**, *34*, 151–175. [CrossRef]
12. Shi, P.; Wang, J.; Xu, W.; Ye, T.; Yang, S.; Liu, L.; Fang, W.; Liu, K.; Li, N.; Wang, M. *World Atlas of Natural Disaster Risk*; Shi, P., Kasperson, R., Eds.; IHDP/Future Earth-Integrated Risk Governance Project Series; Springer: Berlin/Heidelberg, Germany, 2015. [CrossRef]
13. Abbott, P.L. *Natural Disasters*, 10th ed.; McGrew-Hill: New York, NY, USA, 2018; 484p, ISBN 13-978-0078022982.
14. Bobrowsky, P.T.; Marker, B. (Eds.) *Encyclopedia of Engineering Geology*; Springer: Berlin/Heidelberg, Germany, 2018; ISBN 978-3-319-73566-5.
15. Baldo, M.; Bicocchi, C.; Chiocchini, U.; Giordan, D.; Lollino, G. LIDAR monitoring of mass wasting processes: The Radicofani landslide, Province of Siena, central Italy. *Geomorphology* **2009**, *105*, 193–201. [CrossRef]
16. McCalpin, J.; Ferrario, F.; Figueiredo, P.; Livio, F.; Grützner, C.; Pisarska-Jamroży, M.; Quigley, M.; Reicherter, K.; Rockwell, T.; Štěpančíková, P.; et al. New developments in onshore paleoseismic methods, and their impact on Quaternary tectonic studies. *Quat. Int.* **2023**, *664*, 59–76. [CrossRef]
17. Tonkin, T.N.; Midgley, N.G.; Cook, S.J.; Graham, D.J. Ice-cored moraine degradation mapped and quantified using an unmanned aerial vehicle: A case study from a polythermal glacier in Svalbard. *Geomorphology* **2016**, *258*, 1–10. [CrossRef]
18. Elliott, J.R.; Walters, R.J.; Wright, T.J. The role of space-based observation in understanding and responding to active tectonics and earthquakes. *Nat. Commun.* **2016**, *7*, 13844. [CrossRef]
19. Chen, W.; Sun, Z.; Han, J. Landslide susceptibility modeling using integrated ensemble weights of evidence with logistic regression and random forest models. *Appl. Sci.* **2019**, *9*, 171. [CrossRef]
20. Hill, C.L. Geomorphological Survey. In *The Encyclopedia of Archaeological Sciences*; Wiley Blackwell: Hoboken, NJ, USA, 2018; pp. 1–4.
21. Tavares, A.O.; Pato, R.L.; Magalhaes, M.C. Spatial and temporal land use change and occupation over the last half century in a peri-urban area. *Appl. Geogr.* **2012**, *34*, 432–444. [CrossRef]
22. Skidmore, A. *Environmental Modelling with GIS and Remote Sensing*; Skidmore, A., Ed.; CRC Press: Boca Raton, FL, USA; Taylor and Francis: New York, NY, USA, 2017; 266p.
23. Zhang, K.; Xue, X.; Hong, Y.; Gourley, J.J.; Lu, N.; Wan, Z.; Hong, Z.; Wooten, R. iCRESTRIGRS: A coupledmodeling system for cascading flood-landslide disaster forecasting. *Hydrol. Earth Syst. Sci.* **2016**, *20*, 5035–5048. [CrossRef]
24. Brunetti, M.T.; Melillo, M.; Peruccacci, S.; Ciabatta, L.; Brocca, L. How far are we from the use of satellite rainfall products in landslide forecasting? *Remote Sens. Environ.* **2018**, *210*, 65–75. [CrossRef]
25. Govi, M.; Turitto, O. *Ricerche Bibliografiche per un Catalogo Sulle Inondazioni, Piene Torrentizie e Frane in Valtellina e Valchiavenna*; Supplemento a GEAM, Quaderni di Studi e di Documentazione; Associazione Mineraria Subalpina: Torino, Italy, 1994; 249p. (In Italian)
26. Yevjevich, V. Floods and society. In *Coping with Floods*; Rossi, G., Harmancioğlu, N., Yevjevich, V., Eds.; NATO ASI Series; Springer: Dordrecht, The Netherlands, 1994; Volume 257. [CrossRef]
27. Luino, F.; Belloni, A.; Padovan, N.; Bassi, M.; Bossuto, P.; Fassi, P. Historical and geomorphological analysis as a research tool for the identification of flood-prone zones and its role in the revision of town planning: The Oglio basin (Valcamonica—Northern Italy). In Proceedings of the 9th Congress of the IAEG, Durban, South Africa, 16–20 September 2002; pp. 191–200.
28. Esposito, E.; Porfido, S.; Violante, C. (Eds.) *Il Nubifragio Dell'ottobre 1954 a Vietri sul Mare-Costa di Amalfi, Salerno*; GNDCI-CNR: Rome, Italy, 2004. (In Italian)
29. Tropeano, D.; Turconi, L. Using Historical Documents for Landslide, Debris Flow and Stream Flood Prevention. Applications in Northern Italy. *Nat. Hazards* **2004**, *31*, 663–679. [CrossRef]
30. Tropeano, D.; Luino, F.; Turconi, L.; Agangi, A.; Audisio, C.; Biddoccu, M.; Chiarle, M.; Casazza, M.; Cirio, C.G.; Fassi, P.; et al. *Eventi di Piena e Frana in Italia Settentrionale Nel Periodo 2002–2004*; SMS: Torino, Italy, 2006; 158p. (In Italian)
31. Devoli, G.; Morales, A.; Høeg, K. Historical landslides in Nicaragua-collection and analysis of data. *Landslides* **2007**, *4*, 5–18. [CrossRef]
32. Macdonald, N. On epigraphic records: Valuable resource in reassessing flood risk and long-term climate variability. *Environ. Hist.* **2007**, *12*, 136–140. [CrossRef]
33. Porfido, S.; Esposito, E.; Alaia, F.; Molisso, F.; Sacchi, M. The use of documentary sources for reconstructing flood chronologies on the Amalfi rocky coast (southern Italy). In *Geohazard in Rocky Coastal Areas*; Violante, C., Ed.; Geological Society: London, UK, 2009; pp. 173–187, ISBN 978-1-86239-282-3. [CrossRef]
34. Foscari, G.; Esposito, E.; Mazzola, S.; Porfido, S.; Sciarrotta, S.; Santoro, G. *Lo Alluvione. Il Disastro del 1773 a Cava Tra Memoria Storica e Rimozione*; Edisud: Salerno, Italy, 2013; pp. 9–31, ISBN 978-88-95154-87-9. (In Italian)
35. Hutař, J.; Melichar, M. The long decade of digital preservation in heritage institutions in the Czech Republic: 2002–2014. *Int. J. Digit. Curation* **2015**, *10*, 173–183. [CrossRef]
36. McEwen, L.; Garde-Hansen, J.; Holmes, A.; Jones, O.; Krause, F. Sustainable flood memories, lay knowledges and the development of community resilience to future flood risk. *Trans. Inst. Br. Geogr.* **2017**, *42*, 14–28. [CrossRef]
37. Luino, F.; Turconi, L. *Eventi di Piena e Frana in Italia Settentrionale Nel Periodo 2005–2016*; SMS: Torino, Italy, 2017; 478p. (In Italian)
38. Sangster, H.; Jones, C.; Macdonald, N. The co-evolution of historical source materials in the geophysical, hydrological and meteorological sciences: Learning from the past and moving forward. *Prog. Phys. Geogr.* **2018**, *42*, 61–82. [CrossRef]

39. Garnier, E.; Lahournat, F. Japanese stone monuments and disaster memory–Perspectives for DRR. *Disaster Prev. Manag.* **2022**, *31*, 1–12. [CrossRef]
40. Naylor, S.; Macdonald, N.; Bowen, J.P.; Endfield, G. Extreme weather, school logbooks and social vulnerability: The Outer Hebrides, Scotland, in the late nineteenth and early twentieth centuries. *J. Hist. Geogr.* **2022**, *78*, 84–94. [CrossRef]
41. Sarconi, M. *Istoria de' Fenomeni Del Tremoto Avvenuto Nelle Calabrie, e Nel Valdemone Nell'anno 1783 Posta in Luce Dalla Reale Accademia Delle Scienze, e Delle Belle Lettere di Napoli*; Campo: Napoli, Italy, 1784. (In Italian)
42. Konvitz, J. *Cartography in France 1660–1848*; Le Roy, L., Ed.; University of Chicago Press: Chicago, IL, USA, 1987.
43. Forty, S.; Swift, M. *Historical Maps of the Napoleonic Wars*; Brassey's: London, UK, 2003; 144p.
44. Radding, L.; Western, J. What's in a name? Linguistics, geography, and toponyms. *Geogr. Rev.* **2010**, *100*, 394–412. [CrossRef]
45. Dell'O, E. Historicizing vulnerability: Place-names, risk and memory in the Mont Blanc area. *AIMS Geosci.* **2019**, *5*, 493–508. [CrossRef]
46. Newhall, B. *The History of Photographyfrom 1839 to the Present*; The Museum of Modern Art: New York, NY, USA, 1988; 320p, ISBN 100870703811/139780870703812.
47. House, E. *A History of Photography*; Taschen: Koln, Germany, 2012; 768p, ISBN 103836540991.
48. Cosgrove, D.; Fox, W.L. *Photography and Flight*; Reaktion Books: London, UK, 2010; 146p.
49. Padley, G. *The Story of Aerial Photography (150 Years of Breathtaking Imagery)*; Laurence King Publishing: London, UK, 2019; 256p.
50. Luino, F.; Belloni, A.; Turconi, L.; Faccini, F.; Mantovani, A.; Fassi, P.; Marincioni, F.; Caldiroli, G. An historical geomorphological approach to flood hazard management along the shores of an alpine lake (Northern Italy). *Nat. Hazards* **2018**, *94*, 471–488. [CrossRef]
51. Iwaka, K.; Kozuki, Y.; Yamanaka, R.; Tanabe, S.; Murakami, H. Values and Applications of Earthquake and Tsunami Stone Monuments in Tokushima. *J. Jpn. Soc. Civ. Eng. Ser. B2 (Coast. Eng.)* **2011**, *67*, I_1261–I_1265. [CrossRef]
52. Luino, F.; Ramasco, M.; Susella, G. *Atlante dei Centri Abitati Instabili Piemontesi*; Monograph: Torino, Italy, 1993; 245p. (In Italian)
53. Gizzi, F.T.; Masini, N. Historical Earthquakes and Damage Patterns for Potenza (Basilicata, Southern Italy). *Ann. Geophys.* **2007**, *50*, 599–611.
54. Gizzi, F.T.; Potenza, M.R.; Zotta, C. 23 November 1980 Irpinia–Basilicata earthquake (Southern Italy): Towards a full knowledge of the seismic effects. *Bull. Earthq. Eng.* **2012**, *10*, 1109–1131. [CrossRef]
55. Schenk, G.J. Managing natural hazards: Environment, society, and politics in Tuscany and the Upper Rhine Valley in the Renaissance (1270–1570). In *Historical Disasters in Context: Science, Religion, and Politics*; Janku, A., Schenk, G.J., Mauelshagen, F., Eds.; Routledge: New York, NY, USA; London, UK, 2012; pp. 31–53.
56. Blöschl, G.; Kiss, A.; Viglione, A.; Barriendos, M.; Böhm, O.; Brazdil, R.; Coeur, D.; Demaree, G.; Llasat, M.C.; MacDonald, N.; et al. Current European flood-rich period exceptional compared with past 500 years. *Nature* **2020**, *583*, 560–566. [CrossRef] [PubMed]
57. Gizzi, F.T.; Potenza, M.R. The Scientific Landscape of November 23rd, 1980 Irpinia-Basilicata Earthquake: Taking Stock of (Almost) 40 Years of Studies. *Geosciences* **2020**, *10*, 482. [CrossRef]
58. Glaser, R.; Kahle, M. Reconstructions of droughts in Germany since 1500–Combining hermeneutic information and instrumental records in historical and modern perspectives. *Clim. Past* **2020**, *16*, 1207–1222. [CrossRef]
59. Elleder, L.; Kašpárek, L.; Šírová, J.; Kabelka, T. Low water stage marks on hunger stones: Verification for the Elbe from 1616 to 2015. *Clim. Past* **2020**, *16*, 1821–1846. [CrossRef]
60. Vitali, S. *Gli Archivi di Stato Italiani Fra Memoria Nazionale e Identità Locali*; Società Editrice Il Mulino: Bologna, Italy, 2011; pp. 119–129. (In Italian) [CrossRef]
61. Archivio Centrale Dello Stato. Available online: https://acs.cultura.gov.it/ (accessed on 4 April 2023).
62. Archivio di Stato di Campobasso. *La frana di Rocchetta al Volturno*; Archivio di Stato di Campobasso: Genio Civile, Italy, 1906. (In Italian)
63. Palmieri, W. Uomini e dissesti: Frane e alluvioni nell'Ottocento molisano. In *Storia del Molise in età Contemporanea*; Massullo, G., Ed.; Donzelli Editore: Rome, Italy, 2006; pp. 205–241. (In Italian)
64. Brunetti, D. L'archivio comunale dall'Unità al 1897. In *Ministero Dei Beni e Delle Attività Culturali e Del Turismo Direzione Generale Archivi*; Modus Sistemas: Rome, Italy, 2016; 372p. (In Italian)
65. Medolago, G. La rovina del Goglio a Gromo e Valgoglio nel 1666. In *Disastri e Comunità Alpine*; ISTA, Printed by The Factory on Behalf of Borè srl: Rome, Italy, 2019; pp. 59–76. (In Italian)
66. Monumenta Germaniae Historica MGH. Available online: www.dmgh.de (accessed on 4 April 2023).
67. Freiburger Zeitung. Available online: https://www.ub.uni-freiburg.de/recherche/digitale-bibliothek/freiburger-historische-bestaende/freiburger-zeitung (accessed on 4 April 2023).
68. Tambora. Available online: https://tambora.org (accessed on 4 April 2023).
69. Riemann, D.; Glaser, R.; Kahle, M.; Vogt, S. The CRE tambora.org–New data and tools for collaborative research in climate and environmental history. *Geosci. Data J.* **2016**, *2*, 63–77. [CrossRef]
70. Damm, B.; Klose, M. The landslide database for Germany: Closing the gap at national level. *Geomorphology* **2015**, *249*, 82–93. [CrossRef]
71. Kreibich, K.; Schröter, K.; Bubeck, P.; Kunz, M.; Mahlke, H.; Parolai, S.; Khazai, B.; Daniell, J.; Lakes, T. A review of multiple natural hazards and risks in Germany. *Nat. Hazards* **2014**, *74*, 2279–2304. [CrossRef]

72. Kempe, M. Mind the next flood! Memories of natural disasters in Northern Germany from the sixteenth century to the present. *Mediev. Hist. J.* **2006**, *10*, 327–354. [CrossRef]
73. Behre, K.E. Die Veränderungen der niedersächsischen Küstenlinien in den letzten 3000 Jahren und ihre Ursachen. *Probl. Der Küstenforschung Im Südlichen Nord.* **1999**, *26*, 9–33. (In German)
74. Behre, K.E. Coastal development, sea-level change and settlement history during the later Holocene in the Clay District of Lower Saxony (Niedersachsen), northern Germany. *Quat. Int.* **2004**, *112*, 37–53. [CrossRef]
75. Glaser, R.; Stangl, H. Historical floods in the Dutch Rhine delta. *Nat. Hazards Earth Syst. Sci.* **2003**, *3*, 605–613. [CrossRef]
76. Himmelsbach, I.; Glaser, R.; Schönbein, J.; Riemann, D.; Martin, B. Reconstruction of flood events based on documentary data and transnational flood risk analysis of the upper Rhine and its French and German tributaries since AD 1480. *Hydrol. Earth Syst. Sci.* **2015**, *19*, 4149–4164. [CrossRef]
77. Brázdil, R.; Kundzewicz, Z.W.; Benito, G. Historical hydrology for studying flood risk in Europe. *Hydrol. Sci. J.* **2006**, *51*, 739–764. [CrossRef]
78. Bürger, K.; Dostal, P.; Seidel, J.; Imbery, F.; Barriendos, M.; Mayer, H.; Glaser, R. Hydrometeorological reconstruction of the 1824 flood event in the Neckar River basin (southwest Germany). *Hydrol. Sci. J.* **2006**, *51*, 864–877. [CrossRef]
79. Herget, J.; Meurs, H. Reconstructing peak discharges for historic flood levels in the city of Cologne, Germany. *Glob. Planet. Chang.* **2010**, *70*, 108–116. [CrossRef]
80. Roggenkamp, T.; Herget, J. Reconstructing peak discharges of historic floods of the River Ahr, Germany. *Erdkunde* **2014**, *68*, 49–59. [CrossRef]
81. Grünthal, G. The history of historical earthquake research in Germany. *Ann. Geophys.* **2004**, *42*, 631–643. [CrossRef]
82. Lycosthenes, C.; Wolfharth, K.; Wolffard, K. *Prodigiorium ac Ostentorum Chronicon, Quae Prater Naturae Ordinem*; per Henricum Petri: Basel, Switzerland, 1557; 670p.
83. von Hoff, K.E.A. *Chronik der Erdbeben und Vulcan-Ausbrüche*; I. Teil; Justus Perthes: Gotha, Germany, 1840; 470p.
84. von Hoff, K.E.A. *Chronik der Erdbeben und Vulcan-Ausbrüche*; II. Teil; Justus Perthes: Gotha, Germany, 1841; 406p.
85. Sieberg, A. *Beiträge Zum Erdbebenkatalog Deutschlands und Angrenzender Gebietefür die Jahre 58 Bis 1799*; Mitt. Deutsch. Reichs-Erdbebendienst: Jena, Germany, 1940; 112p. (In German)
86. Sponheuer, W. *Erdbebenkatalog Deutschlands und der Angrenzenden Gebiete für die Jahre 1800–1899*; Mitt. Deutsch. Erdbebendienst: Berlin, Germany, 1952; 195p. (In German)
87. Lersch, B.M. *Erdbebenchronik für die Zeit Von 2362 v. Chr. Bis 1897*; Springer: Aachen, Germany, 1897. (In German)
88. Macdonald, N.; Sangster, H. High magnitude flooding across Britain since A.D. 1750. *Hydrol. Earth Syst. Sci.* **2017**, *21*, 1631–1650. [CrossRef]
89. Haigh, I.; Ozsoy, O.; Wadey, M.P.; Nicholls, R.J.; Gallop, S.L.; Wahl, T.; Brown, J.M. An improved database of coastal flooding in the United Kingdom from 1915 to 2016. *Sci. Data* **2017**, *4*, 170100. [CrossRef] [PubMed]
90. Bowen, J.P.; Macdonald, N. A dreadful phenomenon described and improved: Reverend John Fletcher's account of the Buildwas earthquake of 1773. *J. Hist. Geogr.* **2019**, *64*, 72–84. [CrossRef]
91. Murphy, C.; Wilby, R.L.; Matthews, T.; Horvath, C.; Crampsie, A.; Ludlow, F.; Noone, S.; Brannigan, J.; Hannaford, J.; McLeman, R.; et al. The forgotten drought of 1765–1768: Reconstructing and re-evaluating historical droughts in the British and Irish Isles. *Int. J. Climatol.* **2020**, *40*, 5329–5351. [CrossRef]
92. Hawkins, E.; Burt, S.; McCarthy, M.; Murphy, C.; Ross, C.; Baldock, M.; Brazier, J.; Hersee, G.; Huntley, J.; Meats, R.; et al. Millions of historical monthly rainfall observations taken in the UK and Ireland rescued by citizen scientists. *Geosci. Data J.* **2023**, *10*, 246–261. [CrossRef]
93. Musson, R.M.W. A critical history of British earthquakes. *Ann. Geophys.* **2004**, *47*, 597–609.
94. Macdonald, N.; Naylor, S.; Bowen, J.P.; Harvey-Fishenden, A.; Graham, E. Understanding weather futures based on the past: A case of Stornoway, Outer Hebrides. *Scott. Geogr. J.* **2023**, *78*, 84–94. [CrossRef]
95. Kjeldsen, T.R.; Macdonald, N.; Lang, M.; Mediero, L.; Albuquerque, T.; Bogdanowicz, E.; Brázdil, R.; Castellarin, A.; David, V.; Fleig, A.; et al. Documentary evidence of past floods in Europe and their utility in flood frequency estimation. *J. Hydrol.* **2014**, *517*, 963–973. [CrossRef]
96. Endfield, G.H.; Veale, L.; Royer, M.-J.; Bowen, J.P.; Davies, S.; Macdonald, N.; Naylor, S.; Jones, C.; Tyler-Jones, R. Extreme weather in the UK: Past, present and future—event details from the TEMPEST database. *Cent. Environ. Data Anal.* **2017**. [CrossRef]
97. Biblioteca de Catalunya (Library of Catalonia), Section Manuscripts, Ms. 485, Bartolomé de Monfar, "Cronicó de Guillem Mascaró". 1531. 1 Volume. Available online: https://mdc.csuc.cat/digital/collection/manuscritBC/id/28989/rec/1 (accessed on 4 April 2023).
98. Thorndycraft, V.; Barriendos, M.; Benito, G.; Rico, M.; Casas, A. The catastrophic floods of A.D. 1617 in Catalonia (NE Spain) and their climatic context. *Hydrol. Sci. J.* **2006**, *51*, 899–912. [CrossRef]
99. Pino, P.; Alberola, A.; Balasch, C.; Barriendos, M.; Gil, S.; Grau-Satorras, M.; Mazón, J.; Pérez Morales, A.; Tuset, J. Major flood events reconstruction from a multi-proxy approach. The case study of November 1617 flood event in the Mediterranean Basins of Iberian Peninsula. In Proceedings of the 18th EGU General Assembly, European Geosciences Union, Wien, Austria, 8–13 April 2018.
100. Martin-Vide, J.; Barriendos, M. The use of rogation ceremony records in climatic reconstruction: A case study from Catalonia (Spain). *Clim. Chang.* **1995**, *30*, 201–221. [CrossRef]
101. Barriendos, M. Climatic variations in the Iberian Peninsula during the late Maunder Minimum (AD 1675-1715): An analysis of data from rogation ceremonies. *Holocene* **1997**, *7*, 105–111. [CrossRef]

102. Oliva, M.; Ruiz-Fernández, J.; Barriendos, M.; Benito, G.; Cuadrat, J.M.; García-Ruiz, J.M.; Giralt, S.; Gómez-Ortiz, A.; Hernández, A.; López-Costas, O.; et al. The Little Ice Age in Iberian mountains". *Earth Sci. Rev.* **2018**, *177*, 175–208. [CrossRef]
103. Barriendos, M.; Barriendos, J.; Hernández, M.; Gil-Guirado, S.; Olcina-Cantos, J. Drought variability in the Spanish Mediterranean Basin during the Dalton Solar Minimum period (1790–1830). In Proceedings of the EGU General Assembly 2023, Vienna, Austria, 24–28 April 2023; EGU23-3976. [CrossRef]
104. Allan, R.; Endfield, G.; Damodaran, V.; Adamson, G.; Hannaford, M.; Carroll, F.; Macdonald, N.; Groom, N.; Jones, J.; Williamson, F.; et al. Toward integrated historical climate research: The example of Atmospheric Circulation Reconstructions over the Earth. *Wires Clim. Chang.* **2016**, *7*, 164–174. [CrossRef]
105. Europeana. Available online: https://www.europeana.eu/it (accessed on 4 April 2023).
106. Gizzi, F.T. The electronic trading site eBay as a useful tool for obtaining historical data on natural events. *Comput. Geosci.* **2009**, *35*, 1950–1957. [CrossRef]
107. Le Roy Ladurie, E. *Histoire du Climat Depuis L'an Mil*; FLAMMARION: Paris, France, 1983.
108. Alexandre, P. *Le Climat in Europe au Moyen Age*; l'École des Hautes études en Sciences Sociales: Paris, France, 1987; 827p.
109. van Engelen, A.F.V.; Buisman, J.; Ijnsen, F. A Millennium of Weather, Winds and Water in the Low Countries. In *History and Climate*; Jones, P.D., Ogilvie, A.E.J., Davies, T.D., Briffa, K.R., Eds.; Springer: Boston, MA, USA, 2001. [CrossRef]
110. Jakubowski-Thiessen, M. Die großen Mandränken. Sturmfluten in Nordfriesland. In *(Hrsg.): Das Große Nordfriesland-Buch*; Steensen, T., Ed.; Verlag Ellert & Richter: Hamburg, Germany, 2000; pp. 122–133. (In German)
111. Büntgen, U.; Tegel, K.; Nicolussi, M.; McCormick, D.; Frank, V.; Trouet, J.O.; Kaplan, F.; Herzig, K.-U.; Heussner, H.; Wanner, J.; et al. 2500 Years of European Climate Variability and Human Susceptibility. *Science* **2011**, *331*, 578–582. [CrossRef]
112. Büntgen, U.; Urban, O.; Krusic, P.J.; Rybníček, M.; Kolář, T.; Kyncl, T.; Ač, A.; Koňasová, E.; Čáslavsky, J.; Esper, J.; et al. Recent European drought extremes beyond Common Era background variability. *Nat. Geosci.* **2021**, *14*, 190–196. [CrossRef]
113. Wanner, H. *Klima und Mensch—Eine 12'000-jährige Geschichte Hardcover*; Haupt Verlag: Bern, Switzerland, 2016; 276S.
114. Glaser, R.; Stangl, H.; Lang, M. Floods in Central Europe Since AD 1300 And Their Regional Context. In *Colloque SHF "Etiages et Crues Extrémes Régionaux en Europe"*; Taylor & Francis: Lyon, France, 2004; pp. 63–72.
115. Cook, E.R.; Seager, R.; Kushnir, Y.; Briffa, K.R.; Büntgen, U.; Frank, D.; Krusic, P.J.; Tegel, W.; van der Schrier, G.; Andreu-Hayles, L.; et al. Old World megadroughts and pluvials during the Common Era. *Sci. Adv.* **2015**, *1*, e1500561. [CrossRef] [PubMed]
116. Camenisch, C.; Keller, K.M.; Salvisberg, M.; Amann, B.; Bauch, M.; Blumer, S.; Brázdil, R.; Brönnimann, S.; Büntgen, U.; Campbell, B.M.S.; et al. The Early Spörer Minimum—A Period of Extraordinary Climate and Socio-Economic Changes in Western and Central Europe. *Clim. Past* **2016**, 1–33. Available online: http://www.clim-past-discuss.net/cp-2016-7/ (accessed on 4 April 2023).
117. Sudhaus, D.; Seidel, J.; Bürger, K.; Dostal, P.; Imbery, F.; Mayer, H.; Glaser, R.; Konold, W. Discharges of past flood events based on historical river profiles. *Hydrol. Earth Syst. Sci.* **2008**, *12*, 1201–1209. [CrossRef]
118. Weikinn, C. *Quellentexte Zur Witterungsgeschichte Europas von der Zeitwende bis Zum Jahre 1850*; Akademie Verlag: Berlin, Germany, 1958.
119. Pfaff, C.H. *Über die Strengen Winter Vorzüglich des Achtzehnten Jahrhunderts und über den Letzt Verflossenen Winter von 1808–1809*; Academischen Buchhandlung: Freiberg, Germany, 1809.
120. Pötzsch, C.G. *Chronologische Geschichte der Großen Wasserfluthen des Elbstroms Seit Tausend und Mehr Jahren*; Waltherische Hofbuchhandlung: Dresden, Germany, 1784.
121. Undine Informationsplattform. Available online: https://undine.bafg.de/index.html (accessed on 30 May 2023).
122. Barriendos, M.; Ruiz-Bellet, J.L.; Tuset, J.; Mazón, J.; Balasch, J.C.; Pino, D.; Ayala, J.L. The "Prediflood" database of historical floods in Catalonia (NE Iberian Peninsula) AD 1035–2013, and its potential applications in flood analysis. *Hydrol. Earth Syst. Sci.* **2014**, *18*, 4807–4823. [CrossRef]
123. Martin, B.; Giacona, F.; Furst, B.; Edelblutte, C.; Holleville, N.; Vitoux, M.C.; Glaser, R.; Himmelsbach, I.; Schönbein, J.; Heitz, C.; et al. ORRION: A Specific Information Sharing Tool to (re)Build a "Flood Risk Culture" in the Rhine Graben (France–Germany). *E3SWeb Conf.* **2016**, *7*, 18. Available online: https://www.e3sconferences.org/articles/e3sconf/abs/2016/02/e3sconf_flood2016_15005/e3sconf_flood2016_15005.html (accessed on 30 May 2023). [CrossRef]
124. Woodruff, S.D.; Worley, S.J.; Lubker, S.J.; Ji, Z.; Freeman, J.E.; Berry, D.I.; Brohan, P.; Kent, E.C.; Reynolds, R.W.; Smith, S.R.; et al. ICOADS Release 2.5: Extensions and enhancements to the surface marine meteorological archive. *Int. J. Climatol.* **2011**, *31*, 951–967. [CrossRef]
125. García-Herrera, R.; Können, G.P.; Wheeler, D.A.; Prieto, M.R.; Jones, P.D.; Koek, F.B. CLIWOC: A Climatological Database for the World's Oceans 1750–1854. *Clim. Chang.* **2005**, *73*, 1–12. [CrossRef]
126. Pfister, C. Euro-Climhist, Module Switzerland, Release 2. In *Euro-Climhist*; Pfister, C., Rohr, C., Eds.; Informationssystem zur Witterungs- und Klimageschichte; Cambridge University Press: Cambridge, UK, 2015. Available online: www.euroclimhist.unibe.ch (accessed on 30 April 2023).
127. Wang, P.; Lin, K.H.; Liao, Y.C. Construction of the REACHES climate database based on historical documents of China. *Sci. Data* **2018**, *5*, 180288. [CrossRef]
128. Stahl, K.; Kohn, I.; Blauhut, V.; Urquijo, J.; De Stefano, L.; Acácio, V.; Dias, S.; Stagge, J.H.; Tallaksen, L.M.; Kampragou, E.; et al. Impacts of European drought events: Insights from an international database of text-based reports. *Nat. Hazards Earth Syst. Sci.* **2016**, *16*, 801–819. [CrossRef]
129. Kaspar, F.; Zimmermann, K.; Polte-Rudolf, C. An overview of the phenological observation network and the phenological database of Germany's national meteorological service (DeutscherWetterdienst). *Adv. Sci. Res.* **2015**, *11*, 93–99. [CrossRef]

130. Cram, J.; Chow, C.E.; Sachdeva, R.; Needham, D.M.; Parada, A.E.; Steele, J.A.; Fuhrman, J.A. Seasonal and interannual variability of the marine bacterioplankton community throughout the water column over ten years. *ISME J.* **2015**, *9*, 563–580. [CrossRef]
131. National Centers for Environmental Information. Available online: https://www.ncdc.noaa.gov/dataaccess/paleoclimatologydata/datasets/historical (accessed on 15 May 2023).
132. Mächel, H.; Kapala, A.; Behrendt, J.; Simmer, C. Rettung Historischer Klimadaten in Deutschland: Das KLIDADIGI-Projekt des DWD. *Klimastatusbericht* **2008**, 103–118. Available online: https://www.dwd.de/DE/leistungen/klimastatusbericht/publikationen/ksb2008_pdf/a7_2008.pdf?__blob=publicationFile&v=1 (accessed on 15 May 2023).
133. PAGES. Available online: https://pastglobalchanges.org/ (accessed on 15 May 2023).
134. McKay, N.; Emile-Geay, J. The Linked Paleo Data framework–a common tongue for paleoclimatology. *Clim. Past* **2016**, *12*, 1093–1100. [CrossRef]
135. Wilhelm, B.; Ballesteros Cánovas, J.A.; Macdonald, N.; Toonen, W.H.J.; Baker, V.; Barriendos, M.; Benito, G.; Brauer, A.; Corella, J.P.; Denniston, R.; et al. Interpreting historical, botanical, and geological evidence to aid preparations for futurefloods. *Wires Water* **2019**, *6*, e1318. [CrossRef]
136. Khider, D.; Emile-Geay, J.; McKay, N.; Gil, Y.; Garijo, D.; Ratnakar, V.; Garcia, M.A.; Bertrand, S.; Bothe, O.; Brewer, P.; et al. PaCTS 1.0: A Crowdsourced Reporting Standard for Paleoclimate Data. *Paleoceanogr. Paleoclimatol.* **2019**, *34*, 1570–1596. [CrossRef]
137. Old Weather. Available online: https://oldweather.org/ (accessed on 28 April 2023).
138. Freeman, E.; Woodruff, S.D.; Worley, S.J.; Lubker, S.J.; Kent, E.C.; Angel, W.E.; Berry, D.; Brohan, P.; Eastman, R.; Gates, L.; et al. ICOADS release 3.0: A major update to the historical marine climate record. ICOADS release 3.0 A major update Hist. *Mar. Clim. Rec. Int. J. Climatol.* **2016**, *37*, 2211–2232. [CrossRef]
139. Weather Austria. Available online: https://www.weatheraustria.net/ (accessed on 15 May 2023).
140. Rabus, A. Recognizing Handwritten Text in Slavic Manuscripts: A Neural-Network Approach Using Transkribus. *Scr. e-Scr.* **2019**, *19*, 9–32.
141. Matuschek, O. Data-Mining in den Reisetagebüchern James Silk Buckinghams 1815/1816. Ph.D. Thesis, Albert-Ludwigs-Universität Freiburg, Faculty of Environment and National Research, Freiburg, Germany, 2014. (In German)
142. Yzaguirre, A.; Smit, M.; Warren, R. Newspaper archives + text mining = rich sources of historical geo-spatial data. *IOP Conf. Ser. Earth Environ. Sci.* **2016**, *34*, 012043. [CrossRef]
143. Kang, Y.; Park, C. A Multi-Risk Approach to Climate Change Adaptation, Based on an Analysis of South Korean Newspaper Articles. *Sustainability* **2018**, *10*, 1596. [CrossRef]
144. Leydecker, G. Erdbebenkatalog für Deutschland mit Randgebieten für die Jahre 800 bis 2008. (Earthquake catalogue for Germany and adjacent areas for the years 800 to 2008). *Geol. Jahrb.* **2011**, *E59*, 1–198. (In German)
145. Federal Institute for Geosciences and Natural Resources. Available online: https://www.bgr.bund.de/DE/Themen/Erdbeben-Gefaehrdungsanalysen/Seismologie/Seismologie/Erdbebenauswertung/Erdbebenkataloge/historische_Kataloge/germany.html (accessed on 25 June 2023).
146. Mallet, R. *Great Neapolitan Earthquake of 1857—The First Principles of Observational Seismology*; Chapman & Hall: London, UK, 1862; 399p.
147. Almagià, R. Studi geografici sulle frane in Italia, vol. II, Roma. *Mem. Soc. Geogr. It.* **1907**, *13*, 342.


**Disclaimer/Publisher's Note:** The statements, opinions and data contained in all publications are solely those of the individual author(s) and contributor(s) and not of MDPI and/or the editor(s). MDPI and/or the editor(s) disclaim responsibility for any injury to people or property resulting from any ideas, methods, instructions or products referred to in the content.

land

MDPI

*Article*

# Documentary Evidence of 17th Century Landcover and Climate Change in Northern China and Mongolia Compared to Modern Spectral Greening Trends

**Michael Kempf** [1,2]

[1] Physical Geography, Institute of Environmental Social Science and Geography, University of Freiburg, Schreiberstr. 20, 79085 Freiburg, Germany; michael.kempf@geographie.uni-freiburg.de
[2] Department of Archaeology and Museology, Faculty of Arts, Masaryk University, Arne Nováka 1, 60200 Brno, Czech Republic

**Abstract:** Fighting land degradation of semi-arid and climate-sensitive grasslands are among the most urgent tasks of current eco-political agenda. Particularly, northern China and Mongolia are prone to climate-induced surface transformations, which were reinforced by the heavily increased numbers of livestock during the 20th century. Extensive overgrazing and resource exploitation amplified regional climate change effects and triggered intensified land degradation that forced policy-driven interventions to prevent desertification. In the past, however, the regions have been subject to continuous shifts in environmental and socio-cultural and political conditions, which makes it particularly difficult to distinguish into regional anthropogenic impact and global climate change effects. This article presents analyses of historical written sources, palaeoenvironmental data, and Normalized Difference Vegetation Index (*NDVI*) temporal series from the Moderate Resolution Imaging Spectroradiometer (*MODIS*) to compare landcover change during the Little Ice Age (*LIA*) and current spectral greening trends over the period 2001–2020. Results show that decreasing precipitation and temperature records triggered increased land degradation during the late 17th century in the transition zone from northern China and Inner Mongolia Autonomous Region to Mongolia. From current climate change perspectives, modern vegetation shows enhanced physical vegetation response related to an increase in precipitation (*Ptotal*) and temperature (*T*). Vegetation response is strongly related to *Ptotal* and *T* and an increase in physical plant condition indicates local to regional grassland recovery compared to the past 20-year average.

**Keywords:** climate change; Little Ice Age; NDVI; historical climatology; documentary sources; MODIS; spectral greening; land-use; governance

**Citation:** Kempf, M. Documentary Evidence of 17th Century Landcover and Climate Change in Northern China and Mongolia Compared to Modern Spectral Greening Trends. *Land* **2022**, *11*, 100. https://doi.org/10.3390/land11010100

Academic Editors: Fabio Luino, Mariano Barriendos Vallvé, Emmanuel Garnier, Fabrizio Terenzio Gizzi, Ruediger Glaser, Christoph Gruetzner, Walter Palmieri, Sabina Porfido, Heather Sangster and Laura Turconi

Received: 29 November 2021
Accepted: 6 January 2022
Published: 8 January 2022

**Publisher's Note:** MDPI stays neutral with regard to jurisdictional claims in published maps and institutional affiliations.

**Copyright:** © 2022 by the author. Licensee MDPI, Basel, Switzerland. This article is an open access article distributed under the terms and conditions of the Creative Commons Attribution (CC BY) license (https://creativecommons.org/licenses/by/4.0/).

## 1. Introduction

Climate and land cover changes, heavy grazing, and agricultural and resource exploitation contribute significantly to land degradation and desertification processes in sensitive arid and semi-arid regions of Earth [1–8]. Particularly, seasonal vegetation cover plays a major role in the ecosystem's functionalities, affecting soil development, sediment deposition, water infiltration rate, and wind-driven erosion during high-cover and low-cover periods and within the spatial patterns of species differentiation [9–11]. From a historical perspective, seasonal vegetation dynamics control transhumance (seasonal nomadic), socio-cultural, and socio-economic strategies, which nowadays have turned into politically motivated intensified sedentary patterns with regional and supra-regional environmental overstraining. In many cases, severe surface damage and sandy desertification were caused through increased livestock grazing [6,12–15]. The system-inherent interactions of land degradation, climate forcing, anthropogenic impact, and ecological functionalities have been recently emphasized by multiple authors, who suggested complexity not only within physically, but also socio-culturally controlled systems [5,12,16,17].

Particularly, China's Inner Mongolia Autonomous Region and Mongolia have experienced massive political and economic development during the past decades, which enabled a strong transformation of the social, rural, and environmental life [18–22], followed by governmental grassland restoration projects and policies to prevent desertification [23–25]. Although the modern anthropogenic impact on semi-arid environments of the region has recently been emphasized by many authors [13,19,26–28], isolating the climatic signal affecting land degradation processes from human-induced landcover change still provides a great challenge [27,29].

In this article, historical documentary sources from 1688 AD were used to evaluate non-standardized measures of climatic and surface conditions during the Little Ice Age (LIA) in northern China and Mongolia and to compare them to modern landcover development, partly deriving from satellite hyperspectral imagery, Copernicus Global Land Service data, and historical and current climate proxy datasets. The historical data allows the surface vulnerability and land transformation processes through intensified wind-blown sand transport during the exceptional cold and dry period of the so-called Maunder Minimum of the Little Ice Age to be traced [30–35]. The comparison of surface conditions during the late 17th century AD further enables the evaluation of current global climate change and the cross-validation of the strong anthropogenic overprint in semi-arid grasslands of northern China and southern Mongolia [21]. Here, a particular focus is put on global spectral greening trends and vegetation response to global warming. Eventually, this article emphasizes the applicability of historical written sources to understand not only past but also current climate change effects on the local to the regional scale, a methodological problem, which has recently gained further momentum [17,36–39].

## 2. Materials and Methods

### *2.1. Environmental Settings*

The core research area covers southern Mongolia, China's Inner Mongolia Autonomous Region, and parts of China north of Beijing (Figure 1). Mongolia is a landlocked country north of China with a highly continental climate, extremely cold and dry winters, and short and hot summers [40]. After long-term summer droughts, climate extreme events in winter (*dzud*) have frequently led to severe livestock perish, which caused a strong socio-economic crisis due to a domestic product market dependency of about 20% [41,42]. Inner Mongolia is situated to the south at the northern margins of China and stretches from northeast to the northwest (37°30′–53°23′ N, 97° 10′–125°50′ E) [43]. Most of the plateau-like elevated region is dominated by extensive grasslands, which are characterized by various types of steppe vegetation and a great sensitivity to climate and land-use change [44–46]. The climate is monsoon-controlled, arid to semi-arid with cold and dry winters and hot and more humid conditions during summer and towards the subhumid north-eastern part [43,44]. Different climatic zones have developed under a prevailing continental climate, with temperate and semi-humid conditions in the east and more semi-arid and arid conditions towards the western part [21]. Mean monthly precipitation ranges from 0–200 mm (long-term average < 200 mm [47]) with a peak during July and September (Figure 2), temporally limiting plant growth [21]. In combination with the high environmental vulnerability and climate extremes, the strongly increased water consumption for agricultural purposes, animal husbandry, and particularly intensified state-controlled mining activities has locally amplified the drought risk of the region and led to a sequence of water shortages [42,47–50].

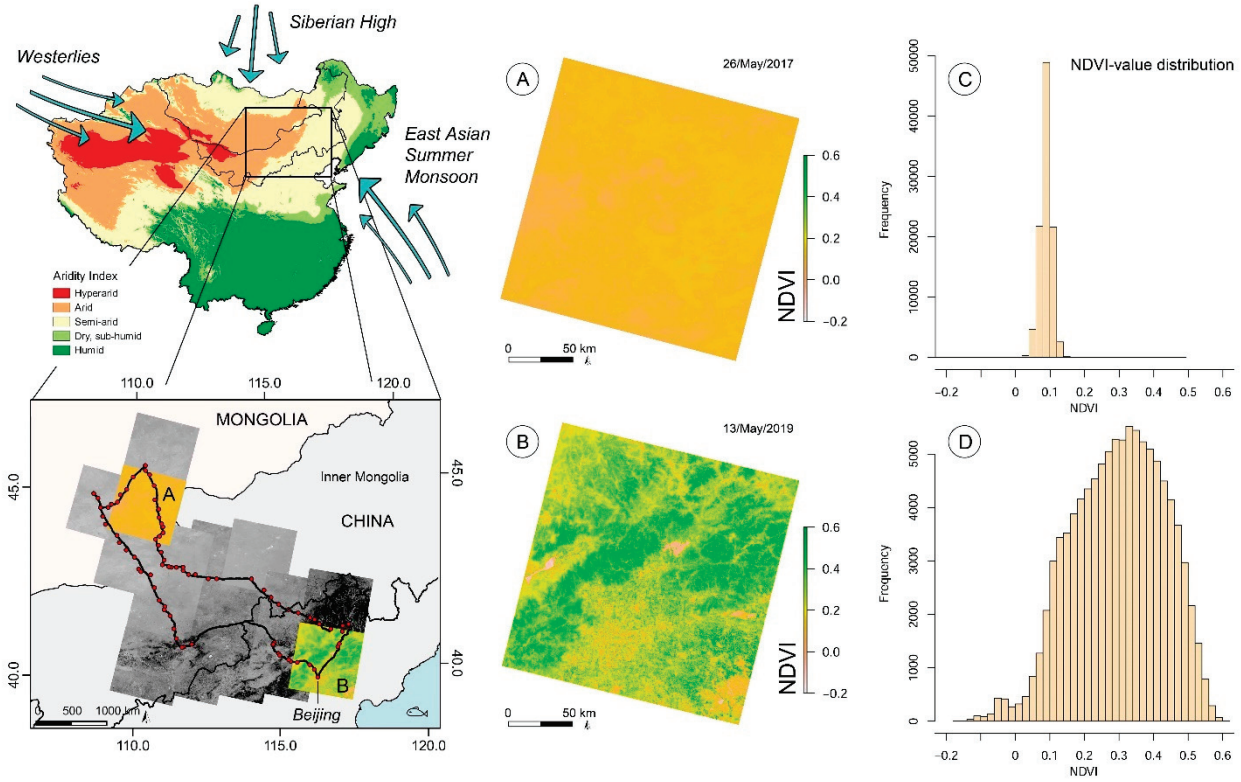



**Figure 1.** The study area in northern China and the southern part of Mongolia, covering approximately 433,425 km$^2$. A set of medium resolution Landsat-OLI-8 hyperspectral satellite image sets the extent of the temporal series reference area (USGS, last accessed 5 January 2021). Vegetation indices (NDVI) allow for the evaluation of surface conditions through reflectance characteristics and eventually the differentiation into bare areas, vegetation-covered areas, and modern built-up (compare sections A and B). The threshold histograms (**C**,**D**) show the signal's differences of two comparison sections in the north with extensive sand cover (**A**,**C**) and the south over Beijing with mosaic vegetation cover and extensive built-up (**B**,**D**). The aridity index is based on the Global Aridity Index and Potential Evapotranspiration Climate Database v2 [51].

### *2.2. Route Reconstruction and Historical Environmental Analysis*

A comparison of historical written sources [52] and environmental data attributes was carried out to evaluate modern land degradation and desertification dynamics in northern China and southern Mongolia. Historical data derived from a day-by-day diary, documented by the French missionary Jean-François Gerbillon in the year 1688 during his employment at the imperial court at Beijing. While he was travelling from Beijing through Inner Mongolia and Mongolia during the period from the 30 May to the 6 October 1688, Gerbillon documented climatic and surface conditions as well as general environmental, social, cultural, and political phenomena [53]. From the documentary sources, a route model was reconstructed using terrain-dependent least-cost-path (LCP) analysis. The model is based on surface roughness and slope gradients because directional movement patterns were emphasized only in cardinal directions [54–56]. For this reason, a digital elevation model was downloaded from the United States Geological Survey (USGS, SRTM 1-arc-second/30 m resolution [57]) and resampled to a 100 m grid size. The route model was calculated in QGIS (QGIS Geographic Information System. QGIS Association. http://www.qgis.org, last accessed 5 January 2022) using a cumulative friction surface and movement directions between the single stopping points. Around the reconstructed route, a 20 km buffer was created to visualize the historical environmental conditions within a suitable range. The corridor does not represent the accessibility of the area but was chosen to interpolate the reconstructed point-based data to a raster. Climatic conditions were

classified on a discrete scale from 1–6 with very hot (6), hot (5), warm (4), moderate (3), cold (2), and very cold (1). Wind speed was estimated using cardinal directions and four classes from calm (0), breeze (1), wind (2) to storm (3). Surface conditions were distinguished according to the Copernicus Global Land Cover collection using the classification into bare/sand (0), herbaceous (1), shrub (2), cropland/grassland (3), forest/mixed (4), built-up (5), and water surface (6) [58,59]. Climatic and surface data were interpolated within a 20 km range along the route to allow for comparison with modern landcover datasets. The data was then compared to modern land cover and temperature variations using the Copernicus Global Land Cover 100 m collection from 2019 [58] and precipitation and temperature comparison datasets [60,61].

### *2.3. Comparison Environmental Data*

To measure the relationship between climate variables and vegetation feedback, a global NDVI monthly time series dataset (2000–2020) was acquired from the Earthdata server of the USGS (https://lpdaac.usgs.gov/products/mod13c2v006/, last accessed 16 April 2021) [62]. The data has a complete spectrum for the period 2001–2020. The year 2000 is incomplete and was partly removed for the trend analysis. The aridity index (Figure 1) is based on the Global Aridity Index and Potential Evapotranspiration Climate Database v2 [51] and was cropped to the administrative boundaries of Mongolia and China to visualize the broader environmental context of the study area. Because desertification and land degradation processes are strongly connected to windspeed and surface erosion, the historical wind direction and intensity were compared to modern data extracted from the Global Windatlas [63].

Due to the temporal variation of the surface and the climatic conditions, the study area was differentiated into equal monthly sectors using Voronoi polygons. Monthly maximum temperature and precipitation totals were plotted in each sector to trace the seasonal variability in Inner Mongolia and southern Mongolia over the summer period. To cross-check the historical data results, a set of comparison climate data was acquired from the National Centers for Environmental Information (NOAA, last accessed 5 January 2021) and plotted using a locally estimated scatterplot smoother (LOESS) [64] and the R environment (R: A language and environment for statistical computing. R Foundation for Statistical Computing, Vienna, Austria. URL https://www.R-project.org/, last accessed 5 January 2022) with smoothing parameters 1, 0.5, and 0.3. Temperature anomaly and reconstructed temperature is based on a stalagmite from Shihua Cave, Beijing, China and instrumental meteorological records [65]. Long-term streamflow variation of the River Kherlen derived from the dataset by Pederson and colleagues and spatial and temporal tree-ring replication and nested model methods by Davi and colleagues [7,66]. Streamflow variation of the river Selenge in Mongolia is based on tree-ring-width chronologies [67] and precipitation reconstruction in north-eastern Mongolia and for two regions in China derived from tree-ring-width data [7,68].

### *2.4. NDVI Temporal Anomalies, Trend Analysis, and Environmental Parameter Correlation*

To trace the response of plant growth to precipitation and temperature variation in the study area, a temporal series of NDVI from MODIS/Terra Vegetation Indices Monthly L3 Global 0.05Deg CMG V006 imagery was created, which provide a pixel size of 5600 m and cover the period 2002–2020. Monthly total precipitation and monthly temperature were extracted from the CRU (Climate Research Unit) dataset [61]. The data comes in .nc file format and can be read and extracted using the ncdf4 package by David Pierce. Precipitation and temperature were used to compare climate change signals to global spectral greening trends [69,70]. Particularly, the early growing phase in Inner Mongolia [71] is sensitive to trends in precipitation and temperature variability, which impacts the growth behavior. A Spearman's rank correlation was performed on raster annual time series stacks to analyze the spatial relationship between climate variables and vegetation response across China and Mongolia. Spectral greening and browning trends as well as trends in precipitation and

temperature variability were identified using a pixel-wise raster analysis in R. The method and the workflow is well-described by Martin Brandt (2013) and is publicly available from the website (https://matinbrandt.wordpress.com/2013/11/15/pixel-wise-time-series-trend-anaylsis-with-ndvi-gimms-and-r/, last accessed, 28 December 2021).

The recent vegetation behavior in northern China and Mongolia was analyzed for yearly anomalies compared to the long-term record from 2000–2020. For this reason, the mean total NDVI value ($m$) and yearly average NDVI values were calculated from the cumulated monthly MODIS datasets. The standard deviation ($SD$) was calculated for all values and subtracted from and added to the multiannual mean value ($m - SD$; $m + SD$) to create the range of the standard deviation for the period 2000–2020. Consequently, annual NDVI anomalies were calculated by distinguishing into positive or negative deviation from the standard deviation range. For each year, the ($m + SD$) was subtracted from the annual mean NDVI value and all values $\leq 0$ were removed. According to the lower limits of the standard deviation range, ($m - SD$) was subtracted from each annual mean NDVI value and all values $\geq 0$ were removed. Eventually, a set of raster layer was generated, which shows negative and positive annual NDVI anomalies compared to the long-term temporal series of 20 years. Additionally, the histograms and density estimations of the anomaly value distribution were plotted to visualize the trends in physical plant activity (see the Supplementary Materials to this article). From the time series, a temporal plot and linear regression analyses were calculated to visualize the development in physical plant conditions in the study area. These anomaly datasets allow an understanding of the recent surfaces transformations in northern China to be obtained and comparison of them to past and current climate change models.

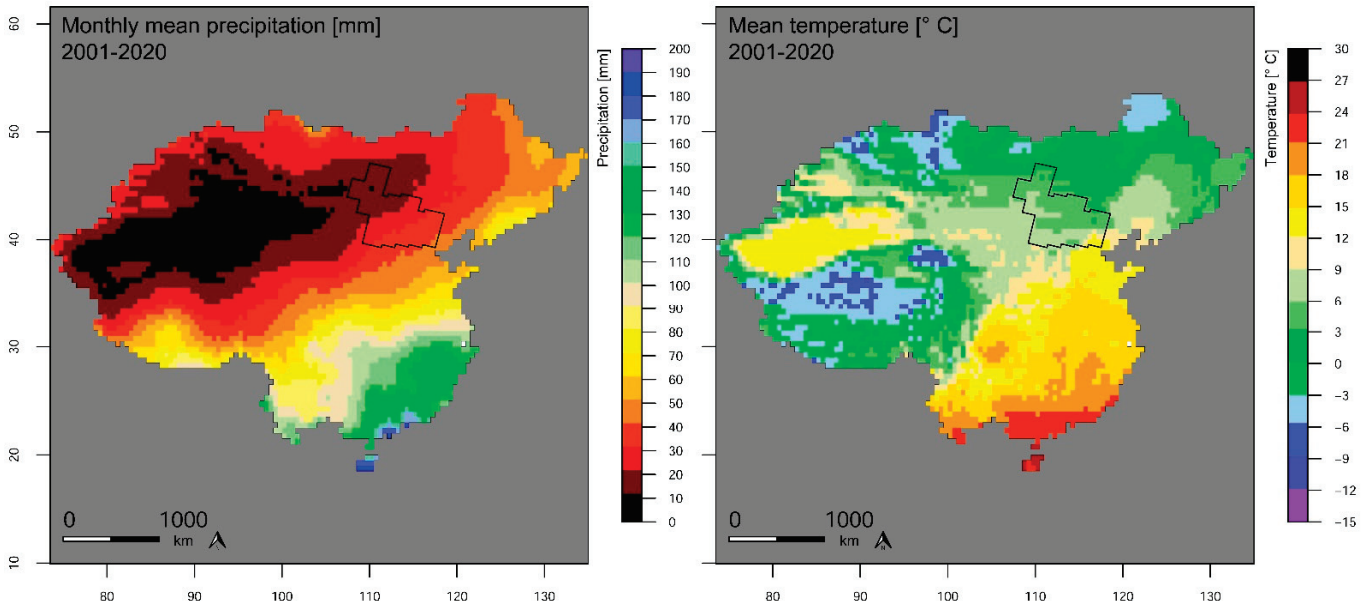



**Figure 2.** Multiannual average monthly total precipitation and mean temperature over the period 2001–2020, based on CRU TS4.05 (Climatic Research Unit Time Series) gridded data of month-by-month variation [61].

## 3. Results and Discussion

Today, the transition zone from northern China to Inner Mongolia and Mongolia is characterized by a pronounced landcover gradient from moderate forested areas in the south and the south-east to increasingly semi-arid and arid conditions towards the Mongolian Plateau and the extensive grasslands of Inner Mongolia and Mongolia (Figure 3). The Copernicus data highlights the modern landcover sequences and compares topographical features for each landcover class in the study area. Forested zones are mostly abundant

in lower elevated areas of the subhumid belt north of Beijing. With increasing elevation, patterns of herbaceous grassland and shrubs prevail. Towards the north-west, extensive sandy lands occur with a mean elevation of about 1000 m a.s.l. Croplands are frequently interspersed into semi-arid grassland patches, which points towards an active anthropogenic land-use. Figure 3 further visualizes the historical route patterns and the daily camps of the travels of Gerbillon from 1688. From these route reconstructions, a cross-validation of hermeneutic sources and modern landcover and climate data was derived.

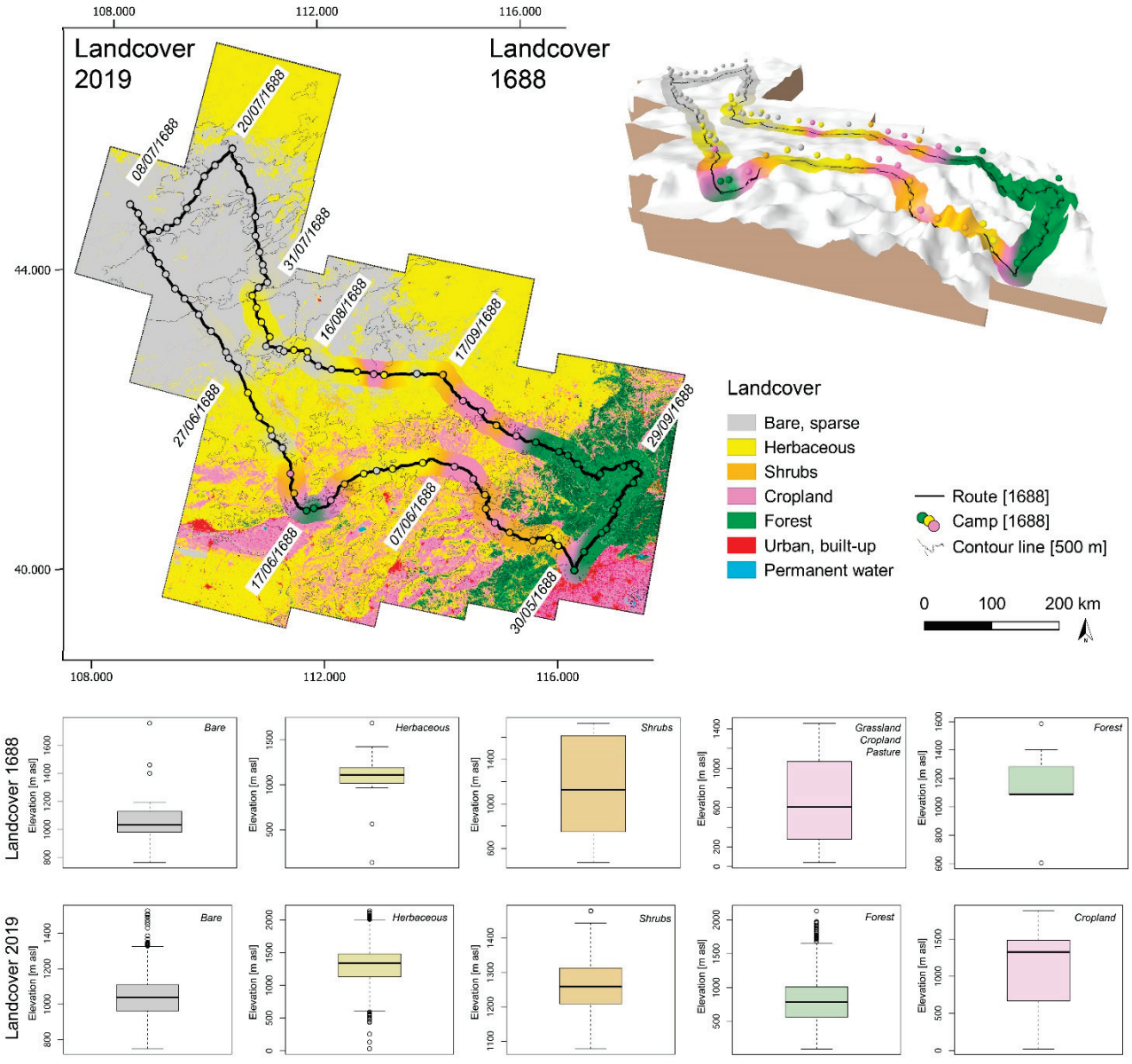



**Figure 3.** Landcover in the study area in 2019 and 1688 compared to topographical elements and the historical route reconstruction from 1688 [53,57,58]. The reconstructed landcover of 1688 is overlaid on modern Copernicus landcover data from 2019. During May to October 1688, Gerbillon crossed large parts of northern China and southern Mongolia and turned back to Beijing after half a year. He reported weather as well as surface and vegetation conditions and enabled the reconstruction of past landcover conditions during the Maunder Minimum of the Little Ice Age.

### *3.1. Historical Landcover Change and Environmental Reconstruction*

A route was reconstructed from the historical data, which starts at Beijing on the 30 May 1688. Travelling to the north-west, the group crossed the mountain range north of China's capital before entering the Mongolian Plateau on the first week of June. According to topographical changes, the landcover transformed rapidly from forested to sparsely forested and herbaceous surfaces, and then to shrubland, grassland, and steppe vegetation from the south-east to the north-west (Figure 3). During the first week, Gerbillon reported from small-scale agricultural crop production, which were interspersed into extensive grasslands. Furthermore, he frequently highlighted the absence of field systems despite the high suitability for intensive agricultural utilization of the region, which was connected to a prior nomadic lifestyle of the local population [21,22,72,73]. The weather conditions were generally very dry with very high temperatures during the onset of June and more humid and moderate conditions during the second half of the month when the group turned to the south-west and crossed extensive sandy grasslands with poor vegetation cover and bare hilltops (Figure 4). On the 17 June, they reached Hohhot, which is located on the Tumuochuan Plain and surrounded by the Hetao Plateau to the south and the Daqing Mountain to the north [74]. The average temperature (6.7 °C) and the annual total precipitation (400 m/a) at Hohhot are low, which supports a semi-arid steppe climate [74]. Both the modern data and the historical landcover reconstruction indicate forested zones in the area, which are probably connected to the lower elevation compared to the surrounding hills. After the 17 June, the group moved northwards, and the vegetation cover declined according to an increase in aridity and windspeed (Figure 5). After the 27th, Gerbillon reported from bare lands with no vegetation but loose sand coverage until the 31 July 1688. In contrast to the 2019 landcover, the 1688 landcover reconstruction shows increasing herbaceous vegetation patterns after the 31 July despite continuously very dry conditions during August. The surface description of the following period until the 17 September again differs considerably from modern landcover data. There is a signal towards more herbaceous and shrubby vegetation and increasing agricultural exploitation during the late 17th century. During the rest of September, the group travelled continuously to the east and entered the forested mountains around the 22 September. Compared to the modern data, the extent of the forested areas reached further to the north and the north-west, which is most likely linked to strong modern human impact, forest management and climate change during the first half of the 20th century [75]. Climatic conditions were reported to be very dry and extremely cold during October 1688, which aligns with the climatic tendency towards a drier and cooler period around 1700 AD and the climate depression during the Maunder Minimum of the LIA. From the palaeoenvironmental reconstructions, 1688 can be considered an extremely anomalous year compared to the long-term average and marks the transition into a generally colder and drier phase that lasts until about 1715/30 AD [35].

These findings are further supported by the windspeed model and the average wind direction from 1688 compared to modern data [63]. The diary reports continuously blowing wind with local extreme events and massively increased sand transport and dune activity. The reconstruction indicates an increase in windspeed and a general change in wind direction during the LIA (Figure 5). During the past decades, the landcover became even more vulnerable to wind erosion due to the locally decreased vegetation cover and intensified overgrazing, which reactivated sand depositions and enabled dust transportation and dune development. The accumulation of coarse particles further supported the degradation of cropland and pasture [76–79]. Sand and dust storms over Inner Mongolia were not only enhancing erosion and accumulation of fine-grained particles in the semi-arid steppe region but also led to the transportation of dust and high concentrations of particulate pollutants into the area of Beijing [80–82].

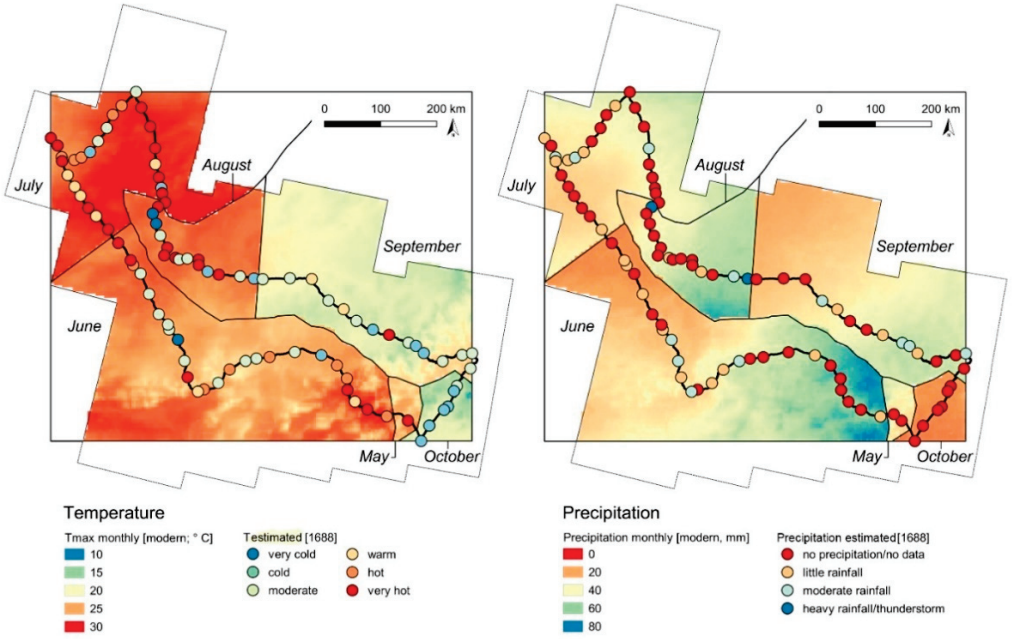



**Figure 4.** Average monthly temperature and precipitation grid in the study area from May to October. The reconstructed climatic conditions from 1688 were plotted on top of the modern dataset to highlight differences and similarities during the Little Ice Age [53,60,61].

To cross-validate the hermeneutic sources, historical and current environmental conditions in the study area were evaluated using palaeoenvironmental proxies from different data sources [7,65–68] and interpolated datasets from modern weather stations [60,61]. Monthly total precipitation in Inner Mongolia and Mongolia shows a significantly positive trend compared to the reference period 2001–2020 [11,83]. Palaeoclimate show a tendency towards greater annual variation (Figure 6). As expected from global climate change models [84–87], the reconstructed temperature increased significantly during the past 500 years and particularly during the period 2001–2020. Reconstructed streamflow runoff in Mongolia is connected to the precipitation variability, and an increase in rainfall triggered peaks in runoff totals. However, there is no negative trend in river runoff during the past 400 years. It is particularly striking that the year 1688, which marks the peak of the Maunder Minimum of the LIA, can be characterized as an exceptionally cold and dry year compared to the long-term average. The period 1675 to 1715, which is characterized by a sunspot minimum and decreased solar activity, is clearly visible in the temperature reconstruction from the tree-ring width and peaks around 1700 [65]. The minimum could have affected the East Asian Summer Monsoon (EASM) according to the 11-year solar cycle [88,89]. The precipitation records of Urgun Nars [7] show a negative trend during the Maunder Minimum, pointing towards decreased humidity transport into semi-arid and arid Mongolia caused by a potential decline and a southward shift of the EASM [90,91].

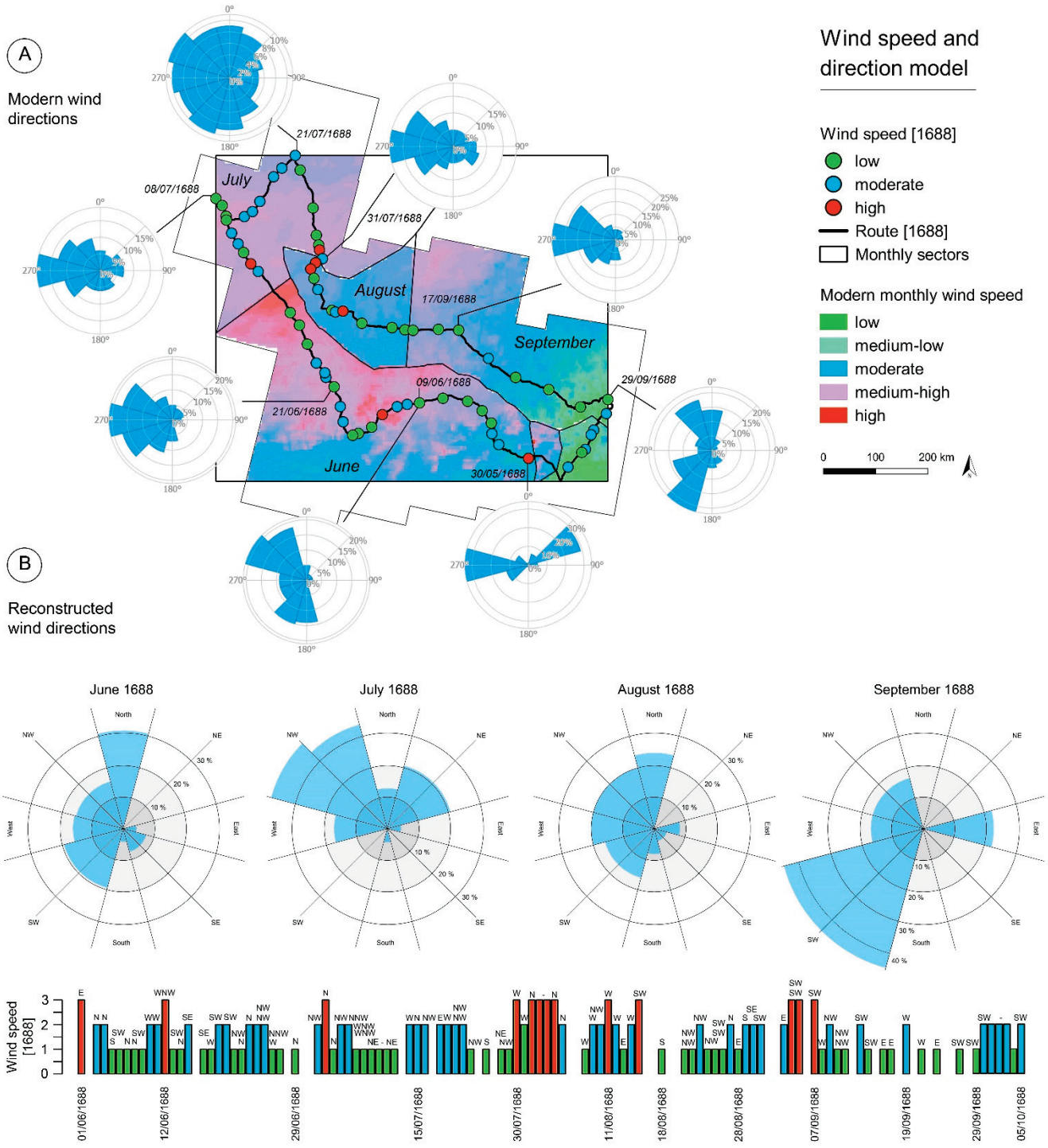



**Figure 5.** (**A**) Modern average monthly windspeed diagrams of the study area from May to October [63]. (**B**) Reconstructed wind directions for June–September 1688. May and October did not provide sufficient data. The reconstructed windspeeds and directions were plotted with modern datasets to underline the current trend towards increased windspeed, north-western wind direction, and sand transport and enhanced desertification risk.

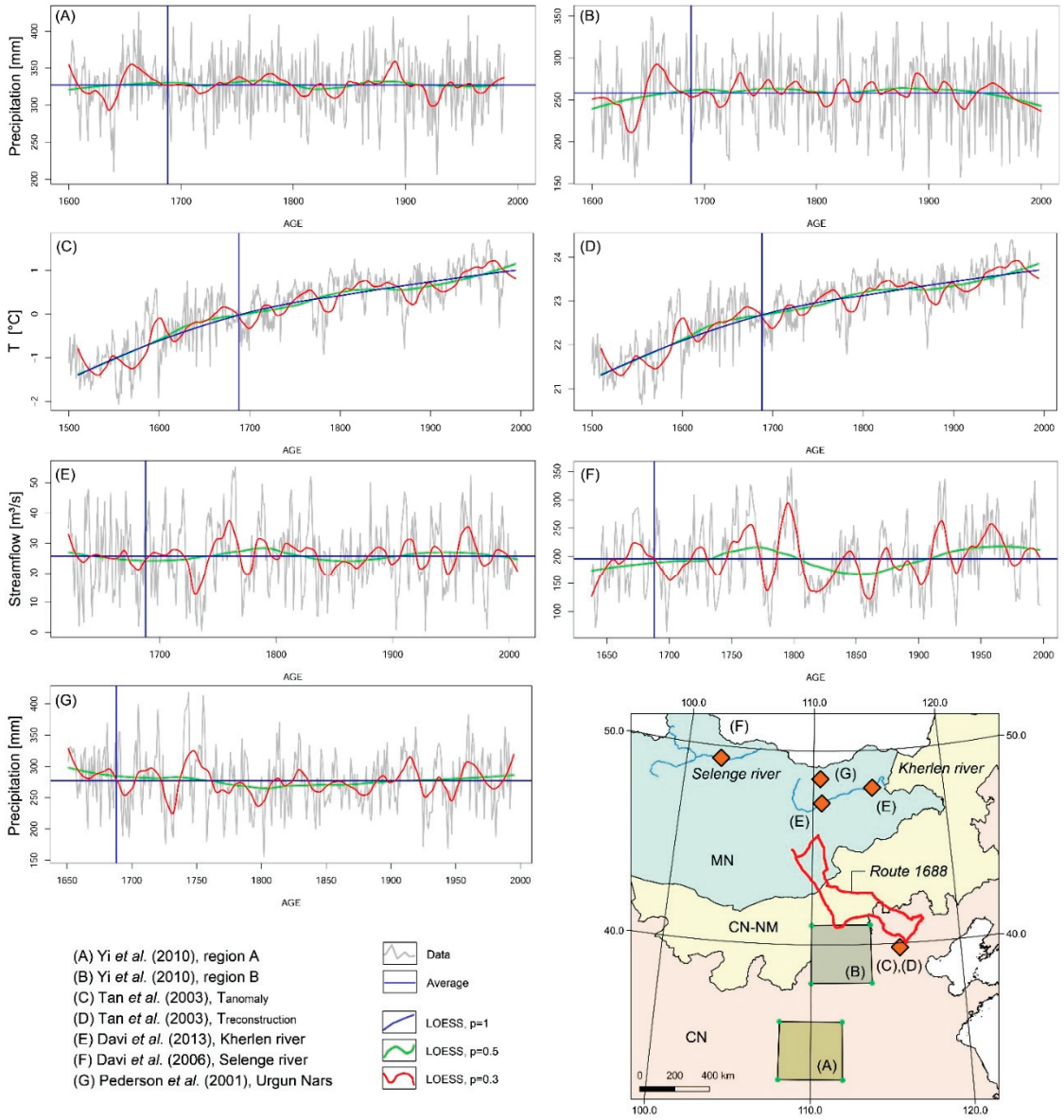



**Figure 6.** Paleoclimate reconstruction from six study sites in China and Mongolia. Raw data acquired from NOAA-National Centers for Environmental Information (last accessed 5 January 2021) and plotted by the author using a locally estimated scatterplot smoother (LOESS) and R software [64]; smoothing parameters 1 (blue line, plot C, D), 0.5 (green line), 0.3 (red line). The year 1688 is marked with a vertical, the average value with a horizontal blue line. (**A**,**B**): Precipitation reconstruction based on tree-ring chronologies for two regions in China [68]. (**C**): Temperature anomaly and (**D**): reconstructed temperature based on a stalagmite from Shihua Cave, Beijing, China and instrumental meteorological records [65]. (**E**): River Kherlen long-term streamflow variation based on [7] and spatial and temporal tree-ring replication and nested model methods [66]. (**F**): Streamflow variation of the river Selenge in Mongolia based on tree-ring-width chronologies [67]. (**G**): Precipitation reconstruction in north-eastern Mongolia based on tree-ring-width data [7].

### *3.2. Modern Climatic and Surface Transformation Processes*

Modern NDVI time series were used to monitor vegetation canopy changes and surface transformations linked to climate change and anthropogenic overstraining. Vegetation indices of subsequent months and years and on various spatial scales allow for temporal in-depth observations of physical plant behavior or drought periods and are a common tool in remote sensing of ecological and climatic processes [92–97]. As derived

from the Copernicus landcover data and the aridity index, the north-western parts of China and Mongolia reveal significantly low plant physiological activity and bare and sandy areas. This accounts for most of the transitional zone between China and Mongolia. The long-term MODIS NDVI temporal series from 2000–2020 show a significantly positive trend in spectral greening in most regions across China and Mongolia (Figures 7 and 8). Particularly, the early growing season is the most important period to determine vegetation dynamics [71,98]. According to Ren et al. (2012), who highlighted the variability of rainfall and temperature as the most important driving factor of vegetation dynamics in Inner Mongolia, the results from the NDVI trend analyses confirm the strong relationship between precipitation development and vegetation response over China and Mongolia (Figure 9). Temperature increased significantly in the study area during the past two decades [99] and a positive trend in multiannual variation has been observed in precipitation totals [100]. In this context, Tong et al. (2017) reported from the eastern part of Inner Mongolia, where NDVI values increased between 1984 and 2013. The correlation between NDVI and precipitation and NDVI and temperature in the study area, which is most-likely connected to seasonal variation in precipitation totals in eastern Inner Mongolia and the annual cycle, can be confirmed for the period 2001–2020 (Figure 9) [15,99–101].

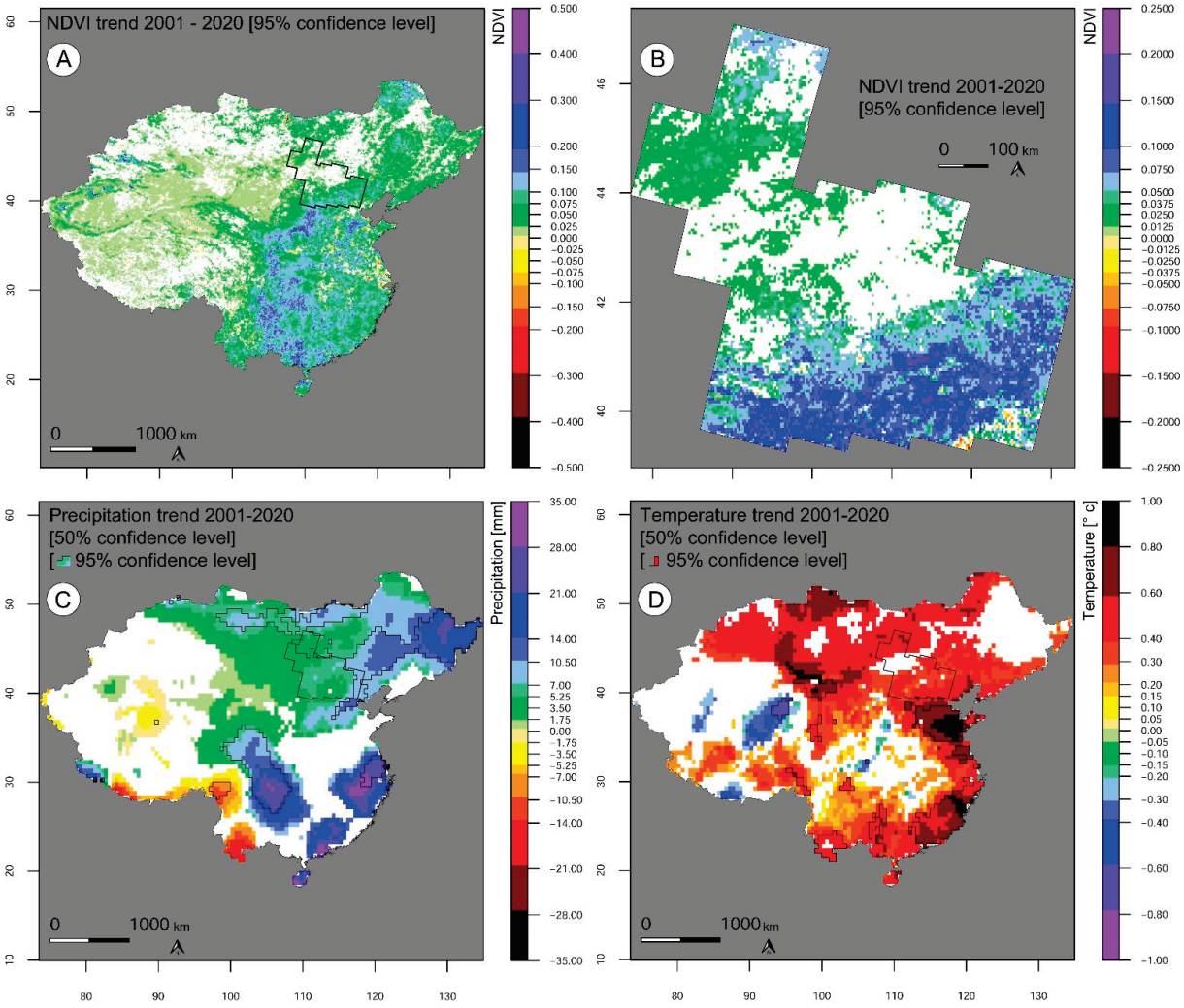



**Figure 7.** Trend analysis of vegetation response to climate change over the period 2001–2020. (**A**) MODIS NDVI trend analysis with a 95% confidence level; (**B**) cropped research core area with NDVI trends; (**C**) precipitation trends with 50% and 95% confidence level; (**D**) temperature trends with 50% and 95% confidence level. White areas show a lower significance level.

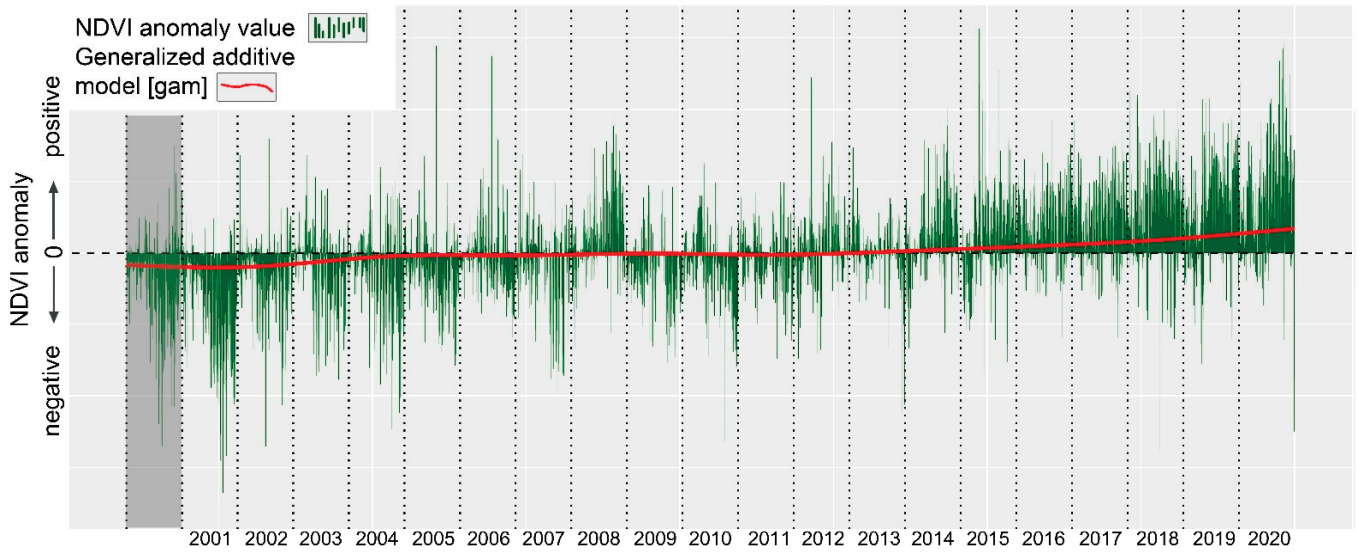



**Figure 8.** Temporal series of annual NDVI anomalies in China and Mongolia compared to the reference period 2001–2020. From the data, a clear trend in positive vegetation growth anomalies can be observed, particularly since 2015. The MODIS dataset for 2000 is incomplete and is marked in grey.

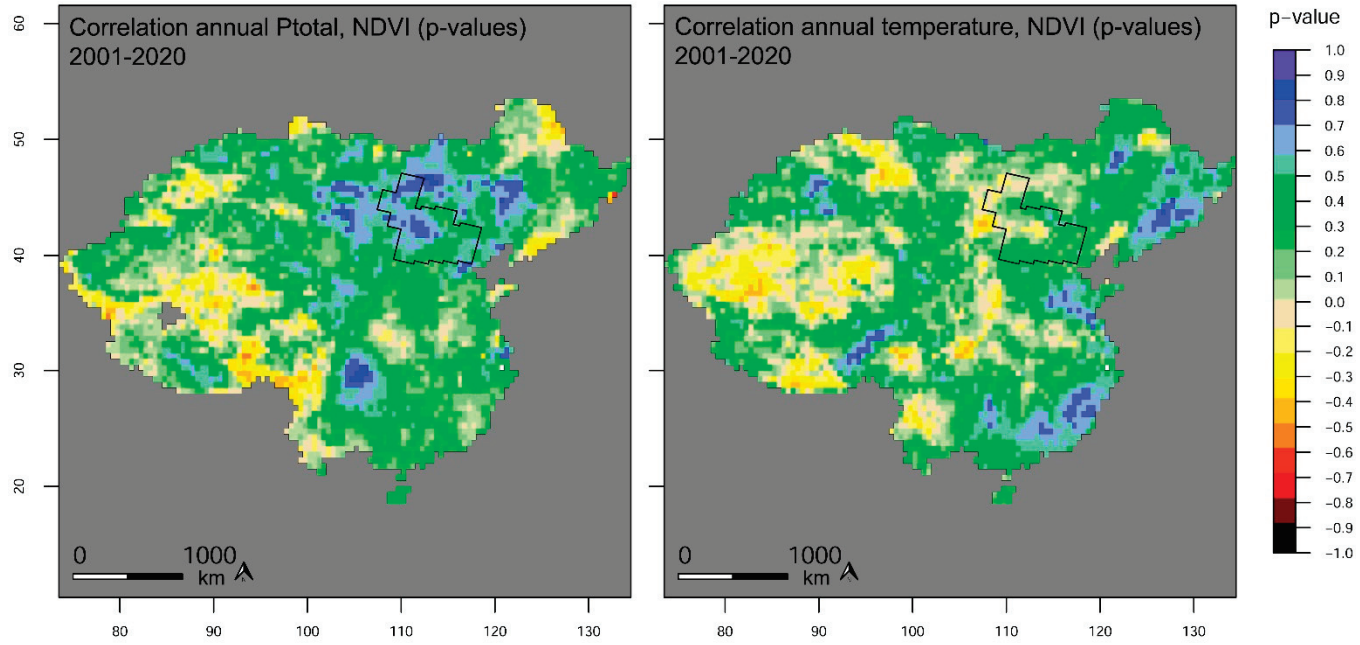



**Figure 9.** Correlation of annual Ptotal sums and NDVI and temperature and NDVI over the period 2001–2020. Greening trends in the study area are strongly correlated to an increase in precipitation.

### *3.3. Vegetation Response to Anthropogenic Surface Transformation*

These results contribute to the discussion about the complexity of aboveground net primary productivity (ANPP) in grasslands and annual, interannual, seasonal, and previous-year precipitation variability as reported from Inner Mongolia and North America short-grass steppe [96,102–107]. There is a stronger spatial gradient of the sensitivity to and the relationship between precipitation and maximum temperature in desert steppe vegetation than in the subhumid forest zones [106,108,109]. This could highlight the anthropogenically induced origin of local desertification processes through grazing activity after the growing

season, which amplified the vulnerability and decreased the resilience to global climate change of Inner Mongolia's grassland and steppe vegetation [109,110]. Grazing activity in Inner Mongolia's grasslands temporally peaks from July to September, when plant growth terminates [98]. As seen from the MODIS trend analysis, there is a clear trend towards vegetation recovery, linked to higher precipitation totals and an increase in temperature. An increasing temperature during the early growing season would therefore advance the spring phenological phases; however, decreased soil moisture would delay them [111].

Recent articles have shown that land degradation has reduced considerably during the past 20 years and that desert extent reduction is not primarily caused by a reduction in human grazing activity but rather by an increase in precipitation [112]. Guo et al. (2020) reported a decrease in active desertification; however, this is mostly restricted to the more sub-humid northern part of Mongolia and the eastern parts of Inner Mongolia and does not totally affect the transitional zone between Inner Mongolia's and Mongolia's grasslands [112]. Cao et al. (2019; 2018a; 2018b) reported significantly reduced numbers of livestock in the Qinghai-Tibetan Plateau between 2001 and 2013 as a result of China's livestock reduction policy and that grazing activity cannot solely be considered the trigger of extensive grassland degradation [11]. The authors furthermore point out that, due to market development, industrialization, population dynamics, and socio-cultural and socio-political transformation processes, the feedbacks of climate change, anthropogenic overprint, and land degradation are manifold and thoroughly interwoven [11,113,114]. Land degradation in northern China has increased constantly since the 1950s and peaked during the 1970s and 1980s and again until the beginning of the 21st century after when it decreased continuously [25,70]. According to Fang et al. (2021), the grassland productivity can be considered stable at least since 2009 [97]. From the anomaly model (Figure 8), a clear trend towards positive vegetation growth behavior can be observed since 2015 and the anomaly raster maps for the period 2015–2020 show significant trends to overall positive vegetation feedback compared to the reference period 2000–2020 (see the Supplementary Materials to this article). The raster trend analysis shows similar results for the extensive grasslands. However, large parts do not show significant vegetation trends.

There is ongoing debate about whether desertification processes are caused by anthropogenic overstraining and particularly overgrazing activity or by climate change phenomena [108,112,115,116]. Climate change and natural response cycles have been determined to trigger land degradation and the human impact caused extensive desertification at variable scales. The complexity of human-natural global change and the feedbacks are particularly visible in semi-arid climate-sensitive areas of Earth, where strong local anthropogenic impacts on short temporal scales have led to massively increased mobility of both humans and livestock after surface transformation and consequently the degradation of neighboring boundary zones [70]. This has led to a rapid decrease of the ecosystem's functionality and landscape connectivity and enhances surface degradation through aeolian processes and dust accumulation. Subsequent dry years, hot drought phenomena, and rising temperatures during the early growing season and summer can further strengthen the vulnerability of the steppe grassland in northern China, despite a temporal increase in physical plant condition [117–119].

The results presented in this article show that over the entire study area, there is a significant increase in spectral greening and interannual vegetation variability, which is correlated to an increase in precipitation and temperature. These results show that decreasing grassland degradation during the 21st century can be related to climate change and increasing precipitation. Consequently, during a period of decreased precipitation totals and temperature, land degradation is supposed to advance significantly, as can be seen from the evaluation of the historical written sources and the reconstructed surface conditions during the 17th century in the study area. This points towards the climate-sensitive ecosystem functionalities of the grasslands at the transition zone from Northern China's Inner Mongolia Autonomous Region to Mongolia and the vulnerability of the region to intensified anthropogenic impact. The historical data not only highlights the

rapidly decreasing ecosystem resilience during the Little Ice Age but also how sensitive the region is to a strongly increasing number of livestock and changing socio-cultural and socio-political parameters and agendas [120]. Under recent climate change and regionally increasing heavy precipitation events and precipitation totals, grassland recovery and expansion could probably have been initiated earlier in the 20th century. However, the development was significantly delayed by strongly increased numbers of livestock and political influence in the region during the second half of the last century. The subsequent governmental restrictions to combat (human-induced) desertification processes in the region have eventually demonstrated success only since about 2015.

## 4. Conclusions

Northern China's and Mongolia's climate sensitive semi-arid regions experienced severe desertification during the 20th century, mostly linked to massively intensified livestock grazing activity, resource exploitation, and agricultural crop production, which increased water consumption and enhanced surface erosion. During the past decades, however, China's policy-driven decision-making processes pushed local to regional programs to prevent land degradation and stabilize sandy areas and grasslands in order to decrease the potential of future soil erosion, surface transformation, and dust transport—a crucial factor, particularly in the context of Beijing's high vulnerability to increased numbers of sandstorms. The actual cause and effect of desertification processes, however, is still heavily debated and it is yet unsolved whether local surface transformations are triggered by regional climate change feedbacks or whether they are connected to anthropogenically induced system transformation and governmental decision-making. It is a matter of fact that both are rooted in the human impact on the landscape functionalities, and land degradation and desertification mirror only the ultimate collapse and loss of resilience to withstand enhanced climatic or human pressure. From the results presented here, a strong relationship between environmental change and land degradation processes can be derived. This questions the recent impact of livestock grazing on the semi-arid regions of northern China and southern Mongolia. No negative trend in land degradation is seen from the long-term NDVI time series, but a significant increase in spectral greening and positive vegetation growth anomalies between 2000 and 2020. China's government sought to restore extensive grasslands to maintain the regional population and one of the Earth's largest and growing livestock. In the future, however, increasing seasonal variability in precipitation and significantly increasing temperature and drought risk during the growing season could re-enhance the climatic pressure on semi-arid landscapes and thus negatively affect grassland development.

To evaluate modern landcover transformation, historical climatological analysis and hermeneutics were merged with long-term palaeoenvironmental data. Documentary sources were used to reconstruct surface transformation and climate development during the LIA and to compare 17th century land degradation processes to modern desertification trends in semi-arid northern China and Mongolia. For this reason, written sources from 1688 were evaluated to extract a temporal series of landcover conditions for the period May to October 1688, a year that falls into a period of reduced sunspot activity and solar energy flux during the LIA. Palaeoenvironmental proxy have shown that precipitation and temperature records decreased during the Maunder Minimum (1675 to 1715 AD). 1688 is reported to peak with extreme climatic conditions by tree-ring-width and stalagmite composition analyses. According to written sources, the year was characterized by extremely low temperatures during the late grazing season of September and the onset of October and extremely dry conditions and severely high temperatures during the summer rainy season, which caused massive livestock perish in the region. Even though the evaluation of hermeneutically deduced historical environmental data remains strongly subjective, it represents an additional source to measure the dimension of human landcover change on the long-term scale. This is particularly important in grasslands and steppe vegetation areas, which are the Earth's most climate-sensitive resources.

**Supplementary Materials:** The following are available online at https://www.mdpi.com/article/10.3390/land11010100/s1, Figure S1: NDVI anomalies.

**Author Contributions:** Research design, analyses, and writing: M.K. All authors have read and agreed to the published version of the manuscript.

**Funding:** This research received funding from the European Union, Operational Programme Research, Development and Education—Project, "Postdoc2MUNI" (No. CZ.02.2.69/0.0/0.0/18_053/0016952), Masaryk University, Brno, Czech Republic.

**Institutional Review Board Statement:** Not applicable.

**Informed Consent Statement:** Not applicable.

**Data Availability Statement:** All data underlying this article are publicly available on the internet.

**Acknowledgments:** I would like to thank two reviewers for their constructive critics.

**Conflicts of Interest:** The author declares no conflict of interest.

## References

1. UN. *United Nations Convention to Combat Desertification in Countries Experiencing Serious Drought and/or Desertification, Particularly in Africa*; Document A/AC. 241/27, 12. 09. 1994 with Annexes; United Nations: New York, NY, USA, 1994.
2. UNCCD. *Land Degradation Neutrality Reports 2019–2020*; UN: Bonn, Germany, 2020.
3. Cowie, A.L.; Penman, T.D.; Gorissen, L.; Winslow, M.D.; Lehmann, J.; Tyrrell, T.D.; Twomlow, S.; Wilkes, A.; Lal, R.; Jones, J.W.; et al. Towards sustainable land management in the drylands: Scientific connections in monitoring and assessing dryland degradation, climate change and biodiversity. *Land Degrad. Dev.* **2011**, *22*, 248–260. [CrossRef]
4. Vogt, J.V.; Safriel, U.; von Maltitz, G.; Sokona, Y.; Zougmore, R.; Bastin, G.; Hill, J. Monitoring and assessment of land degradation and desertification: Towards new conceptual and integrated approaches. *Land Degrad. Dev.* **2011**, *22*, 150–165. [CrossRef]
5. Herrmann, S.M.; Hutchinson, C.F. The changing contexts of the desertification debate. *J. Arid Environ.* **2005**, *63*, 538–555. [CrossRef]
6. Zhao, H.-L.; Zhao, X.-Y.; Zhou, R.-L.; Zhang, T.-H.; Drake, S. Desertification processes due to heavy grazing in sandy rangeland, Inner Mongolia. *J. Arid Environ.* **2005**, *62*, 309–319. [CrossRef]
7. Pederson, N.; Jacoby, G.C.; D'Arrigo, R.D.; Cook, E.R.; Buckley, B.M.; Dugarjav, C.; Mijiddorj, R. Hydrometeorological Reconstructions for Northeastern Mongolia Derived from Tree Rings: 1651–1995. *J. Clim.* **2001**, *14*, 872–881. [CrossRef]
8. Burrell, A.L.; Evans, J.P.; de Kauwe, M.G. Anthropogenic climate change has driven over 5 million km$^2$ of drylands towards desertification. *Nat. Commun.* **2020**, *11*, 3853. [CrossRef] [PubMed]
9. Lin, Y.; Han, G.; Zhao, M.; Chang, S.X. Spatial vegetation patterns as early signs of desertification: A case study of a desert steppe in Inner Mongolia, China. *Landsc. Ecol.* **2010**, *25*, 1519–1527. [CrossRef]
10. Aguiar, M.R.; Sala, O.E. Patch structure, dynamics and implications for the functioning of arid ecosystems. *Trends Ecol. Evol.* **1999**, *14*, 273–277. [CrossRef]
11. Cao, J.; Adamowski, J.F.; Deo, R.C.; Xu, X.; Gong, Y.; Feng, Q. Grassland Degradation on the Qinghai-Tibetan Plateau: Reevaluation of Causative Factors. *Rangel. Ecol. Manag.* **2019**, *72*, 988–995. [CrossRef]
12. Geist, H.J.; Lambin, E.F. Dynamic Causal Patterns of Desertification. *BioScience* **2004**, *54*, 817. [CrossRef]
13. Conte, T.J.; Tilt, B. The Effects of China's Grassland Contract Policy on Pastoralists' Attitudes towards Cooperation in an Inner Mongolian Banner. *Hum. Ecol.* **2014**, *42*, 837–846. [CrossRef]
14. Taylor, J.L. Negotiating the Grassland: The Policy of Pasture Enclosures and Contested Resource Use in Inner Mongolia. *Hum. Organ.* **2006**, *65*, 374–386. [CrossRef]
15. Guo, E.; Wang, Y.; Wang, C.; Sun, Z.; Bao, Y.; Mandula, N.; Jirigala, B.; Bao, Y.; Li, H. NDVI Indicates Long-Term Dynamics of Vegetation and Its Driving Forces from Climatic and Anthropogenic Factors in Mongolian Plateau. *Remote Sens.* **2021**, *13*, 688. [CrossRef]
16. Weber, K.T.; Horst, S. Desertification and livestock grazing: The roles of sedentarization, mobility and rest. *Pastor. Res. Policy Pract.* **2011**, *1*, 19. [CrossRef]
17. Glaser, R.; Kahle, M. Reconstructions of droughts in Germany since 1500–combining hermeneutic information and instrumental records in historical and modern perspectives. *Clim. Past* **2020**, *16*, 1207–1222. [CrossRef]
18. Cincotta, R.P.; Yanqing, Z.; Xingmin, Z. Transhumant Alpine Pastoralism in Northeastern Qinghai Province: An Evaluation of Livestock Population Response during China's Agrarian Economic Reform. *Nomadic Peoples* **1992**, *30*, 3–25.
19. Jordan, G.; Goenster, S.; Munkhnasan, T.; Shabier, A.; Buerkert, A.; Schlecht, E. Spatio-temporal patterns of herbage availability and livestock movements: A cross-border analysis in the Chinese-Mongolian Altay. *Pastor. Res. Policy Pract.* **2016**, *6*, 12. [CrossRef]
20. Glindemann, T.; Wang, C.; Tas, B.M.; Schiborra, A.; Gierus, M.; Taube, F.; Susenbeth, A. Impact of grazing intensity on herbage intake, composition, and digestibility and on live weight gain of sheep on the Inner Mongolian steppe. *Livest. Sci.* **2009**, *124*, 142–147. [CrossRef]

21. Wu, J.; Zhang, Q.; Li, A.; Liang, C. Historical landscape dynamics of Inner Mongolia: Patterns, drivers, and impacts. *Landsc. Ecol.* **2015**, *30*, 1579–1598. [CrossRef]
22. Neupert, R.F. Population, Nomadic Pastoralism and the Environment in the Mongolian Plateau. *Popul. Environ.* **1999**, *20*, 413–441. [CrossRef]
23. Zhang, Y.; Wang, Q.; Wang, Z.; Yang, Y.; Li, J. Impact of human activities and climate change on the grassland dynamics under different regime policies in the Mongolian Plateau. *Sci. Total Environ.* **2020**, *698*, 134304. [CrossRef]
24. Zhang, H.; Fan, J.; Cao, W.; Harris, W.; Li, Y.; Chi, W.; Wang, S. Response of wind erosion dynamics to climate change and human activity in Inner Mongolia, China during 1990 to 2015. *Sci. Total Environ.* **2018**, *639*, 1038–1050. [CrossRef]
25. Xue, Z.; Kappas, M.; Wyss, D. Spatio-Temporal Grassland Development in Inner Mongolia after Implementation of the First Comprehensive Nation-Wide Grassland Conservation Program. *Land* **2021**, *10*, 38. [CrossRef]
26. Cao, J.; Yeh, E.T.; Holden, N.M.; Qin, Y.; Ren, Z. The Roles of Overgrazing, Climate Change and Policy as Drivers of Degradation of China's Grasslands. *Nomadic Peoples* **2013**, *17*, 82–101. [CrossRef]
27. Harris, R.B. Rangeland degradation on the Qinghai-Tibetan plateau: A review of the evidence of its magnitude and causes. *J. Arid Environ.* **2010**, *74*, 1–12. [CrossRef]
28. Kakinuma, K.; Okayasu, T.; Sasaki, T.; Jamsaran, U.; Okuro, T.; Takeuchi, K. Rangeland management in highly variable environments: Resource variations across the landscape mediate the impact of grazing on vegetation in Mongolia. *Grassl. Sci.* **2013**, *59*, 44–51. [CrossRef]
29. Zhang, C.; Xia, W.; Luan, X.; Zhuang, H.; Khan, T.U.; Zhang, G.; Wu, S. Use of historical data to assess the impact of climate change and anthropogenic disturbance on the black-billed capercaillie (*Tetrao urogalloides*) in northeast China. *Glob. Ecol. Conserv.* **2020**, *22*, e00972. [CrossRef]
30. Eddy, J.A. The Maunder Minimum. *Science* **1976**, *192*, 1189–1202. [CrossRef] [PubMed]
31. Shindell, D.T.; Schmidt, G.A.; Mann, M.E.; Rind, D.; Waple, A. Solar forcing of regional climate change during the Maunder Minimum. *Science* **2001**, *294*, 2149–2152. [CrossRef]
32. Lean, J. Evolution of the Sun's Spectral Irradiance Since the Maunder Minimum. *Geophys. Res. Lett.* **2000**, *27*, 2425–2428. [CrossRef]
33. Eddy, J.A. The Maunder Minimum: A reappraisal. *Sol. Phys.* **1983**, *89*, 195–207. [CrossRef]
34. Luterbacher, J.; Rickli, R.; Xoplaki, E.; Tinguely, C.; Beck, C.; Pfister, C.; Wanner, H. The Late Maunder Minimum (1675–1715)—A Key Period for Studying Decadal Scale Climatic Change in Europe. *Clim. Chang.* **2001**, *49*, 441–462. [CrossRef]
35. Usoskin, I.; Solanki, S.K.; Krivova, N.; Hofer, B.; Kovaltsov, G.A.; Wacker, L.; Brehm, N.; Kromer, B. Solar cyclic activity over the last millennium reconstructed from annual 14C data. *Astron. Astrophys.* **2021**, *649*, A141. [CrossRef]
36. Dorward, P.; Osbahr, H.; Sutcliffe, C.; Mbeche, R. Supporting climate change adaptation using historical climate analysis. *Clim. Dev.* **2020**, *12*, 469–480. [CrossRef]
37. Blöschl, G.; Kiss, A.; Viglione, A.; Barriendos, M.; Böhm, O.; Brázdil, R.; Coeur, D.; Demarée, G.; Llasat, M.C.; Macdonald, N.; et al. Current European flood-rich period exceptional compared with past 500 years. *Nature* **2020**, *583*, 560–566. [CrossRef]
38. Erfurt, M.; Skiadaresis, G.; Tijdeman, E.; Blauhut, V.; Bauhus, J.; Glaser, R.; Schwarz, J.; Tegel, W.; Stahl, K. A multidisciplinary drought catalogue for southwestern Germany dating back to 1801. *Nat. Hazards Earth Syst. Sci.* **2020**, *20*, 2979–2995. [CrossRef]
39. Erfurt, M.; Glaser, R.; Blauhut, V. Changing impacts and societal responses to drought in southwestern Germany since 1800. *Reg. Environ. Chang.* **2019**, *19*, 2311–2323. [CrossRef]
40. Struck, J.; Bliedtner, M.; Strobel, P.; Schumacher, J.; Bazarradnaa, E.; Zech, R. Leaf wax n-alkane patterns and compound-specific δ13C of plants and topsoils from semi-arid and arid Mongolia. *Biogeosciences* **2020**, *17*, 567–580. [CrossRef]
41. Angerer, J.; Han, G.; Fujisaki, I.; Havstad, K. Climate Change and Ecosystems of Asia with Emphasis on Inner Mongolia and Mongolia. *Rangelands* **2008**, *30*, 46–51. [CrossRef]
42. Suzuki, Y. Conflict Between Mining Development and Nomadism in Mongolia. In *The Mongolian Ecosystem Network*; Yamamura, N., Fujita, N., Maekawa, A., Eds.; Springer: Tokyo, Japan, 2013; pp. 269–294. ISBN 978-4-431-54051-9.
43. Chen, J.; Huang, D.; Shiyomi, M.; Hori, Y.; Yamamura, Y.; Yiruhan. Spatial heterogeneity and diversity of vegetation at the landscape level in Inner Mongolia, China, with special reference to water resources. *Landsc. Urban Plan.* **2007**, *82*, 222–232. [CrossRef]
44. Xiao, X.; Ojima, D.S.; Parton, W.J.; CHen, Z.; Chen, D. Sensitivity of Inner Mongolia Grasslands to Climate Change. *J. Biogeogr.* **1995**, *22*, 643–648. [CrossRef]
45. Wang, J.; Brown, D.G.; Agrawal, A. Climate adaptation, local institutions, and rural livelihoods: A comparative study of herder communities in Mongolia and Inner Mongolia, China. *Glob. Environ. Chang.* **2013**, *23*, 1673–1683. [CrossRef]
46. Mu, S.; Yang, H.; Li, J.; Chen, Y.; Gang, C.; Zhou, W.; Ju, W. Spatio-temporal dynamics of vegetation coverage and its relationship with climate factors in Inner Mongolia, China. *J. Geogr. Sci.* **2013**, *23*, 231–246. [CrossRef]
47. Zhang, R.; Zhao, X.; Zuo, X.; Degen, A.A.; Li, Y.; Liu, X.; Luo, Y.; Qu, H.; Lian, J.; Wang, R. Drought-induced shift from a carbon sink to a carbon source in the grasslands of Inner Mongolia, China. *CATENA* **2020**, *195*, 104845. [CrossRef]
48. Huang, J.; Xue, Y.; Sun, S.; Zhang, J. Spatial and temporal variability of drought during 1960–2012 in Inner Mongolia, north China. *Quat. Int.* **2015**, *355*, 134–144. [CrossRef]
49. Pei, Z.; Fang, S.; Wang, L.; Yang, W. Comparative Analysis of Drought Indicated by the SPI and SPEI at Various Timescales in Inner Mongolia, China. *Water* **2020**, *12*, 1925. [CrossRef]

50. Wang, L.; Wang, L.; Liu, Y.; Chen, W. The 2017–2018 Winter Drought in North China and Its Causes. *Atmosphere* **2019**, *10*, 60. [CrossRef]
51. Trabucco, A.; Zomer, R. Global Aridity Index and Potential Evapotranspiration (ET0) Climate Database v2. *CGIAR Consort Spat. Inf.* **2018**, *10*. [CrossRef]
52. Liu, Y.; Fang, X.; Dai, J.; Wang, H.; Tao, Z. Could phenological records from Chinese poems of the Tang and Song dynasties (618–1279 CE) be reliable evidence of past climate changes? *Clim. Past* **2021**, *17*, 929–950. [CrossRef]
53. Watts, J. (Ed.) *The General History of China: Containing a Geographical, Historical, Chronological, Political and Physical Description of the Empire of China, Chinese-Tartary, Corea and Thibet*; Dr Jay Watts: London, UK, 1739.
54. Herzog, I. Least-cost Paths–Some Methodological Issues. *Internet Archaeol.* **2014**, *36*. [CrossRef]
55. Howey, M.C.L. Multiple pathways across past landscapes: Circuit theory as a complementary geospatial method to least cost path for modeling past movement. *J. Archaeol. Sci.* **2011**, *38*, 2523–2535. [CrossRef]
56. Kempf, M. Paradigm and pragmatism: GIS-based spatial analyses of Roman infrastructure networks and land-use concepts in the Upper Rhine Valley. *Geoarchaeology* **2019**, *34*, 797–808. [CrossRef]
57. Earth Resources Observation and Science (EROS) Center. Shuttle Radar Topography Mission (SRTM) 1 Arc-Second Global. 2017. Available online: https://www.usgs.gov/centers/eros/science/usgs-eros-archive-digital-elevation-shuttle-radar-topography-mission-srtm-1 (accessed on 5 January 2022).
58. Buchhorn, M.; Smets, B.; Bertels, L.; de Roo, B.; Lesiv, M.; Tsendbazar, N.-E.; Herold, M.; Fritz, S. Copernicus Global Land Service: Land Cover 100m: Collection 3: Epoch 2019: Globe. 2020. Available online: https://zenodo.org/record/3939050#.YdkSPFkRVhE (accessed on 5 January 2022).
59. Buchhorn, M.; Smets, B.; Bertels, L.; de Roo, B.; Lesiv, M.; Tsendbazar, N.-E.; Li, L.; Tarko, A. Copernicus Global Land Service: Land Cover 100m: Version 3 Globe 2015–2019: Product User Manual. 2020. Available online: https://zenodo.org/record/4723921#.YdkSVVkRVhE (accessed on 5 January 2022).
60. Fick, S.E.; Hijmans, R.J. WorldClim 2: New 1-km spatial resolution climate surfaces for global land areas. *Int. J. Clim.* **2017**, *37*, 4302–4315. [CrossRef]
61. University of East Anglia Climatic Research Unit; Harris, I.C.; Jones, P.D. CRU TS4.05: Climatic Research Unit (CRU) Time-Series (TS) Version 4.05 of High-Resolution Gridded Data of Month-by-Month Variation in Climate (Jan. 1901–Dec. 2020). 2021. Available online: https://catalogue.ceda.ac.uk/uuid/c26a65020a5e4b80b20018f148556681 (accessed on 5 January 2022).
62. Didan, K. MOD13C2 MODIS/Terra Vegetation Indices Monthly L3 Global 0.05Deg CMG V006. 2015. Available online: https://lpdaac.usgs.gov/products/mod13c2v006/ (accessed on 5 January 2022).
63. Technical University of Denmark. Global Wind Atlas 3.0: A Free, Web-Based Application Developed, Owned and Operated by the Technical University of Denmark (DTU). 2020. Available online: https://globalwindatlas.info/ (accessed on 5 January 2022).
64. Cleveland, W.S. Robust Locally Weighted Regression and Smoothing Scatterplots. *J. Am. Stat. Assoc.* **1979**, *74*, 829–836. [CrossRef]
65. Tan, M.; Liu, T.; Hou, J.; Qin, X.; Zhang, H.; Li, T. Cyclic rapid warming on centennial-scale revealed by a 2650-year stalagmite record of warm season temperature. *Geophys. Res. Lett.* **2003**, *30*, 1–4. [CrossRef]
66. Davi, N.K.; Pederson, N.; Leland, C.; Nachin, B.; Suran, B.; Jacoby, G.C. Is eastern Mongolia drying? A long-term perspective of a multidecadal trend. *Water Resour. Res.* **2013**, *49*, 151–158. [CrossRef]
67. Davi, N.K.; Jacoby, G.C.; Curtis, A.E.; Baatarbileg, N. Extension of Drought Records for Central Asia Using Tree Rings: West-Central Mongolia. *J. Clim.* **2006**, *19*, 288–299. [CrossRef]
68. Yi, L.; Yu, H.; Xu, X.; Yao, J.; Su, Q.; Ge, J. Exploratory Precipitation in North-Central China during the Past Four Centuries. *Acta Geol. Sin.-Engl. Ed.* **2010**, *84*, 223–229. [CrossRef]
69. Lemordant, L.; Gentine, P. Vegetation Response to Rising $CO_2$ Impacts Extreme Temperatures. *Geophys. Res. Lett.* **2019**, *46*, 1383–1392. [CrossRef]
70. Feng, L.; Jia, Z.; Li, Q. The dynamic monitoring of aeolian desertification land distribution and its response to climate change in northern China. *Sci. Rep.* **2016**, *6*, 39563. [CrossRef]
71. Gong, Z.; Kawamura, K.; Ishikawa, N.; Goto, M.; Wulan, T.; Alateng, D.; Yin, T.; Ito, Y. MODIS normalized difference vegetation index (NDVI) and vegetation phenology dynamics in the Inner Mongolia grassland. *Solid Earth* **2015**, *6*, 1185–1194. [CrossRef]
72. Cui, J.; Chang, H.; Burr, G.S.; Zhao, X.; Jiang, B. Climatic change and the rise of the Manchu from Northeast China during AD 1600–1650. *Clim. Chang.* **2019**, *156*, 405–423. [CrossRef]
73. Chen, Q. Climate shocks, dynastic cycles and nomadic conquests: Evidence from historical China. *Oxf. Econ. Pap.* **2015**, *67*, 185–204. [CrossRef]
74. Fan, P.; Chen, J.; John, R. Urbanization and environmental change during the economic transition on the Mongolian Plateau: Hohhot and Ulaanbaatar. *Environ. Res.* **2016**, *144*, 96–112. [CrossRef] [PubMed]
75. Yu, D.; Zhou, L.; Zhou, W.; Ding, H.; Wang, Q.; Wang, Y.; Wu, X.; Dai, L. Forest management in Northeast China: History, problems, and challenges. *Environ. Manag.* **2011**, *48*, 1122–1135. [CrossRef]
76. Hoffmann, C.; Funk, R.; Reiche, M.; Li, Y. Assessment of extreme wind erosion and its impacts in Inner Mongolia, China. *Aeolian Res.* **2011**, *3*, 343–351. [CrossRef]
77. Zhao, H.-L.; Yi, X.-Y.; Zhou, R.-L.; Zhao, X.-Y.; Zhang, T.-H.; Drake, S. Wind erosion and sand accumulation effects on soil properties in Horqin Sandy Farmland, Inner Mongolia. *CATENA* **2006**, *65*, 71–79. [CrossRef]

78. Li, F.-R.; Kang, L.-F.; Zhang, H.; Zhao, L.-Y.; Shirato, Y.; Taniyama, I. Changes in intensity of wind erosion at different stages of degradation development in grasslands of Inner Mongolia, China. *J. Arid Environ.* **2005**, *62*, 567–585. [CrossRef]
79. Jiang, L.; Xiao, Y.; Zheng, H.; Ouyang, Z. Spatio-temporal variation of wind erosion in Inner Mongolia of China between 2001 and 2010. *Chin. Geogr. Sci.* **2016**, *26*, 155–164. [CrossRef]
80. Guo, J.; Rahn, K.A.; Zhuang, G. A mechanism for the increase of pollution elements in dust storms in Beijing. *Atmos. Environ.* **2004**, *38*, 855–862. [CrossRef]
81. Hu, W.; Niu, H.; Zhang, D.; Wu, Z.; Chen, C.; Wu, Y.; Shang, D.; Hu, M. Insights into a dust event transported through Beijing in spring 2012: Morphology, chemical composition and impact on surface aerosols. *Sci. Total Environ.* **2016**, *565*, 287–298. [CrossRef] [PubMed]
82. Yang, X.; Xu, B.; Jin, Y.; Qin, Z.; Ma, H.; Li, J.; Zhao, F.; Chen, S.; Zhu, X. Remote sensing monitoring of grassland vegetation growth in the Beijing–Tianjin sandstorm source project area from 2000 to 2010. *Ecol. Indic.* **2015**, *51*, 244–251. [CrossRef]
83. Zhang, Y.; Xu, X.; Liao, Z.; Han, Z.; Ji, G.; Liang, W.; Liu, T. Response of surface runoff to land use and land cover change and its impact on Daihai Lake shrinkage in Inner Mongolia, China. *Appl. Clim.* **2021**, *144*, 555–569. [CrossRef]
84. Alverson, K.D.; Pedersen, T.F.; Bradley, R.S. (Eds.) *Paleoclimate, Global Change and the Future*; Springer: Berlin/Heidelberg, Germany, 2003; ISBN 978-3-642-55828-3.
85. Esper, J.; Cook, E.R.; Schweingruber, F.H. Low-frequency signals in long tree-ring chronologies for reconstructing past temperature variability. *Science* **2002**, *295*, 2250–2253. [CrossRef]
86. Jones, P.D.; Briffa, K.R.; Barnett, T.P.; Tett, S.F.B. High-resolution palaeoclimatic records for the last millennium: Interpretation, integration and comparison with General Circulation Model control-run temperatures. *Holocene* **1998**, *8*, 455–471. [CrossRef]
87. Mann, M.E.; Bradley, R.S.; Hughes, M.K. Global-scale temperature patterns and climate forcing over the past six centuries. *Nature* **1998**, *392*, 779–787. [CrossRef]
88. Chen, W.; Zhou, Q.; Xue, X. Solar cycle modulation of the relationship between the boreal spring Northern Atlantic Oscillation and the East and Southeast Asian summer climate. *Meteorol. Atmos. Phys.* **2020**, *132*, 287–295. [CrossRef]
89. Zhang, J.; Zhou, X.; Jiang, S.; Tu, L.; Liu, X. Monsoon Precipitation, Economy and Wars in Ancient China. *Front. Earth Sci.* **2020**, *8*, 317. [CrossRef]
90. Lan, J.; Xu, H.; Lang, Y.; Yu, K.; Zhou, P.; Kang, S.; Zhou, K.; Wang, X.; Wang, T.; Cheng, P.; et al. Dramatic weakening of the East Asian summer monsoon in northern China during the transition from the Medieval Warm Period to the Little Ice Age. *Geology* **2020**, *48*, 307–312. [CrossRef]
91. Zeng, Y.; Chen, J.; Zhu, Z.; Li, J.; Wang, J.; Wan, G. The wet Little Ice Age recorded by sediments in Huguangyan Lake, tropical South China. *Quat. Int.* **2012**, *263*, 55–62. [CrossRef]
92. Wei, B.; Xie, Y.; Wang, X.; Jiao, J.; He, S.; Bie, Q.; Jia, X.; Xue, X.; Duan, H. Land cover mapping based on time-series MODIS-NDVI using a dynamic time warping approach: A casestudy of the agricultural pastoral ecotone of northern China. *Land Degrad. Dev.* **2020**, *31*, 1050–1068. [CrossRef]
93. Fensholt, R.; Proud, S.R. Evaluation of Earth Observation based global long term vegetation trends—Comparing GIMMS and MODIS global NDVI time series. *Remote Sens. Environ.* **2012**, *119*, 131–147. [CrossRef]
94. Gu, J.; Li, X.; Huang, C.; Okin, G.S. A simplified data assimilation method for reconstructing time-series MODIS NDVI data. *Adv. Space Res.* **2009**, *44*, 501–509. [CrossRef]
95. Kempf, M.; Glaser, R. Tracing Real-Time Transnational Hydrologic Sensitivity and Crop Irrigation in the Upper Rhine Area over the Exceptional Drought Episode 2018–2020 Using Open Source Sentinel-2 Data. *Water* **2020**, *12*, 3298. [CrossRef]
96. Ren, S.; Yi, S.; Peichl, M.; Wang, X. Diverse Responses of Vegetation Phenology to Climate Change in Different Grasslands in Inner Mongolia during 2000–2016. *Remote Sens.* **2018**, *10*, 17. [CrossRef]
97. Fang, X.; Wu, J.; He, C. Assessing human-environment system sustainability based on Regional Safe and Just Operating Space: The case of the Inner Mongolia Grassland. *Environ. Sci. Policy* **2021**, *116*, 276–286. [CrossRef]
98. Ren, H.; Schönbach, P.; Wan, H.; Gierus, M.; Taube, F. Effects of grazing intensity and environmental factors on species composition and diversity in typical steppe of Inner Mongolia, China. *PLoS ONE* **2012**, *7*, e52180. [CrossRef]
99. Tong, S.; Zhang, J.; Bao, Y. Spatial and temporal variations of vegetation cover and the relationships with climate factors in Inner Mongolia based on GIMMS NDVI3g data. *J. Arid Land* **2017**, *9*, 394–407. [CrossRef]
100. Zhang, Y.; Liang, W.; Liao, Z.; Han, Z.; Xu, X.; Jiao, R.; Liu, H. Effects of climate change on lake area and vegetation cover over the past 55 years in Northeast Inner Mongolia grassland, China. *Appl. Clim.* **2019**, *138*, 13–25. [CrossRef]
101. Liu, X.; Tian, Z.; Zhang, A.; Zhao, A.; Liu, H. Impacts of Climate on Spatiotemporal Variations in Vegetation NDVI from 1982–2015 in Inner Mongolia, China. *Sustainability* **2019**, *11*, 768. [CrossRef]
102. Ma, W.; Liu, Z.; Wang, Z.; Wang, W.; Liang, C.; Tang, Y.; He, J.-S.; Fang, J. Climate change alters interannual variation of grassland aboveground productivity: Evidence from a 22-year measurement series in the Inner Mongolian grassland. *J. Plant Res.* **2010**, *123*, 509–517. [CrossRef] [PubMed]
103. Lauenroth, W.K.; Sala, O.E. Long-Term Forage Production of North American Shortgrass Steppe. *Ecol. Appl.* **1992**, *2*, 397–403. [CrossRef]
104. Knapp, A.K.; Smith, M.D. Variation among biomes in temporal dynamics of aboveground primary production. *Science* **2001**, *291*, 481–484. [CrossRef] [PubMed]

105. Oesterheld, M.; Loreti, J.; Semmartin, M.; Sala, O.E.; Oesterheld, M.; Semmartin, M. Inter-Annual Variation in Primary Production of a Semi-Arid Grassland Related to Previous-Year Production. *J. Veg. Sci.* **2001**, *12*, 137. [CrossRef]
106. Li, C.; Wang, J.; Hu, R.; Yin, S.; Bao, Y.; Ayal, D.Y. Relationship between vegetation change and extreme climate indices on the Inner Mongolia Plateau, China, from 1982 to 2013. *Ecol. Indic.* **2018**, *89*, 101–109. [CrossRef]
107. An, N.; Price, K.P.; Blair, J.M. Estimating above-ground net primary productivity of the tallgrass prairie ecosystem of the Central Great Plains using AVHRR NDVI. *Int. J. Remote Sens.* **2013**, *34*, 3717–3735. [CrossRef]
108. Na, L.; Na, R.; Zhang, J.; Tong, S.; Shan, Y.; Ying, H.; Li, X.; Bao, Y. Vegetation Dynamics and Diverse Responses to Extreme Climate Events in Different Vegetation Types of Inner Mongolia. *Atmosphere* **2018**, *9*, 394. [CrossRef]
109. Yao, Y.; Liu, Y.; Wang, Y.; Fu, B. Greater increases in China's dryland ecosystem vulnerability in drier conditions than in wetter conditions. *J. Environ. Manag.* **2021**, *291*, 112689. [CrossRef] [PubMed]
110. Zhang, X.; Wang, J.; Gao, Y.; Wang, L. Variations and controlling factors of vegetation dynamics on the Qingzang Plateau of China over the recent 20 years. *Geogr. Sustain.* **2021**, *2*, 74–85. [CrossRef]
111. Huang, W.; Ge, Q.; Wang, H.; Dai, J. Effects of multiple climate change factors on the spring phenology of herbaceous plants in Inner Mongolia, China: Evidence from ground observation and controlled experiments. *Int. J. Clim.* **2019**, *39*, 5140–5153. [CrossRef]
112. Guo, X.; Chen, R.; Thomas, D.S.G.; Li, Q.; Xia, Z.; Pan, Z. Divergent processes and trends of desertification in Inner Mongolia and Mongolia. *Land Degrad. Dev.* **2021**, *32*, 3684–3697. [CrossRef]
113. Cao, J.; Li, M.; Deo, R.C.; Adamowski, J.F.; Cerdà, A.; Feng, Q.; Liu, M.; Zhang, J.; Zhu, G.; Zhang, X.; et al. Comparison of social-ecological resilience between two grassland management patterns driven by grassland land contract policy in the Maqu, Qinghai-Tibetan Plateau. *Land Use Policy* **2018**, *74*, 88–96. [CrossRef]
114. Cao, J.; Xu, X.; Deo, R.C.; Holden, N.M.; Adamowski, J.F.; Gong, Y.; Feng, Q.; Yang, S.; Li, M.; Zhou, J.; et al. Multi-household grazing management pattern maintains better soil fertility. *Agron. Sustain. Dev.* **2018**, *38*, 6. [CrossRef]
115. Wang, F.; Pan, X.; Wang, D.; Shen, C.; Lu, Q. Combating desertification in China: Past, present and future. *Land Use Policy* **2013**, *31*, 311–313. [CrossRef]
116. Miao, L.; Moore, J.C.; Zeng, F.; Lei, J.; Ding, J.; He, B.; Cui, X. Footprint of Research in Desertification Management in China. *Land Degrad. Dev.* **2015**, *26*, 450–457. [CrossRef]
117. Li, H.; He, S.; Gao, Y.; Chen, H.; Wang, H. North Atlantic Modulation of Interdecadal Variations in Hot Drought Events over Northeastern China. *J. Clim.* **2020**, *33*, 4315–4332. [CrossRef]
118. An, Q.; He, H.; Nie, Q.; Cui, Y.; Gao, J.; Wei, C.; Xie, X.; You, J. Spatial and Temporal Variations of Drought in Inner Mongolia, China. *Water* **2020**, *12*, 1715. [CrossRef]
119. Ying, H.; Zhang, H.; Zhao, J.; Shan, Y.; Zhang, Z.; Guo, X.; Rihan, W.; Deng, G. Effects of spring and summer extreme climate events on the autumn phenology of different vegetation types of Inner Mongolia, China, from 1982 to 2015. *Ecol. Indic.* **2020**, *111*, 105974. [CrossRef]
120. Chen, J.; John, R.; Shao, C.; Fan, Y.; Zhang, Y.; Amarjargal, A.; Brown, D.G.; Qi, J.; Han, J.; Lafortezza, R.; et al. Policy shifts influence the functional changes of the CNH systems on the Mongolian plateau. *Environ. Res. Lett.* **2015**, *10*, 85003. [CrossRef]

land

MDPI

*Article*

# Multisource and Multilevel Investigations on a Historical Landslide: The 1907 Servigliano Earth Flow in Montemurro (Basilicata, Southern Italy)

**Mario Bentivenga [1], Fabrizio Terenzio Gizzi [2,*], Giuseppe Palladino [3], Marco Piccarreta [1], Maria Rosaria Potenza [2], Angela Perrone [4], Jessica Bellanova [4], Giuseppe Calamita [4] and Sabatino Piscitelli [4]**

[1] Department of Sciences, University of Basilicata, 85100 Potenza, Italy; mario.bentivenga@unibas.it (M.B.); marco.piccarreta@posta.istruzione.it (M.P.)
[2] Institute of Heritage Science, National Research Council (ISPC-CNR), Area della Ricerca, C.da S. Loja, Tito, 85050 Potenza, Italy; mariarosaria.potenza@cnr.it
[3] Department of Geology and Geophysics, School of Geosciences, University of Aberdeen, Aberdeen AB24 3FX, UK; giuseppe.palladino@abdn.ac.uk
[4] Institute of Methodologies for Environmental Analysis (CNR-IMAA), Area della Ricerca, C.da S. Loja, Tito, 85050 Potenza, Italy; angela.perrone@imaa.cnr.it (A.P.); jessica.bellanova@imaa.cnr.it (J.B.); giuseppe.calamita@imaa.cnr.it (G.C.); sabatino.piscitelli@imaa.cnr.it (S.P.)
* Correspondence: fabrizioterenzio.gizzi@cnr.it

**Abstract:** Italy is one of the European countries most affected by landslides. In order to mitigate the risk, the analysis of such phenomena should involve a broad spectrum of studies to understand the geological and geomorphological properties of the unstable areas, the geometric features of the landslides and the causes of their trigger, the evolution over time, and the works of risk mitigation taken as well as their effectiveness over time. This article is concerned with multidisciplinary investigations on a historical earth flow occurred in Montemurro (Basilicata, Southern Italy) in 1907. We analyse unpublished archive sources strictly coupled with new geological and geomorphological surveys. Furthermore, to gain information on the geometrical features of the landslide body, geophysical prospections (ERT) is used alongside the field surveys. Lastly, to gain insight on the landslide triggering factors, we employed historical–climatological analysis: in particular, we made use of the monthly simple daily intensity index (SDII) to evaluate extreme events and the standardised precipitation index (SPI) to consider previous wetness conditions. The earth flow was triggered on 26 February 1907 and the main movement lasted about one week, involving several buildings, including those of cultural interest. Historical documentary investigations and historical climatological analysis both indicate that the earth flow was triggered by a preceding heavy rain period, which independent historical sources suggest also caused the activation of landslides over a wider area around Montemurro. Currently, the earth flow is NE–SW oriented, extends for a length of ~1.1 km, and has an average width of ~220 m. The landslide is in a dormant activity phase. From a methodological point of view, the research stresses the importance of integrated approaches to investigate natural hazards, particularly by the use of historical data. This research may be of interest to academics, practitioners, and policymakers for both the methodological approach followed and results gained, useful in view of both risk mitigation and territorial planning of landslide-prone areas.

**Keywords:** geological features; historical landslide; cultural heritage; archive sources; historical rainfall; risk mitigation; electrical resistivity tomography (ERT); southern Apennine; Basilicata region; Agri Valley

**Citation:** Bentivenga, M.; Gizzi, F.T.; Palladino, G.; Piccarreta, M.; Potenza, M.R.; Perrone, A.; Bellanova, J.; Calamita, G.; Piscitelli, S. Multisource and Multilevel Investigations on a Historical Landslide: The 1907 Servigliano Earth Flow in Montemurro (Basilicata, Southern Italy). *Land* **2022**, *11*, 408. https://doi.org/10.3390/land11030408

Academic Editor: Domenico Calcaterra

Received: 26 January 2022
Accepted: 5 March 2022
Published: 10 March 2022

**Publisher's Note:** MDPI stays neutral with regard to jurisdictional claims in published maps and institutional affiliations.

**Copyright:** © 2022 by the authors. Licensee MDPI, Basel, Switzerland. This article is an open access article distributed under the terms and conditions of the Creative Commons Attribution (CC BY) license (https://creativecommons.org/licenses/by/4.0/).

## 1. Introduction

Of all European countries, Italy is among the most affected by landslides [1]. The Italian Landslide Inventory (IFFI) Project has recorded 620,808 events affecting an area of 23,700 km$^2$, equal to 7.9% of the national territory [2].

After earthquakes, landslides are the natural hazards that have caused the highest number of victims and amount of damage to inhabited centres, infrastructure, the environment, and cultural heritage. Since after the Second World War, there has been an increase in the risk of landslides due to the growing human pressure on the territory, with an expansion of the urban layout, often involving unstable areas [2]. In the last 50 years (1966–2015), landslides and floods have caused 1947 deaths, 69 missing people, 2534 injured people, and 412,087 evacuated and homeless people [3].

In order to both mitigate the hydrogeological risk and improve the territorial planning, the knowledge of both current and potentially hazardous landslides requires an in-depth and multisource analysis, such as geological, geomorphological, geophysics, and historical to obtain information on the features of unstable areas, the geometry of landslides, the causes of triggering of historical events, and the evolution of the phenomena over time, and so on.

The studies of landslides by different disciplines and competencies among researchers is increasingly required for a wider and deeper understanding of natural hazards, particularly landslides, involving geological, geomorphological, and geotechnical investigations [4]; lidar investigations [5,6]; and geological, geotechnical, and geophysical methods [7–9]. Historical data are also used in landslide studies for different purposes. For example, in order to assess the dynamics of reservoir bank landslides and shoreline abrasion at active zones, Yermolaev et al., (2021) [10] used the integration of laser scanning, unmanned aerial vehicles (UAV), global navigation satellite systems (GNSS), and historical imageries; Tropeano & Turconi (2004) [11] suggested the use of historical documents to both increase public awareness of natural hazards and inform the selection of proper civil protection strategies; and Carrara et al., (2003) [12] used geomorphological data and historical sources to assess landslide hazard.

Using a multilevel and integrated approach, the article is concerned with the investigations on earth flow in Montemurro, a village that falls within the domain of the Apennine chain and occupies the left slope of the high Val d'Agri in the Basilicata region (southern Italy). The region, a real open-air laboratory for multidisciplinary and interdisciplinary research [13], is particularly prone to earthquakes and landslides, which also cause heavy damage to towns and cultural heritage sites, forcing some to be abandoned [14–17].

The article is organized into three main sections: (1) Materials and Methods, where the approaches followed are delineated in detail; (2) Results and Discussion, where we describe the geological and geomorphological characteristics of the Montemurro area, the electrical resistivity tomography (ERT) investigations performed on the landslide, the scrutiny of unpublished historical sources, and a historical climatic analysis; and (3) Conclusions, including the limitations of the research as well as future perspectives.

## 2. Materials and Methods

### *2.1. The Study Area and the Regional Geological Setting*

Montemurro is a village located in the Agri Valley in the southern part of the Basilicata region (Southern Italy, Figure 1) at an altitude of 723 m a.s.l. on a relief elongated in a NE–SW direction.

The Agri Valley is a Quaternary intermontane basin located in the hinterland of the southern Apennines. This basin is part of an east verging fold-and-thrust belt developed as an accretionary wedge from the late Oligocene to the early Pleistocene due to the eastward migration of the Apenninic arc [18–21] (Figure 2).

The present-day configuration of the basin is related to different extensional and transtensional tectonic phases that took place between the Lower Pleistocene and the Holocene, along the fault system known as Val d'Agri Fault System (VAFS) [26,27].

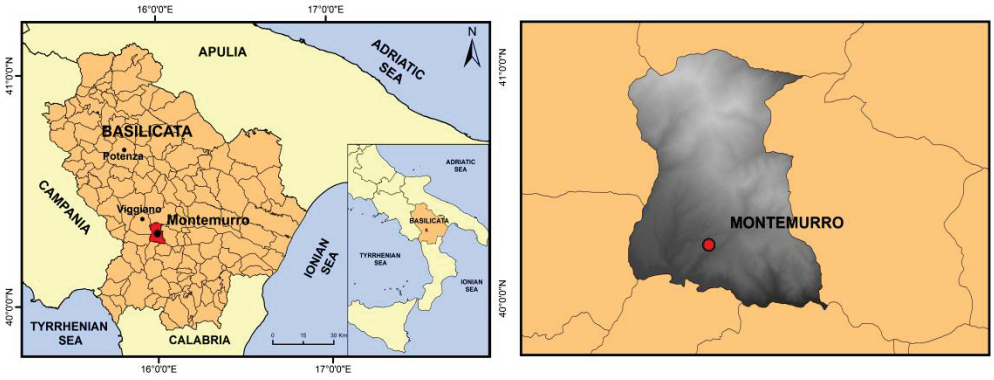



**Figure 1.** Geographical sketch showing the location of the study area. The sketch also includes the location of Viggiano municipality to which the next sections also refer.

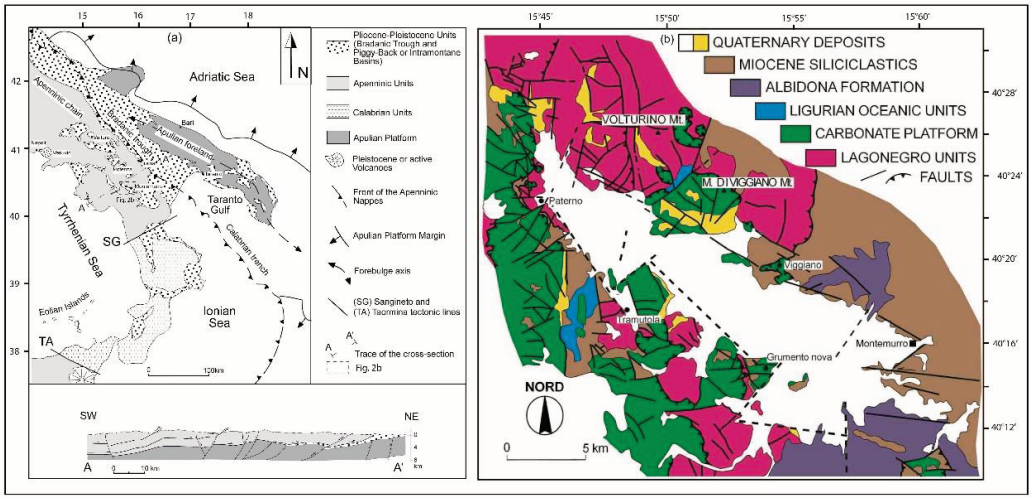



**Figure 2.** (**a**) Geological sketch map of the southern Apennine and geological cross section [22–24]; (**b**) geological map of the Agri Valley basin [25].

VAFS consists of numerous left-lateral strike-slip faults oriented N120°, associated with compatible kinematics left transtensive faults oriented at N90°/N110° and right, oriented at N30°, in addition to left-lateral transpressive faults oriented at N130°/N150°. The development of these structures involved the Galaino breccias [28] Lower Pleistocene in age, cropping out along the north-western edge of the basin of the high Agri valley. The morphogenetic evolution of the valley would have started from the erosion of a mature landscape, with a small subaerial energy gradient, defined in literature as "summit paleosurface" of Upper Pliocene to lower Pleistocene age offset by faults and currently preserved at different altitudes varying between about 1000 and 1400 m. The syntectonic sedimentary infill of the Agri Valley Basin (AVB) includes a succession only partially exposed at the surface for an overall thickness of approximately 100 m in the south-eastern portion of the basin and sometimes in the north-western part, which is schematized in literature in the following way, starting from the oldest terms:

- /Breccia di Galaino—slope breccias and equivalent units of the Middle-Lower Pleistocene;
- Complesso dell'Agri (Agri Complex)—gravel-conglomeratic and sandy-clayey succession of the middle-upper Pleistocene;
- Terrazzi fluviali, conoidi di deiezione, alluvioni recenti e attuali (Fluvial terraces, fans, recent and actual alluvial deposits)—different orders of terraces correlated to colluvial deposits and slopes in equilibrium with the current morpho-climatic structure of the valley (Upper Pleistocene—present).

In the south-eastern portion of the AVB, the units of the "Agri Complex" and the late Pleistocene–Holocene sediments crop out. The first sediments are correlated to ancient local base levels, which reach heights even above 700 m a.s.l. The latter are different orders of terraces characterised by very small area dimensions and thickness, with progressively lowered base levels up to the current 500 m above a.s.l.

### *2.2. The Methods*

The multilevel and cross-correlated methodological approach (Figure 3) adopted in the research includes geological and geomorphological surveys, geophysical investigations, historical documentary analysis, and historical climatological studies. In particular, we performed new geological and geomorphological surveys, electrical resistivity tomography (ERT) investigations aimed at improving the knowledge of the geometry of the landslide body, analysis of unpublished archive sources to obtain information on the landslide features and its activity over time, and historical climatological investigations to identify the landslide triggering factors.

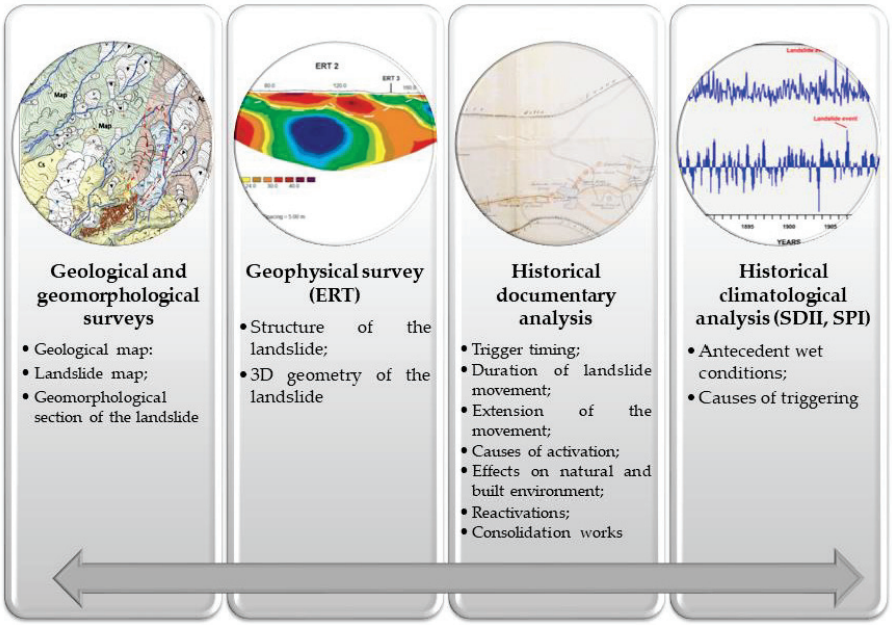



**Figure 3.** The four main methodological steps followed for the investigation on the historical landslide. For each step, the specific aims are itemized.

#### 2.2.1. Electrical Resistivity Tomography (ERT)

In this work, the electrical resistivity tomography geophysical technique was used [29–33] to reconstruct the geometry of the landslide body and to identify the shear surfaces that separate the landslide body from the bedrock [34–36].

The ERT technique consists of the injection of a direct electrical current (I) into the ground through two electrodes and the measurement of the voltages (V), revealing the direction and amount of current flow in the subsurface, through another couple of electrodes. The electrodes can be arranged on the ground by using different arrays, each of which is characterized by a geometric factor (K). The measured apparent resistivities (rho_a), obtained by combining I, V and K, can be inverted into true resistivities (rho) by applying an inversion method. In this paper, the inversion software RES2DINVX32 (version 3.71.118), based on the smoothness-constrained least-squares method [30,37,38], was applied to obtain two-dimensional subsurface resistivity models from the apparent resistivity pseudosections.

2.2.2. The Historical Approach

Historical data can be divided in four main groups [39]:

(a) those that directly record change or occurrence of a natural event (e.g., flood and landslide);
(b) those that indirectly provide data which can be used to suggest causal or explanatory models (e.g., climatic records);
(c) other supporting surveys that include relevant information (e.g., geological surveys);
(d) phenological records which deal with timing (e.g., time of wet season groundwater response).

In our analysis, historical data, particularly that from groups (a) and (b), were considered. Archive documentation was analysed to identify the chronology of the trigger and reactivations of the landslide, the causes of them, the damage effects, the consolidation works planned, and their efficacy over time. Further, climatic records were analysed to determine the cause of the landslide.

The Archive Analysis

The study was carried out mainly through the scrutiny of documentation produced by the *Commissariato Civile per la Basilicata* (CCB) [1]. The sources are currently preserved in the *Archivio di Stato di Potenza* (National State Archive of Potenza), in the chief town of the Basilicata region.

CCB was established with the law for Basilicata No. 140 of 31 March 1904, also known as the Zanardelli law, and it was suppressed in 1923. CCB was founded as a body responsible for planning, design, and execution of a large number of infrastructure works in Basilicata, as well as for the management of the related funds. Therefore, its aim was also to build infrastructure to consolidate the towns affected by hydrogeological instability [40]. The analysis of documents produced by this body allowed increasing the completeness of both data related to the chronology of the trigger and reactivations of the landslide and the effects caused by the mass movement within the deeper and wider landscape of knowledge of the hydrogeological instability of the Montemurro area.

Beyond these documents, other sources derived from the direct consultation of the *Archivio Storico Nazionale del Dipartimento della Protezione Civile* [2] (National Historical Archive of the Civil Protection Department in Rome), before the same archive was transferred to the State Archive of Rome.

The sources of that archive amount to about 15,000 documents relating to disasters that occurred in Italy since 1908. The archive arose from several acquisitions from other bodies that were responsible for civil protection before the birth of the Civil Protection Department, established in 1982 at the Presidency of the Council of Ministers [41]. Sources from this archive were useful for analysing the planned partial shifting of Montemurro due to the occurrence of the 1907 Servigliano landslide and the consolidation works performed in the town as well as its efficacy over time. In addition to the archive sources, magazines contemporary to the landslide were also taken into consideration, with particular attention to photographic reporting.

On the whole, the documents analysed were written between the end of the 19th century to the sixties of the 20th century over approximately 60 years. In particular, the most useful typologies of documents consulted were: correspondence between the mayor of Montemurro and CCB; correspondence between the Ministry of Public Works and CCB; technical administrative documentation relating to the consolidation works carried out by firms; correspondence between the Civil Engineer Body and CCB; and resolutions of the CCB board as well as Montemurro town council.

Historical Climatic Analysis

Monthly rainfall and the monthly number of rainy days were collected from the National Hydrographic Service [42]. The data cover the climatological norms in 1885–1914. The aim was to correlate the investigated landslide event with the climate conditions in

terms of triggering rainfall and antecedent wetness condition. However, the lack of daily data prevented a detailed analysis for extreme events. To overcome these limitations, we used the monthly simple daily intensity index (SDII) to evaluate extreme events and the standardized precipitation index (SPI) [43] to evaluate previous wetness condition.

SDII represents the ratio between monthly rainfall amount and the number of rainy days that month. It is expressed as mm·day$^{-1}$.

SPI was used to quantify the precipitation deficits on multiple time scales (1, 3, 6, 12, 24, and 48 months), thus allowing drought conditions to be described for a range of meteorological, agricultural, and hydrological applications. The index was computed by fitting an appropriate probability density function (PDF) to the frequency distribution of precipitation summed over the time scale of interest (usually from 3 to 24 months).

Computation of the SPI involved fitting a gamma function to a given time series of precipitation, with the probability density function (PDF) defined as:

$$g(x) = \frac{1}{\beta^{\alpha}\Gamma(\alpha)} x^{\alpha-1} e^{-x/\beta} \; for \; x > 0,$$

where $\alpha > 0$ is a shape parameter, $\beta > 0$ is a scale parameter, $x > 0$ is the amount of precipitation and $\Gamma(\alpha)$ is the gamma function. Fitting the distribution to the data requires $\alpha$ and $\beta$ to be estimated for each month of the year and for each time aggregation. The parameters $\alpha$ and $\beta$ can be estimated as follows:

$$\alpha = \frac{1}{4A}\left(1 + \sqrt{1 + \frac{4A}{3}}\right), \; \beta = \frac{\underline{x}}{\alpha} \qquad with \; A = lnln\,(\underline{x}) - \frac{\sum lnln\,(x)}{n}$$

where $n$ is the number of observations. The cumulative distribution function (CDF) $G(x)$ is defined as:

$$G(x) = \int_0^x g(x)dx = \frac{1}{\beta^{\alpha}\Gamma(\alpha)} \int_0^x x^{\alpha-1} e^{-x/\beta} dx \, ,$$

Due to the possibility to have several zero values in a sample set, since the gamma distribution is undefined for $x = 0$, the CDF for the gamma distribution is modified as:

$$H(x) = q + (1 - q)\, G(x),$$

where $q$ is the probability of zero precipitation, given by the ratio between the number of zeros in the precipitation series (m) and the number of observations (n). The CDF is then transformed into the standard normal distribution to yield the *SPI* as:

$$z = SPI = -\left(t - \frac{c_0 + c_1 t + c_2 t^2}{1 + d_1 t + d_2 t^2 + d_3 t^3}\right), \; t = \sqrt{ln\left(\frac{1}{(H(x))^2}\right)} \quad for \; 0 < H(x) < 0.5,$$

$$z = SPI = +\left(t - \frac{c_0 + c_1 t + c_2 t^2}{1 + d_1 t + d_2 t^2 + d_3 t^3}\right), \; t = \sqrt{ln\left(\frac{1}{(1 - H(x))^2}\right)} \quad for \; 0.5 < H(x) < 1,$$

where $c_0$, $c_1$, $c_2$, $d_1$, $d_2$ and $d_3$ are mathematical constants.

Although the SPI index follows a classification restricted only to drought periods, it has become customary to use the index to classify wet periods as well. Table 1 reports the climatic classification according to the SPI, provided by the National Drought Mitigation Center (NDMC, http://drought.unl.edu, accessed on 18 November 2021).

**Table 1.** Climate classification according to the standardized precipitation index (SPI) values.

| SPI Value | Class | Probability (%) |
|---|---|---|
| SPI $\geq$ 2.0 | Extremely wet | 2.3 |
| 1.5 $\leq$ SPI < 2.0 | Severely wet | 4.4 |
| 1.0 $\leq$ SPI < 1.5 | Moderately wet | 9.2 |
| 0.0 $\leq$ SPI < 1.0 | Mild wet | 34.1 |
| −1.0 $\leq$ SPI < 0.0 | Mild drought | 34.1 |
| −1.5 $\leq$ SPI < −1.0 | Moderate drought | 9.2 |
| −2.0 $\leq$ SPI < −1.5 | Severe drought | 4.4 |
| SPI < −2.0 | Extreme drought | 2.3 |

## 3. Results and Discussions

### *3.1. Geological and Geomorphological Settings of the Montemurro Area*

#### 3.1.1. Geological Setting

A new geological survey allowed us to delineate in detail the geological structure of the area, the stratigraphic relationships, and the tectonic structures affecting the different outcropping formations, as shown in the geological map in Figure 4.

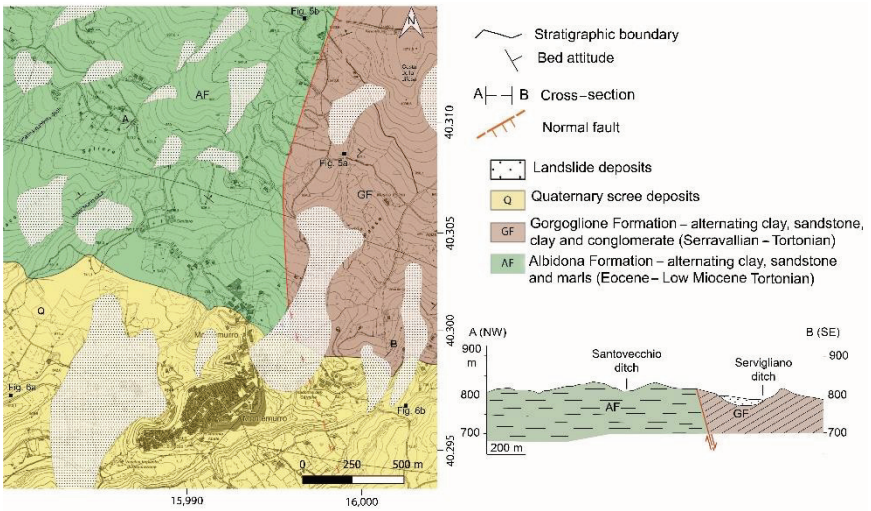



**Figure 4.** Geological map of the study area. The map also shows the site where the photos in Figures 5 and 6 (Figure 5a,b and Figure 6a,b) were taken.

The outcropping rocks can be assigned to both the Gorgoglione Formation [44], which constitutes the pre-Quaternary bedrock of the studied area, and Quaternary alluvial.

The Gorgoglione Formation was deposited in a piggy-back basin during the compression phase of the Apennine orogeny, which gave rise to the Irpino Basin [45–51]. The Gorgoglione Formation consists of a succession made up of massive, well-cemented, coarse sandstones, with variable colouring from whitish to yellowish, alternating with grey pelitic intervals or polygenic and polymetric conglomerate with abundant sandy matrix (Figure 5a). The formation shows a general bed attitude with the beds dipping mainly towards the NE, which gives rise to the reliefs that dominate the inhabited centre of Montemurro at an altitude of about 1000 m a.s.l. However, the northern part of the urban area of Montemurro was built directly on the Miocene arenaceous substrate. The remaining part of the village was built on Quaternary deposits.



(**a**) (**b**)

**Figure 5.** Pre-Quaternary bedrock: (**a**) outcrop the Gorgoglione Formation; (**b**) outcrop the Albidona Formation. The site where the photos were taken is reported in Figure 4. (Photoes taken by Bentivenga M.)

Other outcrops of the Gorgoglione Formation were identified in the north-western part of the study area, along the deep valley cut by the erosion of the Saliere, Notar Mario, and Scannamogliera ditches.

The pre-Quaternary bedrock, which is better exposed along incisions and ditches, consists of banks of whitish quartz sandstones.

The Miocene substrate also crops out along the right side of the Scazzero ditch, southwest of the town of Montemurro, coinciding witha tectonic structure with a NE–SW trend that involves the Pleistocene sands. In this outcrop, the Gorgoglione Formation is very tectonised.

In the rest of the study area, the arenaceous sequence prevails, with more or less extensive outcrops consisting mainly of greyish quartz limestone sandstones with marly or centimetric clay intercalations belonging to the Albidona Formation (Figure 5b).

The arenaceous beds show thicknesses ranging from a few decimetres to a few meters. Beds with a greater thickness show an evident normal gradation [52]. The contact between pelitic and the arenaceous intervals is generally sharp. In the Passo San Vito area, intraformational sliding structures (slumps) have been observed.

In the study area, the Gorgoglione Formation rests discordantly on the Albidona Formation, which extensively emerges further west. Pleistocene sandy deposits lie unconformably above the Gorgoglione Formation. The stratigraphic contact between the two formations is rarely exposed within the surveyed area since it is commonly covered by slope and/or landslide debris. The on-lap geometry of the contact occurs at Largo S. Antonio, 710 m a.s.l., in the Montemurro centre.

The Quaternary succession exposed in the area consists of middle Pleistocene-Holocene wedge-shaped continental clastic deposits [53]. These unconformably lie on the Gorgoglione Formation deposits. These are deposits associated with alluvial plains and alluvial plains and correspond to those identified in the intermediate and upper range of the Val d'Agri complex, as described by Di Niro et al., (1992, 1995) [54,55].

More recently, these Pleistocene deposits were described by Zembo et al., (2010) [56]. They consist of poorly graded conglomerates and clast-supported gravels, with a reddish sandy matrix alternating with sandy gravels. The clasts are mainly derived from the Gorgoglione Formation. Rarely, calcarenitic, siliceous, igneous, and metamorphic clasts are also observed. The dimensions range from centimetric to decimetric and are generally slightly rounded. These deposits crop out at the top of the morphological terrace on which the south-western part of the Montemurro village rests, along the incision of the Santovecchio ditch and along the right side of the Scannamogliera ditch. The best exposed outcrops can be seen on the subvertical walls on the left of the Scazzero ditch (Figure 6b).



(**a**) (**b**)

**Figure 6.** (**a**) Outcrops of sandy sediments in the southern part of the Montemurro; (**b**) conglomerates outcropping near the village. The site where the photos were taken is reported in Figure 4. (Photoes taken by Bentivenga M.)

In the southern part of the studied area, the deposits consist of sands, from coarse to very fine, interstratified with clays and clayey silts with colours varying from grey to olive green. Sometimes, the finer horizons have a high content in organic matter and are also characterized by ferrous reddish-brown or calcareous whitish concretions. Upwards, a gradual increase in grain size can be observed in gravels and massive conglomerates with heterometric clasts of various kinds and sandy matrix of red-brown colour. Conglomerates are often interstratified with coarse sands and lens-shaped silty bodies [57,58] (Figure 6a).

The morphological structural framework of the area was carried out on the basis of observations made on aerial photos and in the countryside during the geological survey. Furthermore, a previous geoelectric survey [57] greatly supported the understanding of the geology of the area by interpreting the numerous tomographic profiles.

The morphological evolution of the area is conditioned by two main mainly normal fault systems, with NW–SE and NE–SW trends, and part of a regional system known as the Val d'Agri fault system (VAFS, [27] and references therein).

On the one hand, the NW–SE system created a stepped structure, which favoured the development of a structural depression with significant deepening towards SW of the pre-Quaternary substrate represented by the Gorgoglione Formation. The most important fault of this system is transtensive, with an Apennine trend, south of the Montemurro cemetery. A similar structure is found further upstream along the provincial road that connects Montemurro to Viggiano (Figure 1) and places the Miocene substrate in contact with the Quaternary sandy deposits, in correspondence with a box-like structure due to two other transtensive faults with an anti-Apennine course. Another contact between the Miocene substrate and the Quaternary deposits was observed close to the inhabited centre of Montemurro, in correspondence with a normal fault, which lowers the south-western part. On the other hand, the NE–SW dislocation system, with an anti-Apennine trend, consists of faults with a prevalently normal component but with often antithetical vergences that favour the development of horst and graben-type structures. This system influences the arrangement of the ridges, stretched in the NE–SW direction, and the trend of the hydrographic network. One of the most important structures of this system is represented by a fault with a prevalently normal component along the Scazzero ditch. Corresponding to this is contact between the Miocene substrate, which emerges along the right side of the ditch and the Quaternary deposits outcropping on the opposite side.

Other recognisable morphological elements are the terraced surfaces, consisting of alluvial deposits and bordered by escarpments with high slopes. Among these, the most evident are the flat surface on which part of the town of Montemurro was built and the vast area called "I Piani", separated from the previous one by the incision of the Scazzero

ditch. The morphological terrace, on the hydrographic left of the ditch, still preserves the morphology of the old fan, which consists of a residual edge, similar to that which can be observed south of the cemetery.

3.1.2. Geomorphological Setting

The results of the new geomorphological analysis carried out in the studied area are reported in the sketch map of Figure 7.

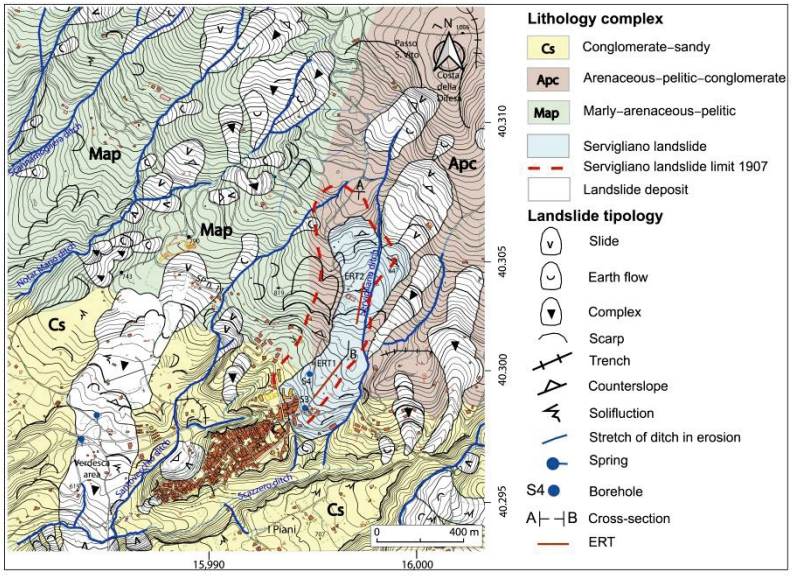



**Figure 7.** Landslide map of the study area.

The western side of the village of Montemurro is characterized by an obvious slope change controlled by the different strength of the outcropping lithologies. The presence of alternating turbidite sandstones, siltstones, and silty clays in the northern sector produces steeper slopes than the southern sector, where Quaternary deposits consisting of conglomerates, sands, and clays outcrop.

The area is characterized by a wide geomorphological instability involving the entire right slope from the Scazzero ditch, 810 to 590 m a.s.l. and 1500 m in length. Landslides mainly affect Quaternary continental deposits of the Val d'Agri Basin and, in the topmost slope sector, the Gorgoglione Formation sandstones. In some cases, it is possible to recognize landslide main scarps, minor scarps, terrace-like features, and counterslopes, which are particularly pronounced along the southern sector of the slope. Geomorphological trenches in the foothills of fault scarps and landslide niches have also been observed.

An impressive pre-1954 quiescent landslide involved the entire area delimited by the road from Montemurro to the cemetery to the north, by the Montemurro high to the east, by the conoid south-westward of the cemetery to the west and by the Scazzero ditch to the south. The damaged area is about 40 ha, and subsoil geological structures have been completely reworked and altered. The entire area is still active and has been affected by many smaller landslide events. Now, the main landslide activity affects the slope in the Verdesca area, where significant evidence of ongoing activity has been observed; this consists of structural damage to infrastructure and anthropic buildings (e.g., dislocation of SP n. 11 road tunnel box, warping of retaining walls, and deformation of road embankments, road surfaces, and old man-made structures; Figure 7 [57–61]).

The area has been affected by a complex landslide, about 700 m long and 325 m wide, developed between 675 and 590 m a.s.l., with a maximum elevation difference of about 85 m between the upper and the lower portions of the landslide body. The size of the damaged area is about 20 ha. The steepness of the landslide body in the accumulation area is about 14°, while it is about 12° in the source area. In the upper sector, this landslide is a

rotational slide, evolving, in the lower part, into a flow [62,63]. The landslide foot has been affected by further superficial movements, due to the continuous erosion of the Scazzero ditch, whose course is diverted in relation to the zone accumulation.

3.1.3. The Servigliano Landslide

The comparison between the current landslide map of the area and historical sources (see Section 3.3.1. allowed us to geometrically identify the Servigliano landslide. The mass movement was activated on 26 February 1907 and originated near Coste della Difesa, north-east of Montemurro village, where the niches of detachment, and affects much of the southern slope of "Passo di San Vito" (1050 m a.s.l.) (Figure 7).

The Servigliano landslide of 1907 can be classified as an "earth flow", extends for about 1000 m, and has an average width of about 280 m. The depletion zone is located at about 1050 m a.s.l. while the toe zone foot reaches 700 m a.s.l. covering a difference in level of 350 m (Figure 8). The last evident reactivation of the landslide took place in June 1921.

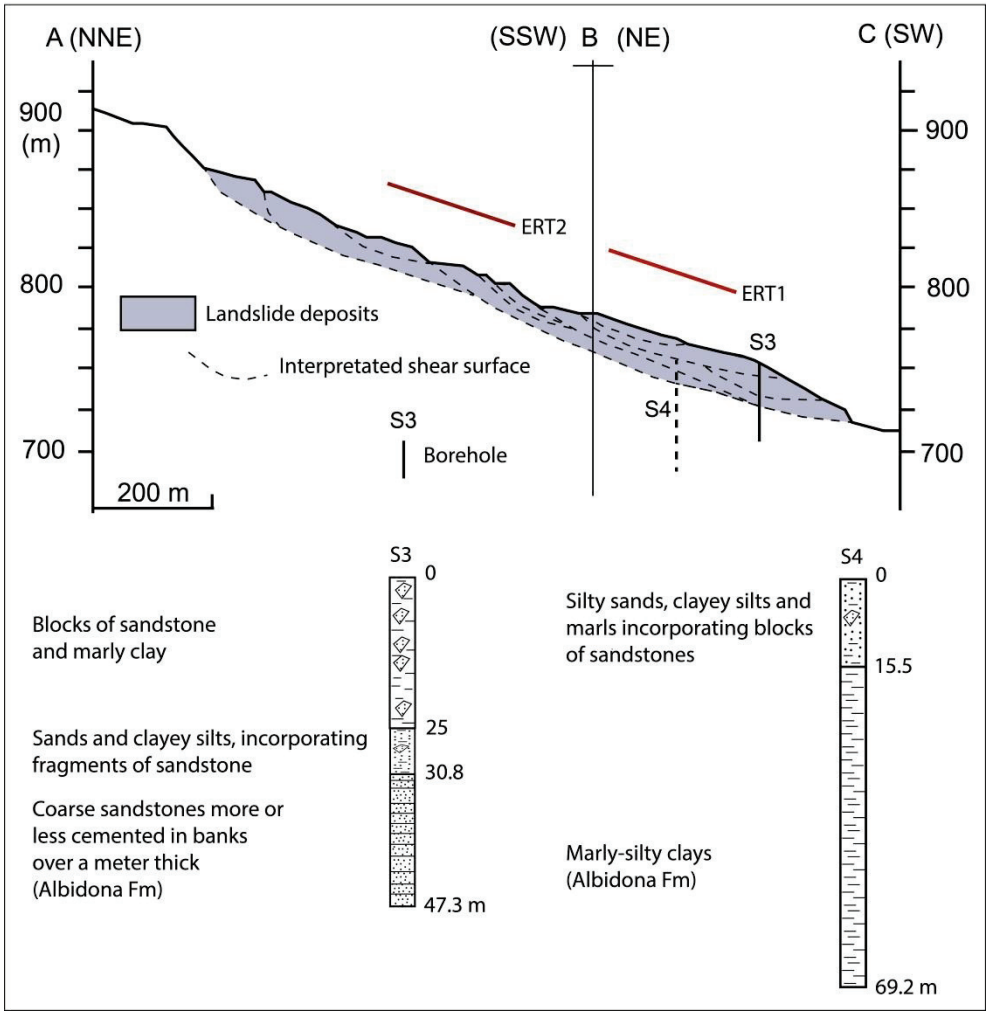



**Figure 8.** Geomorphological section of the Servigliano landslide of 1907 with superimposed boreholes according to Lentini & Schilirò (1982) [3]. For sections outline (A-B and B-C) see Figure 7. The Figure also shows the location of ERT (see Section 3.2.).

The landslide body has an average slope of about 10°. Over time, the main landslide body has been affected by smaller and more superficial landslides that have mainly affected the toe zone, caused by the continuous erosion exerted by the Scazzero ditch that flows in the south-eastern part of Montemurro. The landslide movement mainly affected the deposits of the Gorgoglione Formation, while only in the terminal part, near the town, did

it involve the Quaternary deposits. During the activation in 1907, the landslide partially filled the Servigliano ditch, and the foot of the landslide involved the north-eastern part of the urban area, causing significant damage, to then reach the Scazzero ditch. The deposits of the landslide toe zone are delimited on the left by the terminal part of the Servigliano ditch and on the right by a small ditch that feeds down Santovecchio ditch. In particular, the Servigliano landslide begins with two very distinct escarpments that have generated evident terraces beyond which, towards the bottom, the landslide body evolves by flow. The elongated landslide channel extends from NNE to SSW. In the terminal part, landslide deposits have assumed a fan arrangement north of the town and the Scazzero ditch, which flows in the south-eastern part of Montemurro.

There are no data available concerning the depth of the sliding surface, which would be necessary to reconstruct the geometry of the landslide body. Inside the landslide body, two sources for surfacing the piezometric surface were identified, located at the base of detachment niches. Currently, the Servigliano landslide of 1907 appears to be dormant.

### *3.2. Electrical Resistivity Tomography (ERT)*

The measurements were carried out along two profiles by using the georesistivimeter Syscal Pro Switch 48 connected to multielectrode cables with 48 electrodes arranged following the Wenner–Schlumberger array and spaced 5 m from each other. The obtained resistivity models were 235 m long and reached an investigation depth of about 40 m (Figure 9). ERT results were interpreted taking into account the geological and geomorphological setting of the area and the borehole data (S3 and S4).

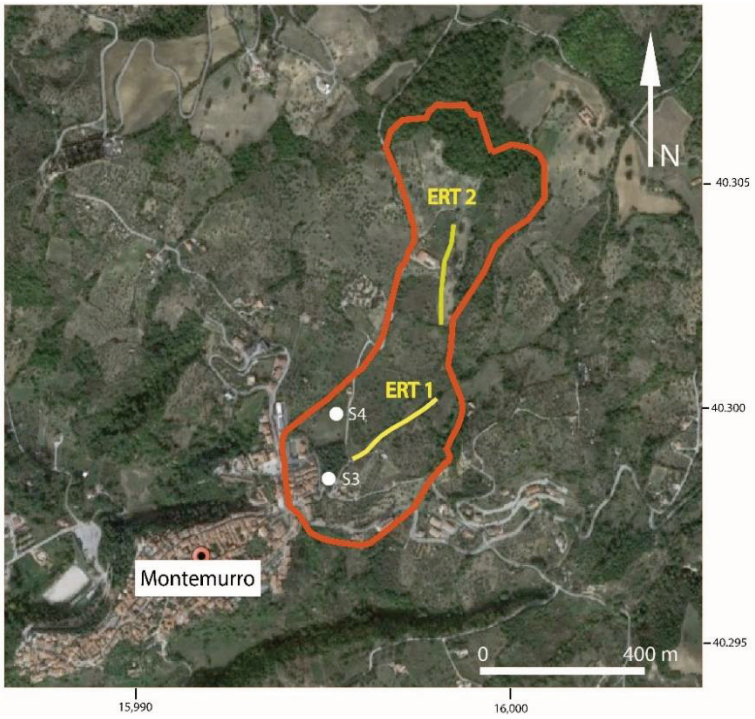



**Figure 9.** Traces of the two ERT (in yellow) and the limit of the Servigliano landslide (in orange). Satellite image from Google Earth™. The map also shows the two boreholes (S3 and S4).

ERT Analysis and Interpretation

ERT were carried out in two different sectors of the landslide parallel to the main axis of the body. They are characterised by a resistivity range limited between 10 and 40 ohm·m, mainly due to the clayey matrix of the terrains outcropping in the area.

ERT1 (Figure 10), located in the landslide foot, shows a succession of resistive and conductive layers, up to 20–25 m in depth, overlying a thicker conductive layer. In the deep portion of the ERT, in the south-western side, an increase of the resistivity is observed.

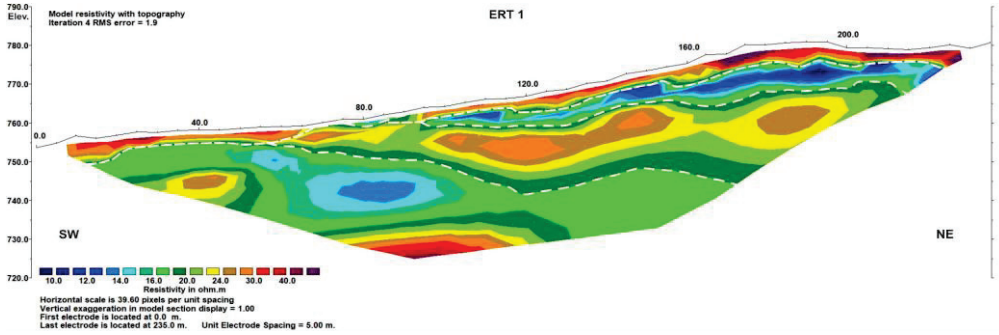



**Figure 10.** Electrical resistivity tomography (ERT 1) carried out parallel to the landslide body along the landslide foot. Dashed white lines outline possible sliding surfaces. Elev.: elevation above sea level.

According to the stratigraphical information inferred by the boreholes (S3 and S4) and the outcropping terrains in the area (Albidona Formation), the resistivity distribution characterising the first 20–25 m of the subsoil could be due to the presence of silty sands, clayey silts, and marls layers incorporating blocks of sandstones. The thicker and deeper conductive layer could be associated with the marly-silty clays and the deep resistive sector could be associated with a bank of cemented sandstones. The dashed white lines, drawn in the ERT, outline possible sliding surfaces related to different reactivations of the landslide body.

ERT 2 was carried out parallel to the landslide body along the middle part (Figure 11). The resistivity model shows an almost piano-parallel electrostratification. According to the geological map (Figure 4), the succession of resistive and conductive layers could be associated with sandstone/conglomerate and clay material, respectively (Gorgoglione Formation). Supposed sliding surfaces (dashed white lines), up to 15 m in depth and related to different reactivations of the landslide body, are delineated on the electrical image.

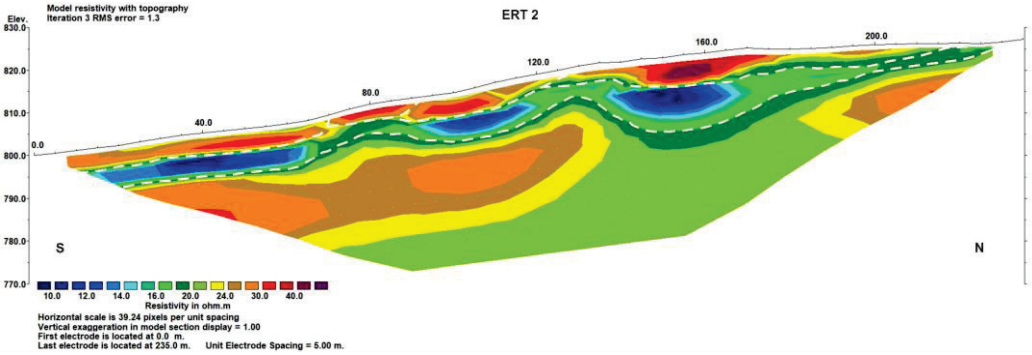



**Figure 11.** Electrical resistivity tomography (ERT 2) carried out parallel to the landslide body along the middle part. Dashed white lines outline possible sliding surfaces. Elev.: elevation above sea level.

### *3.3. The 1907 Landslide Analysed by Historical Data*

#### 3.3.1. The Contribution of Archive Sources

The municipal area of Montemurro is prone to landslides, as also testified by previous studies. For example, Almagià (1910) [64] reported some mass movements starting from the first half of the 19th century. Such phenomena were also triggered by seismic activity, such as the earthquake of Lagonegro of 20 November 1836 (Mw 5.9, [65]), and particularly the disastrous 16 December 1857 Basilicata earthquake (Mw 7.1, [65]) which caused a giant landslide in Montemurro. In the decades following the 1857 earthquake, particularly in the last two decades of the nineteenth century and the early twentieth century, Almagià also refers to further landslides in the southern portion of the town and in many areas around it.

In the following years, and in particular in 1907, a wide landslide was activated at north-east of the historical centre, in the Servigliano area. To improve the knowledge on this landslide, we performed a wide investigation on unpublished archive sources.

The landslide was triggered in the early hours of 26 February 1907 (Figure 12). The phenomenon occurred after eight days of intense rainfall, during which a quantity of water fell equivalent to one third of the rain that fell in the entirety of rainiest year of the previous 22 years. In this period, other landslides were triggered in the municipalities within a radius between 8 and 45 km, such as in San Martino d'Agri (March 1907), 8 km south of Montemurro; Aliano (spring 1907), 20 km east; Senise (1906–winter 1907), 25 km south-east; Tursi (15 February 1907), 40 km east; Teana (between 10 and 15 February 1907), 45 km south [64,66] [4].

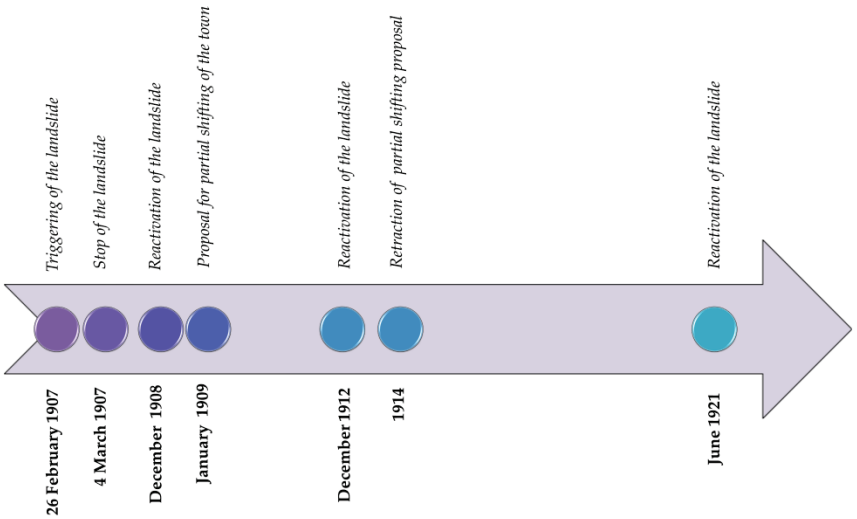



**Figure 12.** Timeline of the main events of the Servigliano landslide as inferred from the scrutiny of archive sources.

The area hit by the Servigliano landslide was not known, at least until 1907, as susceptible to sliding down. In fact, in the aftermath of the devastating 1857 Basilicata earthquake, which razed the entire town to the ground, the Servigliano area was even hypothesised as a place suitable to transfer and rebuild the town. Moreover, technical documents related to the consolidation plan of the landslides in Montemurro dating back to the end of the 20th century (1899) do not include the Servigliano area. These findings are also in line with the analysis of the historical topographic map of the area (scale 1:50,000) whose survey was carried out by the *Istituto Topografico Militare* (Military Topographical Institute) in a period between the sixties and seventies of the nineteenth century [5] (ITM, 1862–1876). Indeed, the contour lines of this map do not supply evidence of morphology related to the landslide.

The ground movement had a height of about 40 m in the detachment area. The landslide destroyed, in the following hours and days, the entire *Rione Carmine* (Carmine quarter) consisting of about thirty houses, the church, and the Servigliano Chapel, as well as many other houses in the *Rione Concerie* (Concerie Quarter), at the edge of the north-eastern part of the town. The movement also caused extensive damage to local road infrastructures and sewage collectors and very serious damage to the olive groves and vineyards, which were destroyed (Figure 13). Fortunately, the landslide did not cause deaths since the inhabitants were able to evacuate their homes.

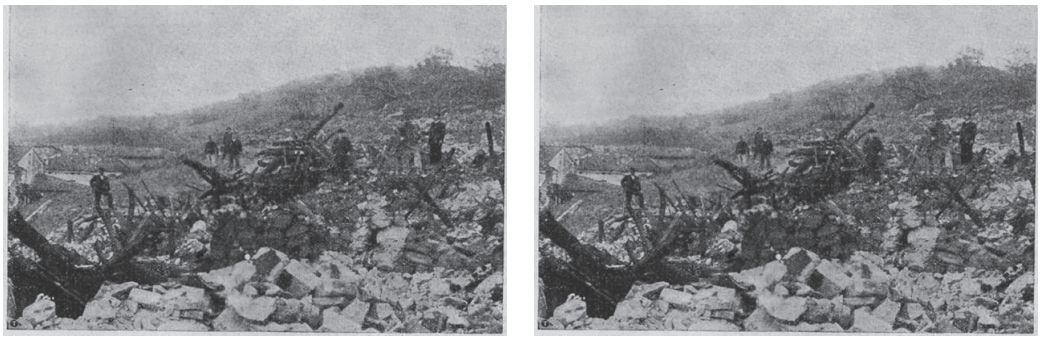


**Figure 13.** The landslide body (**left**, **right**) and the damage caused to a retaining wall (**right**) (Source: [67], private archive of Gizzi F.T.).

On the third day, the landslide body was overestimated to have a length of about 2 km and a width of comparable dimensions. Four days after the first movement, the landslide continued to move, damaging some houses located on the rocky spur that still today characterises the entrance to the town from the *Rione Concerie*.

The movement of the front of the landslide stopped on 4 March, about a week after its triggering, when the works of clearing the rubble, completed in September 1907, and diversion of the waters also began. In fact, multiple depressions were formed inside the landslide body, which led to the formation of ponds (Figures 14 and 15).

To mitigate the residual risk related to houses located close to the landslide front (10 m high) towards the built-up area, further drainage works of the stagnant water were planned between 1907 and 1909, as well as the hydraulic forestry arrangement of the ditches below the inhabited and unstable areas. In fact, about 15 months after the trigger of the earth flow, water stagnation continued to cause movements of the landslide, so much so that the town council requested further reclamation work by CCB.



**Figure 14.** Ponds on the landslide body (Source: [67], private archive of Gizzi F.T.).

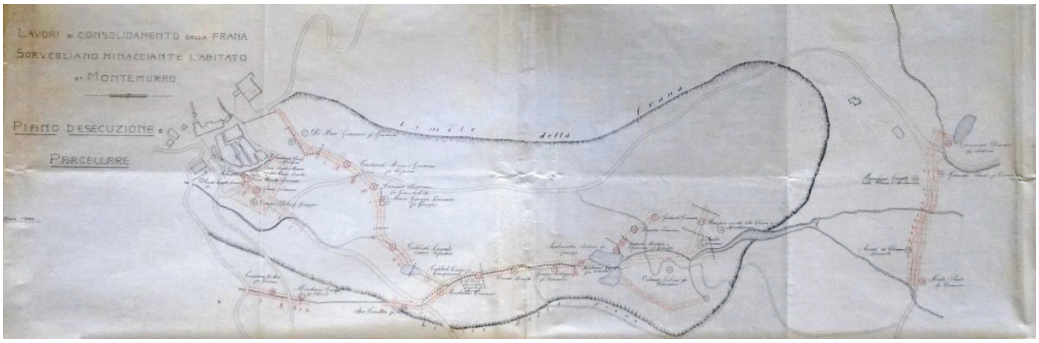



**Figure 15.** Map of the Servigliano landslide, as portrayed in the *Piano d'esecuzione e parcellare* (work plan and cadastral parcel plan for expropriation) in November 1916. The map displays the planimetric extension of the landslide in which both the landslide lakes (in blue) and drainage and consolidation works (in yellow) are reported. [6] The landslide boundary ("limite della frana" on the map) was imposed over the current landslide map of the area (Figure 7). Original drawing to scale 1:2000.

Works planned in 1907–1909 included the removal of the landslide deposit close to the town and the building of a retaining wall at the foot of the unstable body. In June 1911 some works were carried out including clearing of the debris that had partially invaded the town, construction of a retaining wall, and excavation of drainage ditches for the drainage of water from the landslide drainage. Civil engineers did not consider the drainage sufficient, and several homeowners in *Rione Concerie* in December 1912 complained about the movement of the landslide and the presence of stagnant water in the unstable body, especially in summer. However, the construction of the supporting wall at the foot of the landslide body was ineffective because towards the end of December 1908 part of the wall collapsed while the remaining portion was heavily damaged, thus evidencing progression of the earth flow movement.

The late motion of the landslide brought about the proposal to partially move the town, with particular regard to the first row of buildings placed on the landslide front. The proposal was put forward in January 1909 on the basis of Law No. 445 of 1908, which aimed to supply economic provisions to strengthen or transfer the towns affected by landslides. However, the transfer was slow and bureaucratic and the proposal was abandoned definitively in 1914. This occurred because owners had already voluntarily rebuilt the landslide-damaged homes in other areas of the town and the landslide area was involved in extensive consolidation work in the 4 years following the trigger of the mass movements. Furthermore, after 1914, this same area underwent extensive and definitive consolidation works to strongly mitigate the risk. The project was authorised by the Ministry of Public Works in January 1912 and included the expropriations for public interests aimed at executing the consolidation works, including the drainage of rain and spring water from the landslide area by masonry gutters. However, the landslide was still moving in December 1912.

In January 1915 and December 1916, due to the persistent rains, landslides were also triggered in other urban areas. This activity required the attention of the authorities for the safety of the inhabitants and the execution of consolidation works.

In November 1916, consolidation work on the Servigliano landslide was yet to be carried out. From the analysis of the direct survey of the area, as reported in the project of the consolidation works drawn up by the Royal Corps of Civil Engineers dating back to 15 November 1916, the extension of the landslide was evaluated in a maximum length of ~1.1 km, with a maximum width of ~400 m and a minimum width of ~300 m (Figure 15). At that date, significant residual areas of water stagnation still persisted, as the map at Figure 15 shows.

The landslide was reactivated at the beginning of June 1921 when the first houses facing the landslide front began to be obstructed again by the chaotic mass, which was likely also caused by the lack of arrangement of the surface waters in the body of the landslide.

The landslide consolidation works, however, had likely not been carried out by this date; the Mayor of Montemurro in a telegram to the Ministry of the Interior controversially emphasised that "[ . . . ] Invano la Giunta Comunale ed il Consiglio hanno fatto voto per la sistemazione di detta frana [ . . . ]. Quando i danni saranno irreparabili allora arriverà l'opera riparatrice che potrà essere anche di pannolini caldi [ . . . ]" (It was in vain that the town councils voted for the consolidation of the landslide [ . . . ]. When the damage is irreparable, then the remedial work will arrive, which may also include hot napkins [ . . . ]) [7].

The civil engineers of Potenza in the general consolidation interventions of the town of Montemurro scheduled in the 1960s still indicated numerous works as necessary, including drainage, waterproofing of the streets of the town, and the construction of retaining walls. The area involved in the works also included the north-east portion of the town facing the landslide.

#### 3.3.2. Historical Climatic Data Analysis and Interpretation

The monthly total rainfall from 1885 to 1914 was analysed and the results are shown in Figure 16. For each year, the monthly rainfall was added together to realise the total annual rainfall. Then, the average annual rainfall from 1885 to 1914 was calculated. It corresponded to 780.2 mm·year$^{-1}$. The SDII index shows a high variability from one year to another, with three main peaks in September 1905, February 1907, and August 1908. In February 1885, a landslide event worth mentioning in the chronicles of the time occurred [68]. The monthly rainfall in February 1907 was 369.5 mm, a large amount corresponding to more than half of the average annual precipitation. In the same month, 15 rainfall events were recorded, which means that February 1907 was almost always rainy and was also characterised by a very high SDII index (24.63 mm·day$^{-1}$). This data supports the idea that an extreme rain event may have triggered the landslide. Further, the SPI analyses add new concerns about the previous wetness conditions. In this study, we applied SPI on short-term scales (3 months), as this time span can better describe the wetness conditions, i.e., preceding rainfall or extreme rainy events, which trigger the landslide. The graphical analysis in Figure 16 clearly shows that the investigated landslide is a rainfall-induced landslide. It emerges that the landslide was not triggered by an isolated high magnitude/low frequency rainfall event.

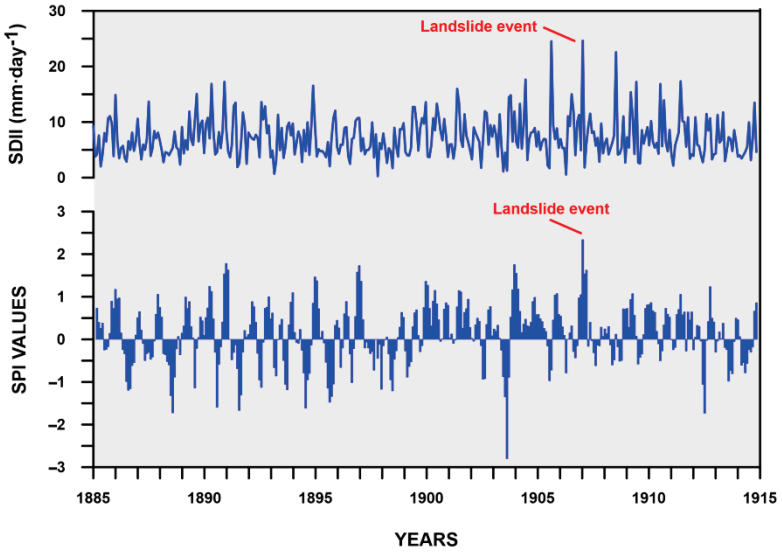



**Figure 16.** Monthly simple daily intensity index (SDII) vs monthly standardized precipitation index values over 3 months (SPI 3) from 1885 to 1915. The investigated landslide took place at the maximum peak of both the indexes.

The SPI peak in February 1907 was anticipated by several previous high SPI values, which suggests that previous wetness conditions contributed to the landslide triggering

by saturating the soil. This condition is completely missing in the cases of September 1905 and August 1908, which did not cause landslides. Therefore, the data strongly support the hypothesis that the landslide event was anticipated by strong soil saturation due to abundant rains that fell over several days until the extreme event of 26 February 1907. This interpretation is consistent with the results of previous studies carried out on landslides throughout the region [69,70].

## 4. Conclusions, Limitations, and Perspectives

The investigation of the 1907 Servigliano landslide entailed a multisource of information that was analysed using a multidisciplinary and interdisciplinary approach.

New field surveys allowed us to identify the geological and geomorphological features of the area as well as the features of the landslide body. The landslide is an earth flow, NE–SW oriented, which currently extends for a length of ~1.1 km with an average width of ~220 m. ERT investigations were undertaken to complement the field surveys, thus better defining the structure and geometrical properties of the landslide body such as width, length, and depth of the main shear surface whose maximum depth can be placed approximately around 30 m.

In order to define the timeline of the trigger, the movement of the mass along the slope, the extension of the unstable body, the reactivations over time, and the consolidation works carried out, the field surveys were also accompanied and fed by the analysis of coeval-to-landslide historical documents. Furthermore, historical climatological data around the period of the trigger of the mass movement suggested that the 1907 landslide was caused by prolonged heavy rain with consequent soil saturation. Such a statement is consistent with the circumstance that the period saw the reactivation of landslides in some municipalities around Montemurro.

The landslide, the last reactivation to which the historical sources refer, occurred in 1921, is currently in a dormant activity phase. This is testified by both the geomorphological indicators and visual inspection of buildings and infrastructures, especially those with linear development, which do not show evidence of landslide-related damage.

However, the research has some limitations. To improve the landslide model, further boreholes should be drilled in the high-medium portion of the landslide body. Furthermore, to define the state of activity, additional investigations are required, such as the spaceborne interferometric synthetic aperture radar (*InSAR*) technique. These aspects will be considered in future research. At the present state of knowledge, the research suggests that consolidation and drainage works carried out over the decades in the landslide area seem effective. Therefore, the need for their constant maintenance is emphasised here.

From a methodological point of view, the results confirm that the integration of different sources of information as well as multiple competencies, such as geological, geomorphological, historical documentary, historical climatological, and geophysical, can greatly improve the understanding of the hazard phenomenon. In particular, historical studies based on primary documentation complement the geomorphological surveys and the geophysical investigations oriented to build the landslide model. From this perspective, we stress the importance for those responsible for land management to arrange and update natural hazard digital repositories made up of documents selected from the range of sources currently preserved in hundreds of archives, both public and private. The stipulation of specific partnership agreements between state and local archives and institutions in charge of territorial planning and mitigation of natural risks could be a useful tool. In order to encourage these partnerships, the Italian Ministry of Culture could set up a national campaign to alert administrators, stakeholders, and policymakers to the potential of historical sources in investigating natural hazards.

The use of archival data for natural hazard investigation could also be facilitated through specific citizen science projects, especially those involving younger generations and students with the support of researchers and specialists. Indeed, archives are rich in historical documentation, but the sources are usable only once they are digitised, which

allows people and institutions to effortlessly search for the information they need. Moreover, citizen science projects would have the further aim of increasing individuals' natural hazard risk perception, which is low in Italy.

**Author Contributions:** Conceptualization, M.B. and F.T.G.; methodology, M.B. and F.T.G.; software, S.P., A.P., J.B. and G.C.; validation, M.B. and F.T.G.; data curation: all the authors; writing—original draft preparation, all authors; writing—review and editing, M.B. and F.T.G.; supervision, M.B. and F.T.G. All authors have read and agreed to the published version of the manuscript.

**Funding:** This research received no external funding.

**Acknowledgments:** The authors are grateful to the municipal administration of Montemurro and in particular to the mayor for their logistical support during the geophysical survey. The authors wish to thank three anonymous reviewers for their careful reading of the manuscript and their insightful comments and suggestions.

**Conflicts of Interest:** The authors declare no conflict of interest.

## Notes

[1] ASDPC (Archivio Storico del Dipartimento della Protezione Civile, Roma). Currently, the historical archive is no longer available to the Civil Protection Department, but it is deposited in the State Archive of Rome.
ASPZ (Archivio di Stato di Potenza).
ACM (Archivio Comunale di Montemurro).
[1a] ASPZ. Commissariato Civile di Basilicata—Opere pubbliche Comune di Montemurro Anno 1909 (Classe 3a Categ. L Fasc. 1). Disegni—Allegato n° 2 (Pianta della parte bassa dell'abitato di Montemurro Scala 1:2000) al Progetto di Consolidamento redatto dal Corpo Reale del Genio Civile di Potenza. Potenza, 19/04/1899.
[2a] ASPZ. Commissariato Civile di Basilicata—Opere pubbliche Comune di Montemurro Anno 1909 (Classe 3a Categ. L Fasc. 1). Telegramma del prosindaco Angelo Pardi al Commissariato Civile per la Basilicata riguardante la frana di Montemurro. Montemurro, 26/02/1907.
[3a] ASPZ. Commissariato Civile di Basilicata—Opere pubbliche Comune di Montemurro Anno 1909 (Classe 3a Categ. L Fasc. 1). Telegramma del prosindaco Pardi al Commissariato Civile per la Basilicata riguardante la frana di Montemurro. Montemurro, 27/02/1907.
[4a] ASPZ. Commissariato Civile di Basilicata—Opere pubbliche Comune di Montemurro Anno 1909 (Classe 3a Categ. L Fasc. 1). Telegramma del Sindaco Santalucia inviato al Commissario Civile riguardante la frana di Montemurro. Montemurro, 27/02/1907.
[5a] ASPZ. Commissariato Civile di Basilicata—Opere pubbliche Comune di Montemurro Anno 1909 (Classe 3a Categ. L Fasc. 1). Telegramma del Ministro Gianturco inviato al Commissario Civile per la Basilicata riguardante la frana di Montemurro. Roma, 27/02/1907.
[6a] ASPZ. Commissariato Civile di Basilicata—Opere pubbliche Comune di Montemurro Anno 1909 (Classe 3a Categ. L Fasc. 1). Telegramma a firma Ing. Alfinito inviato al Commissario Civile riguardante la frana di Montemurro e danni. Montemurro, 02/03/1907.
[7a] ASPZ. Commissariato Civile di Basilicata—Opere pubbliche Comune di Montemurro Anno 1909 (Classe 3a Categ. L Fasc. 1). Telegramma a firma Ing. Alfinito inviato al Commissario Civile riguardante la frana Montemurro. Montemurro, 02/03/1907.
[8a] ASPZ. Commissariato Civile di Basilicata—Opere pubbliche Comune di Montemurro Anno 1909 (Classe 3a Categ. L Fasc. 1). Telegramma a firma Ing. Alfinito inviato al Commissario Civile riguardante la frana Montemurro. Montemurro, 05/03/1907.
[9a] ASPZ. Commissariato Civile di Basilicata—Opere pubbliche Comune di Montemurro Anno 1909 (Classe 3a Categ. L Fasc. 1). Lettera del Commissariato Civile di Basilicata al Ministero dei LL.PP. di Roma—Gabinetto riguardate Montemurro. Difesa dell'abitato contro le frane. Potenza, 14/03/1907.
[10a] ASPZ. Commissariato Civile di Basilicata—Opere pubbliche Comune di Montemurro Anno 1908 (Classe 3a Categ. F Fasc. 1). Verbale del Consiglio del Commissariato Civile per la Basilicata riguardante l'approvazione della perizia riguardante i lavori di consolidamento dei Burroni Libritti e Sant'Antuono. S.l., 26/03/1907.
[11a] ASPZ. Commissariato Civile di Basilicata—Opere pubbliche Comune di Montemurro Anno 1909 (Classe 3a Categ. L Fasc. 1). Verbale del Consiglio del Commissariato Civile per la Basilicata (delibera n° 443—Prot. 2842) riguardante il Progetto esecutivo dei lavori di consolidamento delle frane minaccianti l'abitato di Montemurro. S.l., 26/03/1907.
[12a] ASPZ. Commissariato Civile di Basilicata—Opere pubbliche Comune di Montemurro Anno 1909 (Classe 3a Categ. L Fasc. 1). Verbale del Consiglio del Commissariato Civile per la Basilicata (delibera n° 445—Prot. 2848) riguardante Perizia sommaria delle opere di somma urgenza per lo sgombero parziale e sistemazione della frana Sorvegliano presso l'abitato di Montemurro. S.l., 26/03/1907.
[13a] ASPZ. Commissariato Civile di Basilicata—Opere pubbliche Comune di Montemurro Anno 1908 (Classe 3a Categ. F Fasc. 1). Lettera del Ministero dei LL.PP. di Roma al Commissario Civile per le opere pubbliche in Basilicata riguardante Sistemazione dei fossi sottostanti l'abitato di Montemurro. Roma, 24/04/1907.

[14a] ASPZ. Commissariato Civile di Basilicata—Opere pubbliche Comune di Montemurro Anno 1909 (Classe 3a Categ. L Fasc. 1). Lettera del Commissariato Civile di Basilicata al Ministero dei LL.PP. di Roma—Servizio Basilicata e Calabria riguardante Montemurro. Consolidamento della frana di Sorvegliano. Potenza, 30/07/1907.
[15a] ASPZ. Commissariato Civile di Basilicata—Opere pubbliche Comune di Montemurro Anno 1909 (Classe 3a Categ. L Fasc. 1). Telegramma del Commissariato Civile di Basilicata al Ministero dei LL.PP. di Roma riguardante Frana Sorvegliano. Potenza, 14/09/1907.
[16a] ASPZ. Commissariato Civile di Basilicata—Opere pubbliche Comune di Montemurro Anno 1909 (Classe 3a Categ. L Fasc. 1). Verbale del Consiglio del Commissariato Civile per la Basilicata—Perizia sommaria per variazioni di opere nello sgombero della frana di Sorvegliano presso l'abitato di Montemurro. A.l., 30/09/1907.
[17a] ASPZ. Commissariato Civile di Basilicata—Opere pubbliche Comune di Montemurro Anno 1909 (Classe 3a Categ. L Fasc. 1). Verbale di consegna dei lavori da parte dell'Impresa Francesco Gervasi. Montemurro, 21/11/1907.
[18a] ASPZ. Commissariato Civile di Basilicata—Opere pubbliche Comune di Montemurro Anno 1909 (Classe 3a Categ. L Fasc. 1). Verbale del Consiglio Comunale di Montemurro in seduta straordinaria con Ordine del giorno: bonifica della frana Sorvegliano. Montemurro, 17/05/1908.
[19a] ASPZ. Commissariato Civile di Basilicata—Opere pubbliche Comune di Montemurro Anno 1909 (Classe 3a Categ. L Fasc. 1). Verbale di sospensione lavori di consolidamento delle frane minaccianti l'abitato di Montemurro. Potenza, 02/12/1908.
[20a] ASPZ. Commissariato Civile di Basilicata—Opere pubbliche Comune di Montemurro Anno 1908 (Classe 3a Categ. F Fasc. 1). Certificato di fine lavori redatto dall'Ingegnere Capo del Corpo Reale del Genio Civile di Potenza al Cottimista Gervasi Francesco. Potenza, 26/12/1908.
[21a] ASPZ. Commissariato Civile di Basilicata—Opere pubbliche Comune di Montemurro Anno 1909 (Classe 3a Categ. L Fasc. 1). Telegramma del sindaco Lauria al Prefetto riguardante Caduta muraglione nel Rione Conceria. Montemurro, 27/12/1908.
[22a] ASPZ. Commissariato Civile di Basilicata—Opere pubbliche Comune di Montemurro Anno 1908 (Classe 3a Categ. F Fasc. 1). Lettera dell'Ingegnere Capo del Corpo Reale del Genio Civile al Prefetto Commissario Civile di Potenza riguardante Proposta di trasferimento di parte dell'abitato di Montemurro. Potenza, 19/01/1909.
[23a] ASPZ. Commissariato Civile di Basilicata—Opere pubbliche Comune di Montemurro Anno 1908 (Classe 3a Categ. F Fasc. 1). Lettera dell'Ingegnere Capo del Corpo Reale del Genio Civile al Prefetto Commissario Civile di Potenza riguardante Lavori di sistemazione dei fossi sottostanti all'abitato di Montemurro: Contratto di cottimo 23/06/1908. Cottimista Gervasi Francesco fu Domenico. Potenza, 20/02/1909.
[24a] ASPZ. Commissariato Civile di Basilicata—Opere pubbliche Comune di Montemurro Anno 1909 (Classe 3a Categ. L Fasc. 1). Verbale dei preliminari accordi sui provvedimenti da adottarsi per il consolidamento della frana di Sirvigliano. Territorio comunale di Montemurro, 05/05/1909.
[25a] ASPZ. Commissariato Civile di Basilicata—Opere pubbliche Comune di Montemurro Anno 1909 (Classe 3a Categ. L Fasc. 1). Lettera dell'Ingegnere Capo del Corpo Reale del Genio Civile al Prefetto Commissario Civile per la Basilicata riguardante Lavori consolidamento e risanamento abitato di Montemurro. Potenza, 23/06/1909.
[26a] ASPZ. Commissariato Civile di Basilicata—Opere pubbliche Comune di Montemurro Anno 1909 (Classe 3a Categ. L Fasc. 1). Lettera dell'Ingegnere Capo del Corpo Reale del Genio Civile al Prefetto Commissario Civile per la Basilicata riguardante Consolidamento abitato di Montemurro. Potenza, 30/06/1909.
[27a] ASPZ. Commissariato Civile di Basilicata—Opere pubbliche Comune di Montemurro Anno 1909 (Classe 3a Categ. L Fasc. 1). Lettera dell'Ingegnere Capo del Corpo Reale del Genio Civile al Prefetto Commissario Civile per la Basilicata riguardante Consolidamento abitato di Montemurro. Potenza, 29/08/1909.
[28a] ASPZ. Commissariato Civile di Basilicata—Opere pubbliche Comune di Montemurro Anno 1909 (Classe 3a Categ. L Fasc. 1). Telegramma del sindaco Robilotta al Prefetto riguardante Fosso Libritti. Montemurro, 22/03/1910.
[29a] ASPZ. Commissariato Civile di Basilicata—Opere pubbliche Comune di Montemurro Anno 1908 (Classe 3a Categ. F Fasc. 1). Lettera del Ministero dei LL.PP. di Roma al Prefetto Commissario Civile di Potenza riguardante Collaudo dei lavori di sistemazione dei fossi sottostanti all'abitato di Montemurro eseguiti dal cottimista Domenico Padula. Roma, 28/07/1910.
[30a] ASPZ. Commissariato Civile di Basilicata—Opere pubbliche Comune di Montemurro Anno 1908 (Classe 3a Categ. F Fasc. 1). Lettera del Ministero dei LL.PP. di Roma al Prefetto Commissario Civile di Potenza e all'Ingegnere Capo del Corpo Reale del Genio Civile riguardante Lavori di sistemazione dei fossi sottostanti all'abitato di Montemurro eseguiti dal cottimista Domenico Padula. Roma, 02/05/1911.
[31a] ASPZ. Commissariato Civile di Basilicata—Opere pubbliche Comune di Montemurro Anno 1909 (Classe 3a Categ. L Fasc. 1). Lettera dell'Ingegnere Capo del Corpo Reale del Genio Civile al Prefetto Commissario Civile per la Basilicata ed al Ministero LL.PP. riguardante Lavori complementari richiesti dal Comune per l'atto della consegna per lo sgombero della frana Sorvegliano. Potenza, 06/06/1911.
[32a] ASPZ. Commissariato Civile di Basilicata—Opere pubbliche Comune di Montemurro Anno 1909 (Classe 3a Categ. L Fasc. 1). Lettera di alcuni cittadini di Montemurro al Prefetto di Potenza riguardante Rione Conceria. Montemurro, 29/11/1912.
[33a] ASPZ. Commissariato Civile di Basilicata—Opere pubbliche Comune di Montemurro Anno 1909 (Classe 3a Categ. L Fasc. 1). Lettera del Sindaco di Montemurro al Prefetto di Potenza riguardante Lavori di consolidamento nel Rione Orto di Merola. Montemurro, 24/04/1913.
[34a] ASPZ. Commissariato Civile di Basilicata—Opere pubbliche Comune di Montemurro Anno 1915 (Classe 3a Categ. B Fasc. 1).

Lettera dell'Ingegnere Capo reggente del Corpo Reale del Genio Civile al Prefetto Commissario Civile di Potenza riguardante il Progetto dei lavori di consolidamento della frana "Sorvegliano" minacciante l'abitato di Montemurro. Potenza, 30/09/1913.
[35a] ASPZ. Commissariato Civile di Basilicata—Opere pubbliche Comune di Montemurro Anno 1908 (Classe 3a Categ. F Fasc. 1). Lettera dell'Ingegnere Capo del Corpo Reale del Genio Civile al Prefetto Commissario Civile di Potenza riguardante Rioni Carmine e Concerie. Potenza, 12/03/1914.
[36a] ASPZ. Commissariato Civile di Basilicata—Opere pubbliche Comune di Montemurro Anno 1915 (Classe 3a Categ. B Fasc. 1). Lettera dell'Ingegnere Capo del Corpo Reale del Genio Civile al Prefetto Commissario Civile di Potenza riguardante Progetto di consolidamento della frana "Sorvegliano". Potenza 19/06/1914.
[37a] ASPZ. Commissariato Civile di Basilicata—Opere pubbliche Comune di Montemurro Anno 1915 (Classe 3a Categ. B Fasc. 1). Atti del Tribunale di Potenza riguardante la Controversia tra il Sig. Pietro di Mase ed il Comune di Montemurro. Potenza, 13/01/1915.
[38a] ASPZ. Commissariato Civile di Basilicata—Opere pubbliche Comune di Montemurro Anno 1915 (Classe 3a Categ. L Fasc. 1). Telegramma del Sindaco Robilotta al Commissariato civile per le opere pubbliche e per i rimboschimenti nella Basilicata riguardante smottamenti in Montemurro. Montemurro, 27/01/1915.
[39a] ASPZ. Commissariato Civile di Basilicata—Opere pubbliche Comune di Montemurro Anno 1915 (Classe 3a Categ. L Fasc. 1). Telegramma del Sindaco Robilotta al Commissariato civile per le opere pubbliche e per i rimboschimenti nella Basilicata riguardante le zone di Tempa Scaliello, Tempa Madonna Abbondanza, Fosso Libritti, Fosso Civalupo. Montemurro, 29/01/1915.
[40a] ASPZ. Commissariato Civile di Basilicata—Opere pubbliche Comune di Montemurro Anno 1915 (Classe 3a Categ. B Fasc. 1). Lettera dell'Ingegnere Capo del Corpo Reale del Genio Civile al Prefetto Commissario Civile di Potenza riguardante Consolidamento abitato (Rimboschimento dei burroni Civolupo, Verdesca e Libritti). Potenza 30/01/1915.
[41a] ASPZ. Commissariato Civile di Basilicata—Opere pubbliche Comune di Montemurro Anno 1915 (Classe 3a Categ. B Fasc. 1). Telegramma Ministero LL.PP. riguardante Tempa Scaliello. Roma, febbraio 1915.
[42a] ASPZ. Commissariato Civile di Basilicata—Opere pubbliche Comune di Montemurro Anno 1915 (Classe 3a Categ. B Fasc. 1). Lettera dell'Ingegnere Capo del Corpo Reale del Genio Civile al Prefetto Commissario Civile di Potenza riguardante Frane in Montemurro Rione Libritti—Rione San Nicola—Tempa Scaliello). Potenza, 14/02/1915.
[43a] ASPZ. Commissariato Civile di Basilicata—Opere pubbliche Comune di Montemurro Anno 1915 (Classe 3a Categ. B Fasc. 1). Telegramma del Sindaco Robilotta riguardante Tempa Scaliello. Montemurro, 24/02/1915 (ore 18.40).
[44a] ASPZ. Commissariato Civile di Basilicata—Opere pubbliche Comune di Montemurro Anno 1915 (Classe 3a Categ. B Fasc. 1). Telegramma del Sindaco Robilotta riguardante Tempa Scaliello. Montemurro, 24/02/1915 (ore 18.49).
[45a] ASPZ. Commissariato Civile di Basilicata—Opere pubbliche Comune di Montemurro Anno 1915 (Classe 3a Categ. B Fasc. 1). Lettera del Prefetto di Potenza all'Ing. Capo dell'Ufficio Genio Civile di Potenza riguardante richiesta sopralluogo in località Tempa Scalieddo. Potenza, 24/02/1915.
[46a] ASPZ. Commissariato Civile di Basilicata—Opere pubbliche Comune di Montemurro Anno 1915 (Classe 3a Categ. B Fasc. 1). Telegramma del Sindaco Robilotta al Prefetto riguardante Tempa Scaliello. Montemurro, 08/03/1915.
[47a] ASPZ. Commissariato Civile di Basilicata—Opere pubbliche Comune di Montemurro Anno 1909 (Classe 3a Categ. L Fasc. 1). Telegramma a firma Cugno al Commissariato civile per le opere pubbliche e per i rimboschimenti nella Basilicata riguardante i lavori sotto Casa Cugno. Montemurro, 05/11/1915.
[48a] ASPZ. Commissariato Civile di Basilicata—Opere pubbliche Comune di Montemurro Anno 1909 (Classe 3a Categ. L Fasc. 1). Telegramma del Sindaco Robilotta al Commissariato civile per le opere pubbliche e per i rimboschimenti nella Basilicata riguardante i lavori sotto Casa Cugno e Casa Brescia. Montemurro, 11/11/1915.
[49a] ASPZ. Commissariato Civile di Basilicata—Opere pubbliche Comune di Montemurro Anno 1909 (Classe 3a Categ. L Fasc. 1). Telegramma della Signora Isabella Cugno al Prefetto di Potenza. Montemurro, 15/11/1915.
[50a] ASPZ. Commissariato Civile di Basilicata—Opere pubbliche Comune di Montemurro Anno 1909 (Classe 3a Categ. L Fasc. 1). Telegramma del Sindaco Robilotta al Prefetto di Potenza riguardante smottamento sotto Casa Cugno. Montemurro, 16/11/1915.
[51a] ASPZ. Commissariato Civile di Basilicata—Opere pubbliche Comune di Montemurro Anno 1909 (Classe 3a Categ. L Fasc. 1). Telegramma del Sindaco Robilotta al Commissariato civile per le opere pubbliche e per i rimboschimenti nella Basili-cata riguardante continui smottamenti nelle zone Coste Libritti, Civalupo e Verdesca. Montemurro, 09/01/1916.
[52a] ASPZ. Commissariato Civile di Basilicata—Opere pubbliche Comune di Montemurro Anno 1915 (Classe 3a Categ. B Fasc. 1). Cartografia redatta dall'Ing. di 1A classe del Corpo Reale del Genio Civile di Potenza—Ufficio Speciale per le Opere Idrauliche e di bonifica riguardante Lavori di consolidamento della frana Sorvegliano minacciante l'abitato di Montemurro—Piano di esecuzione e parcellare. Potenza, 15/11/1916.
[53a] ASPZ. Commissariato Civile di Basilicata—Opere pubbliche Comune di Montemurro Anno 1908 (Classe 3a Categ. F Fasc. 1). Telegramma del Sindaco Robilotta di Montemurro al Commissariato civile per le opere pubbliche e per i rimboschimenti nella Basilicata riguardante franamenti in località Tempa Scaliendo. Montemurro, 12/12/1916.
[54a] ASPZ. Commissariato Civile di Basilicata—Opere pubbliche Comune di Montemurro Anno 1908 (Classe 3a Categ. F Fasc. 1). Telegramma del Sindaco Robilotta di Montemurro al Commissariato civile per le opere pubbliche e per i rimboschimenti nella Basilicata riguardante la Zona Civalupo. Montemurro, 16/02/1917.
[55a] ASPZ. Commissariato Civile di Basilicata—Opere pubbliche Comune di Montemurro Anno 1908 (Classe 3a Categ. F Fasc. 1). Telegramma del Sindaco Robilotta di Montemurro al Commissariato civile per le opere pubbliche e per i rimboschimenti nella

Basilicata riguardante la Zona Civalupo. Montemurro, 26/02/1917.
[56a] ASPZ. Commissariato Civile di Basilicata—Opere pubbliche Comune di Montemurro Anno 1915 (Classe 3a Categ. B Fasc. 1). Telegramma del Sindaco Robilotta di Montemurro al Commissariato civile per le opere pubbliche e per i rimboschimenti nella Basilicata riguardante la Frana Sorvigliano. Montemurro, 03/06/1921.
[57a] ASPZ. Commissariato Civile di Basilicata—Opere pubbliche Comune di Montemurro Anno 1915 (Classe 3a Categ. B Fasc. 1). Telegramma del Sindaco Robilotta di Montemurro al Commissariato civile per le opere pubbliche e per i rimboschimenti nella Basilicata riguardante la frana di Rione Concerie. Montemurro, 25/06/1921.
[58a] ASPZ. Commissariato Civile di Basilicata—Opere pubbliche Comune di Montemurro Anno 1915 (Classe 3a Categ. B Fasc. 1). Cartografia redatta dall'Ing. di 1A classe del Corpo Reale del Genio Civile di Potenza—Ufficio Speciale per le Opere Idrauliche e di bonifica riguardante Lavori di consolidamento della frana Sorvegliano minacciante l'abitato di Montemurro—Piano di esecuzione e parcellare. Potenza, 15/11/1916.

2 [59a] ASDPC. Ministero dei Lavori Pubblici—Direzione Generale Servizi Speciali. Lettera del Prefetto Commissario Civile di Basilicata al Ministro dei LL.PP. Direzione Generale dei Servizi Speciali di Roma riguardante Proposta di trasferimento della prima fila di case del Rione orientale Concerie, poste in vicinanza della frana di Sorvegliano del 1907. Potenza, 25/02/1909.
[60a] ASDPC. Ministero dei Lavori Pubblici—Direzione Generale Servizi Speciali Lettera del Corpo Reale Genio Civile—Ufficio Superiore di Ispezione al Ministero dei LL.PP.—Direzione Generale dei Servizi Speciali di Roma riguardante Spostamento parziale abitato di Montemurro. Bari, 20/09/1911.
[61a] ASDPC. Ministero dei Lavori Pubblici—Direzione Generale Servizi Speciali. Lettera del Corpo Reale Genio Civile—Ufficio Superiore di Ispezione al Ministero dei LL.PP.—Direzione Generale dei Servizi Speciali di Roma riguardante Lavori di consolidamento abitato di Montemurro. Bari, 27/11/1911.

3 [62a] ACM. Indagini geognostiche nell'abitato di Montemurro. Relazione geologico-tecnica (e annessi sondaggi geognostici) di Lentini, F.; Schilirò, F. per conto della Regione Basilicata. Catania. 1982.

4 [63a] ASDPC. Ministero dei Lavori Pubblici—Direzione Generale Servizi Speciali. Consiglio del Commissariato Civile della Basilicata. Progetto consolidamento frane minaccianti abitato Senise. 30 November 1908.

5 [64a] ASPZ. Carte geografiche e topografiche. ITM, Foglio n° 85, Montemurro (Parte Occidentale).

6 [58a] See above for complete reference.

7 [56a] See above for complete reference.

## References


1. Herrera, G.; Mateos, R.M.; García-Davalillo, J.C.; Grandjean, G.; Poyiadji, E.; Maftei, R.; Filipciuc, T.C.; Jemec Auflič, M.; Jež, J.; Podolszki, L.; et al. Landslide databases in the Geological Surveys of Europe. *Landslides* **2018**, *15*, 359–379. [CrossRef]
2. Trigila, A.; Iadanza, C.; Bussettini, M.; Lastoria, B. *Dissesto Idrogeologico in Italia: Pericolosità e Indicatori di Rischio*; ISPRA: Rome, Italy, 2018. (In Italian)
3. CNR-IRPI. *Rapporto Periodico sul Rischio Posto alla Popolazione Italiana da Frane e Inondazioni*; CNR-IRPI: Turin, Italy, 2017; (In Italian). Available online: https://it.readkong.com/page/anno-2018-polaris-cnr-3726344 (accessed on 18 November 2021).
4. Cascini, L.; Cuomo, S.; Guida, D. Typical source areas of May 1998 flow-like mass movements in the Campania region, Southern Italy. *Eng. Geol.* **2008**, *96*, 107–125. [CrossRef]
5. Eeckhaut, M.V.D.; Poesen, J.; Verstraeten, G.; Vanacker, V.; Nyssen, J.; Moeyersons, J.; Beek, L.P.H.v.; Vandekerckhove, L. Use of LIDAR-derived images for mapping old landslides under forest. *Earth Surf. Processes Landf.* **2007**, *32*, 754–769. [CrossRef]
6. Lasaponara, R.; Coluzzi, R.; Gizzi, F.T.; Masini, N. On the LiDAR contribution for the archaeological and geomorphological study of a deserted medieval village in Southern Italy. *J. Geophys. Eng.* **2010**, *7*, 155–163. [CrossRef]
7. Malehmir, A.; Bastani, M.; Krawczyk, C.M.; Gurk, M.; Ismail, N.; Polom, U.; Perss, L. Geophysical assessment and geotechnical investigation of quick-clay—A Swedish case study. *Near Surf. Geophys.* **2013**, *11*, 341–352. [CrossRef]
8. Mantovani, M.; Devoto, S.; Forte, E.; Mocnik, A.; Pasuto, A.; Piacentini, D.; Soldati, M. A multidisciplinary approach for rock spreading and block sliding investigation in the north-western coast of Malta. *Landslides* **2013**, *10*, 611–622. [CrossRef]
9. Bentivenga, M.; Giocoli, A.; Palladino, G.; Perrone, A.; Piscitelli, S. Geological and geophysical characterization of the Brindisi di Montagna Scalo landslide (Basilicata, Southern Italy). *Geomat. Nat. Hazards Risk* **2019**, *10*, 1367–1388. [CrossRef]
10. Yermolaev, O.; Usmanov, B.; Gafurov, A.; Poesen, J.; Vedeneeva, E.; Lisetskii, F.; Nicu, I.C. Assessment of Shoreline Transformation Rates and Landslide Monitoring on the Bank of Kuibyshev Reservoir (Russia) Using Multi-Source Data. *Remote Sens.* **2021**, *13*, 4214. [CrossRef]
11. Tropeano, D.; Turconi, L. Using historical documents in landslide, debris flow and stream flood prevention. Applications in Northern Italy. *Nat. Hazards* **2004**, *31*, 663–679. [CrossRef]
12. Carrara, A.; Crosta, G.; Frattini, P. Geomorphological and historical data in assessing landslide hazard. *Earth Surf. Processes Landf.* **2003**, *28*, 1125–1142. [CrossRef]
13. Gizzi, F.T.; Proto, M.; Potenza, M.R. The Basilicata region (Southern Italy): A natural and 'human-built' open-air laboratory for manifold studies. Research trends over the last 24 years (1994–2017). *Geomat. Nat. Hazards Risk* **2019**, *10*, 433–464. [CrossRef]
14. Gizzi, F.T.; Bentivenga, M.; Lasaponara, R.; Danese, M.; Potenza, M.R.; Sileo, M.; Masini, N. Natural Hazards, Human Factors, and "Ghost Towns": A Multi-Level Approach. *Geoheritage* **2019**, *11*, 1533–1565. [CrossRef]

15. Angela, P.; Canora, F.; Giuseppe, C.; Jessica, B.; Vincenzo, S.; Panebianco, S.; Nicola, T.; Sabatino, P.; Luigi, V.; Angelo, D.; et al. A multidisciplinary approach for landslide residual risk assessment: The Pomarico landslide (Basilicata Region, Southern Italy) case study. *Landslides* **2021**, *18*, 353–365. [CrossRef]
16. Gizzi, F.T. Identifying geological and geotechnical influences that threaten historical sites: A method to evaluate the usefulness of data already available. *J. Cult. Herit.* **2008**, *9*, 302–310. [CrossRef]
17. Gizzi, F.T.; Potenza, M.R.; Zotta, C. 23 November 1980 Irpinia–Basilicata earthquake (Southern Italy): Towards a full knowledge of the seismic effects. *Bull. Earthq. Eng.* **2012**, *10*, 1109–1131. [CrossRef]
18. Gueguen, E.; Doglioni, C. Lithospheric boudinage in the western Mediterranean back-arc basin. *Terra Nova* **1997**, *9*, 184–187. [CrossRef]
19. Parotto, M.; Praturlon, A. The Southern Apennine Arc. In *Geology of Italy. Special Volume of the Italian Geological Society of the IGC 32 Florence*; Crescenti, U., D'Offizi, S., Merlino, S., Sacchi, L., Eds.; Società Geologica Italiana: Roma, Italy, 2004; pp. 33–58.
20. Bucci, F.; Novellino, R.; Guglielmi, P.; Prosser, G.; Tavarnelli, E.; Guzzetti, F.; Cardinali, M.; Gueguen, E.; Guglielmi, P.; Adurno, I. Frontal collapse during thrust propagation in mountain belts: A case study in the Lucania Apennines, Southern Italy. *J. Geol. Soc.* **2014**, *171*, 571–581. [CrossRef]
21. Bucci, F.; Tavarnelli, E.; Novellino, R.; Palladino, G.; Guglielmi, P.; Laurita, S.; Prosser, G.; Bentivenga, M. The History of the Southern Apennines of Italy Preserved in the Geosites Along a Geological Itinerary in the High Agri Valley. *Geoheritage* **2019**, *11*, 1489–1508. [CrossRef]
22. Bentivenga, M.; Coltorti, M.; Prosser, G.; Tavarnelli, E. A new Interpretation of Terraces in the Taranto Gulf: The Role of Extensional Faulting. *Geomorphology* **2004**, *60*, 383–402. [CrossRef]
23. Bentivenga, M.; Coltorti, M.; Prosser, G.; Tavarnelli, E. Recent extensional faulting in the Gulf of Taranto area: Implications for nuclear waste storage in the vicinity of Scanzano Ionico (Basilicata). *Boll. Soc. Geol. Ital.* **2004**, *123*, 391–404. (In Italian)
24. Bentivenga, M.; Foresi, L.M.; Prestera, A.; Prosser, G.; Sabia, M. Structures located at the front of a thrust and fold belt: The Craco area (Southern Apennines, Italy). *Boll. Soc. Geol. Ital.* **2005**, *124*, 367–376.
25. Giano, S.I. Geomorphology of the Agri intermontane basin (Val d'Agri-Lagonegrese National Park, Southern Italy). *J. Maps* **2016**, *12*, 639–648. [CrossRef]
26. Cello, G.; Gambini, R.; Mattioni, L.; Mazzoli, S.; Read, A.; Tondi, E.; Zucconi, V. Geological analysis of the High Agri Valley (Lucanian Apennines, Southern Italy). *Mem. Soc. Geol. Ital.* **2000**, *55*, 149–155.
27. Cello, G.; Gambini, R.; Mazzoli, S.; Read, A.; Tondi, E.; Zucconi, V. Fault zone characteristics and scaling properties of the Val d'Agri Fault System (Southern Apennines, Italy). *J. Geodyn.* **2000**, *29*, 293–307. [CrossRef]
28. Giano, S.I.; Lapenna, V.; Piscitelli, S.; Schiattarella, M. New geological and geophysical data on the structural pattern of the quaternary slope deposits in the Agri high valley, southern Apennines. *Alp. Mediterr. Quat.* **1997**, *10*, 589–594.
29. Griffiths, D.H.; Barker, R.D. Two-dimensional resistivity imaging and modelling in areas of complex geology. *J. Appl. Geophys.* **1993**, *29*, 211–226. [CrossRef]
30. Loke, M.H.; Barker, R.D. Rapid least-squares inversion of apparent resistivity pseudosections by a quasi-Newton method. *Geophys. Prospect.* **1996**, *44*, 131–152. [CrossRef]
31. Giano, S.I.; Lapenna, V.; Piscitelli, S.; Schiattarella, M. Electrical imaging and self-potential surveys to study the geological setting of the Quaternary slope deposits in the Agri High Valley (Southern Italy). *Ann. Geophys.* **2000**, *43*, 409–419.
32. Schmutz, M.; Albouy, Y.; Guérin, R.; Maquaire, O.; Vassal, J.; Schott, J.J.; Descloîtres, M. Joint electrical and time domain electromagnetism (TDEM) data inversion applied to the Super Sauze earthflow (France). *Surv. Geophys.* **2000**, *21*, 371–390. [CrossRef]
33. Perrone, A.; Lapenna, V.; Piscitelli, S. Electrical resistivity tomography technique for landslide investigation: A review. *Earth Sci. Rev.* **2014**, *135*, 65–82. [CrossRef]
34. Mauritsch, H.J.; Seiberl, W.; Arndt, R.; Romer, A.; Schneiderbauer, K.; Sendlhofer, G.P. Geophysical investigations of large landslides in the Carnic region of southern Austria. *Eng. Geol.* **2000**, *56*, 373–388. [CrossRef]
35. Lapenna, V.; Lorenzo, P.; Perrone, A.; Piscitelli, S.; Rizzo, E.; Sdao, F. High-resolution geoelectrical tomographies in the study of the Giarrossa landslide (Potenza, Basilicata). *Bull. Eng. Geol. Environ.* **2003**, *62*, 259–268. [CrossRef]
36. Bellanova, J.; Calamita, G.; Giocoli, A.; Luongo, R.; Macchiato, M.; Perrone, A.; Uhlemann, S.; Piscitelli, S. Electrical resistivity imaging for the characterization of the Montaguto landslide (southern Italy). *Eng. Geol.* **2018**, *243*, 272–281. [CrossRef]
37. Sasaki, Y. Resolution of resistivity tomography inferred from numerical simulation. *Geophys. Prospect.* **1992**, *40*, 453–464. [CrossRef]
38. Loke, M.H. *RES2DINVx64 ver. 4.10 with Multi-Core and 64-bit Support for Windows 7/8/10. Rapid 2-D Resistivity & IP Inversion using the Least-Squares Method. Geoelectrical Imaging 2-D & 3-D*; Geotomo Software SDN BHD: Gelugor, Malaysia, 2020.
39. Ibsen, M.-L.; Brunsden, D. The nature, use and problems of historical archives for the temporal occurrence of landslides, with specific reference to the south coast of Britain, Ventnor, Isle of Wight. *Geomorphology* **1996**, *15*, 241–258. [CrossRef]
40. Verrastro, D. L'istituzione del Commissariato civile per la Basilicata. In *Basilicata Regione Notizie*; 2000; Volume 97, pp. 85–92. (In Italian). Available online: https://consiglio.basilicata.it/archivio-news/files/docs/10/48/74/DOCUMENT_FILE_104874.pdf (accessed on 8 December 2021)
41. Civil Protection Departement, Presidency of the Council of Ministers. Historical Archive. Available online: https://www.protezionecivile.gov.it/ (accessed on 10 January 2022).

42. Eredia, F. *Osservazioni Pluviometriche Raccolte a Tutto L'anno 1915*; Tipografia Nazionale Bertero; Ministero dei Lavori Pubblici, Consiglio Superiore delle Acque, Ispettorato del Servizio Idrografico: Roma, Italy, 1919. (In Italian)
43. McKee, T.B.; Doesken, N.J.; Kleist, J. The relationship of drought frequency and duration to time scales. In Proceedings of the Eighth Conference on Applied Climatology, Anaheim, CA, USA, 17–22 January 1993; pp. 179–184.
44. Selli, R. Il Paleogene nel quadro della geologia dell'Italia Meridionale. *Mem. Soc. Geol. Ital.* **1962**, *3*, 733–789.
45. Boenzi, F.; Ciaranfi, N. Stratigrafia di dettaglio del "Flysch di Gorgoglione" (Lucania). *Mem. Soc. Geol. Ital.* **1970**, *9*, 65–79.
46. Ciaranfi, N. Il Flysch di Gorgoglione. *Boll. Sev. Geol. d'Ital.* **1972**, *92*, 101–114. (In Italian)
47. Colella, A. Medium-scale tractive bedforms and structures in Gorgoglione Flysch (Lower Miocene, southern Apennines, Italy). *Boll. Soc. Geol. Ital.* **1979**, *98*, 483–494.
48. Carbone, S.; Lentini, F. Migrazione neogenica del sistema Catena-Avampaese nell'Appennino meridionale: Problematiche paleogeografiche e strutturali. *Riv. Ital. Paleontol. Stratigr.* **1988**, *96*, 271–295. (In Italian)
49. Carbone, S.; Catalano, S.; Lentini, F.; Monaco, C. Le unità stratigrafico-strutturali dell'Alta Val d'Agri (Appennino Lucano) nel quadro della evoluzione del sistema catena–avanfossa. *Mem. Soc. Geol. Ital.* **1988**, *41*, 331–341. (In Italian)
50. Boiano, U. Anatomy of a siliciclastic turbidite basin: The Gorgoglione Flysch, Upper Miocene, southern Italy: Physical stratigraphy, sedimentology and sequence stratigraphy framework. *Sediment. Geol.* **1997**, *107*, 231–262. [CrossRef]
51. Butler, R.W.H.; Tavarnelli, E. The structure and Kinematics of substrate entrainment into high-concentration sandy turbidites: A field example from Gorgoglione "flysch" of southern Italy. *Sedimentology* **2006**, *53*, 655–670. [CrossRef]
52. De Luca, V.; Bentivenga, M.; Cavalcante, F.; Lezzerini, M.; Marano, C.; Palladino, G.; Prosser, G. Geological features, physical and mechanical properties of the Gorgoglione building stone of Basilicata (Southern Italy). *Geoheritage* **2019**, *11*, 1621–1629. [CrossRef]
53. Giano, S.I. Quaternary alluvial fan systems of the Agri intermontane basin (southern Italy): Tectonic and climatic control. *Geol. Carpath.* **2011**, *62*, 65–76. [CrossRef]
54. Di Niro, A.; Giano, S.I.; Santangelo, N. Primi dati sull'evoluzione geomorfologica e sedimentaria del bacino dell'alta Val d'Agri (Basilicata). *Studi Geologici Camerti* **1992**, *1*, 257–263. (In Italian)
55. Di Niro, A.; Giano, S.I. Evoluzione geomorfologica del bordo orientale dell'Alta Val d'Agri (Basilicata). *Studi Geologici Camerti* **1995**, *2*, 207–218. (In Italian)
56. Zembo, I. Stratigraphic architecture and quaternary evolution of the Val d'Agri intermontane basin (Southern Apennines, Italy). *Sediment Geol.* **2010**, *223*, 206–234. [CrossRef]
57. Gueguen, E.; Bentivenga, M.; Colaiacovo, R.; Margiotta, S.; Summa, V.; Adurno, I. The Verdesca landslide in the Agri Valley (Basilicata, Southern Italy): A new geological and geomorphological framework. *NHESS* **2015**, *15*, 2585–2595. [CrossRef]
58. Bentivenga, M.; Palladino, G.; Caputi, A. Development of the Pietra Maura landslide and interactions with the Marsico Nuovo dam (Basilicata, Italy). *Geogr. Fis. Dinam. Quat.* **2012**, *35*, 13–22. [CrossRef]
59. Bentivenga, M.; Capolongo, D.; Palladino, G.; Piccarreta, M. Geomorphological map of the area between Craco and Pisticci (Basilicata, Italy). *J. Maps* **2014**, *11*, 267–277. [CrossRef]
60. Bentivenga, M.; Piccarreta, M. Geomorphological map of Pisticci area (Basilicata, Southern Italy). *J. Maps* **2016**, *12*, 220–226. [CrossRef]
61. Bentivenga, M.; Bellanova, J.; Calamita, G.; Capece, A.; Cavalcante, F.; Gueguen, E.; Guglielmi, P.; Murgante, B.; Palladino, G.; Perrone, A.; et al. Geomorphological and geophysical surveys with In-SAR analysis applied to the Picerno earth flow (southern Apennines, Italy). *Landslides* **2021**, *18*, 471–483. [CrossRef]
62. Varnes, D.J. Slope movements. Types and processes. In *Landslides: Analysis and Control*; Transportation Research Board: Washington, DC, USA, 1978; pp. 11–13.
63. Cruden, D.M.; Varnes, D.J. Landslide types and processes. In *Landslides: Investigation and Mitigation, Transportation Research Board Special Report, 247*; Turner, A.K., Schuster, R.L., Eds.; National Academy Press: Washington, DC, USA, 1996; pp. 36–75.
64. Almagià, R. Studi geografici sopra le frane d'Italia. Volume II, L'Appennino centrale e meridionale—Conclusioni generali. *Mem. Soc. Geogr. Ital.* **1910**, *14*, 1–432. (In Italian)
65. Rovida, A.; Locati, M.; Camassi, R.; Gasperini, P. The Italian earthquake catalogue CPTI15. *Bull. Earthq. Eng.* **2020**, *18*, 2953–2984. [CrossRef]
66. *La Stampa*, 16 February 1907.
67. *La Domenica del Corriere*, 24 March 1907.
68. Cinti, A.; Coppola, L.; Bromhead, E.N. Cultural Heritage and physical environment: A geo-archeological approach to the analysis of interaction and risk factors. In *Geotechnical Engineering for the Preservation of Monuments and Historic Sites*; Bilotta, E., Flora, A., Lirer, S., Viggiani, C., Eds.; Balkema Book; CRC Press: Boca Raton, FL, USA, 2013; pp. 257–264.
69. Piccarreta, M.; Capolongo, D.; Bentivenga, M.; Pennetta, L. Precipitation and dry-wet cycles influence on badland development in a semi-arid area of Basilicata region (Southern Italy). *Geogr. Fis. Dinam. Quat.* **2005**, *7*, 281–289.
70. Lazzari, M.; Piccarreta, M.; Manfreda, S. The role of antecedent soil moisture conditions on rainfall-triggered shallow landslides. *Nat. Hazards Earth Syst. Sci.* **2018**, 1–11. [CrossRef]

land

MDPI

*Article*

# Torrential Hazard Prevention in Alpine Small Basin through Historical, Empirical and Geomorphological Cross Analysis in NW Italy

**Laura Turconi [1,*], Domenico Tropeano [1], Gabriele Savio [1], Barbara Bono [1], Sunil Kumar De [2], Marco Frasca [3] and Fabio Luino [1]**

[1] Istituto di Ricerca per la Protezione Idrogeologica, Consiglio Nazionale delle Ricerche, Strada della Cacce 73, 10135 Torino, Italy; tropeano.domenico@libero.it (D.T.); g_savio@libero.it (G.S.); barbara.bono@irpi.cnr.it (B.B.); fabio.luino@irpi.cnr.it (F.L.)
[2] Department of Geography, North-Eastern Hill University, Shillong 793022, Meghalaya, India; desunil@nehu.ac.in
[3] Independent Researcher, Via Rossetti 7, 10154 Torino, Italy; marcofrasca@hotmail.it
* Correspondence: laura.turconi@irpi.cnr.it

**Abstract:** Debris flow is one of the most dangerous natural processes in mountain regions and it occur in a wide variety of environments throughout the world. In the Italian Alps, some tens of thousands of damaging debris flow and, in general, torrential floods associated to intense sediment transport in secondary catchments have been documented in the last 300 years. These have caused socio-economic damage, damage to anthropogenic structures or infrastructures and in many cases casualties. Often, in the same basins, the occurrence of debris-flow processes recurs many years later. Prediction can often be spatial and based on the magnitude of the largest known process, while the temporal forecast is the most uncertain. It is also possible to increase the resilience of the population and of the territory. The present study aims at investigating different levels of debris-flow hazard in urban areas on Alpine alluvial fans and proposes a strategy for debris-flow prevention based on historical research and on a simplified analytical approach, methods that also involve relatively low costs. For such analysis, Ischiator stream catchment (ca. 20 km$^2$) and its alluvial fan (NW Italy) were selected. This area was partly affected by historical torrential flood associated to intense sediment transport and debris-flow processes. Present-day instability conditions along the slope and the stream network were detected and synthesized through surveys and aerial photo interpretation integrated by satellite images (period 1954–2021). An estimation of the potential amount of moving detritus, referred to as debris flow, was carried out regarding the June 1957 debris-flow event, based on the predictive models. The individual hazard index value was estimated based on different methods. The results indicate that 56% of the area is exposed to flood associated to intense sediment transport hazard, which fluctuates from high to very high levels; such results are supported by debris-flow historical records. Since today almost half of the settlement (Bagni di Vinadio) is located on potentially risk-exposed areas, the urban evolution policy adopted after the 1957 event failed to manage the risk connection to debris-flow activity.

**Keywords:** geomorphological analysis; debris supply prediction; historical data; debris flow and torrential hazard; resilience

**Citation:** Turconi, L.; Tropeano, D.; Savio, G.; Bono, B.; De, S.K.; Frasca, M.; Luino, F. Torrential Hazard Prevention in Alpine Small Basin through Historical, Empirical and Geomorphological Cross Analysis in NW Italy. *Land* **2022**, *11*, 699. https://doi.org/10.3390/land11050699

Academic Editor: Fabrizio Battisti

Received: 12 April 2022
Accepted: 5 May 2022
Published: 7 May 2022

**Publisher's Note:** MDPI stays neutral with regard to jurisdictional claims in published maps and institutional affiliations.

**Copyright:** © 2022 by the authors. Licensee MDPI, Basel, Switzerland. This article is an open access article distributed under the terms and conditions of the Creative Commons Attribution (CC BY) license (https://creativecommons.org/licenses/by/4.0/).

## 1. Introduction

Debris-flow events are particularly dangerous to life and settlements because of their high velocities and the destructive force of the mass involved. Debris flows are capable of destroying homes, roads and bridges, sweeping away vehicles, knocking down trees and obstructing streams and roadways with thick deposits of mud and large stony debris, and they are obviously able to cause victims [1–3]. Debris flows are typically associated

with periods of heavy rainfall or rapid snowmelt [4,5]. Under the action of heavy rainfall, the eluvial–colluvial cover of the slopes can be saturated and fluidized, giving rise to shallow landslides; these landslides are often at the origin of the debris-flows triggering. In addition, the areas burned by forest and brushfires can prove critical. In extremely dry soils, the drainage action on the water ceases, the transpiration action of the plants decreases and so does the ability of the same plants to retain the underlying soil. This means that in the event of heavy rainfall, land affected by fires or severe drought is more prone to landslides (e.g., [6–10]). Knowing the behavior, trigger mode and dynamic processes of debris flow, through detailed historical investigation, can serve to prevent and mitigate harmful effects [11–23]. In some geomorphological conditions, the alluvial fan processes tend to follow more predictable patterns [24–26] and floods associated to intense sediment transport may remain within defined channels as they discharge down slope [27,28]. Even if there is always some degree of unpredictability of the debris-flow hazard on all alluvial fans, some portions of these different hazard levels can be defined. The risk related to debris flows has also been enlarged with the increase of urbanization on alluvial fans. Consequently, detailed debris-flow hazard assessments and associated risk are necessary. Detailed investigation of a number of cases can contribute to a better understanding of the problem and help to identify possible strategies for forecasting and prevention.

The importance of the cognitive phase in identifying and applying debris-flow risk mitigation procedures in alluvial fan areas has been recently highlighted by several contributions from the scientific community that has been working for decades to identify empirical methods and algorithms for estimating debris potential [29–31], as well as in relation to debris flow's destructive power [32,33]. The attention for debris-flow assessment is further enhanced when coupled with urban planning [34,35] and natural hazard maps (e.g., [36]).

Through an accurate historical analysis, more than 5,000 debris-flow events or floods with intense solid transport, damaging effects and often victims, have been identified in the Italian Alps [13,37,38] (Figure 1).

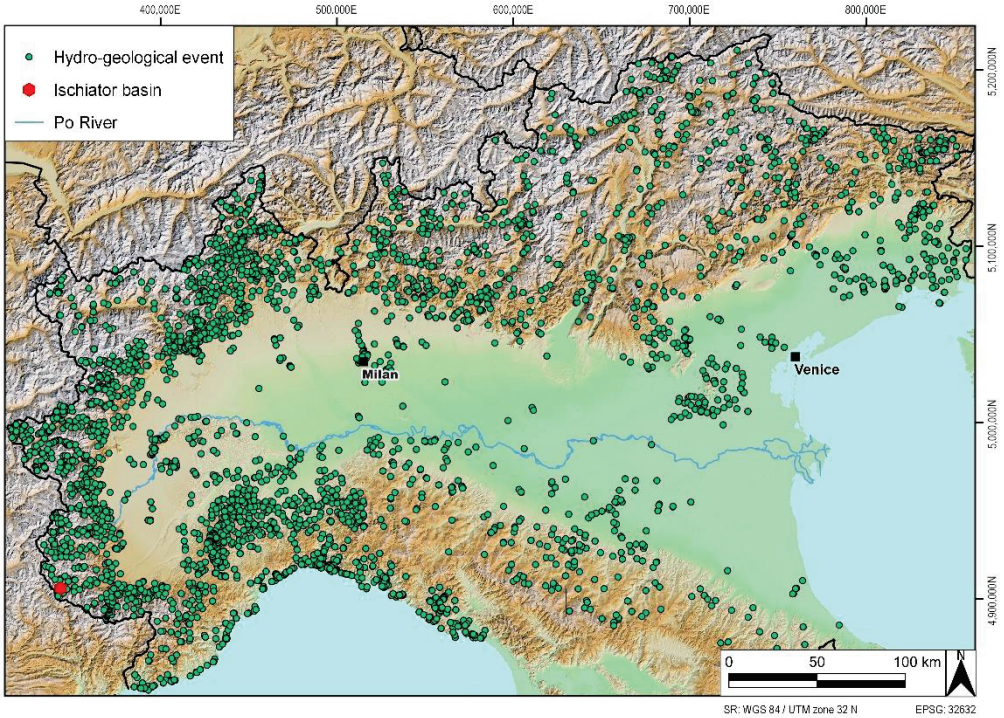



**Figure 1.** Distribution of the torrential processes that have produced damage, and often casualties, in the last 250 years in the Italian Alps. Historical research was conducted by the authors up to 1970, while, for subsequent events, surveys were also carried out in the affected areas.

Similar processes are also recognized in various mountainous parts of Italy [39–41]. From this survey, the magnitudes were obtained of historical debris-flow processes, in some of them also the economic damages and the triggering causes. Many watercourses show processes with high frequency (one case every year), or only once a century, strongly limiting the risk awareness and the overall attention (social, urban planning, etc.). The fact that the frequency of debris-flow events is very low leads to a lack of attention to potential damaging effects. Moreover, for other geo-hydrological processes, if a rather long period of time elapses between an event and the previous one, there is generally a loss of individual or collective historical memory, thus increasing the risk of exposure due to little or no perception of the latent hazard.

An in-depth study on vulnerable areas is therefore necessary to understand possible mitigation strategies, especially where there are historical, cultural, economic and social conditions that are binding for the existing anthropic fabric, even if small. In fact, areas vulnerable to geo-hydrological processes are portions of the territory exposed to potential damages; logically, exposed structures and assets should be removed or displaced from the damaging action of debris flow.

In some cases, however, vulnerable areas are closely linked to the territory by the natural resources to which they are bound (mining areas, energy resources, economic, cultural, historical, etc.) and cannot be relocated. It is therefore necessary to recognize vulnerable areas by analyzing various factors in detail, including past events and the geomorphological peculiarities in which they are located. This cognitive process is a first step towards increasing resilience. The above reflections have pushed the authors to illustrate one of the 800 documented debris-flow cases of catchment in Piedmont, in northwestern Italy [16]. The study aims at proposing a strategy for debris-flow prevention based on historical research and on a simplified analytical approach. The Ischiator catchment (municipality of Vinadio, Cuneo Province, Western Alps) was chosen as an exemplification for this complementary study. The Ischiator basin is also known as Vallone dei Bagni, Valley of "Baths", for its historical thermal-water housing (spa). Bagni di Vinadio is a small alpine village which, thanks to its centuries-old tradition and its high-quality thermal waters, hosts tourism linked to resorts and spa activities. The tourism attraction of Bagni di Vinadio thermal baths has been known since the Roman Age.

In the Italian alpine mountains, there are dozens of spas that boast a long cultural, social and economic history linked to the natural waters that flow at temperatures of up to 60 °C; these structures have been known since Roman times. Due to the therapeutic properties of the waters, Bagni di Vinadio has been described since the 16th century. During the Royal Savoy period, the site rose to prominence as a place of residence and treatment for officers of the royal army. The first nucleus of buildings intended to exploit the beneficial properties of the waters, dating back to the mid-eighteenth century, underwent subsequent extensions and a radical transformation at the beginning of the twentieth century; in more recent years, it has been joined by a Grand Hotel, now equipped with a beauty farm, conference center and sports areas. The other spas in the surrounding area have a similar history. However, these sites are subject to periodic damaging effects of debris flow: in the area at least two other spas have been seriously damaged by flood events associated to intense sediment transport (Terme of Pigna village, about 60 km southeast of Vinadio for the 2014 event [42] and Terme of Valdieri village, about 20 km from Vinadio, repeatedly damaged by the events of June 1957, June 2000, November 2016, 2019 and 2–3 October 2020) (Figure 2). By their nature, therefore, thermal sites cannot be relocated to less vulnerable locations and must be preserved as places of culture and history, with a long track record of resilience.

For hazard assessment and implementation of mitigation strategies, all cognitive tools must be made available [43]. Detailed digital terrain models are sometimes not available, nor are significant precipitation datasets available to assess refined thresholds for triggering debris flows, so only integrated studies can provide adequate support, both in the preparation of event scenarios and in the planning of mitigation measures.



(**a**) (**b**)

**Figure 2.** Effects of floods associated to intense sediment transport on thermal facilities close to Bagni di Vinadio (fewer than 60 km away) for recent events: (**a**) Terme di Pigna [42], 2014 event and (**b**) Terme di Valdieri (photo by the authors during surveys for the severe event occurring in October 2020).

In the case study of the Ischiator catchment, the fan area is exposed to various degrees of debris-flow hazard. A detailed study has provided the validation of magnitude-estimating models, checking morphological analysis of the fan as compared with the hazard zoning of areas affected with different severity by the June 1957 event, confirming once again the importance of historical data [2,44–46].

The Ischiator catchment, for a long while, has undergone torrential processes; man-made protection works since long ago had been conducted by the Italian Forestry State Corps to cope with the rushing floods associated with high sediment discharge. Historical research has revealed numerous technical documents referring to interventions planned or underway, especially from the late 1800s to the first half of the 1900s. Traces of works or artefacts (especially weirs) in a poor state of conservation were also observed during the surveys. The hydraulic works still present are located in the terminal sector of the main shaft or along the tributaries close to the basin closure.

## 2. General Settings

### *2.1. Geology and Geomorphology of the Ischiator Catchment*

The Ischiator catchment (length 7 km, maximum width 2.8 km) runs straight from SW to NE, at the height of Monte Vaccia turns 90° towards the SE and joins the Vallone Corborant at Bagni di Vinadio (altitude 1300 m a.s.l.).

The Ischiator catchment is located northeastward of the Corborant Peak (Figure 3), which belongs to the crystalline Argentera massif (Maritime Alps) [47]. The bedrock outcrops extensively appear on the left slope along the valley, while the right slope is masked by vegetation, especially in the middle-lower valley stretch. An important shear zone, namely the Valletta Shear Zone (VSZ) [48], also known as the Ferriere–Mollières Line [49], crosses the valley from NW–SE, separating two major geo-lithological and geomorphological ambits (Figure 3).

The landscape is the product influenced by marine climates that have enhanced the modelling effects of glaciation; for a long time, glacial tongues have cut deep into valleys and helped shape the valley floor, periodically replenishing its margins with immense quantities of debris derived from the demolition of valley sides and high cirques. The upper geo-morphological sector, with its typical glacial conformation, in which several small alpine lakes are inserted, presents vast steps and almost entirely bare thresholds, with more abundant accumulations of detrital and morainic masking as one proceeds downstream (including rock glaciers).

The lower sector of the Ischiator basin, angled at 90° to the middle and upper parts, is incised in a "V" shape by river erosion. Both slopes are covered by woodland, and the slopes are largely covered by a modest thickness of soil with little pedogenetic evolution.

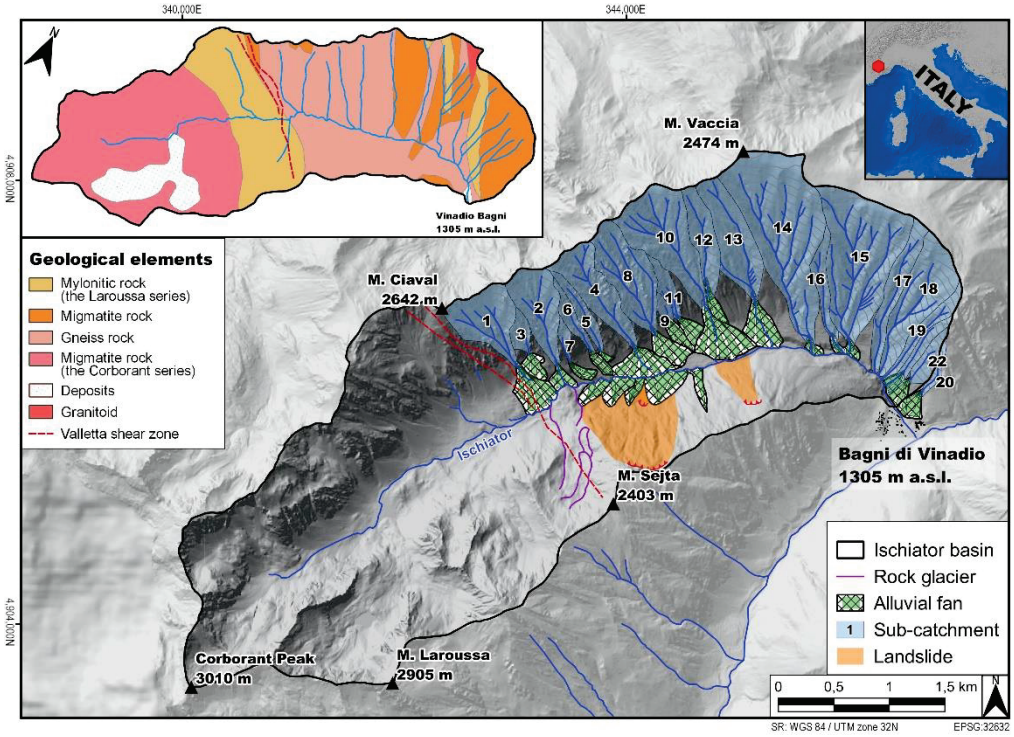



**Figure 3.** Geology–geomorphology and slope instability processes in the Ischiator catchment (1:10,000 scale). The area investigated is shown with n. 22 subcatchments (the Comba Vaccia torrent, detailed in the text, is n. 14). In the outer limit of the map, the geographical coordinates in the UTM–WGS84 system, zone 32T, are shown.

According to Sacchi [50], the Ischiator valley can be subdivided from S–W to N–E into three units: the Corborant series, the Laroussa series and M. Sejta rocks. The Corborant series is composed of two types of alternatively outcropping migmatites: the Mount Corborant peak (3007 m a.s.l.) is the highest point in the crest that divides the catchment, and towards the origin of Ischiator, is composed of occhiadine gneiss. The Laroussa series is exposed along both sides of the valley and comprised between some mylonitic strips and the Corborant series [47,50]. Downward to the VSZ, the Monte Sejta rock complex occurs [47]. The prevailing facies along both slopes in the lowest part of the valley are biotitic anatessite, chloritic and biotitic gneiss, amphibolite and amphibolite gneiss and aplitic granite. The Monte Sejta peak, (2407 m) and the northwest and southeast facing slopes, are mainly sculpted in biotitic anatessite; in such rocks the metasomatic process has attained its maximum intensity, even without producing the anatessitic granite [49]. Some authors consider the Argentera massif as a whole [46]; it consists of the Terrane Gesso–Stura–Vésubie (GSV) to the NE and the Terrane Tinée to the SW, separated by the Ferriere–Mollières cutting area [51,52]. The two terranes are characterized by distinct lithological associations and metamorphic evolutions [53].

Through field recognition, it is easy to understand the cause of accelerated erosion along the left slope, especially where the valley makes a right-angle bend, just upward to the alluvial fan on which the Bagni di Vinadio village is located. In this area, the left valley slope is incised in cloritic–biotitic, greenish to dark grey finely-grained gneiss, scarcely or not schistose, combined in alternance with two large mylonitic strips. Inside such gneiss, a micrograined, aplitic granite is inserted, anatessi-originated and sharply connected to the gneiss without transitional facies [50].

In general, both the morphology of the main valley and the tributaries are deeply molded by the Würm glacial exaration processes (Figure 4). The main glacier was mainly fed by the head cirque and a minor glacier was inflowing from the right slope. Along the longitudinal valley profile, four main valley steps are found [54]. Quaternary terrains are

found along the whole valley axis near the streambed and correspond to scree slope and remnants of glacial deposits.



**Figure 4.** A bird's-eye down-valley view of the Ischiator catchment, upper part: typical U-shaped slopes owing to the glacial activity.

At the inflow of the Ischiator in the Vallone dei Bagni, a multiple fan topography is developed, made by debris-flow deposits of different age. Right of the torrent, near the main housing of Bagni di Vinadio, a widely expanded remnant of the oldest deposits still exists, where the most recent urban growth has taken place; a high terrace scarp connects such deposit to the present-day alluvial fan.

The present study area belongs to a high-relief energy-dominated area, with sharply-dipping slopes; in the lower reach, the right slope has stronger relief energy than the opposite south-facing slope.

### *2.2. Hydro-Meteorological Hazards and Vulnerability in Case Studies*

The Ischiator basin is located in the alpine context, where torrential processes and debris flows occur very frequently (Figure 1 and Table 1). Historical research has shown that tributary streams do not suffer equally from the effects of extreme weather events; in fact, each sub-basin is configured with its own geo-hydrological activity, with its own timing of reactivation of unstable processes, as observed in other Alpine contexts [55]. The study of past events, therefore, allows the recognition of a natural predisposition to debris flows, providing reliable scenarios of occurrence for magnitude and damaging effects in the areas of invasion; however, only targeted studies of long historical series can provide indications on the possible thresholds of occurrence and timing of possible reactivation [56,57].

Numerous rehabilitation works have been carried out in the Ischiator basin since the second half of the 19th century (especially those carried out in the period 1951–1953 and those to repair the damage caused by the 1957 debris flow), for which a large amount of historical documentation was found. However, the situation of geo-hydrological instability has worsened considerably, as was noted during recent inspections.

**Table 1.** Main flood associated to intense sediment transport, debris flow and hydrogeological processes occurred in the Ischiator catchment, organized per 50 years periods. For any period, a level of severity was assigned (low = L, medium = M, high = H and very high = VH) based on all available documentary information [58,59]. Details for all events can be found in the Table A1.

| Date | Number of Events | Intensity |
|---|---|---|
| Ante 1850 | 6 | H to VH |
| 1851–1900 | 3 | H to VH |
| 1901–1950 | 1 | H |
| 1951–2000 | 5 | M to VH |
| Post 2000 | 1 | L |

Another important landscape-shaping agent in the catchment is the stream activity, with numerous deeply incised drainage segments, along which (also avalanche-triggered) instability processes are diffused. The final valley reach is characterized by sharp incisions, especially along the left slope, with intense accelerated erosion events, shallow slides and tectonically induced weathering as a first step toward the rockfall process. Since the early 20th century up to the sixties, such critical sites have been modified due to slope regulation and reforesting works accompanied by check dams building in the ravines to avoid rapid degradation. The main left-bank tributary of the Ischiator stream, the Comba Vaccia torrent (n. 14 in Figure 3), is still regarded as a major problematic area because it is incised in debris slope deposits, in glacial reworked deposits, mixed avalanche and in debris-flow-triggered materials (Figure 5). In the vicinity of the Bagni di Vinadio village (Figure 3), on the right slope, such lower-valley reach sharply changes in dip, roughly forming a 90° angle. This is only possible due to the occurrence of tectonic elements crossing perpendicularly with the main valley axis in this area. Such conditioning is the main cause of the instability processes (Figures 5–7) and of the accelerated erosion in the ravines on the left side of the valley.



**Figure 5.** A horizontal pan of the left slope of the Ischiator catchment, showing widely exposed bare detritus, as it appeared in 1957 (archives of the IRPI-CNR, Torino, unpublished).

The stream characteristics are rapidly evolving in the final reach above the intra-mountain stream stretch, giving rise to an inclined bed profile or fall. Immediately below such a fall, the Ischiator stream forms a deep and rectilinear incision and produces debris deposits having acquired a notable amount of kinetic energy.

In the second half of such reach, the channel is embedded more markedly in the valley bottom, presently filled with glacial deposits in the form of a narrow gorge. In this stretch, erosion and bedload transport processes prevail, accompanied by the tributary ravines in the left slope which supply sufficient amount of coarse debris during extreme rainfall. To reduce the effects of rushing floodwater associated to intense sediment transport, several check dams and weirs were built along the main stream and tributaries. In the lowest reach, the torrent flows through a canyon-shaped gorge, then debouches onto the alluvial fan.

Elevated fan deposits belong to the older formation, while the lower deposits close to the stream belong to the newer formation. This double-shaped fan mostly extends towards the right, composed of rocky slope, and its old, elevated portion supports a large part of the Bagni di Vinadio housing. As frequently happens in mountain regions, the recently built settlement occupies active an alluvial fan sector, due to which sudden debris flow during huge floods generally turns towards the right; while in the left side of the channel above the thermal water housing, a large pier-made embankment hinders another diversion toward an old and ephemeral channel.



**Figure 6.** Present-day slope degradation processes on the left slope of the Ischiator torrent. Several deep ravines are infilled by huge detrital amounts, which feed the drainage network.



**Figure 7.** A detail of the head zone of a ravine out of those shown in Figure 6. The highly unstable conditions of the highly fractured bedrock can be noticed, as well as the debris mantle continuously filling up the stream incisions.

## 3. Materials and Methods

### *3.1. Census of Regulation and Protection Hydraulic Works*

The present-day situations of instability over the slopes and along the stream network were detected and synthesized in detail through photointerpretation (images available for the period 1954–2016, Table 2), satellite images (Google Earth®, available in medium resolution since 2012) and field surveys (summer and autumn 2007, summer 2008–after 30 May event, summer 2021). The photointerpretation was conducted by a single operator

in order to maintain an overall uniform grade of subjectivity. Technical records, projects and documents were consulted and confronted to improve objectivity for the regulation and protection of hydraulic works description and for the instability evaluation.

**Table 2.** Detail of the data image source.

| Years | Data Description | Data Source/Archive |
|---|---|---|
| 1954 | Stereoscopic aerial images B/W of T. Stura valley | CNR-IRPI Archive |
| 1963 | Stereoscopic aerial images B/W of Piedmont Region | CNR-IRPI Archive |
| 1975 | Stereoscopic aerial images B/W of Piedmont Region | CNR-IRPI Archive |
| 1991 | Stereoscopic aerial images B/W of Piedmont Region | CNR-IRPI Archive |
| 2000 | Stereoscopic aerial images B/W–2000 flood event effects in the Piedmont Region | CNR-IRPI Archive |
| 2010 | Stereoscopic aerial images—Infrared | Piedmont Region webgis |
| 2009–2011 | Stereoscopic aerial images—Shadowed relief | Piedmont Region webgis |
| 2016 | Stereoscopic aerial images color—Flood event effects in Piedmont Region | Piedmont Region webgis |
| 2021 | Satellite images | GoogleEarth |

All the regulating and protection works executed in the catchment (93 artifacts in total, as check dams, weirs, repulsory levees, embankments, levees, bridges and wades) were mapped using GIS in order to understand whether the interventions wer effective in reducing critical situations in the stream network (Figure 8).

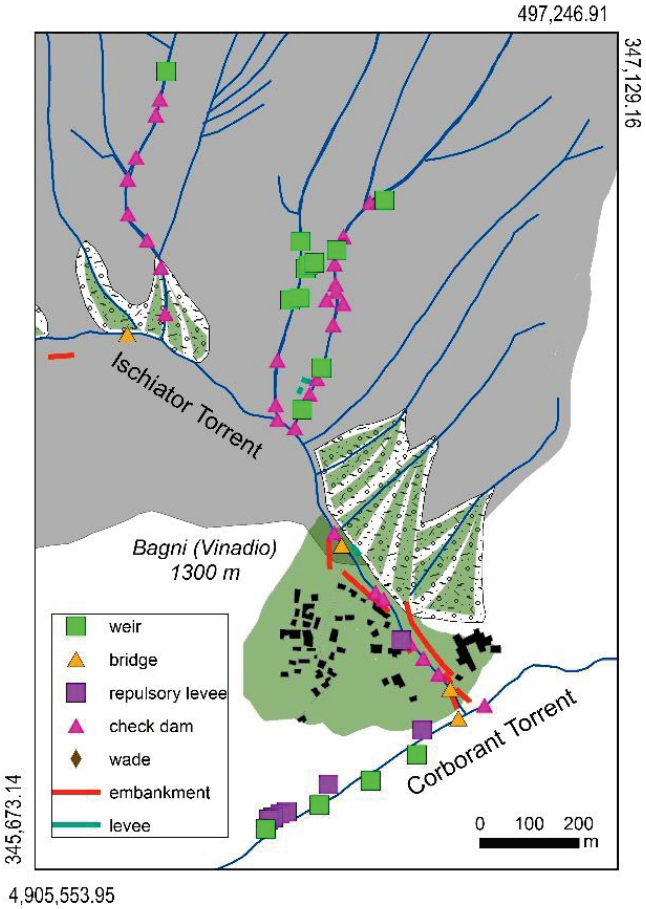



**Figure 8.** A detail of GIS map with the database of the interventions in the stream network (check dams, weirs, repulsory levees, embankments levees, bridges and wades are shown).

The inherent technical data were collected, geo-referenced and arranged in form of the SICOD (Sistema Informativo Catasto Opere di Difesa—Informative System of Defense

Work Cadastre managed by each Italian Region) database set up by the Piedmont Region; such a database aims to review the up-to-date efficiency conditions of the regulation works and other artifacts along the alpine stream network realized in the past.

### *3.2. Method for Magnitude Debris-Flow Evaluation*

The problems arising out of the flow regime of the Ischiator torrent mainly depend upon its mass sediment transport capacity produced by the first-order incisions. An estimation of the potential amount of moving detritus, in case of an extraordinary rainfall event, was carried out based on two predictive models [60,61]. For such estimation, the Ischiator catchment was divided into n. 22 minor subcatchments along the left-valley slope and SW-exposed topography having similar morphology, elevation and vegetal cover (Table 3); for every subcatchment, the bedrock is mainly gneiss and anatessite granite (Figure 3). The number of subdivisions corresponds to the natural minor tributary of the lower geo-morphological sector of the Ischiator basin, which corresponds to the principal debris source of debris-flow processes.

**Table 3.** Morphometric parameters of the subcatchment of the Ischiator basin.

| Catchment Number (See Figure 3) | Effective Area ($km^2$) | Average Slope % |
|---|---|---|
| 1 | 0.353 | 79.17 |
| 2 | 0.316 | 77.88 |
| 3 | 0.071 | 89.92 |
| 4 | 0.367 | 97.83 |
| 5 | 0.118 | 106.37 |
| 6 | 0.092 | 106.09 |
| 7 | 0.036 | 90.13 |
| 8 | 0.461 | 93.20 |
| 9 | 0.039 | 101.87 |
| 10 | 0.569 | 80.95 |
| 11 | 0.085 | 93,87 |
| 12 | 0.227 | 76.95 |
| 13 | 0.395 | 76.34 |
| 14 | 1.072 | 70.33 |
| 15 | 0.899 | 72.36 |
| 16 | 0.129 | 71.25 |
| 17 | 0.232 | 70.47 |
| 18 | 0.449 | 73.48 |
| 19 | 0.122 | 73.36 |
| 20 | 0.044 | 87.83 |
| 21 | 0.098 | 75.49 |
| 22 | 0.094 | 80.99 |

The first predictive model [60] is calibrated for catchments in the Western and Central Alps and is thus suitable for the present study area. The second one [61] was suggested for another application in the Western Alps (e.g., [62]). The results from these two methods are almost similar (such values differed by 3,000 $m^3$ over total volumes, accounting for 80,000 $m^3$). It must be said that the Tropeano and Turconi method [60] operates on the existing or potential instability conditions inside the whole catchment system (Figure 9), while the Hungr method [61] is suitable for estimating the final product of the actual instability agents, i.e., the virtual detritus supply available for unit length along homogeneous segments of the stream network only (Figure 10).

The [61] method should express a more major potential for sediments than that of [60]. The latter, in fact, implies simplifications in the ambit of the different typologies of incipient instability, attributing to any of these univocal mobilization modalities concerning depth of unstable layer and triggering time for its motion, even if they refer to broad-scale situations. The consequence is that the larger the catchment is it widens the doubtfulness about dynamic propensity of the portions of detritus cover far from the stream-flow incisions.

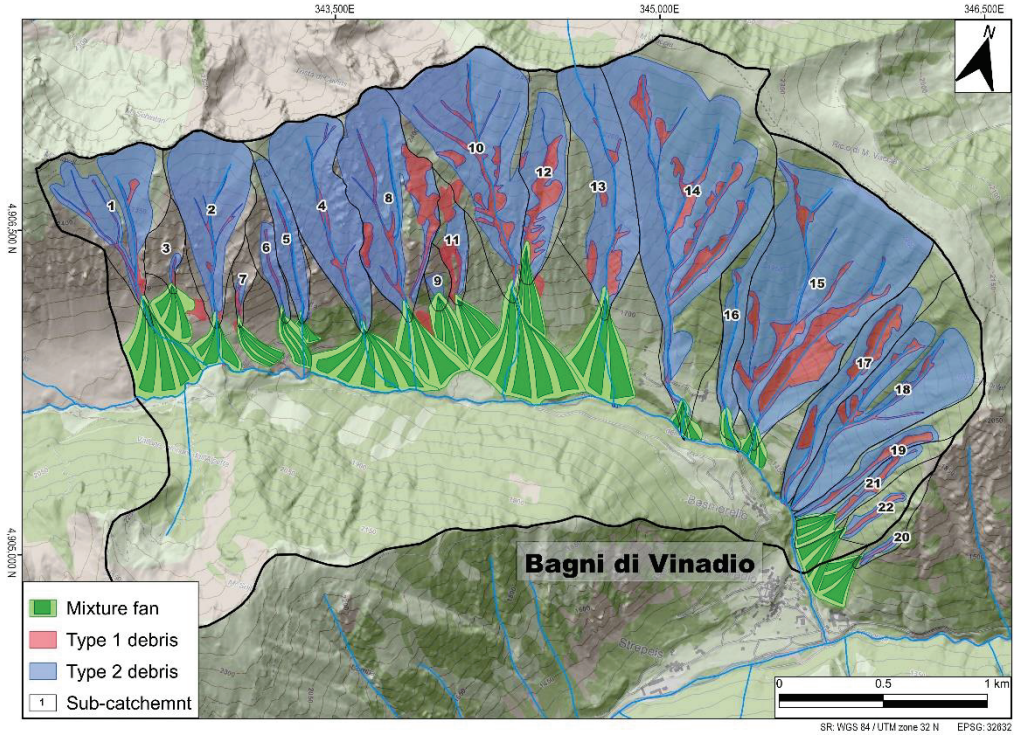



**Figure 9.** Identification of the areas of movable detritus along the secondary hydrographic network immediately available for mass transport (red areas) and of the areas of unstable debris cover, potentially movable along the slopes of the respective basins due to slope processes (landslides) activated during torrential events (blue areas). Tropeano and Turconi method [60].

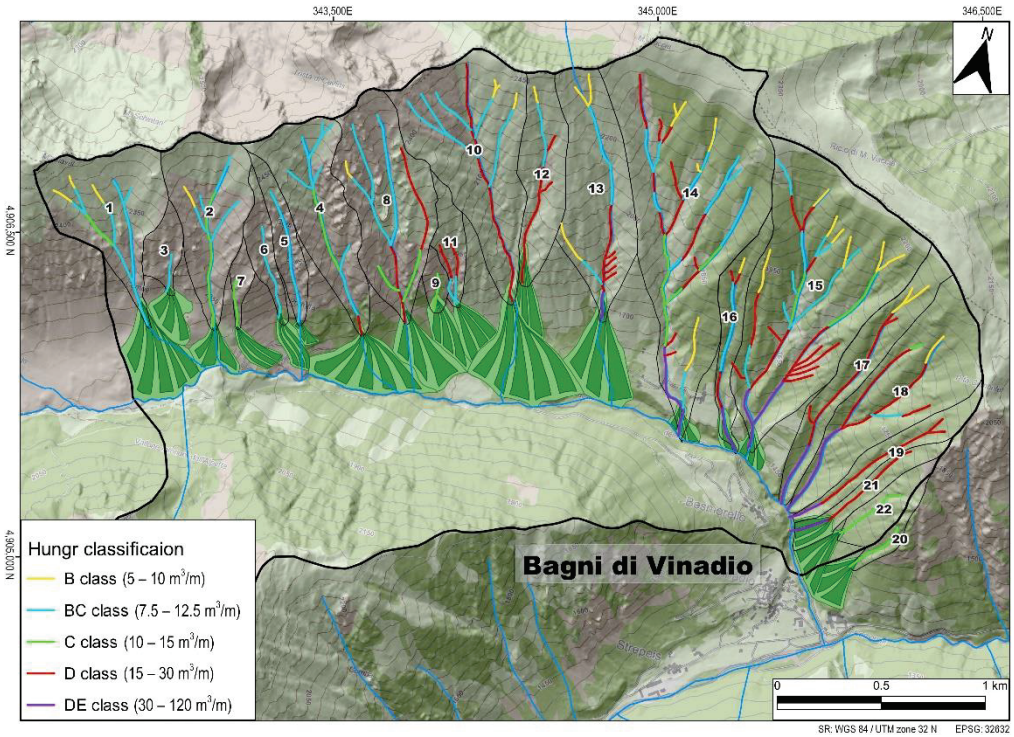



**Figure 10.** Subdivision of the secondary catchment areas of the sub-basins according to the potential debris production (expressed in cubic meters of debris per linear meter), according to the Hungr method [61].

In the Hungr method [61], such problems do not exist because in all channel segments problems do not arise over the provenance of flow detritus. This may imply an exceedingly high-estimated amount of material movement produced through the catchment dynamics (processes). In addition, the authors used the Turconi and Tropeano formula [63], which takes into account all relevant morphometric parameters of the catchment, data generated through historical analysis to estimate frequency factor (f), field mapping and photointerpretation. The subcatchments were sub-divided into areas of <10 $km^2$, in order to obtain good results.

The general expression is:

$$M = \left(AE\ tgs\ r\ h\ (1+n)^{f}\right)/1000_{tot} \quad (1)$$

where:

M: evaluation of magnitude of debris supply;
AE: actual catchment area ($m^2$) computed as A/cos (Iv);
tgs: average slope gradient (Iv) [%];
r: proportionality coefficient (between 0 and 1), that is the ratio between surface extent of the loose materials directly liable to be carried downstream and actual catchment area;
h: average thickness (m) of the debris package which could be delivered into the stream network;
n: adimensional coefficient comprised between 0 and 10, expressing the potential debris availability in case of an exceptional event (e.g., slope failure)/actual catchment area. The closer the value of the coefficient "n" is to n. 10, the greater the level of instability in the basin, and consequently, the amount of material that can implement the debris mixture.
f: frequency factor, expressing the number of events occurring in a standard time lapse equal to 100 years.

In order to define the physical characteristics of all subcatchments, morphometric parameters were previously computed (Table 3). Data from historical archives are very much useful for the debris flow's occurrence (e.g., [2,12,64,65]). From historical records, the number of debris-flow events for each subcatchment was collected to draw the frequency factor (f). The evaluation of the frequency of debris flows helps in understanding the relations between basin conditions, basin morphological evolution, sediment supply processes and debris-flow occurrence. In this case, the estimated return time for the most severe events in the Ischiator basin was considered equal to 100 years. the events of 1664, 1754, 1853 and 1957 were documented: the June 1957 event was the only severe event in the last 100 years. However, at least four medium-intensity events affected the main stream and some tributaries (the events of 1926, 1979, 1987 and 2000). In view of this, two different values were assigned to the frequency factor: f = 1.00, considering one severe event every 100 years; f = 0.25, considering four events in a century. This led to a double set of results that can probably be considered as a minimum and a maximum of the estimate of the movable debris potential.

Through geomorphological interpretation of aerial photographs and intensive field investigation, the areal extent of the debris/soil mantle and its thickness were assessed (factor h) for defining r, h and n coefficients. The approach illustrated above concerns the determination of both the actual subcatchment area and the surface occupied either by active debris/sediment deposits and/or by sediments in temporary equilibrium [66].

### *3.3. Hazard Map*

Based on the estimation of debris, potential data calibration was conducted for the settled area of Bagni di Vinadio to prepare a hazard map of 1:5000 scale of the Ischiator fan area, solely based on the geomorphologic method proposed by Aulitzky [67], modified by Ceriani [68].

Some methods are available for debris-flow hazard mapping [14,27,69,70] and for debris-flow hazard modeling [71–73]; the applicability of those methods is restrained by the

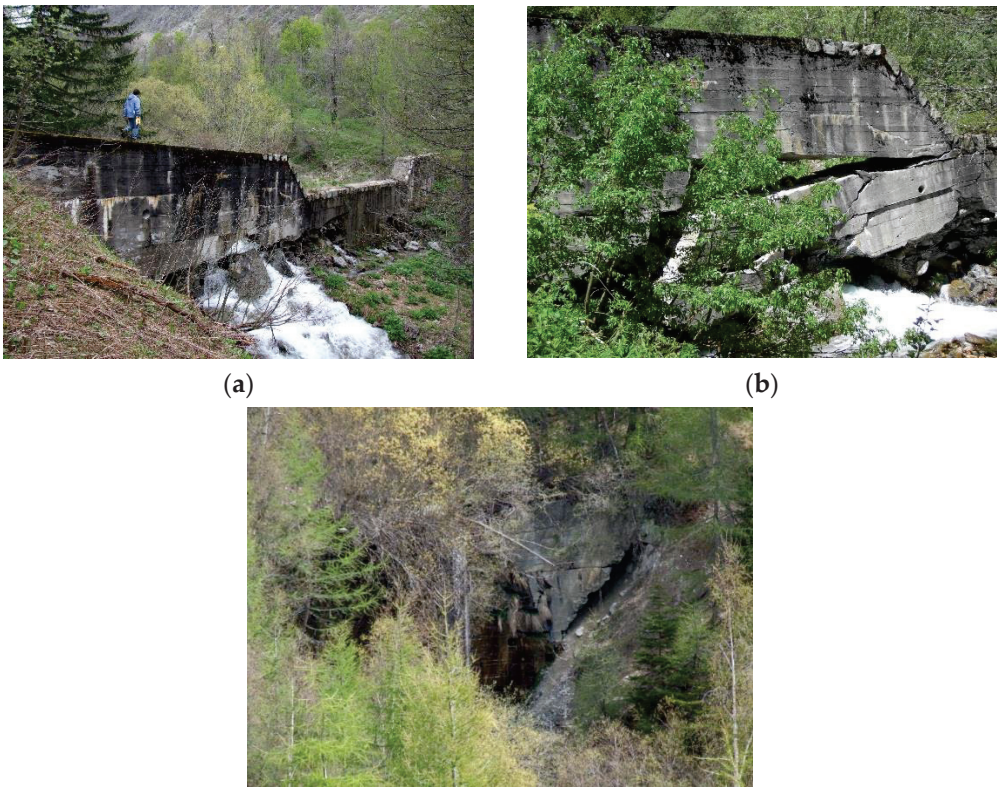
typology of the input data; in fact, some applications require the estimation of the thickness of deposits, grain-size characteristics, or precise definition of the area affected by several debris-flow events [74]; however, such data are not available for the present study area. For the present study, the [68] method was used because it is commonly used by some regional geological surveys in the Italian Alps. It is purely based on the geomorphological approach and fits with the debris-flow-exposed fan area.

An analytical comparison was made between the effects of the June 1957 intense debris flow, the hazard map and the urban growth of Bagni di Vinadio during the 1954–2021 period, deduced from historic and cartographic documents.

## 4. Results

### *4.1. State of the Hydraulic Defence Works*

The census of the works by type, and state of conservation of the same, has made it possible to define that the situation of instability of the slopes and watercourses is considerably aggravated by the general state of abandonment of the works that are no longer maintained. It must also be taken into account that most of the repairs and check dams are at present out of order: 88% of these appears totally filled up by detritus, 71% out of such artifacts need to urgently be restored, being damaged and/or unbroken; 67% of counter-dams are almost buried under detritus, amongst these, 50% are cracked or eroded (Figure 11a–c). Such a scenario is impending above a settled area at potential risk of debris flow.



(**a**) (**b**)

(**c**)

**Figure 11.** Overall and detailed view (**a**,**b**, respectively) of a channel-bed-regulating concrete dam (photo taken on 20 May and 23 June 2008). Notice how the situation has worsened due to a debris-flow event that occurred on 28–30 May 2008. Following further debris-flow events, the conditions of the existing structures along the Ischiator stream were even more worrying for their stability due to the amount of detrital material that would suddenly reach the streambed in case of collapse of the dam (**c**, in summer 2021).

The current defensive system is still based on the old embankment wall and repellent works that should ward off direct erosive activity of water flows (Figure 12). For a number of years, the competent administration has been considering projects for the containment of debris by means of a storage area, but these have not yet been implemented.



(**a**) (**b**)

**Figure 12.** Image of the embankment wall (**a**) and of the erosion repulsion structure (**b**), respectively, longitudinal and transversal to the direction of the water flows, realized after 1957 and still representing the defense system for the built-up area partly visible on the right bank.

*4.2. Debris-Flow Magnitude*

An advantage of the predictive methods of [61,63], instead of others proposed in the literature, is that they are based on a practical examination of the onsite characters of the potential detritus amounts; intense ground-truth verification was carried out through photointerpretation throughout the study area. It is important to note that a little part of the output of debris-flow processes along the ravines of the left-valley slope of the Ischiator catchment comes down the mainstream channel. The main flow in this case acts as a conveyor belt, and channel morphology is conditioning the debris pulses downstream; deposits occur on flattish, even-distributed stream stretches and more acutely dipping channel stretches, resulting in the river cross-section narrowing and controlling the delivery of the debris and sediments.

The main flow in its lower reach interplays with tributaries. In this sector, there is a lack of fan deposits, although high sediment delivery capacity remained in the past. Among the processes occurring in the left slope, the true sediment delivery part in the Ischiator valley, debris flows largely prevail and the materials come down the major stream as they attain the confluence. Such processes evenly occur along a stretch of some 4 km, in which the ravines combine with the main flow along with an estimated detritus of 30,000 $m^3$. Thus, the final stream stretch, just upstream to the fan apex, produces huge amounts of debris flow carried down the major stream. This was verified in the field using the method of Aulitzky [67]. As per the "frequency factor" technique [63], the total estimated debris amount delivered from the ravines in the left slope into the main stream ranges between 250,000 $m^3$ and 530,000 $m^3$, computed using as "frequency factor" values 0.25 and 1.00, respectively. Moreover, the Hungr method [61] yields a debris-supply value range between 410,000 $m^3$ and 915,000 $m^3$ (min–max, respectively) (Figure 13).

In spite of the apparent discrepancy between the cumulative values reported above, the result is almost similar for both the methods for single subcatchments. In most cases, the estimated values in both the methods result in a similar order of magnitude (thousands or ten thousands $m^3$). In order to apply the Hungr method [61], multitemporal aerial photographs were analyzed, avoiding onsite calibration for some sites due to the inaccessibility in some incisions. Applying both the methods, it is found that the major portion of the predicted debris amount belongs to the Comba Vaccia ravine (Figure 3), and the values are 26.5% and 18.4% of the whole, respectively; historical documents also suggest that the Comba Vaccia tributary is the main contributor of the solid charge to the main torrent.

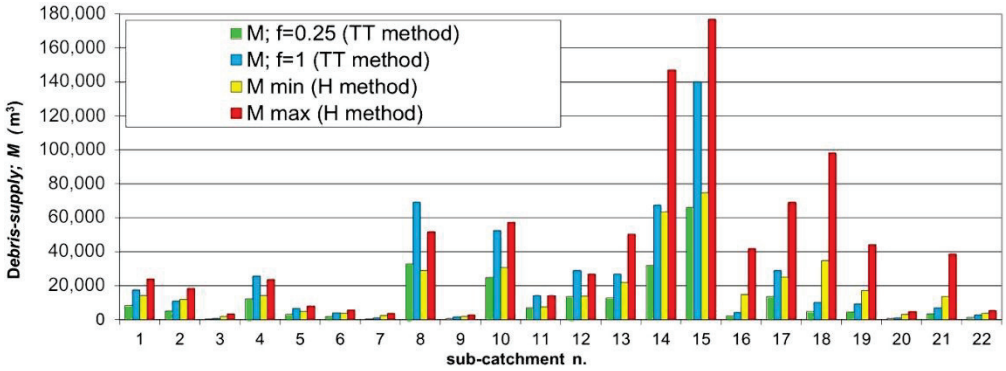



**Figure 13.** A comparison between max–min debris-supply values, estimated by the Hungr [61] method (H method) and the debris-supply values computed using "recurrence interval factors" 0.25 and 1, respectively by the Tropeano and Turconi [60] method (TT method).

### *4.3. Hazard Map*

Several documents and images, as well as the photographs taken just after the 1957 event, justifies the reliability of the [56] method, and it shows that 55.5% of the area classified as exposed to high or very high debris-flow danger was in reality affected by such an historical event (Figure 14). While just fewer than half of the settlement is edified on potentially risk-exposed area, this means that the urban planning policy adopted after the 1957 event did not take into account the numerous documents of the past, nor the morphology of the sites; the land-use planning has not managed the real risk associated with torrential activity.

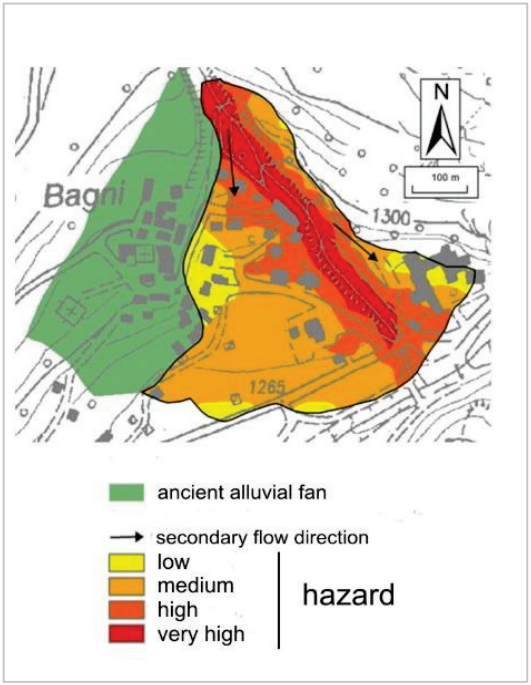



**Figure 14.** A detail of the hazard zoning map of the alluvial fan on which the Bagni di Vinadio inhabited area has grown.

Multitemporal aerial photographs indicate that urban growth of the settlement took place during the 1954–2021 period and a large part of housing developed just in the right-central sector of the fan area with the highest danger potential, and the amount of coarse sediment deposits could be of several thousand $m^3$. The spatio-temporal occurrence of debris-flow events was assessed based on several historical documents [2]. A diachronous appraisal of the landscape evolution throughout the last centuries was prepared from old

manuscripts, historical reports, technical documents, local memory booklets and newspapers, both found in local and CNR-IRPI archives. A rare document dating back to 1775 depicts (Figure 15) the Ischiator torrent as it appeared in the painter's eyes. Both from pictures and from the legend of it, it is clearly found that a channel branch in the left was flowing very close to the thermal-water housing (already in use at such a time) and a branch of the channel bared since old times through the boulder dam already cited. In fact, above the edifice, the legend bears the inscription 'Ripari' (repairs, protections). We do not know if such a term should refer to a planned or already existing kind of embankment, or simply to a refuge location in case of a super-elevated flood associated to intense sediment transport that is naturally immune to debris-flow effects. The right branch of the Ischiator is depicted as more incise and larger than the left one, which in turn appears as longer and forming several bends. A reference is also reported about the location of the old parish, which was possibly destroyed by the right branch of the torrent, and the new parish was rebuilt after the event.

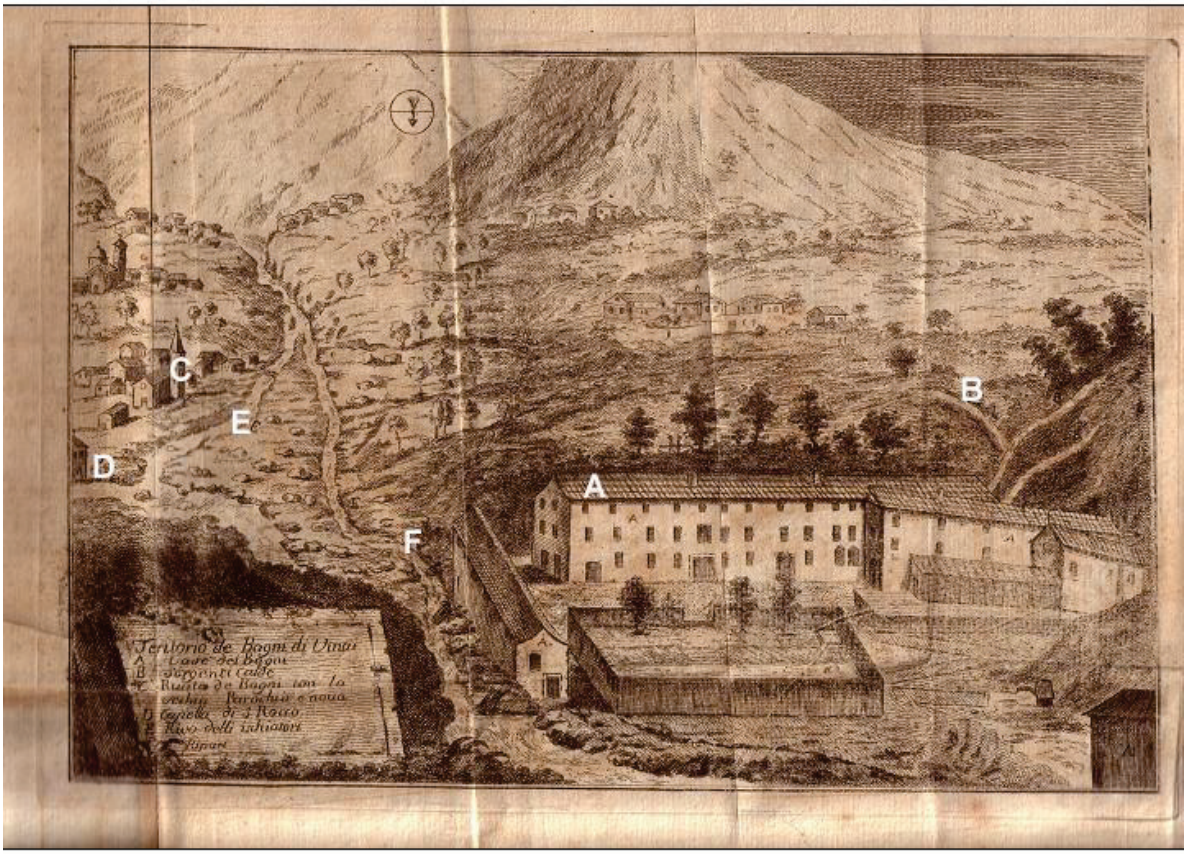



**Figure 15.** A rare lithograph reproduction dating back 1775 in which the Bagni thermal housing, on the Ischiator alluvial fan, is depicted (**A**), as well as the thermal springs (**B**). Other inscriptions are the old Bagni village (**C**) and the ruins of the San Rocco Chapel (**D**), partly destroyed by debris flow occurring in 1754 by the Ischiator torrent (**E**). Defense structures (**F**) are also depicted.

From both photointerpretation and field survey, it can be hypothesized that in reality an historical channel branch on the right of the fan used to exit, which is scarcely recognizable today due to intensive anthropogenic influence. At last, the coarse bedload transport events that took place before 1775 affecting the Bagni di Vinadio area were characterized by large or gigantic blocks in the border of fields, as portrayed in the lithograph, which presumably are the remnants of old alluvial fan deposits.

The present-day fan area of the Ischiator stream is exposed to various degrees of debris-flow hazard over 0.084 km$^2$, i.e., over 88.2% of it. In order to define the area covered by deposits left by the June 1957 debris flow, which is deemed the largest to have occurred

in the last century, a cross-control was drawn between the computed map and historical evidence (Figure 16).

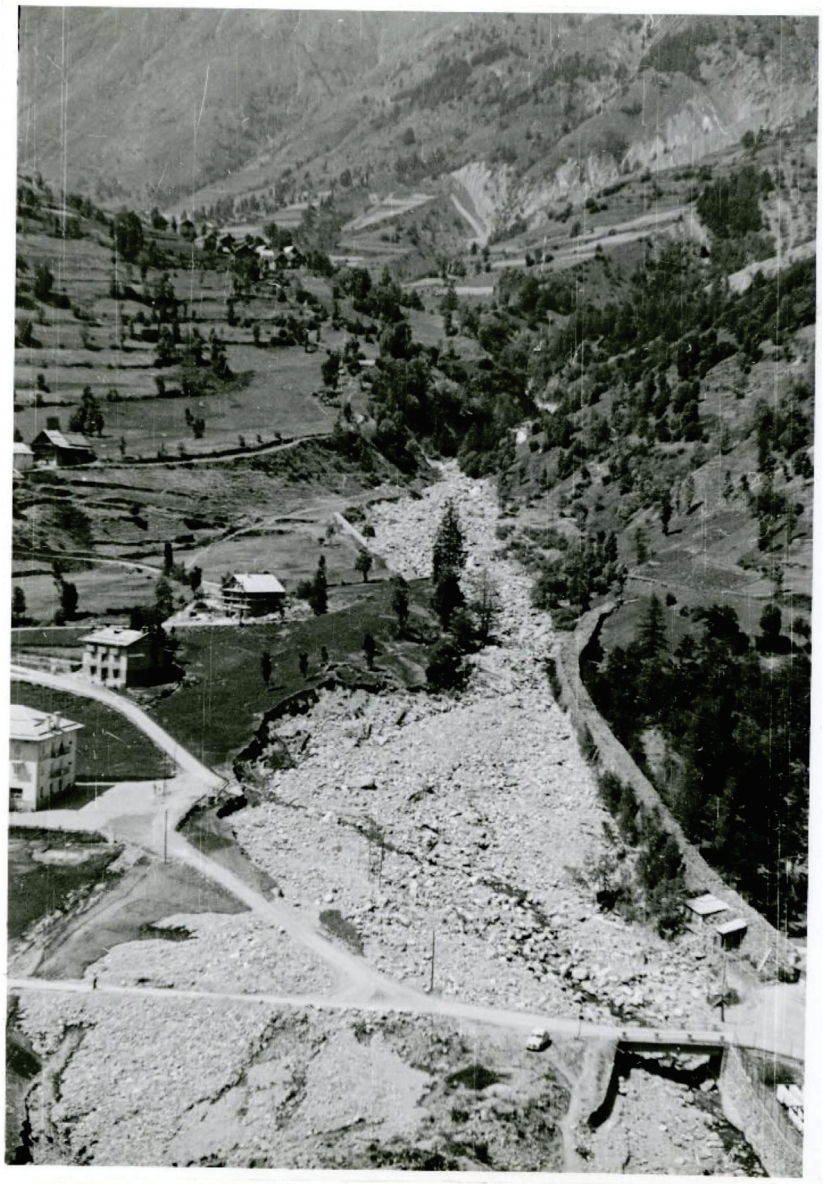


**Figure 16.** Coarse channel bottom, debris-flow deposits and bank erosion processes that occurred in June 1957 on the alluvial fan of the Ischiator stream near the Bagni di Vinadio built-up area, looking upstream (archives of the IRPI-CNR, Torino, unpublished).

## 5. Discussion

The Ischiator basin is in a high state of degradation and geo-hydrological instability, aggravated by the neglect of defense and mitigation works for the torrential processes.

Four series of magnitude values were plotted on a same graph, and one may find that they are as a whole overlapping; in some cases, in spite of some discrepancies, the trend of estimations is good. In addition to this, it is important to note that the best fit between the values found in the two methods above reported concerns about the small catchments (areas fewer than 1 $km^2$): as the area increases, the span of discrepancy arises in the predicted magnitude values (Figures 17 and 18).

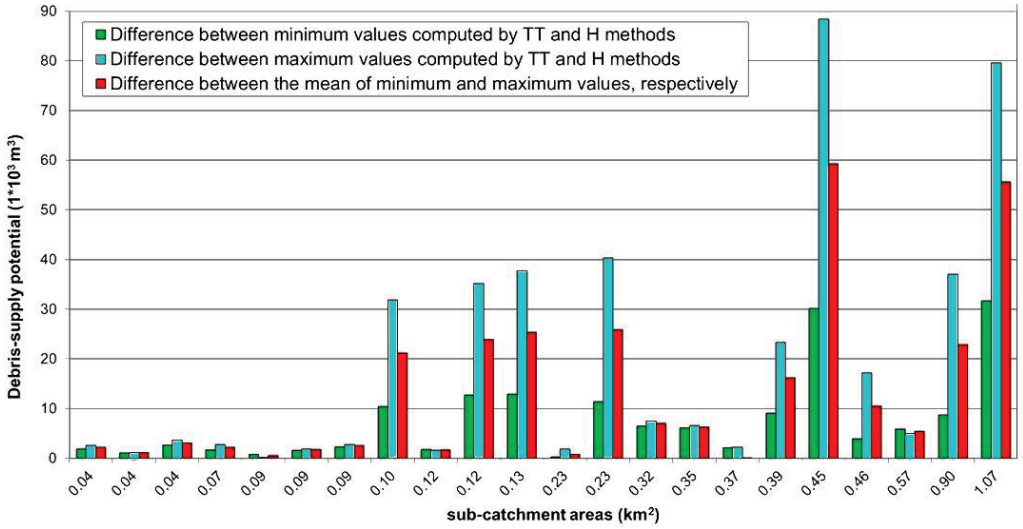



**Figure 17.** Comparison between the numerical discrepancies of the values of potential debris supply for every subcatchment in relation to its area. Such analysis was carried out to evaluate which pair of values (max, min and average), obtained with the (TT) and (H) methods [47,48,50], could have the best fit. It results that the discrepancy between the minimum values offer a more significant result, with a discrepancy of fewer than 10,000 cubic meters on average.

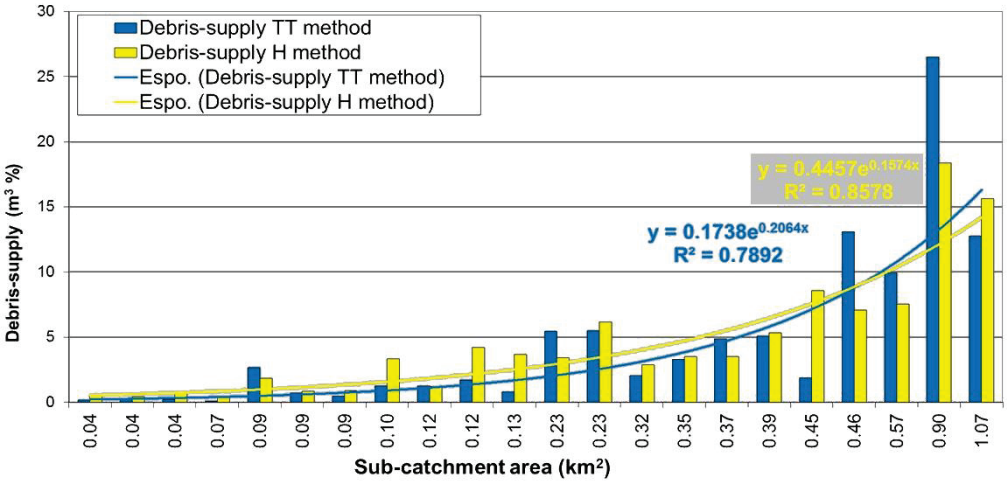



**Figure 18.** Minimum values of the debris-supply volumes calculated with TT and H formulae for each sub-basin; this graph appears rather meaningful when checking the soundness of the analytical comparison between the two methods. Exponential curves are in link with the basin areas.

During the last decades, the study of debris flow has strongly increased processes knowledge in terms of hazard and risk assessments [75–77]. Several approaches have examined debris-flow hazard assessments through GIS statistical analysis (e.g., [78,79]) or dynamic approaches with interpretation of aerial or satellite images [72,80–85]. Specific studies at the local cases are not so common, and often numerical models based on fieldwork are necessary to determine the hazard in the debris-flow deposition areas [14,61,70,86–90].

This study focuses on potentially re-activable paroxysmal processes in the Ischiator catchment, along the stream network and especially the main channel; these carry a huge amount of coarse detritus and bedload deposits, severely endangering the fan area. Although such a phenomenon in the lowermost channel stretch has been quiescent for decades, the study evidences possible critical situations along the minor tributaries directly inflowing in the main stream just above the fan apex.

There are several critical factors that require complex investigations and ad hoc assessments to contain the damaging effects of debris flow and torrential processes. These factors

are: (1) the high vulnerability of the urbanized areas located along the alluvial fan of the Ischiator stream; (2) the high danger induced by the debris flow along the hydrographic network; (3) the impossibility of relocate these buildings, which are bound to the natural resource of thermal waters, which offer an important resource at a local level with no other attractive resources if not linked to excursion tourism.

## 6. Conclusions

In the Alps, there are numerous sites with a long economic or cultural tradition bound to the territory (thermal areas, religious or sacred places, geosites, etc.). They are often located in isolated locations with high exposure to debris flow or flood associated to intense sediment transport. Therefore, mitigation strategies must be implemented to reduce potential damage and increase resilience. In this paper, several themes are addressed with this aim: on the one hand, the evaluation of the magnitude of the natural process with different methods compared, on the other hand a classification of the areas with increasing criticality, by means of simple and locally rapid tools to propose, compared with historical and geomorphological data.

The integration of the research methodology proposed in this paper allowed to evaluate that 55.5% of the area in case of a debris-flow event would most probably be severely damaged. In fact, if a risk analysis and risk map would be developed, all this area would be classified at high or very high risk. This area corresponds to the one concerned by the historical event of 1957, taken as a reference. In the Ischiator stream case, the critical geo-hydrological condition is very much clear and documented in detail, but the same cannot be said for other catchments in the alpine chain. It is also important to note that urbanistic choices have once more been underestimated for the possible occurrence of natural processes, which may act unpredictably with the dynamics and evolution of triggering conditions, startup and re-activation of phenomena. Unfortunately, these factors were not linked with the temporal sequences of human activities. This study should offer opportunities to think about risk-reducing and land-management activity in advance, increasing the attention of the community.

While a hazard analysis focuses on natural processes, the method of risk analysis additionally includes the qualitative or quantitative valuation of elements exposed to these hazards, i.e., their individual values and the associated vulnerability [91–94]. This would initiate a system of hazard assessment, mitigation and reduction in the existing hazards and integrated programming aimed at the identification of mitigation measures. These also include the concept of "compulsory insurance": a well-established tool in several states but not yet consolidated in the Italian reality.

In this paper, we also tried to highlight the elements of the geomorphological and geological analysis, integrated by historical knowledge of the processes that have affected a specific area. These elements often provide essential hazard information for fast and low-cost identification of critical elements. Additional investigation of the elements of risk can be submitted through the multidisciplinary integration and comparison of methods already known in the literature, which are often used in nonsectoral and integrated approaches, preferring those more complex and difficult to validate.

**Author Contributions:** Conceptualization and methodology, L.T. and D.T.; validation, F.L., L.T. and M.F.; investigation, L.T., D.T., G.S. and M.F.; resources, L.T. and G.S.; data curation, D.T., B.B. and L.T.; writing—original draft preparation, L.T. and D.T.; writing—review and editing, L.T., D.T., F.L., B.B. and S.K.D.; supervision, S.K.D.; project administration, L.T.; funding acquisition, L.T. and F.L. All authors have read and agreed to the published version of the manuscript.

**Funding:** The research activity is financed by: ARTEMIDE Project (Archive ThEMatic Imaging Aerophotography of Events) (http://www.irpi.cnr.it/en/project/artemide/; accessed on 10 December 2020), supported by Compagnia di San Paolo Italian National Foundation, Project CNR Number DTA. AD004216; DEBRIS FLOW Valcamonica CNR IRPI Project, supported by Lombardy Region (Italy) Project CNR Number DTA. AD003599.

**Institutional Review Board Statement:** Not applicable.

**Informed Consent Statement:** Not applicable.

**Data Availability Statement:** All stereoscopic aerial images used in this study for the period 1954–2000 belongs to Italian CNR-IRPI Archives. Stereoscopic aerial images for infrared, shadowed relief and flood event effects in Piedmont Region (respectively 2010, 2009–2011 and 2016) can be found on Piedmont Region webgis [59]. Satellite images for 2021 are from Google Earth. All other data presented in this study are authors-made.

**Acknowledgments:** Persons in charge of National Forestry Corp, Major of Vinadio town as well inhabitants are kindly acknowledged for providing information and data. The authors are grateful to the editor and the learned reviewers for their valuable comments and for upgrading the paper.

**Conflicts of Interest:** The authors declare no conflict of interest.

## Appendix A

**Table A1.** Main flood, debris flow and hydrogeological processes occurred in the Ischiator catchment. For all events a level of severity was assigned (low = L, medium = M, high = H, very high = VH) based on all available documentary information.

| Date | Damage Description | Data Source | Intensity |
|---|---|---|---|
| Middle of the 18th Century | Destruction of the former buildings on the right side of the Ischiator alluvial fan. | CNR-IRPI Archive | VH |
| 17 August 1754 | A votive chapel in Bagni destroyed by the Ischiator flood. | Archive of the Vinadio Municipality | H |
| 26–27 August 1834 | The flooding of the Ischiator Stream removed the access bridge to the Vinadio spa. | Archive of the Vinadio Municipality | H |
| October 1839 | Several roads and crossings damaged. | Archive of the Vinadio Municipality | H |
| 1842 | Eroded bridge abutments in the Bagni di Vinadio district. | Archive of the Vinadio Municipality | H |
| October 1846 | Damage to various roads and crossings totalling LIT 2931 (equivalent to approximately EUR 15000 today). | Archive of the Vinadio Municipality | H |
| 3 August 1853 | A debris flow with high magnitude produces deep bank erosion, triggering lateral landslides. The spa was flooded with debris. The existing longitudinal defences on the side of the stream were destroyed. The military barracks were also flooded. | Archive of the Vinadio Municipality | VH |
| 10 July 1873 | An intense flood removes bridges along the Stura Stream. | Archive of the Vinadio Municipality | H |
| May 1894 | Damage to the spa bridge. | Archive of the Vinadio Municipality | VH |
| October–November 1926 | The huge amount of solid matter transported along the Ischiator Stream caused the removal of several bridges, others seriously damaged, and serious damage to roads, houses and hydraulic regulation works. | Archive of the Vinadio Municipality | H |
| 13–14 June 1957 | Damage to the bridge over the Ischiator near the spa; damage also to the banks near the spa. Several weirs in the tributaries of the Ischiator were damaged (e.g. in the Comba Vaccia basin). The Ischiator Stream brought considerable debris to the alluvial fan, diverting its course and constituting a very serious danger for the inhabitants of the Bagni di Vinadio district. | CNR-IRPI Archive | VH |
| 18–19 May 1977 | Damage to the access bridge to the village of Bagni di Vinadio, bank erosion. The floods have brought considerable solid transport. Debris removal and rectification of the riverbed planned. | Archive of Italian Forestry Corps | M |
| 1979 | The threat to the houses in the Ischiator alluvial fan was particularly serious: the waters overflowed the right bank in the area of the Spa hotel. | Dott. Geol. P.F. Sorzana, personal comunication | H |
| 24–25 August 1987 | The intense rainfall triggered widespread mobilisation and transport of debris along the minor incisions on the left-hand side of the slope, also causing some road closures. | Dott. Geol. P.F. Sorzana, personal comunication | H |
| 13 June 2000 | Intense torrential flooding concomitant with that of the main watercourse, considerable debris deposits in Pianche di Vinadio. | AVI Project [58] | H |
| June 2020 | The steep slope below the municipal road was affected by a rapid debris flow. There was no direct damage to human infrastructures, but a possible retrogressive development of the landslide could involve the municipal road and the aqueduct. The landslide material reached the Ischiator Stream riverbed. | ARPA Piemonte [59] | L |

## References


1. Govi, M.; Turitto, O. *Recent and Past Floods in Northern Italy, River Flood Disasters*; ICSU SC/IDNDR Workshop: Koblenz, Germany, 1997; pp. 13–32.
2. Tropeano, D.; Turconi, L. Using historical documents in landslide, debris flow and stream flood prevention. Applications in Northern Italy. *Nat. Hazards* **2004**, *31*, 663–679. [CrossRef]
3. Stoffel, M.; Wyżga, B.; Marston, R.A. Floods in mountain environments: A synthesis. *Geomorphology* **2016**, *272*, 1–9. [CrossRef]
4. Mostbauer, K.; Kaitna, R.; Prenner, D.; Hrachowitz, M. The temporally varying roles of rainfall, snowmelt and soil moisture for debris flow initiation in a snow-dominated system. *Hydrol. Earth Syst. Sci.* **2018**, *22*, 3493–3513. [CrossRef]
5. Sassa, K.; Fukuoka, H.; Fawu, W. Mechanism and risk assessment of landslide-triggered-debris flows: Lesson from the 1996.12. 6 Otari debris flow disaster, Nagano, Japan. In *Landslide Risk Assess*; Balkema: Rotterdam, The Netherlands, 2018; pp. 347–356.
6. Armanini, A.; Michiue, M. *Recent Development on Debris-Flows*; Springer: New York, NY, USA, 1997; pp. 163–165.
7. Cannon, S.H.; Powers, P.S.; Savage, W.Z. Fire-related hyperconcentrated and debris flows on Storm King Mountain, Glenwood Springs, Colorado, USA. *Environ. Geol.* **1998**, *35*, 210–218. [CrossRef]
8. Cannon, S.H.; Gartner, J.E. Wildfire-related debris flow from a hazards perspective. In *Debris-Flow Hazards and Related Phenomena*; Springer Praxis Books; Springer: Berlin/Heidelberg, Germany, 2005; pp. 363–381. [CrossRef]
9. Conedera, M.; Tinner, W.; Neff, C.; Meurer, M.; Dickens, A.F.; Krebs, P. Reconstructing past fire regimes: Methods, applications, and relevance to fire management and conservation. *Quat. Sc. Rev.* **2009**, *28*, 555–576. [CrossRef]
10. Riley, K.L.; Bendick, R.; Hyde, K.D.; Gabet, E.J. Frequency-magnitude distribution of debris flows compiled from global data, and comparison with post-fire debris flows in the western U.S. *Geomorphology* **2013**, *191*, 118–128. [CrossRef]
11. Gees, A. Analyse historischer und seltener Hochwasser in der Schweiz. Bedeutung für das Bemessungshochwasser. *Geogr. Bernensia* **1997**, *53*, 1–156. (In Germany)
12. Barnikel, F.; Becht, M. A historical analysis of hazardous events in the Alps the case of Hindelang (Bavaria, Germany). *Nat. Hazards Earth Syst. Sci.* **2003**, *3*, 625–635. [CrossRef]
13. Tropeano, D.; Turconi, L. Geomorphic classification of alpine catchments for debris-flow hazard reduction. In Proceedings of the Debris-Flow Hazards Mitigation: Mechanics, Prediction and Assessment, Davos, Switzerland, 10–12 September 2003; Millpress Science Publishers: Rotterdam, The Netherlands, 2003; pp. 1221–1232, ISBN 90-77017-78-X.
14. Hürlimann, M.; Copons, R.; Altimir, J. Detailed debris flow hazard assessment in Andorra: A multidisciplinary approach. *Geomorphology* **2006**, *78*, 359–372. [CrossRef]
15. Lega, M.; Casazza, M.; Turconi, L.; Luino, F.; Tropeano, D.; Savio, G.; Ulgiati, S.; Endreny, T. Environmental Data Acquisition, Elaboration and Integration: Preliminary Application to a Vulnerable Mountain Landscape and Village (Novalesa, NW Italy). *Engineering* **2018**, *4*, 635–642. [CrossRef]
16. Turconi, L.; Nigrelli, G.; Conte, R. Historical datum as a basis for a new GIS application to support civil protection services in Northwestern Italy. *Comput. Geosci.* **2014**, *66*, 13–19. [CrossRef]
17. Papa, M.N.; Sarno, L.; Vitiello, F.S.; Medina, V. Application of the 2D Depth-Averaged Model, FLATModel, to Pumiceous Debris Flows in the Amalfi Coast. *Water* **2018**, *10*, 1159. [CrossRef]
18. Stancanelli, L.M.; Musumeci, R.E. Geometrical Characterization of Sediment Deposits at the Confluence of Mountain Streams. *Water* **2018**, *10*, 401. [CrossRef]
19. Luino, F.; Nigrelli, G.; Turconi, L.; Faccini, F.; Agnese, C.; Casillo, F. A proper land-use planning through the use of historical research. *Disaster Adv.* **2016**, *9*, 8–19.
20. Apollonio, C.; Balacco, G.; Novelli, A.; Tarantino, E.; Piccinni, A.F. Land use change impact on flooding areas: The case study of Cervaro basin (Italy). *Sustainability* **2016**, *8*, 996. [CrossRef]
21. Luino, F.; Paliaga, G.; Roccati, A.; Sacchini, A.; Turconi, L.; Faccini, F. Anthropogenic changes in the alluvial plains of the Tyrrhenian Ligurian basins. *Rend. Online Soc. Geol. Ital.* **2019**, *48*, 10–16. [CrossRef]
22. Paliaga, G.; Faccini, F.; Luino, F.; Turconi, L. A spatial multicriteria prioritizing approach for geohydrological risk mitigation planning in small and densely urbanized Mediterranean basins. *Nat. Hazards Earth Syst. Sci.* **2019**, *19*, 53–69. [CrossRef]
23. Roccati, A.; Luino, F.; Turconi, L.; Piana, P.; Watkins, C.; Faccini, F. Historical Geomorphological Research of a Ligurian Coastal Floodplain (Italy) and Its Value for Management of Flood Risk and Environmental Sustainability. *Sustainability* **2018**, *10*, 3727. [CrossRef]
24. Giraud, R.E. *Guidelines for the Geologic Evaluation of Debris-Flow Hazards on Alluvial Fans in Utah: Utah Geological Survey*; Miscellaneous Publication: Salt Lake City, UT, USA, 2005; Volume 6, 16p.
25. Pankaj, J.; van Westen, C.; Jetten, V. Quantitative assessment of landslide hazard along transportation lines using historical records. *Landslides* **2011**, *8*, 279–291. [CrossRef]
26. Chen, Y.; Qiu, Z.; Li, B.; Yang, Z. Numerical Simulation on the Dynamic Characteristics of a Tremendous Debris Flow in Sichuan, China. *Processes* **2018**, *6*, 109. [CrossRef]
27. FEMA. *Guidelines and Specifications for Flood Hazard. Mapping Partners, Appendix G: Guidance for Alluvial Fan Flooding Analyses and Mapping*; Federal Emergency Management Agency: Hyattsville, MD, USA, 2003; pp. 1–33. Available online: https://www.fema.gov/sites/default/files/nepa/Guidelines_and_Specifications_for_Flood_Hazard_Mapping_Partners_Appendix_G-Guidance_for_Alluvial_Fan_Flooding_Analyses_and_Mapping__Feb_2002_.pdf (accessed on 25 May 2020).

28. House, P.K. Using geology to improve floodplain management on alluvial fans: An example from Laughlin, Nevada. *J. Am. Water Resour. Ass.* **2005**, *41*, 1–17. [CrossRef]
29. Chang, T.-C.; Wang, Z.-Y.; Chien, Y.-H. Hazard assessment model for debris flow prediction. *Environ. Earth Sci.* **2010**, *60*, 1619–1630. [CrossRef]
30. Luna, B.Q.; Blahut, J.; Camera, C.; van Westen, C.; Apuani, T.; Jetten, V.; Sterlacchini, S. Physically based dynamic run-out modelling for quantitative debris flow risk assessment: A case study in Tresenda, northern Italy. *Environ. Earth Sci.* **2014**, *72*, 645–661.
31. Turconi, L.; De, S.K.; Demurtas, F.; Demurtas, L.; Pendugiu, B.; Tropeano, D.; Savio, G. An analysis of debris-flow events in the Sardinia Island (Thyrrenian Sea, Italy). *Environ. Earth Sci.* **2013**, *69*, 1509–1521. [CrossRef]
32. He, S.; Liu, W.; Li, X. Prediction of impact force of debris flows based on distribution and size of particles. *Environ. Earth Sci.* **2016**, *75*, 298. [CrossRef]
33. Holub, M.; Suda, J.; Fuchs, S. Mountain hazards: Reducing vulnerability by adapted building design. *Environ. Earth Sci.* **2012**, *66*, 1853–1870. [CrossRef]
34. Bathrellos, G.D.; Gaki-Papanastassiou, K.; Skilodimou, H.D.; Papanastassiou, D.; Chousianitis, K.G. Potential suitability for urban planning and industry development by using natural hazard maps and geological—Geomorphological parameters. *Environ. Earth Sci.* **2012**, *66*, 537–548. [CrossRef]
35. Bathrellos, G.D.; Skilodimou, H.D.; Chousianitis, K.; Youssef, A.M.; Pradhan, B. Suitability estimation for urban development using multi-hazard assessment map. *Sci. Total Environ.* **2017**, *575*, 119–134. [CrossRef]
36. Bathrellos, G.D.; Karymbalis, E.; Skilodimou, H.D.; Gaki-Papanastassiou, K.; Baltas, E.A. Urban flood hazard assessment in the basin of Athens Metropolitan city, Greece. *Environ. Earth Sci.* **2016**, *75*, 319. [CrossRef]
37. Guzzetti, F.; Tonelli, G. Information system on hydrological and geomorphological catastrophes in Italy (SICI): A tool for managing landslide and flood hazards. *Nat. Hazards Earth Syst. Sci.* **2004**, *4*, 213–232. [CrossRef]
38. SICI Project—Information System on Hydrological and Geomorphological Catastrophes. Available online: www.sici.irpi.cnr.it/ (accessed on 21 December 2021).
39. Blahut, J.; Horton, P.; Sterlacchini, S.; Jaboyedoff, M. Debris flow hazard modelling on medium scale: Valtellina di Tirano, Italy. *Nat. Hazards Earth Syst. Sci.* **2010**, *10*, 2379–2390. [CrossRef]
40. Cama, M.; Lombardo, L.; Conoscenti, C.; Rotigliano, E. Improving transferability strategies for debris flow susceptibility assessment: Application to the Saponara and Itala catchments (Messina, Italy). *Geomorphology* **2017**, *288*, 52–65. [CrossRef]
41. Aronica, G.T.; Brigandí, G.; Morey, N. Flash floods and debris flow in the city area of Messina, north-east part of Sicily, Italy in October 2009: The case of the Giampilieri catchment. *Nat. Hazards Earth Syst. Sci.* **2012**, *12*, 1295–1309. [CrossRef]
42. Luino, F.; Turconi, L. *Eventi di Piena e Frana in Italia Settentrionale Nel Periodo 2005–2016*; SMS: Moncalieri, Italy, 2017; 476p, ISBN 978-88-903023-8-1.
43. Lee, T.-L.; Chen, C.-H.; Pai, T.-Y.; Wu, R.-S. Development of a Meteorological Risk Map for Disaster Mitigation and Management in the Chishan Basin, Taiwan. *Sustainability* **2015**, *7*, 962–987. [CrossRef]
44. Luino, F.; Belloni, A.; Turconi, L.; Faccini, F.; Mantovani, A.; Fassi, P.; Caldiroli, G. A historical geomorphological approach to flood hazard management along the shore of an alpine lake (northern Italy). *Nat. Hazards* **2018**, *94*, 471–488. [CrossRef]
45. Audisio, C.; Turconi, L. Urban floods: A case study in the Savigliano area (North-Western Italy). *Nat. Hazards Earth Syst. Sci.* **2011**, *11*, 2951–2964. [CrossRef]
46. Coeur, D.; Lang, M. The Contribution of Historical Data for the Understanding of Floods and Risk Prevention. *Floods* **2017**, *1*, 227–239. [CrossRef]
47. Sacchi, R. Notizie geologiche sulla dorsale M. Sejta—M. Corborant (Massiccio dell'Argentera). *Atti Soc. It. Sc. Nat.* **1961**, *100*, 397–406. (In Italian)
48. Faure-Muret, A. Etudes géologique sur le massif de l'Argentera-Mercantour et ses enveloppes sédimentaires. Thèse Sc., Mém. Serv. Carte géol. France, Paris. *Imp. Nat.* **1955**, *1*, 1–336. (In French)
49. Malaroda, R. Carta Geologica del Massiccio dell'Argentera alla scala 1:50.000 e Note Illustrative. *Mem. Soc. Geol. It.* **1970**, *9*, 557–663. (In Italian)
50. Sacchi, R. Geologia della regione a sud-ovest di Vinadio (Massiccio Cristallino dell'Argentera). *Boll. Serv. Geol. It.* **1959**, *LXXXI*, 223–256. (In Italian)
51. Rubatto, D.; Schaltegger, U.; Lombardo, B.; Compagnoni, R. Complex Paleozoic magmatic and metamorphic evolution in the Argentera Massif (Western Alps) resolved with U-Pb dating. *Schweiz. Mineral. Und Petrogr. Mitt.* **2001**, *81*, 213–228.
52. Rubatto, D.; Ferrando, S.; Compagnoni, R.; Lombardo, B. Carboniferous high-pressure metamorphism of Ordovician rotoliths in the Argentera Massif (Italy), Southern European Variscan belt. *Lithos* **2009**, *116*, 65–76. [CrossRef]
53. Baietto, A.; Perello, P.; Cadoppi, P.; Martinotti, G. Alpine tectonic evolution and thermal water circulations of the Argentera Massif (South-Western Alps). *Swiss J. Geosci.* **2009**, *102*, 223–245. [CrossRef]
54. Sacco, F. Il Gruppo dell'Argentera. In *Estr. Memorie della Reale Accademia delle Scienze di Torino*; Serie II; Accademia delle Scienze di Torino: Torino, Italy, 1911; Volume LXI. (In Italian)
55. Tropeano, D.; Turconi, L. Predictability of the Mass Transport of Sediments in Alpine Catchments. The Case Study of T. Thuras (NW Italy). Available online: http://www.interpraevent.at/palm-cms/upload_files/Publikationen/Tagungsbeitraege/2000_3_321.pdf (accessed on 15 November 2021).

56. Pan, H.-L.; Jiang, Y.-J.; Wang, J.; Ou, G.-Q. Rainfall threshold calculation for debris flow early warning in areas with scarcity of data. *Nat. Hazards Earth Syst. Sci.* **2018**, *18*, 1395–1409. [CrossRef]
57. Hirschberg, J.; Badoux, A.; McArdell, B.W.; Leonarduzzi, E.; Molnar, P. Limitations of rainfall thresholds for debris-flow prediction in an Alpine catchment. *Nat. Hazards Earth Syst. Sci.* **2021**, *2021*, 1–26. [CrossRef]
58. AVI Project. Available online: http://avi.gndci.cnr.it/welcome_en.htm (accessed on 15 November 2021).
59. ARPA Piemonte. Available online: http://webgis.arpa.piemonte.it/geodissesto/sifrap/sifrap_ii_liv_scheda.php?cod_frana=004-61130-00 (accessed on 1 March 2022).
60. Tropeano, D.; Turconi, L. *Valutazione Del Potenziale Detritico in Piccoli Bacini Delle Alpi Occidentali e Centrali*; CNR-GNCDI: Perugia, Italy, 1999; pp. 1–151, (In Italian, with English Abstr.).
61. Hungr, O.; Morgan, C.; Kellerhals, R. Quantitative analysis of debris torrent hazards for design of remedial measures. *Can. Geotech. J.* **1984**, *21*, 663–667. [CrossRef]
62. Ambrogio, S.; Turconi, L. Analisi geomorfologica di dettaglio per la valutazione del potenziale detritico: L'esempio del mud-flow del 17 giugno 2003, Comune di Novalesa (Val Cenischia, Provincia di Torino). In Proceedings of the AIQUA Congress: 'La Geologia del Quaternario in Italia: Temi Emergenti e zone d'ombra´, Roma, Italy, 16–18 February 2004. (In Italian).
63. Turconi, L.; Tropeano, D. Ermittlung von Geschiebefrachten in wildbächen von Westlichen und Zentralen italienische Alpen. *Wildbach Lawinenverbau* **2000**, *63*, 37–47. (In English)
64. Chen, H.-W.; Chen, C.-Y. Warning Models for Landslide and Channelized Debris Flow under Climate Change Conditions in Taiwan. *Water* **2022**, *14*, 695. [CrossRef]
65. Luino, F. Sequence of instability processes triggered by heavy rainfall in northwestern Italy. *Geomorphology* **2005**, *66*, 13–39. [CrossRef]
66. Lyu, L.; Wang, Z.; Cui, P.; Xu, M. The role of bank erosion on the initiation and motion of gully debris flows. *Geomorphology* **2017**, *285*, 137–151. [CrossRef]
67. Aulitzky, H. Preliminary two-fold classification of torrents. In *Mitteilungen der Forstlichen Bundesvers*; Mitteilungen der Forstlichen Bundesversuchsanstalt: Wien, Austria, 1980; pp. 243–256.
68. Ceriani, M.; Fossati, D.; Quattrini, S. Valutazione delle pericolosità idrogeologica sulle conoidi alpine; esempio della metodologia di Aulitzky applicata al conoide del torrente Re di Gianico, Valcamonica (Brescia). *Alpi Centrali. Idraul. E Costr. Idraul. Conf.* **1998**, *3*, 15–26. (In Italian)
69. Pelletier, J.D.; Mayer, L.; Pearthree, P.A.; House, P.K.; Klawon, J.E.; Vincent, K.R. An integrated approach to flood hazard assessment on alluvial fans using numerical modeling, field mapping, and remote sensing. *Geol. Soc. Am. Bull.* **2005**, *117*, 1167–1180. [CrossRef]
70. Glade, T. Linking debris-flow hazard assessments with geomorphology. *Geomorphology* **2005**, *66*, 189–213. [CrossRef]
71. van Westen, C.J. The modeling of landslide hazards using GIS. *Surv. Geophys.* **2000**, *21*, 241–255. [CrossRef]
72. Lin, P.S.; Lin, J.Y.; Hung, J.C.; Yang, M.D. Assessing debris-flow hazard in a watershed in Taiwan. *Eng. Geol.* **2002**, *66*, 295–313. [CrossRef]
73. Melelli, L.; Taramelli, A. An example of debris-flows hazard modelling using GIS. *Nat. Hazards Earth Syst. Sci.* **2004**, *4*, 347–358. [CrossRef]
74. Zhao, Y.; Meng, X.; Qi, T.; Chen, G.; Li, Y.; Yue, D.; Qing, F. Modeling the Spatial Distribution of Debris Flows and Analysis of the Controlling Factors: A Machine Learning Approach. *Remote Sens.* **2021**, *13*, 4813. [CrossRef]
75. Fiebiger, G. Structures of debris flow countermeasures. In *Debris-Flow Hazards Mitigation: Mechanics, Prediction and Assessment*; Chen, C.H., Ed.; ASCE: New York, NY, USA, 1997; pp. 596–605.
76. Heinimann, H.R.; Hollenstein, K.; Kienholz, H.; Krummenacher, B.; Mani, P. *Methoden zur Analyse und Bewertung Von Naturgefahren, Umwelt—Materialen, 85*; BUWAL: Bern, Switzerland, 1998; p. 247p. (In German)
77. Jakob, M.; Hungr, O. *Debris-Flow Hazards and Related Phenomena, XLII*; Springer: Berlin/Heidelberg, Germany, 2005; p. 739. ISBN 978-3-540-27129-1.
78. Guzzetti, F.; Carrara, A.; Cardinali, M.; Reichenbach, P. Landslide hazard evaluation: A review of current techniques and their application in a multi-scale study, central Italy. *Geomorphology* **1999**, *31*, 181–216. [CrossRef]
79. Audisio, C.; Nigrelli, G.; Pasculli, A.; Sciarra, N.; Turconi, L. A Gis Spatial Analysis Model for Landslide Hazard Mapping Application in Alpine Area. *Int. J. Sustain. Dev. Plan.* **2017**, *12*, 883–893. [CrossRef]
80. Mark, R.K.; Ellen, S.D. Statistical and simulation models for mapping debris-flow hazard. In *Geographical Information Systems in Assessing Natural Hazards*; Carrara, A., Guzzetti, F., Eds.; Kluwer Academic Publishers: Dordrecht, The Netherlands, 1995; pp. 93–106.
81. Iverson, R.M.; Reid, M.E.; Lahusen, R.G. Debris-flow mobilization from landslides. *Annu. Rev. Earth Planet. Sci.* **1997**, *25*, 85–138. [CrossRef]
82. Hofmeister, R.J.; Miller, D.J.; Mills, K.A.; Hinkle, J.C.; Beier, A.E. *GIS Overview Map of Potential Rapidly Moving Landslide Hazards in Western Oregon*; IMS22-Text; Oregon Department of Geology and Mineral Industries: Portland, OR, USA, 2002; 52p.
83. Huggel, C.; Kääb, A.; Haeberli, W. Regional-scale models of debris flows triggered by lake outbursts: The 25 June 2001 debris flow at Täsch (Switzerland) as a test study. In *Proceedings of the 3rd International Conference on Debris-Flow Hazards Mitigation*; Rickenmann, D., Chen, C., Eds.; Millpress: Rotterdam, The Netherlands, 2003; pp. 1151–1162.

84. Vallance, J.W.; Cunico, M.L.; Schilling, S.P. *Debris-Flow Hazards Caused by Hydrologic Events at Mount Rainier, Washington*; Open-File Report 03-368; USGS: Vancouver, BC, Canada, 2003.
85. Pallas, R.; Vilaplana, J.M.; Guinau, M.; Falgas, E.; Alemany, X.; Munoz, A. A pragmatic approach to debris flow hazard mapping in areas affected by Hurricane Mitch: Example from NW Nicaragua. *Eng. Geol.* **2004**, *72*, 57–72. [CrossRef]
86. Aleotti, P.; Polloni, G.; Tropeano, D.; Turconi, L. Numerical modeling to determine risk scenarios in an alpine alluvial fan. *Manag. Inf. Syst.* **2004**, *9*, 153–162.
87. Pasuto, A.; Soldati, M. An integrated approach for hazard assessment and mitigation of debris flows in the Italian Dolomites. *Geomorphology* **2004**, *61*, 59–70. [CrossRef]
88. Hussin, H.Y.; Quan Luna, B.; van Westen, C.J.; Christen, M.; Malet, J.-P.; van Asch, T.W.J. Parameterization of a numerical 2-D debris flow model with entrainment: A case study of the Faucon catchment, Southern French Alps. *Nat. Hazards Earth Syst. Sci.* **2012**, *12*, 3075–3090. [CrossRef]
89. Chen, H.X.; Zhang, L.M. EDDA 1.0: Integrated simulation of debris flow erosion, deposition and property changes. *Geosci. Model. Dev.* **2015**, *8*, 829–844. [CrossRef]
90. Schraml, K.; Thomschitz, B.; McArdell, B.W.; Graf, C.; Kaitna, R. Modeling debris-flow runout patterns on two alpine fans with different dynamic simulation models. *Nat. Hazards Earth Syst. Sci.* **2015**, *15*, 1483–1492. [CrossRef]
91. Luino, F.; Turconi, L.; Petrea, C.; Nigrelli, G. Uncorrected land-use planning highlighted by flooding: The Alba case study (Piedmont, Italy). *Nat. Hazards Earth Syst. Sci.* **2012**, *12*, 1–18. [CrossRef]
92. Wang, Y.; Nie, L.; Zhang, M.; Wang, H.; Xu, Y.; Zuo, T. Assessment of Debris Flow Risk Factors Based on Meta-Analysis—Cases Study of Northwest and Southwest China. *Sustainability* **2020**, *12*, 6841. [CrossRef]
93. Notti, D.; Giordan, D.; Cina, A.; Manzino, A.; Maschio, P.; Bendea, I.H. Debris Flow and Rockslide Analysis with Advanced Photogrammetry Techniques Based on High-Resolution RPAS Data. Ponte Formazza Case Study (NW Alps). *Remote Sens.* **2021**, *13*, 1797. [CrossRef]
94. Roccati, A.; Paliaga, G.; Luino, F.; Faccini, F.; Turconi, L. GIS-Based Landslide Susceptibility Mapping for Land Use Planning and Risk Assessment. *Land* **2021**, *10*, 162. [CrossRef]

land

MDPI

*Article*

# Landscape, Memory, and Adverse Shocks: The 1968 Earthquake in Belìce Valley (Sicily, Italy): A Case Study

**Gianni Petino [1], Maria Donata Napoli [2] and Mario Mattia [3,*]**

[1] Department of Political and Social Sciences, Università degli Studi di Catania, 95131 Catania, Italy; petinog@unict.it
[2] Department of Design and Applied Arts, Accademia di Belle Arti di Palermo, 90134 Palermo, Italy; donata.napoli@abapa.education
[3] Istituto Nazionale di Geofisica e Vulcanologia—Osservatorio Etneo, 95125 Catania, Italy
* Correspondence: mario.mattia@ingv.it

**Abstract:** The interaction between humans and nature dramatically reveals the role of sudden and destructive events in the progressive and never-ending trend of depletion of the territorial dimension of the Belìce Valley (Valle del Belìce, Sicily, Italy). If on the one hand a tragic event, such as the earthquake of 1968, that destroyed towns and villages in the Belìce Valley, represented a moment of pain and suffering for local communities and their territories, on the other, more than 50 years after the event, we are able to shed light on the reaction to the earthquake effects through an in-depth analysis of the heritage of the physical and immaterial rubble. Our research is aimed at framing, through special geovisual tools, the paths of this rebuilding process and to verify whether the "new" interaction of humans and nature has reached an acceptable balance. After introducing the concept of landscape and investigating some local manifestations within the Belìce Valley, we tackle the technical question of re-photography as a powerful and quick method for observing the territorial changes that occurred after the earthquake. This approach is based on the collection of historical photographs and, subsequently, onsite activities for the creation of a contemporary archive of images. The method used for comparing the images was that of re-photographic overlapping, a useful technique to compare different moments of the history of a landscape and to analyze the effectiveness of the process of rebuilding. Finally, this analysis introduces us to a new perspective where in our opinion, it is possible to frame some features of the Belìce Valley and some more general aspects that are useful for other territories hit by destructive events and having to face choices related to the future of their communities.

**Keywords:** repeat photography; re-photography; territory; landscape; visual geography; earthquake

**Citation:** Petino, G.; Napoli, M.D.; Mattia, M. Landscape, Memory, and Adverse Shocks: The 1968 Earthquake in Belìce Valley (Sicily, Italy): A Case Study. *Land* **2022**, *11*, 754. https://doi.org/10.3390/land11050754

Academic Editors: Mariano Barriendos Vallvé and Fabio Luino

Received: 4 April 2022
Accepted: 17 May 2022
Published: 20 May 2022

**Publisher's Note:** MDPI stays neutral with regard to jurisdictional claims in published maps and institutional affiliations.

**Copyright:** © 2022 by the authors. Licensee MDPI, Basel, Switzerland. This article is an open access article distributed under the terms and conditions of the Creative Commons Attribution (CC BY) license (https://creativecommons.org/licenses/by/4.0/).

## 1. Introduction

Understanding the territorial changes that occur over time, from a geo-historical point of view and, also and above all, as a consequence of events such as seismic ones, requires the preliminary introduction of the human-nature binomial through the concepts of territory and landscape. A typical definition of territory includes reference to the presence of a subject, the person who through their actions transforms a part of a geographical space. In the field of tourism studies and the tourism market, the concept was further implemented, delegating the territory the fundamental function of retaining the signs of the history of the communities that inhabited it and of maintaining a dense network of relationships and interrelationships among the many resources that distinguish it.

The landscape is the image of the territory, its visual rendering. According to several authors, the landscape is the union of the sensorial aspects of a place, both physical and human, falling under the direct observation of an individual, and constitutes the concrete synthesis of all those factors that led to the use of space by humans, according to a wide variety of responses to environmental opportunities [1,2]. The different ways of

responding to environmental opportunities and adversities have molded the use and design of the territory to take on various types of landscape, for example the great variability of the most "frequent" forms of agricultural or urban landscapes, thus defining the new «croûte technique à la surface du globe» (agglomerated crust on the Earth's surface) [3] constituted by the human superstructure of production of goods for subsistence and living, vital functions for humans. Going beyond the basic functions of human beings, landscape evolution is enriched with elaborative interventions by humans; still, the natural component will always be present, to a varying degree, to signify its inseparable role in human life itself. From these "combined works of nature and of man" [4], the concept of cultural landscape is derived. The "culture" variable is therefore added to the landscape forms, meaning that the landscape is enriched by the vision of the individual or of the communities.

If culture is a landscape variable, the cultural landscape is the staging of the culture of the individual or of the community where a certain common degree of culture is recognized and shared. As Sauer [5] writes, later reiterated by Vallega [6], "the cultural landscape is fashioned out of a natural landscape by a culture group. Culture is the agent, the natural area is the medium, the cultural landscape the result". The result, namely the staging of the territorial schedule, is a cultural action based simplistically on the combination of humans and nature. If humans build their cities and plow their fields, they do it following their own cultural, material, and immaterial pattern. The "sensible experience" of Hellpach [7] is probably strategic since it inserts the action of looking (the landscape of others), aesthetically connoting the experience and, consequently, inserting observers/users of the landscape into the equation and, therefore, a potential market. However, who chooses what to stage? Which and how many cultures, hegemons and subordinates operate in the same spaces as in the case of agricultural ones? Luginbühl [8] and Donadieu [9] attempt to answer this question and agree on the complexity of its vision and its components. This complexity arises from the choice, along paths of economic enhancement of the strengths of a territory, of some products over others according to "the landscapes to be exhibited". The selection of landscape images over others "induces inevitable transformations in the social composition of those who live in that area induced by the increase in property income", and when this happens in an unbalanced way, we could have the phenomenon of rural gentrification [10]. Consequently, each territory will have its own territorial configuration characterized, in broad terms, by objective as well as political and socio-economic aspects. The former comprise the different natural conditions and specific characteristics that derive from socio-economic and cultural choices and events inherited from the past. The latter includes aspects linked to the current territorial organization, dependent on elaborative choices of the territory still in progress or recently concluded and therefore still modifiable, in whole or in part. The human-nature binomial referred to also includes the "nature" component as an essential component of human action, but also as an autonomous agent, often in contrast with the human project, to the point of devastating it both in a material and immaterial sense. Therefore, nature is an agent, but also a medium and a result. This is the case of the earthquake in the Belìce Valley in 1968. It is certainly a natural phenomenon which by manifesting itself, has changed the actions of humans. The earthquake deprived the valley of its territorial specificity. The reconstruction has transformed the natural event into a social event as well, and this led to an identity crisis. The collective action, often multidirectional, uncoordinated, and frequently late, produced cultural landscapes that are difficult to interpret. The re-writing the spaces made by humans has produced deep wounds, some of which are more devastating than the natural event that caused them, due to the decisions taken and the prolonged duration of recovery.

One of the ways to observe these changes is through the cultural stimuli that come from the free forms of art or the more or less codified ones of science [11,12]. It is in cataloging catastrophic events such as this and their aftermath that the re-photographic exercise proposed here finds its perfect application, i.e., an attempt to tell the ways of inhabiting the territory even when nature poses sudden, devastating obstacles, completely disinterested to human projects.

More than 50 years later it may be difficult to identify the original pattern of territorial action. Thanks to the photographic archive of the newspaper L'Ora (acquired by the Sicilian Region and kept at the Sicilian Regional Library "Alberto Bombace" in Palermo) and observation in the field, we contribute to the debate on the conservation of the memory of places and possible perspectives, creating an intermediate "photograph" that preserves what has not yet been lost. The final product of the re-photographic practice becomes the 'witness' to be passed on to the local communities in order to recover their identity through bottom-up participation tools such as the establishment of ecomuseums, one of the most successful forms of "staging" the heritage that cannot be contained within traditional museums except in dematerialized form. Re-photography, therefore, will be used here as a medium for reading the changes in the territory also by those who, despite living in those places, do not know their genesis.

## 2. Study Area

### *2.1. The Belìce Valley*

The Belìce Valley is located in the western part of Sicily, shared between the territories of the three former provinces of Palermo, Trapani, and Agrigento. It is a predominantly hilly area and coincides broadly with the hydrographic basin of the Belìce River, which covers an area of almost a thousand square kilometers; the 94 km long river course (the 5th longest river in Sicily) originates in the municipality of Poggioreale at the confluence of the Belìce Sinistro and Belìce Destro (Figure 1). The valley is geographically divided into an "upper" and "lower" valley; there are 23 municipalities whose territory is partly or totally attributable to the river basin, almost all characterized by a small surface and low population density. Table 1 shows the demographic evolution of the most severely damaged municipalities by the earthquake, on the basis of the Mercalli scale (between VIII and X).

**Table 1.** Demographic evolution of the municipalities most affected by the earthquake. Source: ISTAT Population Census.

| Cities/Years | 1861 | 1911 | 1961 | 2011 | 2020 |
|---|---|---|---|---|---|
| Gibellina | 5419 | 6646 | 6410 | 4264 | 3836 |
| Montevago | 3122 | 3113 | 3008 | 3015 | 2734 |
| Partanna | 12,012 | 16,174 | 13,011 | 10,854 | 10021 |
| Poggioreale | 3338 | 3074 | 2698 | 1534 | 1394 |
| Salaparuta | 3555 | 3015 | 2943 | 1721 | 1596 |
| Salemi | 13,035 | 20,549 | 15,364 | 10,871 | 10,114 |
| Santa Margherita di Belìce | 7474 | 8494 | 7811 | 6544 | 6104 |
| Santa Ninfa | 6486 | 7522 | 5826 | 5095 | 4842 |
| Vita | 3911 | 5474 | 3748 | 2139 | 1819 |
| Camporeale | 3169 | 5749 | 6093 | 3448 | 3029 |
| Contessa Entellina | 3364 | 2117 | 2669 | 1865 | 1536 |

The main economic resource is agro-food production and the cultivation of the olive tree followed by the cultivation of the vine. Among the other crops making up the landscape mosaic, it is worth mentioning the yellow melon which was recently rediscovered and promoted through festivals.

The landscape of the Belìce Valley tells many things and, among these, the slow process of de-territorialization as an effect of the depopulation. However, to think that it was the 1968 earthquake that triggered the population exodus is a mistake; according to some initial observations, it is possible to discern the dynamics against the trend of what we have always believed that they were the dynamics of "crisis" increasingly originating in the absence of specific services and attractiveness in the work sector and in the use and "spending" of free time.

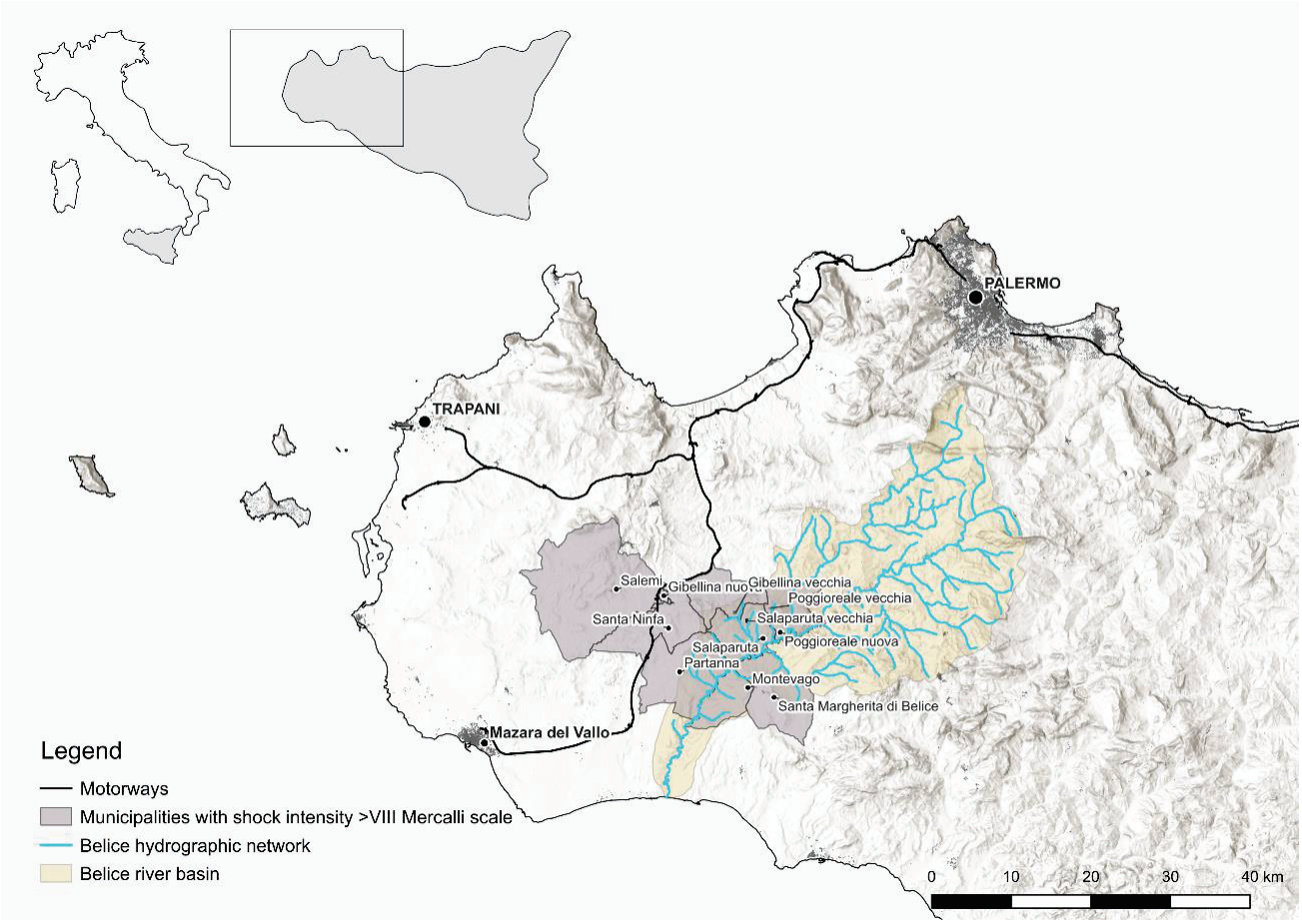



**Figure 1.** Framing of the area. Source: ISTAT data.

Two tragic "big events", such as the two world wars, had already affected the Italian territory, causing a significant loss of population. The Italian industrial golden age (1958–1963) continued the depletion of the population and investments toward other areas of the country, consequently subtracting vitality, both in the narrow and broader sense of the term, from less interesting areas and geographically more distant from the economic centers of Italy. Already before the 1968 earthquake, depopulation in the region was well underway (Figure 2). In any case, the focus of this work is on the effects of the 1968 earthquake on the Belìce Valley, although the depopulation process started in the beginning of the 20th century (and that can be extended to many other areas of Sicily) and deserves its own specific analysis.

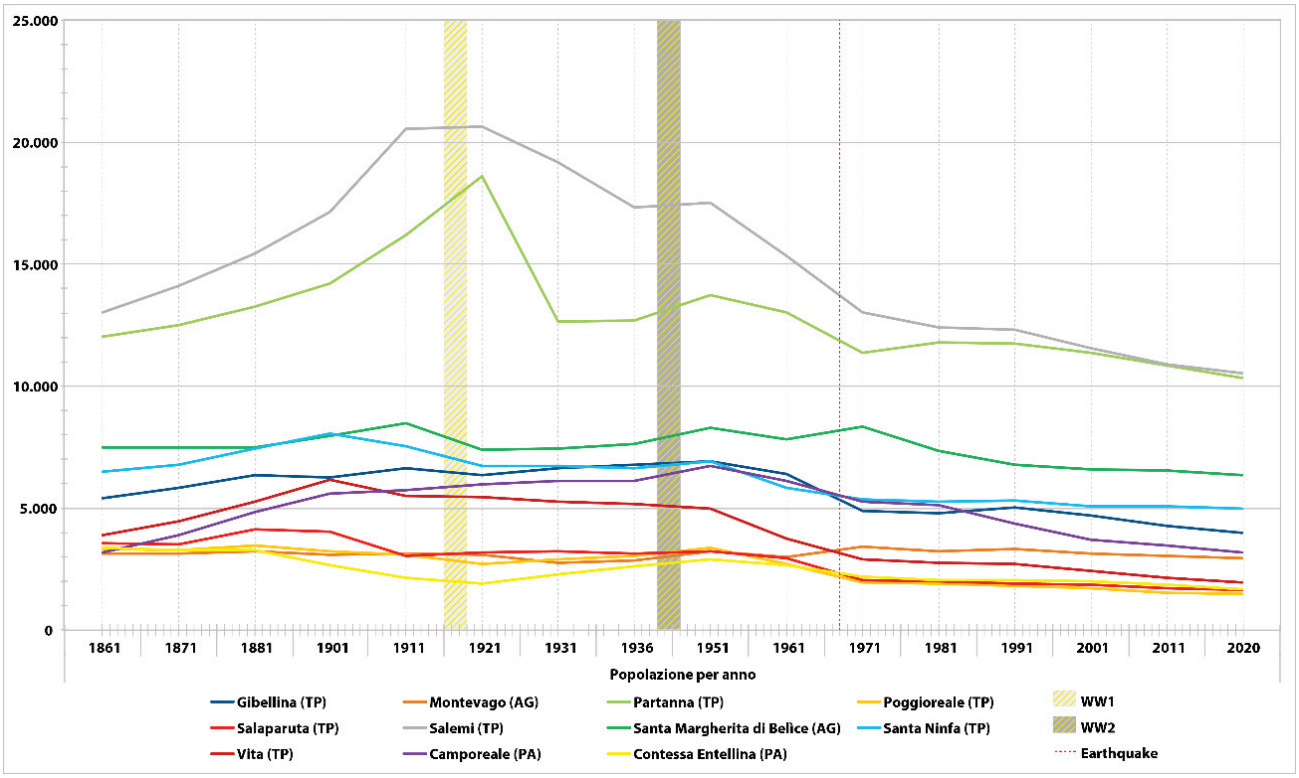



**Figure 2.** Population trends and relationships with major historical events (1861–2020). Source: ISTAT data.

From a geological point of view, the Belice Valley area in SW Sicily represents the westernmost part of the Sicilian Fold and Thrust Belt (hereafter, SFTB, Figure 3A), a south-verging contractional belt segment of the wider Appennine-Maghrebian orogenic system, the suture zone between the colliding Africa and European plates [13,14]. The SFTB is the result of the Neogene-Quaternary tectonic processes during which a pre-orogenic configuration (formed at that time by both platform and open-shelf rock series, i.e., the African continental paleo-margin) has been progressively shortened to form a wide thrusting system. The westernmost segment of the SFTB (i.e., the studied area), consists of NE-SW trending structural domains composed of several, thrust-bounded, foreland-verging tectonic blocks (Figure 3B) at present interposed between two extensional domains, the Tyrrhenian Basin to the north and the stretched Sicily channel region to the south (Figure 3A). Deep seismic explorations in the area [15,16], revealed the structural architecture of SW Sicily as formed by two overlapping thrust wedges separated by a regional decollement. Accordingly, the seismotectonic processes that involve this region appear to be related to ongoing compressional activity along deep-seated, high-angle thrust contacts that at a shallower crustal level, display flat-ramp geometries of deformation.

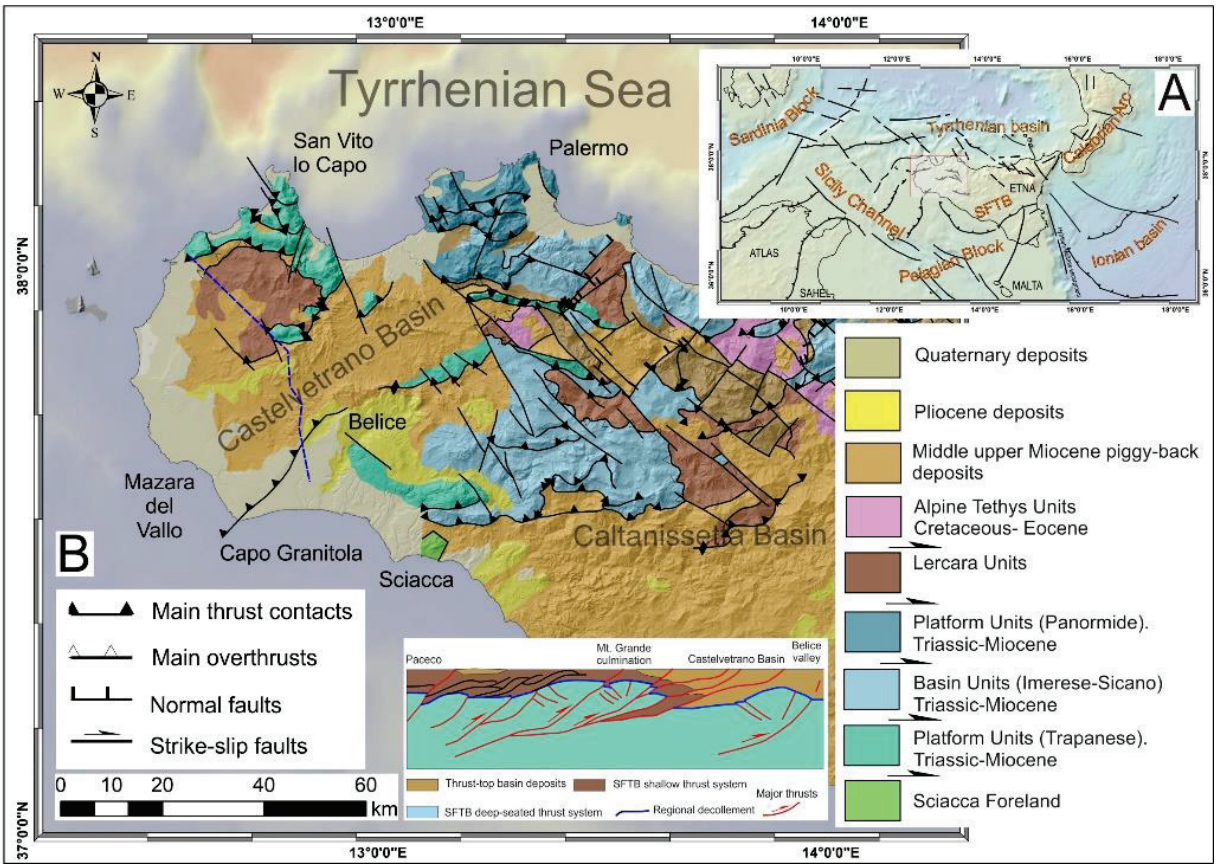



**Figure 3.** (**A**) Tectonic model of the Central Mediterranean region where SFTB occur. Lines represent the main faults. Lines with triangles represent the main contractional tectonic features. (**B**) Geological sketch map of central western Sicily (from Finetti et al., [17] modified) showing the main tectonic units and contacts, the latter consisting mostly of thrust and strike-slip faults. From Barreca et al., [18], modified.

### *2.2. The 1968 Earthquake*

At 2.01.09 (GMT) on 15 January 1968, a wide area of western Sicily was hit by a 6.41 Mw earthquake [19–23], the main shock of a high frequency seismic swarm (more than 300 events) that shook the region for almost a month (from 14th to 25th January 1968) (Figure 4). The disastrous event, the strongest seismic event recorded in Western Sicily in historical time, was preceded by a series of minor events (on 14 January with $4.84 < Mw < 5.1$) and followed by several aftershocks. Among these, the events on the 16 and 25 January reached the magnitude of 5.45 and 5.37, respectively [19–24]. The seismic event caused about 370 deaths and severe damage to 14 villages facing the Belìce River valley. Four of these (Gibellina, Poggioreale, Salaparuta and Montevago—see Figure 1) were completely destroyed (Figures 5 and 6). Ground effects related to the 1968 earthquakes were generally scarce and occurred mainly at the northern limb of Belìce syncline and consisted of moderate landslides, mud upraising along fractures and escape of fluids [25,26]. Sand blows and fissures related to liquefaction phenomena were observed along the Belìce River alluvial plain [27].

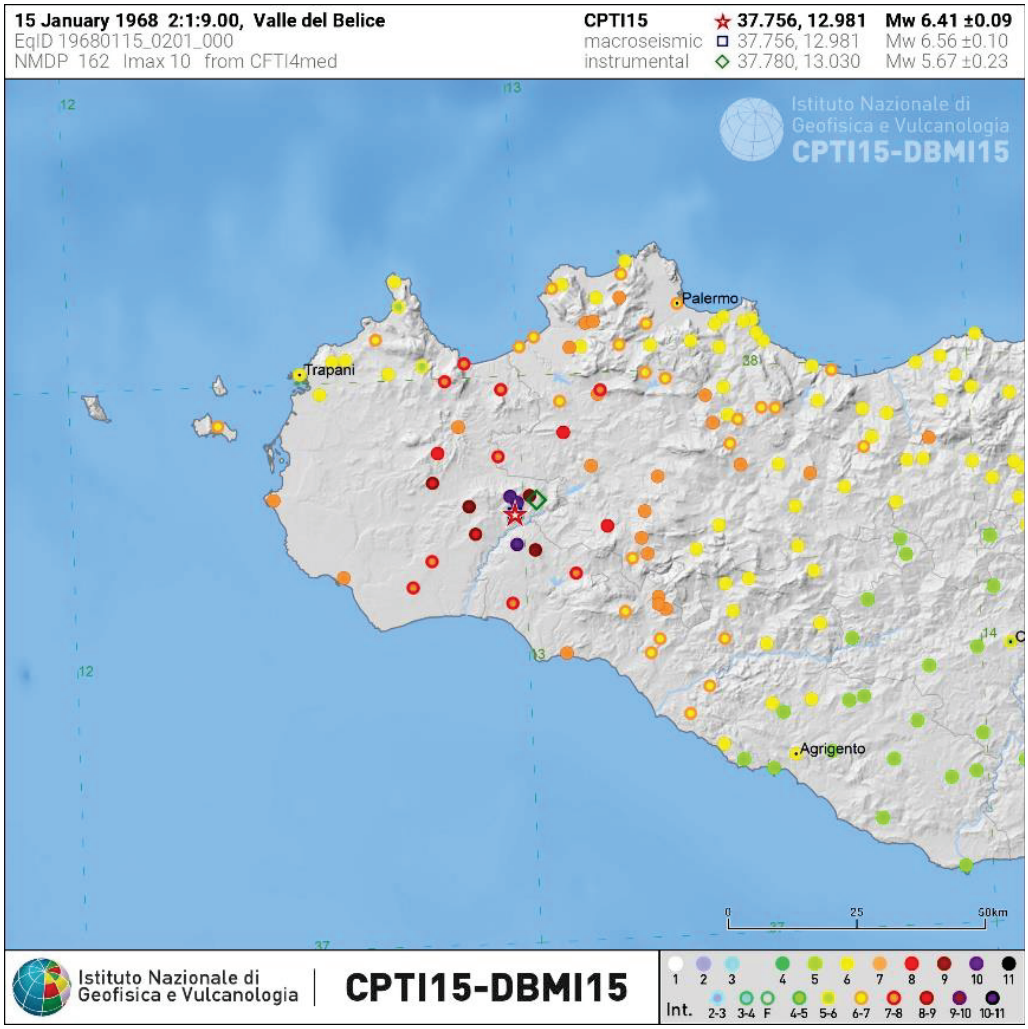



**Figure 4.** Seismic intensity map of 15 January 1968 Belìce earthquake from INGV CPTI (Catalogo Parametrico dei Terremoti Italiani) ver. 4.0 [21–23].



**Figure 5.** Montevago after the earthquake. Photo: Archivio de L'Ora, Biblioteca Regionale Siciliana "Alberto Bombace", Palermo.



**Figure 6.** Intervention of the early volunteers. Photo: Archivio de L'Ora, Biblioteca Regionale Siciliana "Alberto Bombace", Palermo.

### *2.3. The Belice Valley after the Earthquake*

A completely new dynamic affected the entire Belìce Valley after the earthquake: the stark reality of the destruction of entire urban settlements followed by the top-down rewriting of future local identities, which accelerated the processes of de-territorialization [28]. The ties between large sections of the population, who chose to look elsewhere for better living conditions, were severed from their territory, so to speak. The strategy of the government bodies in the wake of the earthquake seemed to facilitate the population decrease in the Belìce Valley as if less population would equal less expenditure of economic resources in the reconstruction and support of local populations (Figures 7 and 8).




**Figure 7.** "Flying" ticket offices of the FF. SS. (Italian railway company), 22 January 1969; free train tickets were available for the entire population of the Belìce Valley for every destination. Photo: Archivio de L'Ora, Biblioteca Regionale Siciliana "Alberto Bombace", Palermo.




**Figure 8.** Refugee departures from Palermo station, 27 January 1968. Photo: Archivio de L'Ora, Biblioteca Regionale Siciliana "Alberto Bombace", Palermo.

Among other things, the earthquake led to the foundation of new cities, such as the "new" Gibellina (about 10 km from the original site and rebuilt in a part of the village of Salemi territory), the "new" Poggioreale (3 km away from the original site) and the "new" Salaparuta (also 3 km away from the original site), to which it is possible to add Montevago. The choice of building new settlements rather than directly intervening in damaged buildings has distant and complex roots. First of all, following the earthquake of 1693, it was preferred to relocate the most affected centers; the city of Noto was thus moved downstream from the original position for better accessing the site and to reduce risk factors. Similarly, without neglecting the possible presence of less legitimate interests, in the case of reconstruction in the Belìce Valley, the first legislative interventions suggested proceeding rapidly with the demolitions and with the abandonment of areas considered geologically unhealthy [29], identifying the most suitable areas further downstream. However, the de-localized reconstructions mark and add further wounds to those not yet or not at all healed as a result of the earthquake.

For each of them it is possible to carry out the complicated task of evaluating the results ex-post in social, economic, and environmental terms. What happened since 1970, the year of the refoundation of Gibellina starting with the construction of the Chiesa Madre (Figure 9), can be read in history books, a history of errors but also that of farsightedness: it is hard to forget the town planning variations that, from 1979 to 1996, were necessary to overcome planning errors [30]. At the same time, it is important to point out the "vision" of Ludovico Corrao (mayor from 1970 to 1994) of a city of art, a city that would have risen thanks to the "gift" of an impressive number of land art interventions that have delivered a city tailored to social networks or, in modern terms, was "instagrammable".

Instead, what happened in Poggioreale and Salaparuta is something different. If we remove Corrao's vision from the history of Gibellina, perhaps we have summarized what really happened in these two most unfortunate centers. The alienating architectures still present in both municipalities remind us of impressive investments of money on pharaonic structures, as in the case of the square of Poggioreale (Figure 10), or the urban center with no identity of Salaparuta (Figure 11) of which only a direct, personal, and immersive experience can enable us to understand.



**Figure 9.** Chiesa Madre, Gibellina, project by Ludovico Quaroni (1970). Photo by the authors, Gibellina 2020.



**Figure 10.** Piazza Elimo, Poggioreale nuova, project by Paolo Portoghesi (1988). Photo by the authors, Poggioreale Nuova 2020.

From a cultural point of view, the "modern" Belìce Valley took its first steps in the 1980s. For this reason, we must go back to the new Gibellina which had already taken shape and in which the primary infrastructure works, carried out first, definitively realized the drawing developed by the technicians of the Institute for the Development of Social Housing (ISES) [30].



**Figure 11.** Salaparuta city center. The "new" Chiesa Madre is visible in the background. Photo by the authors, Salaparuta 2020.

As the cultural excitement around the figure of the sociologist Danilo Dolci waned, after he had animated the hearts and minds of the inhabitants of Belìce long before the earthquake, accompanying them in the struggles for agrarian reform and for a solution to long-standing water problems, Gibellina was to become the catalyst center of a cultural and creative turn, forerunner of the attractive use of art and culture and for a long time incomprehensible to the inhabitants themselves. To guide the cultural turn, first of Gibellina and of the Valley immediately afterwards, was Ludovico Corrao, another leading figure in the area, who continued change and, to the present day, provided us with a path of re-territorialization that is not yet fully accomplished but which places Gibellina in both art history as well as in history books. What the mayor Corrao argued was that the reconstruction should also have gone through new identity processes and liberation from welfare logics; to do this it was necessary to lay the foundations of a local development capable of culturally and economically rooting what would have been the new settlement [31]. Corrao's new (territorial) identity was a mix of essential services and works of art, the latter with the dual function of making beautiful what could usually be considered "urban" and serving as an attractor of new economies, such as tourism. While the city of Gibellina was enriched, thanks to imposing urban plans and with the help of great artists, Corrao called upon Alberto Burri to intervene on the ruins of the original site; thus, between 1984 and 1985, the Cretto was created, one of the most important site-specific land art works in the world which by pouring concrete, incorporated the rubble of the old Gibellina, replicating its structure and urban layout. The Cretto and the new Gibellina (Figure 12) created the metaphorical container, both inside and outside the city, for Ludovico Corrao to fill. Overcoming local criticisms and dislike, he created the first season of the Orestiadi in 1981, an international festival of arts that year after year, for 40 seasons, brought world-class personalities to perform in bagli[1], squares and amphitheaters in the new Gibellina and the Cretto. The scale of the event has extended in time and space, even outside the city limits, stimulating the hospitality industry in the towns of the Valley.

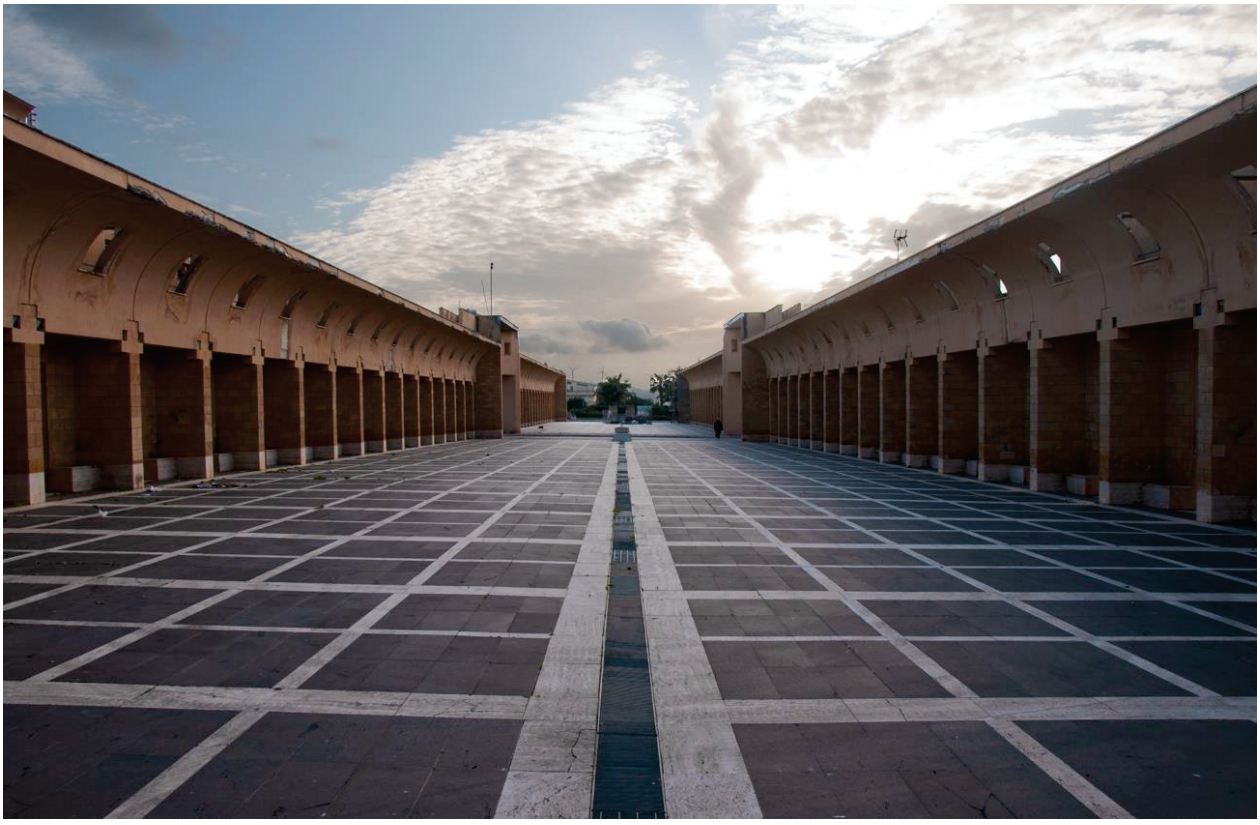


**Figure 12.** Sistema delle Piazze, Gibellina, project by Franco Purini and Laura Thermes (1990). Photo by the authors, Gibellina 2020.

## 3. Methodology

The practice of re-photography, widely used in geographical, geological, anthropological, and natural science studies, is useful to compare the changes in any type of landscape over time. If this practice came about with photography itself, its consolidation as an analysis technique began in the early 1980s with Rogers' research on the use of document comparison through photographic techniques [32,33]. From that moment on, thanks also to the introduction, diffusion, and ever-increasing quality of digital cameras, the adoption of the photographic technique took place with increasing frequency, leading to the enrichment of methodologies and fields of use.

At the time of its introduction, photography replaced painting in the role of documenting data, amplifying the skills of the modern scholar, the evolution of the 'typographic man', through the descriptive potential of the image and transforming it into a 'graphic man' [34]. While painting shifts its field of application to the representation of inner worlds and creative processes, photography (still) seems the perfect tool to faithfully reproduce reality, so the documentary spirit immediately supports the development of the technique. This desire to document includes war reports by Roger Fenton (Crimean War, 1854–56) or Matthew Brady (American Civil War, 1861–65), for example, but also photographic surveys for the construction of large infrastructures, as in the case of the Central Pacific railway line (Sacramento-Odgen, 1861–85) whose realization was documented by Alfred A. Hart, or the later photographic campaigns (1935–44) promoted by the American Farm Security Administration to understand and contrast effects of the Great Depression and worked on by great photographers such as Walker Evans and Dorothea Lange, among others.

*Re-Photography as a Territorial Documentation Technique*

The first application of re-photography as a scientific instrument is an evolution of photogrammetry, and is attributed to the German glaciologist Sebastian Finsterwalder who, at the end the nineteenth century, conducted a photogrammetric analysis of the Tyrolean Alps [35]. The comparison between images taken after a year at photographic stations that remained in the same position allowed him to observe the transformation of the glaciers. Later, the technique was adopted to detect geomorphological modifications of places of naturalistic, cultural, and/or tourist interest [36], to set up ecological surveys of natural habitats [37], to detect changes in the landscape and urban settlements [38,39], up to the first major projects financed by public and private institutions, such as the Carnegie Institution of Washington, which allowed the collection over time of a very consistent corpus of images [40] (see, for example, the collection of the Desert Laboratory, founded in 1903, now part of the University of Arizona and active with dozens of projects in progress)[2].

Beyond the technique and its rigorous use in the scientific and statistical field, the comparison of images of the same subject over time has subsequently taken on a cultural value through the approach of a group of photographers, mostly Americans, who renewed the genre of landscape photography. In the mid-seventies, in fact, there were two important experiences for the change in pace in landscape photography: on the one hand the publication of "The New West, Landscapes Along the Colorado Front Range" (1974) by Robert Adams [41], on the other, the organization in New York of the exhibition "New Topographics" (1975) [42] with the participation of a large number of photographers. The American landscape of the first half of the century, for example the one shown through Ansel Adams' copious body of work, is thus revised and deromanticized, made more real and less idealized by directing the gaze, and the shots, toward what might not necessarily be positive changes in the American territory: urban expansion, infrastructure, and decay—all changes due to human action and inaction [43]. From then on, the cultural approach to the photographic technique developed in Mark Klett's work[3], to which is due, among other things, the adoption of the *re-photography* contraction rather than *repeat photography*, in the French Mission DATAR[4] or in the work of Camilo Jose Vergara[5], among others.

The photographic technique is today enriched with digital capture and display systems that amplify the possibilities of image production and comparison, accelerating all research and subsequent analysis phases. Then there are also all those devices (satellites, drones) and software (GIS, Google Earth) that allow previously impossible points of view. As mentioned, the use of photography has allowed, since the end of the nineteenth century, the comparison of different types of landscape and, today more than ever, it appears to be a very useful tool to verify the state of the environment and the resilient capacity of areas, for example those affected by disasters (earthquakes, fires or hydrogeological disasters).

More than 50 years after the earthquake in the Belìce Valley and starting from the rich archive of the newspaper L'Ora[6], now acquired by the Sicilian Regional Library "Alberto Bombace" of Palermo, we had the opportunity to observe the images taken in the villages of the Valley immediately after the earthquake and in the following months and years; a few images from the Archive made before 1968 (i.e., Figures 16 and 19), some of which are in color, are an exception. The places devastated by the shocks and documented by the many photographic reports were, by default, already fragile places due to the absence of schools, hospitals, hospices, and roads, due to family diasporas caused by emigration and persistent poverty [44]. Among the many images, we chose to focus on those of the hardest hit places, i.e., those where the force of the earthquake had made itself felt the most: Gibellina, Poggioreale, Salaparuta, Montevago, Santa Margherita di Belìce, Partanna, Santa Ninfa, and Salemi. Before physically going to the Valley, we therefore carefully studied the images and information in our possession to prepare an itinerary along pre-established stages, identifying in the images the fiducial markers to look for through geographic internet services such as Google Maps, Open-StreetMap and Google Earth (Figure 13). The photographic campaign was carried out in the same period of the year in which the earthquake occurred (January 1968–January 2020), searching for the places where the

selected photos were taken. Among these, in addition to those of the damaged centers, there were many images of the sites where the emergency shelters had been prepared, namely the tent villages and, later, the barrack camps[7], destined to remain as signs of a never-ending emergency. In this way, we started from the most easily traceable places due to the presence of buildings or recognizable elements, then identified the less immediate locations, thanks to the intersection of data and profiles of the landscape (Figures 14 and 15).

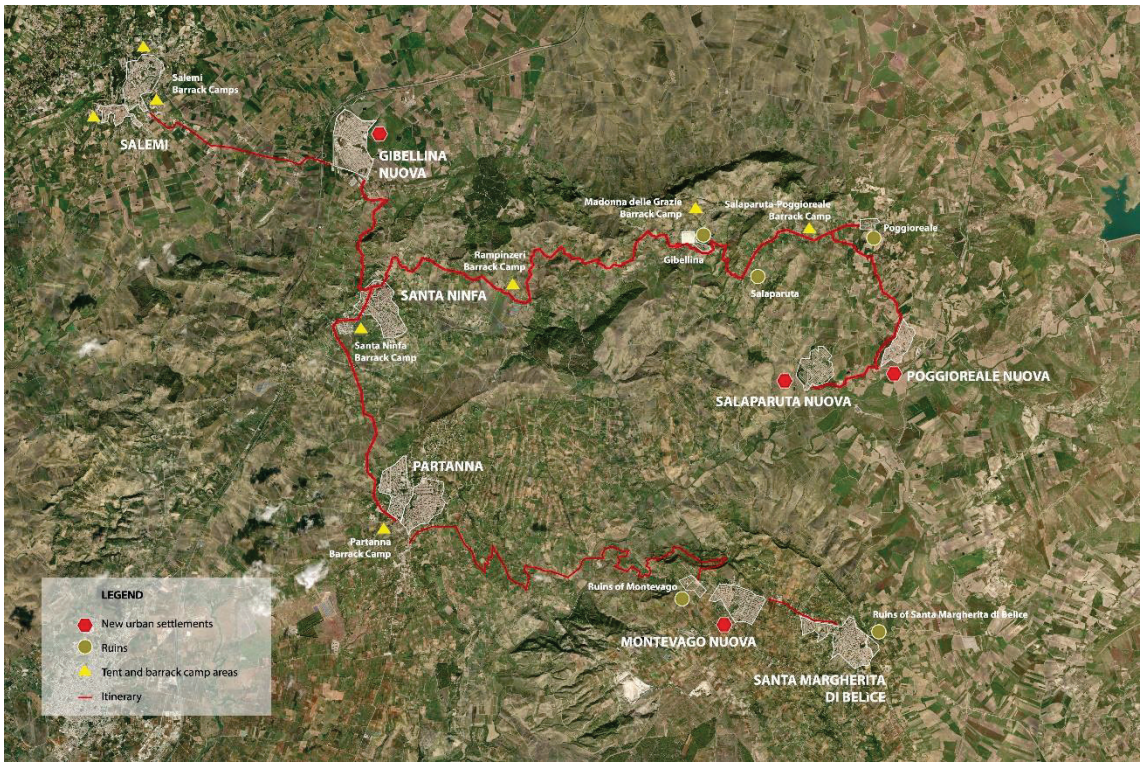



**Figure 13.** Selected locations and itinerary. Source: our elaboration on Google base map.



**Figure 14.** Old Gibellina destroyed by the earthquake. Photo: Archivio de L'Ora, Biblioteca Regionale Siciliana "Alberto Bombace", Palermo. Photo by the authors, Gibellina 2020.



**Figure 15.** Cretto, project by Alberto Burri (1984–89, completed in 2015). Photo by the authors, Gibellina 2020.

## 4. Results: The Application of the Re-Photographic Method in the Belìce Valley

The center of Gibellina, seen from Provincial Road 5 Gibellina-Salaparuta in the aftermath of the earthquake, appears as a dusty pile of rubble distributed along the ridge between two small hills (Figure 14). The comparison with the contemporary image partially restores the feeling one has when visiting the places of the old center[8]: Alberto Burri's artistic intervention, visible from a great distance, is a large funeral shroud that covers most of the site, holding the ruins of the destroyed buildings under it; it is a veil that does not erase the wound but provides dignity, incorporating the object and the place in a work of art that remains there and continues to confront the landscape and communities, representing "the deep structure of the relation between human and space" [45] (Figure 15).

What has changed? The place, previously alive and vital, has remained frozen in a moment of half a century ago; the roads have remained unchanged; the same applies to the profiles of the mountains on the horizon, with the exception of the natural landscape that has continued to live and has taken over its spaces. The "Gibellinesi" (inhabitants of Gibellina) were re-located about 10 km away, within "an immoderate, obstinately euphoric reconstruction project" [46] (Recalcati, 2018) that seems to have almost been created specifically for the social approach of contemporary photography.

Referring to the reinterpretation of the landscape proposed by Klett, Vergara, and others, the approach we adopted intended to propose not only a combination but also an image processing. In particular, through the overlapping of archive and contemporary images, we obtained photographic palimpsests that contribute to the narration of a story of a place and a community, of an event, of conditions of continuity or discontinuity between two moments [47]. Past and present coexist starting from elements that have survived changes due to nature and man but, by adopting Munteán's vision which implies Benjamin's theory of ruin[9] as an allegory of history, the contemporary image has almost a cathartic function since it "unlocks the optical unconscious and pours its contents back into the landscape", while the historical image becomes an allegory of transience and defeat, depending on whether you see it from a natural or artificial point of view [47]. In this sense, among Mark Klett's projects, After the Ruins[10] is particularly interesting since it combines the images of San Francisco taken immediately after the 1906 earthquake and those re-photographed a hundred years later, allowing precise reflections on the sense of fragility and temporariness and, as one would say today, of the resilience of places [48]. In Figure 16, for example, two images of Santa Margherita di Belìce: some pieces of an ancient color photo of the current Piazza Matteotti, prior to 1968, are superimposed on a contemporary image. The re-photographed buildings are Palazzo Filangeri Cutò (on the

left) and the former Chiesa Madre (on the right), today headquarters of the Municipality and of the Gattopardo Museum in the first case, of the Museum of Memory in the second. The first structure has undergone very few changes, while some parts of the second have been 'saved', mainly visible inside the current museum; the rest was instead rebuilt while maintaining a volume that allows, even in this case, to remember the original religious building. Additionally, in this case, at the moment of our photographic survey, the town seemed almost uninhabited and the only figures that populate the image are those present in the photograph of the past. Because of the depopulation of the Valley, the places are now in fact oversized compared to the real people living there.



**Figure 16.** Re-photographic overlap between Cathedral and Palazzo Cutò (Photo: Maggio for L'Ora, Archivio de L'Ora, Biblioteca Regionale Siciliana "Alberto Bombace", Palermo) and Piazza Giacomo Matteotti (Photo by the authors, Santa Margherita di Belìce 2020).

Figure 17 overlaps a historical image of some men waiting in front of the municipal offices located inside the barracks of the Salaparuta Village, along Provincial Road 5, and the current photovoltaic panels installed on the concrete platforms that once served as a base for the same barracks. On the ground are still traces of makeshift paving used to limit the dustiness of the walkable sections, while the hills in the background repeat the shapes and vegetation exactly, as if not a minute had passed. Likewise, there seems to have been no time lag between the overlapping images in Figures 18–20: in the background are the color photographs taken during our survey, to which we added the black and white images preserved in the archive of L'Ora. In Figure 18, after 35 years the rubble of Montevago still remained and, in the meantime, the inhabited center was moved slightly, preferring to abandon the buildings and leaving them as an open wound; we see other ruins in Figure 19, with the superimposition of a moment of daily life in Santa Margherita di Belìce prior to 1968. Instead, in Figure 20, the reconstruction introduces new forms in the recovered center of Santa Ninfa.



**Figure 17.** Villaggio Salaparuta, people at the temporary barrack camp town hall (Photo: Scafidi for L'Ora, Archivio de L'Ora, Biblioteca Regionale Siciliana "Alberto Bombace", Palermo) and photovoltaic system in the Salaparuta area (Photo by the authors, Salaparuta 2020).



**Figure 18.** Montevago, 14 January 1985 (Photo: Archivio de L'Ora, Biblioteca Regionale Siciliana "Alberto Bombace", Palermo) and Ruins of the Chiesa Madre (Photo by the authors, Montevago 2020).



**Figure 19.** Santa Margherita di Belìce (Photo: Scafidi for L'Ora, Archivio de L'Ora, Biblioteca Regionale Siciliana "Alberto Bombace", Palermo) and Ruins of the Chiesa Madre (Photo by the authors, Montevago 2020).



**Figure 20.** Santa Ninfa. Mayor Bellafiore in front of the Casa del Popolo under construction (Photo: Archivio de L'Ora, Biblioteca Regionale Siciliana "Alberto Bombace", Palermo) and Casa del Popolo (Photo by the authors, Santa Ninfa 2022).

## 5. Discussion: Digital Territories and Geographical Readings

The digital transformation of the territory, through photography, was necessary for the diachronicity of the events to be compared: year zero, that of the 1968 earthquake, from which we drew from a large photographic archive, and the field work from the 2020 re-photographic campaign to detect the most recent territorial configuration. Among all the photographic material of the past, a selection was made of the documentation concerning the municipalities most affected by the earthquake. Some photographs were then selected that had specific and useful characteristics for research, i.e., well-identified and recognizable landscape elements, such as reference points still intact or naturalistic details that have remained almost unchanged, considering at least two types of problems: time, more than fifty years having passed, and the event, i.e., the earthquake, a particularly active action in changing the order of things.

The results of our analysis left us perplexed. On the one hand, we observed mechanisms of economic recovery essentially linked to the oenological sector, and timid, although lasting, attempts to build a territorial cultural armor, even if limited to some areas; however, the most important consideration is linked to a certain sense of "emptiness". Empty cities, regardless of the reconstruction paths undertaken, abandoned or museified ruins, empty countryside or with little crop variability, some wind farms and some photovoltaic systems, but overall we could say an empty territory. More than one question arises about the fate of the Belìce Valley. The re-photographic exercise completed here, more than advancing new hypotheses about the changes underway and the future of the area, allows us to make brief reflections that corroborate what can still be deduced through direct observation. A wider re-photographic plan over time, as also hoped for by Klett [48] regarding his project on San Francisco, would certainly allow an accurate reading of the territorial and cultural processes, while although these 50 years have been interminable for the local communities, they are probably too short a period of time to be able to read the changes in a territory that seems to have remained "frozen".

Re-photography has often been used in geomorphological [35–39] or sociological [43,48,49] investigations. The availability of digital technologies has now naturally spread the practice of re-photography, both for the part concerning the initial research and for that linked to the production of images (immediate verification of the results) and to the post-production (overlapping and processing). However, if today re-photographic projects are ever more numerous, including those linked to seismic events[11], these are mainly based on the layout and on the platforms that enable an interactive comparison of the images. The limits of this visual approach, therefore also of this work, could be linked to the ability of photography, and of re-photography, to detect qualitative changes but limit quantitative ones, unless a rigid analytical practice has been followed in all phases [50]; at the same time, it is a tool that allows an effective narrative restitution of physical and social phenomena [49].

All the studies done so far, including our contribution, suggest museifying what remains (the ruins), or even better ecomuseifying[12], i.e., making them available to the affected communities, so that they can participate with and contribute in their strengthening, protection and enhancement. In fact, starting from the assumption that treating the territory, the community, and the heritage individually is not useful, then only through the practices of active citizenship and considering the heritage as a common resource, can it be said that the territory as a whole coincides with the community itself, with its own history and culture—a history and culture also shaped by adverse shocks, such as an earthquake and a pandemic, to which one can succumb or react, but whose memory must also be preserved as a performative instrument [51].

## 6. Conclusions

From a cultural point of view, the "modern" Belìce Valley took its first steps in the 1980s. From an economic viewpoint, it is possible to trace a timid rebirth in the 1990s with the extension of viticulture and the birth of cooperative wineries that received an impulse for their development from the earthquake itself; the two aspects would finally meet only

a few years later. Despite these steps, even if diluted over time, the problem of "delay in development" still seems present. More than fifty years have passed since the earthquake devastated the area, but the socio-economic delay of large parts of this territory is still evident. The persistent depopulation trends accentuate the sense of "emptiness", as if to underline the useless, if not damaging, top-down reconstruction path carried out with various economic and political interventions.

The 'museification' of part of the ruins or the construction of de-historicized "villages" has not led to much more than some visits by tourists or land art enthusiasts. The experience of viticulture is important but most likely it will not be enough to draw new economic and cultural trajectories capable of changing the fate of the Valley. From the cultural point of view, the last two editions of the Orestiadi, despite the pandemic, which constitutes another adverse shock, would suggest that a part of the territory wants to live, produce, and stand out.

In this case, the re-photography shows first of all the inhomogeneity of the interventions carried out[13]: on the one hand the unique case of Gibellina (which coincides with Ludovico Corrao's vision) of a "civic art factory" [52], of a place in the making that also confronts "the eventual decline of the great interpretative plots of modernity" [53]; on the other, a series of similar (but far less successful) attempts to create new centers, built starting from precise urban planning and safety provisions, but which remained mostly anonymous. In addition, the abandonment of the ruins has frozen the landscape of the past, perhaps leaving it as a warning, perhaps as a sign of the inability to take care of it, thus leaving nature the task of erasing them completely. In this sense, the re-photographic approach can help to preserve and re-propose an archaeology of post-seismic phenomenology through a comparison that allows us to observe the changes (or the perpetration) of a status; in this way, memory could be preserved, showing the signs still visible on the territory, in line with the conservation objectives of the historical, cultural and landscape heritage of the ecomuseum networks.

Finally, another aspect that must be considered is the possibility to use re-photography as a tool to improve risk perception and resilience. In the Belìce Valley, up to the 1968 earthquake, a low estimated seismic risk induced no earthquake disaster mitigation measures and no disaster management. From this point of view, the immediate impact of images where the effects of an earthquake are superimposed on old urban or natural environments could be usefully used in schools and public offices to enhance the communities' earthquake risk perception and resilience. Additionally, the results of the re-photography can be integrated in earthquake vulnerability assessments that help identify the most vulnerable areas of the Valley, based on past damage. These kinds of evaluations are the first steps toward understanding the seismic risk in Belìce Valley, and to elaborate and subsequently implement risk mitigation strategies.

**Author Contributions:** G.P.: Conceptualization, Data curation, Methodology, Writing—Original draft preparation; M.D.N.: Conceptualization, Visualization, Writing—Original draft preparation; M.M.: Conceptualization, Data curation, Supervision, Writing—Reviewing and Editing. All authors have read and agreed to the published version of the manuscript.

**Funding:** This research received no external funding.

**Institutional Review Board Statement:** Not applicable.

**Informed Consent Statement:** Not applicable.

**Data Availability Statement:** Not applicable.

**Acknowledgments:** Although the conceptual framework of the study was developed jointly, Gianni Petino drafted paragraphs 1, 2 (Sections 2.1 and 2.3) and 5; Maria Donata Napoli paragraphs 3 and 4, and Mario Mattia the paragraph 2 (Sections 2.1 and 2.2) and 6. The authors thank J. S. Wilson, Indiana University—Purdue University Indianapolis (USA), and Daniel Knudsen, Indiana University Bloomington, for revisions and suggestions and Stephen Conway for the revision of English language. The archive images are kept in the Sicilian Regional Library "Alberto Bombace", partner of the "Belìce

+ 50" Project which is being developed with the National Institute of Geophysics and Volcanology (INGV), the Academy of Fine Arts of Palermo and the University of Catania. This study was partially supported by the Departmental Research Plan Fund (PIA. CE. RI.) 2020–2022, University of Catania, entitled "Local development and community between environmental, social and health emergencies: communication, law, political thought and territory to the test of SARS-CoV-2", and from the research project "Progetto Belìce + 50" in collaboration with the Academy of Fine Arts of Palermo, the National Institute of Geophysics and Volcanology (INGV) and the Sicilian Regional Library "Alberto Bombace" of Palermo, for the collection, analysis and interpretation of data and in the decision to submit the article for publication. The authors also thank two anonymous reviewers and the editors for their constructive comments.

**Conflicts of Interest:** The authors report no conflict of interest. The authors alone are responsible for the content and writing of this article.

## Notes

1 Bagli are buildings built around an open space, a kind of courtyard.

2 https://tumamoc.arizona.edu/active-research-projects (accessed on 6 July 2020).

3 http://www.markklettphotography.com/rephotographic-survey-project (accessed on 20 July 2020).

4 https://missionphotodatar.cget.gouv.fr/mission (accessed on 14 July 2020).

5 https://camilojosevergara.com/About-This-Project/1/ (accessed on 1 March 2022).

6 L'Ora was an important news and investigation newspaper, published in Palermo from 1900 to 1992.

7 Baraccopoli Rampinzeri, Baraccopoli Madonna delle Grazie, Baraccopoli di Salaparuta, Baraccopoli Santa Lucia, Baraccopoli Montevago, Baraccopoli Giammuzzello.

8 Gibellina Nuova (the new Gibellina) was rebuilt 10–15 km away, in the territory of the municipality of Salemi.

9 Munteán refers to the post-doctoral essay "The Origin of German Tragic Drama" (1928), in which Walter Benjamin recognizes an allegory of history in the shape of the ruins: «The allegorical physiognomy of the nature-history, which is put on stage in the Trauerspiel, is present in reality in the form of the ruin. In the ruin history has physically merged into the setting. And in this guise history does not assume the form of the process of an eternal life so much as that of irresistible decay. Allegory thereby declares itself to be beyond beauty. Allegories are, in the realm of thoughts, what ruins are in the realm of things».

10 http://www.markklettphotography.com/after-the-ruins/nmcvfola2oh4900n9txo8j622fxq5s (accessed on 15 July 2020).

11 See, for example, Shawn Clover's projects based on the earthquakes in San Francisco (1906) and Loma Prieta (1989) (https://shawnclover.com/thenandnowmashups, accessed on 23 April 2022), or Igor Baloh Parin's combinations of images of the Slovenian city of Breginj, before and after the 1976 Friuli earthquake (https://www.re.photos/en/profile/Parin/, accessed on 23 April 2022).

12 "The ecomuseum is a participatory practice of enhancing the tangible and intangible cultural heritage, elaborated and developed by the local community also through an entity organized in the perspective of sustainable development", Carta di Catania, 2007.

13 The images shown here are part of a larger group of re-photographic elaborations.

## References

1. Lowenthal, D. Geography, Experience, and Imagination: Towards a Geographical Epistemology. *Ann. Assoc. Am. Geogr.* **1961**, *51*, 241–260. [CrossRef]
2. Lucchesi, F. Sviluppi teorici e tematiche di indagine negli studi di Geografia Umanistica: I paesaggi letterari e quelli cinematografici. *ACME Ann. Fac. Lett. Filos. Dell'univ. Degli Studi Milano* **2012**, *65*, 193–220.
3. George, P. *La Geografia nella Società Industriale*; FrancoAngeli: Milano, Italy, 1976; ISBN 978-8-82042-225-7.
4. WHC. *Operational Guidelines for the Implementation of the World Heritage Convention*; UNESCO World Heritage Centre: Paris, France, 2008.
5. Sauer, C. The Morphology of Landscape. *Geography* **1925**, *2*, 315–350.
6. Vallega, A. *Geografia Culturale: Luoghi, Spazi, Simboli*; UTET: Turin, Italy, 2003.
7. Hellpach, W. *Geopsiche: L'uomo, il Tempo, il Clima, il Suolo e il Paesaggio*; Paoline: Rome, Italy, 1969.
8. Luginbühl, Y. *La Mise en Scène du Monde. Construction du Paysage Européen*; CNRS Editions: Paris, France, 2012; ISBN 978-2-27107-501-7.
9. Donadieu, P. *Sciences du Paysage: Entre Théories et Pratiques*; Lavoisier: Paris, France, 2012; ISBN 978-2-74301-405-6.
10. Napoli, M.D.; Petino, G. Il prodotto attrae, il territorio accoglie. Analisi dell'offerta turistica di due areali produttivi IGP siciliani. In *Annali del Turismo*, 4th ed.; Edizioni Geoprogress: Novara, Italy, 2017; pp. 153–175.
11. Turco, A. *Configurazioni della Territorialità*; FrancoAngeli: Milan, Italy, 2010.
12. Dell'Agnese, E.; Tabusi, M. (Eds.) *La Musica Come Geografia: Suoni, Luoghi, Territori*; SGI: Rome, Italy, 2016; pp. 5–12. ISBN 978-8-88869-298-2.

13. Dewey, J.F.; Helman, M.L.; Turco, E.; Hutton, D.H.W.; Knott, S.D. Kinematics of the Western Mediterranean. In *Alpine Tectonics*; Coward, M.P., Dietrich, D., Park, R.G., Eds.; Geological Society of London: London, UK, 1989; pp. 265–283.
14. Ben-Avraham, Z.; Boccaletti, M.; Cello, G.; Grasso, M.; Lentini, F.; Torelli, L.; Tortorici, L. Principali domini strutturali originatisi dalla collisione neogenico-quaternaria nel Mediterraneo centrale. *Mem. Soc. Geol. Ital.* **1990**, *45*, 453–462.
15. Catalano, R.; D'Argenio, B.; Torelli, L.; Argenio, B.; Torelli, L. A geological section from Sardinia Channel to Sicily Straits based on seismic and field data. In *The Lithosphere in Italy: Advances in Earth Science Research*; Boriani, A.B., Piccardo, M., Vai, G.B., Eds.; Italian National Commitee for the International Lithosphere Program: Rome, Italy, 1989; pp. 110–128.
16. Catalano, R.; Franchino, A.; Merlini, S.; Sulli, A. Central western Sicily structural setting interpreted from seismic reflection profiles. *Mem. Soc. Geol. Ital.* **2000**, *55*, 5–16.
17. Finetti, I.R.; Lentini, F.; Carbone, S.; Del Ben, A.; Di Stefano, A.; Forlin, E.; Guarnieri, P.; Pipan, M.; Prizzon, A. Geological outline of Sicily and Lithospheric Tectono-dynamics of its Tyrrhenian Margin from new CROP seismic data. In *CROP PROJECT: Deep Seismic Exploration of the Central Mediterranean and Italy*; Finetti, I.R., Ed.; Elsevier: Amsterdam, The Netherlands, 2005.
18. Barreca, G.; Bruno, V.; Dardanelli, G.; Guglielmino, F.; Brutto, M.L.; Mattia, M.; Pipitone, C.; Rossi, M. An integrated geodetic and InSAR technique for the monitoring and detection of active faulting in southwestern Sicily. *Ann. Geophys.* **2020**, *63*, 1–11. [CrossRef]
19. De Panfilis, M.D.; Marcelli, L. Il periodo sismico della Sicilia occidentale iniziato il 14 Gennaio 1968. *Ann. Geophys.* **1968**, *21*, 343–421. [CrossRef]
20. Anderson, H.; Jackson, J. Active tectonics of the Adriatic Region. *Geophys. J. Int.* **1987**, *91*, 937–983. [CrossRef]
21. Rovida, A.; Locati, M.; Camassi, R.; Lolli, B.; Gasperini, P. The Italian earthquake catalogue CPTI15. *Bull. Earthq. Eng.* **2020**, *18*, 2953–2984. [CrossRef]
22. Rovida, A.; Locati, M.; Camassi, R.; Lolli, B.; Gasperini, P.; Antonucci, A. *Catalogo Parametrico dei Terremoti Italiani (CPTI15), Versione 3.0*; Istituto Nazionale di Geofisica e Vulcanologia (INGV): Rome, Italy, 2021. [CrossRef]
23. Rovida, A.; Locati, M.; Camassi, R.; Lolli, B.; Gasperini, P.; Antonucci, A. *Catalogo Parametrico dei Terremoti Italiani (CPTI15), Versione 4.0*; Istituto Nazionale di Geofisica e Vulcanologia (INGV): Rome, Italy, 2022. [CrossRef]
24. Bottari, A. Attività sismica e neotettonica della Valle del Belice. *Ann. Geophys.* **1973**, *26*, 55–84. [CrossRef]
25. Michetti, A.M.; Brunamonte, F.; Serva, L. Paleoseismological Evidence in the Epicentral Area of the January 1968 Earthquakes, Belice, Southwestern Sicily. In *Perspectives in Paleoseismology*; Serva, L., Slemmons, D.B., Eds.; A.E.G.: Los Angeles, CA, USA, 1995; pp. 127–139.
26. Bosi, C.; Cavallo, R.; Francaviglia, V. Aspetti geologici e geologico-tecnici del terremoto della Valle del Belice del 1968. *Mem. Soc. Geol. Ital.* **1973**, *12*, 81–130.
27. Haas, J.E.; Ayre, R.S. *The Western Sicily Earthquake of 1968*; National Academy of Engineering Report; National Academy of Science: Washington, DC, USA, 1969; p. 70.
28. Caldo, C. L'insediamento nella valle del Belice (Sicilia) in relazione al terremoto del 1968. *Riv. Geogr. Ital.* **1973**, *3*, 294–312.
29. Aprile, M. Il Terremoto del Belice o del Fraintendimento. In *La Furia di Poseidon. Messina 1908 e Dintorni*; Campione, G., Ed.; Silvana Editoriale: Milan, Italy, 2009; pp. 221–234.
30. Badami, A. *Gibellina, la Città che Visse Due Volte. Terremoto e Ricostruzione nella Valle del Belice*; FrancoAngeli: Milan, Italy, 2020; ISBN 8-89-179024-9.
31. Abbate, G.; Fede, M.S.D. Le città della Valle del Belice in Sicilia a cinquant'anni dal terremoto. In *La Città Altra. Storia e Immagine della Diversità Urbana: Luoghi e Paesaggi dei Privilegi e del Benessere, Dell'isolamento, del Disagio, della Multiculturalità*; Capano, F., Pascariello, M.I., Visone, M., Eds.; Federico II University Press e CIRICE: Napoli, Italy, 2018; pp. 579–586; ISBN 978-8-89993-003-5.
32. Rogers, G.F. *Then and Now—A Photographic History of Vegetation Change in the Central Great Basin Desert*; University of Utah Press: Salt Lake City, UT, USA, 1982; ISBN 978-0-87480-206-1.
33. Rogers, G.F.; Malde, H.E.; Turner, R.M. *Bibliography of Repeat Photography for Evaluating Landscape Change*; University of Utah Press: Salt Lake City, UT, USA, 1984; ISBN 978-0-87480-239-9.
34. McLuhan, M. *The Gutenberg Galaxy: The Making of Typografic Man*; University of Toronto Press: Toronto, ON, Canada, 1962.
35. Finsterwalder, S. *Die Photogrammetrie in den Italienischen Hochalpen*; Verlag Der Deutsche Alpenvereins: Wien, Austria, 1890. [CrossRef]
36. Bryan, K.; Rue, E.C.L. Persistence of Features in an Arid Landscape: The Navajo Twins, Utah. *Geogr. Rev.* **1927**, *17*, 251–257. [CrossRef]
37. Clements, F.E. *Research Methods in Ecology*; The University Publishing Company: Lincoln, NE, USA, 1905.
38. Shantz, H.L.; Marbut, C.F. *The Vegetation and Soils of Africa*; National Research Council and American Geographical Society: New York, NY, USA, 1923.
39. Shantz, H.L.; Turner, B.L. *Photographic Documentation of Vegetational Changes in Africa over a Third of a Century*; University of Arizona: Tucson, AZ, USA, 1958.
40. Webb, R.H.; Boyer, D.E.; Turner, R.M. (Eds.) *Repeat Photography: Methods and Applications in the Natural Sciences*; Island Press: Washington, DC, USA, 2010.
41. Adams, R. *The New West: Landscapes along the Colorado Front Range*; Colorado Associated University Press: Louisville, KY, USA, 1974; ISBN 978-3-86930-900-2.
42. Salvesen, B. (Ed.) *New Topographics*; Steidl: Göttingen, Germany, 2009; ISBN 978-3-86521-827-8.

43. Campbell, N. *The Cultures of the American New West*; Routledge: London, UK, 2000.
44. Sciascia, L. Quelli lì. *L'Ora* **1968**, *68*, 12.
45. Messina, G. Old Gibellina: The map, the world, the Aleph. *Cult. Geogr.* **2019**, *27*, 317–323. [CrossRef]
46. Recalcati, M. Le lacrime e l'opera. In *Alberto Burri. Il Grande Cretto di Gibellina*; Recalcati, M., Ed.; Magonza: Arezzo, Italy, 2018; ISBN 978-8-89875-668-1.
47. Munteán, L. Rephotography and the Ruin of the Event. *Transform. J. Media Cult.* **2016**, *28*, 1–12.
48. Klett, M.; Lundgren, M.; Fradkin, P.L.; Solnit, R.; Breuer, K. *After the Ruins, 1906 and 2006: Rephotographing the San Francisco Earthquake and Fire*; University of California Press: Oakland, CA, USA, 2006; ISBN 978-0-52024-556-3.
49. Burton, C.; Mitchell, J.T.; Cutter, S. Evaluating post-Katrina recovery in Mississippi using repeat photography. *Disasters* **2011**, *35*, 488–509. [CrossRef] [PubMed]
50. Puschmann, O.; Eiter, S.; Fjellstad, W.; Krogli, S.O. Preparing Future Flashbacks—Repeat Photography as a Method in Landscape Monitoring. *Nibio-Pop* **2018**, *4*, 1–6.
51. De Varine, H.D. *L'ecomuseo Singolare e Plurale*; Utopie Concrete: Gemona del Friuli, Italy, 2021.
52. Bonito Oliva, A. *Paesaggio con Rovine*; Edizione Fondazione Orestiadi: Gibellina, Italy, 1992.
53. Frazzetto, G. *La Mano e la Stella*; Edizioni Orestiadi: Gibellina, Italy, 2007; ISBN 978-8-89509-802-9.

land

MDPI

*Article*

# Flood Hazard Index Application in Arid Catchments: Case of the Taguenit Wadi Watershed, Lakhssas, Morocco

**Mustapha Ikirri [1], Farid Faik [1], Fatima Zahra Echogdali [1], Isabel Margarida Horta Ribeiro Antunes [2], Mohamed Abioui [1,*], Kamal Abdelrahman [3], Mohammed S. Fnais [3], Abderrahmane Wanaim [1], Mouna Id-Belqas [1], Said Boutaleb [1], Kochappi Sathyan Sajinkumar [4,5] and Adolfo Quesada-Román [6]**

[1] Department of Earth Sciences, Faculty of Sciences, Ibn Zohr University, Agadir 80000, Morocco; mustapha.ikirri@edu.uiz.ac.ma (M.I.); f.faik@uiz.ac.ma (F.F.); fatimazahra.echogdali@edu.uiz.ac.ma (F.Z.E.); a.wanaim@uiz.ac.ma (A.W.); mouna.id-belqas@edu.uiz.ac.ma (M.I.-B.); s.boutaleb@uiz.ac.ma (S.B.)
[2] Institute of Earth Sciences, Pole of University of Minho, 4710-057 Braga, Portugal; imantunes@dct.uminho.pt
[3] Department of Geology & Geophysics, College of Science, King Saud University, Riyadh 11451, Saudi Arabia; khassanein@ksu.edu.sa (K.A.); mfneis@ksu.edu.sa (M.S.F.)
[4] Department of Geology, University of Kerala, Thiruvananthapuram 695 581, Kerala, India; sajinks@keralauniversity.ac.in
[5] Department of Geological & Mining Engineering & Sciences, Michigan Technological University, Houghton, MI 49931, USA
[6] Department of Geography and Water and Global Change Observatory, University of Costa Rica, San José 2060, Costa Rica; adolfo.quesadaroman@ucr.ac.cr
* Correspondence: m.abioui@uiz.ac.ma

**Citation:** Ikirri, M.; Faik, F.; Echogdali, F.Z.; Antunes, I.M.H.R.; Abioui, M.; Abdelrahman, K.; Fnais, M.S.; Wanaim, A.; Id-Belqas, M.; Boutaleb, S.; et al. Flood Hazard Index Application in Arid Catchments: Case of the Taguenit Wadi Watershed, Lakhssas, Morocco. *Land* **2022**, *11*, 1178. https://doi.org/10.3390/land11081178

Academic Editors: Fabio Luino, Mariano Barriendos Vallvé, Emmanuel Garnier, Fabrizio Terenzio Gizzi, Ruediger Glaser, Christoph Gruetzner, Walter Palmieri, Sabina Porfido, Heather Sangster and Laura Turconi

Received: 2 June 2022
Accepted: 25 July 2022
Published: 28 July 2022

**Publisher's Note:** MDPI stays neutral with regard to jurisdictional claims in published maps and institutional affiliations.

**Copyright:** © 2022 by the authors. Licensee MDPI, Basel, Switzerland. This article is an open access article distributed under the terms and conditions of the Creative Commons Attribution (CC BY) license (https://creativecommons.org/licenses/by/4.0/).

**Abstract:** During the last decade, climate change has generated extreme rainfall events triggering flash floods in short periods worldwide. The delimitation of flood zones by detailed mapping generally makes it possible to avoid human and economic losses, especially in regions at high risk of flooding. The Taguenit basin, located in southern Morocco, is a particular case. The mapping of the flood zones of this basin by the method of the Flood Hazard Index (FHI) in a GIS geographic information systems environment was based on the multi-criteria analysis, taking into consideration the seven parameters influencing these extreme phenomena, namely rainfall, slope, flow accumulation, drainage network density, distance from rivers, permeability, and land use. Average annual rainfall data for 37 years (1980 to 2016) was used in this study for floodplain mapping. A weight was calculated for each parameter using the Analytical Hierarchy Process (AHP) method. The combination of the maps of the different parameters made it possible to draw up a final map classified into five risk intervals: very high, high, moderate, lower and very lower presenting, respectively, 8.04%, 20.63%, 31.47%, 15.36%, and 24.50% of the area of the basin. The reliability of this method was tested by a Flood susceptibility analysis. The results generated by the Flood Hazard Index (FHI) model are similar to those of previous historical events. Realistic and applicable solutions have been proposed to minimize the impact of these floods as much as possible.

**Keywords:** climate change; Flood Hazard Index (FHI); Taguenit Wadi catchment; AHP; flood susceptibility; Morocco

## 1. Introduction

Water scarcity is an omnipresent reality, and with soaring demand in the future; it will continue to be a precious resource. Nonetheless, manifestations of hydrological processes, as the main cause of contrasting catastrophes, such as floods, and water–deficient events, such as droughts and desertification, owing to the effects of climate change [1,2], also require an evaluation of stakeholder actions and potential mismanagement. Meanwhile, the scenario of arid regions is difficult due to the scarcity of flow data detailing, absence of floods, and difficulty in performing natural tracing or continuous monitoring of the

flow [3,4]. However, the occurrence and intensity of rain events and floods represent a real risk in arid regions for water resources management.

Floods have the greatest potential for destruction among all natural hazards, which increasingly affect many people and their activities. In recent decades, the world has been affected by severe flooding, causing thousands of deaths, disruption of economic activities, and infrastructure destruction [2,5,6]. The flooded phenomena have been studied by several researchers, particularly in the development of theories, numerical models, and statistical methodologies, to describe flood behavior and space–time evolution [7–9].

Morocco, located in North–West Africa, is characterized by arid and semi-arid river watersheds, is facing unpredictable rainfall patterns and is subject to various hydrological constraints [9,10]. However, several Morocco regions have been subject to a considerable history of flooding phenomena, and they led to losses of human life amounting to 100 deaths in 1950, 730 deaths in 1995, and 500 deaths in 2014. In parallel, the estimated economic losses reached 2,200,000US$ in 2001 and 5,200,000US$ in 2014 [11–13].The regions of the western Anti-Atlas, particularly in the southwest, have been affected by numerous flooding events. In 1995, the date of the last major flood affected the regions of Lakhssas and Sidi Ifni, inducing enormous and catastrophic damage. Three houses collapsed, and 50 houses were severely damaged while 55 were partially damaged. The famous flood that occurred on 28 November 2014 affected Sidi Ifni city [14]. A flood hazard has still loomed large over the years due to population growth and socioeconomic development, as well as climate change due to global warming. The Taguenit Wadi catchment, located in the Lakhssas region (west coast), has recorded numerous big extensive floods, with prominent floods during 2006, 2010, and 2014, causing damage to infrastructure, loss of soil, and untold suffering to the population. Because of their proximity, the Lakhssas and Sidi Ifni regions are often affected at the same time by the same storm or rainfall events. In the Lakhssas region, the violence of the 2014 floods eroded the riverbanks, taking with them the entire surrounding infrastructure. Roads, often built along the wadi beds, were destroyed, isolating the Lakhssas town. Landslides also blocked roads. On the left bank, 50 houses were flooded. The people living in them were forced to take refuge on terraces while waiting for help. During the floods, three deaths were recorded in the Sidi Ifni province. The material losses were, however, very important, including significant damage to vital infrastructure (roads, water, electricity, sanitation, and fixed and mobile telephone networks) [14]. This calls for regular characterization and river monitoring to protect the various infrastructures and human activities of the area.

Several approaches (geographic information system, remote sensing, and hydraulic models) have made it possible to accurately assess areas at high risk of flooding [15,16]. The most efficient remains hydraulic models since they make it possible to estimate and predict the depth of floods for different return periods [17]. However, they require a large set of measured data, which is not always available [18,19] due to the lack or absence of hydro–meteorological stations, especially in developing countries [17,19].

In recent years, researchers have developed other techniques to predict the impact of high-intensity and short-duration floods, namely the Weights of evidence Model [20], Frequency Ratio [21], Index of Entropy [22], Random Forest [23], Logistic Regression [24], Artificial Neural Network [25], Index of Entropy [26], Analytical Hierarchy Process [27], and Flood Hazard Index (FHI) [8,28]. The latter, widely applied in several regions of the world, has shown its effectiveness.

Flood risks on a basin-scale can be quantified, especially using Flood Hazard Index (FHI) methodologies [12,14,29]. Climate change will trigger more frequent extreme flash floods in arid environments [30–33]. Hence, the study of simulated floods on the Taguenit Wadi catchment and their spatial extension is essential to enable hydraulic operators to determine the extent of flood risk areas. The main aim of the present study is the application of the Flood Hazard Index (FHI) method to determine the most vulnerable flood areas on the Taguenit Wadi catchment.

## 2. Materials and Methods

### *2.1. Geographical Setting of the Taguenit Wadi Catchment*

The Taguenit Wadi catchment, situated in the south part of Morocco between latitudes 29°10′30″ to 29°28′30″ and longitudes 9°52′30″ to 10°43′30″, covers an area of 131.52 km$^2$. The altitude varies between 577 and 1204 m (Figure 1), decreasing overall from east to west. The slopes, which are generally steep, vary from a few degrees (0° and 15°) on the terraces of the tributary riverbeds and downstream of the river basin to 64° on the upstream slopes. The average annual rainfall, recorded at the Adoudou station located 15 km north of the basin, is 133 mm. Aridity increases from west to east, due to the increasing distance from oceanic influences. The average temperature is 26 °C, with a maximum of 45 °C and a minimum of 12 °C [14].

Morocco has highly diverse geomorphology and a variety of landform types [34]. The geomorphology of the basin area is characterized by the dominance of the mountains of the western Anti-Atlas range, with cover vegetation dominated by Argan and euphorbia plants. The river and tributaries flow only after the first rains in October or November. The dominant surface water flow is from SE–NW (Figure 1). The hydrographic network is dense and well-branched, with a specific "Y" shape. The branching of the network is more pronounced upstream than downstream. The time of concentration of the water calculated using the Giandotti equation is 14 h. In this region, flash floods cause much human and material damage, produced by intense rains, resulting in short periods of flooding, usually within several hours. The November 2014 floods caused 100 fatalities as well as the destruction of 200 infrastructures with extensive soil erosion (Figure 2).

The Taguenit Wadi catchment is part of the Lakhssas plateau, located in the Western Anti–Atlas chain, on the west coast of Morocco. It is located between the two Precambrian massifs of Kerdous and Ifni. These geological formations are composed, from bottom to top, of carbonate facies (Tamjout dolomites and lower limestones), dolomitic limestones, marly limestones with intercalations of dolomitic-sandstone, and finally upper limestones [35–37] (Figure 3a). All of the areas are generally faulted, with the main directions of NNE–SSW, NE–SW, E–W, and ENE–WSE. The soil type in the catchment was produced by Working Group World (WRB) Reference Base for Soil Resources [38]. The soil complex is characterized by the dominance of poorly developed anthropogenic soils, namely Calcisols, Leptosols, Luvisols, and Regosols, which respectively occupy 21.13%, 9.20%, 26.99%, and 42.68% of the study area (Figure 3b). The upstream part of the basin with steep slopes is where hard limestone and dolomitic rocks are mainly outcropped. These are depleted by erosion as the topsoil is washed away by rainfall runoff. In the middle part of the basin, we find mainly Leptosols and Calcisols, which result from a saturation of the soils with calcium or magnesium and produce eroded elements of limestone and dolomites upstream of the basin. Their establishment over geological time depends on both periods favorable to pedogenesis and on human action (cultivation), which has a very strong impact on these soils. Finally, in the downstream part, Calcisols are more prevalent, younger than the other types of soil, little differentiated, and more or less stony (pebbles) and of variable texture (often loamy or sandy). They come from alluvial deposits throughout the Quaternary. The analysis of this pedological map gives a good account of the differentiation in an upstream–downstream direction of the types of soils which will behave variably to rainfall events; it emerges from this that the fluviosols located downstream of the basin, partially or saturated with water by the superficial groundwater, will generate runoff "by saturation"; this type of runoff suddenly produces catastrophic floods.

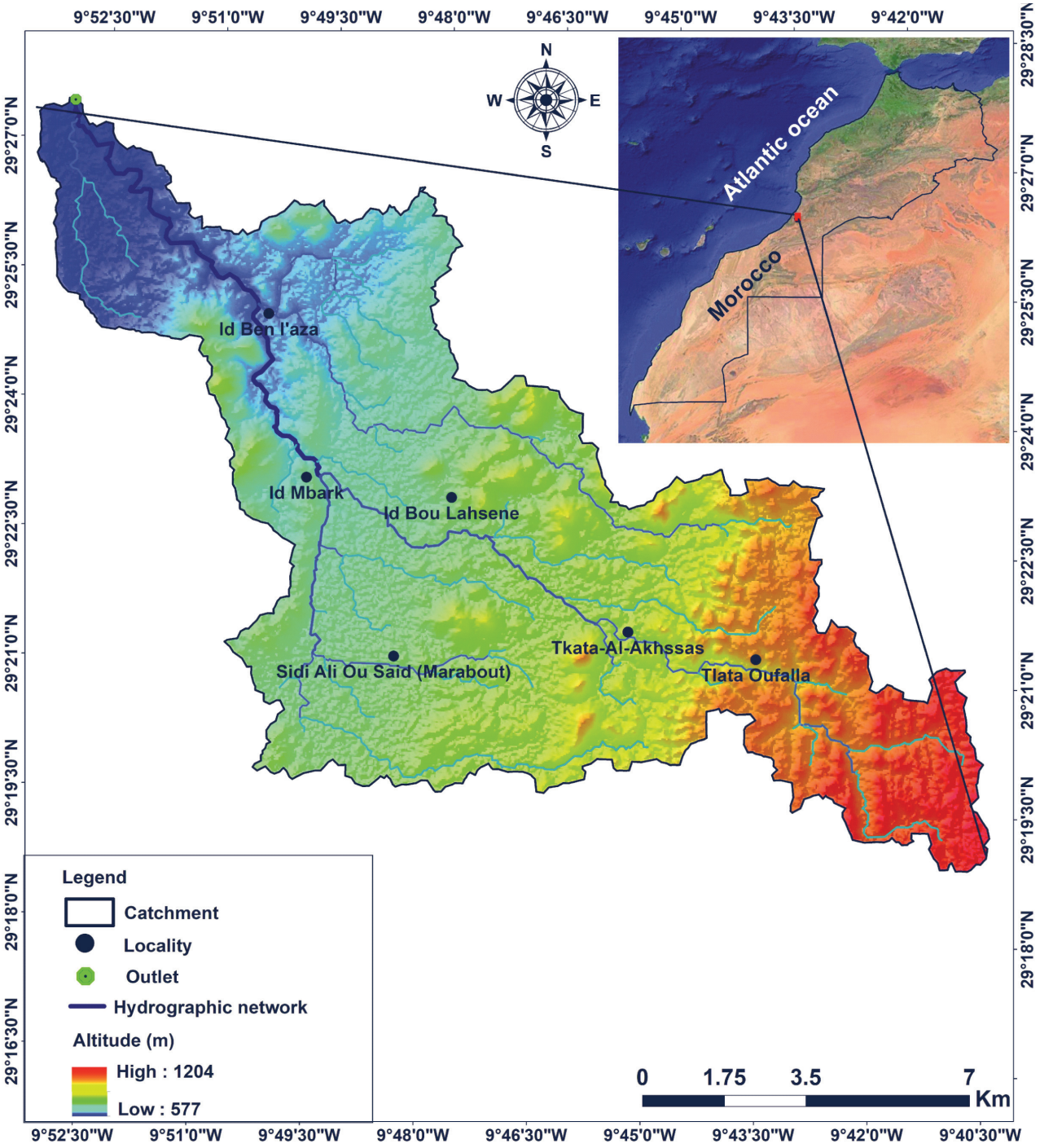



**Figure 1.** Geographic location of Taguenit Wadi catchment.




**Figure 2.** Damage to the infrastructure of the village of Lakhssas during the floods of November 2014. (**a**) Degradation of the National Road N°1; (**b**) Deterioration of the inter-provincial roads connecting Lakhssas village and Ifni city.

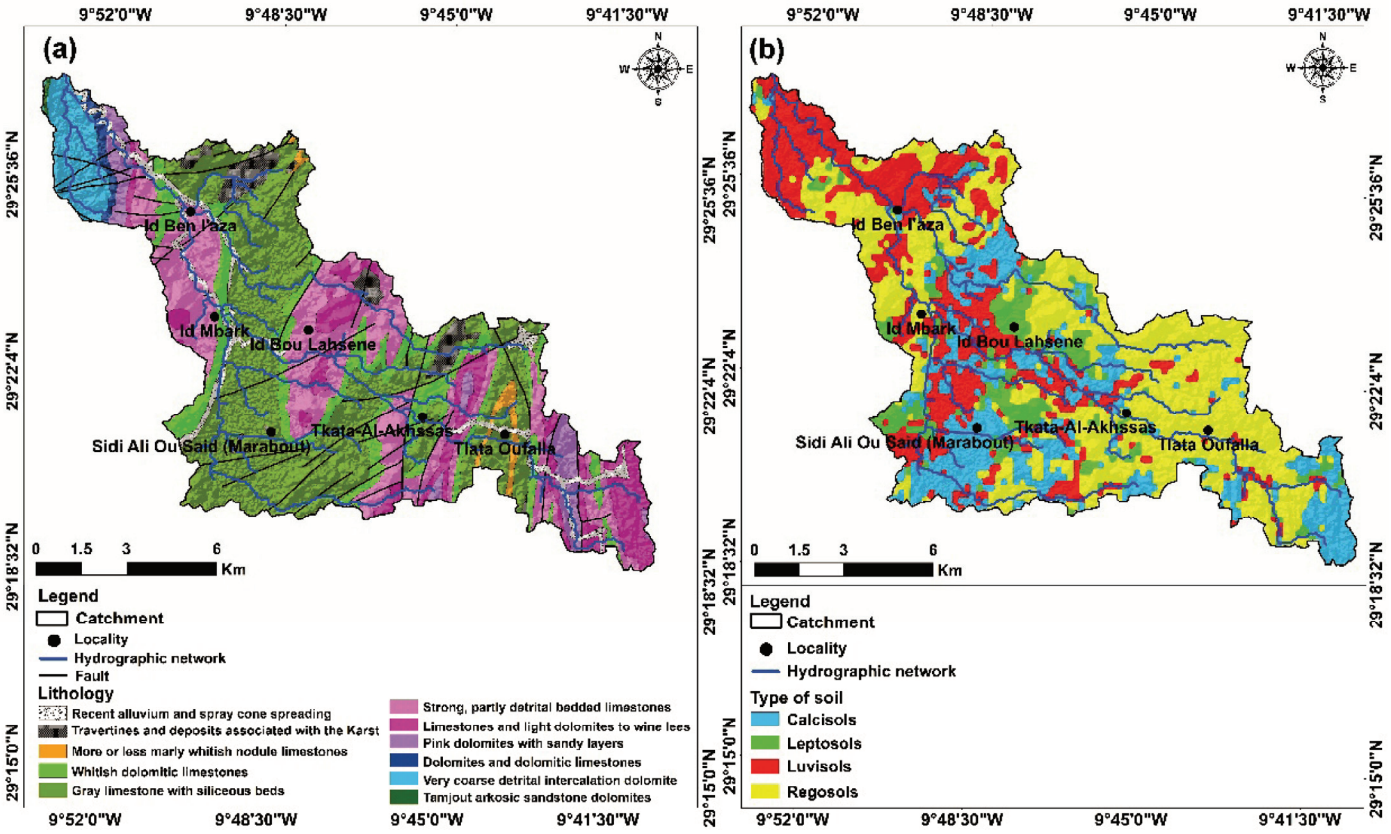



**Figure 3.** Taguenit Wadi River catchment: (**a**) Geological map; (**b**) Soil type map.

### *2.2. Flood Mapping Methodology*

The Flood Hazard Index (FHI) model has been developed to define flood risk areas from a regional perspective [28,29]. The FHI index is intended to identify vulnerable areas of flooding risk.

The Flood Hazard Index (FHI) is based on the Analytical Hierarchy Process (AHP) multi-criteria decision analysis, considering the contribution of weights of seven hydro–geo–morpho–climatic factors, namely Rainfall (R), Slope (S), Flow accumulation (Fa), Drainage Network Density (DND), Distance from Rivers (DFR), Permeability (P), and Land Use (LU). The choice of these factors is theoretically based on their relevance to flood risk (Figure 4).

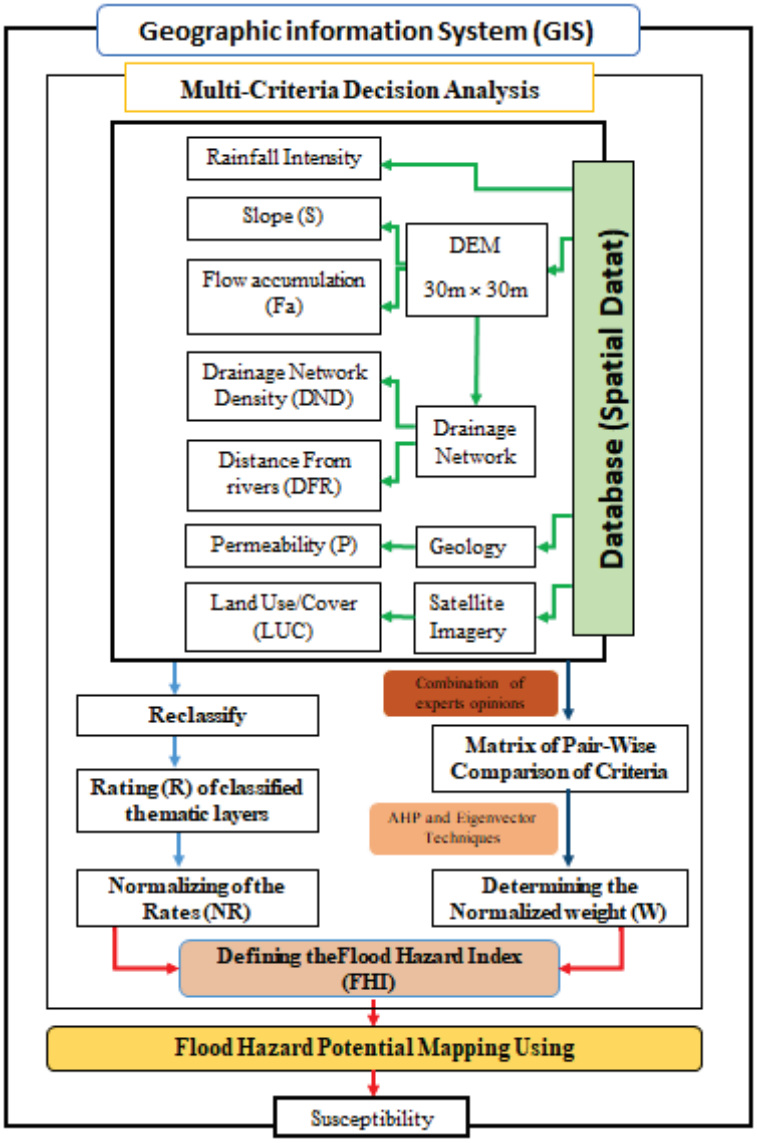



**Figure 4.** Schematic diagram of the integration of hydrological and AHP models in a Geographical Information System (GIS).

### *2.3. Flood Hazard Index (FHI) Factors*

The factors considered in the spatial flood map are extracted from the DEM, with 30 m × 30 m resolution, for slope and flow accumulation, while permeability was extracted from the Lakhssas geological map on a scale of 1:100,000. The drainage network of the area was obtained using DEM data and used to produce the drainage network density and distance from rivers. With regards to rainfall, the spatial distribution map was deduced from a regional extrapolation, including four meteorological stations bordering the basin, namely Adoudou, Taghjijt, Sidi Ifni, and Youssef Ben Tachafine. Land use was obtained using Landsat 8 Oli satellite imagery of the area by supervised classification. All the information was organized in a database using ArcGIS software 10.5.

- Flow accumulation (Fa): Flow accumulation corresponds to the accumulated water flow to a specific cell drained from the cells located upstream. High values of the Fa factor indicate areas of higher concentrated water flow and, therefore, a higher risk of flooding [28,39]. In the study area, this factor varies in a range between 0 and 147.996, with the highest values coinciding with the water flow of the main tributaries of Taguenit Wadi (Table 1; Figure 5a).

- Distance from Rivers (DFR): The spatial distance of a region to the river system is a crucial factor in the delimitation of flood vulnerability zones. As the distance to the river system decreases, the degree of flood risks will increase [14,28,29]. Distances located below 200 m to the river system will correspond to areas of higher flood vulnerability. Otherwise, the areas located away from 400 m to the river system seem to present a lower or absent flood risk. The high flood vulnerability zones are mainly confined to the river networks (Table 1; Figure 5b).
- Drainage Network Density (DND): Drainage network density is proportional to the cumulative water volume from upstream to downstream in the river basin [40,41]. In the Taguenit Wadi catchment, DND values range from 0 to 5.67 m/km$^2$, with the lower class concentrated in the catchment (Table 1; Figure 5c).
- Rainfall (R): For a given area, rainfall is the most important factor related to the occurrence of floods, it has a direct relationship with river flow, and a large amount of rainfall in a short time can generate flash floods in semi-arid regions [1,2]. The annual rainfall data (1980 to 2016) used in this study were collected from Regional Meteorological stations (Taghjijt, Adoudou, Assaka, and Sidi Ifni stations). Thus, a rainfall map was prepared from the annual mean rainfall by inverse distance weighted (IDW) interpolation in ArcGIS 10.4 [39,42]. The annual mean rainfall varies between 122.19 to 137.71 mm/year, with decreased values from the north to the south, and the highest rainfall values are recorded in the southern part of the basin (Table 1; Figure 5d).
- Slope (S): The slope of the area influences surface runoff and water infiltration [39,43]. The slope classes vary between 0 and 64° (Table 1) and were defined according to the model applied by Demek [44]. The lower slope areas are concentrated downstream, while the higher slope areas are concentrated in the mountainous regions, located in the north of the basin (Figure 6a).
- Land use (LU): The type of land use determines the infiltration of rainwater into the soil and the resulting runoff [14,28]. Forests generally favor infiltration through the root system of trees and plants, whereas roads and buildings reduce infiltration of this water and increase surface runoff. In the Taguenit catchment area, the land use data have been reclassified into four classes displayed in Table 1. The village of Lakhssas, located in the center of the basin area and equipped with several infrastructures (e.g., roads, tracks, shops, and dwellings), amplifies the occurrence of floods downstream as it generally contains impermeable materials (Figure 6b).
- Permeability (P): In the Taguenit Wadi catchment, the impermeable or poorly permeable rocks, such as crystalline rocks, promote surface runoff. This factor was reclassified into four classes, varying between 4 to 10, according to models established by Echogdali et al. [29] and Elkhrachy [41]. About 80% of the basin's formations are impermeable or with a low permeability, which offers an environment conducive to a higher probability of strong floods development. Carbonate formations, with lower permeability and strongly favoring runoff, were assigned a weight of 10 (Table 1), while the lowest weight (class 2) was attributed to those with a high permeability corresponding to the Quaternary formations, which extend over 20% of the Taguenit Wadi catchment (Figure 6c).

Each of the seven factors was reclassified, with a rating, according to the impact degree on the flood risk. We assigned values that varied from 2 to 10 as proposed by Kazakis et al. [28], shown in Table 1. They thus indicate the intensity of the flood hazard starting from very low (2), low (4), medium (6), high (8), and very high (10).

**Table 1.** Defined factor classes and corresponding ratings adopted for this study (Source: Collated from various references cited within this paper).

| Factor (Units) | Class | Rating | Weight |
|---|---|---|---|
| Fa: Flow accumulation (Pixels) | 97,503–147,996 | 10 | 2.73 |
| | 45,849–97,503 | 8 | |
| | 23,795–45,849 | 6 | |
| | 6384–23,795 | 4 | |
| | 0–6384 | 2 | |
| DFR: Distance from rivers (m) | 0–33 | 10 | 2.54 |
| | 33–133 | 8 | |
| | 133–377 | 6 | |
| | 377–632 | 4 | |
| | 632< | 2 | |
| DND: Drainage network density ($m/km^2$) | 4.53–5.67 | 10 | 1.43 |
| | 3.40–4.53 | 8 | |
| | 2.26–3.40 | 6 | |
| | 1.13–2.26 | 4 | |
| | 0–1.13 | 2 | |
| R: Rainfall (mm/year) | 134.60–137.71 | 10 | 0.71 |
| | 131.50–134.60 | 8 | |
| | 128.40–131.50 | 6 | |
| | 125.29–128.40 | 4 | |
| | 122.19–125.29 | 2 | |
| LU: Land use (Pixels) | Dwelling | 10 | 0.85 |
| | Wadi | 8 | |
| | Bare ground | 6 | |
| | Vegetation | 2 | |
| S: Slope (Degree) | 0–7 | 10 | 0.55 |
| | 7–15 | 8 | |
| | 15–25 | 6 | |
| | 25–38 | 4 | |
| | 38–64 | 2 | |
| P: Permeability (Pixels) | Impermeable | 10 | 0.40 |
| | Low permeability | 8 | |
| | Average permeability | 6 | |
| | High permeability | 4 | |

### *2.4. Relative Weight of Factors*

The weights of the factors applied in the Taguenit Wadi catchment were determined using AHP (Figure 4) [45,46]. The AHP methodology is a mathematical approach used to characterize complex problems, with a varying number of factors. Once all the factors are hierarchically sorted, a pairwise comparison matrix is constructed to allow meaningful comparison between the assessments of the factors. The relative importance of each factor was determined by five numerical scales, as shown in Table 2.

**Table 2.** Numerical expression of the relative importance of factors.

| Importance | Scale |
|---|---|
| Very important | 1 |
| Moderate | 1/2 |
| Less important | 1/3 |
| Moderately less important | 1/4 |
| Much less important | 1/5 |

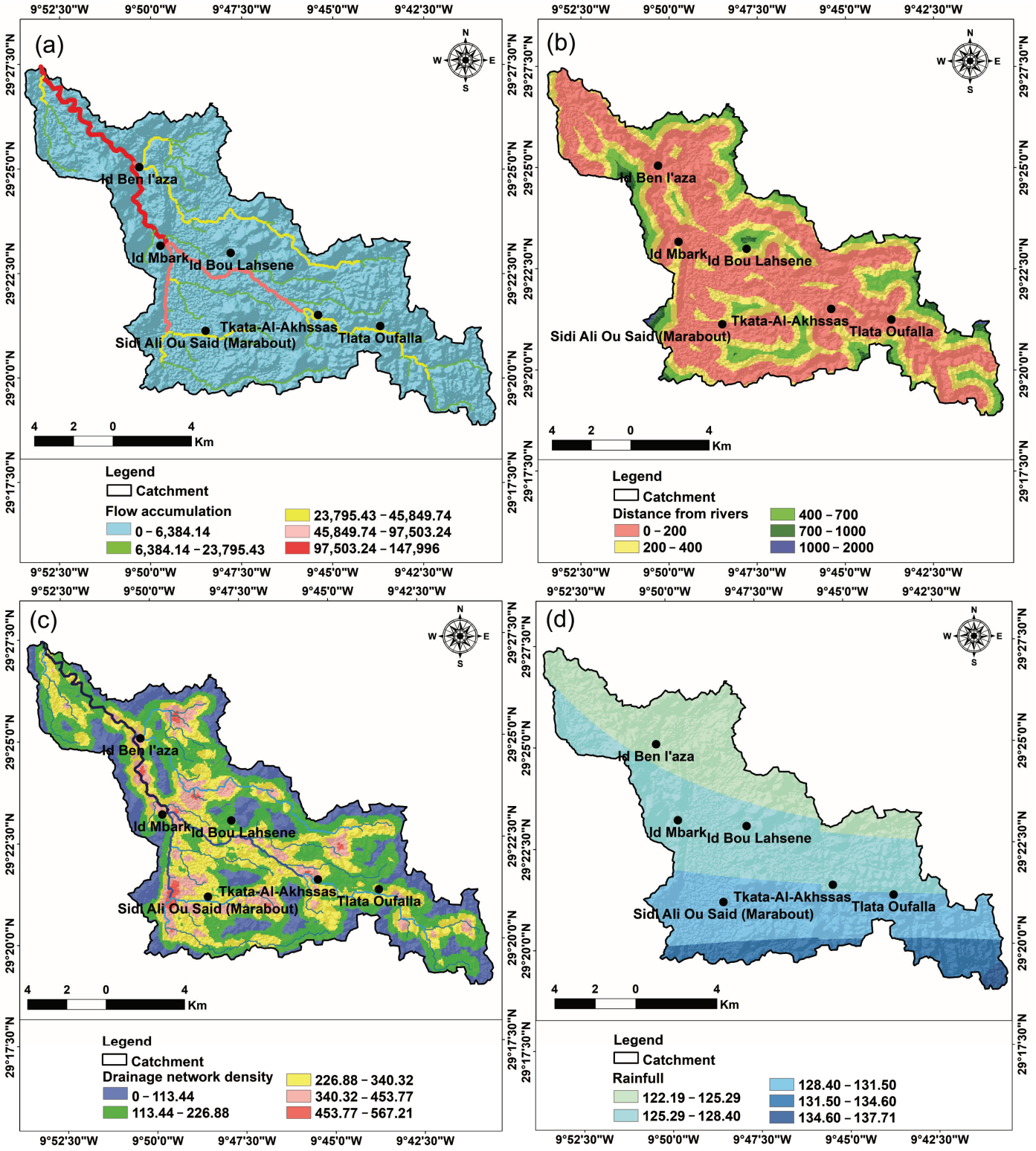



**Figure 5.** Spatial distribution of flood assessment factors in the Taguenit Wadi catchment: (**a**) Flow accumulation; (**b**) Distance from rivers; (**c**) Drainage network density; (**d**) Rainfall.

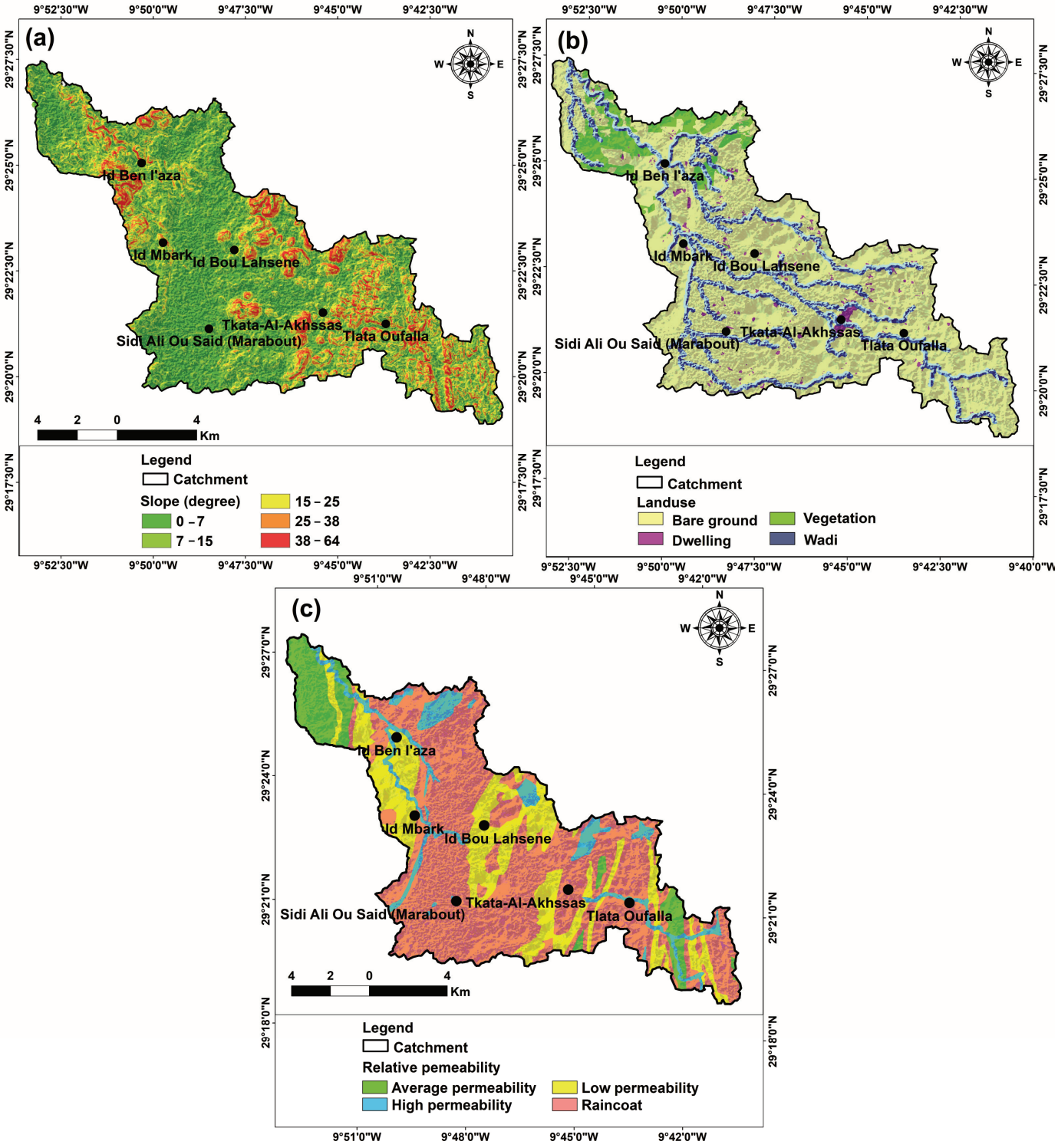



**Figure 6.** Spatial distribution of flood assessment factors in the Taguenit Wadi catchment (continuation): (**a**) Slope; (**b**) Land use; (**c**) Permeability.

The applied matrix is of a dimension 7 × 7, and the diagonal elements are equal to 1. The factors are structured hierarchically in Table 3.

**Table 3.** Pairwise comparison matrix of flood influencing factors for AHP; λmax: maximum value of the comparison matrix, RI: Random indices, CR: consistency ratio.

| Factors | Flow Accumulation | Distance from Rivers | Drainage Network Density | Rainfall | Land Use | Slope | Permeability |
|---|---|---|---|---|---|---|---|
| Flow accumulation | 1 | 2 | 3 | 5 | 3 | 5 | 4 |
| Distance from rivers | 1/2 | 1 | 6 | 4 | 3 | 4 | 6 |
| Drainage network density | 1/3 | 1/6 | 1 | 3 | 2 | 3 | 3 |
| Rainfall | 1/5 | 1/4 | 1/3 | 1 | 2 | 2 | 2 |
| Land use | 1/3 | 1/3 | 1/2 | 1/2 | 1 | 3 | 2 |
| Slope | 1/5 | 1/4 | 1/3 | 1/2 | 1/3 | 1 | 3 |
| Permeability | 1/4 | 1/6 | 1/3 | 1/2 | 1/2 | 1/3 | 1 |
| n = 7 | $\lambda_{max}$ = 7.65 | | | RI = 1.32 | | | CR = 0.08 |

The values presented in each row determine the correlation between two considered factors. The addition of each column value to the comparison matrix and dividing each element of the matrix by its column total could be calculated as the average of the elements in each column of the matrix [45,46]. The normalized weights for individual flood factors are presented in Table 4.

**Table 4.** Normalized weights determined for each flood factor.

| Factors | Flow Accumulation | Distance from Rivers | Drainage Network Density | Rainfall | Land Use | Slope | Permeability | Weight |
|---|---|---|---|---|---|---|---|---|
| Flow accumulation | 0.36 | 0.48 | 0.26 | 0.34 | 0.25 | 0.27 | 0.19 | 2.73 |
| Distance from rivers | 0.18 | 0.24 | 0.52 | 0.28 | 0.25 | 0.22 | 0.29 | 2.54 |
| Drainage network density | 0.12 | 0.04 | 0.09 | 0.21 | 0.17 | 0.16 | 0.14 | 1.43 |
| Rainfall | 0.07 | 0.06 | 0.03 | 0.07 | 0.17 | 0.11 | 0.10 | 0.71 |
| Land use | 0.12 | 0.08 | 0.04 | 0.03 | 0.08 | 0.16 | 0.10 | 0.85 |
| Slope | 0.07 | 0.06 | 0.03 | 0.03 | 0.03 | 0.05 | 0.14 | 0.55 |
| Permeability | 0.09 | 0.04 | 0.03 | 0.03 | 0.04 | 0.02 | 0.05 | 0.40 |

The average of the rows of the normalized matrix represents the corresponding weight (w) of each factor. In the Taguenit Wadi catchment, flow accumulation was considered the most relevant factor in the FHI index, followed by distance from rivers, drainage network density, rainfall, land use, slope, and permeability.

It is necessary to assess the consistency of the determined AHP eigenvector matrix. The consistency of the matrix could be assessed using the consistency ratio (CR) (Equation (1)). This ratio defines the probability of comparison between the consistency index (CI) of the matrix for the ratio index (RI) of a random type of matrix [41].

$$CR = CI/RI \quad (1)$$

With CR as the consistency ratio, CI represents the consistency index, calculated using Equation (2), and RI corresponds to the random index dependent on the number of selected factors (n) (Table 5).

**Table 5.** Random indices (RI) used to calculate the consistency ratio (CR), and n: number of factors selected.

| n | 1 | 2 | 3 | 4 | 5 | 6 | 7 |
|---|---|---|---|---|---|---|---|
| RI | 0 | 0 | 0.58 | 0.9 | 1.12 | 1.24 | 1.32 |

This index was calculated from the average consistency index of a randomly generated sample of 500 pairwise comparison matrices. If the CR value was $\leq$0.10, the matrix was acceptable; and if the CR value was $\geq$0.10, it was necessary to revise the judgments due to the inconsistency.

$$CI = \frac{\lambda_{max} - n}{n - 1} \quad (2)$$

The consistency index (CI) will depend on the $\lambda_{max}$ that corresponds to the maximum value of the comparison matrix, and (n) is the number of factors. The CI was calculated for $\lambda_{max}$ = 7.54, n = 7, and RI = 1.32. The eigenvector $\lambda_{max}$ of the matrix was calculated, and the consistency of all the judgments was also checked, making sure that the AHP method suggested that the obtained CR value was less than or equal to 0.1 [47,48]. Since the value of CR = 0.08, which is less than the threshold (0.1), the consistency of the weights is constant. The seven selected factors were superimposed linearly with their weights calculated previously. The flood risk index was calculated using Equation (3):

$$\text{FHI} = \sum_{i=6}^{n} (\text{wi} * \text{Xi}) \quad (3)$$

With Xi being the classification of the factor at each point, Wi being the weight of each factor, and (n) being number of factors.

In the Taguenit Wadi catchment, Flood Hazard Index (FHI) was applied using Equation (4):

$$\begin{gathered} \text{FHI} = [2.73 \times (\text{Flow accumulation})] + [2.54 \times (\text{Distance From Rivers})] \\ + [1.43 \times (\text{Drainage Network Density})] + [0.71 \times (\text{Rainfall})] + [0.85 \times (\text{Land use})] \\ + [0.55 \times (\text{Slope})] + [0.40 \times (\text{Permeability})] \end{gathered} \quad (4)$$

Flood susceptibility is an analysis to test and evaluate the extent of flooding and to determine the predictive accuracy of the selected model [49]. Some models use the ratio of affected features to total vulnerable features to determine the flood vulnerability of an area [50,51]. The variable 'flood depth' could be added to determine flood susceptibility, as the degree of affected features is directly related to the flood depth. The flood susceptibility was calculated according to Equation (5).

$$S = \frac{R_{affected}}{R_{total}} * 100\% \quad (5)$$

where S is the flood susceptibility score; $R_{affected}$ is the number of affected entities; $R_{total}$ is the amount of total vulnerable entities.

## 3. Results and Discussion

### *3.1. Flood Hazard Index (FHI) Analysis*

Analysis of the results obtained from the linear combination of the selected factors showed that the three most-relevant factors for the determination of flood risk were flow accumulation, distance from rivers, and density of the river system. Five flood risk classes, varying from very low to very high, were defined according to the flood risk map of the Taguenit Wadi catchment (Figure 7). The respective areas corresponding to the different degrees of flood risk varied from 8.29% (very high risk), 20.38% (high risk), 31.47% (moderate risk), 15.36% (low risk), and 24.50% (very low risk) (Table 6). Most flood areas were located on the large flood plains extending westwards from the main Taguenit Wadi. Outside the alluvial zones, with general high flood risk, it should be noted that the zones located downstream of the catchment area, on the way to the Id–Mbark village, were the most vulnerable to high flood occurrences. These areas correspond to the road networks (National Road N°1, provincial roads N°1911, 1918, and tracks), village sites (Lakhssas village, Tlat Oufla, and Idchaoud), and the areas located close to the alluvial banks of the Taguenit Wadi (Figure 7).

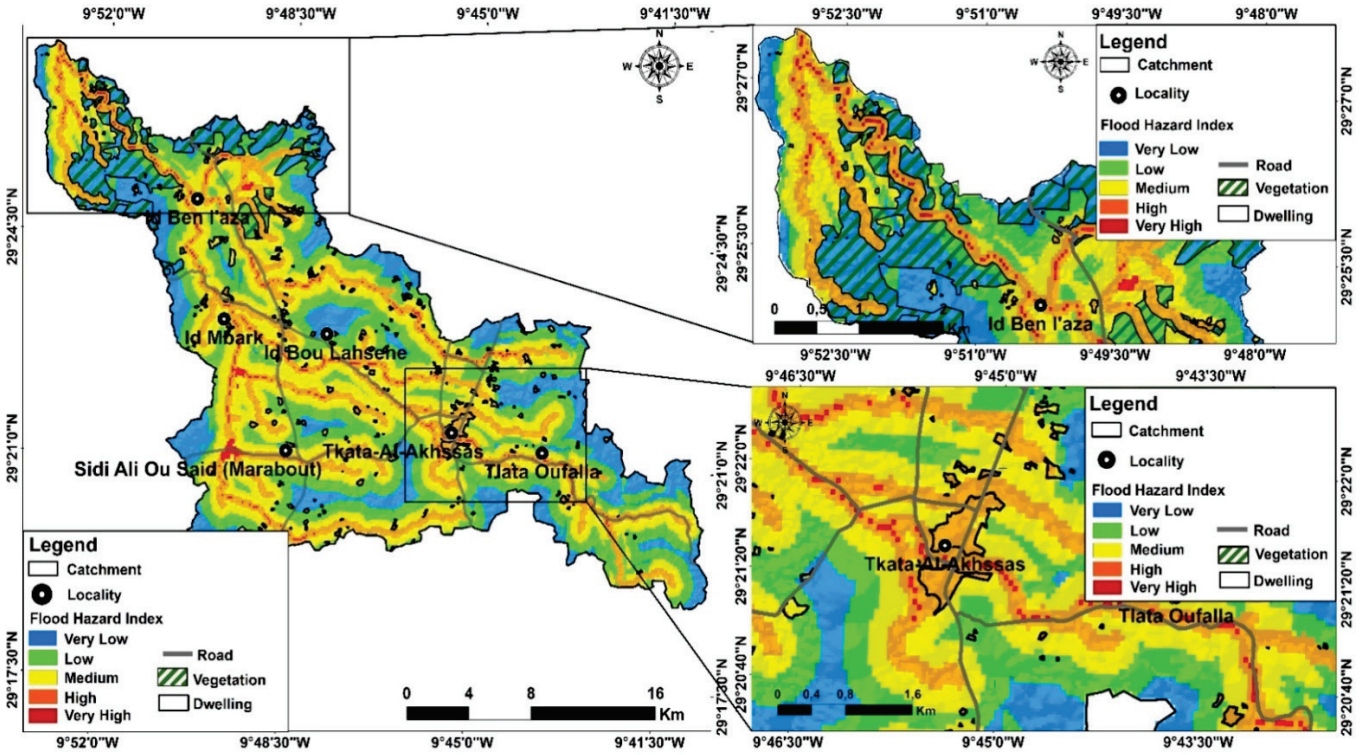



**Figure 7.** Map of areas likely to be flooded in the Taguenit Wadi catchment.

**Table 6.** Percentage of the degree of flood risk areas in the Taguenit Wadi catchment.

| Degree of Flood Risk | Area (km$^2$) | Percentage (%) |
|---|---|---|
| Very high | 10.57 | 8.04 |
| High | 27.13 | 20.63 |
| Medium | 41.34 | 31.47 |
| Low | 20.36 | 15.36 |
| Very Low | 32.16 | 24.50 |

The results of this study corroborated with those found by Kazakis et al. [28] since the two most important factors (flow accumulation and distance from rivers) seemed to be the most influential on flood intensity. Indeed, the respective dominant weights of these two factors in this study were of the order of 3 and 2.1. The comparison of the results of the application of the Flood Hazard Index (FHI) model established to previous historical events shows the reliability of the application of this model. Furthermore, Rahmati et al. [52] and Echogdali et al. [22] evaluated the effectiveness of the Flood Hazard Index (FHI) in identifying potential flood risk areas by comparing it to the results of a HECRAS hydraulic model, respectively, in Bashar River, downstream of Yasooj city and the El Maleh basin in Morocco. The results showed that the Flood Hazard Index (FHI) model was consistently more reliable in accurately predicting flood extent.

In addition to the three factors mentioned above, it seems that the difference in the lateral extension of flood risks in the Taguenit Wadi catchment is also because of the topography of the alluvial plains on either side of the main Wadi. Several topographic profiles transverse to the main river course reflect a variable morphology from one sector to another. The altitude of the Wadi valley varies from 6 m, at the level of the profile; 1 to 10 m at the level of profile 2; and could reach 35 m at the level of profile 6 (Figure 8). The areas of low valley incision automatically induced an overflow of water beyond the minor bed. The strong slopes in the upstream region favored significant confinement of the valleys that limited the lateral extension of river reaches. The village of Lakhssas, the largest and most populous commercial center in the region, with 5000 inhabitants, suffers greatly from these

extreme and repetitive flood events [14]. Of the 50 villages in the study area, only 11 villages are in a low- to a medium-risk flood zone. The remaining 80% of agrarian villages face the danger of flooding risk and occupy the alluvial plains of various tributaries.

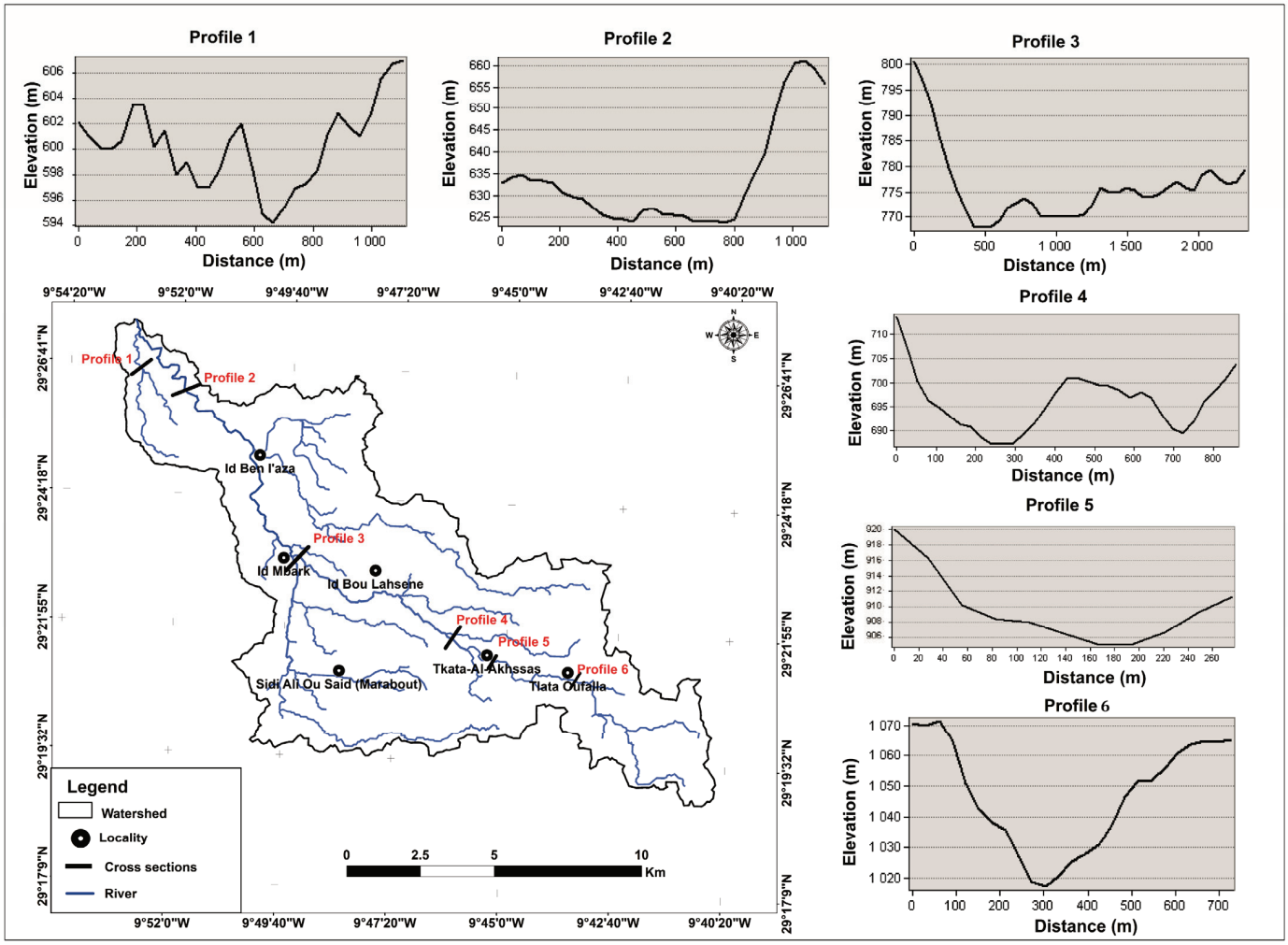



**Figure 8.** Topographic profiles at six cross-sections in the catchment of Taguenit Wadi.

### *3.2. Territorial Planning Implications of Flood Hazard Index (FHI)*

The flood susceptibility test relates the potential damage to the corresponding flood extent for each land-use type. In the catchment of Taguenit Wadi, the flood susceptibility scores for each land use type tended to increase with growing proximity to the main Wadi (Figure 9). The extent of land use damage was therefore significant. The flood susceptibility of three land-use types could be individualized into two different categories: high susceptibility (residential) and medium-to-low susceptibility (roads and agriculture). Residential areas should be avoided in high flood risk areas, while land uses with medium-to-low flood susceptibility (roads and agriculture) are suitable in these flood risk areas. These results will allow for better planning of stream restoration to reduce losses and damages during floods in the Taguenit Wadi catchment.

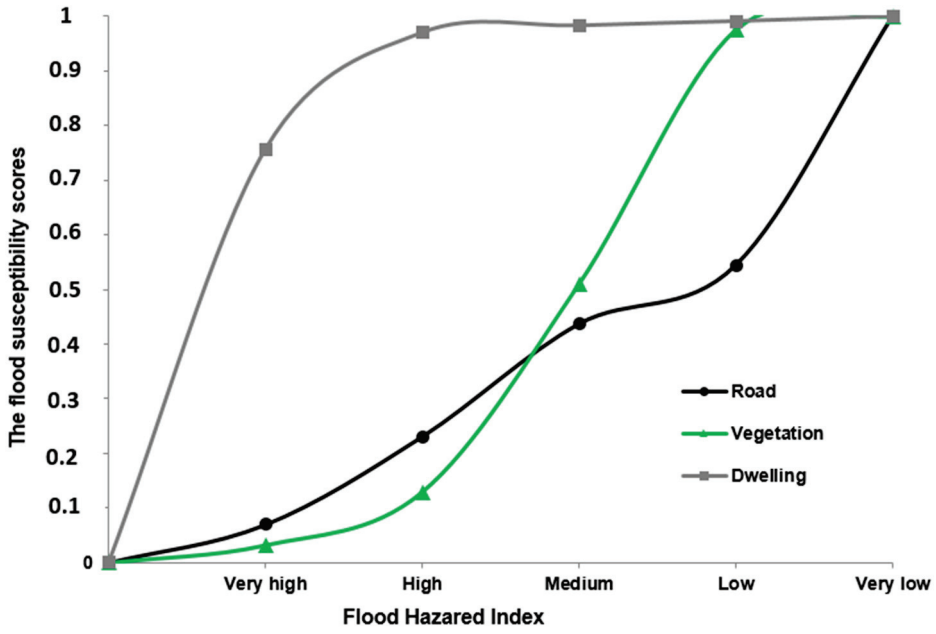



**Figure 9.** Flood Hazard Index (FHI) versus Flood susceptibility scores.

The spatial validation of the lateral extension of flood areas at the level of the Taguenit Wadi catchment was also carried out by the fieldwork observations of the water level during a few floods, especially the one in 2018, and by a survey of the local population. The obtained results from these surveys corroborated with the Flood Hazard Index (FHI) model results. Considering a few differences, the obtained results could be used in future land-use plans on the Taguenit Wadi catchment. In the absence of hydrometric data, the Flood Hazard Index (FHI) model allowed us, despite the limited amount of integrated data, to establish a map of the lateral spread of floods. However, it did not indicate the height of water in these areas, which did not allow us to approach the hazard of these flood zones and at what level where the infrastructures were submerged by water.

The Taguenit Wadi catchment with a high risk of flooding deserves special attention, especially in the habitable, agricultural, and infrastructure areas, to avoid disasters caused by extreme flood events. This basin must be equipped with hydrological and hydraulic infrastructures that allow for regular monitoring of water flows in, at least, three different zones of the main course (e.g., upstream, middle, and downstream). The measured hydrological data should be considered by an intergovernmental regional committee, which could announce warnings in case of high floods to evacuate people, livestock, and property and minimize the associated consequences.

It is important to install an early warning system to give signals during extreme downpours to avoid damage caused by the sudden filling of the Wadi section.

Early warning systems can be employed in arid contexts, as demonstrated in some studies [53,54]. These systems can reduce the risk of flash floods.

On the developmental plans for the Taguenit Wadi catchment, it would be prudent to limit the effect of floods whose origin is at the level of the upstream basin by the construction of a flood control dam. This infrastructure will allow for the reduction of the velocity of floodwater, which will increase the time of contact between the alluvium and the water, and the consequent gradual water infiltration and a strong supply of the alluvial layers largely used by the local farmers. The use of dams in arid environments to reduce flash floods has been used in several regions, and it shows important results [55,56].

On the margin of both the tributaries and Trunk River, it is recommended to develop the slopes with benches, protective sills, and dikes. The purpose of the benches is two-fold: to control water erosion and to reduce surface runoff by promoting infiltration.

The proposed measures and solutions to the Taguenit Wadi catchment, considering the geomorphological characteristics, are represented in Figure 10. In addition, it is important

to set up Flood Risk Management Strategies (FRMS), established by the local authorities, which define prohibition zones and prescription zones, which are constructible under reserve. The implementation of the FRMS will impose an act on the existing to reduce the vulnerability of elements. The challenges to be faced are mainly financial since funding is currently directed towards large basins and agricultural plains of the northern and central regions of Morocco.

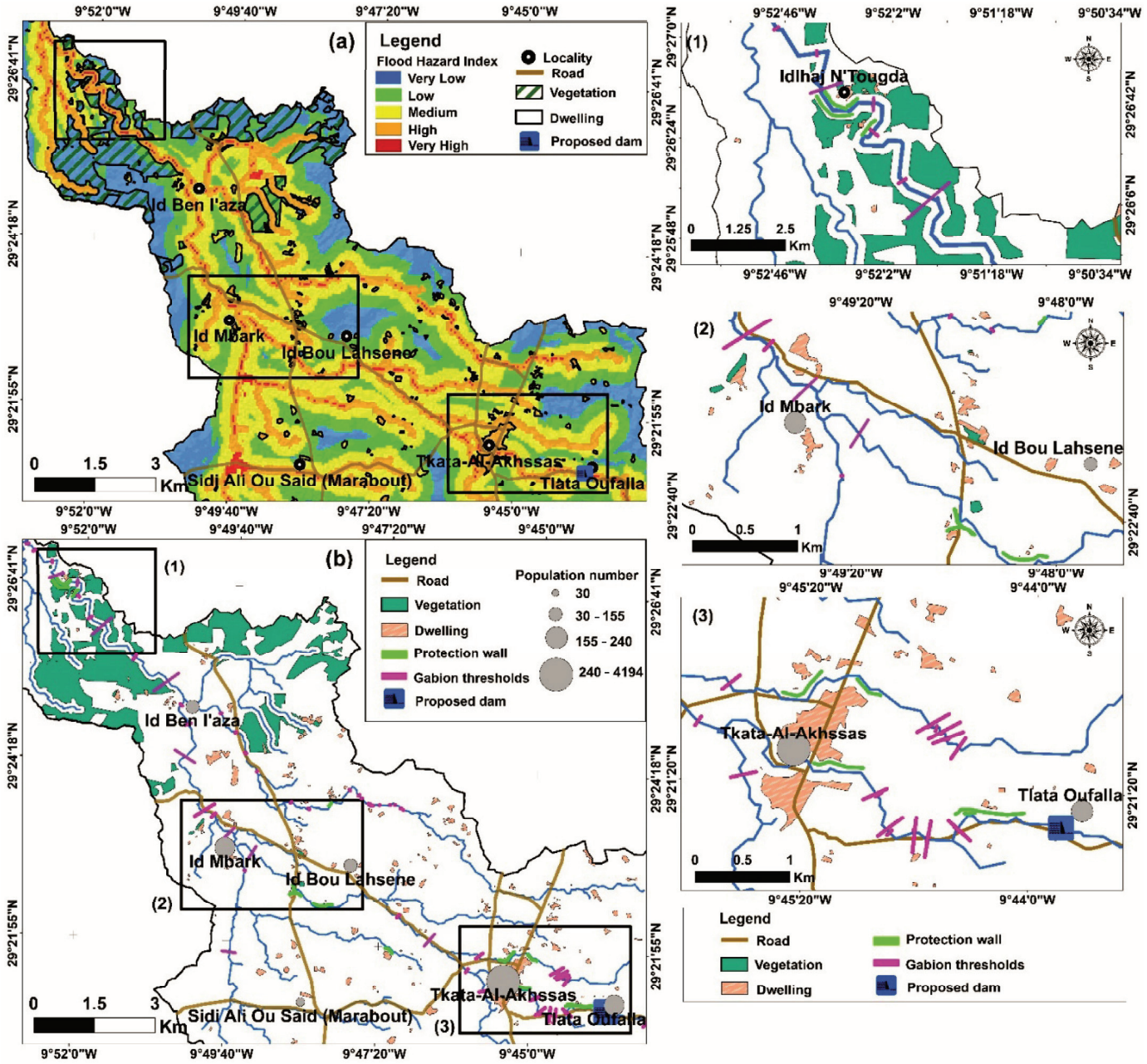



**Figure 10.** Proposed measures to be applied to the Taguenit Wadi catchment. (**a**) Areas likely to be flooded in the Wadi Taguenit watershed; (**b**) Land use, population density in the study area, and proposed measures: (**1**) Details of the downstream part of the basin with the proposed infrastructure; (**2**) Details of the medium flood risk area with medium population density and proposed infrastructure; (**3**) Details of the area most likely to be flooded and most densely populated with proposed infrastructure.

The study of the risks of flooding in the catchment of the Taguenit Wadi (not with monitoring equipment) is of paramount importance in the center of the basin, where the

village of Lakhssas is located, which is the economic engine of the region. Water operators, as well as policymakers, should encourage the strengthening of infrastructure in this basin (e.g., hydrological stations, dams, and levees) to avoid risks related to flooding impacts, mainly associated with extreme events due to storms during the summer season. In the area, it is also recommended to prohibit new constructions in flood-prone areas, in addition to the establishment of a flood warning system involving government sectors (e.g., fire brigade, river basins, the Ministry of Interior, and municipalities). In addition, an afforestation program will be crucial on the alluvial plains to improve the infiltration of water linked to floods. Afforestation can potentially mitigate flood risk by increasing infiltration [57] and mitigating runoff [58]. Dixon et al. [59] showed that floodplain forest restoration of over 10–15% of the total catchment area led to a reduction in a peak discharge of 6% at 25 years post-restoration. The construction of bridges on the main roads exposed to the risk of flooding is also compulsory to avoid the disruption of road traffic, which sometimes lasts several days in times of flood.

## 4. Conclusions

The spatialization of flood risks in the watershed of the Taguenit Wadi using the Flood Hazard Index (FHI) multi-criteria analysis method has made it possible to delimit the areas exposed to flood risks, which must be taken into consideration in future land-use plans.

More than half of the surface of the basin is considered to be an area of very high-to-medium sensitivity to flooding, especially in the downstream part of the basin. The factors most impacting these floods are the flow accumulation followed by the distance from rivers, drainage density, and land use; finally, we must not neglect the impact of the topography of the alluvial zones, which determine the spread of the floods according to the state of the collection of the valley of the main course. The evaluation of the extent of flooding simulated by the Flood Hazard Index (FHI) shows agreement with previous historical events recorded in the study area, which confirms the reliability of the model

Despite the absence of hydrometric data, the Flood Hazard Index (FHI) model proves to be a very important modeling tool for a first approach to the mapping of floodplains, as shown in this case study of the basin.

The results of the application of this model enabled us to propose solutions to avoid the impact of these floods, in this case, the equipment of hydrological stations in three zones of the basin; the construction of a capping dam upstream of the basin, which will make it possible to reduce the speed of water flow and, consequently, gradual infiltration of the latter downstream; the construction of benches and bunds along with the limits of the valleys; and finally, the installation of a vigilance system, allowing the announcement of alerts during heavy floods. However, the Flood Hazard Index (FHI) model also has some limitations. Firstly, it requires a combination of datasets collected from different sources that have a high resolution. These data are not always available at a high resolution. Secondly, another limitation is that the assignment of weights to factors is based on expert opinion, and they can add or remove factors that they judge necessary for the modeling. Finally, it indicates the horizontal extent of the flooding without giving any precision on the depth of water affecting the flooded areas.

**Author Contributions:** Conceptualization, M.I., F.F., M.A. and S.B.; methodology, M.I., I.M.H.R.A., M.A., K.S.S. and A.Q.-R.; software, M.I., F.Z.E. and M.I.-B.; validation, I.M.H.R.A., M.A., K.S.S. and A.Q.-R.; formal analysis, M.I., F.F., F.Z.E., A.W., M.I.-B. and S.B.; investigation, M.I.; resources, M.I.; data curation, M.I.; writing—original draft preparation, M.I., F.F., F.Z.E., A.W., M.I.-B. and S.B.; writing—review and editing, I.M.H.R.A., M.A., K.A., M.S.F., K.S.S. and A.Q.-R.; visualization, M.I.; supervision, F.F., M.A. and S.B.; project administration, M.A.; funding acquisition, K.A. and M.S.F. All authors have read and agreed to the published version of the manuscript.

**Funding:** This research was funded by Researchers Supporting Project number (RSP–2021/249), King Saud University, Riyadh, Saudi Arabia. The funding source was not involved in any way in the conceptualization, writing, and submission of this work.

**Institutional Review Board Statement:** Not applicable.

**Informed Consent Statement:** Not applicable.

**Data Availability Statement:** The data presented in this study are available on request from the corresponding author.

**Acknowledgments:** We thank all reviewers for their valuable comments on this paper. Isabel Margarida Horta Ribeiro Antunes is supported by FCT, Foundation for Science and Technology, I.P., projects UIDB/04683/2020 and UIDP/04683/2020.

**Conflicts of Interest:** The authors declare no conflict of interest.

## References

1. Abdulrazzak, M.; Elfeki, A.; Kamis, A.; Kassab, M.; Alamri, N.; Chaabani, A.; Noor, K. Flash flood risk assessment in urban arid environment: Case study of Taibah and Islamic universities' campuses, Medina, Kingdom of Saudi Arabia. *Geomat. Nat. Hazards Risk* **2019**, *10*, 780–796. [CrossRef]
2. Pinos, J.; Quesada-Román, A. Flood Risk-Related Research Trends in Latin America and the Caribbean. *Water* **2021**, *14*, 10. [CrossRef]
3. El Alfy, M. Assessing the impact of arid area urbanization on flash floods using GIS, remote sensing, and HEC–HMS rainfall–runoff modeling. *Hydrol. Res.* **2016**, *47*, 1142–1160. [CrossRef]
4. Bouramtane, T.; Yameogo, S.; Touzani, M.; Tiouiouine, A.; Ouardi, J.; Kacimi, I.; Valles, V.; Barbiero, L. Statistical approach of factors controlling drainage network patterns in arid areas. Application to the Eastern Anti Atlas (Morocco). *J. Afr. Earth Sci.* **2020**, *162*, 103707. [CrossRef]
5. Tang, J.C.; Vongvisessomjai, S.; Sahasakmontri, K. Estimation of flood damage cost for Bangkok. *Water Resour. Manag.* **1992**, *6*, 47–56. [CrossRef]
6. Lekuthai, A.; Vongvisessomjai, S. Intangible flood damage quantification. *Water Resour. Manag.* **2001**, *15*, 343–362. [CrossRef]
7. Hallegatte, S.; Hourcade, J.C.; Dumas, P. Why Economic Dynamics Matter in Assessing Climate Change Damages: Illustration on Extreme Events. *Ecol. Econ.* **2007**, *62*, 330–340. [CrossRef]
8. Echogdali, F.Z.; Kpan, R.B.; Ouchchen, M.; Id-Belqas, M.; Dadi, B.; Ikirri, M.; Abioui, M.; Boutaleb, S. Spatial Prediction of Flood Frequency Analysis in a Semi-Arid Zone: A Case Study from the Seyad Basin (Guelmim Region, Morocco). In *Geospatial Technology for Landscape and Environmental Management: Sustainable Assessment and Planning*; Rai, P.K., Mishra, V.N., Singh, P., Eds.; Springer: Singapore, 2022; pp. 49–71. [CrossRef]
9. Benkirane, M.; Laftouhi, N.; El Mansouri, B.; Salik, I.; Snineh, M.; El Ghazali, F.E.; Kamal, S.; Zamrane, Z. An approach for flood assessment by numerical modeling of extreme hydrological events in the Zat watershed (High Atlas, Morocco). *Urban Water J.* **2020**, *17*, 381–389. [CrossRef]
10. Heiß, L.; Bouchaou, L.; Tadoumant, S.; Reichert, B. Multi-tracer approach for assessing complex aquifer systems under arid climate: Case study of the River Tata catchment in the Moroccan Anti-Atlas Mountains. *Appl. Geochem.* **2020**, *120*, 104671. [CrossRef]
11. El Alaoui El Fels, A.; Bachnou, A.; Alaa, N. Combination of GIS and mathematical modeling to predict floods in semiarid areas: Case of Rheraya watershed (Western High Atlas, Morocco). *Arab. J. Geosci.* **2017**, *10*, 554. [CrossRef]
12. Echogdali, F.Z.; Boutaleb, S.; Jauregui, J.; Elmouden, A. Cartography of Flooding Hazard in Semi–Arid Climate: The Case of Tata Valley (South-East of Morocco). *J. Geogr. Nat. Disast.* **2018**, *8*, 214.
13. Karmaoui, A.; Messouli, M.; Yacoubi Khebiza, M.; Ifaadassan, I. Environmental Vulnerability to Climate Change and Anthropogenic Impacts in Dryland, (Pilot Study: Middle Draa Valley, South Morocco). *J. Earth Sci. Clim. Chang.* **2014**, *11*, S11.
14. Ikirri, M.; Faik, F.; Boutaleb, S.; Echogdali, F.Z.; Abioui, M.; Al-Ansari, N. Application of HEC–RAS/WMS and FHI models for the extreme hydrological events under climate change in the Ifni River arid watershed from Morocco. In *Climate and Land Use Impacts on Natural and Artificial Systems: Mitigation and Adaptation*; Nistor, M.M., Ed.; Elsevier: Amsterdam, The Netherlands, 2021; pp. 251–270. [CrossRef]
15. Souissi, D.; Zouhri, L.; Hammami, S.; Msaddek, M.H.; Zghibi, A.; Dlala, M. GIS-based MCDM–AHP modeling for flood susceptibility mapping of arid areas, southeastern Tunisia. *Geocarto Int.* **2020**, *35*, 991–1017. [CrossRef]
16. Lyu, H.M.; Zhou, W.H.; Shen, S.L.; Zhou, A.N. Inundation risk assessment of metro system using AHP and TFN-AHP in Shenzhen. *Sustain. Cities Soc.* **2020**, *56*, 102103. [CrossRef]
17. Costache, R.; Tin, T.T.; Arabameri, A.; Crăciun, A.; Ajin, R.S.; Costache, I.; Islam, A.R.M.T.; Abba, S.I.; Sahana, M.; Avand, M.; et al. Flash-flood hazard using deep learning based on $H_2O$ R package and fuzzy-multicriteria decision-making analysis. *J. Hydrol.* **2022**, *609*, 127747. [CrossRef]
18. Fenicia, F.; Kavetski, D.; Savenije, H.H.; Clark, M.P.; Schoups, G.; Pfister, L.; Freer, J. Catchment properties, function, and conceptual model representation: Is there a correspondence? *Hydrol. Process.* **2014**, *28*, 2451–2467. [CrossRef]
19. Luu, C.; Von Meding, J.; Kanjanabootra, S. Assessing flood hazard using flood marks and analytic hierarchy process approach: A case study for the 2013 flood event in Quang Nam, Vietnam. *Nat. Hazards* **2018**, *90*, 1031–1050. [CrossRef]

20. Costache, R.; Pham, Q.B.; Arabameri, A.; Diaconu, D.C.; Costache, I.; Crăciun, A.; Ciobotaru, N.; Pandey, M.; Arora, A.; Ali, S.A.; et al. Flash-flood propagation susceptibility estimation using weights of evidence and their novel ensembles with multicriteria decision making and machine learning. *Geocarto Int.* **2021**, 1–33. [CrossRef]
21. Siahkamari, S.; Haghizadeh, A.; Zeinivand, H.; Tahmasebipour, N.; Rahmati, O. Spatial prediction of flood-susceptible areas using frequency ratio and maximum entropy models. *Geocarto Int.* **2018**, *33*, 927–941. [CrossRef]
22. Al-Abadi, A.M.; Shahid, S. A comparison between index of entropy and catastrophe theory methods for mapping groundwater potential in an arid region. *Environ. Monit. Assess.* **2015**, *187*, 576. [CrossRef] [PubMed]
23. Mosavi, A.; Golshan, M.; Janizadeh, S.; Choubin, B.; Melesse, A.M.; Dineva, A.A. Ensemble models of GLM, FDA, MARS, and RF for flood and erosion susceptibility mapping: A priority assessment of sub-basins. *Geocarto Int.* **2020**, *37*, 2541–2560. [CrossRef]
24. Al-Juaidi, A.E.M.; Nassar, A.M.; Al-Juaidi, O.E.M. Evaluation of flood susceptibility mapping using logistic regression and GIS conditioning factors. *Arab. J. Geosci.* **2018**, *11*, 765. [CrossRef]
25. Hong, H.; Panahi, M.; Shirzadi, A.; Ma, T.; Liu, J.; Zhu, A.X.; Chen, W.; Kougias, I.; Kazakis, N. Flood susceptibility assessment in Hengfeng area coupling adaptive neuro-fuzzy inference system with genetic algorithm and differential evolution. *Sci. Total Environ.* **2018**, *621*, 1124–1141. [CrossRef]
26. Wang, Y.; Fang, Z.; Hong, H.; Costache, R.; Tang, X. Flood susceptibility mapping by integrating frequency ratio and index of entropy with multilayer perceptron and classification and regression tree. *J. Environ. Manag.* **2021**, *289*, 112449. [CrossRef] [PubMed]
27. Ghosh, A.; Kar, S.K. Application of analytical hierarchy process (AHP) for flood risk assessment: A case study in Malda district of West Bengal, India. *Nat. Hazards* **2018**, *94*, 349–368. [CrossRef]
28. Kazakis, N.; Kougias, I.; Patsialis, T. Assessment of flood hazard areas at a regional scale using an index–based approach and Analytical Hierarchy Process: Application in Rhodope–Evros region, Greece. *Sci. Total Environ.* **2015**, *538*, 555–563. [CrossRef]
29. Echogdali, F.Z.; Boutaleb, S.; Elmouden, A.; Ouchchen, M. Assessing Flood Hazard at River Basin Scale: Comparison between HECRAS–WMS and Flood Hazard Index (FHI) Methods Applied to El Maleh Basin, Morocco. *J. Water Resour. Prot.* **2018**, *10*, 957–977. [CrossRef]
30. Kundzewicz, Z.W.; Kanae, S.; Seneviratne, S.I.; Handmer, J.; Nicholls, N.; Peduzzi, P.; Mechler, R.; Bouwer, L.M.; Arnell, N.; Mach, K.; et al. Flood risk and climate change: Global and regional perspectives. *Hydrol. Sci. J.* **2014**, *59*, 1–28. [CrossRef]
31. Sipos, G.; Blanka, V.; Mezősi, G.; Kiss, T.; van Leeuwen, B. Effect of climate change on the hydrological character of River Maros, Hungary-Romania. *J. Environ. Geogr.* **2014**, *7*, 49–56. [CrossRef]
32. Yamamoto, K.; Sayama, T. Impact of climate change on flood inundation in a tropical river basin in Indonesia. *Prog. Earth Planet. Sci.* **2021**, *8*, 5. [CrossRef]
33. Gusarov, A.V.; Sharifullin, A.G.; Komissarov, M.A. Contemporary long-term trends in water discharge, suspended sediment load, and erosion intensity in river basins of the North Caucasus region, SW Russia. *Hydrology* **2021**, *8*, 28. [CrossRef]
34. Dill, H.G.; Kaufhold, S.; Techmer, A.; Baritz, R.; Moussadek, R. A joint study in geomorphology, pedology and sedimentology of a Mesoeuropean landscape in the Meseta and Atlas Foreland (NW Morocco). A function of parent lithology, geodynamics and climate. *J. Afr. Earth Sci.* **2019**, *158*, 103531. [CrossRef]
35. Sdzuy, K.; Geyer, G. The base of the Cambrian in Morocco. In *The Atlas System of Morocco*; Jacobshagen, V.H., Ed.; Springer: Berlin/Heidelberg, Germany, 1988; pp. 91–106. [CrossRef]
36. Benssaou, M.; Hamoumi, N. Le graben de l'Anti–Atlas occidental (Maroc): Contrôle tectonique de la paléogéographie et des séquences au Cambrien inférieur. *Comptes Rendus Geosci.* **2003**, *335*, 297–305. [CrossRef]
37. Soulaimani, A.; Bouabdelli, M. Le Plateau de Lakhssas (Anti–Atlas occidental, Maroc): Un graben fini–précambrien réactivé à l'hercynien. *Ann. Soc. Géol. Nord.* **2005**, *2*, 177–184.
38. IUSS Working Group WRB. World Reference Base for Soil Resources 2014, update 2015. International soil classification system for naming soils and creating legends for soil maps. In *World Soil Resources Reports*; FAO: Rome, Italy, 2015; p. 182.
39. Patrikaki, O.; Kazakis, N.; Kougias, I.; Patsialis, T.; Theodossiou, N.; Voudouris, K. Assessing flood hazard at river basin scale with an index–based approach: The case of Mouriki, Greece. *Geosciences* **2018**, *8*, 50. [CrossRef]
40. Bennani, O.; Druon, E.; Leone, F.; Tramblay, Y.; Saidi, M.E.M. A spatial and integrated flood risk diagnosis: Relevance for disaster prevention at Ourika valley (High Atlas–Morocco). *Disaster Prev. Manag.* **2019**, *28*, 548–564. [CrossRef]
41. Elkhrachy, I. Flash flood hazard mapping using satellite images and GIS tools: A case study of Najran City, Kingdom of Saudi Arabia (KSA). *Egypt J. Remote Sens. Space Sci.* **2015**, *18*, 261–278. [CrossRef]
42. Yoo, C.; Cho, E.; Na, W.; Kang, M.; Lee, M. Change of rainfall–runoff processes in urban areas due to high–rise buildings. *J. Hydrol.* **2021**, *597*, 126155. [CrossRef]
43. Aaron, C.; Venkatesh, M. Effect of Topographic Data, Geometric Configuration and Modeling Approach on Flood Inundation Mapping. *J. Hydrol.* **2009**, *377*, 131–142. [CrossRef]
44. Demek, J. *Manual of Detailed Geomorphological Mapping*; Czechoslovak Academy of Sciences: Prague, Czech Republic, 1972.
45. Saaty, T.L. How to make a decision: The analytic hierarchy process. *Eur. J. Oper. Res.* **1990**, *48*, 9–26. [CrossRef]
46. Saaty, T.L. An exposition of the AHP in reply to the paper "remarks on the analytic hierarchy process". *Manag. Sci.* **1990**, *36*, 259–268. [CrossRef]
47. Saaty, T.L. A scaling method for priorities in hierarchical structures. *J. Math. Psychol.* **1977**, *15*, 234–281. [CrossRef]

48. Saaty, T.L.; Vargas, L.G. (Eds.) The seven pillars of the analytic hierarchy process. In *Models, Methods, Concepts & Applications of the Analytic Hierarchy Process*; Springer: Boston, MA, USA, 2012; Volume 175, pp. 23–40. [CrossRef]
49. Koks, E.E.; Jongman, B.; Husby, T.G.; Botzen, W.J. Combining hazard, exposure and social vulnerability to provide lessons for flood risk management. *Environ. Sci. Policy* **2015**, *47*, 42–52. [CrossRef]
50. Hall, J.W.; Tarantola, S.; Bates, P.D.; Horritt, M.S. Distributed sensitivity analysis of flood inundation model calibration. *J. Hydraul. Eng.* **2005**, *131*, 117–126. [CrossRef]
51. Moel, H.D.; Asselman, N.E.M.; Aerts, J.C.J.H. Uncertainty and sensitivity analysis of coastal flood damage estimates in the west of the Netherlands. *Nat. Hazards Earth Syst. Sci.* **2012**, *12*, 1045–1058. [CrossRef]
52. Rahmati, O.; Zeinivand, H.; Besharat, M. Flood hazard zoning in Yasooj region, Iran, using GIS and multi-criteria decision analysis. *Geomat. Nat. Hazards Risk* **2016**, *7*, 1000–1017. [CrossRef]
53. Sorooshian, S.; Nguyen, P.; Sellars, S.; Braithwaite, D.; Agha Kouchak, A.; Hsu, K. Satellite–based remote sensing estimation of precipitation for early warning systems. In *Extreme Natural Hazards, Disaster Risks and Societal Implications*; Ismail-Zadeh, A., Urrutia Fucugauchi, J., Kijko, A., Takeuchi, K., Zaliapin, I., Eds.; Cambridge University Press: Cambridge, UK, 2014; Volume 1, pp. 99–112.
54. Cools, J.; Innocenti, D.; O'Brien, S. Lessons from flood early warning systems. *Environ. Sci. Policy* **2016**, *58*, 117–122. [CrossRef]
55. Abbasi, N.A.; Xu, X.; Lucas-Borja, M.E.; Dang, W.; Liu, B. The use of check dams in watershed management projects: Examples from around the world. *Sci. Total Environ.* **2019**, *676*, 683–691. [CrossRef] [PubMed]
56. Tarchiani, V.; Massazza, G.; Rosso, M.; Tiepolo, M.; Pezzoli, A.; Housseini Ibrahim, M.; Katiellou, G.L.; Tamagnone, P.; De Filippis, T.; Rocchi, L.; et al. Community and impact based early warning system for flood risk preparedness: The experience of the Sirba River in Niger. *Sustainability* **2020**, *12*, 1802. [CrossRef]
57. Bracken, L.J.; Croke, J. The concept of hydrological connectivity and its contribution to understanding runoff-dominated geomorphic systems. *Hydrol. Process.* **2007**, *21*, 1749–1763. [CrossRef]
58. Broadmeadow, S.; Nisbet, T.R. *Opportunity Mapping for Woodland to Reduce Flooding in the Yorkshire and the Humber Region*; Forest Research Monograph; Forest Research: Surrey, UK, 2010; Volume 1, 64p.
59. Dixon, S.J.; Sear, D.A.; Odoni, N.A.; Sykes, T.; Lane, S.N. The effects of river restoration on catchment scale flood risk and flood hydrology. *Earth Surf. Process. Landf.* **2016**, *41*, 997–1008. [CrossRef]

land

*Article*

# Merging Historical Archives with Remote Sensing Data: A Methodology to Improve Rockfall Mitigation Strategy for Small Communities

**Davide Notti [1], Diego Guenzi [1,*], Rosa Lasaponara [2] and Daniele Giordan [1]**

[1] Italian National Research Council, Research Institute for Geo-Hydrological Protection (CNR-IRPI), Strada delle Cacce 73, 10135 Torino, Italy
[2] Italian National Research Council, Institute of Methodologies for Environmental Analysis (CNR-IMAA), c/da S.Loja, Tito Scalo, 85050 Potenza, Italy
* Correspondence: diego.guenzi@irpi.cnr.it

**Abstract:** Both in the literature and in practical applications, several works have dealt with rockfall analysis and the planning of mitigation measures. It is also possible to find inventories and papers that describe historical events. However, it is challenging to find methodologies or studies about inventorying rockfall mitigation or their efficiency over time. In Italy, many rockfall barriers and other mitigation solutions have been built in the last decades, and one of the most urgent problems is their correct management and maintenance. Lauria, a small town in southern Italy, can be considered an example of this common condition exacerbated by a wildfire in 2017. This work presents a methodology for assessing rockfall risk and creating a geodatabase of mitigation structures focused on small communities. We used digitalization of archival sources to reconstruct and geocode the record of mitigation works. An available database of historical landslides was used to reconstruct the most relevant rockfall events. Moreover, we coupled this with Sentinel-2 images and high-resolution orthophotos to map the wildfire area. Data obtained from the UAV-LiDAR survey were used to map the mitigation structures. The aim was to create a reliable state-of-the-art method, described in an operational monograph, to be used by experts for the design of new rockfall mitigation structures in both an affordable and efficient way. Moreover, we created a simple webGIS and a 3-D interactive view, helpful in disseminating rockfall hazards and mitigation strategies among the population at risk.

**Keywords:** historical archive; LiDAR; rockfall mitigation; wildfire; Sentinel-2; webGIS

**Citation:** Notti, D.; Guenzi, D.; Lasaponara, R.; Giordan, D. Merging Historical Archives with Remote Sensing Data: A Methodology to Improve Rockfall Mitigation Strategy for Small Communities. *Land* **2022**, *11*, 1951. https://doi.org/10.3390/land11111951

Academic Editors: Mariano Barriendos Vallvé, Fabrizio Terenzio Gizzi, Ruediger Glaser, Christoph Gruetzner, Walter Palmieri, Sabina Porfido, Heather Sangster and Laura Turconi

Received: 15 September 2022
Accepted: 30 October 2022
Published: 1 November 2022

**Publisher's Note:** MDPI stays neutral with regard to jurisdictional claims in published maps and institutional affiliations.

**Copyright:** © 2022 by the authors. Licensee MDPI, Basel, Switzerland. This article is an open access article distributed under the terms and conditions of the Creative Commons Attribution (CC BY) license (https://creativecommons.org/licenses/by/4.0/).

## 1. Introduction

Rockfall mitigation needs a multidisciplinary approach [1] including research tools such as inventory maps and susceptibility models [2,3], numerical modelling [4], the effect of extreme events such as wildfires [5], and the design of mitigation structures [6].

Most rockfall events happen in small villages or similar settings and, except for the local communities, they are often overlooked. However, even if limited to a very local scale, rockfalls can threaten several people's lives and restrict access to significant portions of small villages and urbanized areas.

Rockfalls that affect small towns or villages are often little studied, and the local authorities do not have enough resources and technical background to define a long-term strategy to manage rockfall-prone areas. In most cases, local authorities focus only on the immediate resolution of the localized problem without a general overview of a larger extent.

Local administrations often commission their studies on rockfall risk assessments over small areas to different companies that make general assessments without a global view of the problem. Up to a few years ago, these studies were stored in local archives and only in paper format in the town hall. Often, such documents are forgotten or lost. Consequently,

a considerable amount of knowledge cannot be accessed when new studies and projects are made, resulting in difficult evaluation of the affordability of the different scenarios [7].

In the literature, it is possible to find many studies on rockfall modelling and the design of mitigation strategies [8], but few studies have evaluated the degradation of mitigation [1,9]. Moreover, wildfires in several parts of the world, such as the Mediterranean climate regions, exacerbate instability and threaten rockfall mitigation structures [5,10–12]. Thus, correct maintenance of infrastructures to reduce the rockfall risk is critical. For this reason, even good remedial works can be affected by irreversible degradation without a clear maintenance plan. Moreover, these plans are not easily applied and, in the past, they have not been provided by companies. The problem of correct infrastructure maintenance is critical, particularly in areas such as Italy, where many different technical solutions have been adopted in the last three decades. Due to the recent substantial evolution of the rockfall barriers, many ancient installations are not compliant with the actual rules. In addition, in the past the installation of barriers did not require the definition of an adequate maintenance plan. For this reason, in a large part of the country, the most important aspects of rockfall risk reduction are not related to the installation of new solutions but the correct management of already installed ones. In many cases, the only possibility is the replacement of old structures. The replacement, of course, requires a new analysis of the studied area to design the new installations correctly. This procedure is often very complex and the first important element that should be accessible is a detailed description of the state-of-the-art and the implementation of a user-friendly solution for proper support and the upgrade procedures for the installed systems. The digitalization of old archive studies [13–15] is the first low-cost solution to create a (geo)database of available information. Digitalization is often a partial and preliminary solution because the amount of data can be very high. For this reason, using a dedicated document, such as the Operative Monograph (OM) proposed by [16], can add value by making a collating essential information organized in a predefined structure.

The availability of high-resolution DTMs could significantly help study rockfall-prone areas. In recent years, LiDAR [17] and uncrewed aerial vehicles (UAV) [18–20] have mapped areas affected by rockfalls at a very-high resolution and relatively low cost. Moreover, proximal remote sensing techniques also reduce risk for the operators, limiting (or eliminating) the need for direct access to the most dangerous areas [21]. In addition, a very high-resolution DTM can be used to compute a more effective GIS-based rockfall simulation [22]. This work presents a methodology based on digitalizing an old mitigation work archive, and integrating it with ancillary data, high-resolution LiDAR DTM and other remote sensing data. The procedure aims to create an integrated geodatabase of rockfall mitigation works and their state of maintenance. The method was tested on a small site in Lauria municipality, southern Italy, but can be applied on a large scale for scientific applications or risk management plans.

Since the late 1980s, the municipality of Lauria and a regional civil engineering board set up a series of studies and mitigation works. The most important works were done from 1997 to 2001. Several rockfall events happened after the 1996 wildfire and the 1998 earthquake [23]. Geo-structural survey borehole investigation and rockfall modelling were commissioned for this mitigation work. The results of geo-structural surveys and geomechanical analysis were adopted to detect potentially unstable sectors. This important information from past studies risked being forgotten without digitalization and geocoding processes that can allow use of these results in future studies.

In our work, we acquired and digitalized all available documents and studies in the area of interest developed over the last 40 years. We created a geodatabase that identifies all the infrastructures and collects all the available information. The OM and the GIS database can be used to organize large and complex datasets that can be adopted to manage slope instability, and be used by experts or local authorities as a starting point for urban planning, to assess numerical models, or to study rockfall mitigation works. The proposed methodology is the first step toward a better definition of a long-term strategy to reduce the

rockfall risk in urban areas that experts and local authorities must manage. We also created information sources for dissemination, such as a webGIS based on open source software and 3-D models aimed to increase preparedness among the population and simplify access to available information.

This paper is organized as follows. A description of the study area is provided in Section 2, followed by the materials and methods adopted in Section 3 and the results in Section 4. The results are divided into three parts: (i) archive digitalization and the history of rockfall works and events; (ii) remote sensing and LiDAR data, and (iii) a description of the operative monograph and results dissemination. The last two sections of the paper are the discussion (Section 5) and conclusions (Section 6).

## 2. Study Area

The town of the Lauria (Basilicata region, southern Italy) is located in the Apennine belt (Figure 1A).

From a geological point of view, the town is on the northern border of the Lauria Mountains structural unit [24], mainly made by Mesozoic calcareous formation. The lower part of the historical town (Lauria Inferiore) was built at the base of Sant'Elia ridge. According to the CARG Geological map [25], the slope affected by rockfall is located in the Jurassic unit "Alburno-Cevati-Pollino" (Figure 1B). The lithology is represented by dolomitic limestone, with interbedded layers of marl, conglomerate and calcareous sandstone (Figure 1B). The main structural lineament and sub-vertical faults are NNW-SSE, NW-SE, and N-S. The main dipping of the formation is to NW, and some karst processes enhance rock mass fracturation.

The high acclivity of the slope and the complex fracture systems isolate unstable blocks subject to frequent rockfall/toppling events of small-medium volumes. The slope affected by rockfall has a length of about 1 km, and reaches 200 m in height. The average gradient is about 60° in the sector just above the old part of Lauria town Figure 1C. Several buildings are located less than 20 m from the foot of the cliff.

In recent times, events such as severe rainfall (2002), wildfires (1996 and July 2017) and an earthquake (9 September 1998, the epicentre was located about 3 km southeast of Lauria and with a magnitude of Mw = 5.6) [23] have caused significant rockfalls that affected the closest buildings and the road. Fortunately, there have been no fatalities in recent years. In particular, in July 2017, several fires occurred in southern Italy [26], and a large one affected most of the Sant'Elia ridge. The event caused some concern in the local administration, which followed up with investigations to assess the maintenance state of the rockfall defence systems installed.

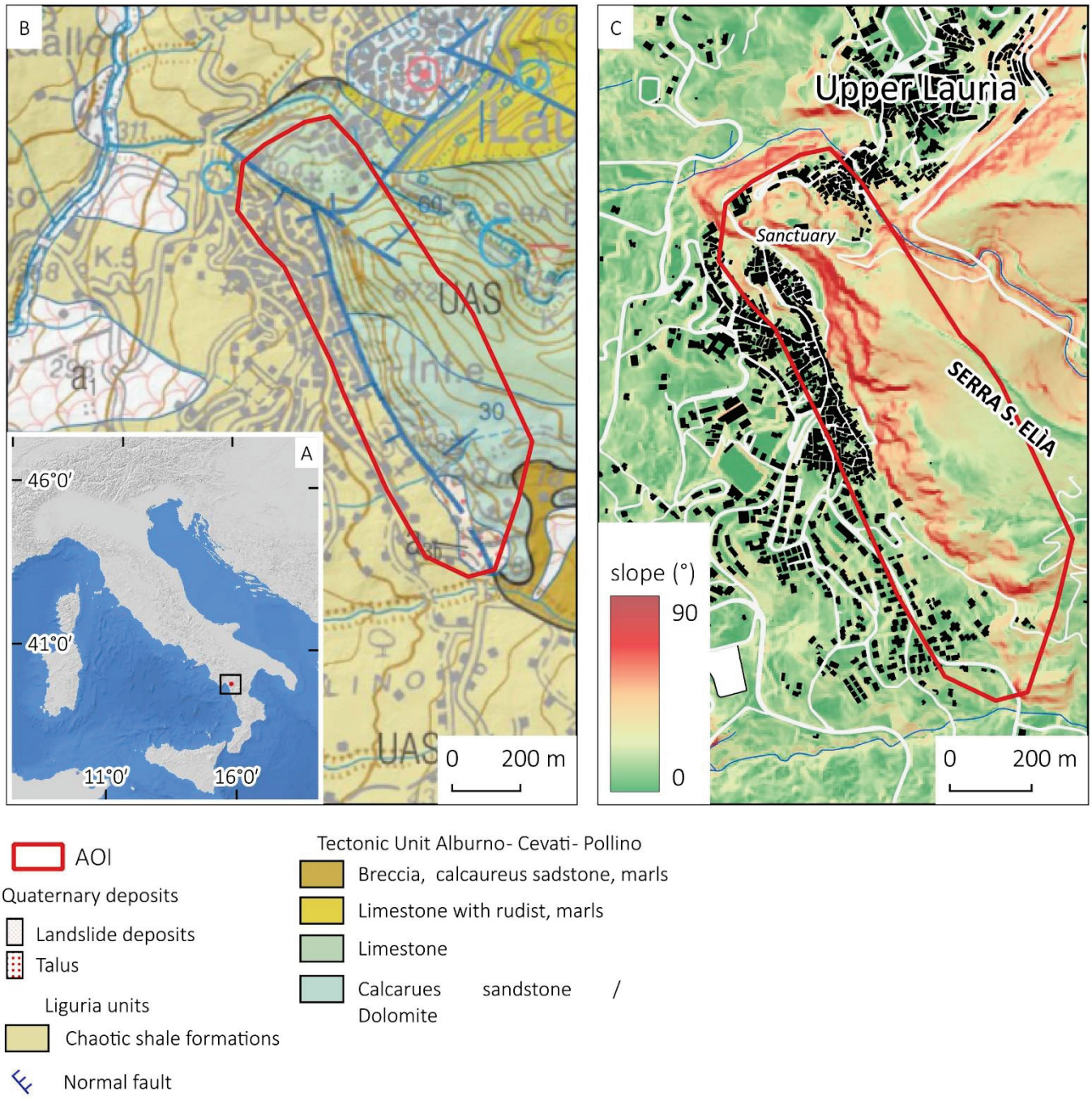



**Figure 1.** (**A**) Location of Lauria case study. (**B**) Geological settings of the study area, adapted with permission from [25] 2014, ISPRA Servizio Geologico d'Italia. (**C**) Acclivity maps of study area based on 5 m DTM of Regione Basilicata.

## 3. Materials and Methods

We created a methodological approach (Figure 2) to build a database of existing knowledge and data for future studies and dissemination to the population. The methodology comprised four steps: (i) data collection; (ii) an organized geodatabase setup; (iii) publication of the OM that collates all the available information on the case study, and (iv) results dissemination.

For data collection, there were four main input types: (i) Lauria municipal archive of mitigation works, (ii) rockfall events and other databases, (iii) creation of the 2017 wildfire map; (iv) DTM Lidar and orthophotos of the study area.

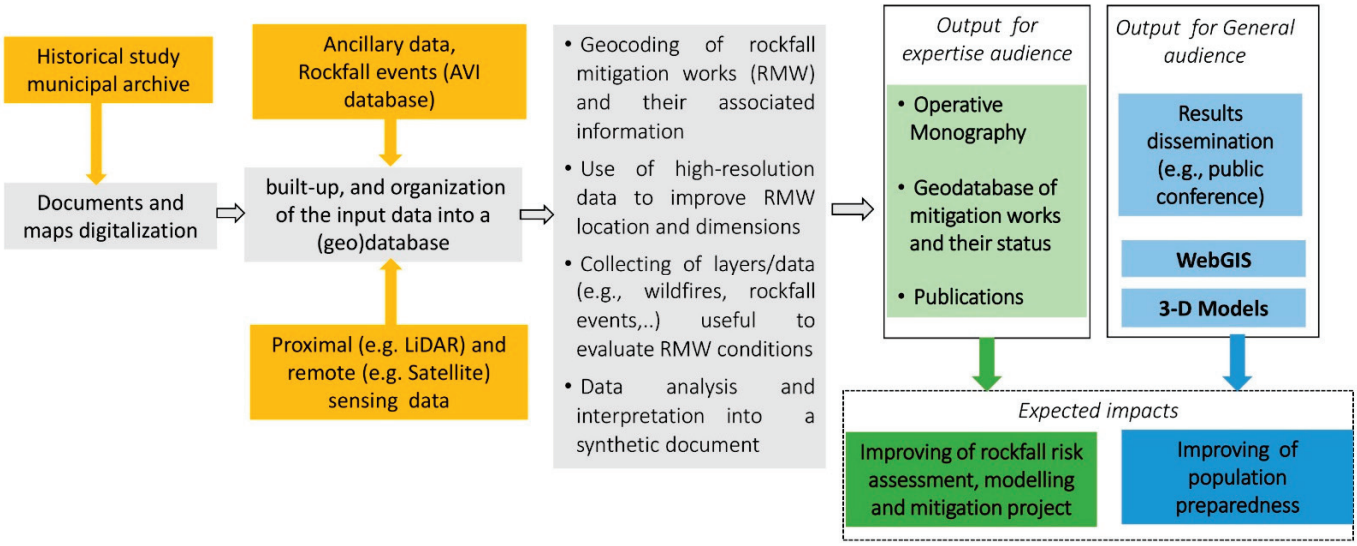



**Figure 2.** Flow chart of the proposed methodology.

The first input deals with the digitalization of old studies, maps and documents from the archive of Lauria municipality and the geocoding of maps on a GIS. We digitized about 70 documents and maps from the Lauria town hall archive (approximately 20 GB of data). Most of them were archived only in paper format in the Lauria town hall. We organized them in a hierarchical structure that follows the original archive's organization (Table 1).

**Table 1.** An example of the hierarchical structure of the database of digitalized documents (translated from an original document made for Lauria municipality).

| Data/Documents Repository | | Document Filename | Shorth Descriptions | Year |
|---|---|---|---|---|
| **Parent** | **Child** | | | |
| 01_1997_ Draft projects | 03_Normative | Tecnhichal_specifications.pdf | Rockfall mitigation works requirements | 1999 |
| | | Barrier_req.pdf | Rockfall barriers requirements | 1999 |
| | 04_Maps | Widespread_instability_map.tif | Preliminary maps of widespread rockfall instability | 1999 |
| | | Punctual_instability_map.tif | Preliminary maps of punctual rockfall instability | 1999 |
| 02_1998 | 01_geomechanicahl | Geomechanical_rel.pdf | Rock mass characterization relation and maps | 1998 |
| 03_Final projects | 03_Certificates | Rokfall_barrier_pr_1500kJ.tif | Rockfall barrier sketch | 2001 |
| | | Rokfall_barrier_cert_1500kJ.pdf | Rockfall barrier certificate | 2001 |
| 04_2002 Rockfall event | 02_Maps | 2002_barrier_maps.tif | Rockfall barriers maps | 2002 |
| | | 2002_restore_maps.tif | Maps of restoration of damaged mitigation works | 2002 |

The second input involved collecting all the available information about rockfall events from historical archives of newspapers. In particular, we added to our project all the data from the "Aree Vulnerate Italiane" (AVI) project led by CNR-IRPI [15], a database of historical landslides and flood events that occurred in Italy until the early 2000s. Other sources of information and geo-data were the Regione Basilicata geoportal [27]

and the national landslide inventory (IFFI project geoportal [28]) and other cartographic services [29].

The third input involved creating a burnt area map of the July 2017 wildfire using the variation of normalized burn ratio ($NBR_{var}$) or dNBR [30] obtained from $NBR_{post}$-$NBR_{pre}$ fire. The NBR is based on the following equation: (NIR − SWIR)/(NIR + SWIR), where NIR is the near-infrared band, while SWIR is the short-wave infrared. This index is widely used in the literature [26,31,32]. We used Sentinel-2 images pre-wildfire and post-wildfire and validated the $NBR_{var}$ map with post-event aerial photos of the Regione Basilicata.

The last input involved the acquisition of very high-resolution DTM and orthophotos based on LiDAR data of the study area. The LiDAR survey was made by an external enterprise and financed by Lauria municipality. The LiDAR used for the survey was a Riegl miniVUX-1 with Applanix APX-20 and Sony A7R Mk III loaded on a DJI MATRICE 600 UAV. The area covered was about 609,260 $m^2$, with an average point density of 176 $pt/m^2$. Using ground control points (GCPs) measured with real-time kinematic positioning of the global navigation satellite system (RTK GNSS) allowed validation of the cloud points, which have an accuracy of 2 cm on the vertical axis. The points cloud was processed to obtain DTM and DSM at 0.5 m of spatial resolution and orthophotos at 0.02 m. The LiDAR data were also managed directly on QGIS using the Whitebox plugin [33] for a detailed analysis of some rockfall barriers.

The second step was creating an organized database, in which the studies and project materials were sorted based on the year of production, works certification and typology. At the same time, through GIS software, we created a geodatabase of rockfall mitigation works, main rockfall events and other ancillary data. The mitigation structures were geolocated with the help of a high-resolution LiDAR orthophoto. We also did a ground survey to take photos of the most representative mitigation structures.

In the third step, we created the OM [16] that represents a practical (and standardized) organization of what we already know about the studied phenomenon.

The OM is a document for an expert audience and was delivered confidentially to Lauria municipality. The document contains six main chapters: (1) summary of available ancillary data; (2) geological/geomorphological and structural settings based on previous studies; (3) state of the art of the mitigation work, including the certificate and calibration; (4) description of LiDAR and orthophoto product; (5) webGIS and 3-D models metadata; (6) final consideration and suggestion for future studies. In particular, in the last section, essential information and data currently missing are suggested for implementing the geodatabase. In the conceptual scheme of OM, all the new information produced will be collected in the database and will update the OM in a positive feedback circle. In the case of rockfall mitigation work, these actions could, for example, include a new geomechanical survey or a deep investigation of the maintenance status of rockfall barriers.

The last considered step involves the dissemination of results. This phase aims to increase the population's awareness and knowledge about rockfall risk. The main products consist of a webGIS built on free software, and 3-D models for interactive visualization of the affected areas.

To create the webGIS of Lauria rockfall mitigation works, we used GeoServer and MapStore services. The GeoServer [34] is a web mapping software for geo-data dissemination. GeoServer is a Free and Open-Source Software (FOSS) server, written entirely in Java that allows users to store, view and edit geospatial data. Designed for interoperability, it publishes data from any major spatial data source using open standards [35,36].

MapStore [37] is a professional FOSS cartography and geographical information platform based on a topological map model that allows creating webGIS services using the WMS obtained from, for example, GeoServer.

To create a 3-D interactive view of the mitigation works (that can be used with any browser without installing GIS or other software), we used the Qgis2threejs plugin for QGIS [38]. The LiDAR DTM was used as an elevation layer to create several high-resolution 3-D view models with different layers.

## 4. Results

Archive digitization, remote sensing and LiDAR data, and the dissemination of results allowed us to produce a detailed and updated state-of-the-art rockfall document. The result forms the basis for further works and decisions for experts and Lauria authorities. In the next section, the main outputs are discussed.

### *4.1. Archive Digitization and History of Rockfall Works and Events*

The digitization of the archives and the search in all available databases allowed us to reconstruct the history of rockfall events and mitigation works, as summarised in Table 2.

**Table 2.** History of main rockfall events and mitigation work from historical archives.

| Events/Action | Date | Source |
|---|---|---|
| Rockfall (generic report) | 1970 | AVI project [39] |
| Rockfall (report on mitigation strategy) | 1983 | AVI project [40] |
| Rockfall event | 1996-11 | parliamentary question [41] |
| Rockfall mitigation study start | 1997 | Lauria archive [42] |
| Rockfall triggered by an earthquake | 1998-09 | Lauria archive [43] |
| Rockfall mitigation works ends | 2001 | Lauria archive [44] |
| Rockfall damaged some mitigation structures | 2002-01 | Lauria archive [45] |
| Restoration of damaged structures | 2002 | Lauria archive [46] |
| Rockfall triggered by fires | 2017 | Local newspaper [47] |
| State of the art of mitigation work | 2021 | OM and webGIS of CNR-IRPI [48] |
| Start of the restoration of mitigation structures | 2022 | Lauria municipality [49] |

For instance, in the AVI project archive it was possible to find the following information [40]: "The corps of Civil Engineers intervened in 1983 for the scaling of a stone volume. In 1983 the Prefecture assigned to the municipality of Lauria an amount of 50 million Italian lire necessary to cover the hospitality costs of the families temporarily evacuated. The recommended intervention methods are divided into two phases: (1) survey carried out by expert rock climbers aimed at carrying out scaling of completely detached boulders, cementing of the surface blocks in the process of detachment, nailing and application of electro-welded mesh; (2) implementation of active tie rods and simultaneous installation of monitoring instrumentation consisting of crackmeters, depth strain gauge bars, fixed inclinometer columns, and load cells".

Another source of documented rockfall events came from a parliamentary question of 1996 [41].

"In the night between 22 and 23 November 1996, during a violent storm, a rockfall of limestone rock occurred in Lauria (PZ), with an estimated volume of a few cubic meters. The detachment occurred from a pinnacle of the ridge overlooking the San Giacomo district. After a jump of about 100 m, the boulders reached the underlying collection basin, delimited by the rockfall wall. Large rock fragments overpassed the concrete barrier and reached the adjacent service road at 416 m, damaging two cars. Another large boulder hit a house breaking through the roof and the underlying brick floor. Fortunately, no people were involved in the rockfall".

After the 1998 earthquake [23], a technical report on rock mass characterization was commissioned through an utmost urgency procedure [43]. The geomechanical study detected several areas with critical potential instability related to discontinuities that isolate wedges and blocks prone to fall, even if they have small to moderate volumes. Some details of geomechanical station sm11 (Table S1) and a summary map (Figure S1), polar diagram of the fracture system (Figure S2), and table (Table S2) of the geomechanical survey are reported in the Supplementary Materials.

In January 2002, a few weeks after the conclusion of the remedial work, a rockfall located near an unstable sector detected in the 1998 report, partially destroyed the new

barriers and nets. The defences were restored a few months later. These are the last documented works and studies on the unstable cliff of Sant'Elia Ridge.

In the last 20 years, no new risk mitigation projects have been done, and no maintenance work has been planned for the installed structure. In 2017, another wildfire that hit the area of Mount Sant'Elia caused new small rockfalls. In 2022 preliminary maintenance work commissioned by Lauria Municipality was started.

The results of digitization, geocoding, and database creation are shown in the following figures. The analogic maps (Figure 3A) of the ubication of the rockfall mitigation structures were digitized and geocoded in a geodatabase containing the most relevant information available in the report (Figure 3B). For instance, for each installation, it is possible to know the type and the number of anchors, eyebolt anchor and the mesh used (e.g., double-twisted hexagonal wire mesh). We also include a sketch of the rockfall barrier's design and other structures (Figure 3C). The sketch can be directly downloaded from a link in the vector database.

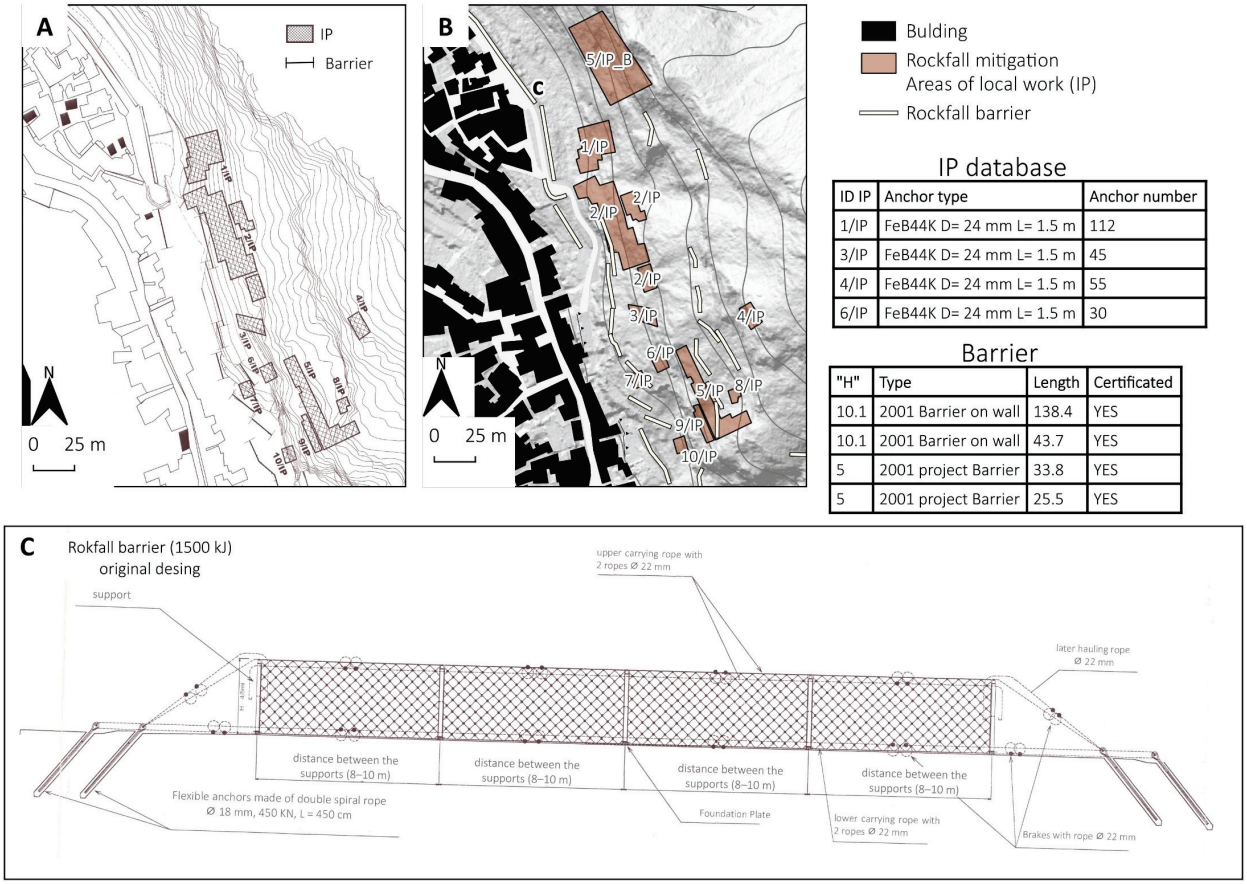



**Figure 3.** (**A**) Original map of local mitigation work (IP sectors) and rockfall barrier (Lauria municipal archive [44]). (**B**) Digitized map overlapped to hillshade LiDAR, with an example of tables database information. (**C**) Digitized sketch of 1500 kJ barrier (Lauria municipal archive [44]).

When feasible, we also classified rockfall barriers by their age of construction or design using available reports. We also included some photos taken on the ground (e.g., photos 1, 2 and 3 in Figure 4) to show their current condition. The LiDAR and the high-resolution orthophoto have been fundamental for detecting and accurately geocoding barriers located in the upper part of the slope and covered by vegetation (Figure 4B). The classification of the barrier is only qualitative, an accurate classification needs an expert survey (e.g., from a structural engineer) to assess the maintenance status of the barriers. This task was not within our competence and was suggested as a recommended action in the operative monograph.

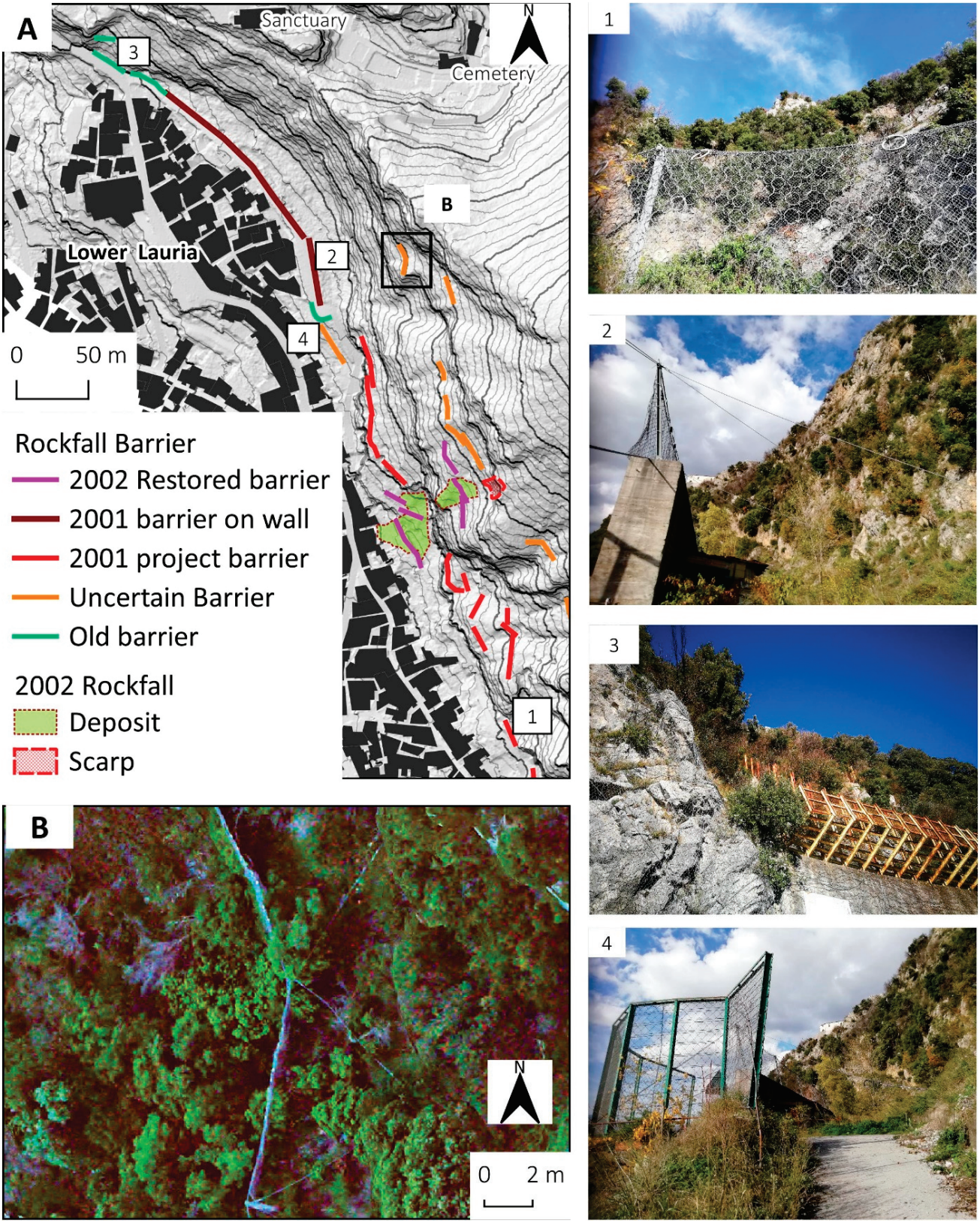
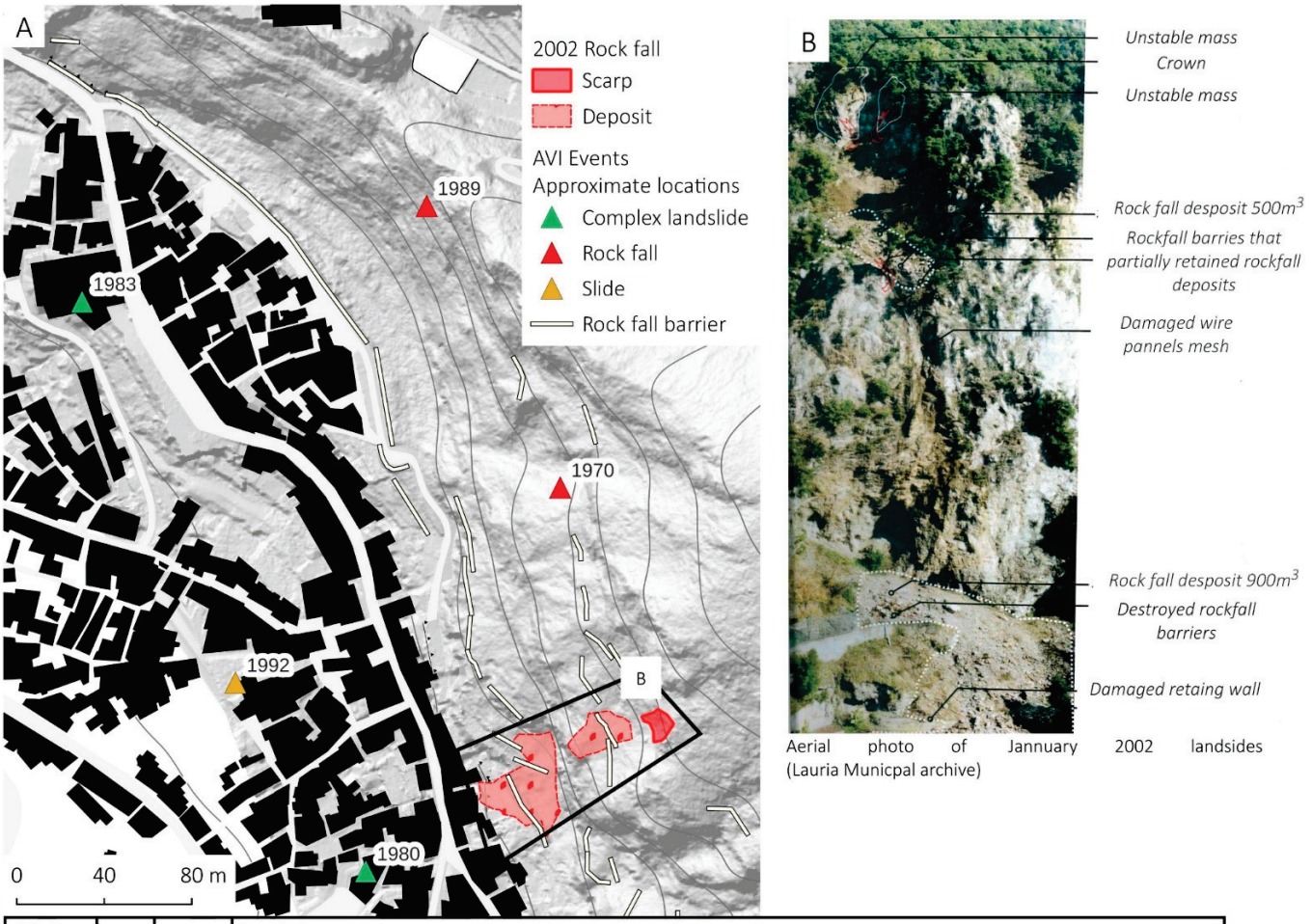



**Figure 4.** Example of digitized and geocoded rockfall barriers. (**A**) Classification of the barriers with the location of some representative photos (taken in February 2020 field survey). Photo 1 shows a certified rockfall barrier of 2001. Photo 2 shows a 1500 kJ barrier installed over a wall. Photos 3 and 4 show an old barrier (pre-2001) without documentation. (**B**) Barrier of uncertain age detected with UAV LiDAR and orthophoto (details in Figure 7).

Figure 5A show the location of events from the AVI database that occurred in the lower sector of Lauria town. Geolocation was improved from the original database using the text reference, but it is still approximate. The same map reports the location of the January 2002 rockfall event. The map and the aerial photo taken a few days after the rockfall (Figure 5B) comes from a report from the Lauria archive.




| AVI_ID | year | type | Description |
|---|---|---|---|
| 2,000,288 | 1,989 | Rock fall | The Armo ridge is made up of carbonate rocks stratified in large banks crossed by numerous families of fractures and fissures. These isolate rock wedge, even of considerable size, especially between Punta San Giovanni and the Cerruti region |
| 2,400,176 | 1,970 | Rock fall | Rockfall from the collapse of fractured roc blocks, which occurred in very steep slope corresponding to fault lines, exposed to the action of atmospheric agents. They affected the inhabited area of Lauria Inferiore. |

**Figure 5.** (**A**) Approximate location of AVI events and 2002 rockfall with related database information in the table. (**B**) Aerial images of rockfall available in the post-event report (source: Laura municipal archive [45]).

### *4.2. Remote Sensing and LiDAR*

The creation of the 2017 wildfire map (Figure 6) was essential to estimate potential damage to rockfall works. The availability of pre-wildfire (Figure 6A), and post-wildfire (Figure 6B) Sentinel-2 images allowed us to calculate $NBR_{var}$ (Figure 6C). We used the $NBR_{var}$ with post-event aerial photos of Regione Basilicata [38] to map the area of the 2017 wildfires with reasonable accuracy. The map of $NBR_{var}$ was used to estimate the potential damage to barriers (Figure 6D). The maps show that wildfires affected most of the study area. These results show that the fires could have damaged many fences, as documented in other sites [5]. After the wildfire, the reduction of vegetation protection (roots and dense shrubs) had unchained several meta-stable blocks and talus along the slope, causing an increase of small rockfalls with a similar process described by [12]. Fortunately, vegetation

recovery was relatively rapid. During the 2019 surveys, evidence of the wildfire had almost disappeared, as confirmed by the LiDAR orthophoto of 2020, showing very dense active vegetation (Figure 7A).

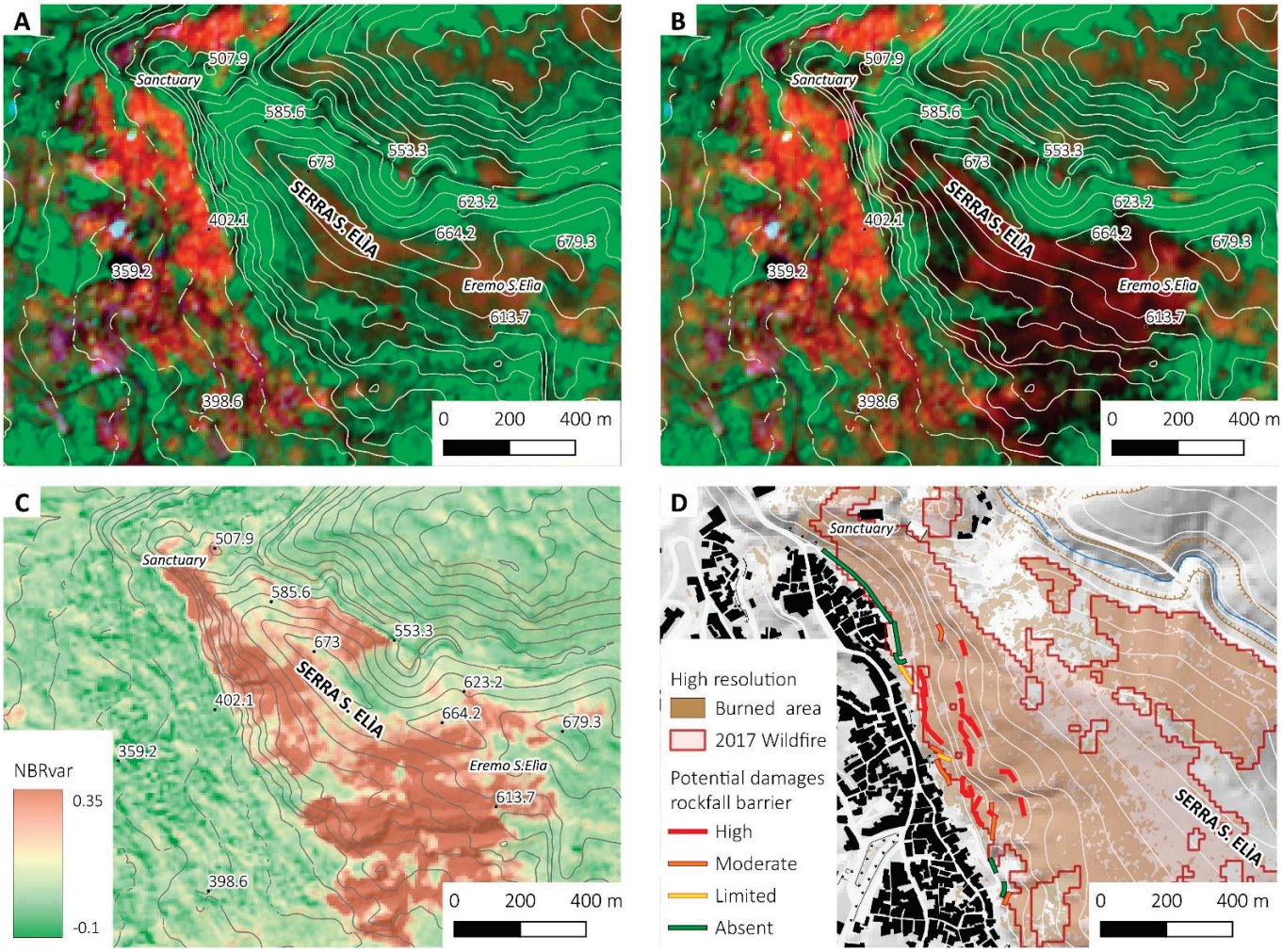



**Figure 6.** (**A**) Pre-event Sentinel-2 image (2017-07-02). (**B**) Post-event Sentinel-2 image (2017-07-12). (**C**) $NBR_{var}$ index. (**D**) Map of burnt areas with estimated damages to rockfall barriers.

The UAV-LiDAR survey allowed us to obtain a very high-resolution orthophoto and DTM. The derived products, such as the slope gradient and the hill shade, have unprecedented details identifying the areas with high rockfall hazards. With a spatial resolution of 0.02 m, the orthophoto allowed us to detect some rockfall barriers surrounded by dense vegetation (Figure 7A). The combined use of LiDAR point cloud data classified by intensity allowed us to detect the shape and accurately geocode the barriers (Figure 7B,C). Moreover, the derived interpolated DSM allowed us to estimate the height of some fences (e.g., about 3 m in Figure 7D). The data show that their dimension agrees with a sketch of the 2001 project. The high-resolution DTM could also increase the accuracy of GIS-based rockfall runout models, such as the QPROTO plugin for QGIS [22].

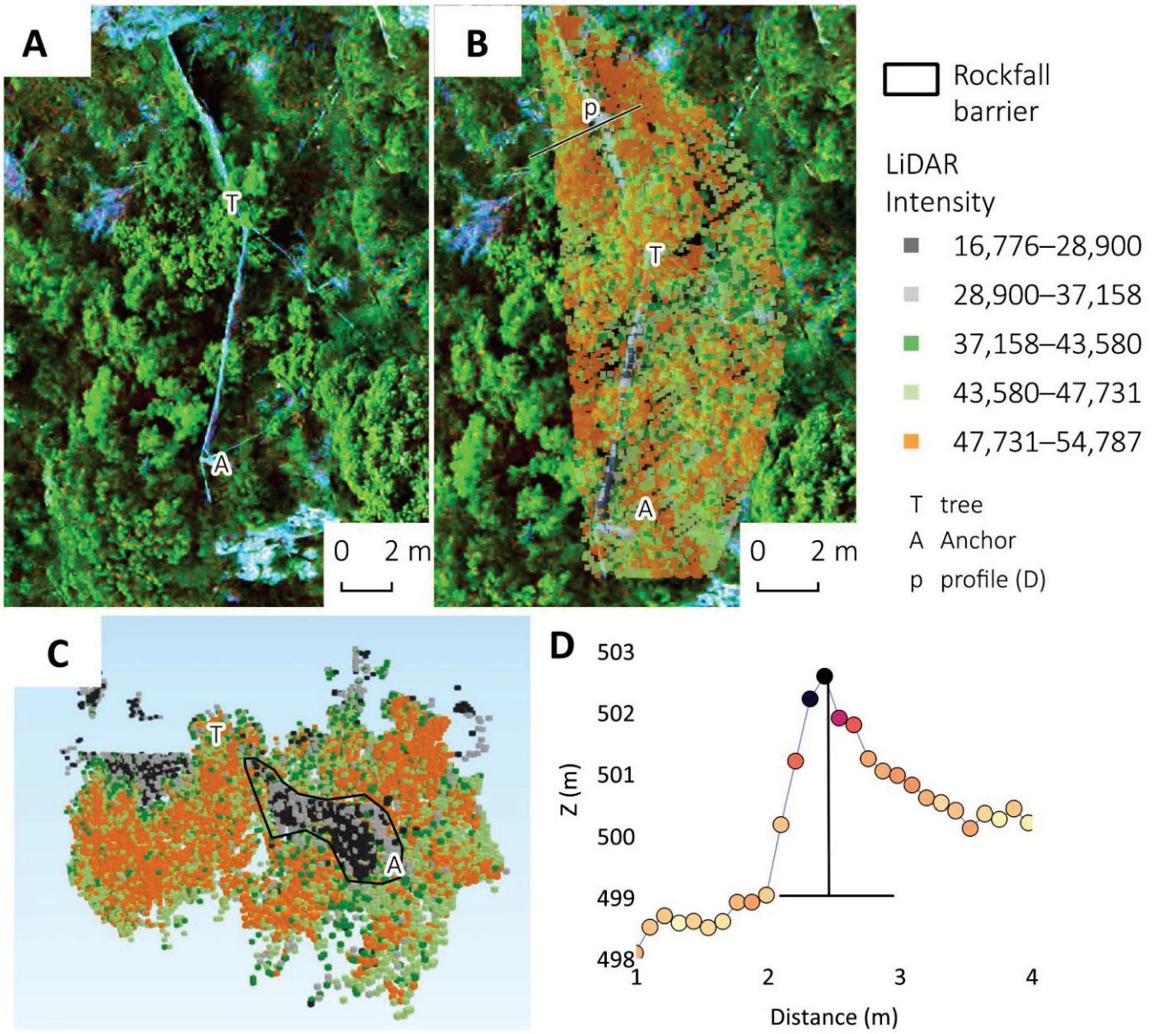



**Figure 7.** An example of a rockfall barrier in a steep slope detected on orthophoto and confirmed by LiDAR point cloud. (**A**) Orthophoto with 10 cm of spatial resolution. (**B**) Sampled LiDAR point cloud classified by intensity. (**C**) A 3-D view of the LiDAR point cloud. (**D**) Vertical barrier profile based on LiDAR data interpolated in 10 cm DSM.

### *4.3. Operative Monograph and Results Dissemination*

The OM of the Lauria case study mainly focuses on (i) the structure of the database and GIS data; (ii) the available geological settings; (iii) a list of previous rockfall events; (iv) a report on rockfall mitigation work history and qualitative maintenance status, and (v) results of UAV-LiDAR survey. A document of about 40 pages was delivered confidentially to Lauria municipality at the end of 2020. In the OM, we highlighted some critical aspects, such as:

- the lack of data about the maintenance of rockfall works in the past few decades;
- the difficulty of collecting old certifications of the works;
- the need to update rock mass characterization and numerical modelling;
- the importance of constantly updating the digital database of mitigation and geocoding;

- the importance of planning rockfall mitigation strategies over a large scale (e.g., coordination with regional authorities) to optimise resources;
- the need for dissemination materials for the population of Lauria hamlet, in collaboration with an expert that worked on planning.

The dissemination phase aimed to produce simple-to-understand representations of results available to the general public which were provided as a demonstration during a meeting with public authorities. The webGIS contains a simplified version of the digitized GIS database with the most representative layers, the position of barriers, the 2002 rockfall, and the burnt areas.

The MapStore web application also allows adding widgets with a better explanation of the layer contents. A simplified English version of the webGIS is available at this link: http://irpi-geop.to.cnr.it:8080/mapstore/#/viewer/openlayers/12 (accessed on 14 September 2022).

The creation of some 3-D models (e.g., Figure 8A,B) allows an easy consultation of the database for non-experts. Several data can be overlapped into models, where single elements can be investigated directly on the browser, with a hyperlink to other information pages.

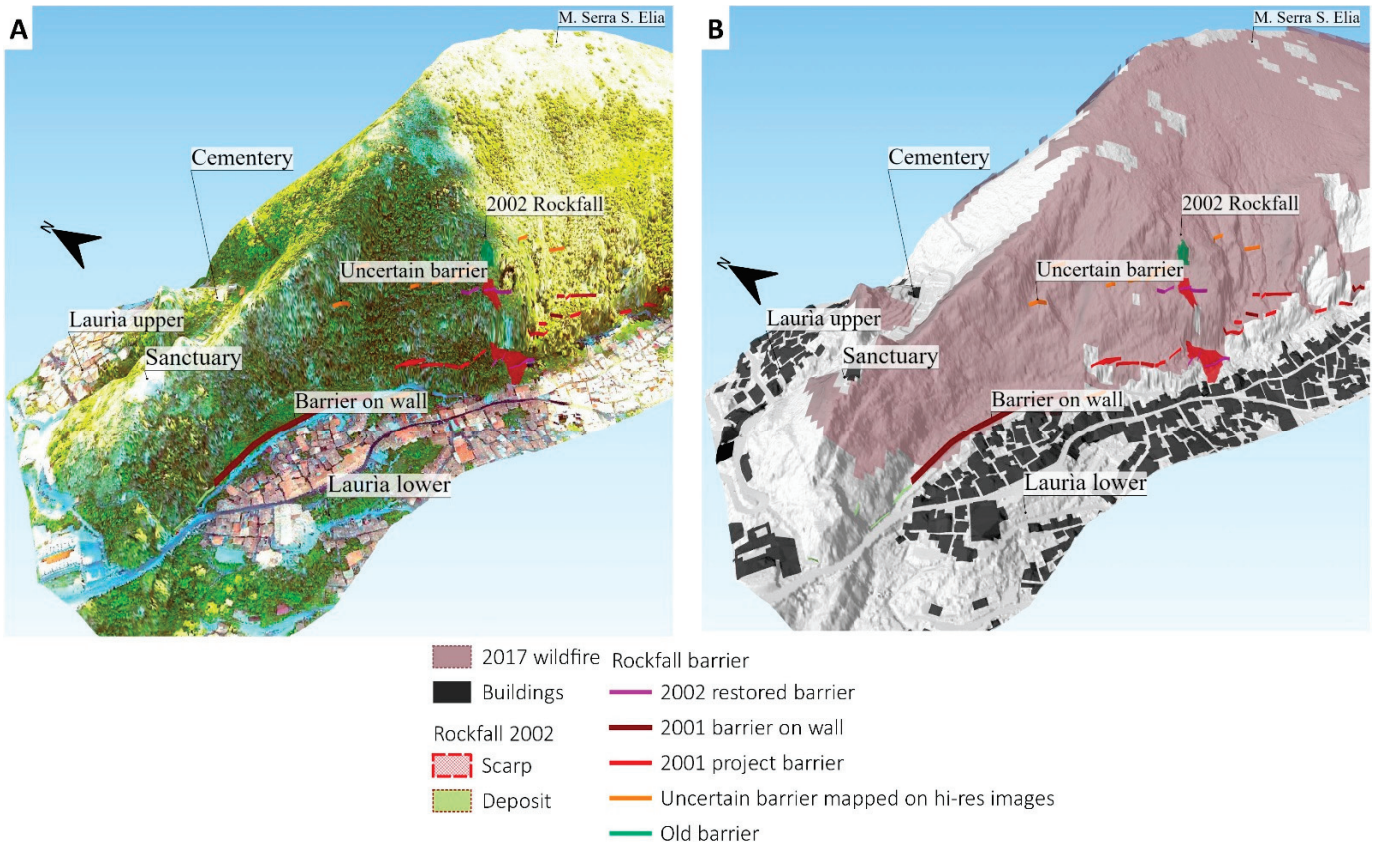



**Figure 8.** Exported 3-D view of the study area based on DTM LiDAR with rockfall barriers overlapped, obtained with the Qgis2threejs plugin [29]. (**A**) 3-D view with overlapped orthophoto. (**B**) 3-D view with overlapped shaded relief and burnt area. The 3-D views are available on the Zenodo platform [50].

## 5. Discussion

In the past few decades, in Italy and in many other parts of the world, vast numbers of rockfall mitigation structures (active and passive) have been installed but, for most of them, their state of maintenance, and the changes that occurred to the surrounding slope are not known.

A system that can manage and monitor the state of the structures and the slope is fundamental for detecting an increase of rockfall susceptibility, particularly if external events such as wildfires have damaged these structures. A geodatabase supported by OM can provide essential suggestions for implementing new studies and projects when the structures become inadequate. It is also necessary to highlight how many infrastructures were built with criteria that are not compliant with current regulations, e.g., Eurocode regulations [51]. An approach like the one we proposed can provide a complete picture of mitigation works and their characteristics to organize an ordinary/extraordinary maintenance plan to support progressive updating of older systems with modern and more functional structures.

In addition, a geodatabase of mitigation structures can be overlapped with all other ancillary data or model results that deal with rockfalls (e.g., the areas affected by wildfire or runout models).

The main difficulties that limit the creation of an updated database are the lack of resources, knowledge and personnel in small communities. Moreover, usually at a regional or national scale, there is no coordination and collection of small projects made locally.

One of the very few examples of a complete public inventory of rockfall mitigation works was made in South Tirol (Bolzano province) [52]. From their webGIS [53], it is possible to download the dataset that contains information about the type of rockfall mitigation, the vulnerable element (e.g., road) and the related contract. In the literature, there are no other clear examples of such databases.

For these reasons, we believe that our work has created an initial procedure to manage rockfall mitigation work and their state of conservation that can be integrated with other methodologies to manage rockfalls along the road network [3,54]. The test made at a local slope scale in Lauria Town can be used as starting point for regional application.

The OM, combined with a geodatabase, allows both authorities and experts to focus on the data and implement knowledge of mitigation works. In an updated version of OM, we will add to the "suggestion and comments" section a summary table with the current status of the data (e.g., Table 3). In a future update, other information could be related to priority, cost-benefit analysis [7,55] and the feasibility of the suggested action.

**Table 3.** Lauria case study. Summary of suggested actions aimed to implement the database of rockfall mitigation work. Current status legend P = partial or old data, X = missing data/information, V = complete and updated data.

| Dataset/Study | Current Status | Notes |
|---|---|---|
| Geomechanical study | P | Only a technical report aged 1998 is available, a new study with more precise geocoding is suggested. |
| DTM | V | The new HR LiDAR DTM cover all the affected slope. |
| Numerical modelling | X | Runout modelling based on HR DTM could help design the restoration of mitigation structures. |
| Maintenance status information | X | An in-situ analysis, made by experts, is necessary to evaluate the structural condition of existing mitigation work. |
| Rockfall event database | P | A more systematic inventory of rock fall events is necessary. |
| Geodatabase/webGIS | V | They need to be updated when new data are available. |
| Dissemination | P | Public engagement on rockfall risk is necessary |

For instance, in the municipal archive of Lauria, there is a geomechanical characterization of rock mass technical reports. However, this study was made under an urgent

mandate, with imprecise geolocation of geomechanical stations. For this reason, in a dedicated section of the OM, we recommend making a new rock mass characterization with newly refined methods and rockfall simulations based on high-resolution LiDAR DTM.

Our study also describes the importance of updating and improving the landslide historical events database and related tools. This historical recording is one of the leading research fields in CNR-IRPI [15,56–58]. The associated remedial works should be part of a future database. In this sense, the future metadata repository will help data distribution. For example, at this link, there is a prototype of the CNR-IRPI data catalog: https://catalog.irpi.cnr.it/geonetwork/srv/eng/catalog.search#/home (accessed on 14 September 2022).

## 6. Conclusions

We present a methodological approach aimed at creating an affordable standardized, replicable approach to manage, catalogue and monitoring rockfall mitigation structures. The problem of correctly managing rockfall barriers and, more generally, all adopted solutions for rockfall risk mitigation has often been underestimated. There is a wide literature dedicated to rockfall risk reduction, but few studies have considered the importance of correct management and maintenance of adopted solutions. Much infrastructure was built more than thirty years ago, without a clear idea of the most challenging future events. Update of already installed infrastructures can involve extensive maintenance or replacement. This is a challenging activity in small municipalities, where the local authorities sometimes do not have sufficient technical knowledge to manage this effort. In this paper, we present a typical example of this situation. Lauria is a municipality that has invested many resources in the last decades to protect the town from rockfall risk. Nowadays, the most critical problems are assessing the effectiveness of the installed solutions and evaluating the need for new ones. The necessity of an effectiveness evaluation was amplified by the effect of wildfires that occurred in 2017 that involved areas in which rockfall barriers had been installed since early 1970. To support the municipality, we developed and proposed a procedure targeted at the needs of small communities. The method is based on creating a geodatabase, OM and in disseminating results. The approach also combines traditional archive digitization with remote sensing data from satellite images to high-resolution LiDAR surveys. We tested our methodology for the small town of Lauria (southern Italy). We obtained detailed state-of-the-art and qualitative maintenance conditions for mitigation works. The database shows that the most recent studies were made more than 20 years ago, and no significant maintenance works have been done on the structures. The documentation analysis pointed out the lack of an updated geomechanical study of the whole rockfall-prone area.

The LiDAR data with high-resolution orthophoto allowed precise geocoding of the barrier to estimate 3-D dimensions and an evaluation of vegetation cover. A future step could be integrating the geodatabase of mitigation works with high-resolution DTM LiDAR to produce detailed rockfall modelling to improve the estimation of impact energy on structures.

In addition, we mapped the area affected by the wildfire, and the resulting potential damage to structures, with Sentinel-2 satellite data. The combined use of Sentinel-2 and aerial images showed that the 2017 wildfire potentially damaged most rockfall barriers and other mitigation structures.

The acquired knowledge summarized in the OM is a starting point that experts may use to do more accurate modelling and design a more appropriate structure to mitigate rockfall risk. We also think that the local authorities should use this approach and our results as a reference for exhaustive studies and to plan mitigation work.

We also created products focused on the general public, such as the webGIS and interactive 3-D models, as we believe that population preparedness and knowledge about natural hazards and risk mitigation strategies are essential for choosing the best affordable and safe measures by decision-makers.

**Supplementary Materials:** The following supporting information can be downloaded at: https://www.mdpi.com/article/10.3390/land11111951/s1, Figure S1: Lauria, map of potential rockfall/topple instability for each geomechanical station; Table S1: sm11: main parameter of measured discontinuities; Table S2: Description of some significant rock mass characterization stations; Figure S2: Original polar diagram of the average orientation of the discontinuity systems of the slope affected by rockfall.

**Author Contributions:** Conceptualization, D.N. and D.G. (Daniele Giordan); methodology, D.N. and D.G. (Daniele Giordan); software (WebGIS), D.G. (Diego Guenzi); validation, D.N., D.G. (Diego Guenzi); investigation, D.N. and D.G. (Daniele Giordan); resources, D.G. (Daniele Giordan); data curation, D.N. and D.G. (Diego Guenzi); writing—original draft preparation, D.N.; writing—review and editing, D.N., D.G. (Diego Guenzi) and D.G. (Daniele Giordan); visualization, D.N.; supervision, D.G. (Daniele Giordan); project administration, D.G. (Daniele Giordan) and R.L.; funding acquisition, D.G. (Daniele Giordan) and R.L. All authors have read and agreed to the published version of the manuscript.

**Funding:** This research received no external funding.

**Data Availability Statement:** The data used in this work can be obtained from the authors under reasonable request.

**Acknowledgments:** The authors would like to acknowledge the Lauria Municipality for making its archive available and committing to and funding the LiDAR acquisition.

**Conflicts of Interest:** The authors declare no conflict of interest.

## References

1. Scavia, C.; Barbero, M.; Castelli, M.; Marchelli, M.; Peila, D.; Torsello, G.; Vallero, G. Evaluating Rockfall Risk: Some Critical Aspects. *Geosciences* **2020**, *10*, 98. [CrossRef]
2. Depountis, N.; Nikolakopoulos, K.; Kavoura, K.; Sabatakakis, N. Description of a GIS-Based Rockfall Hazard Assessment Methodology and Its Application in Mountainous Sites. *Bull. Eng. Geol. Environ.* **2020**, *79*, 645–658. [CrossRef]
3. Cignetti, M.; Godone, D.; Bertolo, D.; Paganone, M.; Thuegaz, P.; Giordan, D. Rockfall Susceptibility along the Regional Road Network of Aosta Valley Region (Northwestern Italy). *J. Maps* **2021**, *17*, 54–64. [CrossRef]
4. Agliardi, F.; Crosta, G.B.; Frattini, P. Integrating Rockfall Risk Assessment and Countermeasure Design by 3D Modelling Techniques. *Nat. Hazards Earth Syst. Sci.* **2009**, *9*, 1059–1073. [CrossRef]
5. Sarro, R.; Pérez-Rey, I.; Tomás, R.; Alejano, L.R.; Hernández-Gutiérrez, L.E.; Mateos, R.M. Effects of Wildfire on Rockfall Occurrence: A Review through Actual Cases in Spain. *Appl. Sci.* **2021**, *11*, 2545. [CrossRef]
6. Toe, D.; Mentani, A.; Govoni, L.; Bourrier, F.; Gottardi, G.; Lambert, S. Introducing Meta-Models for a More Efficient Hazard Mitigation Strategy with Rockfall Protection Barriers. *Rock Mech. Rock Eng.* **2018**, *51*, 1097–1109. [CrossRef]
7. Galve, J.P.; Cevasco, A.; Brandolini, P.; Piacentini, D.; Azañón, J.M.; Notti, D.; Soldati, M. Cost-Based Analysis of Mitigation Measures for Shallow-Landslide Risk Reduction Strategies. *Eng. Geol.* **2016**, *213*, 142–157. [CrossRef]
8. Strada, C.; Tagnin, S.; Mottironi, M.; Larcher, V.; Villa, G.; Mair, V. Management of Rock Fall Risk on the Main Roads of Southtirol. In *Engineering Geology for Society and Territory-Volume 2*; Springer: Berlin/Heidelberg, Germany, 2015; pp. 1829–1833.
9. Marchelli, M.; De Biagi, V.; Peila, D. A Quick-Assessment Procedure to Evaluate the Degree of Conservation of Rockfall Drapery Meshes. *Frat. Ed Integrità Strutt.* **2019**, *13*, 437–450. [CrossRef]
10. de Graff, J.V.; Gallegos, A.J. The Challenge of Improving Identification of Rockfall Hazard after Wildfires. *Environ. Eng. Geosci.* **2012**, *18*, 389–397. [CrossRef]
11. De Graff, J.V.; Shelmerdine, B.; Gallegos, A.; Annis, D. Uncertainty Associated with Evaluating Rockfall Hazard to Roads in Burned Areas. *Environ. Eng. Geosci.* **2015**, *21*, 21–33. [CrossRef]
12. Melzner, S.; Shtober-Zisu, N.; Katz, O.; Wittenberg, L. Brief Communication: Post-Wildfire Rockfall Risk in the Eastern Alps. *Nat. Hazards Earth Syst. Sci.* **2019**, *19*, 2879–2885. [CrossRef]
13. Turconi, L.; Tropeano, D.; Savio, G.; Bono, B.; De, S.K.; Frasca, M.; Luino, F. Torrential Hazard Prevention in Alpine Small Basin through Historical, Empirical and Geomorphological Cross Analysis in NW Italy. *Land* **2022**, *11*, 699. [CrossRef]
14. Taylor, F.E.; Malamud, B.D.; Freeborough, K.; Demeritt, D. Enriching Great Britain's National Landslide Database by Searching Newspaper Archives. *Geomorphology* **2015**, *249*, 52–68. [CrossRef]
15. Guzzetti, F.; Cardinali, M.; Reichenbach, P. The AVI Project: A Bibliographical and Archive Inventory of Landslides and Floods in Italy. *Environ. Manag.* **1994**, *18*, 623–633. [CrossRef]
16. Giordan, D.; Cignetti, M.; Wrzesniak, A.; Allasia, P.; Bertolo, D. Operative Monographies: Development of a New Tool for the Effective Management of Landslide Risks. *Geosciences* **2018**, *8*, 485. [CrossRef]
17. Robiati, C.; Eyre, M.; Vanneschi, C.; Francioni, M.; Venn, A.; Coggan, J. Application of Remote Sensing Data for Evaluation of Rockfall Potential within a Quarry Slope. *ISPRS Int. J. Geo-Inf.* **2019**, *8*, 367. [CrossRef]

18. Sarro, R.; Riquelme, A.; García-Davalillo, J.C.; Mateos, R.M.; Tomás, R.; Pastor, J.L.; Cano, M.; Herrera, G. Rockfall Simulation Based on UAV Photogrammetry Data Obtained during an Emergency Declaration: Application at a Cultural Heritage Site. *Remote Sens.* **2018**, *10*, 1923. [CrossRef]
19. Santangelo, M.; Alvioli, M.; Baldo, M.; Cardinali, M.; Giordan, D.; Guzzetti, F.; Marchesini, I.; Reichenbach, P. Brief Communication: Remotely Piloted Aircraft Systems for Rapid Emergency Response: Road Exposure to Rockfall in Villanova Di Accumoli (Central Italy). *Nat. Hazards Earth Syst. Sci.* **2019**, *19*, 325–335. [CrossRef]
20. Giordan, D.; Adams, M.S.; Aicardi, I.; Alicandro, M.; Allasia, P.; Baldo, M.; De Berardinis, P.; Dominici, D.; Godone, D.; Hobbs, P. The Use of Unmanned Aerial Vehicles (UAVs) for Engineering Geology Applications. *Bull. Eng. Geol. Environ.* **2020**, *79*, 3437–3481. [CrossRef]
21. Menegoni, N.; Giordan, D.; Perotti, C.; Tannant, D.D. Detection and Geometric Characterization of Rock Mass Discontinuities Using a 3D High-Resolution Digital Outcrop Model Generated from RPAS Imagery–Ormea Rock Slope, Italy. *Eng. Geol.* **2019**, *252*, 145–163. [CrossRef]
22. Castelli, M.; Torsello, G.; Vallero, G. Preliminary Modeling of Rockfall Runout: Definition of the Input Parameters for the QGIS Plugin QPROTO. *Geosciences* **2021**, *11*, 88. [CrossRef]
23. Michetti, A.M.; Ferreli, L.; Esposito, E.; Porfido, S.; Blumetti, A.M.; Vittori, E.; Serva, L.; Roberts, G.P. Ground Effects during the 9 September 1998, Mw = 5.6 Lauria Earthquake and the Seismic Potential of the "Aseismic" Pollino Region in Southern Italy. *Seismol. Res. Lett.* **2000**, *71*, 31–46. [CrossRef]
24. Canora, F.; Rizzo, G.; Panariello, S.; Sdao, F. Hydrogeology and Hydrogeochemistry of the Lauria Mountains Northern Sector Groundwater Resources (Basilicata, Italy). *Geofluids* **2019**, *2019*, 7039165. [CrossRef]
25. Bonardi, G.; Cinque, A.; De Capoa, P.; Di Staso, P.; Esposito, P.; Giuda, D.; Mazzoli, S.; Parente, M.; Radoičić, R.; Sgrosso, A.; et al. *Note Illustrative della Carta Geologica D'italia Alla Scala 1:50.000—Goglio 521 Lauria*; Dipartimento Difesa del Suolo, Servizio Geo: Abruzzo, Italy, 2016.
26. Lasaponara, R.; Tucci, B.; Ghermandi, L. On the Use of Satellite Sentinel 2 Data for Automatic Mapping of Burnt Areas and Burn Severity. *Sustainability* **2018**, *10*, 3889. [CrossRef]
27. RSDI—Geoportale della Basilicata RSDI—Geoportale della Basilicata 2015. Available online: https://rsdi.regione.basilicata.it/ (accessed on 28 October 2022).
28. ISPRA IFFI—Inventario dei Fenomeni Franosi in Italia. Available online: https://www.progettoiffi.isprambiente.it/ (accessed on 28 October 2022).
29. Ministero Transizione Ecologica—Italian Government Geoportale Nazionale. Available online: http://www.pcn.minambiente.it/mattm/ (accessed on 28 October 2022).
30. Miller, J.D.; Thode, A.E. Quantifying Burn Severity in a Heterogeneous Landscape with a Relative Version of the Delta Normalized Burn Ratio (DNBR). *Remote Sens. Environ.* **2007**, *109*, 66–80. [CrossRef]
31. Cocke, A.E.; Fulé, P.Z.; Crouse, J.E. Comparison of Burn Severity Assessments Using Differenced Normalized Burn Ratio and Ground Data. *Int. J. Wildland Fire* **2005**, *14*, 189–198. [CrossRef]
32. Morresi, D.; Marzano, R.; Lingua, E.; Motta, R.; Garbarino, M. Mapping Burn Severity in the Western Italian Alps through Phenologically Coherent Reflectance Composites Derived from Sentinel-2 Imagery. *Remote Sens. Environ.* **2022**, *269*, 112800. [CrossRef]
33. Lindsay, J.B. The Whitebox Geospatial Analysis Tools Project and Open-Access GIS. In Proceedings of the GIS Research UK 22nd Annual Conference, The University of Glasgow, Glasgow, UK, 16–18 April 2014; pp. 16–18.
34. Open Source Geospatial Foundation GeoServer. Available online: https://geoserver.org/ (accessed on 7 September 2022).
35. Cignetti, M.; Guenzi, D.; Ardizzone, F.; Allasia, P.; Giordan, D. An Open-Source Web Platform to Share Multisource, Multisensor Geospatial Data and Measurements of Ground Deformation in Mountain Areas. *ISPRS Int. J. Geo-Inf.* **2019**, *9*, 4. [CrossRef]
36. Núñez-Andrés, M.A.; Lantada Zarzosa, N.; Martínez-Llario, J. Spatial Data Infrastructure (SDI) for Inventory Rockfalls with Fragmentation Information. *Nat. Hazards* **2022**, *112*, 2649–2672. [CrossRef]
37. GeoSolutions MapStore. Available online: https://www.geosolutionsgroup.com/technologies/mapstore/ (accessed on 7 September 2022).
38. Minoru, A. Qgis2threejs Plugin Document—Qgis2threejs Plugin 2.4 Documentation. Available online: https://qgis2threejs.readthedocs.io/en/docs/ (accessed on 22 July 2020).
39. Guadagno, M. Landslide inventory record N. 2400176. SICI—Sistema Informativo Catastrofi Idrogeologiche (Information System for Hydrogeological Disasters). Istituto di Ricerca per la Protezione Idrogeologica (IRPI) del Consiglio Nazionale delle Ricerche e Gruppo Nazionale per la Difesa dalle Catastrofi Idrogeologiche (GNDCI) del Consiglio Nazionale delle Ricerche. Available online: http://wwwdb.gndci.cnr.it/php2/avi/frane_tutto.php?numero_frana=2400176&lingua=en (accessed on 14 September 2022).
40. Guadagno, M. Landslide Inventory Record N. 2000288. SICI—Sistema Informativo Catastrofi Idrogeologiche Idrogeologiche (Information System for Hydrogeological Disasters)—Istituto di Ricerca per la Protezione Idrogeologica (IRPI) del Consiglio Nazionale delle Ricerche e Gruppo Nazionale per la Difesa dalle Catastrofi Idrogeologiche (GNDCI) del Consiglio Nazionale delle Ricerche. Available online: http://wwwdb.gndci.cnr.it/php2/avi/frane_tutto.php?numero_frana=2000288&lingua=en (accessed on 14 September 2022).

41. Pitella, G. Interrogazione A Risposta Scritta 4/05725 Presentata da Pittella Giovanni Saverio in Data 1996-11-28—(Parliamentary Question 4/05725 Submitted by Pittella Giovanni Saverio on 28 November 1996). Available online: http://dati.camera.it/ocd/aic.rdf/aic4_05725_13 (accessed on 13 July 2022).
42. Lauria Town Hall. Progetto dell'intervento definitivo per il consolidamento della parete rocciosa dell'Armo. Capitolato d'appalto. Ministero dell'Interno—Coordinamento della Protezione Civile ORDINANZA N.2632/97 (Final design for the consolidation of Armo rockfall prone slope. Tender specifications. Ministry of the Interior—Civil Protection ORDER N.2632/97). Reserved unpublished report (Italian). 1997.
43. Lauria Town hall. Lavori di somma urgenza volti a fronteggiare l'aggravamento del dissesto idrogeologico della parete rocciosa dell'armo, a seguito del sisma del 09/09/98. Relazione sui lavori della 2/a fase di Somma Urgenza—Ispezioni e rilievo geostrutturale in parete (Highly urgent works aimed at mitigating the worsening of the instability of the Armo slope, following the earthquake of 09/09/98. Geostructural survey report). Reserved unpublished report (Italian). 1998.
44. Lauria Town Hall. Intervento definitivo per il consolidamento della parete rocciosa dell'Armo (Final project for the consolidation of the Armo cliff). Comune di Lauria, Provincia di Potenza. Reserved unpublished report (Italian). 2001.
45. Lauria Town Hall. Relazione sulle ispezioni ed i rilievi in parete condotti lungo il tratto di versante del costone roccioso "Armo" interessato dai fenomeni di crollo del 23.01.02 e proposte per il successivo risanamento e per la sistemazione delle aree ad esso sottostanti (Report the filed surveys conducted along the slope affected by the 23 jannuary 2002 rockfall on Costone dell'Armo ridge and proposals for the subsequent rehabilitation and restoring of the damaged works). Reserved unpublished report (Italian). 2002.
46. Lauria Town Hall. Progetto esecutivo per il ripristino imposto dalla frana sul Costone Armo del 23 gennaio 2002 (executive project for the resotorinf of mimitgation works damage by 2002 rockfall). Città di Lauria Provincia di Potenza Settore Assetto ed Uso del Territorio Servizio Lavori Pubblici. Reserved unpublished report (Italian). 2002.
47. Infopinione. Lauria, Abitazioni Minacciate da Incendio: Le Immagini (Lauria, Houses Threatened by Fire: The Images). 2017. Available online: https://www.infopinione.it/index.php/2017/07/11/lauria-abitazioni-minacciate-incendio-le-immagini/ (accessed on 14 September 2022). (In Italian)
48. Giordan, D.; Notti, D.; Guenzi, D. Analisi e webGIS delle opere di difesa Costone dell'Armo Lauria (PZ). [43]Analyss and webGSI of rockfall mitigation work of Armo ridge (Lauria, PZ). Operative Monography commissioned by Lauria Municipality, CNR-IRPI. Reserved unpublished report (Italian). 2020.
49. Lauria Town Hall. Lavori di Ripristino della Funzionalità e Sicurezza delle Reti Paramassi sul Costone Armo Sovrastante L'abitato di Lauria (Works to Restore the Efficiency of the Rockfall Nets on the Armo Ridge Upstream of the Town of Lauria). 2021. Available online: https://www.comune.lauria.pz.it/wp-content/uploads/2021/10/AVVISO-ESITI-DI-GARA.pdf (accessed on 13 September 2022). (In Italian)
50. Notti, D.; Guenzi, D. 3-D View of a Slope Affected by Rockfall. 2022. Available online: https://zenodo.org/record/6875771 (accessed on 13 September 2022).
51. Vagnon, F.; Bonetto, S.; Ferrero, A.M.; Harrison, J.P.; Umili, G. Eurocode 7 and Rock Engineering Design: The Case of Rockfall Protection Barriers. *Geosciences* **2020**, *10*, 305. [CrossRef]
52. Laura, G.; Strada, C. The Role of Rockfall Protection Barriers in the Context of Risk Mitigation: The Case of the Autonomous Province of Bolzano. In *Engineering Geology for Society and Territory—Volume 5*; Springer: Berlin/Heidelberg, Germany, 2015; pp. 397–400.
53. Bolzano Province Protection Structures-Rockfalls Works-Lines. Available online: https://geokatalog.buergernetz.bz.it/geokatalog/#!home&layer=p_bz%3AHazards%3AProtectionStructures-RockfallsWorks-Lines (accessed on 27 July 2022).
54. Giordan, D.; Cignetti, M.; Godone, D.; Bertolo, D.; Paganone, M. Definition of an Operative Methodology for the Management of Rockfalls along with the Road Network. *Sustainability* **2021**, *13*, 7669. [CrossRef]
55. Ortiz, R.; Castro, L.; Marambio, S. A Methodology for Semi-Quantitative Analysis of Rockfall Hazards and Cost-Benefit-Based Mitigation Design. In *Rock Mechanics for Natural Resources and Infrastructure Development*; CRC Press: Boca Raton, FL, USA, 2019; pp. 352–359, ISBN 0-367-82317-9.
56. Tropeano, D.; Turconi, L. Using Historical Documents for Landslide, Debris Flow and Stream Flood Prevention. Applications in Northern Italy. *Nat. Hazards* **2004**, *31*, 663–679. [CrossRef]
57. Napolitano, E.; Marchesini, I.; Salvati, P.; Donnini, M.; Bianchi, C.; Guzzetti, F. LAND-DeFeND–An Innovative Database Structure for Landslides and Floods and Their Consequences. *J. Environ. Manag.* **2018**, *207*, 203–218. [CrossRef] [PubMed]
58. Petrucci, O.; Polemio, M. The Use of Historical Data for the Characterisation of Multiple Damaging Hydrogeological Events. *Nat. Hazards Earth Syst. Sci.* **2003**, *3*, 17–30. [CrossRef]

land

MDPI

*Article*

# Historical Floods on the Spanish Mediterranean Basin: A Methodological Proposal for the Classification of Information at High Spatio–Temporal Resolution—AMICME Database (CE 1035–2022)

**Jordi Tuset [1], Mariano Barriendos [2,*] and Josep Barriendos [3]**

[1] Fluvial Dynamics Research Group (RIUS), University of Lleida, 25198 Lleida, Spain
[2] Institute of Environmental Assessment and Water Research (IDAEA-CSIC), 08034 Barcelona, Spain
[3] Department of Geography, University of Alicante, 03690 San Vicente del Raspeig, Spain
* Correspondence: mariano.barriendos@idaea.csic.es

**Abstract:** The uncertainties raised by climate change in the Mediterranean region justify a detailed study on rainfall regime over a long time scale. This study is not just about reconstructing and characterizing climate variability, but also identifying the hydrometeorological episodes of greater severity and low frequency. These phenomena, such as floods and droughts, affect the availability of water resources, generate casualties and have significant impacts on human activity. In this context of global warming, knowledge of past extreme hydrometeorological events has gained importance over time. Moreover, the ability to classify these past extreme events in order to compare them with current ones strengthens research capabilities. For this reason, this paper proposes a multivariable classification system for flood episodes, both historical and recent. The classification considers the physical conditions of a flood, its damage to structures and its social impacts. The proposed methodology has been applied to the AMICME flood database for the Spanish Mediterranean catchment areas from CE 1035 to 2022. This paper shows the application of this methodology for six flood episodes from different centuries and locations. It has been possible to display all the indexed information for the different flood cases of every episode through cartographic summary representations. Results prove the adaptability of the classification system to different hydrographical and historical contexts.

**Keywords:** classification tools; climatic hazards; databases; documentary sources; flood events; historical floods

**Citation:** Tuset, J.; Barriendos, M.; Barriendos, J. Historical Floods on the Spanish Mediterranean Basin: A Methodological Proposal for the Classification of Information at High Spatio–Temporal Resolution—AMICME Database (CE 1035–2022). *Land* **2022**, *11*, 2311. https://doi.org/10.3390/land11122311

Academic Editor: Deodato Tapete

Received: 5 November 2022
Accepted: 14 December 2022
Published: 16 December 2022

**Publisher's Note:** MDPI stays neutral with regard to jurisdictional claims in published maps and institutional affiliations.

**Copyright:** © 2022 by the authors. Licensee MDPI, Basel, Switzerland. This article is an open access article distributed under the terms and conditions of the Creative Commons Attribution (CC BY) license (https://creativecommons.org/licenses/by/4.0/).

## 1. Introduction

### *1.1. Research Background*

The uncertainties posed by climate change in the Mediterranean region justify a detailed study of the behaviour of its rainfall regimes. It is not only a matter of reconstructing and characterising climate variability, but also of identifying the most severe and infrequent hydrometeorological events. These phenomena, such as torrential rainfall that cause floods, affect the availability of water resources and generate casualties and important impacts on human activity. It is therefore suitable that the study of these phenomena should address both the physical–atmospheric and the social impact aspects in an integrated approach.

The problem with the study of extreme hydrometeorological events is their low frequency. There is little experience and knowledge of them during the instrumental period, which covers only the 20th century. Their detection, reconstruction and analysis over long time periods requires the preparation of information beyond the instrumental records, using various sources that provide proxy–data for periods of several centuries and even millennia [1]. Flood events of magnitude and hydrological behaviour are identified, providing more precise knowledge about frequencies and their temporal variability at

different scales, whether from sedimentological records or from historical documentary sources [2]. This reduces uncertainties regarding the challenge of climate change and makes it possible to prepare preventive or territorial planning measures to deal with the effects of the most severe episodes, or the increased frequency of events of medium severity.

Information on past floods has the difficulty of being largely available in qualitative formats. Historical documentary sources accumulate a large number of episodes, but their information is descriptive and only partially quantifiable. Therefore, adaptation by means of cataloguing and classification criteria are required in order to have a quantitative component for analyses of the information obtained on broad spatial and temporal scales. Largely, this information is unpublished and is gradually recovered in different research projects or during the preparation of local/regional studies or academic papers. Therefore, the creation and application of specific methodological tools that could take advantage of these information retrieval efforts for the creation of large, unified databases is justified.

A common procedure for the classification of individual historical floods involves the use of indices that reflect the degree of severity of the episode [3–6]. The classification according to impact depends on human exposure to floods and reported damages. These are not always directly related to the physical magnitude of the flood, as they depend more on the degree of exposure and vulnerability of the affected person at any given time. Disentangling the different categories of information (hazard, exposure and vulnerability) from historical documentation and the role played by each of them requires a multivariable and quantitative classification approach that has not yet been explored. However, when episode information is detailed, authors classify according to the causes of the flood [7] or the value of the peak flow [8], although the determination of the peak flow may not be easy or accurate [9]. The reality is that there is no agreement on what the components of a good classification are, let allow a unified method [7], as the classification system depends on the input information and the intended treatment of the classified data.

### *1.2. Objectives and Structure*

The main objective of this paper is to present a numerical system (qualitative) of classification of historical flood events. This system seeks to differentiate the magnitude of the hydrological response (physical processes) from the impact on society, since there is not always a direct relationship between the danger and the damage caused. Moreover, the method must be able to work with different types of flood events (pluvial floods, fluvial floods, marine storm floods, torrential rainfalls, etc.) and a wide variety of data sources.

This will improve the analysis of a broad time scale in which not only the flood episodes of the historical period but also of the modern instrumental period can be integrated.

The article includes a description of the existing databases on historical floods in different countries. It details the initiatives and the situation in Spain. Finally, the proposed classification system is described with some study cases as an example of the capacity of the proposed system to integrate the information with quantitative and cartographic support.

### *1.3. State of Art of Historical Flood Databases*

#### 1.3.1. Characteristics of Sources and Available Information

The required information for the reconstruction of flood events on a historical level is presented in multiple documentary and bibliographic sources. Examples include: Administrative documentary sources of local civil and ecclesiastical authorities; private documentary sources such as diaries and memoirs; and bibliographic sources, such as local histories or descriptive works on singular episodes. Their common feature is their qualitative character with a limited quantifiable component. A number of different criteria can be applied for the description and characterisation of this information.

Previous fieldwork experience in the Spanish Mediterranean basin has led to a classification based on the reliability of the sources and their information for use in climatic and meteorological reconstructions. To summarise, three types of information sources are identified [10]:

+ Type 1. Primary sources. Information on flood events generated by contemporary eyewitness authors.
  - Subtype (a). Documentary sources.
  - Subtype (b). Local newspapers.
+ Type 2. Secondary sources. Information obtained from primary sources by authors who are not eyewitnesses.
  - Subtype (a). Scientific literature.
  - Subtype (b). Historiographical sources and thematic papers.
+ Type 3. Tertiary sources. Information obtained from secondary sources by non–presencial authors.
  - Subtype (a). Technical reports.
  - Subtype (b). Non–specialized works and social network collections.

For these types of information sources, those of subtype "a" correspond to objective and/or systematic sources, which cover a large part of the events that took place. Those of subtype "b" correspond to subjective and/or sporadic sources, which only cover a part of the events [10].

These criteria may be distant or different from the most common in historiographical research, but they are the ones that have given the best results in the identification and characterisation of extreme natural phenomena on the Spanish Mediterranean River Basins. They have been applied since 2013 in the national PREDIFLOOD and MEDIFLOOD projects without generating problems or operational conflicts in the undertaken projects. Different historical flood chronologies were built following these criteria and methods. The result of the climatic and meteorological analysis shows that preparation of the data is positive [11–14].

The sources of information already have a consolidated methodology for their identification and selection. On a practical level, the sources of information selected as meeting the quality criteria for any research start–up are [10]:

+ Type 1. Administrative documentary sources of local, civil and ecclesiastical authorities for the historical period. Local press for the modern period.
+ Type 2. Local Historiography.
+ Type 3. Various material available on social networks.
+ Epigraphic limnimetric records (Water Flood Marks).
+ Instrumental records.

#### 1.3.2. Studies with "Serial" Information

The qualitative information on floods obtained from historical sources is organised into simple classifications because its aim is to enable the analysis of all types of cases over long periods of time. Flood cases are locations with a documentary record of flood. When flood cases of different locations are produced by the same meteo–hydrological episode, all flood cases are organized and defined like a unique "flood episode". However, in historical time it is frequent that flood episodes only contain information from one flood case. A classification of three categories is generally accepted for flood cases, although with different terminologies and modifications adapted to the hydrological behaviour of the different regions studied.

These criteria are a combination of hydrological evidence and social impacts. In Spain, a classification of three categories has been used [15]:

(1) Ordinary floods: No overflow, no damage.
(2) Extraordinary floods: overflow, damage to property.
(3) Catastrophic floods: overflow, destruction of infrastructure.

The results obtained from this classification are used in studies aimed to identify and characterise patterns of climate variability within the Little Ice Age. It only uses information related to relevant geographical locations, such as large cities or areas with significant infrastructural elements. For these locations, chronologies of flood events are

established and their frequency is analysed. Countless projects have been generated for different European regions and river basins under this pattern, and as more information has become available, new updates have been generated, as in the case of the Spanish Mediterranean River Basins [11,12,15,16]. Recent works are proving that the methodologies used on a continental scale were consistent with the projects to characterise floods in Europe during the 16th century [17], or the most recent example using dozens of chronologies for Europe for the last 500 years [18].

However, information organised in series or chronologies for specific locations, or even their aggregation in regional indices, reduces the analysis capacity. During the information treatment process, a lot of material is discarded because it is outside the selected locations and subsequently is not used. In the process of reconstructing past events, there is always a doubt about the usefulness of any information: can one work with demanding criteria and discard material, or should all the information collected be taken into consideration because it could contribute to a better understanding of the event?

It is reasonable to think that a different organisation of information is needed to tackle work in high spatio–temporal resolution. This approach requires the recovery of as much information as possible, as well as its integrated processing and analysis, by means of a new configuration of criteria. The use of all the information available in historical episodes allows an effective interdisciplinary approach, dealing with meteorological/climatic, hydrological and social aspects. An example of this approach has been the reconstruction of the flash flood event recorded in Catalonia on 23 September 1874, known as "Aiguat de Santa Tecla", which caused 535 deaths in a few hours of river flooding [19].

#### 1.3.3. Current Historical Flood Databases

Current digital resources allow the processing of information from historical sources in a systematic way, exploiting their contents as efficiently as possible. In addition, they make it possible to store large amounts of information in various formats, to organise it and to improve it gradually. These capabilities are driving the creation of large databases on a national and international scale for historical and instrumental information on meteorological variables and extraordinary hydrometeorological events.

The "serial" procedure discussed in the previous section was valid for basic historical climatology, but methodological progress is needed. It seems clear that an intermediate information preparation phase in large databases is desirable for a more flexible and integrated research. The initial objectives can still be achieved, but the capacity for other lines of research is also enhanced. One example is palaeometeorological reconstruction, the classification and typification of severe episodes, or the more precise characterisation of documented impacts and social vulnerabilities in the study of severe hydrometeorological events.

There are several examples of initiatives focusing on the creation of databases on historical weather and climate information. One of the oldest initiatives is the Euro–Climhist database, created by Dr. Christian Pfister of the University of Bern, Switzerland (https://www.euroclimhist.unibe.ch/en/, accessed on 18 November 2022). Other more recent initiatives are at the national level, such as the UK [20,21] or France's BDHI [22]. In Germany, there is an even more comprehensive or ambitious initiative: TAMBORA (the climate and environmental history collaborative research environment). In this database, which also covers information in any format, collaborative mechanisms are proposed so that all citizens can actively participate in it [23]. Currently this database not only compiles information on floods, but also deals with all kinds of climatic and environmental information, such as droughts [24].

A final aspect that shows interest in these initiatives is creation of a thematic network at the international level to promote the exchange of experiences in the field of historical flood events: the Flood Working Group (FWG), sponsored by PAGES (Past Global Changes) Programme.

Spain also offers initiatives aimed at the creation of databases on historical floods. Two episodes of catastrophic floods encouraged the cataloguing of historical episodes. The first

was in October 1982 in Valencia and Murcia Regions and caused 40 fatalities and losses of EUR 300 M [25]. The second was in November 1982 and affected Catalonia Region causing 26 fatalities and estimated losses of EUR 271 M [26].

Based on these episodes, Spanish administrations launched an effort in 1983 to compile information on similar episodes in historical times, creating a national level database organised by river basins: National Catalogue of Historical Floods (CNIH), Civil Protection, Ministry of the Interior, Government of Spain [27].

These works in Spain have been reinforced by the European Directorate 2007/60/CE (European Parliament and European Council), on the assessment and management of flood risks and in Royal Decree 903/2010, of 9 July, on the assessment and management of flood risks. Since 2006, the database has been publicly accessible online and has been updated several times, up to 2014. Following the European Directive, the Hydrographic Demarcations are developing different initiatives for better flood risk management. However, the work on historical episodes is far from the potential offered by the documentary sources of historical archives.

#### 1.3.4. Initiative of the ARCHIVE Association

The interdisciplinary research group that has developed the databases that support the proposed classification system has been active for the last 12 years. It received funding from two national projects (PREDIFLOOD, 2013–2015 and MEDIFLOOD, 2016–2019) that allowed the creation of a historical flood database for Catalonia (AMIC). Its results substantially improved the efforts made in Spain until then (see Tables 1 and 2). The existing indices to assess the quality of historical flood databases are applied to Spanish databases [28]. Coverage Index combines spatial and temporal dimensions of the data (Coverage Index = (area × years)/1,000,000 km$^2$). The combination of the number of flood events with the Coverage Index defines a definitive assessment of the quality of the database (Density Index = number of flood events/Coverage Index). According to these criteria, the CNIH database (2014 version: Density Index 7.5) is clearly improved by the AMIC database (2019 version: Density Index 48.5).

**Table 1.** Coverage and Density Indices for different Spanish flood databases. Updated after Barriendos et al., 2014.

| Flood Databases | Area (km$^2$) | Period (Years) | Episodes (Nr.) | Coverage Index [a] | Density Index [b] |
|---|---|---|---|---|---|
| CNIH. All Spanish Basins. Original version. 1983. | 493,838 | Average * 838 years | 2579 | 413.8 | 6.2 |
| CNIH. All Spanish Basins. Improved version. 2014. | 493,838 | Average * 838 years | 3121 | 413.8 | 7.5 |
| AMIC. Catalonia Basins. Original version. 2014. | 32,114 | 1035–2013 979 years | 1103 | 31.4 | 35.1 |
| AMIC. Catalonia Basins. Improved version. 2019. | 32,114 | 1035–2013 979 years | 1524 | 31.4 | 48.5 |
| AMICME. Spanish Mediterranean Basins. 2021. | 181,644 | 1035–2019 985 years | 3986 | 178.9 | 22.3 |

a: Coverage Index = (area × years)/1,000,000 km$^2$. b: Density Index = Number of Events/Coverage Index (Gaume et al., 2009). *: Average of all Spanish Basins Flood Databases [10].

This research is no longer funded by national projects on an ongoing basis, so an association has recently been established to enable the database to continue (ARCHIVE from the Catalan language: Associació del Risc Climàtic Històric. Impacte, Vulnerabilitat, Exposició/Association of Historical Climate Risk. Impact, Vulnerability, Exposure). The new activity has reinforced the extension of the database to cover rivers draining to the Spanish Mediterranean coast from the French border to the Strait of Gibraltar (AMICME database). According to the flood database evaluation system used [28], the new database

covers a large territory, but for that reason the density index has been temporarily reduced (version 2021: Density Index 22.3). The catalogued flood events include the following information: complete date, affected river and basin, points or municipalities with documented flooding, georeferencing, flood level, material damage and impact to people.

**Table 2.** Detail of the years covered by flood databases of all Spanish Basins contained in CNIH Barriendos et al., 2014.

| River | Period | Years |
|---|---|---|
| Duero | 1483–1985 | 503 |
| Segura | 1482–1982 | 501 |
| Júcar | 1088–1983 | 896 |
| Tajo | 849–1979 | 1131 |
| Ebro | BC49–1984 | 2034 |
| Guadalquivir | 1483–1985 | 503 |
| Norte + Galicia | 1482–1983 | 502 |
| Guadiana | 620–1985 | 1366 |
| Sur | 1544–1983 | 440 |
| Pirineo Oriental | 1483–1983 | 501 |
| Average | | 838 |

## 2. Materials and Methods. Proposal for a Segregated Classification System

### *2.1. Background to the Proposed Methodology*

The capabilities of computer resources make it possible to access a greater quantity and diversity of primary sources, and to efficiently manage the information that can be generated. This context requires renewed methodologies and procedures for cataloguing and classification.

Work on the Spanish Mediterranean River Basins since 1998 employed a three–category quantitative classification system based on a combination of fluvial behaviour and the severity of documented impacts [15]. This system was developed locally for a Catalan coastal sector (Maresme County) with good results for the 18th–20th centuries [29]. The only progress of this classification system has consisted of enriching the number of classification categories to five [10].

The analysis of phenomena at different scales and with different characteristics also makes it advisable to use unified and general methodologies and procedures. The application of specific *ad hoc* methods for each case of study would no longer be efficient, making it difficult to connect different episodes in analyses at different spatio–temporal scales.

The AMICME database presented here is a structure that aims to organise the materials and information collected for floods over a broad time period and in a multidisciplinary environment. It is still a preliminary structure, open to modifications and improvements, and will undoubtedly be further developed as materials from different sources of information are introduced.

There are numerous precedents of flood databases in the context of public administrations in Spain (e.g., CNIH already mentioned). However, their purpose is more directed to the storage of information than the preparation of data for multidisciplinary analysis. The proposal generated by the AMICME database takes maximum advantage of these experiences. However, as far as possible, we have avoided creating a typical database, resulting in a one–off compilation effort, for specific purposes.

The initial idea of having a simple catalogue of cases (geographic point where the flood occurred) and events (episode including all flood cases) evolved into the creation of a complex structure that could accommodate and organise the set of materials recovered from each flood. Additionally, it also evolved into a series of consultation tools to reference and organise access to detailed information when needed for analysis from different approaches.

In order to improve the identification of flood events and facilitate access to that information, it was decided to define a new classification system that could overcome the

limitations of the system in use since 1993 [29]. This first three–level classification system combined fluvial and anthropic aspects without the possibility of differentiation. It also prevented the possibility of linking the occurrence of cases with the extent or complexity of flood events as a whole, since its values were only used in the generation of serial chronologies at annual or seasonal resolution.

After more than 30 years, this paper presents a new classification system that makes it possible to differentiate three dimensions or variables of the phenomenon: the hydraulic behaviour of river floods, the impacts on structural elements and the vulnerability of the population. On the other hand, the extent of the events can also be quantified by distinguishing the affectation by flood case and the number of rivers and river basins involved.

### *2.2. Proposed Segregated Variables*

The proposed classification system organises the information into three different variables, each with a numerical scale of four categories (0 to 3). Separation of the variables allows a more precise analysis according to the objectives of every research, avoiding the integration of different information into the same numerical expression, which produces an irreversible loss of detail. The variables that make it possible to segregate the historical information available for the last 500/750 years on the Spanish Mediterranean coast are the following:

+ Variable 1. Hydraulic behaviour of the river flood.

It responds to the physical behaviour of the hydrometeorological risk (hazard). It is the main component of a climatic risk situation due to excess rainfall because it produces an objective response in the fluvial system that can also be quantified by the reconstruction of the maximum discharge reached by the flood event.

Historical documentation does not preserve instrumental records or systematic magnitude measurements of river floods. However, institutional and private testimonies perfectly identify fluvial behaviour at least in order to be able to classify them by categories.

+ Variable 2. Flood impact on structural elements.

This provides a response to the objective degree of exposure to climate risk. The level of damage caused to permanent constructive elements can be an indicator not only of the overflow level reached but also of the force or speed at which flooding was occurring.

The balance of damages and the description of the most relevant incidents produced by each river flood are the best described elements in the historical documentation. The reason for this is obvious: every affected community must assess the damage and destruction and deal with its repair or reconstruction in order to be able to recover normal activity as soon as possible.

+ Variable 3. Social/personal vulnerability to the flood.

It responds to the subjective degree of vulnerability to the impact. The number of people directly affected by a flood event is not a direct indicator of the severity of the event, but shows the interaction between the event and the social context in which it occurs.

The human component is the most discontinuously documented and reflects highly disparate situations. It is a factor that does not depend on objective factors. Certain perceptions and attitudes can generate situations with different outcomes, ranging from victimless self–protection in the face of a major flood to the loss of human lives in avoidable situations.

### *2.3. Proposed Quantification of Each Variable*

The categories propose their numerical classification from 0 to 3 according to the magnitude or severity of their effects. Their informative elements are different, but it is intended that the scales of the four categories have their numerical expressions assimilable to each other as far as the respective severity level is concerned.

+ Variable 1. Hydraulic Component

The description of every flood case in its natural characteristics in the river system is the element of best objective identification by direct witnesses. Its values are defined according to the behaviour of every river course beyond its normal conditions.

- Value 0: Insufficient information for a definitive classification. When the testimony does not clearly define the behaviour of the water in a river course during an episode, it is prudent not to assign a numerical value to it, pending more precise and reliable information.
- Value 1: *In situ* pluvial flood or marine flood due to marine storm. These are situations in which the river system is barely responsive. After heavy but small–scale rainfall, water is retained and floods low–lying areas. These floods are often aggravated by drainage problems caused by human constructions, such as structural elements or urban development where drainage networks with sufficient capacity have not been provided.
- Value 2: Simple river flood, within the usual river bed. An episode of torrential or prolonged rainfall, when occurring over a wide area, causes an increase in the flows of the river system. If the magnitude of the event is moderate, the event results in an ordinary flood, without ever overflowing the usual bed.
- Value 3: River overflow of any magnitude. Widespread heavy or torrential rainfall of sufficient magnitude causes increases in flow that cannot be assimilated by the usual channel and overflow occurs. The circulation of water in unusual areas is an easily identifiable circumstance.

\+ Variable 2. Structural Component

This category describes the effects on permanent constructions or activities of human origin, with a high exposure but relatively low vulnerability. The severity of the event is transmitted in a gradation of impacts on elements of relatively objective and constant behaviour such as building structures and crops.

- Value 0: Insufficient information for a definitive classification.
- Value 1: Minor disturbance with inconvenience or damage to movable property or temporary exposed activities. These are reversible problems that occur in flood–prone areas, such as basement flooding, damage to vehicles and street furniture.
- Value 2: Moderate damage with loss of movable property and damage to permanent structures. These are situations in which the force of the water affects some built elements with considerable damage. Some examples are hydraulic infrastructures such as protective dams, bridges or watermills, as well as damage to buildings and public roads. In any case, it is damage that requires a repair intervention with an economic cost and significant alterations until normality can be restored.
- Value 3: Severe affectation with partial or complete destruction of permanent structures. The response of the river system to a severe event can result in the partial or complete destruction of any infrastructure or building in the vicinity of the water course. Both in historical and modern times there are elements susceptible to this destruction. The list would be endless. In historical times, in addition to buildings, farms were also sensitive elements where overflows could cause losses due to the washing out of crops and permanent crops (vineyards, fruit trees) and irrigation installations and for regular work (irrigation ditches, warehouses, silos, dams). In modern times, supply installations, often close to water courses, have proved to be significantly sensitive: drinking water distribution networks, sewerage, electricity, gas and communications supplies.

\+ Variable 3. Human Component.

This element of classification appears significantly in the most recent floods and requires a segregated classification of structural impacts due to the special idiosyncrasies of human beings when faced with situations of natural risk. Their responses vary greatly

depending on the cultural background and the existing perception of climate risk and the capacities of the available resources.

- Value 0: Insufficient information for a definitive classification.
- Value 1: Minor affectation with discomfort or displacement for self–protection. These are situations in which the integrity of the population is not threatened, but their usual activities are altered. Mobility is particularly affected, in such a way that routes or schedules are voluntarily or involuntarily modified in journeys and in private and public means of transport.
- Value 2: Moderate affectation with evacuations and/or forced lockdowns. These are situations in which the presence of water is already a threat to the physical integrity of people. In some situations there are spontaneous evacuations or evacuations coordinated by the authorities. There may also be rescues in the face of imminent danger. The population temporarily loses its mobility, and either individually or at the direction of the authorities, movement is restricted and the population is isolated or immobilised.
- Value 3: Serious impact with injuries and fatalities. These are situations in which self–protection decisions or instructions from the authorities are not sufficient to avoid personal injuries and fatalities, either due to the behaviour of the water itself or due to the collapsing construction elements. This category also includes fatalities caused by failure to follow the instructions of the authorities or reckless actions in the course of the ongoing event.

This numerical classification system presents situations that are not well defined or that go beyond the criteria contemplated *a priori*. The main factor to bear in mind with regard to natural phenomenon is that the system is adapted to the most common circumstances typical of the studied area, the Mediterranean Basin, where floods are produced by torrential rainfall events and less commonly by extensive or persistent rainfall. There are other causes of flood events, which are covered by the same classification system even if their occurrence is minimal. Examples are episodes caused by rapid snow melt of large snow–covered areas, or breakage of natural dykes (formed by glaciers or landslides). However, events with human involvement are also recorded and catalogued, such as dam collapse due to natural events and/or technical inefficiencies (i.e., collapse of Puentes Dam, 30 April 1802, Guadalentín River, Lorca city; more than 600 casualties). Rapid emptying of dams due to technical decisions or tactical interest in war situations (i.e., flood episode of 26 July 1938 in Ebro River. During 115 days of Ebro Battle, five flood episodes were provoked to affect crossing attempts on the Ebro River).

Another circumstance that generates a notable impact on the classification system is the detection of spurious episodes, generated with the use of incorrect, erroneous information that does not correspond to a real existing event. In cases of obvious errors, the classification system does not generate numerical values, but rather the indicative "ERR" (from "error", mistake, in the original language).

In this way, an identification code is generated for false or non–existent flood cases. The aim is to prevent their inclusion in any subsequent numerical analysis as if they were a real case. However, they should be identified precisely to recall previous studies that have used such erroneous information and to prevent them from being analysed in future research. If misinformation is completely suppressed, it may reappear in different studies without being detected in time. This should be avoided if possible.

### *2.4. Proposed Numerical Indices for Case Characterisation*

A weighted composite index containing the information of the three variables above is proposed for characterisation of the flood cases. Combining the information from the three variables into a single numerical value allows an integrated analysis of the flood events that constitute each episode. The formula for the Index per flood event ($I_c$) is:

$$I_c = ((x_{\text{natural variable}} \times 3) + (x_{\text{structural variable}} \times 2) + (x_{\text{social variable}} \times 1))/(3 + 2 + 1)$$

where:

$x_{natural\ variable}$ = Index value for variable 1, Hydraulic Component.
$x_{structural\ variable}$ = Index value for variable 2, Structural Component.
$x_{social\ variable}$ = Index value for variable 3, Human Component.

This formula weights each of the three variables that make up the classification system differently, placing greater emphasis on the variables with greater reliability and objectivity. Thus, the natural variable has a higher weighting because it is the phenomenon that is most reliably and consistently identified, as well as being the most objective of the variables. The structural variable has a medium weighting because it objectively reflects damage to build elements, but which are subject to human factors. Finally, the social variable has a neutral valuation due to its susceptibility to assess the vulnerability and exposure of the population affected by the flood. The information records are not subjective or erroneous, but the circumstances in which human casualties occur are inconsistent and with an important random component.

The index by cases generates values similar to those of the previous variables (0 to 3), which facilitates the reading of the data, their comparison and interpretation. It is a summary value that simplifies the information and allows integration by episodes.

## 3. Results. Application of the Classification System

This section provides examples of the application of the possibilities offered by the proposed classification system. The possibility of integrating with cartographic resources the totality of cases of flood events, and for very different historical periods.

This is a methodological initiative for which no previous references have been found in the scientific literature. The integration of historical and modern information has not been a common work in historical flood databases. However, the analysis of low–frequency events makes it increasingly interesting.

### *3.1. Cartographic Representation of Flood Events*

One of the objectives of the proposed classification system is that it allows a direct and synthetic representation of the cases that compose a flood episode. In this sense, we show the cartographic representation of a set of six episodes with different casuistry, which allow us to illustrate the applicability and versatility of the classification system. The episodes represented have been selected according to different criteria:

- Temporal distribution. One episode per century is shown, from the 16th century to the present day. This tests the ability to synthesise flood events over long periods of time.
- Diversity of casuistry. Episodes have been chosen with as many different characteristics of fluvial behaviour and damage as possible, as well as different numbers of data records and different areas affected.

The first of the flood episodes depicted is that of the Kingdom of Valencia on 27 September 1517 (Figure 1). This episode affected multiple river basins included on the Júcar River Hydrographic Demarcation (Júcar River Catchment Authority—according to Spanish Administration, Water Authority Institutions are organized by large Catchment Areas), and has a total of 18 flood cases in different towns and rivers. The representation of the cases of this episode allows us to see their distribution and their location close to important river courses of the Júcar Hydrographic Demarcation. The characteristic of all the cases in this episode is that they reach the maximum level in the natural variable (river overflow), causing serious damage to structures in the affected populations. On the other hand, there are few cases in which there were personal casualties in these villages.

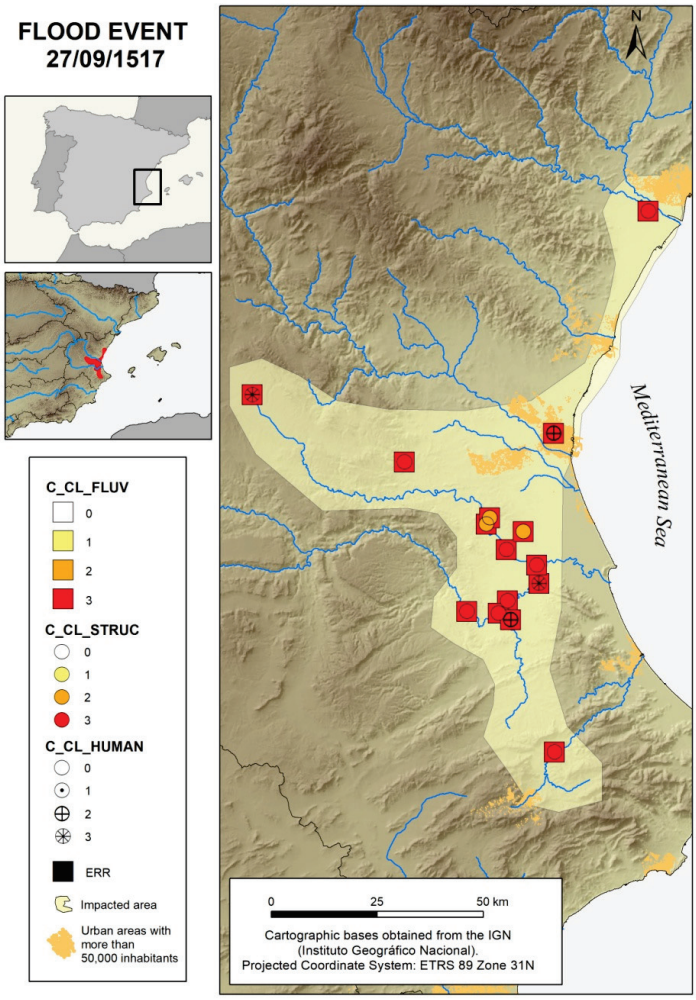



**Figure 1.** Representation of cases for the flood event of 27 September 1517. C_CL_FLUV: Variable 1. Hydraulic behaviour of the river flood. C_CL_STRUC: Variable 2. Flood impact on structural elements. C_CL_HUMAN: Variable 3. Social/personal vulnerability to the flood. ERR: Erroneous or spurious cases. Blue line: Basic fluvial system. Black line: Spanish Hydrographic Demarcations. Urban areas: Population according to 2022 demographic record.

The second episode is that of 2 and 3 November 1617 (Figure 2). This episode affected three different Hydrographic Demarcations, causing 84 cases of flooding. It has been decided not to represent the cases of flooding that occurred in the Júcar Basin in order to focus the mapping on the basins with the highest concentration of cases. Even ignoring remote cases, the magnitude of the episode justifies the division into two different daily maps that represent the dates of the episode with the highest number of impacts. In the case of the impacts caused by the flood on the 2nd of November (Figure 2, left), the effects are concentrated in towns near the Llobregat and Ter rivers in the Internal Catalan Basins. On the other hand, on the following day (Figure 2, right), the effects were more widespread, affecting the headwaters of these river basins more severely and even affecting tributaries of the Ebro river basin, which is much larger. In both cases, it can be seen that this episode is also characterised by a large number of cases in which both the fluvial and structural variables are intense.

The third episode selected is from 14 to 20 November 1716 and caused damage along the Mediterranean coast of the Iberian Peninsula. This episode has 11 flood cases and affected three different Hydrographic Demarcations. This map serves as an example for the representation of episodes with more than one flood case at the same point.

The effects caused by this episode were widely distributed throughout the territory, with the most severe affectations occurring on the 19th and 20th in the city of Girona and, at the same time, in other villages along the Valencian coast (Figure 3, left).

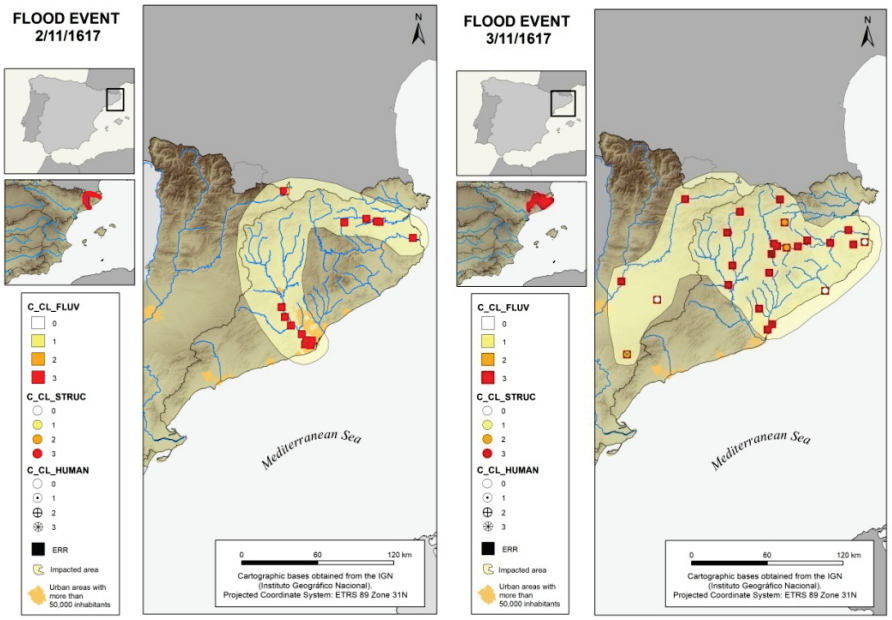



**Figure 2.** (**Left**): Representation of cases for the flood event of 2 November 1617. (**Right**): Representation of cases for the flood event of 3 November 1617. C_CL_FLUV: Variable 1. Hydraulic behaviour of the river flood. C_CL_STRUC: Variable 2. Flood impact on structural elements. C_CL_HUMAN: Variable 3. Social/personal vulnerability to the flood. ERR: Erroneous or spurious cases. Blue line: Basic fluvial system. Black line: Spanish Hydrographic Demarcations. Urban areas: Population according to 2022 demographic record.

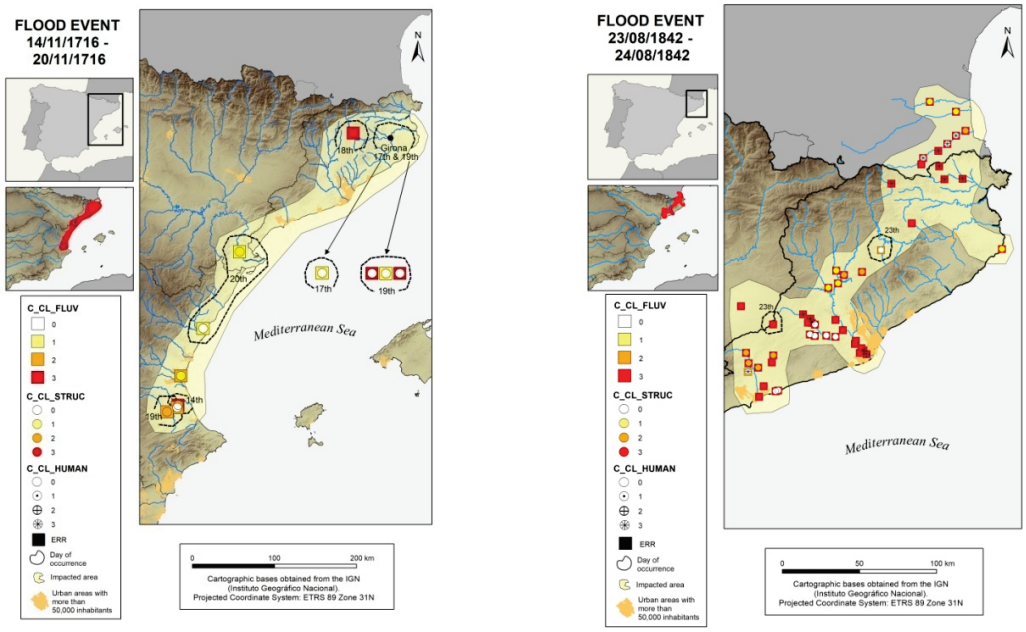



**Figure 3.** (**Left**): Representation of cases for the flood event of 14 to 20 November 1716. (**Right**): Representation of cases for the flood event of 23 and 24 August 1842. C_CL_FLUV: Variable 1. Hydraulic behaviour of the river flood. C_CL_STRUC: Variable 2. Flood impact on structural elements. C_CL_HUMAN: Variable 3. Social/personal vulnerability to the flood. ERR: Erroneous or spurious cases. Blue line: Basic fluvial system. Black line: Spanish Hydrographic Demarcations. Urban areas: Population according to 2022 demographic record.

The episode selected for the 19th century is the one known as "Aiguat de Sant Bartomeu" on 23 and 24 November 1842. This episode affected a total of three Hydrographic Demarcations, causing 57 flood cases. Its affectations were mainly distributed along the coastal area of the Internal Catalan Basins (Catalonia) and the Pyrenean River Basins that run through France (Figure 3, right). This episode is notable for having a few flood cases whose impact on structures was lower than in other episodes. On the other hand, the impact on the population was more significant, causing fatalities in many parts of the affected area.

The fifth episode selected is that of the floods of 7 and 8 September 1973. This episode affected a single Hydrographic Demarcation, the Internal Catalan Basins, and caused 15 flood cases. The effects of this episode were concentrated in two specific areas. On the one hand, the mouth of the Llobregat river, where the river overflow was severe but caused little structural damage. On the other hand, the coastal area north of the city of Barcelona, the major urban area, was equally affected by floods but these caused more structural damage (Figure 4). The impact on the population was limited, focusing on the area of the mouth of the Llobregat river.

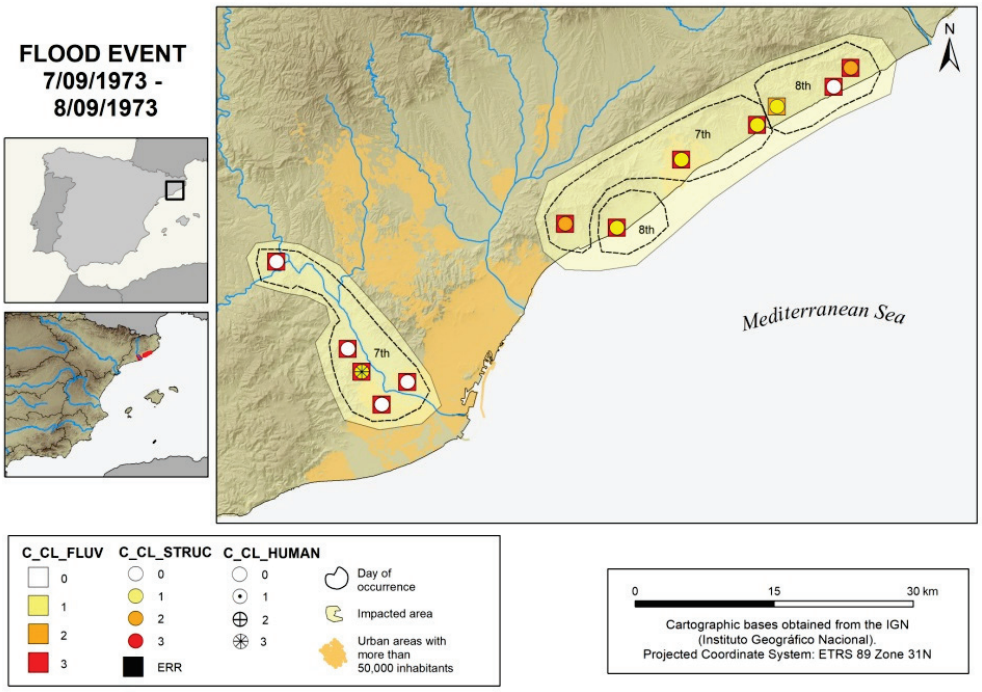



**Figure 4.** Representation of cases for the flood event of 7 and 8 September 1973. C_CL_FLUV: Variable 1. Hydraulic behaviour of the river flood. C_CL_STRUC: Variable 2. Flood impact on structural elements. C_CL_HUMAN: Variable 3. Social/personal vulnerability to the flood. ERR: Erroneous or spurious cases. Blue line: Basic fluvial system. Black line: Spanish Hydrographic Demarcations. Urban areas: Population according to 2022 demographic record.

The last selected episode belongs to the 21st century. It is related to a DANA (Cut–Off Low, or Cold Drop. In Spanish: Depresión Aislada en Niveles Altos) that mainly affected the county of La Vega Baja del Segura in September 2019. This episode affected a total of three Hydrographic Demarcations causing 35 flood cases (Figure 5).

The effects of the DANA had a great media impact due to its repercussions, with various affectations on the urban areas of La Vega Baja del Segura. The river floods were intense, with widespread effects on the population, although the impact on infrastructure was moderate.

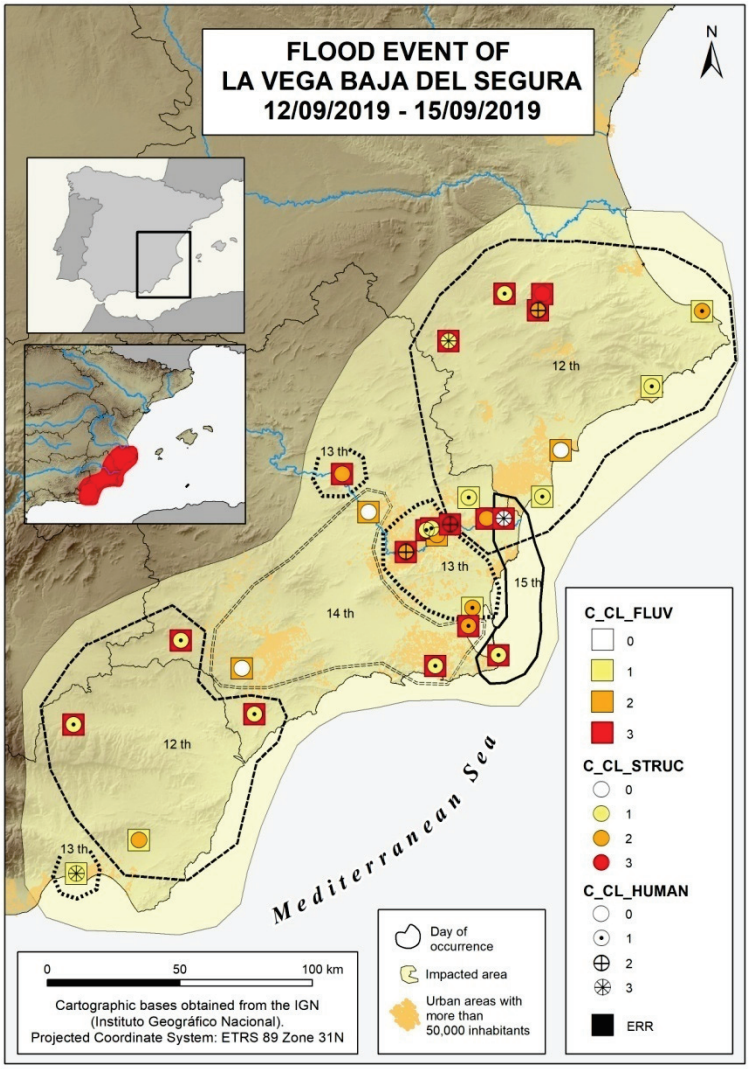



**Figure 5.** Representation of cases for the flood event of 12 to 15 September 2019. C_CL_FLUV: Variable 1. Hydraulic behaviour of the river flood. C_CL_STRUC: Variable 2. Flood impact on structural elements. C_CL_HUMAN: Variable 3. Social/personal vulnerability to the flood. ERR: Erroneous or spurious cases. Blue line: Basic fluvial system. Black line: Spanish Hydrographic Demarcations. Urban areas: Population according to 2022 demographic record.

### *3.2. Numerical Characterisation of Flood Cases*

This section shows the results obtained from the application of the proposed flood episode classification system mentioned above. Numerical values are shown for different episodes in which the information relating to the 3 variables used to calculate the Case Index ($I_c$) is synthesised, as well as the resulting values themselves (Table 3). The table shows the episodes represented in Section 3.1 and other significant ones have been added to provide more casuistry to give more richness to the application test. The aim was to compare the performance of the index with episodes of the greatest possible diversity, from episodes with a large number of cases, such as November 1982, to others with only a single case, a common feature in the oldest historical episodes.

**Table 3.** Results obtained from the application of the index $I_c$ on different flood episodes.

| Event Date | Hydrographic Demarcations | Number of Cases | Hydraulic Component Average | Structural Component Average | Human Component Average | Average of Total $I_c$ |
|---|---|---|---|---|---|---|
| 1193 | 1 | 4 | 2.5 | 1.8 | 1.3 | 2.0 |
| 1193 September | 1 | 1 | 3.0 | 3.0 | 3.0 | 3.0 |
| 1290 | 1 | 1 | 2.0 | 0.0 | 3.0 | 1.5 |
| 1421 October | 2 | 23 | 3.0 | 2.7 | 0.8 | 2.6 |
| 1517 September | 1 | 18 | 3.0 | 2.8 | 0.7 | 2.5 |
| 1617 November | 4 | 84 | 2.9 | 2.6 | 0.2 | 2.4 |
| 1716 November | 3 | 11 | 2.0 | 0.8 | 0.0 | 1.3 |
| 1787 October | 3 | 56 | 2.6 | 2.3 | 0.6 | 2.2 |
| 1793 September | 2 | 14 | 2.7 | 2.3 | 1.2 | 2.3 |
| 1842 August | 3 | 57 | 2.9 | 1.8 | 0.8 | 2.2 |
| 1898 January | 3 | 92 | 2.4 | 1.3 | 0.3 | 1.7 |
| 1907 October | 4 | 154 | 2.7 | 1.6 | 0.2 | 1.9 |
| 1937 October | 2 | 128 | 2.6 | 1.4 | 0.1 | 1.8 |
| 1940 October | 3 | 134 | 3.0 | 1.1 | 0.4 | 1.9 |
| 1962 September | 4 | 58 | 2.8 | 1.3 | 0.3 | 1.9 |
| 1963 September | 7 | 66 | 2.5 | 0.7 | 0.1 | 1.5 |
| 1973 September | 1 | 15 | 2.7 | 0.6 | 0.2 | 1.6 |
| 1982 October | 5 | 44 | 2.0 | 0.3 | 0.4 | 1.1 |
| 1982 November | 6 | 398 | 2.4 | 1.5 | 0.1 | 1.4 |
| 1994 October | 5 | 109 | 2.2 | 0.7 | 0.2 | 1.4 |
| 1996 September | 5 | 65 | 1.1 | 0.1 | 0.1 | 0.6 |
| 2005 October | 4 | 35 | 1.4 | 0.3 | 0.1 | 0.8 |
| 2007 October | 4 | 63 | 1.2 | 0.2 | 0.1 | 0.7 |
| 2019 September | 3 | 35 | 2.3 | 1.4 | 0.9 | 1.8 |
| 2020 January | 5 | 58 | 2.2 | 0.6 | 0.4 | 1.3 |

Shaded rows: flood events already analysed in Section 3.1.

## 4. Conclusions

In view of the information on extreme historical flood events potentially available in documentary and bibliographic sources, a series of preparatory phases are proposed in this paper. Firstly, the original information must be treated with historiographic criteria to make it as reliable and complete as possible [10]. The next step proposed in this paper consists of the development and application of methodological criteria for the generation, cataloguing and classification of historical information in formats that allow subsequent meteorological/climatic and hydraulic/hydrological analysis. It also provides a starting point for future analysis on the social dimension of flood episodes.

The application of new methodological proposals will not in any case allow the data generated to be assimilated to quantitative instrumental information. However, the general objective of this paper is to facilitate the use of qualitative historical information with maximum efficiency in the analysis of severe flood episodes.

The quantitative classification systems by cases and episodes presented in this paper have been tested in the AMICME database with satisfactory results. Despite being applied to episodes with considerably different characteristics, both systems generate indices without spurious or conflicting values. Consequently, their use in large historical flood databases is feasible.

A relevant aspect of the case indexing system ($I_c$) is that it allows the information on the different variables (multivariable) involved in its definition to be kept segregated.

This prevents the loss of detailed information for subsequent research or analysis. This segregation is not easy to manage, but its usefulness takes precedence. The proof of this complexity is the cartographic representations generated for specific episodes. The amount and diversity of information presented has required the design of a rather complex to read symbology. However, it preserves and shows nuances for each of the variables, a positive factor in the overall analysis of the flood episodes.

**Author Contributions:** J.T., creation and development of the methodological tools. M.B., creation and development of the methodological tools, preparation of the state of the art of this subject; writing of the Introduction and Materials & Methods sections. J.B., preparation and application of the methodological tools on the database and the chosen study cases; cartographic representation of six examples of flood episodes. All authors have read and agreed to the published version of the manuscript.

**Funding:** Present work was funded by Prediflood Project, Ministerio de Economía y Competitividad, Spanish Government (Number CGL2012–35071), 2013–2015; and Mediflood Project. Ministerio de Economía y Competitividad, Spanish Government, Number CGL2016–75996–R, 2016–2019.

**Data Availability Statement:** Not applicable.

**Conflicts of Interest:** We do not have any conflict of interest with this work. Nor do we consider that the work and the results affect any ethical aspect.

## References

1. Pfister, C. Die "Katastrophenlücke" des 20. Jahrhunderts und der Verlust traditionalen Risiko–bewusstseins. *Gaia* **2009**, *18*, 239–246. [CrossRef]
2. Thorndycraft, V.R.; Barriendos, M.; Benito, G.; Rico, M.; Casas, A. The catastrophic floods of AD 1617 in Catalonia (northeast Spain) and their climatic context. *Hydrol. Sci. J.* **2006**, *51*, 899–912. [CrossRef]
3. Brázdil, R.; Kundzewicz, Z.W.; Benito, G.; Demarée, G.; Macdonald, N.; Roald, L.A. Historical floods in Europe in the past millennium. In *Changes in Flood Risk in Europe*; Kundzewicz, Z.W., Ed.; IAHS Special Publication 10: Wallingford, UK, 2012; pp. 121–166, ISBN 978-1-907161-28-5. [CrossRef]
4. Glaser, R.; Riemann, D.; Schönbein, J.; Barriendos, M.; Brázdil, R.; Bertolin, C.; Camuffo, D.; Deutsch, M.; Dobrovolný, P.; Van Engelen, A.; et al. The variability of European floods since AD 1500. *Clim. Chang.* **2010**, *101*, 235–256. [CrossRef]
5. Barriendos, M.; Coeur, D. Flood data reconstruction in historical times from non–instrumental sources in Spain and France. In *Systematic, Palaeoflood and Historical Data for the Improvement of Flood Risk Estimation*; Methodological Guidelines; Centro de Ciencias Medioambientales: Madrid, Spain, 2004; pp. 29–42.
6. Sturm, K.; Glaser, R.; Jacobeit, J.; Deutsch, M.; Brázdil, R.; Pfister, C. Floods in Central Europe since AD 1500 and their relation to the atmospheric circulation. *PetermannsGeogr. Mitt.* **2001**, *148*, 18–27.
7. Tarasova, L.; Merz, R.; Kiss, A.; Basso, S.; Blöschl, G.; Merz, B.; Viglione, A.; Plötner, S.; Guse, B.; Schumann, A.; et al. Causative classification of river flood events. *WIREs Water* **2019**, *6*, e1353. [CrossRef]
8. Lang, M.; Fernández-Bono, J.F.; Recking, A.; Naulet, R.; Grau-Gimeno, P. Methodological guide for palaeoflood and historical peak discharge estimation. In *Systematic, Palaeoflood and Historical Data for the Improvement of Flood Risk Estimation*; Methodological Guidelines; Centro de Ciencias Medioambientales: Madrid, Spain, 2004; pp. 43–53.
9. Brázdil, R.; Kundzewicz, Z.W.; Benito, G. Historical hydrology for studying flood risk in Europe. *Hydrol. Sci. J.* **2006**, *51*, 739–764. [CrossRef]
10. Barriendos, M.; Ruiz–Bellet, J.L.; Tuset, J.; Mazón, J.; Balasch, J.C.; Pino, D.; Ayala, J.L. The 'Prediflood' database of historical floods in Catalonia (NE Iberian Peninsula) AD 1035–2013, and its potential applications in flood analysis. *Hydrol. Earth Syst. Sci.* **2014**, *18*, 4807–4823. [CrossRef]
11. Balasch, J.C.; Pino, D.; Ruiz–Bellet, J.L.; Tuset, J.; Barriendos, M.; Castelltort, X.; Peña, J.C. The extreme floods in the Ebro River basin since 1600 CE. *Sci. Total Environ.* **2019**, *646*, 645–660. [CrossRef] [PubMed]
12. Barriendos, M.; Gil-Guirado, S.; Pino, D.; Tuset, J.; Pérez-Morales, A.P.; Alberola-Romà, A.; Costa, J.; Balasch, J.C.; Castelltort, X.; Mazón, J.; et al. Climatic and social factors behind the Spanish Mediterranean flood event chronologies from documentary sources (14th–20th centuries). *Glob. Planet. Chang.* **2019**, *182*, 102997. [CrossRef]
13. Peña, J.C.; Balasch, J.C.; Pino, D.; Schulte, L.; Barriendos, M.; Ruiz–Bellet, J.L.; Prohom, M.; Tuset, J.; Mazón, J.; Castelltort, X. Low-frequency atmospheric variability patterns and synoptic types linked to large floods in the lower Ebro River basin. *J. Clim.* **2022**, *35*, 2351–2371. [CrossRef]
14. Pino, D.; Ruiz-Bellet, J.L.; Balasch, J.C.; Romero-León, L.; Tuset, J.; Barriendos, M.; Mazon, J.; Castelltort, X. Meteorological and hydrological analysis of major floods in NE Iberian Peninsula. *J. Hydrol.* **2016**, *541*, 63–89. [CrossRef]
15. Barriendos, M.; Martín-Vide, J. Secular Climatic Oscillations as Indicated by Catastrophic Floods in the Spanish Mediterranean Coastal Area (14th–19th Centuries). *Clim. Chang.* **1998**, *38*, 473–491. [CrossRef]

16. Barriendos, M.; Rodrigo, F.S. Study of historical flood events on Spanish rivers using documentary data. *Hydrol. Sci. J.* **2006**, *51*, 765–783. [CrossRef]
17. Brázdil, R.; Glaser, R.; Pfister, C.; Dobrovolný, P.; Antoine, J.M.; Barriendos, M.; Camuffo, D.; Deutsch, M.; Enzi, S.; Guidoboni, E.; et al. Flood Events of Selected European Rivers in the Sixteenth Century. *Clim. Chang.* **1999**, *43*, 239–285. [CrossRef]
18. Blöschl, G.; Kiss, A.; Viglione, A.; Barriendos, M.; Böhm, O.; Brázdil, R.; Coeur, D.; Demarée, G.; Llasat, M.C.; Macdonald, N.; et al. Current European flood-rich period exceptional compared with past 500 years. *Nature* **2020**, *583*, 560–566. [CrossRef]
19. Ruiz-Bellet, J.L.; Balasch, J.C.; Tuset, J.; Barriendos, M.; Mazon, J.; Pino, D. Historical, hydraulic, hydrological and meteorological reconstruction of 1874 Santa Tecla flash floods in Catalonia (NE Iberian Peninsula). *J. Hydrol.* **2015**, *524*, 279–295. [CrossRef]
20. Macdonald, N.; Sangster, H. High-magnitude flooding across Britain since AD 1750. *Hydrol. Earth Syst. Sci.* **2017**, *21*, 1631–1650. [CrossRef]
21. Veale, L.; Endfield, G.H.; Davies, S.; Macdonald, N.; Naylor, S.; Royer, M.J.; Bowen, J.; Tyler-Jones, R.; Jones, C. Dealing with the deluge of historical weather data: The example of the TEMPEST database. *Geo Geogr. Environ.* **2017**, *4*, e00039. [CrossRef]
22. Lang, M.; Coeur, D.; Audouard, A.; Villanova-Oliver, M.; Pène, J.P. BDHI: A French national database on historical floods. *E3S Web Conf.* **2016**, *7*, 04010. [CrossRef]
23. Riemann, D.; Glaser, R.; Kahle, M.; Vogt, S. The CRE tambora.org—New data and tools for collaborative research in climate and environmental history. *Geosci. Data J.* **2015**, *2*, 63–77. [CrossRef]
24. Glaser, R.; Kahle, M. Reconstructions of droughts in Germany since 1500—Combining hermeneutic information and instrumental records in historical and modern perspectives. *Clim. Past* **2020**, *16*, 1207–1222. [CrossRef]
25. Pantanada de Tous: 33 Años de la Peor Gota Fría de la Historia Valenciana, ABC 2015. Available online: https://www.abc.es/local-comunidad-valenciana/20151020/abci-aniversario-pantanada-tous-201510201113.html (accessed on 15 December 2022).
26. Pons, M. El temporal de 1982 Desborda los Ríos Pirenaicos y Causa 26 Muertos, El Nacional.cat. 2018. Available online: https://www.elnacional.cat/es/efemerides/marc-pons-temporal-1982-desborda-rios-pirenaicos_322212_102.html (accessed on 15 December 2022).
27. Civil Protection, Catálogo Nacional de Inundaciones Históricas. 2014. Available online: https://www.proteccioncivil.es/catalogo/naturales/cnih/cnih2014/Presentacion.html (accessed on 18 November 2022).
28. Gaume, E.; Bain, V.; Bernardara, P.; Newinger, O.; Barbuc, M.; Bateman, A.; Blaškovičová, L.; Blöschl, G.; Borga, M.; Dumitrescu, A.; et al. A compilation of data on European flash floods. *J. Hydrol.* **2009**, *367*, 70–78. [CrossRef]
29. Barriendos, M.; Pomés, J. *L'aigua a Mataró. Inundacions I Recursos Hídrics (Segles XVIII–XX)*; Caixa d'Estalvis Laietana: Mataró, Spain, 1993; 278p, ISBN 84-606-1496-4.

land

MDPI

*Article*

# The Role of Historical Data to Investigate Slow-Moving Landslides by Long-Term Monitoring Systems in Lower Austria

**Philipp Marr *, Yenny Alejandra Jiménez Donato, Edoardo Carraro, Robert Kanta and Thomas Glade**

Geomorphological Systems and Risk Research, Department of Geography and Regional Research, University of Vienna, Universitätsstraße 7, 1010 Vienna, Austria
* Correspondence: philipp.marr@univie.ac.at

**Abstract:** Landslides are one of the most significant natural hazards worldwide. They can have far-reaching negative impacts on societies in different socio-economic sectors as well as on the landscape. Among the different types and processes that can also affect infrastructure and land use planning, slow-moving landslides are often underestimated. Therefore, studying areas affected by slow movements provide an opportunity to better understand the spatial and temporal patterns of these processes, their forcings, mechanisms, and potential risks. This study aims to investigate the importance of historical data for improving landslide hazard assessment in Lower Austria (Austria), which is particularly prone to landslides. This paper focuses on how historical information formed the basis for the establishment of three long-term landslide monitoring observatories in this region. The analysis conducted highlights the importance of using historical data to better assess the frequency and magnitude relationships and phases of landslide activity. In particular, they can extend the temporal window and provide relevant information on past events and accelerations to improve knowledge of landslide dynamics and the resulting socio-economic impacts. In order to better assess the landslide hazard associated, it is necessary to integrate historical data and monitoring datasets obtained by surface and subsurface methods. Both components allow for the characterization of the spatio-temporal evolution of slow movements and the analysis of the hazard over time. Based on a variety of historical sources, it was possible to install the instruments constituting the long-term landslide monitoring observatories in a meaningful manner. The results demonstrate the influential role of human impact on the stability conditions, which may also contribute to landslide occurrence. In this regard, the attempt to combine historical data and long-term, continuous monitoring systems in the presented landslide observatories can improve landslide risk reduction measures in the region. The integration of different techniques and tools, along with ongoing research and collaboration with local authorities, will further improve our understanding of these slow-moving processes and the development of effective management strategies.

**Keywords:** natural hazard; slow-moving landslides; long-term monitoring; historical data; lower Austria

**Citation:** Marr, P.; Jiménez Donato, Y.A.; Carraro, E.; Kanta, R.; Glade, T. The Role of Historical Data to Investigate Slow-Moving Landslides by Long-Term Monitoring Systems in Lower Austria. *Land* **2023**, *12*, 659. https://doi.org/10.3390/land12030659

Academic Editors: Fabio Luino, Mariano Barriendos Vallvé, Fabrizio Terenzio Gizzi, Ruediger Glaser, Christoph Gruetzner, Walter Palmieri, Sabina Porfido, Heather Sangster and Laura Turconi

Received: 31 January 2023
Revised: 4 March 2023
Accepted: 7 March 2023
Published: 11 March 2023



**Copyright:** © 2023 by the authors. Licensee MDPI, Basel, Switzerland. This article is an open access article distributed under the terms and conditions of the Creative Commons Attribution (CC BY) license (https://creativecommons.org/licenses/by/4.0/).

## 1. Introduction

Natural hazards, such as landslides, have been well known for many decades to pose a serious threat to societies, communities, and individuals worldwide [1–3]. Due to the increasing population pressure and the need for infrastructure, e.g., for transportation systems and agricultural purposes, natural hazards pose a growing threat within various socio-economic dimensions [4,5]. Indeed, landslide phenomena have been increasingly reported in recent decades, causing damage or threatening society in manifold ways [3]. In addition, global climate change is expected to lead to an increase in the frequency and intensity of landslides, potentially leading to increased negative impacts on society in the future [6,7].

According to Cruden and Varnes [8] and Dikau et al. [9], landslides are defined as the movement of rock, debris, or earth down a slope. Only in the case that humans and/or

anthropogenic structures are negatively affected the event will be considered a hazard [10]. Landslides are dynamic systems that commonly occur on hillslopes and in mountainous regions worldwide and are important contributors to landscape evolution [11,12]. These natural phenomena encompass a wide range of mechanisms and processes at different spatial and temporal scales [2]. As a result, understanding the temporal evolution of slope instabilities is a difficult task, as combinations of different controlling factors could exist. Three important factors have been identified to be critical in the kinematic transition from a stable to an actively unstable slope: (i) preconditioning, (ii) preparatory, and (iii) triggering factors [2]. These factors are dynamic, and the inter-dependencies of natural processes and human activities have influences on the spatio-temporal occurrence of landslides [13]. Assessing the driving mechanisms that are causing the instability is useful to deepen hazard analysis and determine adaptation and mitigation strategies to lower the vulnerability of the elements at risk.

In order to reliably assess the driving mechanisms, the hazard, and the consequent risk of current and future landslides, historical data can be of key value [12,14]. In many cases, historical information is an important tool for land use planning and disaster risk mitigation management that should be integrated into the methodological approaches [15]. Historical data can be divided into four categories [16]: (i) data that directly record the occurrence of the event, e.g., drought, flood, landslide, and erosion rates; (ii) data that can be used to identify causal factors, e.g., climatic records; (iii) data that provide additional relevant information, e.g., geological surveys; and (iv) phenomenological data that account for temporal variability of the phenomenon, e.g., groundwater response to precipitation.

However, there is skepticism about the reliability of historical data [17]. Historical data can sometimes omit relevant evidence about the location, date, magnitude, and duration of the event. In addition, each archive has specific temporal and spatial information that makes it difficult to build a homogenous database. Furthermore, most historical archives are biased and record only unusual or catastrophic events, omitting isolated events or those that occurred in uninhabited areas [17,18]. Despite these criticisms, some studies have demonstrated the potential of using historical data for landslide hazard assessment, e.g., in Germany, New Zealand, and Italy (e.g., [19–22]).

Historical data provide important information about landslide activity and processes over a long period of time; however, they are not self-sufficient. In most cases, they are used to complete and enhance the information obtained from geological and geomorphological analyses. Nevertheless, historical data can also be incorporated into landslide monitoring. A continuous record of long-term monitoring is necessary to provide an unbiased temporal database. Furthermore, near-real-time monitoring can provide high-quality data to better understand the dynamics of active landslides and to develop more effective landslide mitigation and adaptation measures, such as early warning systems [23]. Landslide monitoring systems are used worldwide to detect and predict landslide activity [23]. Ground-based landslide monitoring systems typically consist of field sensors on or within the landslide-prone area, a data acquisition system to sample and control the sensors, a communication system to connect data from the field to base-station computers, and software for data processing and dissemination at a base station [23].

The design and implementation of a long-term monitoring system depend on specific considerations based on historical information that vary from site to site [23]. First of all, it is important to take into account the aim of the monitoring, to pinpoint the timing of landslide events, to gather information on the type of landslide to be monitored, the involved material, the activity status, and the physical setting on the site [23,24].

For evaluating the frequency of landslides in a particular area, it is vital to incorporate historical data in the analysis [12]. The availability and quality of historical data are very different and vary from case to case. There are prominent landslides that were dated thousands of years back with geochronological techniques and other events during the last centuries were reported in newspapers or documented by historians [25,26]. Historical data about landslide hazards were also collected in Austria, in particular in Lower Austria, which

is highly prone to landslide events [27–29]. However, there is a lack of studies compiling previous works and data as a basis for the establishment of long-term monitoring systems for landslide hazard assessment.

The European Alps, Austria in particular, are highly impacted by natural hazards affecting settlements and infrastructure [30]. Its topography is characterized by a variety of morphological landscapes, from alluvial flat areas to high-alpine landscapes, in which landslides represent a significant threat to private and public infrastructures, possibly influencing the socio-economic setting. The landslide occurrence in Austria is conditioned by a number of factors, including lithology, geomorphology, and human impact [31]. Deep-seated and shallow landslides are common in many regions of Austria, in particular in those areas situated in areas of the Central Alps comprised of metamorphic rock types and the Flysch Unit (e.g., Lower Austria) [32]. In addition to landslide susceptibility, the infrastructure at risk in Lower Austria is interesting due to the continuing economic losses due to landslides and the availability of historical data [33,34]. As a result, the exposure to landslide hazards considerably involves human activities and local authorities dealing with mitigation actions within the Lower Austrian territory [33,35,36].

Among the different types of landslides occurring in Lower Austria, understanding the dynamics of slow-moving landslides is of particular interest. Considering the difficulties in real-time monitoring of rapid landslides, slow-moving processes provide the opportunity to better study landslide dynamics over a long period of time [37]. Furthermore, the study of these processes is essential because they have often been identified as early deformation signals for fast-moving landslides or cascading hazards that could have catastrophic effects [37]. Complexity and non-uniform spatial and temporal kinematics of slow movements preclude the use of short-term measures to assess landslide processes [37,38]. For this reason, it is important to integrate available historical data with long-term, multi-parameter monitoring approaches in order to assess and mitigate the potential landslide hazard [39,40].

This study aims to prove the importance and added value of the integration of historical data in the long-term continuous monitoring process to improve the hazard assessment of three slow-moving landslides in Lower Austria. The monitoring setups and strategies are similar across the three sites, so-called landslide observatories, in Lower Austria (Hofermühle, Gresten, and Brandstatt observatories). All sites share the use of a variety of methods and sensors to monitor changes in both surface and subsurface conditions. This approach allows us to assess the spatial and temporal relationships between displacement rates and hydro-meteorological inputs, as well as potential land use changes to landslide dynamics. The objectives of this study are threefold:

1. To gather historical data of landslide events in an inventory and to analyze their characteristics in each of the three study sites in Lower Austria.
2. Assess how historical data played an important role in the landslide hazard assessment, in the selection of the study sites in Lower Austria, and the implementation of different methods within the monitoring systems.
3. Explore how historical data lead to coping and response strategies in planning decisions.

## 2. Study Area

The landslide observatories presented in this study are situated in the federal state of Lower Austria. This region covers a total area of approximately 19,000 km$^2$ in north-eastern Austria (Figure 1a,b). The three landslide observatories under investigation are introduced in the next sub-sections as Hofermühle, Gresten, and Brandstatt, respectively (Figure 1c–e). These sites are comparable in terms of natural settings (geological and climatic conditions), land use, and anthropogenic influences, such as drainage systems. However, they show distinct site-specific differences in the number of landslide subsystems, spatial extent, and dynamics.

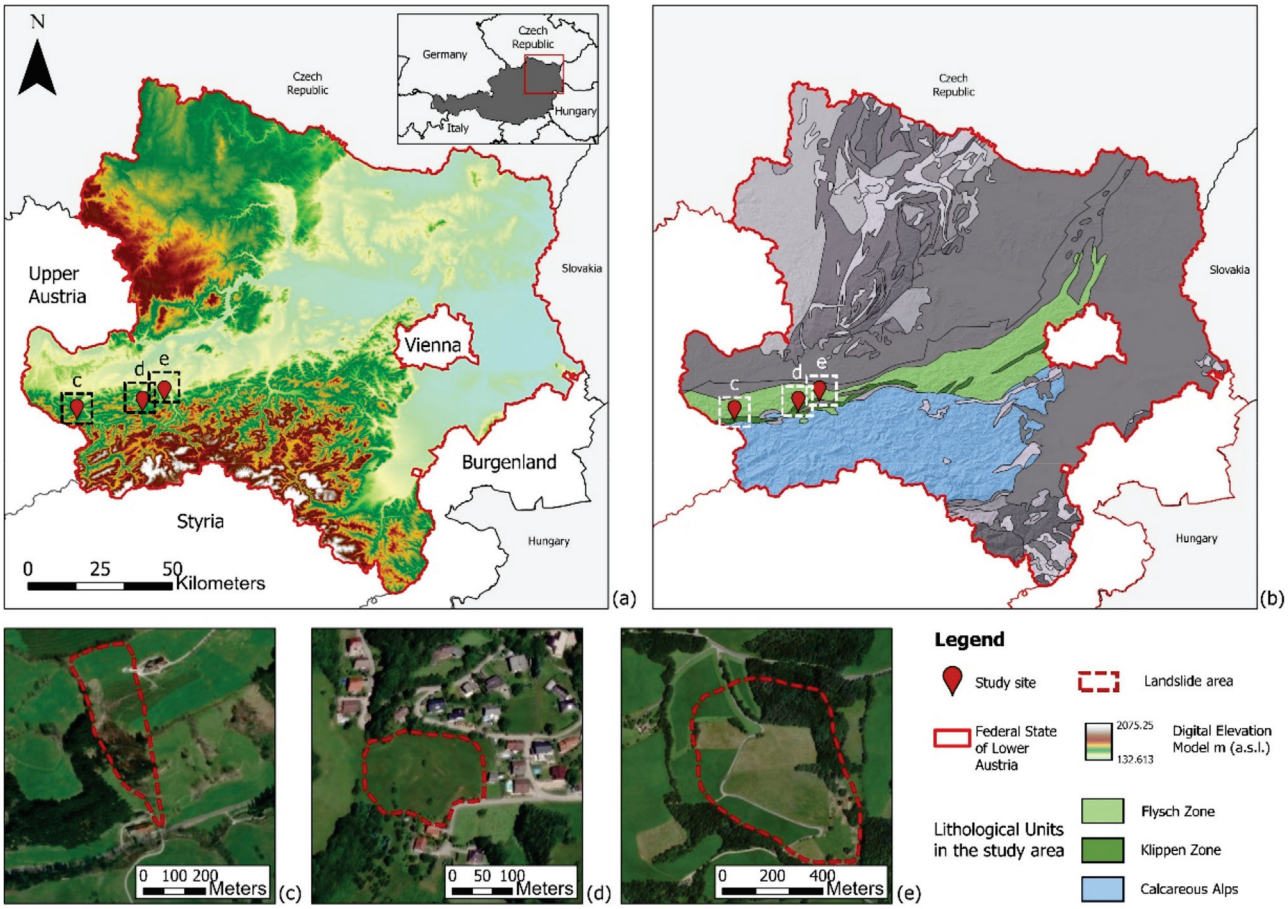



**Figure 1.** Location of the landslide observatories and areas of investigation in Lower Austria. (**a**) Location of the Lower Austria federal state, in north-eastern Austria. Relief shading is based on the Austrian 10 m DEM [41]; (**b**) Geological map in which the lithological units reported are of major interest for the study area (after [42]); (**c**–**e**) Location of the (**c**) Hofermühle, (**d**) Gresten, and (**e**) Brandstatt observatory, respectively, as well as areas affected by landslide displacements in recent years. Satellite images of the landslide sites provided in the ArcGIS Pro 3.0.0 software using World Imagery (Source: Esri, Maxar, Earthstar Geographics, and the GIS User Community).

The study sites are located in a complex geological setting, and it represents the most important predisposing factor driving the landslide occurrence and activity in the region [28,43–45]. Most of the complex, hydrologically triggered slope instabilities described in the previous studies in Lower Austria are predominantly located in the transition zone between the Flysch Zone (FZ) and the Klippen Zone (KZ) Units and the Northern Calcareous Alps (NCA) Unit (Figure 1b). Due to the high content of clay minerals and the corresponding weathering products, the geo-mechanical behavior of these lithological units prompts this area to landslide processes [28,45]. Actually, of the 1100 landslides registered in Lower Austria from 1965 to 2006, 62% were reported in the FZ (42%) and KZ (20%) [46].

Climate conditions are driving both the weathering and the triggering mechanisms of slope instabilities affecting the FZ and KZ lithologies in the study area. Here, the main triggering factors of landslide activity include long-lasting heavy rainfall and rapid snow melting [29,31]. The study area is located in the NE Alpine foreland and it is characterized by a warm temperature and humid climate. Long-term precipitation time series are available from the Histalp project (www.zamg.ac.at/histalp) in order to assess patterns and trends within the European Alps. Here, it is assumed that the meteorological station located in Waidhofen an der Ybbs is a representative location to properly identify the

hydro-meteorological setting of the landslide observatories presented (Figure 2) due to its proximity to the three study sites.

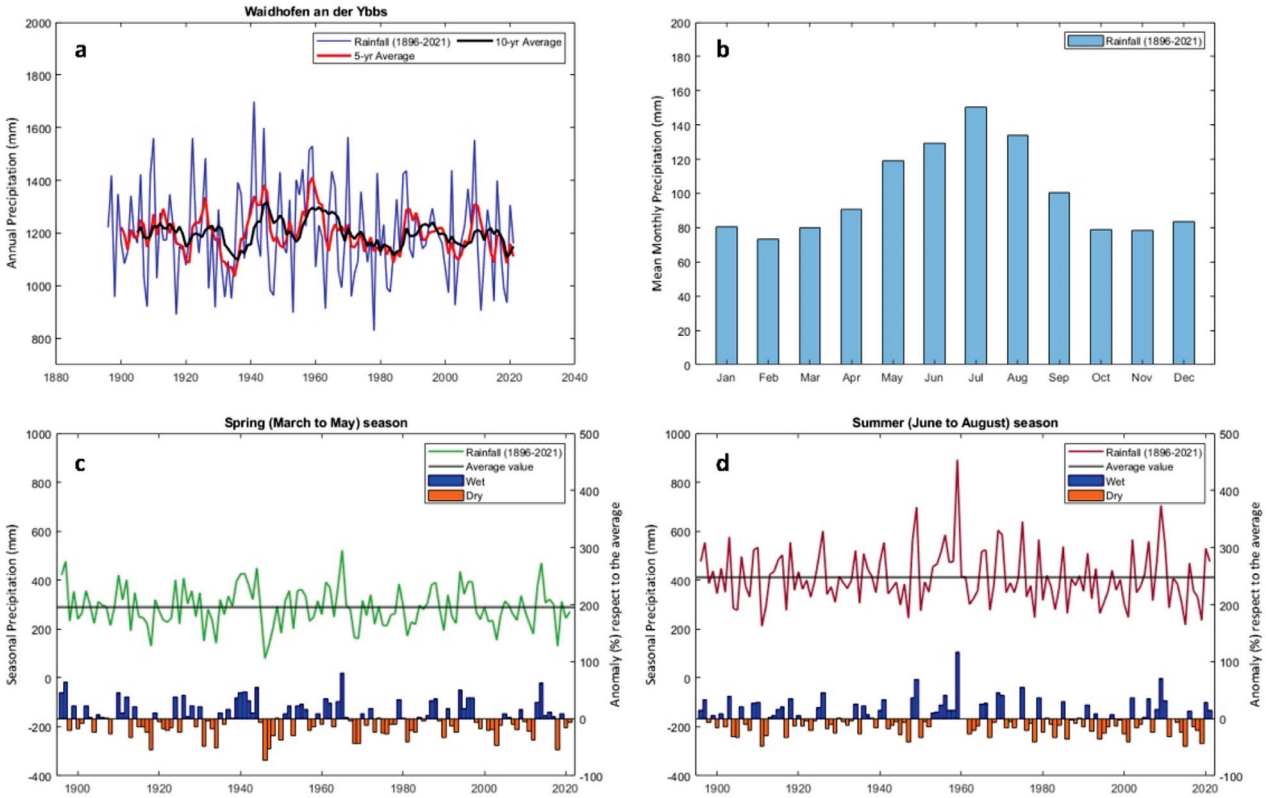



**Figure 2.** Precipitation time series from Waidhofen an der Ybbs meteorological station (period visualized: 1896–2021, data obtained from Histalp project). (**a**) Annual precipitation rate is reported, as well as the 5-years and 10-years average value; (**b**) Monthly mean precipitation amounts; (**c**) Seasonal time series are reported respectively for the spring; (**d**) summer season and rainfall anomalies with respect to the average.

However, since the snow height has not been continuously monitored over time, insights from the contribution of snow melting from the past cannot be proved, but its influence is reported [31,47]. The mean annual precipitation rate is approximately 1197 mm/year (period 1896–2021; data obtained from Histalp project). Although the annual precipitation recorded an alternation across the average value in recent years, the analysis of the rainfall time series exhibits a trend of increased precipitation in the 10-yr average value, especially after 2019 (Figure 2a). Monthly mean precipitation amounts are also reported (Figure 2b), in which summer (June to August, 413 mm) is the dominant precipitation season, and an increasing trend from March to July is evident. Notable changes have not been found in the analysis of the spring season (March to May) time series, where a fluctuation between the dry and wet seasons occurs (Figure 2c). The most interesting and evident changes are shown in the summer season time series (Figure 2d), in which dry periods have become dominant since the late eighties. However, an increasing trend in the precipitation amounts was recorded in the period 2002–2009, showing the highest recorded summer sum of 706 mm in 2009.

### *2.1. Hofermühle Landslide—Konradsheim District*

The Hofermühle monitoring station is a representative landslide located in the northern part of the Redtenbach catchment in the Konradsheim district of Waidhofen an der Ybbs, Lower Austria. The Hofermühle landslide is defined as a complex rotational slow-moving landslide [8] with different spatial and temporal phases of activity [29]. The upper

part of the Hofermühle catchment shows a slow, continuous displacement of mm/cm per year [29]. Furthermore, it was shown that areas which are poorly drained in the slope might be more prone to landslide processes [48]. Historical events have shown that the material from the continuous movement can move towards the torrent, resulting in sporadic fast mudflow processes [29,49].

### *2.2. Gresten Landslide—Scheibbs District*

The Salcher landslide area is located in the central part of the municipality of Gresten, district of Scheibbs, in the western part of Lower Austria. It is an unwooded, east-facing slope with dip angles between 10–20°, which was used as a skiing area until the 1950s [28]. The complex geologic setting of the region is evident in this study site, as the GKZ lies within a band of approximately 2 km between the FZ to the north and the NCA to the south [28]. Historical data and further investigations have confirmed that the slope has been in constant motion for decades [50]. The active landslide area covers 4000 $m^2$, with a potential shear plane of 4 m depth. It corresponds to a slow-moving rotational landslide [8]. The potential accelerations of the landslide pose a constant threat to local communities as residential buildings and roads are located near the active landslide area.

### *2.3. Brandstatt Landslide—Scheibbs District*

The Brandstatt landslide monitoring site is located in the municipality of Gresten, district of Scheibbs in Lower Austria. The study area is a good example of a deep-seated, complex landslide with an area of about 0.2 $km^2$ [51]. It is characterized by a north-facing slope with an inclination of 15–20°, which is mainly used as grassland and pasture. The corresponding subsurface is determined by a complex geological setting where the GKZ is in contact with the inner-Alpine Molasse. Especially in the middle and upper part of the slope, sandstone blocks and deeply weathered soft clay shales are intercalated [51,52]. The lower part is dominated by clastic and carbonate lithologies of the Molasse unit, in which dark grey marls, yellowish sandstones, and grey calcareous sands were found [51]. The slope exhibits wavy deformations patterns, such as bulges and depressions, that are often indications of continuous landslide activity [53].

## 3. Material and Methods

This study of historical landslides was conducted primarily by compiling various types of data from national and regional institutions and scientific journals concerning the three study areas. Regional landslide databases provided by the Geological Survey of Lower Austria were consulted but did not provide sufficient information on the magnitude and intensity of past events in the monitoring areas. Therefore, technical reports from the relevant authorities were also obtained and reviewed. The sources consulted, such as aerial photographs, field reports, and maps, were mainly provided by the Geological Survey of Lower Austria and the Austrian Service of the Torrent and Avalanche Control (WLV). The reviewed databases include the landslide catalog of the Geological Survey of Lower Austria and landslide inventories from previous investigations [45]. Additional information, such as detailed geotechnical and geological information on the study areas, was found in published technical reports [50]. There were some scientific articles describing landslide processes in our study areas, e.g., publications by Petschko et al. [27,45] and Stumvoll et al. [28,29]. Additionally, information on landslides was also compiled from various bachelor and master theses.

These findings were complemented and cross-checked using scientific articles and personal interviews with local residents and staff from local municipalities. All data were extracted, summarized, and integrated into a common landslide database for further analysis. The landslide database was then merged with meteorological data to find significant correlations between landslide dynamics and meteorological conditions. Based on the temporal occurrence of landslides, a temporal probability could be estimated for each study site.

Temporal information was mainly referenced in local technical reports published directly after a landslide occurrence. Spatial information was obtained from extensive field campaigns, historical maps, and aerial photographs of past landslide events. The resulting landslide inventory provided substantial information on past landslides. That information was the necessary input for the subsequent set-up of the respective landslide monitoring programs. The reports primarily included the location, date, and magnitude of the event after it occurred, potential triggering mechanisms, landslide maps, as well as partial information on damage assessment and immediate and long-term actions needed to mitigate the effects of future events. The database also contained information on landslide-prone areas in the three study areas and confirmed the need to establish a long-term monitoring project with continuous application of different methods and installation of sensors in order to extend the sparse single data to detailed knowledge of landslide dynamics in spatio-temporal dimensions.

## 4. Analysis of Historical Landslide Data

### *4.1. Hofermühle Landslide*

The first documented landslide activity in the Hofermühle catchment dates from 2 July 1975 (Figure 3) [47]. This was a large-scale landslide on the orographic right side of the stream [54]. As a consequence, the area was drained after this event. It is unclear to which extent this measure contributed to slope stability, but until 2011 there were no further reported events. According to the report of the WLV, there was major landslide activation in 2011, triggered in the area of the upper orographic left side of the stream [49]. The landslide had a displacement of 2 m in 2 weeks. The last report of landslide activity was recorded on 21 April 2013 [55]. After heavy precipitation on the previous days, the material mobilized in 2011 was saturated in the lower part of the landslide (Figure 4a–c), triggering an mudflow with a velocity of 20 m/h [49], down to the torrent path (Figure 4d,e). Considering the potential risk for the properties located on the alluvial cone, the WLV removed the run-off inhibiting trees in the drainage cross-section, cleared the debris masses, and built a dam at the outlet of the torrent to mitigate potential future events [55,56]. According to the WLV report in 2016, the formation of cracks, inclination of trees, and depressions are indications that the landslide process is still active [54]. Within the last 47 years, the occurrence of three major landslides were detected at the Hofermühle site, whereas their spatial distribution was confined to a particular area of the slope.

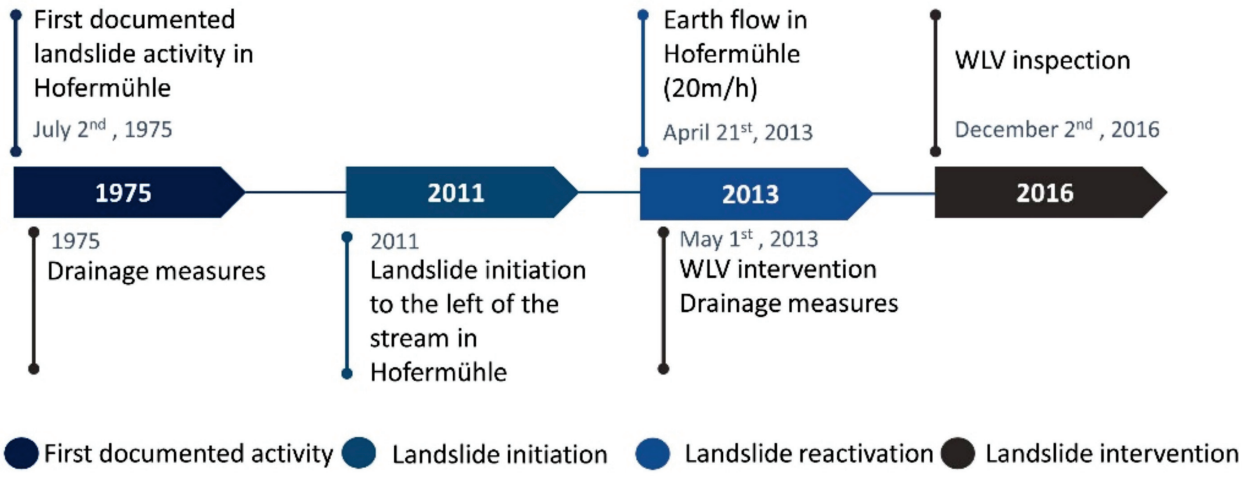



**Figure 3.** Historical information of the landslide activity at the Hofermühle site.

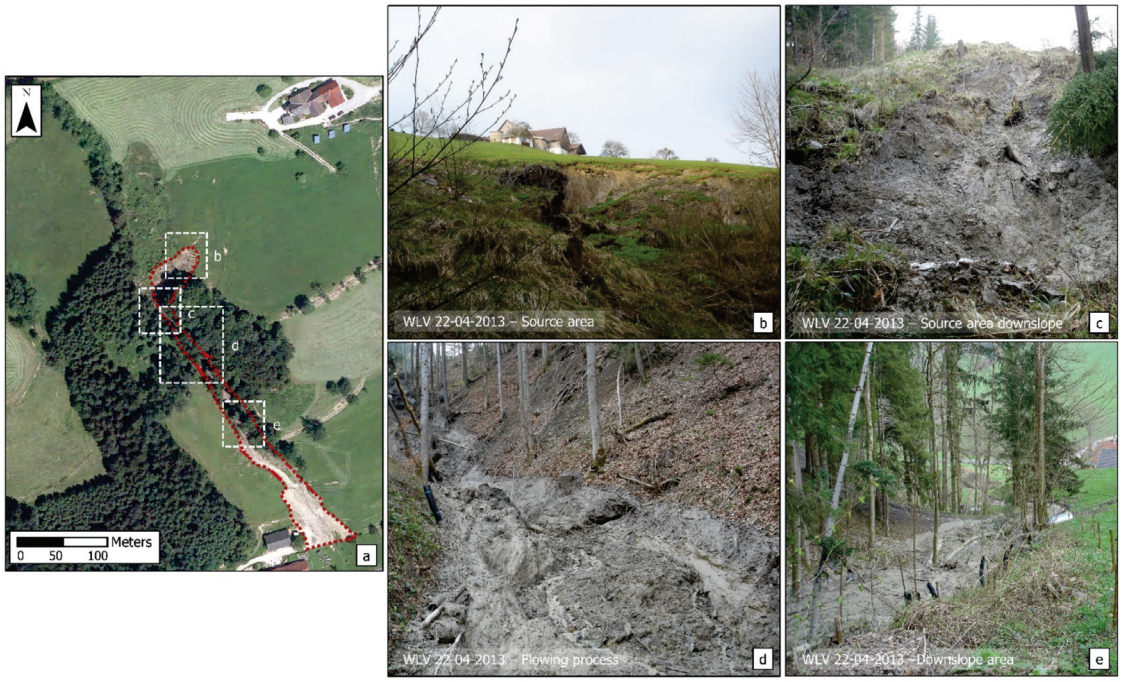



**Figure 4.** Hofermühle earth flow event occurred in 2013. (**a**) Area involved in the runout path of the mobilized material; (**b**,**c**) Sliding processes in the source area; (**d**,**e**) Flowing processes along the Hofermühle torrent path. The orthophoto used in (**a**) is provided by the Federal State Government of Lower Austria [57] whereas the photographs of the 2013 event are provided by the Torrent and Avalanche Control authority (WLV) [49].

### *4.2. Gresten Landslide*

The first signs of horizontal surface movement were observed in the 1950s, as the ski lift pillars in a small skiing slope were tilted [28]. The first recorded landslide activity on the Salcher slope in Gresten dates to 3 July 1975 as a result of a heavy precipitation event (Figure 5) [47]. In that year, a landslide on the eastern slope of the Pichelkegel in the lift area caused the lower support of the lift to tilt downhill, making the road impassable [58]. Consequently, drainage measures were implemented in the fall of 1975 [58]. A few years later, on 31 May 1978, the reactivation of slope movement occurred. The accumulated daily precipitation of 101.9 mm triggered displacement in some parts of the landslide [53,59]. The landslide depression had a width of 10 m along the path and extended upslope to 8 m. At that time, the authorities took measures and recommended that the slope be secured with a layer of stone at the base of the embankment [59]. Subsequently, the depression was filled with bulk material [59].




**Figure 5.** Historical information on the activity of the Salcher landslide in Gresten.

Despite the initiated measures, repeated movements occurred on the slope in August 2006, damaging local infrastructure [60]. These movements were possibly related to the 162.5 mm of precipitation during 1–7 August [28]. In September 2007, a small debris flow occurred to the northeast of the slope [50]. These events highlighted the need for professional monitoring of the Salcher landslide. Therefore, a geotechnical investigation was conducted by the Geological Survey of Austria and the University of Natural Resources and Life Sciences in Vienna, Austria, from 16 April 2007 to 6 June 2008, which included drilling, trenching, and laboratory analysis of the landslide [50].

In June 2009, a 20 cm acceleration of the landslide occurred. This phenomenon was mainly due to the exceptional rainfall that triggered large landslides throughout Lower Austria [60], as was also observed in the meteorological data in Section 2. In view of these past events, the authorities of Lower Austria conducted a monitoring project between 26 April 2007 and 11 November 2012 to perform a geotechnical characterization of the landslide area [60]. Compiling the historical landslide activity and considering landslide initiation and reactivation events, five major events within 47 years have been reported.

### *4.3. Brandstatt Landslide*

The first landslide activity in Brandstatt was documented in the mid-1960s (Figure 6) [52]. According to a report of the Lower Austrian Provincial Government in 1970, a large landslide occurred a few years earlier above the Groß-Schacher property, disrupting the main road over a length of 100 m [52]. After the event, deep drainage ribs were installed, and a double row of wooden piles was laid on the valley side of the road. In 1982 and 1983, a drainage system was installed in the slope due to the constant ground movements that threatened the main road [61]. On 15 May 1985, a reactivation of the landslide occurred. Ground movements were initiated about 12 m above the main road and extended about 50 m across the meadow area adjacent to the valley [61]. After this event, some remedial measures were proposed by the authorities, such as drainage measures, filling the storm drains with permeable material and diverting the collected water [61]. In March 2001, a lawn bulge of 0.5 × 30 m formed. The displacement continued over the next few months and swept the pasture fence standing on top of it. The event was related to the heavy precipitation of the winter of 2000/2001, where precipitation in the alpine foothills reached up to 175% of the long-term value [53]. As a result, further mitigation measures were recommended, such as the installation of deep drains and soundings to determine the optimal drain depth [53]. From 12 April 2007 to 18 May 2009, a geophysical and geotechnical monitoring project was conducted by the Geological Survey of Austria to characterize the landslide area [62]. The results and the corresponding landslide map were published in July 2012 [51]. The historical data of the last 62 years document four major events. Despite the undertaken measures, the landslide is further moving at different speeds in different areas, which leads to continuous road damage that is subsequently repaired by the municipality. Due to this, regular mowing is not possible anymore in part of the area and it is therefore utilized as a grazing area for cattle.

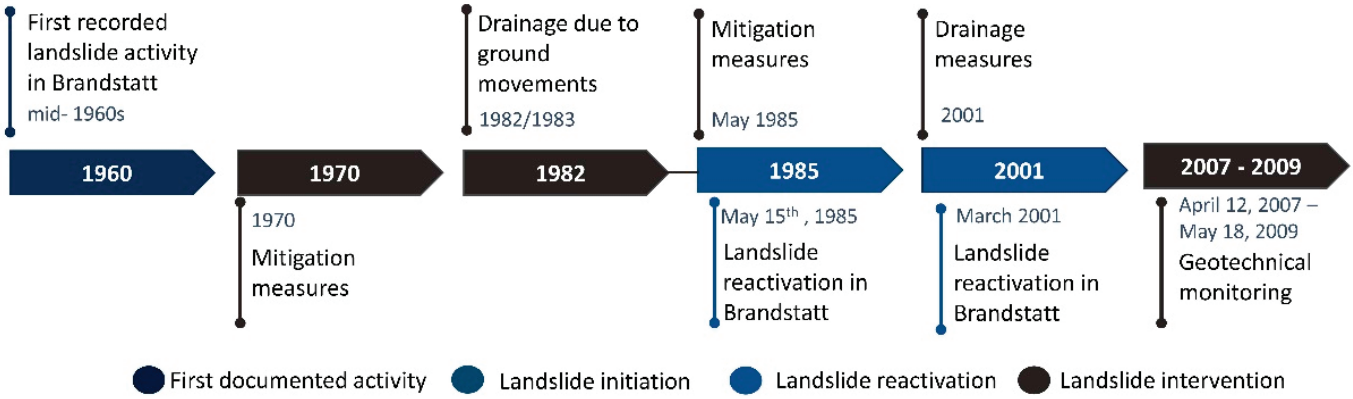



**Figure 6.** Historical information on the landslide activity in Brandstatt site.

## 5. Establishment of Landslide Observatories (2014–Today)

Due to the reported historical data and the continuous socio-economic impacts, the three sites in Lower Austria were selected for the implementation of long-term monitoring systems. The installations within the landslide monitoring sites were initiated in 2014 by the Geomorphological Systems and Risk Research (ENGAGE) working group of the Department of Geography and Regional Research at the University of Vienna; project information at www.noeslide.at (accessed on 30 January 2023). In the initiation phase, this work was accompanied by the Geological Survey of Lower Austria. The selection of the specific locations for the different instruments is based on the analyzed landslide historical data and field observations. The gathered information varies in spatio-temporal resolution, from point measurements with 5-min intervals, e.g., automatic inclinometers, to areal data obtained on a monthly basis, e.g., terrestrial laser scanning or UAV flights. There are a large variety of surface and subsurface methodological approaches at the different landslide observatories. Beside basic installations that are present at every site (e.g., meteorological station), site-specific techniques have been implemented in the respective locations.

### *5.1. Common Monitoring Devices*

In order to achieve comparable data, all landslide observatories are equipped with Campbell Scientific meteorological stations. The stations were installed within the landslide areas in order to obtain continuous, reliable, and site-specific data. These are based on CR1000 or CR1000X data logger and sensors for temperature and humidity (HC2S3), air pressure (CS106), heated precipitation sensors (Young 52202), pyranometers (CMP3 or MS-60), Windsonic4 ultrasonic anemometers, TDR probes (CS605), and piezometers (Geokon 4500AL) (see Tables 1–3). The meteorological stations are connected to permanent power lines. The connection with the data server is either via NL-240 module into an existing WiFi network or directly via LAN cable to provide a permanent internet connection. The external server based at the University of Vienna requests the data every 5 min, controls autonomously if the data are within the defined parameters, and sends warnings by mail in case of any deviation.

**Table 1.** Compilation of the different methods applied and data obtained from Hofermühle. The methods are distinguished between surface (A) and subsurface (B) monitoring approaches. The installations of the meteorological station are added in italics. The obtained data are structured in the same way with additional information on the measurement intervals as footnotes.

| **Methods** | | **Data** | |
|---|---|---|---|
| Surface monitoring (A) | Subsurface monitoring (B) | Data (A) | Data (B) |
| multi-temporal TLS measurements | 4 manual inclinometer (Glötzl NMGD) | high resolution 3D-point cloud [1] | measured values A/B [cm], deformation A/B [cm], borehole profile A/B [cm] [2] |
| multi-temporal UAV measurements | automatic inclinometer (Measurand SAAF) | high resolution DEM [3] | deformation [mm] [4] |
| GPS measurements, measuring stones (finished) | | GPS time series | |
| *Meteorological Station:* | | | |
| *-temperature and humidity (HC2S3)* | 9 TDR probes (CS605) | temp [°C], rel. humidity [%] [4] | permittivity [unitless], electr. conductivity [dS/m], temp. [°C] [4] |
| *-air pressure (CS106)* | 8 piezometers (Geokon 4500AL) | baro. pressure [mbar] [4] | avg. groundwater level [m], avg. temp. [°C] [4] |
| *-heated precipitation sensor (Young 52202)* | | total precip. [mm] [4] | |
| *-precipitation sensor (SBS500)* | | total precip. [mm] [4] | |
| *-pyranometer (CMP3)* | | solar radiance [kW and J, avg] [4] | |

**Table 1.** *Cont.*

| Methods | Data |
|---|---|
| *-Windsonic4 ultrasonic anemometer* | direction [deg.], wind speed [ms, avg] [4] |
| *-mechanical anemometer (034B Met One)* | direction [deg.], wind speed [ms, avg] [4] |
| *-distrometer (OTT Parsivel)* | prec. intensity [mm/h], SYNOP Code, particle quantity, radar reflectivity [dBz] [4] |
| *-heated snow depth sensor (SR50AH)* | distance to ground [m] [4] |

[1] 3–6 months measurement interval; [2] monthly interval; [3] 6 months measurement interval; [4] 5 min measurement interval.

**Table 2.** Compilation of the different methods applied and data obtained from Gresten. The methods are distinguished between surface (A) and subsurface (B) monitoring approaches. The installations of the meteorological station are added in italics. The obtained data are structured in the same way with additional information on the measurement interval as footnotes.

| Methods | | Data | |
|---|---|---|---|
| Surface monitoring (A) | Subsurface monitoring (B) | Data (A) | Data (B) |
| multi-temporal TLS measurements | 3 manual inclinometer (Glötzl NMGD) | high resolution 3D-point cloud [1] | measured values A/B [cm], deformation A/B [cm], borehole profile A/B [cm] [2] |
| multi-temporal UAV measurements (finished) | automatic inclinometer (Glötzl SNMGD) | high resolution DEM [3] | deformation [cm], temp. [°C] [4] |
| GPS and TS measurements, with geodetic plies (finished) | automatic ERT (operated by the GBA) | GPS time series [3] | model of the specific electrical resistance [5] |
| wireless sensor network (finished) | | dislocation measurements [6] | |
| *Meteorological Station:* | | | |
| *-temperature and humidity (HC2S3)* | 3 TDR probes (CS605) | temp [°C], rel. humidity [%] [7] | permittivity [unitless], electr. conductivity [dS/m], temp. [°C] [7] |
| *-air pressure (CS106)* | 5 piezometers (Geokon 4500AL) | baro. pressure [mbar] [7] | avg. groundwater level [m], avg. temp. [°C] [7] |
| *-heated precipitation sensor (Young 52202)* | | total precip. [mm] [7] | |
| *-precipitation sensor (SBS500)* | | total precip. [mm] [7] | |
| *-pyranometer (MS-60)* | | solar radiance [kW and J, avg] [7] | |
| *-Windsonic4 ultrasonic anemometer* | | direction [deg.], wind speed [ms, avg] [7] | |
| *-mechanical anemometer (034B Met One)* | | direction [deg.], wind speed [ms, avg] [7] | |
| *-distrometer (OTT Parsivel)* | | prec. intensity [mm/h], SYNOP Code, particle quantity, radar reflectivity [dBz] [7] | |

[1] daily measurement interval; [2] monthly measurement interval; [3] 3 months measurement interval; [4] 10 min interval; [5] 3 h interval; [6] hourly interval; [7] 5 min measurement interval.

**Table 3.** Compilation of the different methods applied and data obtained from Brandstatt. The methods are distinguished between surface (A) and subsurface (B) monitoring approaches. The installations of the meteorological station are added in italics. The obtained data are structured in the same way with additional information on the measurement interval as footnotes.

| **Methods** | | **Data** | |
|---|---|---|---|
| Surface monitoring (A) | Subsurface monitoring (B) | Data (A) | Data (B) |
| multi-temporal TLS measurements | 5 manual inclinometer (Glötzl NMGD) | high resolution 3D-point cloud [1] | measured values A/B [cm], deformation A/B [cm], borehole profile A/B [cm] [2] |
| multi-temporal UAV measurements | | high resolution DEM [1] | |
| *Meteorological Station:* | | | |
| *-temperature and humidity (HC2S3)* | 9 TDR probes (CS605) | temp [°C], rel. humidity [%] [3] | permittivity [unitless], electr. conductivity [dS/m], temp. [°C] [3] |
| *-air pressure (CS106)* | 3 piezometers (Geokon 4500AL) | baro. pressure [mbar] [3] | avg. groundwater level [m], avg. temp. [°C] [3] |
| *-heated precipitation sensor (Young 52202)* | | total precip. [mm] [3] | |
| *-pyranometer (MS-60)* | | solar radiance [kW and J, avg] [3] | |
| *-Windsonic4 ultrasonic anemometer* | | direction [deg.], wind speed [ms, avg] [3] | |
| *-heated snow depth sensor (SR50AH)* | | distance to ground [m] [3] | |

[1] annual measurement interval; [2] monthly measurement interval; [3] 5 min measurement interval.

Besides surface monitoring, different subsurface monitoring installations are in use. One key technique in landslide research to obtain subsurface dynamics are inclinometers [63–65]. Manual inclinometers are installed at all monitoring sites, which are measured monthly with a vertical inclinometer (Glötzl NMGD type) [28,29,66,67]. It has to be noted that the installation of inclinometers in areas with a movement of more than a few centimeters can lead to a dysfunction of the instrument due to either the breaking of the plastic case or the inability of the measuring probe to fully enter the pipe. Historical data and field observations were considered to identify suitable locations within the landslide body.

### *5.2. Site-Specific Monitoring Devices*

The basic equipped meteorological stations are complemented at the Gresten and Hofermühle landslide observatories by mechanical anemometers (034B Met One), distrometers (OTT Parsivel2), and SBS500 precipitation sensors to measure raindrop size distribution and velocity. These precipitation parameters are considered to be important triggering factors. Hofermühle and Brandstatt are additionally equipped with heated snow depth sensors (SR50AH).

In addition to the subsurface installations being present on every site, there are devices that are specifically installed in order to meet site-specific landslide dynamics. At Hofermühle, an automatic inclinometer (Measurand ShapeArray F type) [29,68] is also operated via a data logger. The data is recorded at five-minute intervals. In Gresten, the automatic inclinometer (Glötzl SNMGD) [69] measures displacements in 10-min intervals. Additionally, the Geosphere Austria (formerly Geological Survey of Austria) operates a fully automatic electrical resistivity tomography monitoring profile that measures every 3 h [69–72].

Time series of terrestrial laser scans open up the possibility of creating high-resolution, multi-temporal digital elevation models (DEMs), which are used to generate runoff models and display surface changes [29,56,73]. Consequently, UAV surveys (DJI Mavic 2 Pro) and TLS measurements (Riegl VZ-6000) are carried out regularly at Brandstatt and Hofermühle. In Gresten, a permanent terrestrial laser scanner (Optech ILRIS-3D) [28,74] has been in operation since 2015. The scans are scheduled daily at noon.

#### 5.2.1. Site-Specific Monitoring—Hofermühle

Dynamic probing of heavy (DPH) subsurface characteristics by the resistance of the different soil layers and the maximum penetration depth can be identified [29]. In order to expand the knowledge about subsurface characteristics, e.g., the detection of potential shearing planes, dynamic probing heavy [75] was performed at 32 locations on 24 August 2017; 17–21 September 2018; 17–19 October 2018; 26–29 March 2019; and 12 March 2020 [29]; using a pneumatic SRS-15 (German type) penetrometer [29]. To complement the information of DPH with sediment samples, nine sediment cores were retrieved via percussion drilling using a GeoTOOL GTR 780V drilling rig on 17–21 September and 17–19 October 2018 [29] and were transported to the laboratory for further analysis.

With the aim of recording purely superficial movement patterns by means of point measurements, around 60 reference points in the form of marked boulder stones were created at the Hofermühle and deposited at the surface. These have been measured about once a month from 2014 to 2019 using manual GPS measurements (Table 1).

#### 5.2.2. Site-Specific Monitoring—Gresten

Approximately 10 DPH surveys took place in Gresten using the same technique as described in Section 5.2.1. In addition, 10 sediment cores were extracted using the GeoTOOL GTR 780V for further analysis [28].

GNSS and total station surveys of geodetic piles were performed by the former Geological Survey of Austria [28,60]. From 2015 to 2019, a wireless network of acceleration sensors was operated on the landslide to register the smallest changes on the surface (Table 2).

#### 5.2.3. Site-Specific Monitoring—Brandstatt

The development of the Brandstatt observatory with permanent installations, such as inclinometers and piezometers, started in the spring of 2022 (Figure 7). Here, the first DPH measurements were carried out. In total, 29 DPH measurements [75] were performed in Brandstatt in 2022 using the same devices as mentioned in Section 5.2.1. The maximum penetration depth was reached at 16.2 m. The GeoTOOL GTR 1100 MF was used for percussion drilling to extract seven sediment cores in the summer of 2022, which are currently being analyzed.

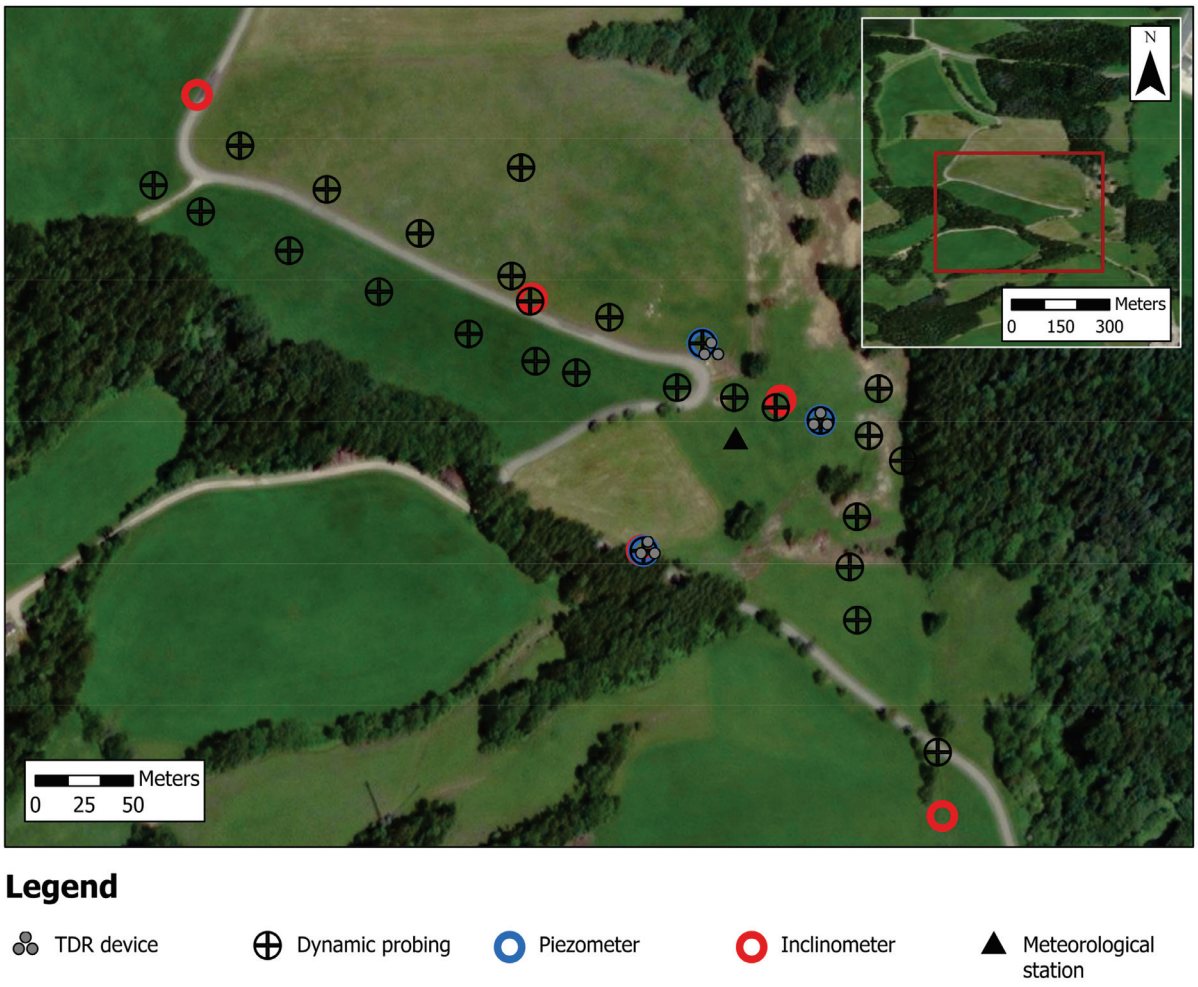



**Figure 7.** Location of DPH (dynamic probing heavy) tests and different monitoring devices, such as piezometers, inclinometers, TDR devices, and the meteorological station at the Brandstatt landslide observatory. Satellite image of the study area provided in the ArcGIS Pro 3.0.0 software using World Imagery (Source: Esri, Maxar, Earthstar Geographics, and the GIS User Community).

## 6. Discussion

Compiling landslide inventories with historical data has several limitations and uncertainties. The collection of all past events is hardly feasible and lacks comprehensiveness. Very often, landslide records are based on events that caused damage to society. Thus, all historical databases contain the minimum landslide information only. This is true for high-frequency/low-magnitude events which were not recorded or did not occur in parts of the study area where it was not noted by the population [14,22]. The longer the event lies in the past, the less probable data about the event can be collected [22]. Notifying landslide events is subjective and can lead to difficulties in accuracy and process identification, also depending on the person's experience. Nevertheless, it can be expected that major events were recorded. The selection of study areas is challenging as researchers are reliant on the support of the landowners. Consequently, potentially interesting areas could not be accessible or only to a limited extent. However, despite these limitations, the collection of historical data was valuable and represents the basis for modern landslide monitoring systems in Lower Austria.

### *6.1. The (Historical) Role of Human Impact and Land Use Planning*

Since historical data extend our knowledge in a given area, this information has proven to be a useful tool for decision-making in landslide hazard contexts and, consequently,

for land use planning [14,76]. One of the most important elements for understanding the potential future damage is tracking, recording, and analyzing past landslides and assessing in the greatest detail the consequences to nature and society [77]. Therefore, landslide inventories are fundamental inputs for frequency reconstructions and comprehensive landslide risk assessments [78]. Historical damage events to private property and infrastructure associated with periodic landslide occurrences have implications for land use planning [79]. Considering that restrictive measures, such as construction bans, could result in significant indirect losses to the detriment of property owners. Urban planners must evaluate the potential loss of life and damage in order to implement more proactive landslide mitigation measures and effective disaster risk reduction measures [79]. In the case of the study sites, most of the land was private, and human losses have not been documented so far. Therefore, there were no significant landslide mitigation measures that could potentially impact property owners. However, it is important to note that land use has changed in the study areas, e.g., with the cessation of ski operations in Gresten and exclusive use as grassland in Brandstatt.

The analysis of historical information has shown that landslides are inevitably linked to anthropogenic activities. Landslide narratives include not only their occurrence but also the previous and subsequent human interventions. In the case of Lower Austria, several measures to mitigate these effects and future occurrences have been implemented. Successive drainage systems were put in place by local property owners, as well as local authorities, to counteract triggering factors that could contribute to the acceleration of landslides. However, it is also a matter of concern that these interventions, as well as land use changes, can also potentially contribute to landslide occurrence [35]. Furthermore, the expected changing precipitation patterns due to global climate change, as well as the frequency and magnitude, complicate future sustainable adaptation and mitigation measures [6].

Landslide occurrence in the study sites was first documented in the mid-1960s to 1970s and must be linked to land use changes that alter hydrological systems. Human interventions exacerbate hazards, add pressure to the systems, and create risk as infrastructure is threatened by these events. In all three study sites, houses, roads, and grassland are at risk of landslide activity. Human activity is often a root cause of landslides, not only by predisposing or triggering them [79] but also as a result of inadequate mitigation. Moreover, inadequate mitigation and adaptation measures can themselves have a negative influence on slope stability and cause landslides.

### *6.2. The Importance of Historical Data in Landslide Monitoring*

It is generally accepted that landslide monitoring should be relevant, feasible, and useful [80]. Historical data should also be incorporated into the planning and design of the monitoring process, as it is an essential source of information on past landslide activity. The integration of historical and real-time data offers a unique opportunity to develop more comprehensive landslide hazard models and mitigation measures. Historical records in the study areas provided information on the type, geometry, frequency, magnitude, and intensity of past landslide events. Considering the above, the historical data were undoubted inputs in the development of the monitoring planning to better understand slow-moving landslide dynamics in Lower Austria.

The monitoring data of the last years confirmed the non-uniform temporal and kinematic landslide behavior [28,29,73]. There are different periods of activity and differential re-activations on the slopes. The historical data improved the understanding of predisposing factors (lithology, tectonics) and triggering factors (heavy rainfall, snow melting). With the help of these data, it was possible to correlate landslide activity to meteorological factors, such as specific precipitation events at the Hofermühle and in Gresten. Since the installation of the monitoring site in Brandstatt has just begun, respective information cannot be obtained yet. Indeed, the analysis of past events plays an important role in

estimating risk, which is a combination of the hazard and the vulnerability of the exposed elements at risk.

Past landslide reports have repeatedly demonstrated that a continuous monitoring process is imperative to better understand landslide dynamics (e.g., [14,22]). Slow-moving landslides, in comparison to rapid landslides, present a unique opportunity for natural disaster prevention by setting in place suitable monitoring systems and modeling the mechanics of their movement [39]. Furthermore, landslides with relatively low moving rates offer the possibility to study the involved processes in depth over a longer period with different phases of activity. This helps to correlate movements to specific potential triggering factors, such as precipitation events and to improve the understanding of the influence of global climate change. Few studies have examined the dependence of landslide failure mechanisms on environmental conditions over time [39,81].

With both the importance of long-term monitoring approaches and the integration of historical information compiled by various stakeholders in Lower Austria recognized, decisions on measuring devices and locations for the monitoring project presented in this work were undertaken. The Hofermühle provides an example of how the integration of available historical landslide data with a long-term, multi-parameter monitoring approach is necessary to assess and mitigate the potential landslide scenario (Figure 8a–c). Historical data have provided information regarding past landslide events in the Hofermühle catchment in order to characterize past hazards. The mudflow that occurred in 2013 at Hofermühle especially revealed that the slow-moving landslide could be partially mobilized and evolve into a fast-flow process towards the main torrent path (Figure 8b). In particular, the estimation of the deposit heights and the run-out distance have been employed to evaluate the landslide risk and design mitigation strategies in the lower part of the slope. Decisions on locations for real-time monitoring have been established in agreement with local authorities for the perspective of disaster risk reduction and adaptation. In this sense, the slope-distributed network has been installed to assess ground displacements (surface and subsurface) and hydrologic parameters in the more active sectors of the unstable slope (Figure 8c) to evaluate potential landslide hazard scenarios and impacts.

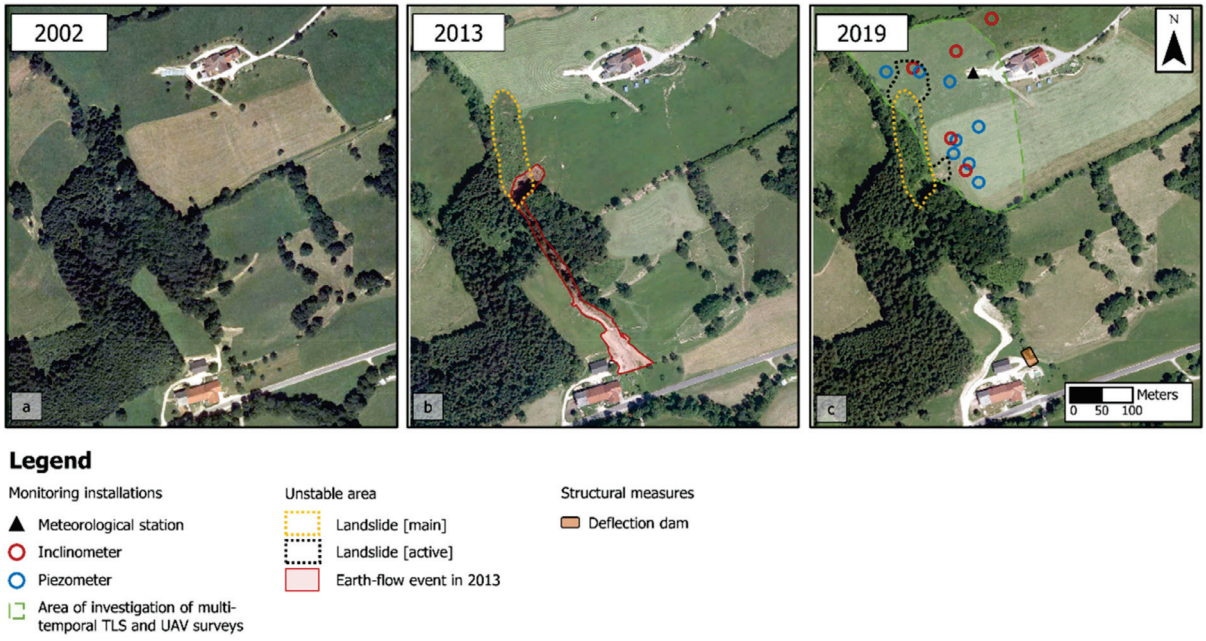



**Figure 8.** Digital orthophoto from (**a**) 2002, (**b**) 2013, and (**c**) 2019 of the Hofermühle landslide. The area affected during the earth-flow event in 2013 is also represented in (**b**). Main areas of investigation are indicated in (**c**), as well as simplified morphological features of the landslide activity. Monitoring installations and structural measures to mitigate a possible landslide are visible in (**c**). Orthophotos are provided by the Federal State Government of Lower Austria [57,82,83].

*6.3. Approaches of Linking Historical Data to Landslide Monitoring*

There are several case studies in the literature that demonstrate the importance of historical data in the decision-making process of implementing long-term monitoring systems to better assess landslide hazards. The Johnson Creek landslide, near Newport, Oregon, was investigated by the United States Geological Survey (USGS) and had a long history of landslides during rainy seasons that continually affected the main highway [23]. A large landslide occurred between January 2002 and February 2003. Therefore, in 2004, the USGS used historical information on landslide processes to install a near-real-time monitoring system at this site. The goal of the near-real-time monitoring system was to better understand the relationship between rainfall and pore pressures that control landslide movement [23]. The monitoring system consisted of a rain gauge, vibrating wire piezometers along a longitudinal section of the slide, inclinometers above the slide plane, and extensometers. In November 2006, the contribution of vertical rainfall infiltration to pore water pressures was evaluated by installing additional sensors within the slide body. Two vertical arrays of six vibrating wire piezometers and dielectric soil moisture content sensors were installed in the central and upper parts of the landslide. Monitoring revealed that pore water pressure increased after rain events and that the landslide moved when pore water pressure exceeded a threshold value [23].

Another case successfully involving historical information are landslides in the London Clay coastal cliffs at Warden Point, Isle of Sheppey, Kent. This area has been continuously monitored since 1971 [84,85]. Historical data were an important contribution to understanding landslide and erosion dynamics in this region. Erosion history information has been obtained from editions of the major Ordnance Survey maps of 1876, 1896, 1931, and 1964. In addition, the first detailed descriptions of landslides in these areas were produced by Hutchinson et al. [86]. According to Dixon and Bromhead [84], new landslides occurred repeatedly in the same sections of the cliff, and therefore 56 piezometers were installed near these past landslides. These monitoring efforts led to the calculation of pore water pressures associated with the eroded landslide mass and the conclusion that first-time landslides occur on slopes that have been steepened due to marine erosion [84].

The studies from Dixon and Bromhead [84] were followed by coastal landslide monitoring in the cliff region of Aldbrough, East Riding of Yorkshire, UK [85]. Since September 2001, the monitoring of deep-seated, rotational landslides has been conducted using Terrestrial LiDAR surveys and UAV photogrammetry. Thirty-eight surveys were carried out until 2017, and twenty-seven surveys were used to calculate volume erosion. In addition to surface monitoring, drilling and laboratory geotechnical investigations were performed. The monitoring based on past landslide events indicated that major landslides occurred every six to seven years. In addition, the integration of the TLS data and the borehole analysis was useful for understanding the role of landslides and their pre-conditioning factors. Moreover, according to the authors, this obtained dataset of past landslides constituted a useful tool for calibrating coastal process modeling.

Another example of the integration of historical data and landslide monitoring is the Cirque des Graves landslides in Normandy [87]. This is a slow-moving and deep-seated coastal landslide that is regularly affected by accelerations with displacements of several meters. Historical information on past landslide activity and the economic and physical conditions has been the rationale for landslide monitoring since 1985 [87]. The authors concluded that a combination of historical data and slope instrumentation was needed to improve knowledge of slope dynamics. Therefore, the monitoring system was installed in strategic locations, and it is based on permanent GNSS receivers and hydro-meteorological observation points. This analysis showed existing linkages between groundwater levels and landslide kinematics to define critical piezometric thresholds that trigger landsliding [87].

## 7. Conclusions

Landslides are natural processes that affect and can influence societal systems in manifold ways. Understanding the evolution of complex landslides is difficult since

their kinematics can depend on the combination of different predisposing and triggering mechanisms. Together with challenges arising from Global Change, including climate change, future landslide dynamics become increasingly complex. Therefore, this demands an even deeper understanding of the processes. In this context, historical data represent an essential element when performing frequency-magnitude analysis for evaluating the potential hazards and risks represented by landslides.

In this study, historical data on landslide events in three areas of Lower Austria were compiled, which represented the basis for the implementation of long-term monitoring systems. The importance of available historical data has been analyzed in order to estimate the landslide frequency and magnitude relationships of the selected slow-moving landslides in the Flysch Zone, a complex and highly susceptible area to sliding processes in Lower Austria. Despite the fact that the study sites are located under similar conditions (geology, tectonics, climate, and land use), the analysis of the historical information has shown that there are considerable differences among the landslide observatories in terms of landslide hazard characteristics. Based on historical data, planning decisions were made to protect infrastructure by building protective structures.

Furthermore, these can extend the chronological window on past events and displacement accelerations in the interest of improving the understanding of landslide processes and their natural and socio-economic impacts. The combination of both surface and subsurface monitoring methods allows for different spatial scales, from point information (e.g., inclinometers) to areal information (e.g., terrestrial laser scans). In this perspective, the attempt to combine historical data and long-term, continuous monitoring systems in the presented landslide observatories allows for an investigation of the spatio-temporal evolution of slow-moving landslides. Based on a variety of historical sources, it was possible to install the instruments constituting the long-term landslide monitoring observatories in a meaningful manner.

In many cases, historical information is an important tool for land use planning and disaster risk mitigation management that should be integrated into methodological approaches. This is stressed by the results of this study, which further shows the importance of historical data in establishing long-term monitoring systems. The non-linear behavior of slow-moving landslides and understanding the predisposing and triggering mechanisms controlling the slope stability remain a challenge, but it could be shown that historical data can contribute to reducing landslide hazards and the potential impacts on the local inhabitants.

## 8. Perspectives

Considering the points raised in this study, there are some challenges, issues, and future plans for the application of historical data in landslide research and landslide observatories. Historical data can support the unraveling of the complex interrelation between human activities and landslide dynamics. However, even if we have historical data, it is challenging to understand and predict the impacts of global climate change due to the non-linear processes involved, such as the change in precipitation patterns, which can change the spatio-temporal frequency and magnitude of hazards in the future. Therefore, it is necessary to carry out a quantitative analysis of landslide hazards through the simulation of future scenarios.

Common early warning models have a high rate of false and missed alarms [80]. Therefore, the monitoring process is a crucial step for implementing an appropriate early warning system [80]. Long-term and multi-parameter landslide monitoring provides a large amount of data that not only proportionate spatio-temporal information about past landslide activity but also facilitates the calculation of empirical thresholds that can be used to predict future landslides [78]. Therefore, early warning models that are based on key hydro-mechanical parameters of deformation and precipitation improve the accuracy and practicality of landslide early warning [80]. In this regard, historical data on landslides are of great importance to estimate the potential future consequences.

The development of a common international procedure for landslide documentation can help to standardize the data for the historical data of the future, which are obtained today. This could help to further stimulate research connected to historical data and improve our understanding of landslides and mitigate their impacts. There are examples, such as initiatives to continuously compile past events within an online portal of the Federal Ministry of Agriculture, Forestry, Regions, and Water Management of the Republic of Austria (www.naturgefahren.at) or the DOMODIS project. Further, the application of innovative methods, such as Artificial Intelligence approaches, could help develop systems to determine thresholds for triggering mechanisms for early warning purposes.

**Author Contributions:** Conceptualization, P.M., Y.A.J.D. and E.C.; methodology, P.M., R.K. and Y.A.J.D.; formal analysis, E.C. and Y.A.J.D.; investigation, P.M., Y.A.J.D. and E.C.; resources, P.M., Y.A.J.D. and E.C.; data curation, E.C. and Y.A.J.D.; writing—original draft preparation, P.M., Y.A.J.D. and E.C.; writing—review and editing, P.M., Y.A.J.D., E.C. and T.G.; visualization, Y.A.J.D. and E.C.; supervision, P.M.; project administration, P.M. and T.G. All authors have read and agreed to the published version of the manuscript.

**Funding:** This research received no external funding. Open Access Funding by the University of Vienna.

**Data Availability Statement:** The data presented in this study are available on request from the corresponding author. The analyzed precipitation series are publicly available in the archived dataset from the Histalp project www.zamg.ac.at/histalp (accessed on 30 January 2023).

**Acknowledgments:** We are thankful for the support from ENGAGE—Geomorphological Systems and Risk Research working group at the Department of Geography and Regional Research at the University of Vienna. A special thanks to Lilly Bucher and Daniele Spedaliere. The University of Vienna provided regular funding and allowed us to build and maintain the monitoring sites. Furthermore, we want to thank the Regional Geological Survey of the Regional Council of Lower Austria for their continuous support, namely Michael Bertagnoli and Joachim Schweigl. Additionally, the regional office of Lower Austria West of the Avalanche and Torrential Control unit of the Federal Ministry of Austria for Agriculture, Forestry, Regions, and Water Management based in Melk provided important support, namely Eduard Kotzmaier. The Geosphere Austria, formerly known as the National Geological Survey of Austria (GBA), provided very useful information. The different municipalities in Gresten, Scheibbs and Waidhofen an der Ybbs welcomed us always warmly and accompanied our research continuously. Finally, without the agreement and the openness of the local landowners, the installation of the monitoring sites would never have been possible. Thanks for your interest and willingness to improve scientific knowledge. We thank the open access funding by the University of Vienna.

**Conflicts of Interest:** The authors declare no conflict of interest.

## References

1. Guzzetti, F.; Carrara, A.; Cardinali, M.; Reichenbach, P. Landslide hazard evaluation: A review of current techniques and their application in a multi-scale study, Central Italy. *Geomorphology* **1999**, *31*, 181–216. [CrossRef]
2. Glade, T.; Crozier, M.J. The Nature of Landslide Hazard Impact. In *Landslide Hazard and Risk*; Glade, T., Anderson, M., Crozier, M.J., Eds.; John Wiley & Sons Ltd.: Hoboken, NJ, USA, 2005; Volume 1, pp. 41–74.
3. Petley, D. Global patterns of loss of life from landslides. *Geology* **2012**, *40*, 927–930. [CrossRef]
4. Casteller, A.; Häfelfinger, T.; Cortés Donoso, E.; Podvin, K.; Kulakowski, D.; Bebi, P. Assessing the interaction between mountain forests and snow avalanches at Nevados de Chillán, Chile and its implications for ecosystem-based disaster risk reduction. *Nat. Hazards Earth Syst. Sci.* **2018**, *18*, 1173–1186. [CrossRef]
5. Vranken, L.; Van Turnhout, P.; Van Den Eeckhaut, M.; Vandekerckhove, L.; Poesen, J. Economic valuation of landslide damage in hilly regions: A case study from Flanders, Belgium. *Sci. Total Environ.* **2013**, *447*, 323–336. [CrossRef] [PubMed]
6. Crozier, M.J. Deciphering the effect of climate change on landslide activity: A review. *Geomorphology* **2010**, *124*, 260–267. [CrossRef]
7. Gariano, S.L.; Guzzetti, F. Landslides in a changing climate. *Earth Sci. Rev.* **2016**, *162*, 227–252. [CrossRef]
8. Cruden, D.M.; Varnes, D.J. *Landslide Types and Processes. Landslides: Investigation and Mitigation*; Special Report 247; Transportation Research Board: Washington, DC, USA, 1996; pp. 36–75.
9. Dikau, R.; Brunsden, D.; Schrott, L.; Ibsen, M.L. *Landslide Recognition. Identification, Movement and Causes*; John Wiley & Sons Ltd.: Chichester, UK, 1996; p. 251.
10. Varnes, D.J. *Landslide Hazard Zonation: A Review of Principles and Practice*; IAEG Commission on Landslides and Other Mass-Movements; UNESCO Press: Paris, France, 1984.

11. Dai, F.C.; Lee, C.F.; Ngai, Y.Y. Landslide risk assessment and management: An overview. *Eng. Geol.* **2002**, *64*, 65–87. [CrossRef]
12. Glade, T.; Albini, P.; Frances, F. An Introduction to the Use of Historical Data in Hazard Assessment. In *The Use of Historical Data in Natural Hazard Assessments*; Glade, T., Albini, P., Frances, F., Eds.; Kluwer Academic Publishers: Dordrecht, The Netherlands, 2001; pp. XVII–XXV.
13. Van Den Eeckhaut, M.; Poesen, J.; Vandekerckhove, L.; Van Gils, M.; Van Rompaey, A. Human-environment interactions in residential areas susceptible to landsliding: The Flemish Ardennes case study. *Area* **2010**, *42*, 339–358. [CrossRef]
14. Carrara, A.; Crosta, G.; Frattini, P. Geomorphological and historical data in assessing landslide hazard. *Earth Surf. Process. Landf.* **2003**, *28*, 1125–1142. [CrossRef]
15. Ray, R.L.; Lazzari, M. Introductory Chapter: Importance of Investigating Landslide Hazards. In *Landslides-Investigation and Monitoring*; IntechOpen: London, UK, 2020; p. 1.
16. Brunsden, D.; Ibsen, M.L. The nature of the European archive of historical landslide data, with specific reference to the United Kingdom. In *Temporal Occurrence and Forecasting of Landslides in the European Community*; Final Report Epoch EC Programme; European Commission, Science Research Development: Brussels, Belgium, 1994; Volume 2.
17. Ibsen, M.L.; Brunsden, D. The nature, use and problems of historical archives for the temporal occurrence of landslides, with specific reference to the south coast of Britain, Ventnor, Isle of Wight. *Geomorphology* **1996**, *15*, 241–258. [CrossRef]
18. Guzzetti, F.; Cardinali, M.; Reichenbach, P. The AVI Project: A bibliographical and archive inventory of landslides and floods in Italy. *Environ. Manag.* **1994**, *18*, 623–633. [CrossRef]
19. Cruden, D.M. Estimating the Risks from Landslides Using Historical Data. In *Landslide Risk Assessment, Proceedings of the International Workshop*; Cruden, D.M., Fell, R., Eds.; Balkema: Rotterdam, The Netherlands, 1997; pp. 177–184.
20. Calcaterra, D.; Parise, M.; Palma, B. Combining historical and geological data for the assessment of the landslide hazard: A case study from Campania, Italy. *Nat. Hazards Earth Syst. Sci.* **2003**, *3*, 3–16. [CrossRef]
21. Esposito, G.; Carabella, C.; Paglia, G.; Miccadei, E. Relationships between Morphostructural/Geological Framework and Landslide Types: Historical Landslides in the Hilly Piedmont Area of Abruzzo Region (Central Italy). *Land* **2021**, *10*, 287. [CrossRef]
22. Glade, T. Landslide Hazard Assessment and Historical Landslide Data—An Inseparable Couple. In *The Use of Historical Data in Natural Hazard Assessments*; Springer: Dordrecht, The Netherlands, 2001; pp. 153–168.
23. Reid, M.E.; Baum, R.L.; Lahusen, R.G.; Ellis, W.L. Capturing Landslide Dynamics and Hydrologic Triggers Using Near-Real-Time Monitoring. In *Landslides and Engineered Slopes. From the Past to the Future*; CRC Press: Boca Raton, FL, USA, 2008; pp. 201–214.
24. Loche, M.; Alvioli, M.; Marchesini, I.; Bakka, H.; Lombardo, L. Landslide susceptibility maps of Italy: Lesson learnt from dealing with multiple landslide types and the uneven spatial distribution of the national inventory. *Earth Sci. Rev.* **2022**, *232*, 104–125. [CrossRef]
25. Calcaterra, D.; Parise, M. The Contribution of Historical Information in the Assessment of Landslide Hazard. In *The Use of Historical Data in Natural Hazard Assessments*; Glade, T., Albini, P., Frances, F., Eds.; Kluwer Academic Publishers: Dordrecht, The Netherlands, 2001; pp. 201–216.
26. Pánek, T. Recent progress in landslide dating: A global overview. *Prog. Phys. Geogr. Earth Environ.* **2014**, *39*, 168–198. [CrossRef]
27. Petschko, H.; Brenning, A.; Bell, R.; Goetz, J.; Glade, T. Assessing the quality of landslide susceptibility maps–case study Lower Austria. *Nat. Hazards Earth Syst. Sci.* **2014**, *14*, 95–118. [CrossRef]
28. Stumvoll, M.J.; Canli, E.; Engels, A.; Thiebes, B.; Groiss, B.; Glade, T.; Schweigl, J.; Bertagnoli, M. The "Salcher" landslide observatory—Experimental long-term monitoring in the Flysch Zone of Lower Austria. *Bull. Eng. Geol. Environ.* **2019**, *79*, 1831–1848. [CrossRef]
29. Stumvoll, M.J.; Schmaltz, E.M.; Kanta, R.; Roth, H.; Grall, B.; Luhn, J.; Flores-Orozco, A.; Glade, T. Exploring the dynamics of a complex, slow-moving landslide in the Austrian Flysch Zone with 4D surface and subsurface information. *Catena* **2022**, *214*, 106–203. [CrossRef]
30. Sebald, J.; Senf, C.; Heiser, M.; Scheidl, C.; Pflugmacher, D.; Seidl, R. The effects of forest cover and disturbance on torrential hazards: Large-scale evidence from the Eastern Alps. *Environ. Res. Lett.* **2019**, *14*, 1–12. [CrossRef]
31. Schweigl, J.; Hervás, J. Landslide mapping in Austria. In *Scientific and Technical Research Series*; Office for Official Publications of the European Communities: Luxembourg:, 2009.
32. Fuchs, S.; Wenk, M.; Keiler, M. Geomorphic Hazards in Austria. In *Landscapes and Landforms of Austria*; Springer: Cham, Switzerland, 2022; pp. 105–117.
33. Lemenkova, P.; Promper, C.; Glade, T. Economic Assessment of Landslide Risk for the Waidhofen ad Ybbs Region, Alpine Foreland, Lower Austria. In Proceedings of the Protecting Society through Improved Understanding, 11th International Symposium on Landslides and the 2nd North American Symposium on Landslides and Engineered Slopes, Banff, AB, Canada, 3–8 June 2012; pp. 279–285.
34. Promper, C.; Glade, T. Landcover Changes for Landslide Risk Evolution–First Results from Lower Austria. In Proceedings of the Protecting Society through Improved Understanding, 11th International Symposium on Landslides and 2nd North American Symposium on Landslides and Engineered Slopes, Banff, AB, Canada, 3–8 June 2012.
35. Promper, C.; Puissant, A.; Malet, J.P.; Glade, T. Analysis of land cover changes in the past and the future as contribution to landslide risk scenarios. *Appl. Geogr.* **2014**, *53*, 11–19. [CrossRef]

36. Promper, C.; Gassner, C.; Glade, T. Spatiotemporal patterns of landslide exposure—A step within future landslide risk analysis on a regional scale applied in Waidhofen/Ybbs Austria. *Int. J. Disaster Risk Reduct.* **2015**, *12*, 25–33. [CrossRef]
37. Lacroix, P.; Handwerger, A.L.; Bièvre, G. Life and death of slow-moving landslides. *Nat. Rev. Earth Environ.* **2020**, *1*, 404–419. [CrossRef]
38. Petley, D.N.; Carey, J.M.; Ng, K.Y.; Massey, C.I.; Froude, M.J. Understanding Patterns of Movement for Slow Moving Landslides. In Proceedings of the 20th NZGS Geotechnical Symposium, Napier, New Zealand, 24–26 November 2017.
39. Li, Y.; Utili, S.; Milledge, D.; Chen, L.; Yin, K. Chasing a complete understanding of the failure mechanisms and potential hazards of the slow moving Liangshuijing landslide. *Eng. Geol.* **2021**, *281*, 10597. [CrossRef]
40. Moradi, S.; Heinze, T.; Budler, J.; Gunatilake, T.; Kemna, A.; Huisman, J.A. Combining Site Characterization, Monitoring and Hydromechanical Modeling for Assessing Slope Stability. *Land* **2021**, *10*, 423. [CrossRef]
41. BMDW. Digital Elevation Model (DEM) Based on Airborne Laserscan Data of the Austrian Federal States Raster Resolution 10 m. In *Bundesministerium für Digitalisierung und Wirtschaftsstandort (BMDW)*; geoland.at, Ed.; data.gv.at (Open Data Österreich); BMDW: Vienna, Austria, 2015.
42. Weber, L. *Flächendeckende Beschreibung der Geologie von Osterreich 1:500.000 im Vektorformat. Exzerpt (Basiskarte Geologie) aus der Metallogenetischen Karte von Osterreich 1:500.000*; Geologische Bundesanstalt: Vienna, Austria, 1997.
43. Thenius, E. *Geologie der Österreichischen Bundesländer in Kurzgefaßten Einzeldarstellungen*; NiederÖsterreich, Geologische Bundesanstalt: Wien, Austria, 1974.
44. Schnabel, W. *The Flysch Zone of the Eastern Alps*; Verlag der Geologischen Bundesanstalt (GBA): Vienna, Austria, 1999; p. 49.
45. Petschko, H.; Bell, R.; Leopold, P.; Heiss, G.; Glade, T. Landslide Inventories for Reliable Susceptibility Maps in Lower Austria. In *Landslide Science and Practice: Volume 1: Landslide Inventory and Susceptibility and Hazard Zoning*; Margottini, C., Canuti, P., Sassa, K., Eds.; Springer: Berlin/Heidelberg, Germany, 2013; pp. 281–286.
46. Gottschling, P. Massenbewegungen. In *Geologie der Österreichischen Bundesländer—Niederösterreich*; Wessely, G., Ed.; Geologische Bundesanstalt: Vienna, Austria, 2006; pp. 335–340.
47. Schwenk, H. Massenbewegungen in Niederösterreich 1953–1990. *Jahrb. Geol. Bundesanst.* **1992**, *135*, 597–660.
48. Orozco, A.F.; Steiner, M.; Katona, T.; Roser, N.; Moser, C.; Stumvoll, M.J.; Glade, T. Application of induced polarization imaging across different scales to understand surface and groundwater flow at the Hofermühle landslide. *Catena* **2022**, *219*, 106–612.
49. Sausgruber, T. *Hofermühlrutschung Waidhofen/Ybbs*; Forsttechnischer Dienst für Wildbach-und Lawinenverbauung: Melk, Austria, 2013.
50. Jochum, B.; Lotter, M.; Ottner, F.; Tiefenbach, K. *Geophysikalische und Ingenieurgeologische Methoden zur Untersuchung von durch Massenbewegungen bedingte Bauschäden in Niederösterreich. BBK-Projekt NC-62/F (2007) und ÜLG-35 (2007)*; Internal Report; Amt der Niederösterreichischen Landesregierung. Geologischer Dienst: Sankt Pölten, Austria, 2008.
51. Schweigl, J. *Abschlussbericht BD1-G-411/011-2009*; Internal Report; Amt der Niederösterreichischen Landesregierung. Geologischer Dienst: Sankt Pölten, Austria, 2012.
52. Amt der Niederösterreichischen Landesregierung. *Gutachten (BD-96-G-1970)*; Internal Report; Amt der Niederösterreichischen Landesregierung: Sankt Pölten, Austria, 1970.
53. Gottschling, P. *Geologisches Gutachten BD1-G-867/1. Landesbaudirektion—Geologischer Dienst. Katastrophenerhebungsblatt. Hinteregger*; Internal Report; Landesbaudirektion. Geologischer Dienst: Sankt Pölten, Austria, 2001.
54. Sausgruber, T. *Protokoll zum Lokalaugenschein Hangprozess Hofermühle/Hofermühlrutschung (3491/13-2016)*; Internal Report; Wildbach- und Lawinenverbauung: Melk, Austria, 2016.
55. Kotzmaier, E. *Aktenvermerk Krojer Rutschung (Hofermühle) 03.05.2013*; Internal Report; Wildbach- und Lawinenverbauung: Melk, Austria, 2013.
56. Stumvoll, M.J.; Schmaltz, E.M.; Glade, T. Dynamic characterization of a slow-moving landslide system—Assessing the challenges of small process scales utilizing multi-temporal TLS data. *Geomorphology* **2021**, *389*, 1–16. [CrossRef]
57. NOEL GV. *Digital Orthophoto*; Department for Hydrology and Geoinformation, Federal State Government of Lower Austria, Ed.; Federal State Government of Lower Austria: St. Pölten, Austria, 2013.
58. Schwenk, H. *Marktgemeinde Gresten, Schiliftanlage der Fa*; Pfeiffer & Kreuse OHG, Erdrutsch; Internal Report; Amt der niederösterreichischen Landesregierung: Sankt Pölten, Austria, 1976.
59. Schwenk, H.; Gresten, G.; Salcher, G. *Gemeinde Gresten, Güterweg Salcher. Erdrutschschaden 1978. Erhebungsbericht und Gutachten des geologischen Dienstes der Baudirektion*; Internal Report; Melk, Austria, 1979.
60. Schweigl, J. *Gresten, Krause (Gst.Nr.1999/1), Bramreiter (Gst.Nr.1999/6) u.Plank (Gst.Nr.1999/7) Katastrophenschaden 2006, Rutschung Salcher, geologischer Abschlussbericht zu den Vermessungen (No. BD1-G-142/001-2007)*; Internal Report; Amt der Niederösterreichischen Landesregierung: Sankt Pölten, Austria, 2013.
61. Hinteregger, H. *Landesbaudirektion—Geologischer Dienst. Katastrophenerhebungsblatt. Geologisches Gutachten. (BD-G-867)*; Internal Report; Landesbaudirektion. Geologischer Dienst: Sankt Pölten, Austria, 1987.
62. Lotter, M.; Jochum, B. *Geophysikalische und Ingenieurgeologische Methoden zur Untersuchung von Durch Massenbewegungen Bedingte Bauschäden in Niederösterreich (BBK-Projekt NC-62/F (2007) und ÜLG-35 (2007))*; Internal Report; Amt der Niederösterreichischen Landesregierung. Geologischer Dienst: Sankt Pölten, Austria, 2010.
63. Simeoni, L.; Mongiovì, L. Inclinometer monitoring of the Castelrotto landslide in Italy. *J. Geotech. Geoenviron. Eng.* **2007**, *133*, 653–666. [CrossRef]

64. Stark, T.D.; Choi, H. Slope inclinometers for landslides. *Landslides* **2008**, *5*, 339–350. [CrossRef]
65. Bordoni, M.; Vivaldi, V.; Bonì, R.; Spanò, S.; Tararbra, M.; Lanteri, L.; Parnigoni, M.; Grossi, A.; Figini, S.; Meisina, C. A methodology for the analysis of continuous time-series of automatic inclinometers for slow-moving landslides monitoring in Piemonte region, northern Italy. *Nat. Hazards* **2022**, *115*, 1115–1142. [CrossRef]
66. Glötzl. *Datasheet Neigungsmessrohre ABS 50, ABS 74, PVC 60, ALU 48*; GLÖTZL Gesellschaft für Baumesstechnik mbH: Rheinstetten, Germany, 2016; p. 2.
67. Glötzl. *Datasheet NMGD Vertikalneigungsmesser*; GLÖTZL Gesellschaft für Baumesstechnik mbH: Rheinstetten, Germany, 2019; p. 1.
68. Measurand. *Datasheet SAAF Model 003*; Measurand: Hanwell, NB, Canada, 2019; p. 6.
69. Hauck, C.; Stumvoll, M.J.; Jochum, B.; Guardiani, C.; Glade, T. The Influence of Hydro-Meteorological Conditions on Landslide Dynamics—An Application to the Salcher Landslide in Gresten, Lower Austria. In *EGU General Assembly Conference Abstracts*; EGU: Vienna, Austria, 2018; p. 15672.
70. Tsourlos, P.; Jochum, B.; Supper, R.; Ottowitz, D.; Kim, J.H. Optimizing Geoelectrical Arrays for Special Geoelectrical Monitoring Instruments. In *Near Surface Geoscience 2016—22nd European Meeting of Environmental and Engineering Geophysics*; European Association of Geoscientists & Engineers: Utrecht, The Netherlands, 2016; Volume 2016, p. 495.
71. Lidauer, S.; Jochum, B.; Ottowitz, D.; Stumvoll, M.J.; Glade, T. Geoelectric long-time monitoring: Changes and pattern within subsurface resistivity during different precipitation events in the Salcher landslide, Gresten (Lower Austria). In *EGU General Assembly Conference Abstracts*; EGU: Vienna, Austria, 2018; p. 12679.
72. Ottowitz, D.; Hoyer, S.; Jochum, B.; Riegler, M.; Preuner, P.; Scolobig, A.; Supper, A. *Long-Term Landslide Monitoring for Understanding of Underlying Dynamic Processes as Basis for an End-User Focused Early Warning—LAMOND*; Geologische Bundesansalt Fachabteilung Geophysik: Vienna, Austria, 2018. [CrossRef]
73. Stumvoll, M.J.; Konzett, M.; Schmaltz, E.M.; Glade, T. Application of UAS to Detect Infrequent and Local Large-Scale Surficial Displacements: Critical Examples from the Fields of Landslide and Erosion Research. In *sUAS Applications in Geography*; Konsoer, K., Leitner, M., Lewis, Q., Eds.; Springer: Cham, Switzerland, 2022; pp. 203–233.
74. Canli, E.; Höfle, B.; Hämmerle, M.; Thiebes, B.; Glade, T. Permanent 3D laser scanning system for an active landslide in Gresten (Austria). *Geophys. Res. Abstr.* **2015**, *17*, 2885.
75. *DIN EN ISO 22476-2:2005*; Geotechnical Investigation and Testing—Field Testing—Part 2: Dynamic Probing. ISO: Geneva, Switzerland, 2005.
76. Schwab, J.; Gori, P.; Jeer, S. *Landslide Hazards and Planning*; American Planning Association: Chicago, IL, USA, 2005.
77. Klose, M.; Damm, B.; Terhorst, B. Databases in geohazard science: An introduction. *Geomorphology* **2015**, *249*, 1–3. [CrossRef]
78. Piacentini, D.; Troiani, F.; Daniele, G.; Pizziolo, M. Historical geospatial database for landslide analysis: The Catalogue of Landslide Occurrences in the Emilia-Romagna Region (CLOCkER). *Landslides* **2018**, *15*, 811–822. [CrossRef]
79. Klose, M.; Maurischat, P.; Damm, B. Landslide impacts in Germany: A historical and socioeconomic perspective. *Landslides* **2016**, *13*, 183–199. [CrossRef]
80. Qiang, X. Understanding the landslide monitoring and early warning: Consideration to practical issues. *J. Eng. Geol.* **2020**, *28*, 360374. [CrossRef]
81. Palis, E.; Lebourg, T.; Tric, E.; Malet, J.-P.; Vidal, M. Long-term monitoring of a large deep-seated landslide (La Clapiere, South-East French Alps): Initial study. *Landslides* **2017**, *14*, 155–170. [CrossRef]
82. NOEL GV. *Digital Orthophoto*; Department for Hydrology and Geoinformation, Federal State Government of Lower Austria, Ed.; Federal State Government of Lower Austria: St. Pölten, Austria, 2002.
83. NOEL GV. *Digital Orthophoto*; Department for Hydrology and Geoinformation, Federal State Government of Lower Austria, Ed.; Federal State Government of Lower Austria: St. Pölten, Austria, 2019.
84. Dixon, N.; Bromhead, E.N. Landsliding in London Clay coastal cliffs. *Q. J. Eng. Geol. Hydrogeol* **2002**, *35*, 327–334. [CrossRef]
85. Hobbs, P.R.N.; Jones, L.D.; Kirkham, M.P.; Holyoake, S.J.; Pennington, C.V.L.; Dashwood, C.; Reeves, H.J. Establishment of a coastal landslide observatory at Aldbrough, East Riding of Yorkshire, UK. *Q. J. Eng. Geol. Hydrogeol* **2020**, *53*, 88–100. [CrossRef]
86. Hutchinson, J.N. *Survey of the Coastal Landslides of Kent*; Building Research Station: London, UK, 1965.
87. Lissak, C.; Macaire, O.; Malet, J.P.; Bitri, A.; Samyn, K.; Grandjean, G.; Davidson, R. Airborne, and ground-based data sources for characterizing the morpho-structure of a coastal landslide. *Geomorphology* **2014**, *217*, 140–151. [CrossRef]


**Disclaimer/Publisher's Note:** The statements, opinions and data contained in all publications are solely those of the individual author(s) and contributor(s) and not of MDPI and/or the editor(s). MDPI and/or the editor(s) disclaim responsibility for any injury to people or property resulting from any ideas, methods, instructions or products referred to in the content.

land

MDPI

*Article*

# Historical Memory as an Effective and Useful Tool for Proper Land Use Planning: Lessons Learnt from Some Italian Cases

**Fabio Luino [1], Fabrizio Terenzio Gizzi [2,*], Walter Palmieri [3], Sabina Porfido [4,5] and Laura Turconi [1]**

[1] Istituto di Ricerca per la Protezione Idrogeologica, Consiglio Nazionale delle Ricerche, Strada della Cacce 73, 10135 Torino, Italy; fabio.luino@irpi.cnr.it (F.L.); laura.turconi@irpi.cnr.it (L.T.)
[2] Istituto di Scienze del Patrimonio Culturale, Consiglio Nazionale delle Ricerche, C.da S. Loja, 85050 Potenza, Italy
[3] Istituto di Studi sul Mediterraneo, Consiglio Nazionale delle Ricerche, Via Guglielmo Sanfelice, 8, 80134 Napoli, Italy; palmieri@ismed.cnr.it
[4] Istituto di Scienze dell'Alimentazione, Consiglio Nazionale delle Ricerche, Via Roma 64, 83100 Avellino, Italy; sabina.porfido@cnr.it
[5] INGV, Osservatorio Vesuviano, Via Diocleziano 328, 80124 Napoli, Italy
* Correspondence: fabrizioterenzio.gizzi@cnr.it

**Abstract:** Many Italian cities and towns have been affected by geological or geohydrological processes. However, due to the loss of historical memory, lessons of the past have been ignored; new urbanized areas have expanded into the same zones where damage and casualties occurred in the past. Despite current practices, researchers are showing how historical data can be among the most valid tools for identifying the most affected and hazardous areas. When the completeness and quality of historical sources are sufficiently high, we can make useful statistical inferences regarding the spatiotemporal variations of natural processes. This information is of great importance for land use planning, as it makes us able to rely not only on the current state of the investigated areas but also on their dynamic evolutionary framework over time. In this article, we present a chronological review of past Italian works describing the occurrence of natural extreme events making use of historical data. Then, we present some Italian case studies in which the awareness of hazards gained by paying attention to past information would have ensured better management of the risk for the benefit of public safety. Finally, the authors stress the need to safeguard, manage, and enhance the large collection of historical data that constitutes Italy's heritage.

**Keywords:** geological and geohydrological processes; historical research; old documents; cultural heritage; land use planning; urbanization; hazard and risk mitigation

**Citation:** Luino, F.; Gizzi, F.T.; Palmieri, W.; Porfido, S.; Turconi, L. Historical Memory as an Effective and Useful Tool for Proper Land Use Planning: Lessons Learnt from Some Italian Cases. *Land* **2023**, *12*, 1751. https://doi.org/10.3390/land12091751

Academic Editor: Thomas Panagopoulos

Received: 7 July 2023
Revised: 28 August 2023
Accepted: 3 September 2023
Published: 8 September 2023

**Copyright:** © 2023 by the authors. Licensee MDPI, Basel, Switzerland. This article is an open access article distributed under the terms and conditions of the Creative Commons Attribution (CC BY) license (https://creativecommons.org/licenses/by/4.0/).

## 1. Introduction

Italy is a young peninsula from a geological point of view: its shape and physical configuration originate from the collision between the African and Eurasian plates that occurred during the Cenozoic. This geological event caused the closure of the Tethys Sea and was accompanied by the compression and piling up of its sediment, which determined the formation of the two important mountain chains that now characterize the Italian territory: the Alps and the Apennines [1,2]. This tectonic evolution is still ongoing, causing remarkable seismic and volcanic activity, which threatens human settlements and activities. The diversity of the Italian landscape is also due to the wide variety of lithotypes, including pre-orogenic basement and successive sedimentary cover [3,4]. This situation, combined with the high population density, especially distributed in coastal areas, makes the peninsula particularly vulnerable to extreme natural events, such as earthquakes and volcanic eruptions, as well as landslides, mud debris flows, and floods.

Looking at Catalogo Parametrico dei Terremoti Italiani (Parametric Catalogue of Italian Earthquakes) [5], we can easily see that earthquakes often occur in areas that have

already been shaken by past events. The strongest historical events occurred in Sicily, in the eastern Alps, and along the central–southern Apennines, from Abruzzo to Calabria. However, major earthquakes have also hit the northern–central Apennines and the Gargano (Apulia) promontory.

Specifically, 75 earthquakes from medium to high magnitude (Mw $\geq$ 5.5) have occurred since 1900, some of which caused heavy losses and had significant environmental effects. The strongest of these was the Mw 7.1 earthquake that destroyed Messina and Reggio Calabria in December 1908 [5–10], causing about 80,000 deaths.

In the last 60 years, the most damaging earthquakes occurred on 6 May 1976 in Friuli Venezia Giulia (Mw 6.5, 989 casualties) [5,11,12], on 23 November 1980 in the Campania–Basilicata region (Mw 6.9, 2914 victims) [5,13–16], and on 6 April 2009 in Abruzzo (Mw 6.3, 309 victims) [5,17,18], as well as the 2016–2017 seismic sequence in Central Italy (299 victims) [5,19–22].

However, it should not be forgotten that Italy also has many volcanoes, at least 10 of which are "active" (which means that they have "woken up" at least once in the last 10,000 years): Etna, Stromboli, Vesuvius, Ischia, Lipari, Vulcano, Pantelleria, Colli Albani, Campi Flegrei, and Isola Ferdinandea. The only two that currently erupt continuously, separated by short intervals, are Etna and Stromboli. When we consider volcanic eruptions that occurred historically in Italy, we are immediately reminded of 79 BC, when there was the great eruption of Vesuvius, which buried the nearby cities of Pompeii and Herculaneum under a cloud of ash and pumice rocks, causing thousands of casualties (based on descriptions in two Epistulae by Gaius Plinius Caecilius Secundus). Vesuvius has apparently been "dormant" (which does not mean extinct) since 1944, but it is perfectly active [23]; the risk linked to Vesuvius is determined by the fact that a densely settled area has developed around it over the centuries, with millions of inhabitants. Mount Etna, in Sicily, is the largest active volcano. The most impressive effusive eruption of Etna in historical times took place in 1669 [24], when lava buried numerous villages, reaching as far as the sea near Catania, with a flow up to 17 km long but without casualties. In recent decades, only Etna and Stromboli have erupted. Etna is usually active, sometimes more so, sometimes less so. In 1979, Mount Etna had a sudden explosion that caused 9 deaths and 23 injuries among a group of tourists on an excursion [25,26]; at that time, the last official order for the evacuation of a town due to an eruption was issued.

In addition to endogenous phenomena, exogenous phenomena also contribute to increasing the risk. Every year, in Italy, hundreds of floods and thousands of landslides occur, affecting the environment and causing severe damage and casualties. The reason for such activity is that Italy is a peninsula with a highly articulated and complex hydrographic network. There are about 1200 rivers, 57 of which are longer than 100 km. Therefore, thousands of torrents and streams make up a very dense network. This inevitably brings a high risk of possible flooding for a large part of the peninsula. In conjunction with rainy periods, landslides can be triggered; they are superficial if the rainfall is short and intense, and deeper if the rainfall lasts for several days. For this reason, we treat them together, defined as geohydrological processes [27].

Although geohydrological processes have been occurring since remote times, they have accelerated considerably since around the end of World War II [28], with numerous serious geohydrological processes devastating Italy, in terms of both human victims and damage to structures and infrastructure. However, it is important to distinguish the different phenomena: on one hand, landslides, mudflows, and debris flows, and on the other hand, floods.

Regarding landslides, the most damaging event, which was world-renowned and widely studied, was the Vajont landslide (Friuli Venezia Giulia, Northern Italy) on 9 October 1963. It is one of the largest mass movements ever to occur in Italy (about 240 million $m^3$). Earth that detached from the slope fell into a large hydroelectric reservoir. The resulting water wave passed over the dam and poured over the Piave Valley floor, sweeping away many villages; in total, 1911 casualties were reported [29,30], but there were probably more.

Concerning mudflows and debris flows, one of the most catastrophic events (considered anthropogenic) took place in July 1985 in Prestavel (Trentino, Northern Italy), when a huge mudflow occurred. The tailing ponds of the Prestavel fluorite mine broke their banks, discharging 180,000 $m^3$ of mud in a matter of minutes onto the small tourist village of Stava. Many houses and hotels were razed to the ground, and there were 269 casualties and many injuries [31,32].

Another large mudflow struck several towns in Campania (Southern Italy), including Sarno, in May 1998. Numerous mudflows invaded the villages, rapidly filling houses and causing as many as 160 casualties [33,34].

Italy also has a very long history of floods. Since the end of the Second World War, some noteworthy floods have occurred. In particular, in November 1951, the famous Polesine (Veneto) flood caused 100 deaths (84 died on a truck). About 100,000 hectares was flooded, and 5674 houses were destroyed or damaged; a total of 33% of the population was forced to leave Polesine after the flood [35].

Fifteen years later, in November 1966, the great flood of Florence occurred (which also involved Veneto, Trentino, and Friuli), with 111 casualties [36]. This flood greatly shocked the international community, especially because of the serious damage to art museums and the national library of Florence [37]. Lastly, we also remember the two great floods of 1994 and 2000 that hit Piedmont in particular, causing very serious damage, with 69 casualties (1994) [38] and 36 casualties (2000) [39,40].

Knowledge of the above-mentioned endogenous and exogenous phenomena was possible thanks to the extensive and critical use of historical sources, in which Italy is particularly rich. The wealth of written sources and their widespread availability come from the different foreign rules and subsequent administrative structures that have succeeded one another over the centuries.

Historical sources can be used to identify urban areas that were affected by extreme natural events in the past; thus, we can understand the impact that these events had on humanity, the built environment, and the territory. The aim is to obtain a powerful tool to prevent the occurrence of hazards and mitigate risks. With this in mind, in this article, we discuss five case studies scattered throughout the peninsula dealing with processes that differ in terms of type, evolution, kinematics, and damage. The five case studies, covering areas affected by both hydrogeological and seismic hazards, can be considered illustrative of how knowledge of the memory of places and humanity's respect for the natural evolution of the territory would have contributed to mitigating the risk of natural hazards to prevent disasters.

Following the Section 1, the article is divided into four main parts: (a) an overview of the main works that made use of historical sources to report on the occurrence of natural hazards in Italy; (b) the Section 3, which describes the approach followed to analyze the five case studies; (c) the Results section, in which the natural hazards that occurred at each of the five sites are analyzed, along with the role of humans in mitigating risks (or not); (d) the Section 5, which provides a critical analysis of the five case studies; and (e) the Section 6, in which the authors sum up the research and propose concrete actions of interest to stakeholders and policymakers with regard to improving the management of natural risks.

## 2. Pioneers in the Use of Historical Sources to Study Natural Hazards in Italy: An Overview

In past centuries, Italian scholars dealt with natural extreme events, which attracted their interest based on the causes of natural processes and their possible repetitiveness over time. Certainly, geological and geomorphological phenomena are among the events that cause concern and spark the imagination; thus, information about them is worth handing down, and people have frequently had the propensity to pass on significant events they have witnessed to posterity. Often, those who witnessed the effects of extreme natural events felt the desire and the need to leave a testimony, perhaps a long narrative or even a

simple description of, for example, the exceptional height reached by the waters of a river or the effects of an earthquake or a landslide on a certain area or town.

### *2.1. Floods and Landslides*

For example, browsing through the pages of an anthology of ancient Latin poets, we can find this passage by Silius Italicus in his *Punica Liber IV* [41], which refers to the Battle of the Trebbia, which took place on 25 December in 218 BC. In epic form, the author describes a violent raging of the river that caused the death of numerous soldiers (Figure 1). Gaius Plinius Caecilius Secundus [42], in his *Naturalis Historia*, told of a landslide that during the great eruption of Vesuvius prevented people from approaching the shoreline. [43]. The poet Dante Alighieri, in *Inferno*, the first canticle of *The Divine Comedy* (about 1320) [44], could not fail to mention the "ruina di Marco" near Rovereto (Trento province, Northern Italy), an area he had known during his travels. It was an area of more than 35 hectares where cyclopean boulders detached from Monte Zugna and were carried downstream by water, diverting the course of the Adige River in prehistoric times [45], an event so terrifying that Dante had to mention it.

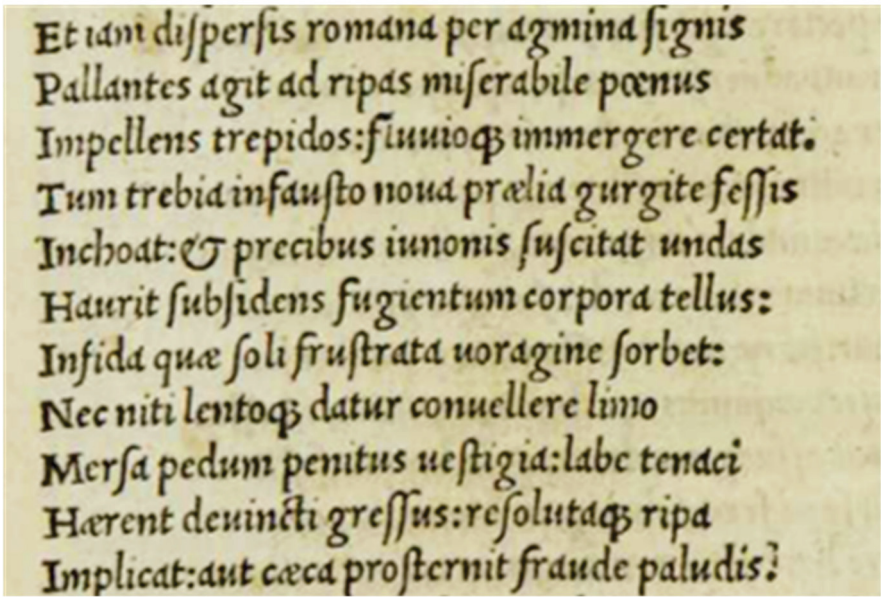

Et iam diſperſis romana per agmina ſignis
Pallantes agit ad ripas miſerabile pœnus
Impellens trepidos: fluuioq; immergere certat.
Tum trebia infauſto noua prælia gurgite feſſis
Inchoat: & precibus iunonis ſuſcitat undas
Haurit ſubſidens fugientum corpora tellus:
Infida quæ ſoli fruſtrata uoragine ſorbet:
Nec niti lentoq; datur conuellere limo
Merſa pedum penitus ueſtigia: labe tenaci
Hærent deuincti greſſus: reſolutaq; ripa
Implicat: aut cæca proſternit fraude paludis?

**Figure 1.** Passage from *Punica Liber IV* by Silius Italicus [41] (verses 570–580) describing the Battle of the Trebbia, in which many soldiers drowned due to a flood.

We can consider the attention paid by the people of Rome, more than 800 years ago, to the heights reached by the waters of the Tiber in the "Urbs Aeterna". Today, walking some distance from the Tiber's riverbed, we can still find some epigraphs, the so-called "flood notches", known also as "little hands", indicating the height reached by the Tiber in the city. Many epigraphs can also be found on the façade of the Basilica di Santa Maria sopra Minerva in Piazza della Minerva, near the Pantheon. The oldest marble plaque, placed at Castel Sant'Angelo, recalls the flood of 6 November 1277, although written sources mention that older flood notches were once present and later disappeared [46].

In Florence, there are also many epigraphs testifying to the various floods of the Arno that hit the city over the centuries. The oldest is from 1333 [47], and the great floods that followed, which occurred in 1547, 1557, 1589, 1740, and 1758 and on 3 November 1844, are commemorated by plaques. The Florence municipality made a census of the epigraphs, and georeferenced them to implement the data in a Web GIS [48]. The Web GIS reports include, in addition to the geographic coordinates of each epigraph's location, the details of the information on the plaque, such as the date of the flood and, above all, the height reached by the floodwaters.

In the Roman period, descriptions of Tiber floods were recorded by Titus Livius (at least eight before 189 BC), Horace and Dione Cassius (nine around the time of Christ's birth), and other Latin authors such as Tacitus and Plinius [49]. Floods in the medieval period and up to 1870 were studied and reported by contemporary writers such as Castiglione [50] and Bonini [51]. Later, other historians sporadically described the floods they witnessed. The records of the earliest period, up to 1870, are essentially based on the chronicles of floods in Rome and the records of flood levels handed down through the generations, as attested by the many tombstones that can still be seen today. Although height measurements from the first hydrometer in Ripetta (Cavour bridge in Rome) have existed since 1782, it was not until 1871, following the great flood of 29 December 1870, that the Ministry of Public Works began to systematically observe the river level daily under normal conditions and hourly during floods, as Di Loreto and Bersani [49] recently reported.

Descriptions of the old catastrophic floods of the Arno River in Florence were published in 1762 by Ferdinando Morozzi [52], a hydraulic engineer, and the work was later resumed in 1845 by Giuseppe Aiazzi [53]. Some historians have gone further, not limiting themselves to describing just one episode [54] but describing in detail different areas of specific regions [55], also mentioning the various disasters that affected the territory. For example, Goffredo Casalis [56], an Italian abbot and historian, completed a tremendous 31-volume work that has become a touchstone for historical research. His dictionary illustrated the civil conditions of every inhabited part of the Sardinian Kingdom, which included four regions of present-day Italy and part of Switzerland and France. Casalis described the morphological characteristics, the geographical position, and the climate of each one; the information is completed by descriptions of historical events of each country, including extreme natural events such as landslides and floods.

Pantanelli and Santi [57], late-19th-century scholars, writing about the Emilian Apennines, stressed that "all or almost all the big landslides of our day are nothing more than a renewal of landslides occurred in periods before the nineteenth century" (translated from Italian).

Shortly thereafter, Santi [58] cited ancient gravitational movements in the Modena area, which destroyed fortresses and towns. Following Santi, there were also numerous reports by Almagià (1907, 1910) in his two important volumes [59,60] focusing on landslides in the Apennine chain.

In 1900, Comandini and Monti [61] published a significant collection of data related to Italy throughout the 19th century. After reviewing many sources (journal articles, books, technical reports) in their work, they provided a good synthesis of all the events for which they had found at least one record, listing all of the storms; dry, rainy, hot, and cold periods; and hydrogeological processes.

Three years later, Berta [62] published a volume on the history of the city of Alessandria from 1168 to 1900; it contains numerous references to flooding originated from the Tanaro and Bormida Rivers, which the city straddles [63].

Returning to the Apennines, in accordance with the oral traditions still widespread in the Langhe Hills (Piedmont), Pullè [64] wrote that "many are the legends of the small town of Frignano that tell of countries swallowed up by the earth or submerged by the waters [. . .] such legends betray the ancient terror I would say almost atavistic of disasters" (translated from Italian). More realistically, in reference to Piacenza and Parma, Almagià [59] wrote that "some local names testify to disasters that occurred in past times" (e.g., "Lacereto, Lama, Rovina, Rovinaglia, and Rovinasso", names of Italian areas affected by past landslides). Toponyms, in fact, are an indispensable complement to historical research in a certain territory; they can provide us with much information that we cannot always find in documents. There are many toponyms throughout the peninsula that recall places where, in the more or less recent past, harmful phenomena occurred. On the slopes, we can find the localities of Ruinon (equivalent to "big ruin") in Valfurva (Lombardy), "Le Rotte" (equivalent to "the breaks") in Bosia (Piedmont), and "Lavini di Marco" ("lavini" is for "landslides"). These toponyms refer to the giant landslides in the Rovereto area (Trentino

Alto Adige) mentioned by Dante in *The Divine Comedy* [44]. In addition, there are the hamlet of Sommarovina ("supreme ruin") in San Giacomo Filippo (Lombardy), and some built-up rivers where mud/debris flows are called "inferno" ("hell") in Omegna (Piedmont), "Rabbia" ("rage") in Sonico (Lombardy), and "Rotolon" ("tumble") in Recoaro T. (Veneto). Moreover, along waterways, there are places such as "Borgata La Rotta" ("break levee") in Moncalieri (Piedmont) along the Po River; "Cascina Malpensata" ("badly thought farm") along the Chisone (Piedmont); up to the banks of the Po in the town of "Alluvioni Cambiò" ("changed by floods") in Piedmont, a town with a singular history behind it [65].

The examples continue for other areas of the peninsula: the term "lama" with all its derivatives, such as "lavina", "lavanga", "calanca", "rovina", "motta" and "smotta", and "sciolle", is emblematic of the traces left throughout Italy by landslides [66].

This concept was taken up for the Piedmontese alpine environment by geographer Giorgio Roletto [67], who stated that "Our mountains still await many revelations from archive research, which on the other hand can never be dispelled by the research done on the ground [. . .]. In the Pellice Valley (Piedmont) has been affirmed the conviction that every hundred years there is a periodic ineluctable return of the flood".

The development of a research sector for the historical reconstruction of geological and geomorphological phenomena in Italy has gradually gained momentum in the scientific community since the 1970s. This research sector makes use of competencies that straddle the humanistic and geological disciplines. For example, since its founding in 1970, the Research Institute for Hydrogeological Protection (IRPI) of the National Research Council (CNR) has specialized in historical research, based on the belief that knowing the past well makes it easier to predict the future. In this way, under the supervision of geologist Mario Govi, director of the Turin IRPI, many researchers have dedicated themselves to the historical investigation of geomorphological phenomena in specific valleys or entire regions. Thus, the idea of developing a national catalogue to collect all historical information concerning the geological–geomorphological processes that have caused damage was born. At the end of the 1980s, the Minister for the Coordination of Civil Protection commissioned the CNR to conduct historical research with the aim of carrying out a census of areas historically affected by geological and hydraulic hazards (landslides and floods). In this way, the Aree Vulnerate Italiane (Italian Affected Sites; AVI) Special Project (1994) was developed [68]. The archive of the project collected historical information related to the natural instability processes that had occurred in Italy since 1917 (much earlier events were also included, albeit sporadically) by searching 100 national and local newspapers. The archive contained over 22,000 pieces of information related to landslides, covering over 18,500 affected locations, and over 7500 pieces of information related to floods, covering 12,000 affected locations. It was considered the first work of its kind on a national scale. Unfortunately, after funding ran out, the project was not continued. The information was later used by many other authors in their works, although the analysis only started in 1918.

Del Din Dall'Armi [69] published an interesting volume, a collection of geohydrological events in a mountainous region of Veneto (an area known as Agordino) particularly prone to instability.

In 1987, the Agency for New Technologies, Energy, and Environment (ENEA) published the Giano Project [70]. The plan was to catalogue hydrogeological instability events in Italy during the 18th and 19th centuries. However, the project was discontinued after only three years, which inevitably affected the completeness and representativeness of the data. Later, in the late 1980s, the Study of Unstable Inhabited Centers (SCAI) Project [71] was promoted by the National Hydrogeological Disaster Defense Group (GNDCI) within the framework of activities for the prediction and prevention of high-risk landslides ("Previsione e prevenzione dei fenomeni franosi a grande rischio"). The aim of the project was to evaluate the instability conditions of some inhabited Italian towns. With detailed and specific investigations, the conditions of instability associated with various types of mass movements affecting inhabited areas and dwellings were mapped and described, with particular attention being given to the safety of buildings and inhabitants. In that study, the

historical reconstruction of past phenomena was a necessary and essential methodological step, with a very important role. The SCAI Project is based on Law No. 445, promulgated in 1908. The law was intended to sustain the investigations on the geological instability of towns to identify both conditions that were dangerous to public safety and situations that required the relocation or consolidation of settlements. Law No. 445 of 1908 classified 1306 inhabited centers to be consolidated and 323 to be relocated throughout the country. Since 1988, several research groups have worked on the project, publishing many papers based on historical analysis and geological–geomorphological studies.

In 1992, Vincenzo Catenacci [72] published a volume of over 300 pages covering major slope instability phenomena that affected Italy from 1945 to 1990. The book was based on data gathered from scientific publications and newspapers, and it was enriched with many photographs.

Another important study was conducted by Govi and Turitto [73]. Following the serious event that occurred in Valtellina (Lombardy) in July 1987, they launched a fact-finding investigation to obtain a picture of similar phenomena occurring in the same territory over the centuries. Their attention was focused on selecting scientific papers and local newspapers that dealt directly or indirectly with the problem of geohydrological processes in the Valtellina Valley (Lombardy). The content of each text was analyzed and summarized, and the types of phenomena reported were highlighted, indicating the degree of technical or purely informative detail in the description. In addition to the names of affected places and the event dates, the resulting damage and any further useful information for characterization were systematically reported.

Luino, in collaboration with some researchers from IRPI Torino, systematically analyzed the hydraulic criticality of five important rivers in Lombardy—the Staffora stream [74], the Pioverna and Serio streams [75], the Oglio River [76], and the Lago Maggiore-Ticino River [77]—using a well-established methodology at the CNR-IRPI in Turin. This geological–geomorphological study was accompanied by a deep historical analysis concerning all past floods (with heights, casualties, and damage) and the subsequent identification of potentially flood-prone areas on the valley floor. At the end, an urban layer was superimposed to verify the suitability of the regulatory plans. The IRPI research method was also considered in the Piedmont and Liguria regions. The whole path of the methodological approach consists in comparing archival findings with field evidence to assess the processes of natural hazards, and their occurrence and magnitude, and arranging all the data in a GIS to be properly managed [78–82].

In the south of Italy, Petrucci, in collaboration with some colleagues, conducted several historical studies [83–86]. These works are the result of a long and patient research process in which he consulted ancient maps and unpublished documents dealing with the geohydrological instability phenomena that have occurred in different areas of Calabria over time.

Another important study area in southern Italy is the Campania region. Especially after the famous Sarno landslide in 1998, studies on landslides and alluvial phenomena that affected that area (and neighboring areas) in historical times have multiplied [87–92].

Tropeano and Turconi [93] published a paper precisely concerning the use of historical data in investigating the prevention of natural hazards such as landslides, debris flows, and floods in northern Italy. They argued that today's processing of archival data allows for possible analytical applications for the structural remediation of natural hazards in built-up areas. In any case, the research results make it possible to raise public awareness of natural hazards and to implement the appropriate civil protection strategies.

Luino et al. [94] conducted extensive historical research on the city of Alba (Piedmont), which was severely affected in November 1994. By comparing old maps and recovering old documents, the authors discovered that large areas of the city had already been affected by severe flooding in the past and that new residential districts and industries (Ferrero confectionery) had sprung up in those areas.

Alluvial phenomena that occurred before the birth of Christ are found in various works, involving both the Po River [95] and the Tiber River [96,97].

In 2014, Lazzari noted the usefulness of historical data in defining geomorphological risk and in subsequent risk assessment in the spatial planning phase. In that paper, he described past studies using historical data [98].

In addition to the conscious need to hand down written memories of such news in an appropriately elaborated form, the cardinal concept that has guided the main activities of all bodies that have collected data over the past 50 years, primarily the CNR-IRPI of Turin, is that exogenous and endogenous phenomena are likely to repeat themselves in space (very often in the same places) and in time (according to extremely variable intervals of recurrence), in ways similar to those in the past.

### *2.2. Earthquakes*

Historical sources are also a significant tool to obtain information on earthquake activity in the past. The earliest "catalogue" of Italian earthquakes goes back to the "paradoxography" literary genre [99], which consists of "paradoxical" objects and events in the natural and human worlds, i.e., things that are strange but true [100]. The first important catalogue of the Italian region was compiled in 1457, at the beginning of the modern age: "De terraemotu libri tres", by politician and humanist Giannozzo Manetti [101]. The book covers the period from antiquity to 1456, with the last date being when the strongest earthquake since the 11th century hit peninsular Italy (Mw 7.2) [5]. After about two and a half centuries, during which other catalogues were also compiled, the monumental work by Marcello Bonito was printed [102]. Bonito made extensive and critical use of original sources to list earthquakes from all over the then known world. However, it was not until the 19th century that a paradigm shift occurred in earthquake data compilation. Indeed, the early 19th century saw the catalogues shifting from a simple list for intellectuals and historians toward a positivistic–scientific interpretation of the correlation between earthquakes and volcanic phenomena [103,104]. Leopoldo Pilla [105] stressed the importance of historical memory to put into practice what we call prevention today: "[. . .] The tremor occurs in one place, and in a short time it devastates [. . .] but the time that destroys everything, still erases the memory of past disasters [. . .]. Thirty, fifty, and one hundred years pass by, and here the trembling again melts the same district, which so that it did not find more attentive than in the previous attack, becomes a new field of death [. . .]" (translated from Italian).

The next "maturation" phase in dealing with historical data was introduced by the "milestone" catalogue by Baratta [106], "I Terremoti d'Italia" ("Italian Earthquakes"). Baratta catalogued the major earthquakes from the first century BC until the end of the 19th century, identifying over 250 seismic centers. He made wide use of historical sources, whose references he provides in the third part of his volume under the title "Saggio di Bibliografia Sismica Italiana" ("Italian Seismic Bibliography"). The relevance of Baratta's work is attested by the fact that it is a source widely used by current compilers of seismic catalogues.

Other national and local catalogues have been published since Baratta's. Among these, the efforts made within the framework of Progetto Finalizzato Geodinamica (Geodynamic Oriented Project; PFG) of the Italian National Research Council (CNR) are worth noting. Indeed, the aim of PFG was to make the most of historical data for practical purposes. The results were "Atlas of Macroseismic Maps of Italian Earthquakes", concerning specific historical–seismological studies of past earthquakes, and "Catalogo dei Terremoti Italiani dall'Anno 1000 al 1980" ("Catalogue of Italian Earthquakes from 1000 to 1980") [107,108].

Improvements in interpreting historical data, new extensive research on unknown earthquakes, and an increase in the quality and completeness of information related to already known past events have led to the following versions of the current catalogues and databases: (1) Parametric Catalogue of Italian Earthquakes, CPTI15 [5], with the associated Database of Italian Macroseismic Database, DBMI15 [109], and (2) the parametric–descriptive Catalogue of Strong Italian Earthquakes, CFTI5Med [110].

The CPTI catalogue, the first version of which dates back to 1999, has been adopted for seismic hazard analysis; it lists about 4900 earthquakes with maximum or epicentral intensity greater than or equal to 5 during the period 1000–2020. The catalogue is supported by DBMI15, which supplies historical source-derived intensity data points useful for assessing the earthquake parameters of CPTI15.

The parametric–descriptive CFTI5Med catalogue includes more than 1600 earthquakes in Italy and the Mediterranean region from 760 BC to 1997. The catalogue represents the (temporary) landing point of a long-term project that had its first outcomes in 1995, with the publication of the first version (CFTI 1). However, this last version was planned to only include earthquakes that occurred in Italy [111]. Later historical studies [112,113] allowed the catalogue to be extended to cover the Mediterranean region. CTI5Med is aimed at helping researchers to retrieve information useful for analyzing and reinterpreting earthquakes from different points of view (e.g., damage, environmental effects, reconstruction, institutional response, and relocation of settlements). For this purpose, it included some original historical sources, transcribed or printed. The historical sources used for the analysis of earthquakes included individual and institutional testimony, sources on literary and naturalistic erudition, gazettes and newspapers, historiographical studies, oral tradition, epigraphs, scientific reports and field surveys, and macroseismic surveys. However, historical data have also been considered in other fields of earthquake research. For example, historical sources can be examined to learn about urban damage patterns caused by past earthquakes in detail, supplying information useful for seismic microzoning purposes [114]. Primary sources were extensively used to map earthquake effects on urban areas in several Italian localities, allowing damage events to be pinpointed at different levels of spatial accuracy depending on the quality and completeness of the sources [115–121].

### *2.3. Volcanoes*

Historical sources are also required to know the eruptive chronology of the most important Italian volcanoes; in addition to field analysis, historical evidence of volcanic activity over at least the last 2000 years is essential. The history of volcanoes cannot be ignored, as it provides a key to interpreting their setting, as well as a view on future activity.

The most important example is certainly the history of Vesuvius, starting from the eruption in 79 AD. The masterful description of this eruption, which destroyed Pompeii and Herculaneum, by Gaius Plinius Caecilius Secundus (61-11 AD) can be considered the best historical documentation regarding the activities of Vesuvius that has been handed down to us from antiquity [122,123]. The term "Plinian eruptions", currently used in volcanology to describe extremely explosive eruptions, comes from the description of Vesuvius by Pliny the Younger. Again, a subplinian eruption occurred in medieval times in 472. This eruption was described by Marcellinus Comite in *Chronicon*; then, many sources provide details on the destructive eruption of Vesuvius in 1631 [123]. This last eruption was well documented by eyewitnesses such as Manzo [124], Braccini [125], and Recupito [126], who described not only the eruptive phases but also the precursor phenomena, the impact on towns, and the consequences for the population and the volcano setting. The history of the most important Italian volcanic complexes in addition to Vesuvius (Campi Flegrei, Etna, etc.) has been collected and described extensively over the centuries, but a systematic study with an analysis of historical sources and direct field observations is due to seismologist and volcanologist Mercalli in 1883 [127]. The study was developed into the publication *Vulcani e fenomeni vulcanici in Italia* (Volcanoes and volcanic phenomena in Italy). Mercalli first proposed a classification of volcanic and seismic phenomena in the Italian region (e.g., Campi Flegrei, Vesuvio, Etna, Isole Eolie, Stromboli, Vulcano, and Pantelleria e Linosa). Currently, the eruptive history of Italian volcanoes is mainly documented by INGV, which publishes daily updates on its institutional website [128].

## 3. Materials and Methods

### *3.1. General Settings of the Case Studies*

In the following subsections, five case studies in Italy concerning different geohydrological and geological hazards are investigated. All five towns or villages considered (Figure 2, Table 1) have been frequently hit by extreme natural events in the past, and we investigated such events, making extensive use of historical sources. Although the natural processes were repeated over time and many historical documents reflect the hazardous nature of these areas, no correct land use planning was adopted [94]. For each case study, both the research methodology and materials used, and the results obtained are discussed in depth.

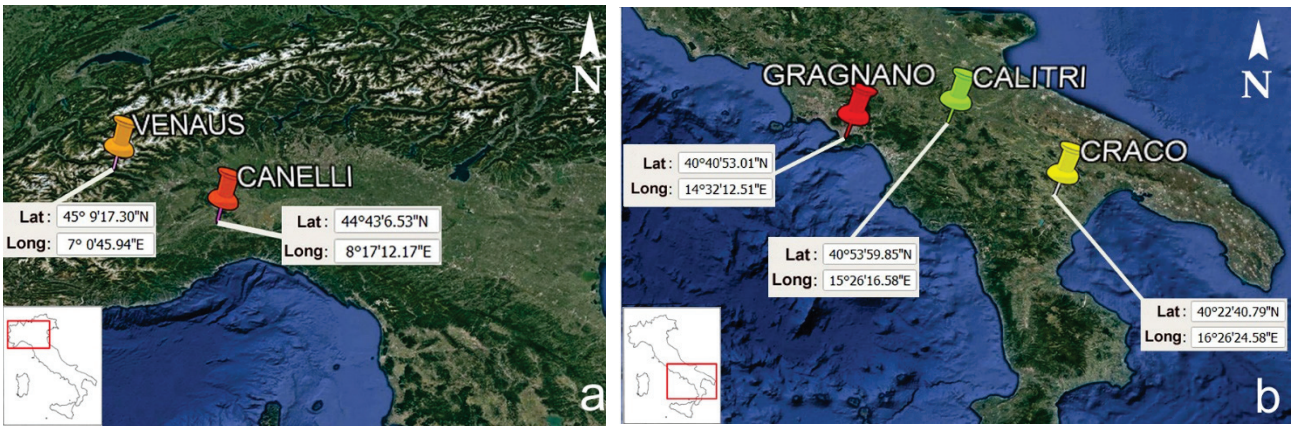



**Figure 2.** The five case studies examined with their geographical coordinates: two in the north (**a**) and three in the south of Italy (**b**) (from Google Earth, modified).

**Table 1.** Case studies: region and province of inhabited centers, and number of inhabitants.

| Town/Village | Region | Province | Inhabitants (2021) |
|---|---|---|---|
| Venaus | Piedmont | Turin | 883 |
| Canelli | Piedmont | Asti | 10,165 |
| Gragnano | Campania | Naples | 28,293 |
| Calitri | Campania | Avellino | 4256 |
| Craco (old town) | Basilicata | Matera | 0 (abandoned) |

### *3.2. Methods*

According to Ibsen and Brunsden [129], historical data can be categorized into four groups: (a) data that directly report the occurrence of natural hazards (e.g., floods, landslides, earthquakes); (b) data that indirectly offer evidence that can support causal or explanatory models (e.g., climatic records); (c) auxiliary surveys that refer to other significant information (e.g., geomorphological surveys); and (d) phenological accounts concerning timing (e.g., changed groundwater levels after rainy periods).

The historical data we considered in our five case studies mainly belonged to groups (a) and (c). The data were used to identify the following: (1) the chronology of the triggers of natural hazards; (2) the features (e.g., magnitude, size) and causes of natural hazards; (3) the toll on human life (dead and wounded); (4) the damage to buildings, infrastructure, and cultural heritage; (5) the environmental consequences, such as primary and secondary effects of earthquakes; (6) the relationship between built-up areas and hazardous areas over time; (7) the transfer of urban areas due to the hazard; (8) consolidation works and their efficacy over time.

To shed light on these aspects, we carried out studies referring to documentary and ichnographic sources derived from (1) State archives, (2) historical archive of the National Department of Civil Protection, (3) municipal archives, and (4) archives of research institutes.

As regards the State archives, they are located in each provincial capital, with about 100 offices being scattered throughout the Italian peninsula. The role of these archives is to safeguard and make the most of documentary heritage and to ensure its public use. They conserve documentation produced by the central and peripheral administrations of the pre-unification states and the archives of the peripheral administrations of the unitary state [130]. In our study, we searched for and analyzed material related to documentation produced by Commissariato Civile per la Basilicata (CCB), preserved at the National State Archive of Potenza, the chief town of the Basilicata region. CCB was a body established by Basilicata Law No. 140 of 31 March 1904. It had a role in the planning and building of public infrastructure in Basilicata, including construction aimed at consolidating the towns affected by slope instability, in an attempt to mitigate the local geohydrological risk [131,132].

The second archive analyzed was Archivio Storico Nazionale del Dipartimento della Protezione Civile (National Historical Archive of the Civil Protection Department) in Rome. The documents were consulted before the historical archive was acquired by Archivio di Stato di Roma (State Archive of Rome). The collection amounts to about 15,000 documents related to disasters that have occurred in Italy since 1908. The archive grew thanks to several acquisitions from other bodies that were responsible for civil protection in Italy before the establishment of the Civil Protection Department of the Presidency of the Council of Ministers in 1982 [133].

The third archives we considered in our research were the municipal historical archives, the documents of which are recorded following a standardized methodology fixed toward the end of the century [134] by a circular by the Ministry of the Interior. These documents are categorized under 15 topics. Researchers interested in studying natural hazards usually focus their efforts on two main subject categories: X, Lavori Pubblici (Public Works), and XV, Pubblica Sicurezza (Public Safety). Research on the five case studies discussed in this article also focused on these two categories.

The fourth repository we analyzed was the historical archive of the IRPI-CNR. In particular, the historical archive of the IRPI of Turin contains over 120,000 unpublished documents concerning landslides and floods that have occurred in the basin of the Po River (the longest river in Italy) since 1800. For some areas, such as the Piedmont region, the available documents date back to the 1700s.

The documents largely consist of descriptive reports following technical inspections, declarations of public disasters, municipal resolutions, reports of instability and damage, field surveys, requests for subsidies, and so on. Much information on topics of interest is included in projects accompanied by floor plans, reports of direct testimonies, interviews, and black-and-white or color photographs. The collection of this documentary heritage was possible thanks to a long search carried out in numerous archives, such as state archives, prefectures, civil engineering offices, municipal archives, and archives of associations and private citizens. To safeguard the documents and make them available to researchers for faster consultation, they were all scanned and converted to Portable Document Format (PDF) files in 2011. Part of the documentation was also included in a relational database for the easier searching and consultation of historical records [135]. For the case studies analyzed in this article, we made extensive use of reports on the occurrence of natural hazards, descriptive reports on post-event inspections, municipal resolutions on remedial works to be carried out, descriptions by competent territorial authorities, maps of the affected areas, and photographs.

Beyond the original documentary records preserved in the public archives, we also considered printed sources, such as field surveys, monographic studies on natural hazards, historical cartography, local historiography, and newspapers. The latter were especially useful for identifying the chronology of natural phenomena and related damage.

In the analysis of natural phenomena and their impact on the built and natural environment, documentary sources from bodies with a public function (e.g., municipalities, civil engineering) were favored. These records usually guarantee higher quality and more

complete information. Furthermore, to both ascertain the reliability of the information retrieved and ensure data completeness, we performed cross-correlation analysis on different historical sources. Overall, for the analysis of the five case studies presented here, the historical sources taken for reference span from the 17th to the 19th century. The next five sections describe, for each locality, specific aspects of the historical records used.

## 4. Results

### *4.1. Belbo Stream and Its Floods in Canelli Town (Northwestern Italy)*

Canelli town, with about 10,400 inhabitants, is located on the valley floor of the Belbo stream (Piedmont—Asti province), a right tributary of the Tanaro River, at an altitude of 155 m a.s.l.; the upper part extends over a hilly area that reaches up to 251 m.

The earliest historical information on flooding originated from the Belbo along the valley floor dates back to the mid-16th century [136]. The large municipal area of Canelli that borders the riverbed of the Belbo has been flooded several times; leaving aside the periods for which the information is incomplete and sometimes difficult to interpret, and considering only from 1800 to the present day, the concentric area turns out to have been inundated at least 17 times, 9 of which were particularly severe. The last disastrous flood occurred on 5 November 1994.

Like almost all inhabited centers, the old nucleus developed in the morphologically higher area, sufficiently distant from the riverbed, especially on the left slope of the Belbo. The valley bottom was still wide in 1852 [137]; the area belonging to the river was occupied exclusively by fields and pastures. The only historical additions were a road bridge that connected the two sides for centuries and the Alessandria–Bra railway, inaugurated in 1865, with the associated embankment and bridge upstream of the town. In 1880, on the right bank, the house closest to the watercourse was about 170 m away (Figure 3a) [138], while on the left bank, most of the houses along the main road were about 120 m from the riverbed, apart from two buildings that pushed toward the stream at a distance of about 50–60 m.

Two violent floods at the end of May 1879 and on 30 March 1892, with an overflowing of the Belbo stream, caused serious damage to the houses, small businesses, and workshops closest to the streambed. Over the years, the land on the valley floor that had remained vacant began to be occupied, mainly by craft workshops and houses. In the last years of the 1800s, the Piedmontese economy was transformed with the establishment of a system of large companies engaged in new types of production, such as the modern mechanical and electrical industry. Canelli, for example, became the headquarters of Gancia, a company internationally renowned for sparkling wines and vermouth. The Belbo valley floor gradually became more urbanized, so while the floods of the Belbo previously only involved the fields located on the valley floor, with the progress of urbanization, the first real problems began.

From 1880 to 1933, the town doubled in area from 1.08 to 2.16 $km^2$ (Figure 3b) [139]. Businesses and homes began to appear on the right bank of the Belbo. In May 1926, a very serious flood occurred: over 100 houses in the capital were flooded, some up to a height of 2.5–3 m. There was serious damage not only to residential buildings but also to farmhouses, companies, craftsmen's shops, and infrastructure. After the substantial post-flood interventions carried out along the banks and on the embankments by civil engineers, it would have been optimal to choose the areas farthest from the Belbo riverbed for buildings. Conversely, in the period between the two world wars, colonization of the territorial strip next to the riverbed of the Belbo continued at a rate of about 9 hectares per year. After a particularly rainy period, on 4 and 12 September, two very serious floods severely affected the economy of the little town. On 4 September, the Belbo stream flooded, overcame the banks, and invaded the whole concentric area on both banks, with heights exceeding 2 m. Several houses collapsed, and there was one casualty. In addition, in this case, the damage to commercial and industrial activities was serious, as many cattle

drowned, the wells of the aqueduct were clogged, and telephone service and post offices were destroyed. Other infrastructure for public use suffered severe damage.

An exceptional flow rate of about 1100 $m^3/s$ was estimated for the Belbo stream. Only 8 days later, incredibly, another great flood occurred in the Belbo. The water invaded the town again and, although reaching a lower level (70 cm less than the level reached 8 days before), advanced with greater violence, causing greater damage than the previous flood. A total of 70 hectares were flooded [140]; in total, 18 houses were destroyed, and 97 were damaged. Damage was estimated at 1 billion and 300 million lire (equivalent to EUR 25 million today). The waters of the Belbo flooded the town again on 11 February 1951 [141] and 10 November 1951; on the latter occasion, the cost for restoring public works and repairing the damage to individual buildings was estimated at EUR 15.5 in today's currency ("Report on the damage of the flood of 10 November 1951"). Despite these very serious events, the urban expansion of the town did not stop; rather, it continued. The built-up areas increased from 4.3 $km^2$ in 1951 to 6 $km^2$ in 1966, at a rate of 11 hectares per year. Historical research also includes two minor floods of the concentric area of Canelli on 10 April 1957 and 30 August 1968 caused by tributaries of the Belbo. However, nothing compared to the events of 2 November 1968. In Canelli, a torrential flood, with a flow of about 300 $m^3/s$ and a duration of 14 h, which was only partially contained within the previously built defense works, caused very serious damage. Occupying a large swath of the valley floor, 10 industrial, 170 artisanal, and 143 commercial companies were affected. The damage to public assets amounted to at least 380 million lire [142] or more than EUR 7 million today. Flooding originated from the Belbo also involved some side canals [140].

Massive works carried were out along the valley floor in the post-flood periods: robust walls, ripraps, and embankments were built upstream and in the concentric area. By the 1970s and 1980s, the last areas of the Belbo River still remained undeveloped. From 1966 to 1991 (Figure 3c,d) [143,144], the built-up area increased from 6.05 to 9.41 $km^2$ at an annual rate of 13.4 hectares per year, greater than that during the period 1951–1966. In particular, upstream of the main bridge on the hydrographic right, just behind the riverbed, a large warehouse was built at the historic Gancia Winery, while on the left bank, several houses were built not far from the stream.

In this urban situation, the great flood of 5 November 1994 occurred (Figure 4), the most serious in the city to date. The floodwaters of the Belbo broke through the railway embankment at the entrance of the town and poured into the town using the main artery as a means of outflow.

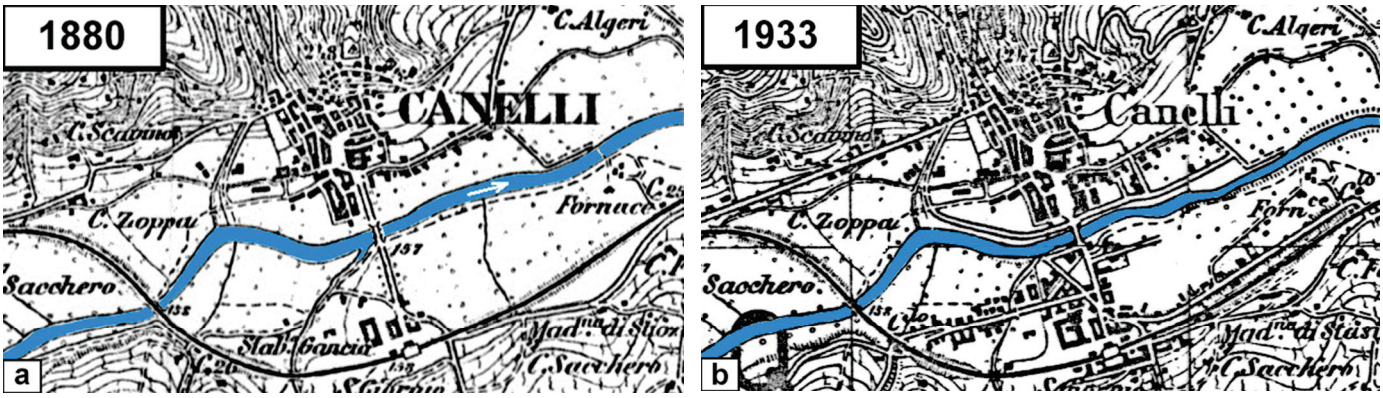



**Figure 3.** *Cont.*

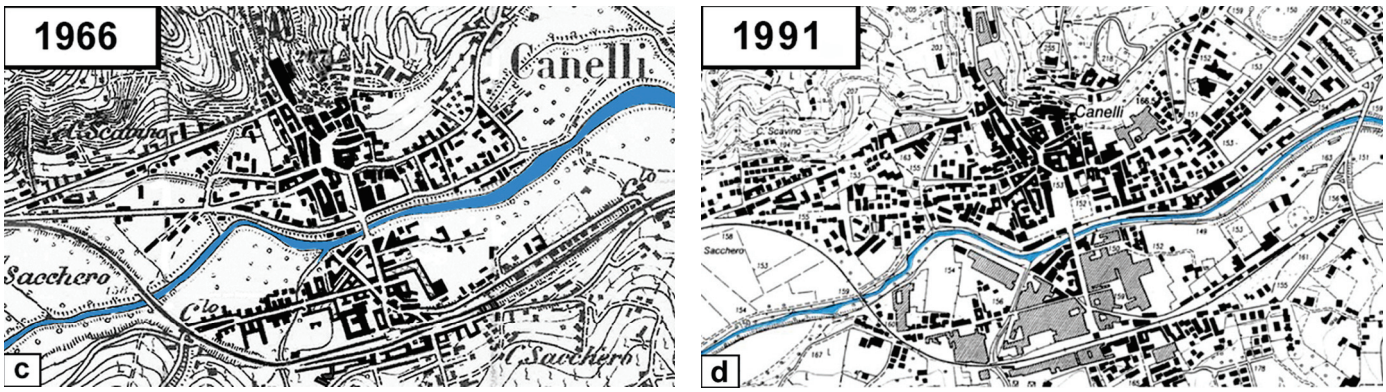



**Figure 3.** Historical reconstruction of Canelli's urban development from historical maps: (**a**) 1880 [138], (**b**) 1933 [139], (**c**) 1966 [143], (**d**) 1991 [144]. The Belbo River is indicated in blue. North is up.

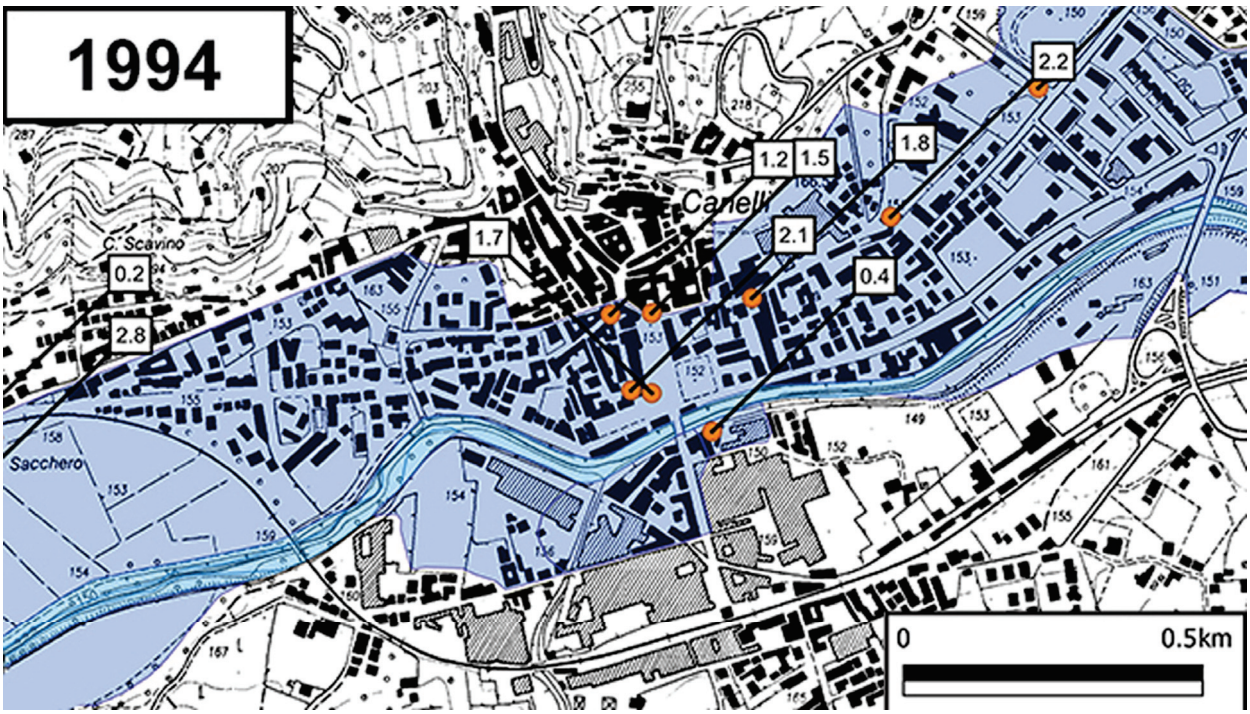



**Figure 4.** Canelli, 5–6 November 1994, with superimposition of area flooded in November 1994 and relative heights (meters) reached by water at ground level [144]. North is up.

Witnesses reported that the water breaking through the railway embankment caused a sudden wave of more than 3 m (Figure 5a). Two inhabitants of buildings located near the breakthrough left their homes, were hit by the water, and drowned. There was also a third victim. The water transported and deposited sediments, floating material, and debris of all kinds in the inhabited areas. The embankment wall slowed the return of floodwaters into the riverbed. Despite the effects of gravity, in the central Piazza Cavour, a comparison of the height of traces left on buildings during the event and the level reported on a plaque referring to the flood of 4 September 1948 shows that the traces associated with the 1948 flood (2.06 m) are 69 cm higher than those from 1994 (1.37 m) (Figure 5b). It is true that the floodwaters in the town did not reach the historical heights of May 1926 and September 1948 (Figure 6), but on such a heavily urbanized valley floor, the damage was proportionally much greater.




**Figure 5.** (**a**) Canelli town center on Monday 7 November 1994. Dark flood mark on perimeter wall of a house in Via Solferino is evident (photo by Canelli Municipality). (**b**) Helicopter view of eastern part of city. Silty clay deposits left by the Belbo on flooded valley floor are evident (photo by F. Luino).




**Figure 6.** Canelli: In Cavour Square, marble marker of famous flood of 4 September 1948 compared with water level (meters) on 5 November 1994 (photo by F. Luino).

*4.2. Forced Abandonment of Craco (Basilicata, Southern Italy)*

The (abandoned) historical center of Craco (Figure 7) is in the Basilicata region (southern Italy). The region, which can be seen as an open-air laboratory for multidisciplinary and interdisciplinary research, is prone to earthquakes and landslides, which have affected towns and cultural heritage over time [145,146].



**Figure 7.** Overview of Craco historical center, now abandoned (photo by F.T. Gizzi).

Craco, among the most famous and iconic "ghost towns" in Italy and the best known on an international scale, sits at about 390 m a.s.l. and extends over a NW-SE oriented ridge, delimited by two streams. Along the slopes of the ridge, allochthonous Cretaceous–Oligocene units are in contact with conglomerates, sands, and clays of Pliocene age. The northeastern slope of the ridge is affected by numerous landslides, some of which develop along the entire slope, up to the bottom of the valley. The southern slope is also marked by instability phenomena, including the Centro Storico (historic center; CS) and Convento (convent; CV) landslides, responsible for damage to buildings and infrastructure, with the subsequent transfer of the town [147].

The first notice regarding the activity of the CS landslide dates to the last decades of the 19th century, when a mass movement was recorded in the southern part of the town [148]. The reactivation of both the CS and CV landslides continued at different rates until the end of the 1940s. Following the landslides, several consolidation works were planned [149–155].

After a period of apparent inactivity, a football field was built on the body of the CS landslide, downstream of the state road surrounding the town [156]. However, the field was destroyed due to reactivation of the CS mass movement [156].

In December 1963 (Figure 8), both landslides reactivated, leading to the technical and administrative transfer procedures of the town [157,158]. The CS landslide reactivated again in January 1965, with partial collapse of the retaining wall built to support SS103 and significant damage to buildings (Figure 9). Because of the 1963 movements, after a field survey performed in early 1964, the technicians of the Italian Geological Service suggested transferring the town: "The phenomenon [landslide] is currently in such an advanced stage as to exclude any possibility of slope consolidation and, consequently, of consolidation of

the town. Therefore, it is necessary to prepare the gradual transfer of the latter [Craco] to a more suitable area" (translated from Italian) [156].

Two possible areas were recommended: the first (Sant'Angelo) was close to the historical center, but with limited extension, and the second was located a few kilometers away (Peschiera) [156]. At first, the municipal administration approved the transfer of the town to the latter site. However, the identification of a transfer location changed in the following years. The technicians of the Geological Service carried out another field survey in June 1964 and suggested transferring the town to the site closer to the historical center [159]. This technical opinion was seen as supporting the widespread discontent among the population due to the socioeconomic disadvantages that would have resulted from transferring to the Peschiera site. Therefore, the municipal administration revoked the decision taken a few years earlier and ratified the Decree of the President of the Republic on 23 April 1965, No. 800, defining that the transfer should take place both at the site close to the historical center and at the site far from it [160].


CRACO
Largo
Machiavelli
Via Mario Pagano
Via M. Pagano
Largo
Alighieri
Largo
Vittorio Emanuele II°
Largo
Garibaldi
Largo
Bandiera
Via
Monte
Via
Fico
Via Cavour
Str. Com. Craco
Via Melchiorre
del Fico
d'Agri
Via S. Maria Giampietro
Via
Val
Risorgimento
Umberto I°
Ht 103
Via Matteotti
Via Nazionale
Via Vittoriana
Via Garibaldi
Via Roma
Via Marconi
Via Principe
Via Cappelli
Via Fontanelle
Via Mazzini
Via Giuliano
Via Fontana
Via Cimitero
Via Cappuccini
Via Cappuccini
Via Cappuccini




(**a**) (**b**)

**Figure 9.** Effects of CS landslide reactivation in Craco in January 1965. (**a**) Area close to the retaining wall, damaged and partially collapsed due to landslide movement; (**b**) same areas with damage to residential buildings in foreground. A counterfort sustaining a building can be seen, indirectly suggesting old movements of the landslide [162].

From this depiction of the events, two observations can be made. The first remark is that the inhabitants and institutions did not consider the repeated mass movements, with the effects that they caused, as a "warning" sign; on the contrary, the areas affected by reactivation were, in some cases, subject to reconstruction. Furthermore, the urban expansion of Craco toward the southern areas of the relief continued in the 19th and 20th centuries even if the retroactive nature of the CS landslide should have advised against this choice. In fact, the urban development of the historic center of Craco can be divided into three main phases [147,163]: (1) the first settlement nucleus (11th–14th centuries), which developed around the Norman Tower; (2) the expansion phase between the 15th and 18th centuries; and (3) the expansion phase that can be dated between the 19th and 20th centuries, a period during which landslide phenomena (in particular CS), despite having largely shown signs of their activity, did not discourage urban development in areas at risk.

The second observation is that, in most cases, the consolidation works were designed and carried out only after the landslide had occurred, thus highlighting the lack of resolute institutional action aimed at preparing an organic plan to try to mitigate the hydrogeological risk in "peacetime" (prior to paroxysmal phenomena). Furthermore, some superficial infrastructure interventions were carried out by technicians and/or workers, such as the construction of retaining walls at the end of the 19th century and a sports field on the landslide body, which certainly contributed to the reactivation of the CS landslide in the late 1950s. There was also no close convergence of actions between national and local bodies to coordinate an organic plan for risk mitigation. Additionally, some of the preventive actions were met with resistance by the inhabitants, who were reluctant to follow the ordinances (e.g., closing of the tanks), thus making efforts to reduce risk somewhat useless.

All of this must be added to the lack of in-depth knowledge of the characteristics of mass movements (particularly the CS landslide), such as the depth of the sliding surface. These considerations can make us hypothesize that the settlement did not acquire resilience over time but gradually lost it, thus facilitating the decision to transfer. As for the latter, during the initial phase (mid-1960s), there was a divergence between the topographical and geological requirements of the new site, favored by the municipal administration, and the socioeconomic ones, claimed by the inhabitants. Therefore, the area initially selected for the transfer was considered inadequate by some of the citizens who were worried about the economic impact on their families. Later, the local government accommodated the citizens' needs and supported the transfer of Craco to two places at different distances from the unstable village. This change in policy, certainly dictated by political opportunity, was also conditioned by two socioeconomic ideas about the development of the area. The first

idea was focused on a paradigm shift in the economic perspective of the inhabitants of Craco to select a place (Peschiera) closer to a developing industrial area (areas of Pisticci and Val Basento), while the second idea considered the historical rural disposition of the inhabitants who emphatically rejected this paradigm shift and vigorously asked for a new settlement closer to the location of the owned land. Obviously, the change in perspective affected the timing and planning of the town transfer.

### *4.3. Gragnano Debris Flows (Naples District)*

Gragnano, in the district of Naples, is almost entirely surrounded by carbonate reliefs that form the first branches of Monti Lattari. This is a geologically unstable area because of its pyroclastic deposits from millennial eruptions of nearby Vesuvius. Fast mudflows in pyroclastites (or, better, volcaniclastic debris flows) from Mount Pendolo have occurred in this area. In Italian, "pendolo" means "pendulum"; it is a toponym that, as has been remarked, "says it all because of its swings once to Pimonte and again, but mostly, toward Gragnano" (translated from Italian) [164].

On 21 January 1841, a debris flow from Mount Pendolo, at that time also known as Mount Suppezza, devastated the crops, ruined some houses, and killed three people. During the night, after two more victimless landslides, a catastrophic mudflow battered "rione Trivoncello", destroyed houses, and buried 103 people. Among them, only 6 were taken out of the rubble alive, although 1 girl did not survive, so the overall number of deaths was 101.

As is often the case with great catastrophes, especially very ancient ones, there is no agreement on the figures; some sources at that time spoke instead of 113 victims. Despite the limited geological knowledge available at the time—the reports and descriptions of hydrogeological instabilities were provided by people other than geologists—at least one contemporary author shows an indisputable awareness of the causes of the phenomenon. Camillo Ranieri wrote that the mountains above Gragnano (Figure 10) are "of calcareous spar mixed with calcium carbonate. The Vesuvius eruptions have blanketed them of layers of lapilli [...]. The heavy rains, especially last January, saturated those soils and lapilli that had abundantly accumulated on limestone rock, and because they could not penetrate into the bowels of the mountain, all materials which blanketed them lost balance: they fell precipitously down for both steepness of the mountain, and enormous weight in comparison with volume, and, overcoming all obstacles, crashed many houses which were unstable and not newly built" (translated from Italian) [165].



**Figure 10.** Two Gragnano landslides triggered in 1841: Mulino Gottoli (**left**) and Trivioncello (**right**) [163].

Ranieri's final reflections are based on strong pessimism regarding the geologic stability of that area: "further rains could do repeat the disasters", he wrote. This is a cautionary tale that came about with awareness of the weakness of those slopes, an admonition that—as often happens with the permanent loss of historical memory of previous disasters—was unable to create widespread awareness, through collective consciousness, of avoiding, especially in the following century, the anthropization of land with a high degree of risk.

It should be remembered, however, that not all historical sources agreed that the catastrophic event was a pyroclastic flow. Geological science still took a pioneering approach in Southern Italy in the 19th century, thus, in an article published at the same time, another architect [166] questioned this point of view. His argument was that the main cause of that crash was determined to be some unspecified "electrical currents coming from the depths of the mountain"; therefore, his conclusion was that there would be no risk in the future.

The catastrophic magnitude of that event could not but leave a mark, and in fact, other writers, in the following decades, pieced together the event scenario [167–171]; at the beginning of the next century, Roberto Almagià [60], the author of a famous treaty on landslides in Italy, recalled that tragedy. However, all these publications and all these witnesses were unable to settle, in the collective consciousness, awareness of the high-risk level of that territory.

To confirm the high-risk level of that area, it should be noted that most of the historical sources above, in addition to the event of 21 January 1841, mentioned a previous episode, the debris flow of 20 January 1764, which destroyed "Rione Bagnulo" in the same municipality, causing the death of 42 people.

More recently, similar events have been reported in scientific work, especially after a similar phenomenon occurred in the neighboring Sarno in May 1998, killing 160 people. The clamor after that disaster was an incentive for carrying out new research to provide a complete picture of debris flows in Campania over the centuries [87,172–174]. These new studies identified another event like what occurred at Mount Pendolo as long ago as October 1540, in the locality of Congiaria. In contemporary times, further debris flows occurred on 20 August 1935, on the east side of the village (contrada Tavernarola), and on 17 February 1963, destroying a farmhouse and burying four people.

Despite this centuries-old sequence of events, and despite the evident risk exposure, the period that began after World War II, under the pressure of significant demographic growth, appears to be characterized by a sort of collective removal of the problem. Gragnano's urban development proceeded in a confused way: wild anthropization characterized by new settlements, usually built with little attention to the geolithological balance of the land. The most emblematic event occurred on 2 January 1971: Upstream of the hotel La Selva, built a few years earlier in a zone exposed to landslide risk, an excavation was carried out to build a house (Figure 11) [175]. After two days of torrential rain, a 7000 $m^3$ mudflow collapsed from the altered hillside and destroyed the hotel and four houses. Six people died, and a wedding procession headed to the hotel was almost involved. But this was not the final event: other mudflows, although much smaller, occurred, including one in February 1987 on a highway and one on 11 January 1997, which destroyed a stable and killed livestock.

### *4.4. The Memory of Earthquake-Induced Instability in Calitri*

The backwards history can start from the last strong seismic event, which struck Southern Italy on 23 November 1980 (Mw 6.9; Io = X MCS) (Figures 12 and 14). The earthquake caused serious damage in almost 800 localities; a total of 75,000 houses were destroyed, and 275,000 were severely damaged. About 3000 people were killed, and 10,000, injured. Fifteen municipalities throughout the Avellino, Salerno, and Potenza provinces were nearly totally destroyed with MCS/MSK level I $\geq$ IX intensity (Figure 12) [13].



**Figure 11.** La Selva Hotel partially destroyed by mudslide of 2 January 1971 [72].

The effects on the natural environment were also devastating, including primary effects such as superficial faults and secondary effects (sensu Michetti et al., 2007) [176] such as landslides (200 were identified), fractures in the soil, hydrological variations, and liquefaction phenomena [177,178].

Calitri, a small village with about 5000 inhabitants in the hinterland of Irpinia in the southern Apennines (Campania region) suffered VIII MCS/MSK and ESI-07 level damage [13,178,179], with six fatalities (Figure 14).

In addition to the damage to buildings, there were multiple environmental effects, such as liquefaction phenomena, ground fractures, and significant gravitational phenomena [177,180,181]. Among the latter, particularly devastating was the extensive landslide movement, approximately 850 m long and about 100 m deep, classified as slump-earth flow, which mobilized 23 million $m^3$ of land, with destructive consequences for the houses in the historic center [180,182–184].

Similar to what happened after the 1980 earthquake (Figure 13), the village had already been affected in the past by sliding phenomena triggered by earthquakes that occurred in 1694, 1805, 1851, 1910, and 1930 in the southern Apennines [179,185,186].

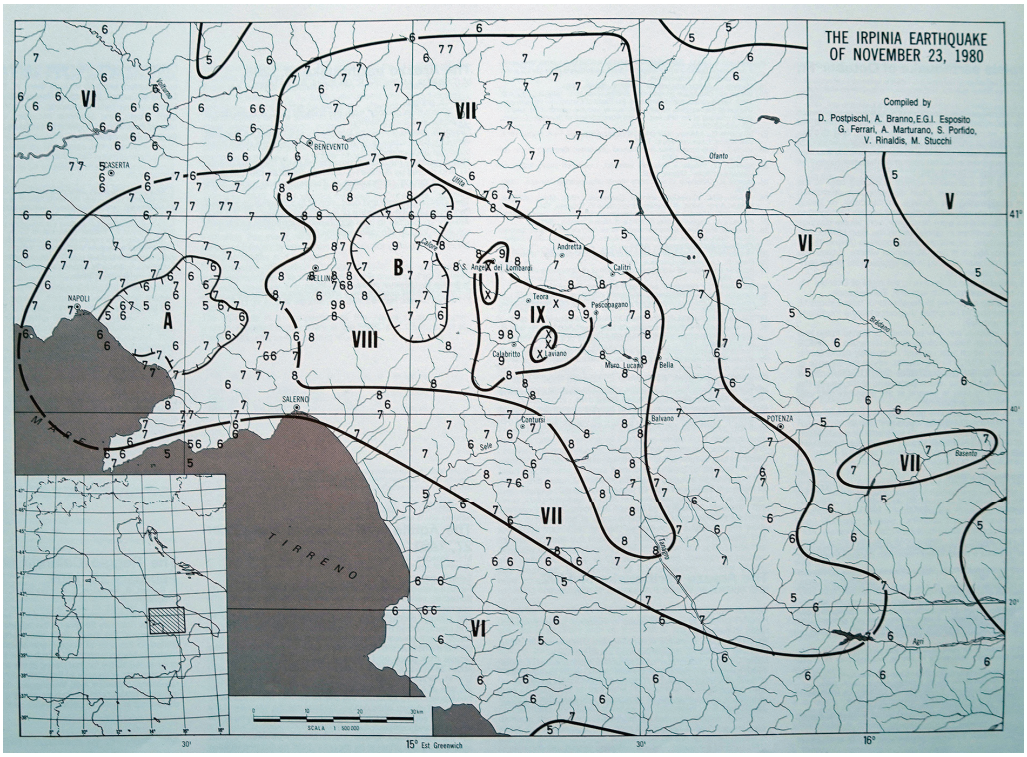



**Figure 12.** Isoseismal lines of 1980 earthquake [13]. Roman numerals (X–IV) indicate the intensity value on the MCS scale. The area marked by the letter (A) corresponds to the Vesuvian attenuation area, instead the letter (B) shows the attenuation area up to two degrees of intensity. Arabic numerals indicate the intensity on the MCS scale at individual locations. North is up.



(**a**) (**b**)

**Figure 13.** Calitri (Avellino province): effects of landslide in the historic center (Courtesy of the "Pro Loco of Calitri"): (**a**) via Matteotti, parallel view of the niche of the landslide triggered by the 1980 earthquake; (**b**) via Matteotti, angular view of the tilting of the retaining wall due to the landslide movement [187].

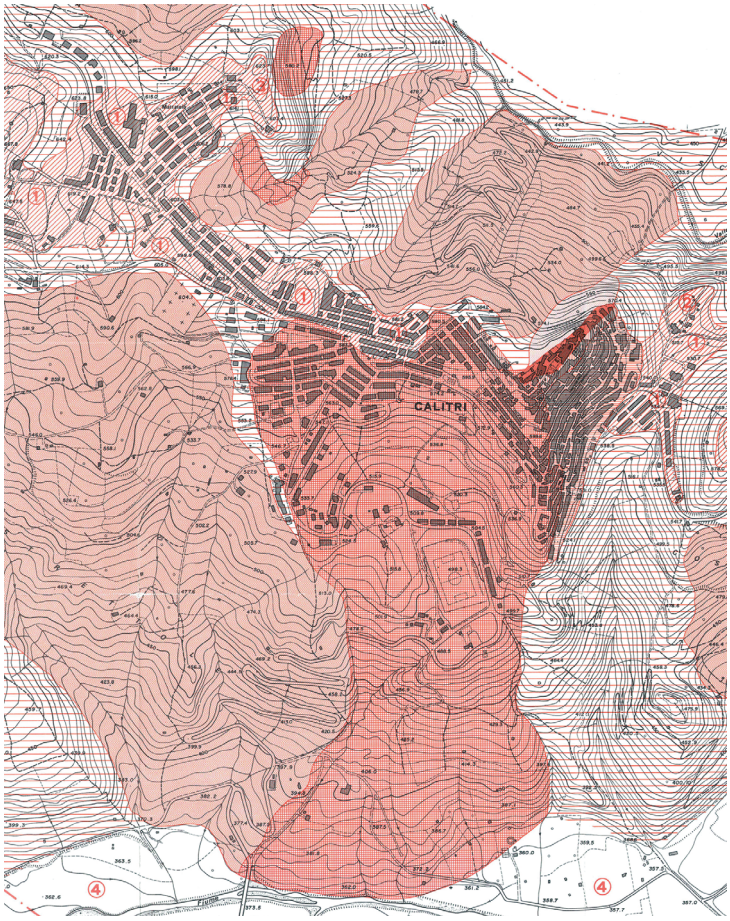



**Figure 14.** Seismic microzonation map of Calitri drawn by Samuelli-Ferretti and Siro [180] for the PFG-CNR immediately after the November 1980 earthquake. "① very good foundation soils; ② moderate foundation soils; ③ bad foundation soils; ④ flat areas with increases in seismic coefficients" North is up.

To understand the evolution of today's landslides, we also need to study what happened in the past, particularly the landslides induced by past earthquakes. Essential to the reconstruction of the process of landslides triggered by earthquakes is appropriately choosing historical documentation contemporary to the seismic events examined. We propose, as an example, significant extracts from original sources related to two strong earthquakes in the southern Apennines: one on 8 September 1694 (epicentral area between the Campania and Basilicata regions: Lat 40.862 Long 15.406) and one on 26 July 1805 (epicentral area in the Molise region: Lat 41.500 Long 14.474). Historical documents are of fundamental importance because they highlight the level of damage not only in the center but also in the surrounding territory, areas that over time could constitute expansion zones to be kept under proper control before being used. After the earthquake of 1694, Calitri, located in the epicenter, was almost completely destroyed, reaching X MCS, with the loss of at least 311 people, as shown by the parish documents of the time (other historical sources report between 700 and 1200 victims).

The earthquake also triggered a landslide phenomenon, which developed from the top of the village, where a castle was located. The movement was characterized by "two very large, very wide, deep openings" (translated from Italian), as an anonymous source of the time described. "At 8… of the fallen September 1694 at about a quarter to 6 p.m. of the Italian clock, … a frightful earthquake made itself felt, shaking the earth for the space of a Creed… The village of Calitri, it is all destroyed, with the churches, houses, and monasteries. The castle of Calitri, situated above a very large mountain in the manner of a

fortress, with bridges, which opened on one side, and fell over the soil, which was below them... In the castle of Calitri, in the two courtyards, two very large openings were made very wide and deep, which make it a great surprise, calculated to be in this village perished about 700 people" (translated from Italian) [188].

The second description refers to the 26 July 1805 earthquake, which mainly devastated the Molise region (Io = XI MCS), with also considerable damage in the Campania region [177,189]. Even though Calitri was located far away, more than 100 km from the epicenter, it experienced the triggering of a large landslide movement, as reported by naturalist physicist G. S. Poli [190]:

"In Calitri's land... on the way to Castiglione, a large piece of land was turned upside down, and in the act of trembling, flames were seen coming out of it... The trees, which had been planted there, sank into the ground as a sign that now you can barely see the tops; and a rustic pagliajo [pile of straw] was completely absorbed in it. The fracture then occurred one mile away from the said land, starting from the Vallone de' Monaci up to the place called the Mountains, extending from East to West for the length of one mile, having the width of five palms. Here, also the land has been furiously upset and undermined, partly absorbed oak trees and almond trees and olive trees, and partly covered and buried them in the same way, which can no longer be seen" (translated from Italian).

The history of Apennine villages such as Calitri is often very complex, since in addition to the natural socioeconomic factors governing development, the role of natural hazards in the territory must also be appropriately considered. In this case, not only hydrogeological instability but also seismic phenomena have played a significant and in some cases even predominant role, and together, they have caused severe damage in the urban context, constrained development, and caused damage to the surrounding natural environment.

Hydrogeological upheaval and seismic hazards can, at times, merge. We must not forget that earthquakes with sometimes very distant epicenters have triggered considerable landslides both within and outside urban centers, which are certainly not negligible contributions to the modification of cultural heritage. Similarly to what happened after the 1980 earthquake, the village of Calitri had already been affected by complex sliding phenomena triggered by earthquakes that occurred in 1694, 1805, 1851, 1910, and 1930.

This is why, when planning the future development of villages, it is desirable to never neglect the historical memory of what happened many centuries ago, which has been passed on to us by detailed historical sources, chronicles, letters, etc. A reading of the recent past can help us understand how much these phenomena have affected people's capacity for resilience and thus their attachment to the territory, even if not always under optimal conditions. Therefore, historical information should represent a systematic approach to obtaining a rich database for the overall assessment of the territorial risk of any technical intervention. This is certainly an important approach, the results of which, in all their complexity, should be provided by administrations to the population as a starting point for responsible and knowledgeable territorial planning.

### *4.5. Debris Flows on Supita Alluvial Fan (Venaus—Turin)*

There are hundreds of historical reports that describe mud–debris flows causing casualties and damage in the alpine basins [93,191]. Often, the predisposing factors are acclivity, debris cover, fractured bedrock, and the presence of unstable boulders along the banks and slopes [192]. The case presented here represents one of many [193] in which the elements of geomorphological and hydraulic risk are merged.

The catchment area of the Supita stream, the right tributary of the Cenischia stream in the middle of the Susa Valley (municipality of Venaus, about 80 km west of Turin), has an average slope of 62% and an area of 2.2 $km^2$, and it develops for about 4.2 km, with an altimetric excursion of over 1500 m between the closing point (720 m) and the highest peak of the watershed ridge (2320 m) located in the northwestern end of the header watershed.

In the terminal section of the basin, the accumulation of debris with significant volume can quickly reach the apex of the alluvial fan due to mud–debris flows [194,195]. The water-

course near the inhabited center flows channeled up to the closing section at the confluence with the Cenischia stream. The distal part of the large fan is blurred with the extensive Cenischia alluvial plain. This includes other contributing factors that recurrently behave similarly to those described and on which there has been detailed research [82,196–199]. The high level of anthropization in the distal and central sections of the Supita alluvial fan obliterates the morphological evidence of torrential dynamics, except for the area close to the apex.

In this area, it is still possible to recognize some secondary channels and elongated lobed shapes parallel to the banks [200]. The "defensive" system is tied to the conformation of the inhabited core, where dedicated spaces for the watercourse are extremely small and undergo alternating mud–debris flows and avalanches [201].

Thanks to the cartographic and iconographic heritage (Figures 15–17), the historical analysis made it possible to identify numerous previous events of debris flow and slope instability that affected the territory of Venaus.




**Figure 15.** Example of historical documents at historical archive of municipality of Venaus from 1714. (**a**) Description and (**b**) detail of territory of Venaus and Supita, extracted from "Carte topographique et militaire du mont Cenis 1821" [202] (last accessed on 25 January 2020). North is up.

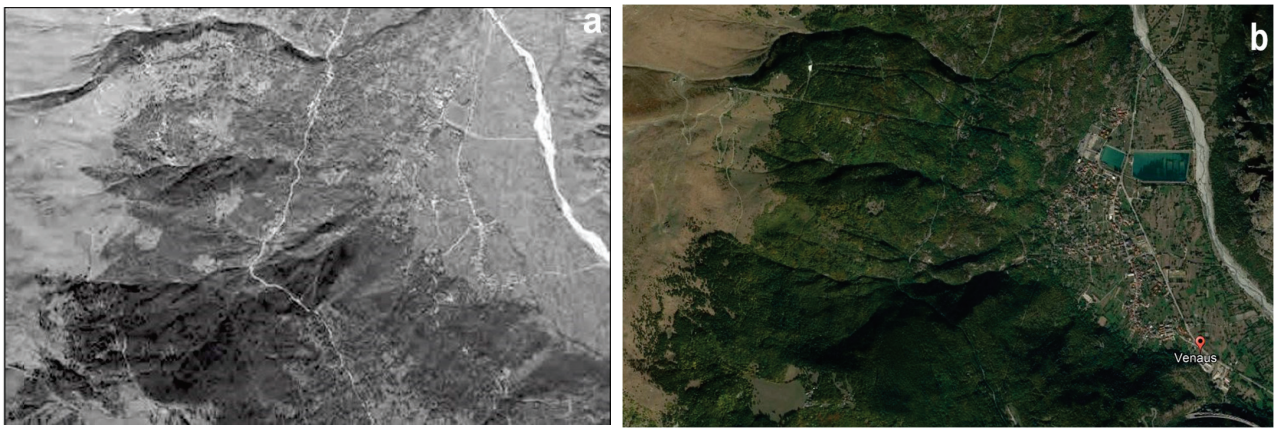



**Figure 16.** Growth of built-up areas in alluvial fan section of Supita stream: (**a**) aerial shot of terminal sector of Supita stream and its alluvial fan in 1953 (Photographies aériennes de la France, Institut national de l'information geographique et forestiere [203]; last accessed on 25 January 2020); (**b**) recent image (Google Earth, 2022). North is up.




**Figure 17.** Effects of May 1977 debris flow (photo: IRPI Archive): (**a**) images of area invaded by debris transported along Supita stream on 29 May 2008; (**b**) aerial view of accumulation in alluvial fan [191].

The main paroxysmal geohydrological and morphological instability events documented for the Supita basin are listed in chronological form in Table 2. In addition to the episodes of debris flow and torrential floods, there are those related to avalanche activity, which historically occurred with high frequency. The SIVA catalogue and the Web GIS of ARPA Piemonte report 11 avalanches that occurred between 1845 and 2020, only 6 of which caused damage.

**Table 2.** Synthesis of mud–debris flows and avalanche events that caused damage in Supita basin. For avalanches, see Web GIS of ARPA Piemonte [204] (last accessed on 20 January 2020). MDF, mud–debris flow; TF, torrential flood; A, avalanche.

| Date | Event | Description | Source |
|---|---|---|---|
| 20–21 May 1728 | MDF | Due to heavy rain on 20 and 21 May, the Cenischia and Supita streams and others transported a large quantity of land and demolished most of the road and some houses, with loss of furniture | Atti delle visite di corrosione per la comunità di Venaus [200] |
| 25 May 1836 | MDF | Clearance of boulder that fell on Moncenisio road in Supita region | Historical Archive of Venaus Municipality |
| 15 January 1845 | A | Civil buildings buried, 6 casualties | ARPA Piemonte Archive |
| 18 January 1885 | A | Civil buildings damaged | ARPA Piemonte Archive |
| April 1904 | MDF | Mass transport along Supita stream, with damage to national road and Mont Cenis; flooded distant land | [205] |
| March 1930 | A | Wooded area damaged; avalanche arrived nearly uphill of Case Costa | ARPA Piemonte Archive |
| March 1934 | A | Avalanche dammed Moncenisio state road | ARPA Piemonte Archive |
| 13–14 June 1957 | TF | Torrential flood of Supita stream with intense solid contribution to fan, damage to crossing and defense works | [200] |
| 19 May 1977 | TF | Supita, powered by three landslides in late evening, partially flooded land in the fan and part of Venaus also due to the undersizing of bridge crossing river | [200] |
| 15 October 2000 | TF | Torrential flooding originated from the Supita stream; at a crossing, outflow surmounted a municipal road; phenomenon also involved a river crossing | [206] |

**Table 2.** *Cont.*

| Date | Event | Description | Source |
|---|---|---|---|
| 29 May 2008 | MDF | At around 7:00 am on 29 May, a significant process of mud–debris flow occurred; after totally obstructing the State Road 25 bridge in Moncenisio, the solid–liquid mixture invaded numerous buildings in the historical center; Supita stream deposit was not contained by retention basin recently built above | [191] |
| 13 April 2008 | A | Mass interrupted one road | ARPA Piemonte Archive |
| 15 December 2018 | A | Avalanche repeatedly hindered transit along main access road to Colle del Moncenisio, destroyed an extensive area of wood, and stopped in the canals about 200 m from some houses below | [195,207] |

## 5. Discussion

The five cases presented in this paper cover the most widespread geological and geomorphological phenomena in the Italian peninsula: floods, landslides, debris flows, and earthquakes. All cases provide evidence showing how events that occurred repeatedly in the same places over time were not appropriately considered in land use planning; we could dramatically state that history has taught nothing.

Take, for example, the case of Canelli, a classic town located near a waterway on the valley floor that has expanded over the decades despite recurring floods (average of one flood every 24 years for the past 160 years) sending unmistakable signals about where not to build. In addition, despite the damage caused by floods, the city administration continued to shortsightedly grant building permits in areas that had been flooded. It always relied on expensive river works that were carried out in post-flood months; unfortunately, for citizens, such works always create an extremely dangerous false sense of security. In Canelli, after the last very serious flood occurred in 1994, a water retention basin was built upstream of the town, with an area of 39 hectares; it is expected to mitigate but certainly not drastically reduce problems associated with future flooding. If the municipal administration had practiced good urban planning over the decades, could the recent floods, and particularly the 1994 flood, have caused less damage? In other words, if they had not built new buildings in the areas closest to the Belbo riverbed and in the most morphologically depressed areas, could much damage have been avoided? Historical mapping and data from retrospective research were used to answer this simple question. By superimposing the inundated area on the Belbo valley floor in November 1994 over the oldest maps, it can be seen that it increased from 0.03 $km^2$ hypothetically inundated in 1880 (20.35% of the total urbanized area) to 0.09 $km^2$ in 1933 (40.35%), 0.25 $km^2$ in 1966 (40.86%), and up to 0.40 $km^2$ in 1994 (39.86%) (Figure 18). Since the proportion remained practically the same from 1933 to 1994, we can say that during this period of construction in Canelli, almost every second building was located in a potentially flood-prone area, despite the repeated severe flooding in the town during the same period.

Canelli is a typical small Italian town located on a valley floor where the acquisition of pertinent riverine areas, not supported by adequate basic knowledge, has inevitably led to the suffering from the effects of river activity, with consequences that are all the more catastrophic the more they are unforeseen. While under ordinary conditions, hydraulic defense works can guarantee a good level of safety, because they can control river processes and limit their effects, it is primarily during extreme events that the rapidity and violence of these processes often disrupt the implemented interventions, leaving the population completely unprepared. A clear example of this is the catastrophic flood of November 1994 in the Canelli area.

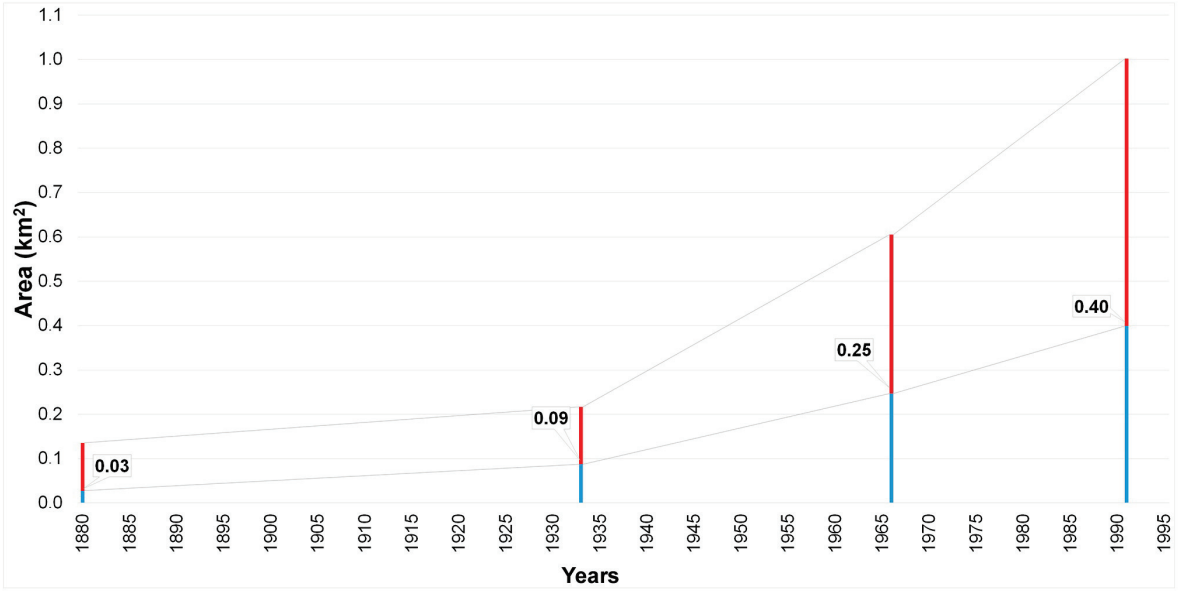



**Figure 18.** Increased urbanized area in Canelli (sum of blue and red), measured on topographical bases of 1880, 1933, 1966, and 1991. Blue indicates percentage of urban area that would have been flooded in those years as extensively as in November 1994.

There have been erroneous land planning choices dictated by the local administrators' need to acquire new land to be urbanized without ascertaining its hazards in advance, despite the rich historical documentation available for such an assessment being evident. Above all, they almost never turn to river geomorphologists, only to hydraulic engineers, who have a softer and more tolerant approach to the problem of land loss. Particularly surprising is the obstinacy and obtuseness of administrators who continue to build in areas that were repeatedly flooded in the past, trusting in mitigation works, as well as fate and in the welfare state. The proposed investigation methodology, applied to the Canelli territory and adaptable to other territorial situations, is based on consultation of historical documentation, consisting of bibliographic, cartographic, and archival material; it represents a first basic approach to gathering the knowledge of areas exposed to flood risk but should be integrated with geomorphological investigation and hydraulic verification for a more precise delimitation of areas that could be flooded following a reference flood [208].

Also interesting is the case of Craco, in Basilicata. From a methodological point of view, two main deductions can be made from this case study. First, the results of the research underline the importance of extensive, in-depth, cross-correlated historical investigation. This is useful to identify both the sequence of occurrence of landslides, and their effects on the built environment and the actions implemented by institutions. In this case, examining historical sources helped to show the weaknesses in the management of the risk chain. In this view, a retrospective analysis can be useful to identify possible actions to be taken to increase the resilience of small settlements and improve the decisions regarding their fate (transfer or in situ reconstruction) in case of disasters triggered by natural hazards.

Regarding risk management, the study highlights the need for close synergy between central and local institutions. Furthermore, the research suggests actively involving the population by making people aware of territorial risks and stimulating the use of adaptation strategies. Regarding post-event management and the possible transfer of inhabited areas subject to natural hazard risk, conducting an in-depth socioeconomic analysis of the territory is essential, as well as considering the old, hazard-affected settlements as places where the identity of local communities is strongly rooted. Furthermore, there should be an emphasis on the valorization and rehabilitation of "ghost towns" throughout Italy. In-depth studies would increase our knowledge of such places, as a preliminary phase in their valorization. In fact, Craco, along with other towns abandoned after extreme natural

events, can be considered an open-air laboratory through which the population, especially young generations, can be informed about natural and geological risks of the territory in which they live.

As for Gragnano, historical research has shown the occurrence of numerous landslide events since ancient times. The pyroclastic coverings deposited on the surrounding mountains as a result of the eruptions of nearby Vesuvius have always made the area particularly fragile. Rapid flows of loose pyroclastites, which are often triggered by violent rainfall events, are widespread throughout the vast area surrounding Vesuvius. The inhabitants of that area remember what happened in nearby Sarno, where, on 5 May 1995, several debris flows caused enormous devastation and the death of more than 160 people. In the Gragnano area, the first known events of this type date back to 1540, and the first catastrophic event was in 1764, when 42 people died. A much more serious event occurred on 21 January 1841, when several landslides killed over 100 people. It should be remembered that these events, although very serious, occurred in a territory that was still scarcely anthropized. The scarce historical memory of what happened, the rapid economic development of that area (Gragnano is world-famous for its numerous pasta factories), and a lack of territorial planning along with a marked increase in population have greatly increased the level of risk. In the decades that followed, further disastrous events occurred, the most significant of which was a landslide in 1971, which destroyed a hotel and killed six people.

Aspects similar to those of Canelli can be considered for Gragnano. Despite the high level of hazard in the area and despite the numerous catastrophic events that have occurred there, safety measures have been sporadic and often ineffective. The loss of historical memory became evident in the second half of the 20th century, when under the impetus of economic growth (Gragnano became world-famous for its pasta production), the extensive use of cement was not compatible with the landslide risk to which it was subjected. Unlike the situation in Canelli, in Gragnano, it is not only a matter of wrong urban planning choices but also an almost total absence of planning: houses, workshops, and industrial sheds are being built illegally. The widespread illegality has been only partially remedied in recent years with the demolition of a few unauthorized buildings by the police. In addition, at least until recent years, no hazard map of the municipal territory has been drawn up; no warning system has been created based on the identification of rain thresholds; no channeling and drainage systems have been built, nor structures to reduce the speed of water.

The history of Apennine villages such as Calitri (Avellino province) may seem even more complex, since in addition to the natural socioeconomic factors governing development, the role of natural hazards within the territory must also be appropriately considered. In this case, not only the geohydrological processes but also seismic phenomena have played a significant and in some cases a predominant role, and together, they have caused severe damage in the urban context, constrained development, and affected the surrounding natural environment.

Geohydrological processes and seismic phenomena can, at times, merge. We must not forget that earthquakes with sometimes very distant epicenters have triggered considerable landslides both within and outside urban centers, which are certainly not negligible contributions to the modification of cultural heritage. Like what happened following the 1980 earthquake, the village of Calitri had already been historically affected by complex sliding phenomena triggered by earthquakes in 1694, 1805, 1851, 1910, and 1930.

This is why, when planning the future development of villages, it is desirable to never neglect the historical memory of what happened many centuries ago, which has been passed on to us in the form of detailed records, chronicles, letters, etc.

A reading of the recent past helps us to understand how much these phenomena have affected people's capacity for resilience and thus their attachment to the territory, even if not always under optimal conditions. Therefore, examining historical information should represent a systematic approach to obtaining a rich database for the overall assessment of territorial risk for any technical intervention. This is certainly an important

approach, the results of which, in all their complexity, should be provided by administrations to the population, as a starting point for responsible and knowledgeable territorial planning choices.

Finally, there is Venaus, in the Cenischia valley (Turin province), a municipality affected by debris flows from the stream that crosses it. The historical research on the Supita stream documents how the paroxysms of avalanche and debris flow connected to the periodic processes described lead to the accumulation of stone and vegetal material in the riverbed, which is constantly available for further debris flows and facilitates mass transport to inhabited areas in conjunction with intense thunderstorms.

As happened in May 2008, a debris flow event can jeopardize the homes, bridges, and roads along the active canal, despite any costly interventions having been carried out. Some critical points remain, essentially regarding the active bed in the fan and the possible reactivation of the secondary channels located at the apex of the fan, according to the scenarios that have already partially materialized in previous cases and to the crossing works that must be able to guarantee the outflow of solid–liquid mixtures. Added to this is periodic forest depletion threatened by avalanches and extensive fires (such as what occurred in October 2017).

Despite the damaging effects on the buildings of Venaus described based on rich historical information, the small town has been resilient over the centuries, having adopted mitigation strategies with a considerable outlay of resources. Despite the recurrence of debris flows and floods in the past, the experience of Venaus and the testimonies collected during CNR-IRPI's research revealed that the basis for the lack of the perception of risk (not only geohydrological but also avalanche risk) among the resident population was a substantial loss of collective memory and a sort of refusal, highlighting the need for interventions aimed at disseminating basic knowledge and encouraging behavior appropriate to the specific vulnerability of an area. Institutions also failed to fully assess the risk inherent in urban transformation and to apply firm intervention measures in the territory, in terms of both post-event reconstruction and urban planning. Different communication and planning practices are necessary to face and mitigate possible and foreseeable risks connected to paroxysmal events. The contribution of technicians, coherently adapted to dissemination, can be central in the implementation of these processes, to avoid the frequent cases in which risk is often denied or not considered, also because of the consequences that effective awareness would entail for the development of projects with a strong impact that is certainly economic but also environmental.

## 6. Conclusions and Perspectives

The historical approach appears to be indispensable from a cognitive perspective for more targeted forecasting, prevention, and risk mitigation activities. These actions are intended to safeguard collective and individual assets as well as public safety in case of risk associated with the occurrence of natural events. In addition to the need to pass on the written memory of such events in an appropriately elaborated form, the most important concept that has guided the main activities of various bodies that deal with territorial issues over the past 50 years is that exogenous and endogenous phenomena are likely to repeat in space (very often in the same places) and over time (according to extremely variable intervals of recurrence) in ways similar to those previously seen.

It is evident that collecting historical data to understand natural processes allows us to considerably improve the cognitive framework developed with typical geological–geomorphological analysis, the main product of which is the mapping of instability, and it certainly better defines some fundamental aspects of territorial hazard and vulnerability assessments aimed at mitigating risks.

Emphasizing the usefulness of the historical approach certainly does not imply underestimating the importance of other types of research of a more distinctly methodological or applicative nature in the vast range of disciplines concerning protection from natural risks; it does mean that retrieving historical data should be considered an indispensable

phase of assessing territorial hazard within a wider methodological approach that includes integration and dialogue among multiple disciplines. However, along with specific competencies and experiences, the recovery and use of historical memory require a considerable commitment of time, which is not always rewarded by fruitful results. The need to have updated databases that are accessible not only to the entire scientific community but also to institutions and technical professions is, therefore, evident.

In recent years, the importance of using historical studies in land use planning has also been emphasized at the regulatory level. In particular, in the assessment of possible flood risk scenarios, it has become indispensable to provide descriptions of past floods that had significant adverse effects on human health, the environment, cultural heritage, and economic activities and that, with high probability, could recur in the future in a similar manner, including the extent of flooding and water flow paths, and the adverse consequences (Art. 4, paragraph 2b of European Directive No. 60/EC issued in 2007, implemented in Italy by Legislative Decree No. 49 issued in 2010). Good examples of the need for planning studies to include information on historical research of past events can also be found in Circular No. 7LAP (1999) of the Piedmont Region (Northern Italy).

In this lengthy paper, the experiences of the authors, who have been using historical data for decades to deal with land instability problems and geological hazards, have been condensed. Italy is unfortunately a peninsula where endogenous and exogenous processes are widespread. Five cases in different areas of the peninsula are presented; for each one, it is amply described how the use of historical data proved to be helpful in the prediction and prevention of instability phenomena.

The historical sources, as extensively described, are mainly preserved in public and private archives. As far as public archives (which make up almost the entirety of those normally consulted) are concerned, it must be emphasized that the state archives are for the most part ordered and indexed. For the archives of individual Italian municipalities, the situation is quite different. The general impression of technicians who rely on them (geologists, engineers, etc.) is that municipal archives are still considered cumbersome and useless by most local administrations. This is why, except in a few municipalities, folders are usually piled up, or in the attic or basement of the town hall, in a dusty, humid room without adequate ventilation, and even more problematically for a scholar, the materials are not inventoried. In this context, digitizing the data seems ideal, which, considering the size and historical importance of the documents, should be the responsibility of each Italian municipality. Such cataloguing would also allow for more rapid and in-depth searches, not only for the aspects covered in this work but also for economic, sociological, and legislative studies, and obviously, it would be very useful for purely bureaucratic, administrative issues.

The hope of all those who work in this field is that the Italian state values historical data, imposing rules and constraints on municipalities to safeguard and use such heritage of inestimable historical and social value for the benefit of the community, contributing to mitigate risks and shape safer cities of tomorrow.

**Author Contributions:** Conceptualization and methodology, F.L., F.T.G., W.P., S.P. and L.T.; validation, F.L., F.T.G., W.P., S.P. and L.T.; investigation, F.L., F.T.G., W.P., S.P. and L.T.; resources, F.L., F.T.G., W.P., S.P. and L.T.; data curation, F.L., F.T.G., W.P., S.P. and L.T.; writing—original draft preparation, F.L., F.T.G., W.P., S.P. and L.T.; writing—review and editing, F.L., F.T.G., W.P., S.P. and L.T.; supervision, F.L.; project administration, F.L., F.T.G., W.P., S.P. and L.T.; funding acquisition, F.L., F.T.G., W.P., S.P. and L.T. All authors have read and agreed to the published version of the manuscript.

**Funding:** This research was funded by FONTES Italian Projects of Relevant National Interest (PRIN), Project CNR Number DTA.AD003.737. The research activity was also sustained by the BEGIN project (DUS.AD017.190, CUP C39J20001760002), financed by Basilicata ERDF-ROP 2014–2020.

**Data Availability Statement:** The sources considered to perform the analyses of the five case studies are freely accessible in the Italian public libraries or archives mentioned in the text and references.

**Conflicts of Interest:** The authors declare no conflict of interest.

## Abbreviation

Word shortening for archive sources (shown in the References in full Italic): ARB—SPIX (Archivio Regione Basilicata—Basilicata Region Archive—c/o Spix); B. (Busta—Portfolio); s.l. (Senza indicazione del luogo—Without indication of place); s.d. (Senza indicazione della data—Without date indication); ASDPC (Archivio Storico Dipartimento della Protezione Civile—Historical Archive of Civil Protection Department), MM.LL.PP. (Ministero dei Lavori Pubblici, Ministry of Public Works), Div. (Divisione—Division), C. (Consolidamenti—Consolidation works), B. (Busta—Portfolio), SNB (Senza Numero Busta—Without portfolio number); ASPZ (Archivio di Stato di Potenza—State Archive of Potenza), CC (Commissariato Civile—Civil Commission), FP (Fondo Prefettura—Prefecture Documents), S2 (Serie 2), Cat. (Categoria—Category), B. (Busta—Portfolio), F. (Fascicolo—File), s.l. (Senza indicazione del luogo—Without indication of place); s.d. (Senza indicazione della data—Without date indication). ACC (Archivio del Comune di Canelli—Canelli Municipality Archive).

## References


1. Desio, A. *Geologia dell'Italia*, 1st ed.; UTET: Torino, Italy, 1973; p. 1081. (In Italian)
2. Dal Piaz, G.V.; Bistacchi, A.; Massironi, M. Geological outline of the Alps. *Episodes* **2003**, *26*, 175–181. [CrossRef]
3. Pasquarè, G.; Venturini, C. *Mapping Geology in Italy*, 1st ed.; Selca: Firenze, Italy, 2004; p. 330, ISBN 88 448 0189 2.
4. Marchetti, M.; Soldati, M.; Vandelli, V. The Great Diversity of Italian Landscapes and Landforms: Their Origin and Human Imprint. In *Landscapes and Landforms of Italy. World Geomorphological Landscapes*, 1st ed.; Soldati, M., Marchetti, M., Eds.; Springer: Cham, Switzerland, 2017. [CrossRef]
5. Rovida, A.; Locati, M.; Camassi, R.; Lolli, B.; Gasperini, P.; Antonucci, A. *Catalogo Parametrico dei Terremoti Italiani (CPTI15)*, 4th ed.; Istituto Nazionale di Geofisica e Vulcanologia (INGV): Bologna, Italy, 2022.
6. Baratta, M. *La Catastrofe Sismica Calabro-Messinese. 28 Dicembre 1908*; Società Geografica Italiana: Roma, Italy, 1910; Volume 2, p. 426. (In Italian)
7. Caciagli, M. Le Tracce del Terremoto del 1908 Nell'ambiente Naturale. In *Il Terremoto e il Maremoto del 28 Dicembre 1908: Analisi Sismologica, Impatto, Prospettive*, 1st ed.; Bertolaso, G., Boschi, E., Guidoboni, E., Valensise, G., Eds.; INGV-DPC: Roma, Bologna, Italy, 2008; pp. 197–214. (In Italian)
8. Porfido, S.; Esposito, E.; Violante, C.; Molisso, F.; Sacchi, M.; Spiga, E. *Earthquakes-Induced Environmental Effects in Coastal Area: Some Example in Calabria and Sicily (Southern Italy)*, 1st ed.; Marine Research at CNR Dta: Venezia, Italy, 2011; Volume DTA/06-2011, ISSN 2239-5172.
9. Barbano, M.S.; Castelli, V.; Pantosti, D.; Pirrotta, C. Integration of historical, archaeoseismic and paleo-seismological data for the reconstruction of the early seismic history in Messina Strait (south Italy): The 1st and 4th centuries AD earthquakes. *Ann. Geophys.* **2014**, *57*, S0192. [CrossRef]
10. Comerci, V.; Vittori, E.; Blumetti, A.M.; Brustia, E.; Di Manna, P.; Guerrieri, L.; Lucarini, M.; Serva, L. Environmental effects of the December 28, 1908, Southern Calabria–Messina (Southern Italy) earthquake. *Nat. Hazards* **2015**, *76*, 1849–1891. [CrossRef]
11. Procházková, D.; Schenková, Z.; Kárník, V. Macroseismic fields of the main Friuli shocks of 1976. *Tectonophysics* **1979**, *53*, 249–259. [CrossRef]
12. Slejko, D.; Neri, G.; Orozova, I.; Renner, G.; Wyss, M. Stress field in Friuli (NE Italy) from fault plane solutions of activity following the 1976 mainshock. *Bull. Seism. Soc. Am.* **1999**, *89*, 1037–1052. [CrossRef]
13. Postpischl, D.; Branno, A.; Esposito, E.; Ferrari, G.; Marturano, A.; Porfido, S.; Rinaldis, V.; Stucchi, M. The Irpinia earthquake of November 23, 1980. In *Atlas of Isoseismal Maps of Italian Earthquakes*, 1st ed.; Postpischl, D., Ed.; Quaderni della Ricerca Scientifica: Roma, Italy, 1985; Volume 114, pp. 152–157.
14. Gizzi, F.T.; Potenza, M.R.; Zotta, C. 23 November 1980 Irpinia-Basilicata earthquake (Southern Italy): Towards a full knowledge of the seismic effects. *Bull. Earthq. Eng.* **2012**, *10*, 1109–1131. [CrossRef]
15. Gizzi, F.T.; Potenza, M.R. The Scientific Landscape of November 23rd, 1980 Irpinia-Basilicata Earthquake: Taking Stock of (Almost) 40 Years of Studies. *Geosciences* **2020**, *10*, 482. [CrossRef]
16. Porfido, S.; Alessio, G.; Gaudiosi, G.; Nappi, R.; Michetti, A.M. 40 Years Later: New Perspectives on the 23 November 1980, Ms 6.9, Irpinia-Lucania Earthquake. *Geosciences* **2022**, *12*, 173. [CrossRef]
17. Galli, P.; Camassi, R.; Azzaro, R.; Bernardini, F.; Castenetto, S.; Molin, D.; Tertulliani, A. Il terremoto aquilano del 6 aprile 2009: Rilievo macrosismico, effetti di superficie ed implicazioni sismotettoniche. *Quaternario* **2009**, *22*, 235–246. (In Italian)
18. Vittori, E.; Di Manna, P.; Blumetti, A.M.; Comerci, V.; Guerrieri, L.; Esposito, E.; Michetti, A.M.; Porfido, S.; Piccardi, L.; Roberts, G.P.; et al. Surface Faulting of the 6 April 2009 $M_w$ 6.3 L'Aquila Earthquake in Central Italy. *Bull. Seismol. Soc. Am.* **2011**, *101*, 1507–1530. [CrossRef]
19. Galli, P.; Peronace, E.; Bramerini, F.; Castenetto, S.; Naso, G.; Cassone, F.; Pallone, F. The MCS intensity distribution of the devastating 24 August 2016 earthquake in central Italy (Mw 6.2). *Ann. Geophys.* **2016**, *59*, 13. [CrossRef]
20. Galli, P.; Castenetto, S.; Peronace, E. The macroseismic intensity distribution of the October 30, 2016 earthquake in central Italy ($M_w$ 6.6). Seismotectonic implications. *Tectonics* **2017**, *36*, 2179–2197. [CrossRef]

21. Rossi, A.; Tertulliani, A.; Azzaro, R.; Graziani, L.; Rovida, A.; Maramai, A.; Pessina, V.; Hailemikael, S.; Buffarini, G.; Bernardini, F.; et al. The 2016–2017 earthquake sequence in central Italy: Macroseismic survey and damage scenario through the EMS-98 intensity assessment. *Bull. Earthq. Eng.* **2019**, *17*, 2407–2431. [CrossRef]
22. Gizzi, F.T.; Kam, J.; Porrini, D. Time windows of opportunities to fight earthquake under-insurance: Evidence from Google Trends. *Humanit. Soc. Sci. Commun.* **2020**, *7*, 61. [CrossRef]
23. Morgan, D.J.; Blake, S.; Rogers, N.W.; DeVivo, B.; Rolandi, G.; Macdonald, R.; Hawkesworth, C.J. Time scales of crystal residence and magma chamber volume from modelling of diffusion profiles in phenocrysts: Vesuvius 1944. *Earth Planet. Sci. Lett.* **2004**, *222*, 933–946. [CrossRef]
24. Branca, S.; De Beni, E.; Proietti, C. The large and destructive 1669 AD eruption at Etna volcano: Re-construction of the lava flow field evolution and effusion rate trend. *Bull. Volcanol.* **2013**, *75*, 694. [CrossRef]
25. Sanderson, T. Direct gravimetric detection of magma movements at Mount Etna. *Nature* **1982**, *297*, 487–490. [CrossRef]
26. Branca, S.; Del Carlo, P. Eruptions of Mt Etna During the Past 3,200 Years: A Revised Compilation Integrating the Historical and Stratigraphic Records. In *Mt. Etna: Volcano Laboratory*; Bonaccorso, A., Calvari, S., Coltelli, M., Del Negro, C., Falsaperla, S., Eds.; AGU: Washington, DC, USA, 2004; Volume 143, pp. 1–27.
27. Canuti, P.; Casagli, N.; Pellegrini, M.; Tosatti, G. *Geo-Hydrological Hazards. Anatomy of an Orogen: The Apennines and Adjacent Mediterranean Basins*; Kluwer Academic Publishers: Alphen aan den Rijn, The Netherlands, 2001; pp. 513–532.
28. ISPRA Rapporto Sulle Condizioni di Pericolosità da Alluvione in Italia e Indicatori di Rischio Associati. In *ISPRA Rep.*; 2021; 353, p. 184. Available online: https://www.isprambiente.gov.it/files2021/pubblicazioni/rapporti/rapporto_alluvioni_ispra_353_16_11_2021_rev2.pdf (accessed on 4 December 2022). (In Italian)
29. Semenza, E.; Ghirotti, M. History of the 1963 Vaiont slide: The importance of geological factors. *Bull. Eng. Geol. Env.* **2000**, *59*, 87–97. [CrossRef]
30. Kilburn, C.R.J.; Petley, D.N. Forecasting giant, catastrophic slope collapse: Lessons from Vajont, Northern Italy. *Geomorphology* **2003**, *54*, 21–32. [CrossRef]
31. Chandler, R.J.; Tosatti, G. The Stava tailings dams failure, Italy, July 1985. *Proc. Inst. Civ. Eng.-Geotech. Eng.* **1995**, *113*, 67–79. [CrossRef]
32. Luino, F.; De Graff, J.V. The Stava mudflow of 19 July 1985 (Northern Italy): A disaster that effective regulation might have prevented. *NHESS* **2012**, *12*, 1029–1044. [CrossRef]
33. Del Prete, M.; Guadagno, F.M.; Hawkins, A.B. Preliminary report on the landslides of 5 May 1998, Campania, southern Italy. *Bull. Eng. Geol. Environ.* **1998**, *57*, 113–129. [CrossRef]
34. Guadagno, F.M.; Forte, R.; Revellino, P.; Fiorillo, F.; Focareta, M. Some aspects of the initiation of debris avalanches in the Campania Region: The role of morphological slope discontinuities and the development of failure. *Geomorphology* **2005**, *66*, 237–254. [CrossRef]
35. Govi, M.; Maraga, F. Inundation on the Po Plain caused by levee breaches. *G. Geol. Appl.* **2005**, *1*, 167–176. [CrossRef]
36. Malguzzi, P.; Grossi, G.; Buzzi, A.; Ranzi, R.; Buizza, R. The 1966 "century" flood in Italy: A meteorological and hydrological revisitation. *JGR Atmos.* **2006**, *111*, D24106. [CrossRef]
37. Arrighi, C.; Brugioni, M.; Castelli, F.; Franceschini, S.; Mazzanti, B. Flood risk assessment in art cities: The exemplary case of Florence (Italy). *J. Flood Risk Manag.* **2018**, *11*, S616–S631. [CrossRef]
38. Luino, F. The flood and landslide event of November 4-6 1994 in Piedmont Region (Northwestern Italy): Causes and related effects in Tanaro Valley. *Phys. Chem. Earth Part A Solid Earth Geod.* **1999**, *24*, 123–129. [CrossRef]
39. Ratto, S.; Bonetto, F.; Comoglio, C. The October 2000 flooding in Valle d'Aosta (Italy): Event description and land planning measures for the risk mitigation. *Int. J. River Basin Manag.* **2003**, *1*, 105–116. [CrossRef]
40. Luino, F. Sequence of instability processes triggered by heavy rainfall in northwestern Italy. *Geomorphology* **2005**, *66*, 13–39. [CrossRef]
41. Damiano, B. (Ed.) *Silius Italicus (88–89 B.C.)–De Secundo Bello Punico. Impressum Lugduni: Expensis Bartholomei Troth, 1514*; Mense Ianuario: Lyon, France, 1514; p. 102.
42. Caecilius, G.P. II *Naturalis Historia*; Letter from Pliny the Younger to Tacitus on the eruption of Vesuvius in 79 AD, Editio Princeps. 1469.
43. Mori, A. Considerazioni sull'erosione accelerata del suolo in Abruzzo. *Boll. Della Soc. Geogr. Ital.* **1968**, *IX*, 67–78. (In Italian)
44. Alighieri, D. *(c. 1320)-La Divina Commedia. Inferno*; Feltrinelli: Milano, Italy, 2021; p. 764. (In Italian)
45. Noriller, G. *I Lavini di Marco Celebrati da Dante*; Sottochiesa, Rovereto, Italy, 1871; p. 237. (In Italian)
46. D'Onofrio, C. *Il Tevere e Roma*, 1st ed.; Ugo Bozzi Editore: Rome, Italy, 1968; p. 275. (In Italian)
47. Gramigni, T. La Memoria Epigrafica Dell'alluvione Dell'Arno Del 1333, in Acqua Nemica. Fiumi, Inondazioni e Città Storiche Dall'antichità Al contemporaneo. In Proceedings of the 29–30 January 2015 Converence, Florence, Italy, 29–30 January 2015. (In Italian)
48. DatiOpen.it. Available online: http://www.datiopen.it/it/opendata/Comune_di_Firenze_Targhe_alluvioni_storiche?fbclid=IwAR0jmZ5u38PjDG9RAYry5wbIFlJ-rkBD8mprQPLiAAT4JZyuB6kQ3vajW6M (accessed on 15 May 2022).
49. Di Loreto, E.; Bersani, P. Le alluvioni storiche del Tevere a Roma, nella memoria delle lapidi e dei dipinti. *Mem. Descr. Carta Geol. D'it.* **2021**, *108*, 209–220. (In Italian)
50. Castiglione, J. *Trattato Dell'inondatione del Tevere*; Facciotto: Rome, Italy, 1599; p. 78. (In Italian)

51. Bonini, F.M. *Il Tevere Incatenato Overo L'arte di Frenar L'acque Correnti*; Francesco Moneta: Rome, Italy, 1663. (In Italian)
52. Morozzi, F. *Dello Stato Antico E Moderno Del Fiume Arno E Delle Cause E De' Rimedi Delle Sue Inondazioni (1762)*; Nella Stamperia di Gio. Batista Stecchi, All'insegna di S. Ignazio Lojola: Firenze, Italy, 1762. (In Italian)
53. Aiazzi, G. *Inondazioni Dell'arno e Notizie Scientifiche Sul Medesimo*; Piatti, T., Ed.; Florence, Italy, 1845. (In Italian)
54. Gherardi, A. *Di Alcune Memorie Storiche Risguardanti L'inondazione Avvenuta in Firenze L'anno 1333*; Archivio Storico Italiano: Florence, Italy, 1873; pp. 240–261. (In Italian)
55. Salvestrini, F. *Libera Città Su Fiume Regale. Firenze e L'ARNO Dall'antichità al Quattrocento*; Nardini, Ed.; Nardini: Florence, Italy, 2005; pp. 51–86. (In Italian)
56. Casalis, G. *Il Dizionario Geografico Storico-Statistico-Commerciale Degli Stati di S. M. il Re di Sardegna, Volume 6*; Maspero Libraio e Cassone e Marzorati Tipografi: Turin, Italy, 1856; p. 790. (In Italian)
57. Pantanelli, D.; Santi, V. *Itinerari, L'APPENNINO Modenese, 900–1164*; Rocca, S., Ed.; Cappelli: Casciano, Italy, 1895; p. 1166. (In Italian)
58. Santi, V. *Le Frane dell'Appennino Modenese*; Antica Tipografia Soliani: Modena, Italy, 1897; p. 104. (In Italian)
59. Almagià, R. *Studi Geografici Sopra le Frane in Italia. Vol. I, L'appennino Settentrionale e il Prealpino Tosco Romano*; Società Geografica Italiana: Rome, Italy, 1907. (In Italian)
60. Almagià, R. *Studi Geografici Sopra le Frane in Italia, II L'appennino Centrale e Meridionale*; Società Geografica Italiana: Rome, Italy, 1910. (In Italian)
61. Comandini, A.; Monti, A. *L'Italia Nei Cento Anni del Secolo XIX (1801–1900) Giorno per Giorno Illustrate*; A. Vallardi: Milan, Italy, 1900; p. 7799. (In Italian)
62. Berta, G. *Cenni di Cronistoria Alessandrina Dall'anno 1168 al 1900*; (re-printed by SEAB: Bologna, Italy, 1977); Tip. G. Jacquemod Figli: Alessandria, Italy, 1903; p. 301. (In Italian)
63. Mandarino, A.; Luino, F.; Turconi, L.; Faccini, F. Urban geomorphology of a historical city straddling the Tanaro River (Alessandria, NW Italy). *JOM* **2020**, *17*, 29–41. [CrossRef]
64. Pullè', F.L. Paesi che se ne vanno. Le frane dell'Appennino Modenese. *Riv. D'italia* **1901**, *3*, 291–315. (In Italian)
65. Rao, R. Villaggi abbandonati fra Tanaro e Po (X-XIX secolo): Una dinamica di lungo periodo. *Archeol. Mediev.* **2017**, *XLIV*, 171–192.
66. Arena, G. Denominazioni varie attribuite alle forme del terreno. In *Atlante dei Tipi Geografici*; IGV: Florence, Italy, 2004; pp. 702–709. (In Italian)
67. Roletto, G. Alcune considerazioni geografiche sull'alluvione del 1728 nell'alta Val Pellice. *L'Universo* **1930**, 895–899. (In Italian)
68. AVI Project. Available online: http://avi.gndci.cnr.it/en/progetto/introprogetto_en.htm (accessed on 5 December 2022).
69. Del Din Dall'Armi, M. *Dissesti Idrogeologici ed Eventi Calamitosi Nell'agordino Dal 1000 al 1966*; Istituto Bellunese di Ricerche Sociali e Culturali: Balluno, Italy, 1986; p. 285. (In Italian)
70. ENEA (1987)-Catalogo cronologico di eventi eccezionali di origine naturale in Italia (1000–1985). *Progetto Giano: Raccolta, Analisi, Elaborazione E Interpretazione Di Informazioni Storiche Sugli Effetti Prodotti Da Eventi Naturali Eccezionali in Italia Dall'anno 1000 al 1985, S.G.A.* Bologna, Italy, 1987; Volume II, p. 501. Available online: http://sici.irpi.cnr.it/storici.htm (accessed on 10 November 2022). (In Italian)
71. GNDCI The SCAI Project. Available online: http://www.gndci.cnr.it/en/scai/welcome_en.htm (accessed on 27 May 2023).
72. Catenacci, V. *Il Dissesto Geologico e Geoambientale in Italia dal Dopoguerra al 1990*; Ist. Poligrafico e Zecca dello Stato: Rome, Italy, 1992; p. 300. ISBN 978-88-240-0286-8. (In Italian)
73. Govi, M.; Turitto, O. Ricerche Bibliografiche Per un Catalogo Sulle Inondazioni, Piene Torrentizie e Frane in Valtellina e Valchiavenna. In *Quaderni di Studi e di Documentazione*; Geam, Ed.; Associazione Mineraria Subalpina: Turin, Italy, 1994. (In Italian)
74. Luino, F.; Tetamo, G.; Belloni, A.; Padovan, N. *Individuazione Delle Zone Potenzialmente Inondabili Dal Punto Di Vista Storico E Geomorfologico Ai Fini Urbanistici: Torrente Staffora (PV)*; Istituto di Ricerca per la Protezione Idrogeologica: Torino, Italy, 1999; p. 55. (In Italian)
75. Luino, F.; Bassi, M.; Fassi, P.; Belloni, A.; Padovan, N. *Individuazione delle Zone Potenzialmente Inondabili dal Punto di Vista Storico e Geomorfologico ai Fini Urbanistici: Torrente Pioverna (Valsassina) e Fiume Serio (Val Seriana)*; Istituto di Ricerca per la Protezione Idrogeologica: Torino, Italy, 2000; p. 60. (In Italian)
76. Luino, F.; Belloni, A.; Padovan, N. Historical and Geomorphological Analysis as a Research Tool for the Identification of Flood-Prone Zones and Its Role in the Revision of Town Planning: The Oglio Basin (Valcamonica-Northern Italy). In Proceedings of the 9th Congress of the IAEG, Durban, South Africa, 16–20 September 2002.
77. Luino, F.; Fassi, P.; Lerbini, M.; Belloni, A.; Caldiroli, G.; Braghin, F. *Individuazione Delle Zone Potenzialmente Inondabili Della Sponda Lombarda Del Lago Maggiore. Ricerca Storica, Studio Geomorfologico Ed Analisi Urbanistica Ai Fini Della Pianificazione Di Emergenza Comunale E Intercomunale*; P.I.C. INTERREG IIIA: Milano, Italy, 2005; p. 366, (In Italian) [CrossRef]
78. Audisio, C.; Turconi, L. Urban floods: A case study in the Savigliano area (North-Western Italy). *NHESS* **2011**, *11*, 2951–2964. [CrossRef]
79. Turconi, L.; Tropeano, D.; Savio, G.; De, S.K.; Mason, P.J. Landscape analysis for multi-hazard preven-tion in Orco and Soana valleys, Northwest Italy. *NHESS* **2015**, *15*, 1963–1972. [CrossRef]
80. Paliaga, G.; Luino, F.; Turconi, L.; Marincioni, F.; Faccini, F. Exposure to Geo-Hydrological Hazards of the Metropolitan Area of Genoa, Italy: A Multi-Temporal Analysis of the Bisagno Stream. *Sustainability* **2020**, *12*, 1114. [CrossRef]

81. Turconi, L.; Casazza, M.; Bono, B.; Luino, F. Increasing geohydrological instability in a valley of the Italian Central Alps: A study in the Anthropocene. *JOM* **2022**, *19*, 2145917. [CrossRef]
82. Turconi, L.; Tropeano, D.; Savio, G.; Bono, B.; De, S.K.; Frasca, M.; Luino, F. Torrential Hazard Prevention in Alpine Small Basin through Historical, Empirical and Geomorphological Cross Analysis in NW Italy. *Land* **2022**, *11*, 699. [CrossRef]
83. Petrucci, O.; Polemio, M. The use of historical data for the characterisation of multiple damaging hydrogeological events. *NHESS* **2003**, *3*, 17–30. [CrossRef]
84. Petrucci, O.; Polemio, M.; Pasqua, A.A. Flash Floods Risk Variation of Steep Drainage Basins in Ca-Labria (Italy) and the Role of Rainfall and Anthropogenic Modifications since 1800. In *Global Change: Facing Risks and Threats to Water Resources*; Servat, E., Demuth, S., Dezetter, A., Daniell, T., Eds.; IAHS Press Ed.: Oxfordshire, UK, 2010; pp. 103–110.
85. Petrucci, O.; Gullà, G. A simplified method for landslide damage scenario assessment based on historical data. *Nat. Hazards* **2010**, *52*, 539–560. [CrossRef]
86. Petrucci, O.; Palmieri, W.; Versace, P. *La difesa del Suolo Nell'ottocento nel Mezzogiorno d'Italia*; Rubbettino: Soveria Mannelli, Italy, 2011; p. 184, ISBN 978-88-95172-02-6. (In Italian)
87. Migale, L.S.; Milone, A. Colate di fango in terreni piroclastici della Campania. Primi dati della ricerca storica. *Rass. Stor. Salernitana* **1998**, *30*, 235–271. (In Italian)
88. Aversano, V.; Ruggiero, G. *Montagna Assassina o Vittima? Per Una Storia del Territorio e Delle Alluvioni di Bracigliano, Quindici, Sarno e Siano*; Laveglia Carlone: Battipaglia, Italy, 2000; p. 330. (In Italian)
89. Porfido, S.; Esposito, E.; Alia, F.; Esposito, G.; Iaccarino, G. Censimento dei Maggiori Dissesti Idrogeo-Logici che Hanno Colpito Quindici in Epoca Storica. In Proceedings of the Giornata Dell'ambiente "Il Dissesto Idrogeologico: Inventario e Prospettive", XIX Giornata Dell'ambiente, Accademia Naz. Dei Lincei, Rome, Italy, 5 June 2001. (In Italian)
90. Porfido, S.; Esposito, E.; Alaia, F.; Molisso, F.; Sacchi, M. The Use of Documentary Sources for Reconstructing Flood Chronologies on the Amalfi Rocky Coast (southern Italy). In *Geohazard in Rocky Coastal Areas*; Violante, C., Ed.; Geological Society London Special Publications: London, UK, 2009; pp. 173–187. [CrossRef]
91. Porfido, S.; Esposito, E.; Molisso, F.; Sacchi, M.; Violante, C. Flood Historical Data for Flood Risk Estimation in Coastal Areas, Eastern Tyrrhenian Sea, Italy. In *Landslide Science and Practice*; Margottini, C., Canuti, P., Sassa, K., Eds.; Springer: Berlin/Heidelberg, Germany, 2011; Volume 5, pp. 103–108, ISBN 978-3-642-31427-8.
92. Foscari, G.; Esposito, E.; Mazzola, S.; Porfido, S.; Sciarrotta, S.; Santoro, G. *Lo Alluvione. Il Disastro Del 1773 A Cava Tra Memoria Storica e Rimozione*; Edisud: Salerno, Italy, 2013; p. 314, ISBN 978–88-95154–87-9. (In Italian)
93. Tropeano, D.; Turconi, L. Using Historical Documents for Landslide, Debris Flow and Stream Flood Prevention. Applications in Northern Italy. *Nat. Hazards* **2004**, *31*, 663–679. [CrossRef]
94. Luino, F.; Turconi, L.; Petrea, C.; Nigrelli, G. Uncorrected land-use planning highlighted by flooding: The Alba case study (Piedmont, Italy). *NHESS* **2012**, *12*, 2329–2346. [CrossRef]
95. Luino, F. Le Inondazioni Storiche del Fiume Po in Particolare dal 1861 a Oggi. In *L'Italia dei Disastri: Dati e Riflessioni Sull'impatto Degli Eventi Naturali 1861–2013. Eventi Estremi e Disastri*; Guidoboni, E., Valensise, G., Eds.; Bonomia University Press: Bologna, Italy, 2013; pp. 109–158. Available online: https://publications.cnr.it/doc/285439 (accessed on 20 October 2022).
96. Di Martino, V.; Belari, M. *Qui Arrivò il Tevere*; Multigrafica: Rome, Italy, 1980; p. 236. (In Italian)
97. Lanzini, M.; Mazza, R.; Capelli, G. Le Antiche Alluvioni del Tevere ed i Dissesti Storici (Prati-Balduina XVII Municipio). In *La Geologia Di Roma: Dal Centro Storico Alla Periferia*; Funiciello, R., Praturlon, A., Giordano, A., Eds.; APAT: Rome, Italy, 2008; Volume 80, pp. 186–194, ISBN 978-88-240-2893-6. (In Italian)
98. Lazzari, M. Utilizzo delle fonti storiche per lo studio della pericolosità e del rischio geomorfologico. *Mem. Descr. Carta Geol. D'it.* **2014**, *XCVI*, 251–260. (In Italian)
99. Camassi, R. Catalogues of historical earthquakes in Italy. *Ann. Geophys.* **2004**, *47*, 645–657. [CrossRef]
100. Geus, K.; Colin, G.K. Paradoxography. In *Oxford Handbook of Science and Medicine in the Classical World*; Keyser, P.T., Scarborough, J., Eds.; Oxford University Press: Oxford, UK, 2018; pp. 431–444.
101. Manetti, G. *De Terraemotu Libri Tres*; Biblioteca Apostolica Vaticana: Vatican City, Italy, 1457. (In Italian)
102. Bonito, M. *Terra Tremante, o Vero, Continuatione de Terremoti, Dalla Creatione del Mondo Sino al Tempo Presente*; : Arnaldo Forni Ed., Bologna, Italy, 1980; Nella Nuova Stampa Delli Socii Dom. Ant. Parrino, e Michele Luigi Mutii, ad Istanza di Dom. Ant. Parrino: Naples, Italy, 1691; p. 822. (In Italian)
103. Guidoboni, E. Method of investigation, typology and taxonomy of the basic data: Navigating between seismic effects and historical contexts. *Ann. Geophys.* **2000**, *43*, 621–666.
104. Gizzi, F.T.; Lazzari, M. Il Dibattito Scientifico sui Terremoti. In *La Città Ferita. Il Terremoto Dello Stretto e la Comunità Internazionale*; Motta, G., Ed.; Franco Angeli Ed.: Milan, Italy, 2008; pp. 129–135, EAN 9788856802658. (In Italian)
105. Pilla, L. *Poche Parole Sul Tremuoto Che Ha Desolato I Paesi Della Costa Toscana*; Vannucchi Ed.: Pisa, Italy, 1846; p. 22. (In Italian)
106. Baratta, M. *I Terremoti d'Italia*; Arnaldo Forni Ed.: Sala Bolognese, Italy, 1901; p. 960. (In Italian)
107. Postpischl, D. *Atlas of Isoseismal Maps of Italian Earthquakes*; Consiglio Nazionale Ricerche, Progetto Finalizzato Geodinamica Ed.: Rome, Italy, 1985; Volume 114, p. 164.
108. Postpischl, D. *Catalogo Dei Terremoti Italiani Dall'anno 1000 Al 1980*; Consiglio Nazionale Ricerche, Progetto Finalizzato Geodinamica Ed.: Bologna, Italy, 1985; p. 239. (In Italian)

109. Locati, M.; Camassi, R.; Rovida, A.; Ercolani, E.; Bernardini, F.; Castelli, V.; Caracciolo, C.H.; Tertulliani, A.; Rossi, A.; Azzaro, R.; et al. Italian Macroseismic Database (DBMI15), v4.0. *INGV* **2022**. (In Italian) [CrossRef]
110. Guidoboni, E.; Ferrari, G.; Mariotti, D.; Comastri, A.; Tarabusi, G.; Sgattoni, G.; Valensise, G. CFTI5Med, Catalogo dei Forti Terremoti in Italia (461 a.C.-1997) e nell'area Mediterranea (760 a.C.-1500). *Ist. Naz. Geofis. E Vulcanol. (INGV)* **2018**. [CrossRef]
111. Boschi, E.; Ferrari, G.; Gasperini, P.; Guidoboni, E.; Smriglio, G.; Valensise, G. *Catalogo dei Forti Terremoti in Italia dal 461 a.C. al 1980*; ING-SGA: Bologna, Italy, 1995; p. 973. (In Italian)
112. Guidoboni, E.; Comastri, A.; Traina, G. *Catalogue of Ancient Earthquakes in the Mediterranean Area up to the l0th Century*; ING-SGA: Bologna, Italy, 1994; p. 504.
113. Guidoboni, E.; Comastri, A. *Catalogue of Earthquakes and Tsunamis in the Mediterranean Area from the 11th to the 15th Century*; INGV-SGA: Bologna, Italy, 2005; p. 1037.
114. Gizzi, F.T. To What Degree Can Historical Seismicity Records Assist in Seismic Microzonation? *Eng. Geol.* **2006**, *87*, 1–12. [CrossRef]
115. Esposito, E.; Laurelli, L.; Porfido, S. Damage pattern in historical centers: Isernia, an example in Southern Italy. *Ann. Geofis.* **1995**, *38*, 663–677. [CrossRef]
116. Gizzi, F.T.; Masini, N. Damage scenario of the earthquake on 23 July 1930 in Melfi: The contribution of the technical documentation. *Ann. Geofis.* **2004**, *47*, 1641–1665. [CrossRef]
117. Tertulliani, A.; Riguzzi, F. Earthquakes in Rome during the past one hundred years. *Ann. Geofis.* **1995**, *38*, 581–590. [CrossRef]
118. Guidoboni, E.; Mariotti, D.; Giammarinaro, M.S.; Rovelli, A. Identification of amplified damage zones in Palermo, Sicily (Italy), during the earthquakes of the last three centuries. *Bull. Seismol. Soc. Am.* **2003**, *93*, 1649–1669. [CrossRef]
119. Gizzi, F.T.; Masini, N. Historical Earthquakes and Damage Patterns for Potenza (Basilicata, Southern Italy). *Ann. Geofis.* **2007**, *50*, 599–611.
120. Gizzi, F.T.; Masini, N. Historical damage pattern and differential seismic effects in a town with ground cavities: A case study from Southern Italy. *Eng. Geol.* **2006**, *88*, 41–58. [CrossRef]
121. Gizzi, F.T. *Il "Terremoto Bianco" del 21 Agosto 1962. Aspetti Macrosismici, Geologici E Risposta Istituzionale. Con la Collaborazione di Maria Rosaria Potenza e Cinzia Zotta. Prefazione di Sergio Castenetto*; Zaccara Editore: Lagonegro, Italy, 2012; p. 736, ISBN 788895-508443. (In Italian)
122. De Carolis, E.; Patricelli, G. *Vesuvius, A.D. 79. The Destruction of Pompeii and Herculaneum*; L'Erma di Bretschneider: Rome, Italy, 2003; p. 140, ISBN 8882651991.
123. Ricciardi, G.P. *Diario del Monte Vesuvio: Venti Secoli di Immagini e Cronache di un Vulcano Nella Città. Volume 3*; ESA ed.: Naples, Italy, 2009; p. 896, ISBN 8895430166. (In Italian)
124. Manzo, G.B. Lettera in materia del Vesuvio scritta da Napoli al Sig. Antonio Bruni a Roma. In *Diario del Monte Vesuvio: Venti secoli di Immagini e Cronache di un Vulcano nella citta*; Ricciardi, G.P., Ed.; Edizioni Scientifiche ed Artistiche: Napoli, Italy, 2009; Volume I, pp. 204–205+220–221. (In Italian)
125. Braccini, C. Relazione dell'incendio fattosi nel Vesuvio alli 16 di Dicembre 1631. In *Diario del Monte Vesuvio: Venti secoli di Immagini e Cronache di un Vulcano nella citta*; Ricciardi, G.P., Ed.; Edizioni Scientifiche ed Artistiche: Napoli, Italy, 2009; Volume I, pp. 198–199+201+208–209 +214+222–224. (In Italian)
126. Recupito, G.C. de vesuviano Incendio nuntius. In *Diario del Monte Vesuvio: Venti secoli di Immagini e Cronache di un Vulcano nella citta*; Ricciardi, G.P., Ed.; Edizioni Scientifiche ed Artistiche: Napoli, Italy, 2009; Volume I, pp. 207+211–212+216–232. (In Italian)
127. Mercalli, G. *Vulcani e Fenomeni Vulcanici in Italia*; Forni Ed.: Sala Bolognese, Italy, 1883; p. 374. (In Italian)
128. INGV. Available online: https://www.ingv.it/en/index.php (accessed on 18 March 2022).
129. Ibsen, M.L.; Brunsden, D. The nature, use and problems of historical archives for the temporal occurrence of landslides, with specific reference to the south coast of Britain, Ventnor, Isle of Wight. *Geomorphology* **1996**, *15*, 241–258. [CrossRef]
130. Ministero della Cultura, Direzione Generale degli Archivi, Archivi di Stato. Available online: https://archivi.cultura.gov.it/istituti-archivistici/archivi-di-stato (accessed on 18 December 2022).
131. Verrastro, D. L'istituzione del Commissariato civile per la Basilicata. *Basilicata Reg. Not.* **2000**, *97*, 85–92. Available online: http://dati.san.beniculturali.it/SAN/produttore_SIAS_san.cat.sogP.28613 (accessed on 8 December 2021). (In Italian)
132. Bentivenga, M.; Gizzi, F.T.; Palladino, G.; Piccarreta, M.; Potenza, M.R.; Perrone, A.; Bellanova, J.; Calamita, G.; Piscitelli, S. Multisource and Multilevel Investigations on a Historical Landslide: The 1907 Servigliano Earth Flow in Montemurro (Basilicata, Southern Italy). *Land* **2022**, *11*, 408. [CrossRef]
133. Civil Protection Department, Presidency of the Council of Ministers. Available online: https://www.protezionecivile.gov.it/en/ (accessed on 10 January 2022).
134. Ministero dell'Interno Regno d'Italia. *Circolare ministeriale 1° Marzo 1897*; n. 17100-2 (c.d. circolare Astengo); Ministero dell'Interno Regno d'Italia: Rome, Italy. (In Italian)
135. Sacco, G.M.; Nigrelli, G.; Bosio, A.; Chiarle, M.; Luino, F. Dynamic taxonomies applied to a web-based relational database for geo-hydrological risk mitigation. *Comput. Geosci.* **2012**, *39*, 182–187. [CrossRef]
136. Tropeano, D.; Terzano, P. Eventi alluvionali nel bacino del Belbo: Tipologia e frequenza dei dissesti in base a notizie storiche. *Bull. Assoc. Mineraria Subalp.* **1987**, *24*, 437–474. (In Italian)
137. Corpo Reale di Stato Maggiore. *Gran Carta degli Stati Sardi in Terraferma-F. LX Acqui*; Scala 1:50.000. Rilievi del 1852; Corpo Reale di Stato Maggiore: Rome, Italy, 1852.

138. Istituto Geografico Militare. F. 69, II SO Canelli. Scala 1:25.000. Rilievi del 1880. In *Dai tipi dell'Archivio Topocartografico dell'Istituto Geografico Militare Italiano*; Original map; Istituto Geografico Militare: Florence, Italy, 1880.
139. Istituto Geografico Militare. F. 69, II SO-Canelli. Scala 1:25.000. Rilievi del 1880, con ricognizioni parziali del 1897. In *Dai tipi dell'Archivio Topocartografico dell'Istituto Geografico Militare Italiano*; Original map; Istituto Geografico Militare: Florence, Italy, 1933.
140. IRES. *Answers to Questionnaires Concerning Hydrogeological Disruptions*; Canelli Municipality: Canelli, Italy.
141. LA STAMPA Magazine. 12 February 1951.
142. ACC. *Dichiarazione del Sindaco di Canelli*; ACC: Canelli, Italy, 1968.
143. Istituto Geografico Militare. F. 69, II SO-Canelli. Scala 1:25.000. Rilievi del 1880, con ricognizioni generali del 1923 e del 1966. In *Dai tipi dell'Archivio Topocartografico dell'Istituto Geografico Militare Italiano*; Original map; Istituto Geografico Militare: Florence, Italy, 1966.
144. Regione Piemonte. Carta Tecnica Regionale: Sezione 193080-Canelli. Scala 1:10.000. In *Dai Rilievi Aerofotogrammetrici del 1991*; Original map; Regione Piemonte: Turin, Italy, 1991.
145. Gizzi, F.T.; Proto, M.; Potenza, M.R. The Basilicata region (Southern Italy): A natural and 'human-built' open-air laboratory for manifold studies. Research trends over the last 24 years (1994–2017). *Geomat. Nat. Hazards Risk* **2019**, *10*, 433–464. [CrossRef]
146. Gizzi, F.T. Identifying geological and geo-technical influences that threaten historical sites: A method to evaluate the usefulness of data already available. *J. Cult. Herit.* **2008**, *IX*, 302–310. [CrossRef]
147. Gizzi, F.T.; Bentivenga, M.; Lasaponara, R.; Danese, M.; Potenza, M.R.; Sileo, M.; Masini, N. Natural Hazards, Human Factors, and "Ghost Towns": A Multi-Level Approach. *Geoheritage* **2019**, *11*, 1533–1565. [CrossRef]
148. *ASPZ, FP, S2, Cat. 89, F. 38F, Q. (1888-92b)-Craco Frana. Lettera del Sottoprefetto del Circondario di Matera al Prefetto di Potenza con Oggetto Craco: Trasmissione del Verbale di Deliberazione del Consiglio Comunale di Craco tenutosi il giorno 2 ottobre 1887*, Matera, Italy, 11 November 1887.
149. *ASPZ, CC, B. 1. (1908)-Lettera del Commissariato Civile di Potenza all'Ingegnere Capo del Genio Civile–Servizio Idraulico di Potenza con Oggetto Consolidamento delle frane minaccianti l'abitato di Craco*, Potenza, Italy, 1 February 1908. (In Italian)
150. *ASPZ, CC, B. 1. (1905)-Lettera dell'Ingegnere Capo del Genio Civile–Ufficio Speciale per le Opere Idrauliche e di Bonifica in Basilicata di Potenza al Prefetto Commissario Civile di Potenza con oggetto consolidamento dell'abitato di Craco–Progetto*, Potenza, Italy, 28 October 1905. (In Italian)
151. *ASPZ, CC, B. 1. (1917)-Processo verbale di consegna a firma dell'ingegnere capo del Genio Civile–Ufficio Speciale per e Opere Idrauliche e di Bonifica In Basilicata di Potenza riguardante i lavori di consolidamento dell'abitato di Craco*, Craco, Italy, 25 November 1917. (In Italian)
152. *ASPZ, CC, B. 1. Lettera Dell'ingegnere Capo Del Genio Civile–Ufficio Speciale Per Le Opere Idrauliche e Di Bonifica In Basilicata al Prefetto Commissario Civile di Potenza Riguardante Craco–Consolidamento dell'abitato*, Potenza, Italy, 18 July 1922. (In Italian)
153. *ASPZ, CC, B. 1. Consiglio del Commissariato Civile per la Basilicata riguardante Craco–Consolidamento dell'abitato: Stralcio con aggiornamento e modifiche dal progetto 28/10/1915 no. 2830.* Potenza, Italy, 30 July 1922. (In Italian)
154. *ASPZ, CC, B. 1. Lettera del Prefetto Commissario Civile al Ministro LL.PP.–Direzione Speciale dei Servizi Speciali di Roma con Oggetto Craco–Consolidamento dell'abitato: Perizia di stralcio 18/07/1922 no. 1967. s.l.* 8 August 1922. (In Italian)
155. *ASPZ, CC, b. 1. Lettera del Sindaco di Craco al Prefetto di Potenza con oggetto Lavori Consolidamento dell'abitato*, Craco, Italy, 4 November 1922. (In Italian)
156. *ASDPC, Trasferimento di Craco, SNB. Relazione Geologica del Dott. Walter Brugner del Servizio Geologico d'Italia riguardante le condizioni di stabilità dell'abitato di Craco (Provincia di Matera)*, Roma, Italy, 2 January 1964. (In Italian)
157. *ASDPC, Div. 29 Matera, C., Colobraro–Craco, B. 4. Lettera del Provveditorato Regionale alle Opere Pubbliche per la Basilicata al Ministero LL.PP. Direzione Generale dei Servizi Speciali Div. 26 con oggetto Craco–Movimenti Franosi*, Potenza, Italy, 13 December 1963. (In Italian)
158. *ASDPC, Div. 29 Matera, C., Colobraro–Craco, B. 4. Telegramma del Provveditorato alle Opere Pubbliche al Ministero LL.PP. Riguardante L'informativa circa la situazione determinatosi nell'abitato di Craco a causa di un vasto movimento franoso. s.l.* 30 December 1963. (In Italian)
159. *ASDPC, Trasferimento di Craco, SNB. Relazione Geologica del Dott. Ing. Amedeo Balboni del Servizio Geologico d'Italia riguardante il trasferimento dell'abitato di Craco (Provincia di Matera)*, Roma, Italy, 26 June 1964. (In Italian)
160. *ASDPC, Trasferimento di Craco, SNB. All. 1 Relazione del Provveditorato Regionale alle Opere Pubbliche per la Basilicata–Ufficio del Genio Civile di Matera- riguardante la proposta di trasferimento parziale dell'abitato di Craco nelle località Peschiera e S. Angelo*, Matera, Italy, 1 April 1968. (In Italian)
161. ARBa–SPIX, B. 305. *Mappa del danneggiamento. s.l., s.d.*
162. *ASDPC, MM.LL.PP. Div.29. Matera, C., Colobraro–Craco, B. 4. Craco–Zona movimento franoso*, Craco, Italy, 17 June 1965. (In Italian)
163. Angelucci, F.; Domenici, F.; Ricci, S. Prime acquisizioni sull'abitato e la torre normanna di Craco (Matera). In *Case e Torri Medievali Indagini Sui Centri Dell'italia Meridionale E Insulare (Sec. XI–XV) Campania, Basilicata, Puglia, Calabria, Sicilia e Sardegna*; Edizioni Kappa: Roma, Italy, 2014. (In Italian)
164. Di Palma, C. Il dissesto idrogeologico dei monti Lattari: Cause e possibili rimedi. In Proceedings of the Convegno Fidapa di Gragnano, Gragnano, Italy, 2 April 2004. Available online: http://www.centroculturalegragnano.it/monti-lattari/ (accessed on 14 October 2022). (In Italian)
165. Ranieri, C. *Sul Funesto Avvenimento Della Notte Del 21 al 22 Gennaio 1841 nel Comune di Gragnano*; Boezio: Naples, Italy, 1841. (In Italian)

166. Montella, N. *Sposizione del Disastro Avvenuto in Gragnano Diretta ad Allontanare il Timore di Ulteriori Pericolic*; Tip. del Petrarca: Naples, Italy, 1841. (In Italian)
167. De Maricourt, L. Un Éboulement a Gragnano. In *Mes Heures De Paresse à Naples*; Goujon et Milon: Paris, France, 1842; pp. 199–206.
168. Gigante, A. Un avvenimento funesto. In *Viaggio da Napoli a Castellammare*; Stamp. dell'Iride: Naples, Italy, 1845; pp. 149–152. (In Italian)
169. De Luca, F.; Mastriani, R. *Dizionario Corografico-Universale dell'Italia, Vol. IV, Parte I*; Civelli: Milan, Italy, 1852; pp. 155–156. (In Italian)
170. Mastriani, F. La frana. In *Il Conte di Castelmoresco, Vol. I*; Tommaso Guerrero and C. Ed.: Naples, Italy, 1855; pp. 5–16. (In Italian)
171. Liguori, F.S. *Cenni Storico Critici Della Città Di Gragnano*; Tip. Spinelli: Naples, Italy, 1863. (In Italian)
172. Celico, P.; Guadagno, F.M. L'instabilità delle coltri piroclastiche delle dorsali carbonatiche in Campania: Attuali conoscenze. *Quad. Di Geol. Appl.* **1998**, *5*, 75–133. (In Italian)
173. Mele, R.; Del Prete, S. Lo studio della franosità storica per la valutazione della pericolosità da frane. Un esempio dell'area di Gragnano (Campania). *Boll. Soc. Geol. Ital.* **1999**, *118*, 91–111. (In Italian)
174. De Riso, R.; Budetta, P.; Calcaterra, D.; Santo, A.; Del Prete, S.; Del Luca, C.; Di Crescenzo, G.; Guarino, P.M.; Mele, R.; Palma, B.; et al. Fenomeni di instabilità dei Monti Lattari e dell'area flegrea (Campania): Scenari di suscettibilità da frana in aree-campione. *Quad. Geol. Appl.* **2004**, *11*, 1–26. (In Italian)
175. Vallario, A. *Sarno: Sei anni dalla Catastrophe*; Guida: Naples, Italy, 2004; pp. 36–37. (In Italian)
176. Michetti, A.M.; Esposito, E.; Guerrieri, L.; Porfido, S.; Serva, L.; Tatevossian, R.; Vittori, E.; Audemard, F.; Azuma, T.; Clague, J.; et al. Environmental Seismic Intensity Scale ESI 2007. *Mem. Descr. Carta Geol. D'italia* **2007**, *74*, 11–20.
177. Porfido, S.; Esposito, E.; Guerrieri, L.; Vittori, E.; Tranfaglia, G.; Pece, R. Seismically induced ground effects of the 1805, 1930 and 1980 earthquakes in the Southern Apennines, Italy. *Ital. J. Geosci.* **2007**, *126*, 333–346.
178. Serva, L.; Esposito, E.; Guerrieri, L.; Porfido, S.; Vittori, E.; Comerci, V. Environmental Effects from some historical earthquakes in Southern Apennines (Italy) and macroseismic intensity assessment. Contribution to INQUA EEE scale project. *Quat. Int.* **2007**, *173–174*, 30–44. [CrossRef]
179. Porfido, S.; Alessio, G.; Gaudiosi, G.; Nappi, R.; Spiga, E. The Resilience of Some Villages 36 Years After the Irpinia-Basilicata (Southern Italy) 1980 Earthquake. In *Advancing Culture of Living with Landslides*; Mikoš, M., Vilímek, V., Yin, Y., Sassa, K., Eds.; Springer: Cham, Switzerland, 2017; pp. 121–133. [CrossRef]
180. Samuelli-Ferretti, A.; Siro, L. (1983a)-Comune di Calitri (AV). In *Indagini di Microzonazione Sismica CNR- PFG, Pubbl. n. 492*; CNR-PFG: Bologna, Italy, 1983; 221p. (In Italian)
181. Porfido, S.; Esposito, E.; Michetti, A.M.; Blumetti, A.M.; Vittori, E.; Tranfaglia, G.; Guerrieri, L.; Ferreli, L.; Serva, L. Areal distribution of ground effects induced by strong earthquakes in the Southern Apennines (Italy). *Surv. Geophys.* **2002**, *23*, 529–562. [CrossRef]
182. Del Prete, M.; Trisorio Liuzzi, G. Risultati dello studio preliminare della frana di Calitri (AV) mobilitata dal terremoto del 23/11/1980. *Geol. Appl. Idrogeol.* **1981**, *16*, 153–165. Available online: https://hdl.handle.net/11586/71536 (accessed on 20 September 2022). (In Italian)
183. Del Gaudio, V.; Wasowski, J. Time probabilistic evaluation of seismically induced landslide hazard in Irpinia (Southern Italy). *Soil Dyn. Earthq. Eng.* **2004**, *24*, 915–928. [CrossRef]
184. Martino, S.; Scarascia Mugnozza, G. The role of the seismic trigger in the Calitri landslide (Italy): Historical reconstruction and dynamic analysis. *Soil Dyn. Earthq. Eng.* **2005**, *25*, 933–950. [CrossRef]
185. Porfido, S.; Esposito, E.; Luongo, G.; Marturano, A. Terremoti ed effetti superficiali: Esempi nell'Appennino meridionale. In Proceedings of the Convegno "Studio Centri Abitati Instabili", Portonovo di Ancona, Italy, 10–12 May 1989. (Published in 1991) (In Italian)
186. Parise, M.; Wasowski, J. Aspetti evolutivi e dato attuale della franosità nei dintorni dell'abitato di Calitri. In Proceedings of the International Conference "La Prevenzione Delle Catastrofi Idrogeologiche: Il Contributo Della Ricerca Scientifica", Alba, Italy, 5–7 November 1996. (In Italian)
187. Pro Loco Calitri. Available online: www.prolococalitri.it (accessed on 3 January 2022).
188. Vera, e distinta Relatione del Terremoto accaduto in Napoli, e parte del suo Regno il giorno 8 di Settembre 1694. *Con il Numero De' morti, e Feriti che Nelle Medesime Sono Restati Sotto delle Pietre*, Per Gio. Francesco Buagni: Napoli, Italy; Roma, Italy. (In Italian)
189. Esposito, E.; Luongo, G.; Marturano, A.; Porfido, S. Il terremoto di S. Anna del 26 luglio 1805. *Mem. Soc. Geol. It.* **1987**, *37*, 171–191. Available online: http://eprints.bice.rm.cnr.it/id/eprint/2761 (accessed on 10 September 2022). (In Italian)
190. Poli, G.S. *Memoria sul Tremuoto de' 26 Luglio del Corrente Anno 1805*; Orsini Ed.: Naples, Italy, 1806; p. 224. (In Italian)
191. Luino, F.; Turconi, L. *Eventi di Piena e Frana in Italia Settentrionale nel Periodo 2005–2016*; Ed. SMS: Moncalieri, Italy, 2017; p. 478, ISBN 8890302380/9788890302381. (In Italian)
192. Luino, F.; De Graff, J.; Roccati, A.; Biddoccu, M.; Cirio, C.G.; Faccini, F.; Turconi, L. Eighty Years of Data Collected for the Determination of Rainfall Threshold Triggering Shallow Landslides and Mud-Debris Flows in the Alps. *Water* **2020**, *12*, 133. [CrossRef]
193. Turconi, L.; Nigrelli, G.; Conte, R. Historical datum as a basis for a new GIS application to support civil protection services in NW Italy. *Comput. Geosci.* **2014**, *66*, 13–19. [CrossRef]

194. Tropeano, D.; Turconi, L. Geomorphic classification of alpine catchments for debris-flow hazard reduction. In Proceedings of the Debris-Flow Hazards Mitigation: Mechanics, Prediction and Assessment, Davos, Switzerland, 10–12 September 2003.
195. ARPA PIEMONTE-Progetto Risknat Programma Operativo di cooperazione transfrontaliera tra Italia-Francia 2007–2013 ALCOTRA nel campo dei rischi idrogeologici, Rapporto di sintesi, in Italian. Available online: https://www.interreg-alcotra.eu/sites/default/files/rfe_2016_finale_wp4.pdf (accessed on 23 October 2022).
196. Turconi, L.; Tropeano, D.; Savio, G. Debris flows in the Marderello catchment in Summer 2005 (Cenischia Valley, Western Italian Alps): A critical rainfall-process analysis. *Wildbach Und Lawinenverbau* **2008**, *72*, 42–61. Available online: http://www.cnr.it/prodotto/i/67023 (accessed on 14 September 2022).
197. Coviello, V.; Arattano, M.; Turconi, L. Detecting torrential processes from a distance with a seismic monitoring network. *Nat. Hazards* **2015**, *78*, 2055–2080. [CrossRef]
198. Pasculli, A.; Cinosi, J.; Turconi, L.; Sciarra, N. Learning Case Study of a Shallow-Water Model to Assess an Early-Warning System for Fast Alpine Muddy-Debris-Flow. *Water* **2021**, *13*, 750. [CrossRef]
199. Turconi, L.; Luino, F.; Gussoni, M.; Faccini, F.; Giardino, M.; Casazza, M. Intrinsic Environmental Vulnerability as Shallow Landslide Susceptibility in Environmental Impact Assessment. *Sustainability* **2019**, *11*, 6285. [CrossRef]
200. Tropeano, D.; Govi, M.; Mortara, G.; Turitto, O.; Sorzana, P.; Negrini, G.; Arattano, M. *Eventi Alluvionali e Frane Nell'italia Settentrionale. Periodo 1975-81*; CNR-IRPI GNDCI: Turin, Italy, 1999; pp. 240–243. (In Italian)
201. ARPA PIEMONTE. *Rapporto Preliminare Sull'evento Alluvionale del 28–30 maggio 2008*; ARPA PIEMONTE: Turin, Italy, 2008; p. 39. (In Italian)
202. Carte Topographique et Militaire du Mont Cenis 1821. Available online: https://upload.wikimedia.org/wikipedia/commons/a/a4/Carte_topographique_et_militaire_du_mont_Cenis_1821.jpg (accessed on 16 December 2022).
203. GEOPORTAIL. Available online: https://www.geoportail.gouv.fr/carte (accessed on 26 July 2022).
204. SIVA: SISTEMA INFORMATIVO VALANGHE Scheda di Caratterizzazione del Sito Valanghivo. Available online: http://webgis.arpa.piemonte.it/webval/valdati_new.php?CODECATE=35_M_TO (accessed on 12 November 2022).
205. Newspaper "The independent", (Susa, year 18, number 18, 24 April 1904); Geologia dell'Ambiente. 2020. Available online: https://www.sigeaweb.it/2012-07-23-20-10-41/supplementi-a-gda/1178-supplemento-gda4-2021.html (accessed on 23 September 2021).
206. REGIONE PIEMONTE. *Rapporto Sull'evento Alluvionale del 13–16 ottobre 2000, Versione 1.1*; Regione Piemonte: Turin, Italy, 2000; p. 82. (In Italian)
207. Bertea, A.; Cordola, M.; Dutto, F.; Longo, F.; Dotta, A.; Caffo, L.; Vangelista, Z.; Fontan, D. Il piano di protezione civile per emergenza valanghe del comune di Venaus. *Neve Valanghe* **2010**, *36*, 36–43. (In Italian)
208. AUTORITÀ DI BACINO DEL FIUME PO Progetto di Piano Stralcio per l'Assetto Idrogeologico, Norme di Attuazione; Autorità di Bacino del Fiume Po: Parma, Italy. 1999, p. 9. Available online: http://www.adbpo.it/download/MorfologiaFluviale/psff_pai/8702All-3_tit_II-Metodo_di_delimit_fasce_fluviali.pdf (accessed on 7 September 2022).

**Disclaimer/Publisher's Note:** The statements, opinions and data contained in all publications are solely those of the individual author(s) and contributor(s) and not of MDPI and/or the editor(s). MDPI and/or the editor(s) disclaim responsibility for any injury to people or property resulting from any ideas, methods, instructions or products referred to in the content.

land

MDPI

*Article*

# Historical Floods and Territorial Planning: Lessons Learned and Opportunities Lost after the Santa Teresa Flood (1879) in the Segura Basin (Spain)

**Antonio Oliva [1,*] and Jorge Olcina [2]**

[1] Interuniversity Institute of Geography, University of Alicante, 03690 San Vicente del Raspeig, Spain
[2] Departament of Regional Geographical Analysis and Physical Geography, University of Alicante, 03690 San Vicente del Raspeig, Spain; jorge.olcina@ua.es
* Correspondence: antoniogeografia1@gmail.com

**Abstract:** Historical cartography is one of the principal tools used in correct flood adaptation and management based on territorial planning. In fact, Directive 2007/60/EC on the assessment and management of flood risks includes the analysis and inventory of historical floods in a river basin for assessing the flood hazard and risk existing in a geographical space. This study seeks to analyse the largest flood registered in the Segura basin, occurring on 14–15 October 1879, which attracted enormous interest on a national and international level. The methodology applied is based on the consultation of historical sources and historical cartography, and the elaboration of maps using GIS, enabling comparisons to be made with current flood zones. The results show that the Santa Teresa flood was very similar to the Spanish National Cartographic Systems for Flood Areas (SNCZI) map for a 500-year return period. Furthermore, it allows the identification of the sensitive points along the course of the river or those prone to burst banks or overflowing, which practically coincide with the current maps and modelling conducted by the official bodies. Furthermore, the buildings in the floodable area in the historical cartography have been counted and reconstructed on a GIS map and the SNCZI. Massive anthropic occupation through the construction of settlements and infrastructures (hospitals, schools, centers for the elderly, roads and railways) in the Guadalentín valley and the Segura River increases the risk of flooding in the study area, despite the numerous control and regulation works carried out in the Segura River basin.

**Keywords:** floods; historical cartography; territorial planning; Santa Teresa flood; Segura basin

**Citation:** Oliva, A.; Olcina, J. Historical Floods and Territorial Planning: Lessons Learned and Opportunities Lost after the Santa Teresa Flood (1879) in the Segura Basin (Spain). *Land* **2024**, *13*, 28. https://doi.org/10.3390/land13010028

Academic Editor: Hariklia D. Skilodimou

Received: 14 November 2023
Revised: 11 December 2023
Accepted: 14 December 2023
Published: 25 December 2023



**Copyright:** © 2023 by the authors. Licensee MDPI, Basel, Switzerland. This article is an open access article distributed under the terms and conditions of the Creative Commons Attribution (CC BY) license (https://creativecommons.org/licenses/by/4.0/).

## 1. Introduction

Floods are natural phenomena that cause major social and environmental impacts throughout the world [1–8]. There are several factors that increase the damage generated by floods, such as: deforestation of the catchment basin of the flows, erosion of soils, obstacles to the water flow, breakage or failure of engineering works, occupation of floodplains, urbanisation and inadequate drainage, deficiencies in territorial planning, and limitations in warning the population in case of emergency or climate change [8,9]. According to Wadgure and Kamble (2022), the areas most prone to floods are: (a) places affected by historical floods; (b) depressed or sunken areas with very little slope; and (c) areas located downstream from dams [4].

The *Special Report on Directive 60/2007/EC of 23 October on the assessment and management of natural risks*, elaborated by the European Court of Auditors indicates that serious floods are becoming more frequent in Europe. In particular, more than double the number of medium-sized or large *flash floods* are being reported than at the end of the 1980s [8].

For Europe, the Representative Concentration Path 8.5 scenario (RCP 8.5) reveals a substantial increase in the frequency of maximum flow, which will affect the population and will exponentially increase economic losses. In fact, future climate modelling shows

an increase in the number of rainfall events associated with 100-year return periods. This means that, in every country in Europe, including Spain, there will be an increase in the frequency of serious floods [10,11].

In Spain, the Ministry for Ecological Transition and Demographic Challenge (hereafter, MITERD) indicates that each year an average of 10 serious flood episodes occur in Spain [12,13] (MITERD, 2018; MITERD, 2020). According to the CCS and the Directorate General for Civil Protection and Emergencies (DGPCE), floods have caused the deaths of 312 people over the last 20 years (2000–2020). The years 2018 and 2019 particularly stand out as 24 and 20 deaths due to floods were recorded, respectively, together with material damage worth EUR 800 million [14–16]

This is due to the increased exposure in floodable areas, which, as indicated by Pérez-Morales et al., (2021), shows that the "property boom" (1996–2006) in Spain gave rise to the increase in the area exposed to floods, particularly on the coast. This situation has translated into a notorious increase in the impact and frequency of floods [17].

However, the number of deaths caused by floods in Spain is falling considerably, due to the construction of more robust housing (in floodable areas) and flood defence works (structural measures), although there has been an increase in the exposure of the population to flash floods in the urban framework [16].

According to the Spanish National Cartographic System for Flood Areas (hereafter, SNCZI) of the MITERD, it is estimated that around 3 million Spaniards live in areas that are at a high risk of flooding, identified during the implementation of the Directive 60/2007/ED on the assessment and management of flood risks.

The climate scenarios for Spain indicate a reduction in the average annual precipitation and the number of rainy days per year [18,19]. However, a greater volume of precipitation has been observed, together with a greater frequency of intense precipitation. These conditions favour an increase in floods [19].

Traditionally, the flood-defence measures implemented throughout the 20th century focused on the so-called "old hydraulic policy" based on structural or hard engineering works, generally in response to the occurrence of a catastrophic event. These types of engineering works comprise the construction of reservoirs, dams, retaining walls, pipelines, bypasses, channelling and, in the most extreme cases, the deviation of flows or the construction of artificial flows [20–22].

These types of actions are immediate solutions requested by the society affected by a flood episode and which, in general, are welcomed by the population, particularly on a local scale, where town councils fight for the regional authorities to finance these infrastructures [16,22]. Although these types of actions usually resolve the problem effectively, it is true that, as well as being very expensive, they divert the problem to other sectors, while generating a "false sense of security" among the population, as it makes people believe that the problem has been resolved and there will be no more flooding [16].

Currently, adaptation measures include a series of actions that are more efficient when adapting to the negative effects of floods. These measures include: prediction measures (real-time weather forecasting and hydrological information systems); prevention measures (flood directive 60/2007/EC): historical analysis, historical mapping of flooded areas, hazard mapping, flood risk mapping and the elaboration of a flood risk management plan; land-use management and planning in the territory, regulation of land uses in accordance with the Regulation of the Public Water Domain, the Water Law, assurance systems, civil protection plans (emergency plans and flood risk adaptation plans (including evacuation) and raising awareness and education about risk; protection measures (mixed, adaptation, and structural measures; recovery of river spaces or *Room of Rivers*; and sustainable urban drainage systems (SUDS) and rainwater storage mechanisms (storm tanks and floodable parks), green solutions or *Nature-Based Solutions* (NBS), green corridors, flood alleviation areas or flood control zones (FCZ), commonly known as sacrifice zones or the adaptation of buildings). We should also include the exploitation or recovery of former water uses and the flood reduction measures of traditional societies.

Directive 60/2007/EC on the assessment and management of flood risk constituted a considerable change in the planning and management of flood risk in the European space, promoting preventive measures based on mapping and territorial planning as basic elements of risk reduction [9]. Maps are a principal tool for the Directive in identifying, accrediting, and preventing flood risk. In order to elaborate the flood hazard and risk maps, Directive 60/2007/EC indicates the need to conduct a preliminary assessment of the flood risk (Art. 4, point 1) using the available information, such as recorded data and long-term evolution studies. Along these lines, the steps in undertaking this assessment are: (a) maps of the river basin district, at the appropriate scale, showing the boundaries of river basins and sub-basins and, where they exist, coastal areas, and showing the topography and land use of the river basin, topography, and land use; (b) a description of the floods occurring in the past (historical) that have had a significant negative impact; (c) a description of significant past flood events where adverse consequences of similar future events can be foreseen; and (d) an assessment of the potential negative consequences of future floods. These data allow a hazard map to be elaborated in accordance with the probabilities of occurrence or return periods with data such as the expanse, depth, and speed of the water. Subsequently, the risk map should include the potential adverse consequences for the affected inhabitants, the type of economic activity affected, the pollution accidentally caused by flooding or the impact on protected areas and any other information that the State considers useful, such as the indication of floodable zones.

When elaborating risk maps and defining flood management measures, studies that include a historical analysis of extreme natural phenomena, in this case floods, have constituted a fundamental tool for identifying the risk existing in a territory and influencing human behaviour, with the aim of informing about floodable areas and preventing their occupation.

Internationally, there are multiple studies using historical data analysis to analyse past climate characteristics and their behaviour in relation to extreme events (droughts, glaciations, floods) [19], reconstruction and estimation of historical flood frequency based on existing historical records, analysis to calculate flood trends in different climatic regions of the world, and even the use of historical flood marks.

Kjeldsen et al. (2014) point out that the analysis of historical flood events from academic application to practice has been limited, but that it serves to estimate the frequency of past floods and to understand future trends. He also highlights the great heterogeneity of methodologies applied when carrying out historical analyses, which generally depend on the data series (short or long) available. The conclusions drawn by the authors indicate that there is considerable potential to improve the reliability of current flood risk assessments by collecting valuable information on past extreme events contained in historical datasets [23].

Mediero et al. (2015) conducted a study based on recorded historical flow data consisting of the longest flow series available in Europe. The methodology applied is interesting since they first chose data from 102 gauging stations from 25 European countries, then identified five major regions (Atlantic, Continental, Scandinavian, Alpine, and Mediterranean) and identified the months with the highest probability of flooding. They also calculated the trend in the magnitude of floods in different periods (every 10 years) throughout the 20th century, obtaining as results a negative trend in the magnitude of floods. This means that there has been a decrease in the number of flood events in the regions analysed [24].

Szczepanek et al. (2022) emphasise the crucial role of flood marks ("this is how far the water reached in the flood of XXXX. . ."). These marks are very useful because they function as a warning system for the population that they are living in a flood zone. In addition, these marks are considered cultural heritage in many cities. In this case, 21 elements of flood marks in Krakow (Poland) are analysed, highlighting the oldest mark in the 16th century. The author also points out that nowadays these flood marks can be recorded by using new technologies (photography with any personal mobile phone), which makes it possible to obtain an image of the flood, to know the magnitude of the flood, and to use these data for better flood management [25].

In Spain, there are numerous studies that analyse the role of historical climatology and its relationship with extreme events (droughts, floods, periods of glaciation in Spain), since the 14th century [26–29], as well as the chronology of extreme flood events through documentary sources [30].

There are also studies of historical analysis of extreme climate episodes, floods, and their consequences [31,32]. In these studies there are detailed analyses of the formation of detailed meteorological situations causing the formation of storm nuclei (in most cases, mesoscale convective systems) causing the largest episodes of precipitation and flooding in the Spanish southeast from 1950 until 1990. In addition, it also includes information related to the effects of floods (affected areas and duration of the flood), evaluations of initial economic costs (after the flood), and final economic costs (total losses due to the flood episode), including aid from the Spanish governments and even the approval of some defence work or actions to repair hydraulic infrastructure [31].

In addition, there are geographical–historical studies that compile historical floods that occurred in different basins. Galván Plaza (2018) analyses the four major historical floods of the Ebro River as it passed through the city of Murcia, from 1643 to 1961, using historical maps and plans of the time. Likewise, he also highlights how man has been occupying and settling in the flood plain of the Ebro River on its left bank, causing greater economic losses with the floods experienced by the Ebro River [33]. Gil Olcina and Canales (2022) have recently published a monograph on the causes and consequences of the floods that occur in the Segura basin, and especially in its final section corresponding to the Alicante region of Vega Baja del Segura. Likewise, the authors compile the most important flood episodes that occurred in the Segura basin, highlighting: 1879, 1946, 1948, 1972, 1973, 1987, 2016, and 2019. They also compile all the information related to the numerous defence plans to regulate the Segura basin to alleviate the effects of the floods from 1879 to 1987 [34].

They also highlight: flood risk analysis studies that currently exist in urban environments in the province of Alicante, where some interesting information related to some municipalities in the Vega Baja del Segura can be found [35]; risk analysis studies that take into account danger (through hydraulic modelling), exposure (identifying areas, land uses, infrastructure, and buildings), and vulnerability studies for different land uses, obtaining flood risk maps in urban environments, as is the case of the Tormes River (Salamanca, Spain) [36]; and works related to the abandonment of traditional irrigation systems for dryland crops (peat irrigation or diversion irrigation, taking advantage of rainwater and formation of floods) that has increased the magnitude of river floods today. They also use historical maps and sketches to identify the abandoned irrigation network and the affected areas of the Abanilla Rambla, explaining the effects on the flooding episode of September 2019. In addition, they also calculate the volume of flow that would have been reduced if these irrigation systems were currently in operation, calculating an estimated value for different return periods [37].

Likewise, studies on the reconstruction and magnitude of floods also stand out through the use of geomorphological evidence, combined with one-dimensional hydraulic modelling and supported with records from documentary sources of the localities. An example is the work of Benito et al. (2010) in which they carried out paleoflood studies along a 2.5 km stretch located at the confluence of the Rambla Mayor (162 $km^2$) and the Carmelo River (210 $km^2$), in the upper basin of the Guadalentín (basin of the Safe). From this analysis they identified at least 10 floods with flows between 15–580 $m^3$ (950–1200); seven floods, in which two floods estimated higher flows between 580–680 $m^3/s$ (1648–1672); seven floods with two flood events greater than 250 $m^3/s$ (1769–1802); four flood episodes, where two episodes stood out with estimated flows between 760–1035 $m^3/s$ (1830–1840), and finally, seven floods of which three events exceeded 880 $m^3/s$ (1877–1900). The conclusion obtained from this work is the anomalous increase in the frequency of large-magnitude floods between 1830 and 1900 [38].

Similarly, studies have also been carried out that are based on other sources, such as old photographs [39], the historical mapping of river courses [40], or the elaboration of

current flood hazard and risk mapping in accordance with historical cartography [41–43], in the Segura basin, and in the cities of Orihuela [42] and Murcia [43].

The rivers have evolved with the societies at the headwaters, along their courses and in the floodplains, giving rise to a series of implications related to territorial planning. However, territorial management and planning are policies that have only been implemented in Spain in the last 50 years. Therefore, they constitute a new aspect for regulating land uses in floodable areas after a flood episode.

As indicated by Giménez-Font (2009), rivers have also been a longstanding primary focal point of cartographic activity in surveying, hydrometrics, engineering, and cartography. The abundant Spanish cartography includes many river maps and plans dating back to the 16th century with exquisite quality, particularly those elaborated in the 18th and 19th centuries. The majority of them are accompanied by a wealth of historical documentation which is increasingly accessible and often with correct interpretations on the capacity of erosion and the changing river courses, which has been an age-old matter of interest and concern for river societies [40].

Historical cartography has been an object of research in itself or has accompanied historical or geographic studies. However, new readings allow us to extract conclusions on a scientific-technical level and also on an environmental level that multiply the possibilities of many old maps which are no longer just a static representation but an element of reference in the study of river morphology and its relationship with the name [40]. In many physical geography studies, historical cartography has been a decisive element of analysis, although it does have its advantages and disadvantages with respect to the scales used and the purpose of the maps [40].

This historical cartography improved in terms of quality and detail throughout the 18th century, which enables us to identify the responses of river systems to human impacts and, in turn, the technical responses which, over the course of about two centuries, were implemented for some of the morphological manifestations of the rivers [40]. In the 19th century, maps of the flooded areas after a flood episode with catastrophic consequences for society (fatalities and economic damage) began to be drawn up. These maps could be considered as the beginning of hazard maps after the event (post-catastrophe).

This study seeks to assess the territorial impacts based on territorial management and planning based on the analysis of the flood episode of 14–15 October 1879 in the Segura basin, located in the south-east of the Spanish peninsula.

The objectives of this study are:

(a) To carry out a historical analysis of the flood of 14–15 October 1879 (Santa Teresa flood) in the Guadalentín river valley and in the middle and lower sections of the Segura river.
(b) Reconstruct the historical map of the flood to study the current situation.
(c) Calculate the total built-up area in the flood zone of the Guadalentín valley and Segura river valley.
(d) Identify lessons learned and missed opportunities for risk reduction from territorial planning.

This study seeks to show the importance of the historical study of extreme flooding events and of historical cartography for the territorial planning of areas at risk. The precise analysis of the areas affected and their comparison with the current territorial reality enable the weight of the territorial planning to be assessed when establishing new land uses after the occurrence of a high-impact flood episode.

## 2. Materials and Methods

### *2.1. Historical Description of the Effects of the October 1879 Flood*

The flood episode of 14 and 15 October 1879, known as the "Santa Teresa flood" as it occurred on the date of the saint's day with the same name, occurred as a result of intense and torrential rains throughout the whole of the Segura basin, with an even greater intensity recorded in the basin of the Guadalentín, which is the principal tributary of the

River Segura. This episode marked a before and after in the history of the basin, particularly in the villages affected [40]. It has been described as one of the deadliest floods in European hydrological records, in the words of the French potamologist Maurice Pardé—the result of the enormous swelling of the River Guadalentín, one of the largest tributaries of the River Segura, classified as "the wildest river in Europe" [34].

Very briefly, a cold drop (gota fria) occurs when a pocket of cold air detaches from the main jet stream in the Gulf of Cádiz and the divergent winds and the sea temperature foster the formation of mesoscale convective systems, which generate abundant and torrential rain [44]. Calvo García-Tornel, Conesa García, and Álvarez Rogel (2001) estimated that the rainfall produced in the headwaters of the River Guadalentín was 600 mm/hour, which, in only one hour, by far exceeded the maximum estimates for 24 h in a 500-year return period [45]. This rainfall was concentrated in the headwaters of the River Guadalentín, giving rise to the sudden flooding of the Rivers Velez and Luchena, whose waters come together at the beginning of the Guadalentín. This brought about the exponential swelling of the Guadalentín close to La Parroquia between the sites of the Valdeinfierno and Puentes reservoirs, reaching a height of 15.5 m [34].

With respect to the flows circulating in the River Guadalentín, it is estimated that the maximum height of the swelling was 4000 $m^3/s$. However, this figure is incorrect, given that the only calculation that is found in the work titled "*El régimen de los ríos peninsulares*" by Masachs (1948) only refers to the maximum swelling in the River Guadalentín as it passes through Totana, estimated at 1300 $m^3/s$, which represents a 10,800-fold increase of its module, for the series of data corresponding to the period 1915 to 1929 [46,47]. This is confirmed by Conesa García (1985), who calculated the maximum volume as it passed through the destroyed Puentes II reservoir at 1744 $m^3/s$, for a river basin level of 971.2 $km^2$. Furthermore, it was estimated that for Puentes de los Carros, with a basin of 2748 $km^2$, the maximum volume would have been 1300 $m^3/s$ [34]. It was also calculated that the River Guadalentín discharged a volume of 58 $hm^3$ as it passed through Lorca, while downstream at the meeting point of the River Guadalentín with the River Segura, the volume contributed by the former was between 30 and 35 $hm^3$ [34].

Such high volumes as these in the River Guadalentín as it passed through Lorca are explained by three reasons: (a) the high amount and intensity of rainfall in the headwaters of the Guadalentín, (b) the siltation of the Valdeinfierno dam and the Puentes II dam, which was destroyed in the 1802 flood, and (c) the insufficient capacity of the Canal del Reguerón (60 $m^3/s$). All of this led the waters of the Guadalentín, when combined with the swelling of the River Segura, to generate floods and catastrophic consequences in the Vega Media and Vega Baja del Segura.

The consequences of the flood in the town and surrounding area of Lorca were very severe. A total of 15.362 ha were flooded by the waters of the River Guadalentín, both in the town and the agricultural lands.

The specific impacts of the flood are listed by González López (2014), who indicates the following: the flooded area in Lorca spanned from the lower part of the San Cristóbal neighbourhood to the door of the parish church, the Calle Mayor (water with a 4–5 m height) and the Charco, Puente de los Carros, and Rambla streets. In the Puerta de San Ginés street, the water covered the roofs. Between the Rueda orchards and the Santa Quiteria bridge, "the avalanche opened a gap in the wall" converting the neighbourhood into a river. The San Diego orchard and the bordering districts were converted into a large lake. In the village beside the river, the water reached the La Merced convent. On the Águilas road, 100 m from the Santa Paula oval and the Tres Puentes promenade "there was a shoreless sea". At this point, the waters almost touched the streets of the town, reaching the doors of the barracks in Aire street where the parish church of San Matero is located. In the sanctuary of Nuestra Señora de las Huertas, the waters covered the pulpit, and in the San Diego church the waters reached the second floor of the building [44].

There is little information about the rural areas further away from the urban nuclei, only that "[t]he districts of La Tova, Fontanares, Jarales, Paca, Avilés, Doña Inés and

Zarzadilla have been so badly affected that none of their farms will be able to produce anything for some years" [44].

Meanwhile, the River Segura also experienced severe swelling, although slightly less than the Guadalentín. Except for the convergence point of the Guadalentín with the Segura, the rest of the swellings of the tributaries of the Segura were not synchronised but successive, and the maximum flow as the waters passed through Murcia was 1890 $m^3/s$. On the morning of 15 October, the flow of the River Segura dropped to 1640 $m^3/s$ and a few hours later it increased again to 1700 $m^3/s$, as a result of the addition of the flows from the upper sub-basins (Rivers Tus, Taibilla, and Mundo), together with the contributions of the upstream watercourses [34]. López Bermúdez and other authors (1978) estimated that the River Segura had a maximum flow of 2500 $m^3/s$ in the city of Murcia on 15 October, resulting in the total flooding of the Vega Media and Vega Baja del Segura until the sea [47].

In the Vega Media, specifically in Murcia, the effects of the flood were devastating for the aforementioned reasons, namely: (a) the reactivation and overflowing of the tributary watercourses of the River Segura on its left side, increasing its flow; (b) the reactivation and overflowing of the watercourses directly falling into the Albatalía and the orchards of Espinardo, Churra, and Monteaguado and the areas of Puente de Tocinos, Arboleja, Urdienca, and Raal, flooding the city of Murcia in the north and east; (c) the increased flow of the River Segura itself as it passed through Murcia estimated at 2500 $m^3/s$; and (d) the works of the Canal de El Reguerón (known as the trench of the devil or death), located at a height of 4 m above the River Segura and with an insufficient hydraulic capacity of 60 $m^3/s$, collected the waters of the flood of the bend in the Guadalentín which met with the swelled flow of the River Segura, leading to the overflowing of both of the rivers in Murcia, flooding its western and southern sectors and increasing the flood in the eastern sector. Murcia was practically isolated by a sheet of water with an average height of 1.5 m throughout the whole of the orchard lands [34].

With respect to the final section of the River Segura or Vega Baja del Segura, Gil Olcina and Canales (2022) highlight that both the town of Orihuela and other municipalities of the Vega Baja (15 in total) were seriously affected by the floods and the overflowing of the River Segura [34].

It is estimated that the flow of the River Segura as it passed through Orihuela was 2000 $m^3/s$. Thanks to prior warning through conches and telegraphs, a higher number of deaths due to the flood were prevented. However, the flood destroyed many buildings and the height of the flood water in the Vega Baja reached 7 m at its lowest points. The figure below shows a sketch of the flood episode (Figure 1).

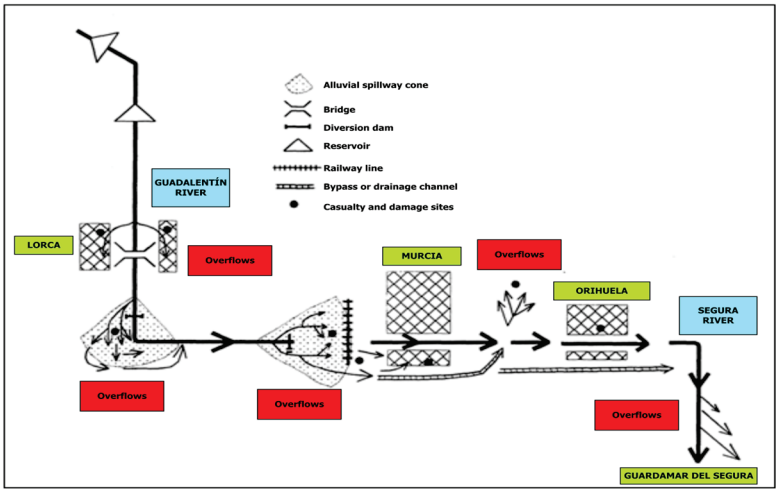



**Figure 1.** Sketch of the flood of October 1879. Source: Adapted from Calvo García-Tornel, Conesa, and Álvarez Rogel (2001) [45].

This flood, the deadliest documented in Spain, aroused widespread solidarity on a national and international level. As indicated by Gil Olcina and Canales (2022), the royal family led the movement of support to the victims: Alfonso XII travelled to the flooded area and visited the most affected areas of the Vega Media and Vega Baja; Queen Isabel, who at that time lived in Paris, sold her jewels to help the victims and support the campaign to collect donations [34].

Furthermore, the news received unprecedented coverage beyond Spain's borders: none of the large floods occurring in Spain had been reported in Europe in the same way as the Santa Teresa flood [34]. The authors add that this was largely due to the intense activity that, supported by Queen Isabel, then living in Paris, was carried out by the Spanish ambassador to that city, who exercised his role rightly and with prestige. His name was Mariano Roca de Togores y Carrasco, the Marquis of Molins, from the eminent lineage from the town of Orihuela of the Counts of Pinohermoso. Among the different initiatives to raise funds in France, which finally amounted to 1,812,000 pesetas, particularly noteworthy due to its originality and size was the launch of 400,000 copies of the *Revue Paris-Murcie*, published by the French Press Committee.

As indicated by Gil Olcina and Canales (2022), the death toll was as follows: a total of 761 people lost their lives in the orchard area of Murcia, 13 in Lorca, two in Librilla and one in Cieza. With respect to material damage, a total of 5762 huts and houses were destroyed, and 2949 ruined; there were crop losses, and 22,469 animals drowned. Furthermore, the damage to the hydraulic infrastructures was enormous, as the irrigation network was completely destroyed across the whole of the area affected together with 129 mills. In Lorca, the total losses were calculated at 1,716,000 pesetas, which was much lower than those estimated by the local assessors at 7,247,871; even greater was the value of the damage in Murcia at 9,011,000 pesetas and 1,539,000 in Orihuela [34] (Table 1).

**Table 1.** Fatalities and material casualties in the Santa Teresa flood.

| Municipalities | Deaths | Property Damage (€ in 2023) |
|---|---|---|
| Lorca | 13 | 6,176,786.90 |
| Murcia | 763 | 7,693,891.21 |
| Orihuela | 2 | 1,311,212.45 |
| **TOTAL** | **778** | **13,870,678.42** |

Source: González López (2014) [44] and Gil Olcina and Canales (2022) [34]. Own elaboration.

### *2.2. Study Area*

The methodology used in this study is based on the compilation of documentation and historical data related to the flood of October 1879 in the Segura basin, in which the Rivers Guadalentín and Segura played a leading role in the catastrophic consequences in several towns in the Region of Murcia, including Lorca and Murcia, and in towns in Alicante located in the valley of the River Segura.

The area of study selected corresponds to the valley of the Rivers Guadalentín and Segura from Contraparada in Murcia to Guardamar del Segura in Alicante where the river meets the Mediterranean Sea. This area has been chosen as it corresponds to the flooded area in the historical flood of October 1879 (the Santa Teresa flood) (Figure 2).

Another map has been prepared to differentiate the three regions that form part of the Guadalentín Valley and the River Segura: Lorca, Murcia, and the region of the Vega Baja del Segura, since throughout the text allusion will be made to these toponymies (Figure 3).

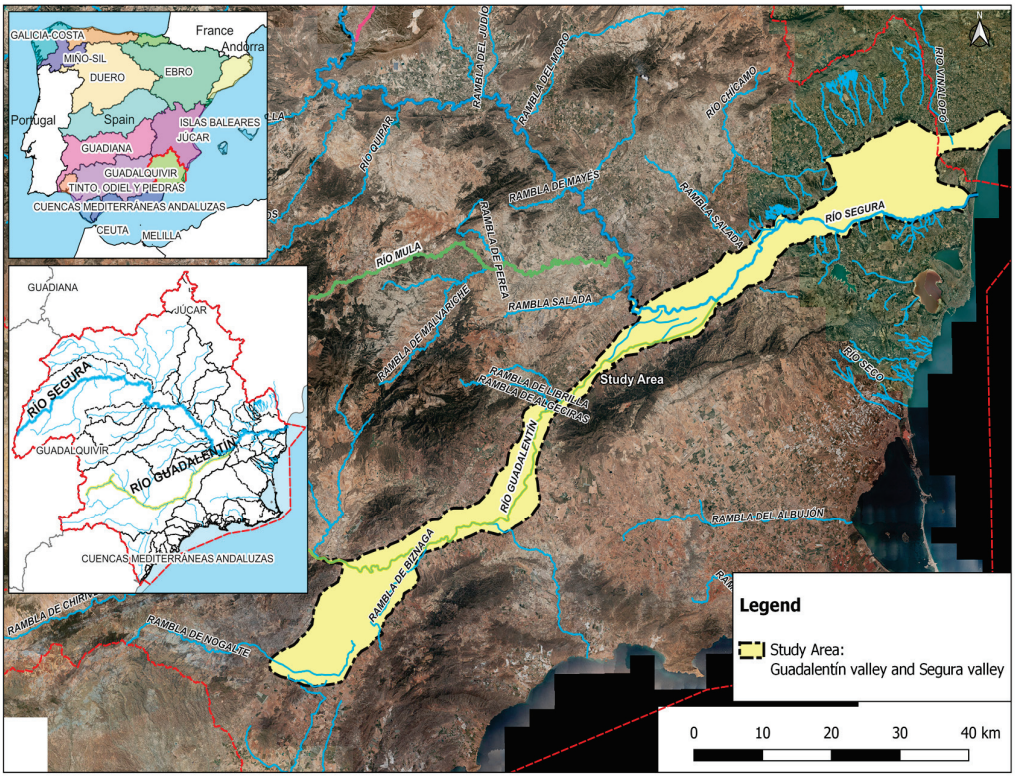



**Figure 2.** Study area: fluvial valley of the Rivers Guadalentín and Segura. Source: National Geographic Institute (IGN) and Segura Hydrographic Confederation (CHS). Own elaboration.

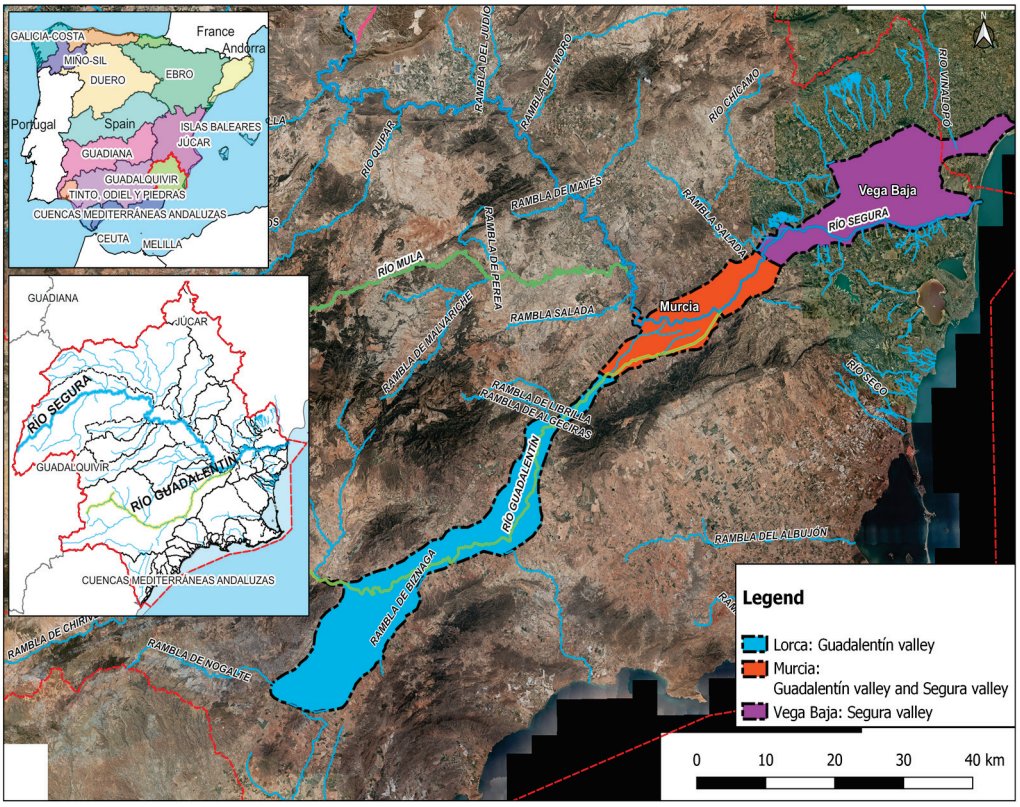



**Figure 3.** The three main regions of the study area. Source: National Geographic Institute (IGN) and Segura Hydrographic Confederation (CHS). Own elaboration.

The Guadalentín and Segura river valleys have experienced numerous floods. The basin organization has counted more than 300 episodes of flooding since the 13th century.

The most catastrophic flood episodes in the Segura basin have coincided with the flooding of the Rivers Guadalentín and Segura, causing numerous deaths and enormous economic damage.

An example of this is the flood of October 1879, an episode of analysis and study in the present research.

It should be pointed out that, from Murcia, the Segura River is incorporated in the so-called Depresión Prelitoral Murciana, characterized by being a valley with little slope, accentuating its flatness from the region of the Vega Baja del Segura. Hence the large number of meanders in the Segura River from Murcia to Orihuela and from Orihuela to Guardamar del Segura.

It should also be noted that, in the Vega Baja del Segura region, the Segura River is higher than its river valley, with a very large flood zone on its left bank. This means that when the Segura River overflows, generally, the greatest catastrophic effects occur on the left bank, and the overflowing waters cannot return to the riverbed. The overflowed waters circulate to the lowest point of the alluvial plain where there is a network of channels that set the stagnant waters in motion. In this way, the waters are transported by this network of channels (azarbes) to the Segura River in its final stretch.

Most floods take between a week and a month and a half to drain, depending on the magnitude of the flood.

### *2.3. Methodology for the Reconstruction of Historical Maps*

The methodology applied in this research consisted of the collection of information and historical maps showing preferential flooding areas, as well as historical maps of floods that have occurred, for example, the flood of October 1879.

Cartographic reconstructions can be carried out in several ways. Two ways can be distinguished: method A and method B. Method A would consist of georeferencing a historical map by adding common points that allow for fitting the historical cartography or plans with current cartography. However, it must be taken into consideration that many historical maps lack the projection used today; they are plans or sketches drawn of large areas (on a county or regional scale) and the result obtained would distort the historical map and the reality of the facts.

For these reasons it was decided to use a methodological alternative: method B (Figure 4). Method B consists of reconstructing historical cartography manually by photointerpretation. The application of this method does not necessarily include georeferencing; one simply uses photointerpretation techniques and creates polygonal layers in shapefile (.shp) format, and prepares it manually with the help of historical descriptions and historical maps.

The result of the manually created layer is a polygonal vector layer that covers the entire flood zone. In this layer itself, groups can be divided based on historical information. In this case, the materials are included as shown on the map drawn up in 1881, which refers to the flood of 1879.

Several studies have been highly useful for the construction of the effects of the flood: the study by González López (2013) gives a detailed description of the areas affected in Lorca, the weak points of the course of the River Guadalentín as it passes through the municipality, the burst banks and obstacles encountered by the floodwater of the river course, and the areas affected downstream past Murcia [44]. It also provides data about personal and economic damage recorded by the municipality after the flood. The recent study by Gil Olcina and Canales (2022) describes in greater detail the causes and consequences experienced in the high and low plains of the River Segura (Murcia, Orihuela, and the floodplains) and provides an inventory of the damage caused by the floods in both towns, the number of mortal victims in the flood episode, and the total material damage [34]. Other studies, such as the one carried out by Calvo García-Tornel, Conesa García, and

Álvarez Rogel (2001) estimate the value of the flooding in the River Guadalentín [45] or that by López Bermúdez and others (1978), which estimates the value of the overflowing of the River Segura [46].

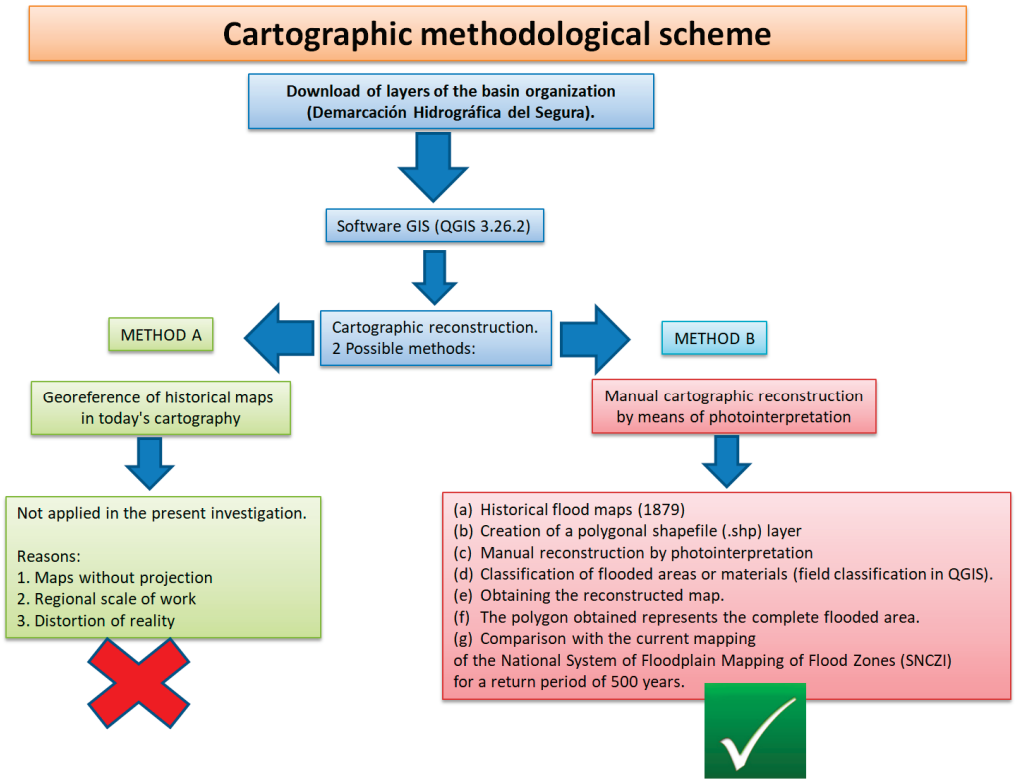



**Figure 4.** Cartographic methodological scheme. Own elaboration.

Historical map documents have been consulted. Illustrations from the period of the effect of the flood have also been used in order to assess the magnitude of the disaster [47]. They have been drawn from the special issue of the publication "*La Ilustración Española y Américana*", published on 30 October 1879. This volume contains a graphic report of the effects of the flood in the city of Murcia by Juan Almagro. They are the only images of the catastrophe that were printed in the press at the time [48]. In this respect, also interesting is the special issue titled "*Paris-Murcie*", in which prestigious French and Spanish writers collaborated: V. Hugo, A. Dumas, O. Feuillet, A. Daudet, E. Littré, E. Zola, G. Mistral, M. Ruiz Zorrilla, M. Roca de Togores (marqués de Molins), E. Castelar, A. Cánovas del Castillo, etc. Also useful is "*Murcia-París*", with articles by renowned Spanish and Murcian authors: J. Echegaray, P. Díaz Cassou, A. Baquero Almansa, R. Serrano Alcázar, J. Martínez Tornel, and Ricardo Gil, among others. Both publications contain very significant illustrations of the effects of the flood in the Segura basin, particularly in the principal urban nuclei, the rural villages, and the hydraulic infrastructures (bridges). All of these written press documents have been consulted in the Digital Newspaper Archive of the Spanish National Library (http://www.bne.es/es/catalogos/HemerotecaDigital/ accessed on 1 November 2023) [48,49] and in the General Archive of the Region of Murcia (https://archivogeneral.carm.es/archivoGeneral/arg.inicio accessed on 1 November 2023) [50,51].

Two historical maps have been compiled and consulted, which can be considered as hazard maps of the time. The first map is a flood hazard map of areas that flood with a certain frequency. After the flood (October 1879), a series of cartographic maps was elaborated that represents the situation of the river and the irrigation network as a disseminator of the flood, with a particular focus on Murcia.

The first historical cartographic map of the flood that is noteworthy is that of Juan Belando (1879), as it constitutes a kind of hazard map, which includes areas of the former

marshlands in Murcia. Furthermore, it distinguishes between three levels of flood hazard: 1: Relative, 2: Large, and 3: Maximum (Figure 5).

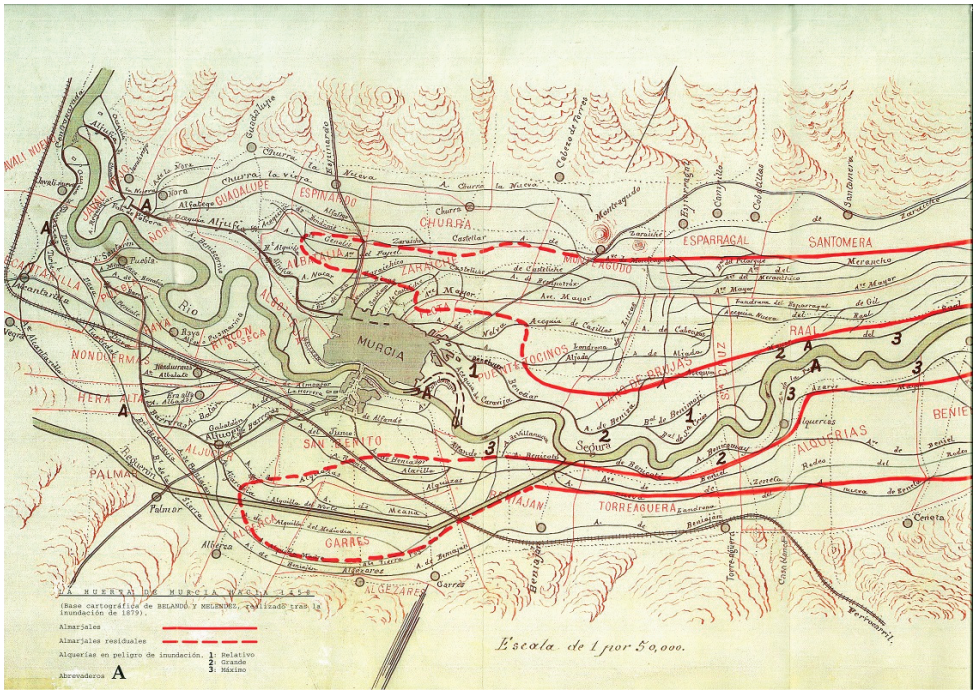



**Figure 5.** Sketch of the huerta of Murcia after the flood of 15 October 1879 drawn up by Juan Belando. Source: Hispanic Digital Library (LDH) (2023) [51].

The second map was published on 30 April 1881 (two years after the flood of October 1879) after the study of the floods that occurred. A sketch was published of the flood with very detailed elements and aspects, such as the height or four types of alluvial materials (sand, sandy silt, semi-compact silt, and compact silt), enabling points of burst banks in the river (overflowing), flooded areas and water accumulation points to be identified (Figure 6).

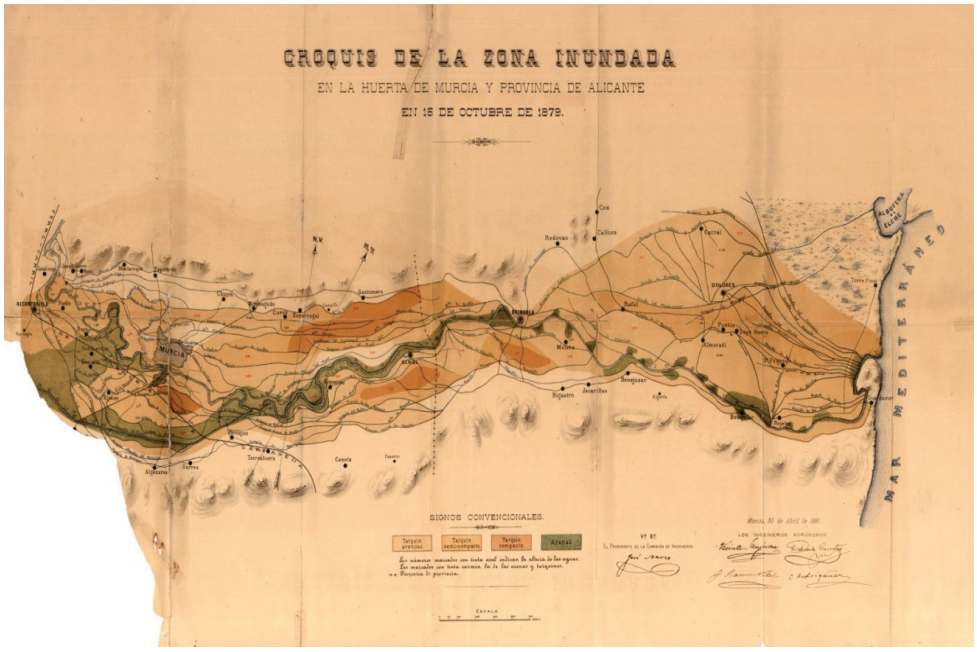



**Figure 6.** Sketch of the flooded area in the huerta of Murcia and Alicante Province. Santa Teresa Flood (14–15 October 1879). Source: National Library of Spain (2023) [51].

Although there are studies that include this map as an example of the effects of the Santa Teresa flood, an exhaustive analysis enables us to identify abundant data and details which are fundamental for understanding the flood episode and the possibility of identifying sensitive points.

These points, shown on the historical map of 1881 as "Arenas", are the most vulnerable points for the overflowing of the Segura River, especially in the sharp bends as it passes through Murcia and at different points of the Vega Baja del Segura.

Furthermore, it was considered necessary to reconstruct cartographically the sketch of the Santa Teresa flood of 1881 in a GIS map (Geographic Information System) to adapt it to the current projections. The methodology to carry out the cartography was performed manually by means of photointerpretation. For this purpose, a vector and polygonal layer was created in shapefile (.shp) format.

A database (BB.DD.) was created in this vector layer. For this purpose, four IDs were created according to the type of material used to draw the 1881 map of the 1879 flood. The four classes created were: "Sands", "Sandy tarquin", "Semi-compact tarquin", and "Compact tarquin".

When the vector layer was created, it appeared as a single polygon and a single colour. In the properties of the vector layer it could be classified according to the selected class "ID" or "Materials". The class "Materials" was chosen and assigned four different colours in relation to the size of the material and its volume in water. Thus, thinner materials were in dark blue and light blue, and thicker or more compact materials were in orange and red.

However, this map only reflects the situation from Contraparada (Murcia) to Guardamar del Segura (Alicante). Therefore, taking into account the detailed description by González López (2013) [44] of Lorca, a map of the flooded area in each municipality was produced, according to the legend of the 1881 sketch. In this way, not only has the Santa Teresa flood map been reconstructed for current projections (SCR UTM Zone 30 N, EPSG: 25830), but it has been expanded to include Lorca, as a novel aspect with respect to traditional investigations (Figure 7).

### *2.4. Calculating the Total Built-Up Area in the Flood Zone of the Guadalentín Valley and Segura River Valley*

After reconstructing the map of the Santa Teresa flood with its flooded areas in Lorca, Murcia and the Vega Baja del Segura, a comparison between the area of the flood and the very latest modelling and cartography of the Spanish National Cartographic Systems for Flood Areas (SNCZI) was made. To consult this layer, a WMS connection was made, given that the results of the modelling were in raster image format and therefore, it was more suitable for consulting the depths than vector format. The layer used corresponded to the flood hazard associated with a 500-year return period.

After obtaining the layers, a single colour was assigned to the flooded area of the Santa Teresa flood (1879) and the WMS image of the SNCZI was superimposed. In this way comparative maps of the flooded area were obtained. Given the similarity of the two floods, other maps were elaborated which reflected the points of weakness, burst banks, overflows, or the presence of barriers or walls that hindered the running of the water and caused more damaging floods in certain areas. In turn, the raster image of the river flood hazard (T500 years) was incorporated to simulate the effect of the Santa Teresa flood in the present day.

The results of Section 3.2 were obtained through the downloading of data from the Land Cover Information System of Spain (hereafter, SIOSE) in high resolution (SIOSE AR), available in the National Geographic Institute (hereafter, NGI). Clip geoprocessing was applied between the layer of the surface area flooded by the Santa Teresa flood and the land uses of the area of study. After obtaining the resulting layer, a selection of attributes was made based on the coverage code (ID_Cove) corresponding to a type of description, related to built-up or artificially consolidated land (Table 2).

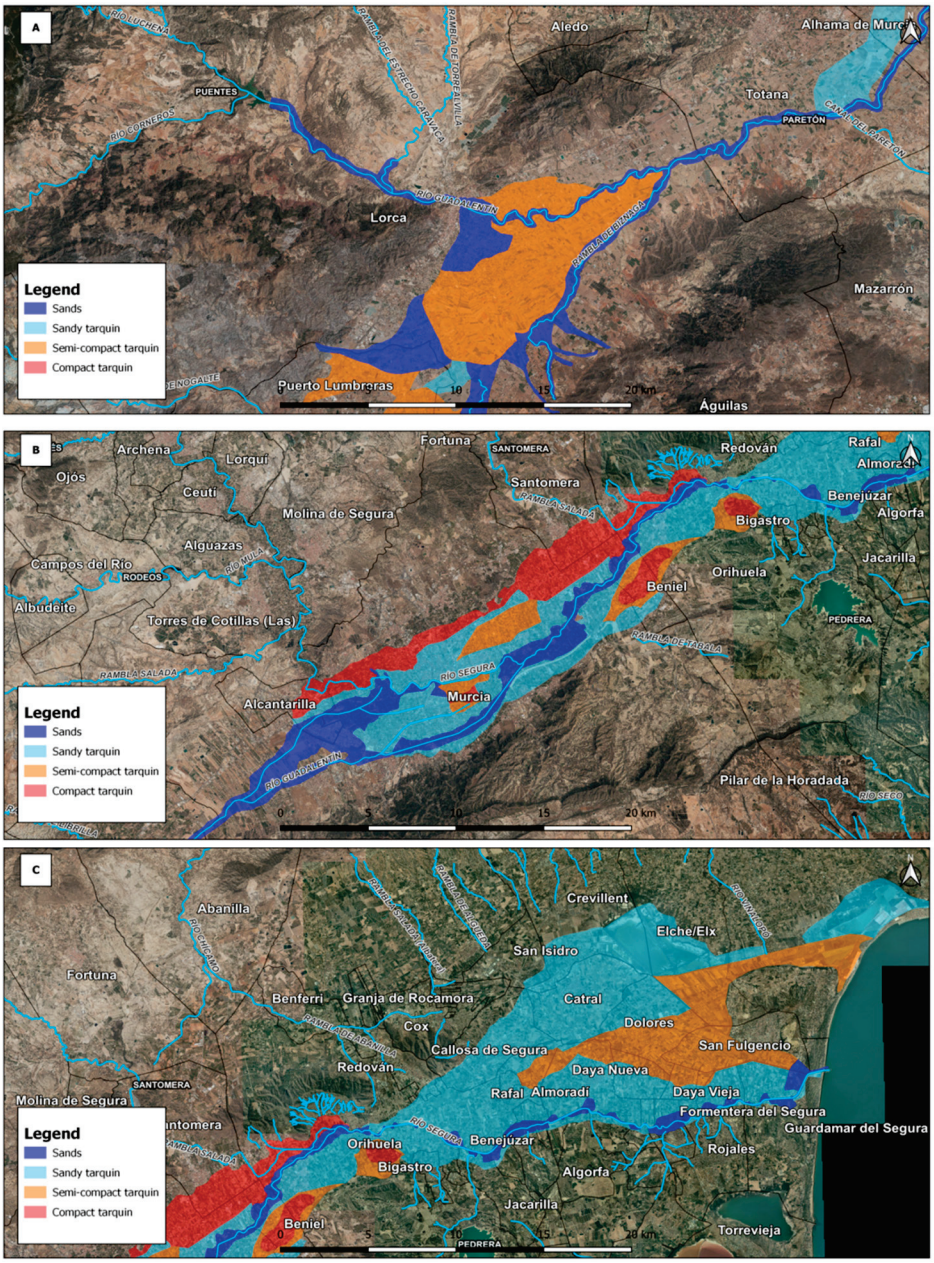



**Figure 7.** Flood zone according to the sketch drawn up in the historical cartography of 1881 after the Santa Teresa flood. Source: Prepared by the authors. Image (**A**) does not appear on the 1881 map, so it has been drawn up based on information from González López (2013) [44] on the effects of the flood in Lorca. Figures (**B**,**C**) have been elaborated according to the 1881 cartography and the descriptions of Gil Olcina and Canales (2022) [34] about the effects of the floods in Murcia and Vega Baja del Segura.

Subsequently, a sum of all of the polygons of each of the previously mentioned land uses was made, obtaining the total built-up or consolidated area.

The results obtained were reflected in a map of consolidated land uses in the floodable area of the Santa Teresa flood and a table of data with their percentage values.

Finally, in the discussion section, the results obtained are analysed, highlighting the importance of taking into consideration historical information and cartography to understand the effects of flood episodes and their implication with the most important aspects of land use planning and river basin management.

**Table 2.** Land cover code according to SIOSE.

| ID_Cove | Description |
|---|---|
| 101 | Buildings |
| 102 | Artificial green area and urban trees |
| 104 | Paved or sealed area |
| 105 | Swimming pools |
| 106 | Ponds and basins |
| 111 | Other constructions |
| 112 | Sports construction |
| 121 | Undeveloped land |
| 122 | Open area |
| 132 | Extraction areas |
| 133 | Landfill sites |
| 140 | Unclassified land transport network |
| 141 | Motorways and dual carriageways |
| 142 | Roads |
| 143 | Urban roads |
| 144 | Roads and paths |
| 145 | Railway tracks |

Source: SIOSE. Own elaboration.

## 3. Results

### *3.1. Comparison between the Cartographic Reconstruction of the October 1879 Flood and the Current Official Mapping of the SNCZI*

The first result obtained from the research was the cartographic reconstruction of the flood of October 1879, based on the historical descriptions of the event and the sketch of the flooded area published in 1881 (two years after the flood).

The classified layer was transformed into a single-colour layer (yellow) that simulated the total flood zone, also known as the hazard envelope.

The SNCZI WMS connection layer was superimposed on this layer for a return period of 500 years. This layer was chosen because it represented the flood of greatest magnitude and extension of the flood zone at present, taking into consideration all the existing river basin regulation works.

Maps A, B, and C show the comparison between the reconstructed mapping of the 1879 flood (yellow colour) and the current flood zone associated with a 500-year return period according to the SNCZI. Image A shows the area affected by the 1879 flood of the River Guadalentín, flooding its alluvial cone in the Murcian town of Lorca. In this image it can be seen that the area flooded in 1879 was larger than that of the SNCZI (T500 years). This is due to the fact that the current modelling takes into account the existing works at the headwaters of the Guadalentín (Valdeinfierno and Puentes III reservoirs).

Figure B shows the town of Murcia, the confluence point between the Rivers Segura and Guadalentín. As can be seen, the area flooded in 1879 (yellow colour) is practically identical to the SNCZI flood hazard mapping (T500 years). It can even be seen that there are areas that were flooded in 1879, and the current modelling does not consider them floodable.

Figure C corresponds to the final stretch of the Segura River, downstream of Murcia, from Orihuela to Guardamar del Segura. The area flooded in 1879 is practically identical to the SNCZI flood hazard mapping (T500 years) although it is even more extensive. Both cartographies show the areas most prone to flooding in the great floods experienced in the Segura basin (Figure 8).

As we can observe in the results obtained, the floodable area is practically identical, except for a few areas. This is due to several reasons: first, the new works constructed (reservoirs, walls, channels) alter the river circulation and protect certain spaces that the SNCZI map detects as non-floodable areas. Second, all of the smaller tributaries (watercourses, gullies, ravines) are not taken into account in the historical map but are represented in the SNCZI map. Third and finally, the confluence of all of the waters generates a large area, in width and height, throughout the whole valley of the Rivers Guadalentín and Segura, together with the anthropological actions in the territory.

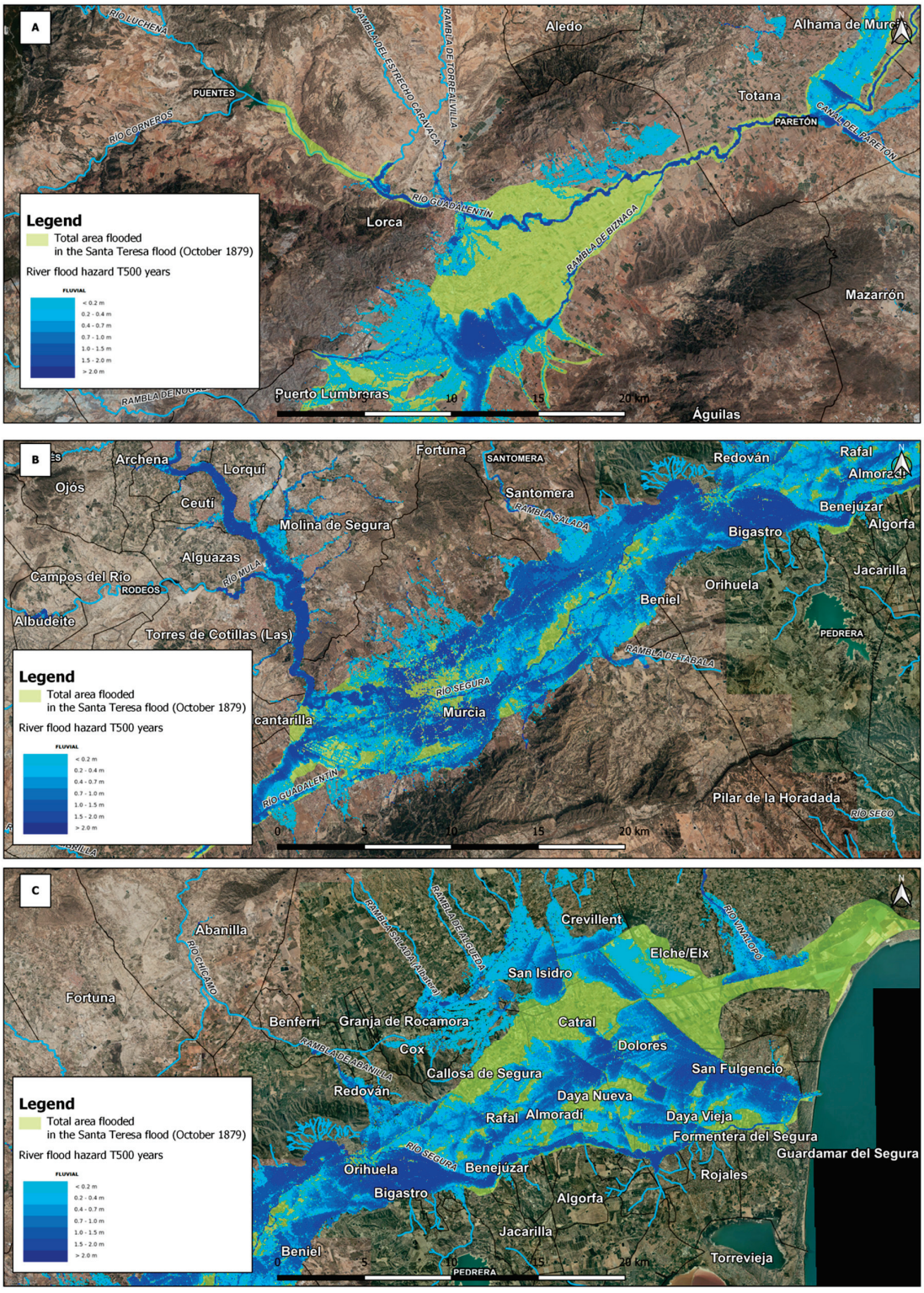



**Figure 8.** Comparison between the total area flooded in the Santa Teresa flood (October 1879) and the current flood hazard mapping for a return period of 500 years, for the middle and lower reaches of the Rivers Guadalentín and Segura. (**A**) is located in the town of Lorca (Murcia). The extent of the October 1879 flood is shown in yellow. The flood hazard mapping of a 500-year return period of the SNCZI is shown in blue. As you can see, the extent of the flooded area is wider. (**B**) is located in the town of Murcia (Murcia). The extent of the October 1879 flood is shown in yellow. The flood hazard mapping of a 500-year return period of the SNCZI is shown in blue. As you can see, the flood zone is

practically the same. (**C**) is located in the Vega Baja del Segura region (Alicante). The extent of the October 1879 flood is shown in yellow. The flood hazard mapping of a 500-year return period of the SNCZI is shown in blue. As can be seen, the flooding area is practically identical, although other affected sectors are shown that are not included in the current cartography.

As the two maps are similar (the reconstructed historical map and the SNCZI map), a map was elaborated of black or conflictive points corresponding to burst banks or overflows of the Rivers Guadalentín and Segura and, in turn, of the direction of the circulation of the flow of the waters in different sections (Figure 9).

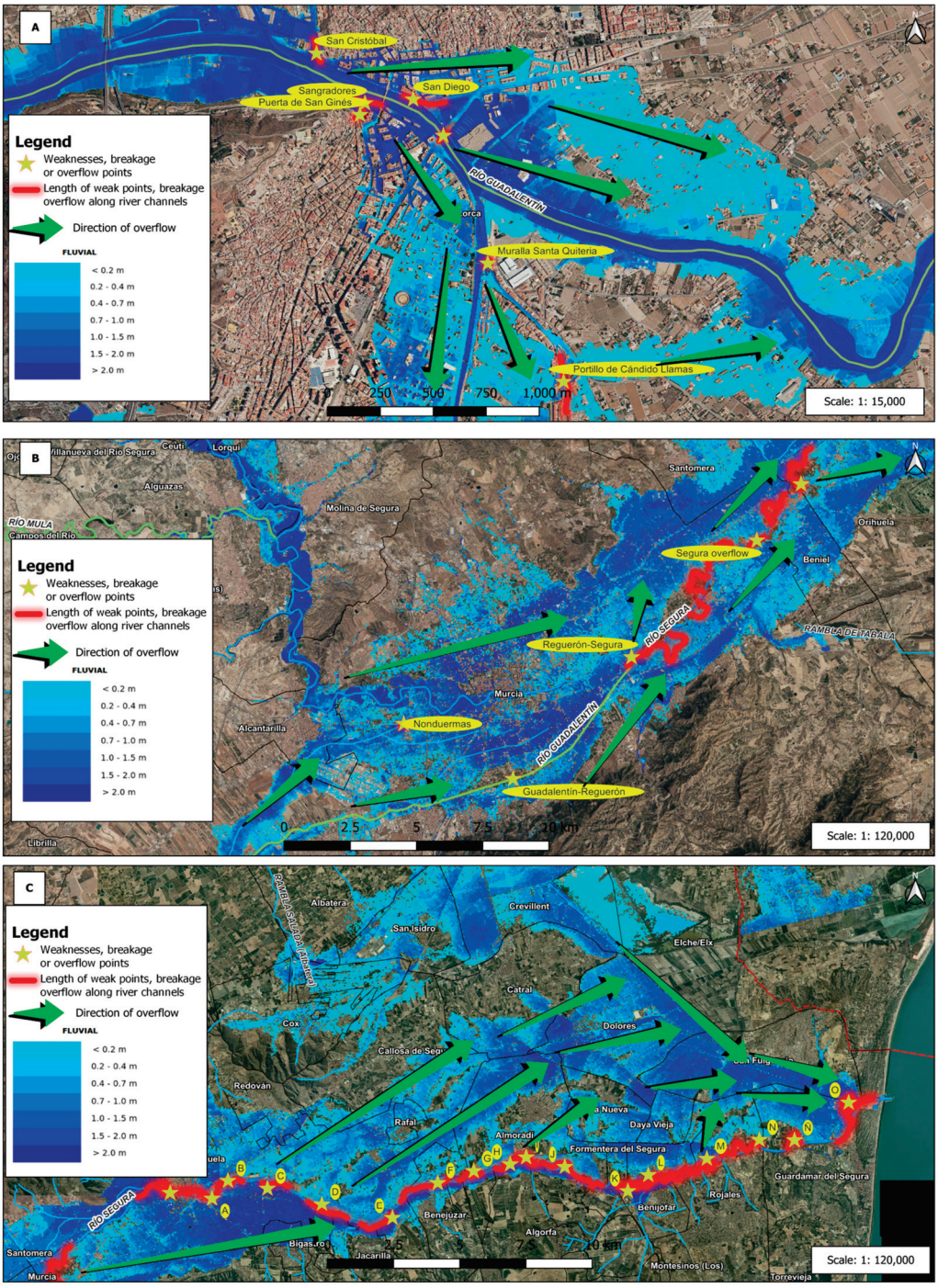



**Figure 9.** Current map with the SNCZI flood hazard mapping for a return period of 500 years and the sensitive points of breakage or overflowing according to the historical mapping of the Santa Teresa

flood (October 1879) of the sketch of the flood of 1881. The green arrows reflect the direction of flow in the overflows. The yellow stars mark points of breakage or overflow of the river course or black spots due to the presence of obstacles. The numerous stars in image C correspond to possible points of breakage or overflow of the Segura River in its final stretch. (**A**) shows the city of Lorca (Murcia) on a more detailed scale. The image shows the flood danger mapping associated with a 500-year return period of the SNCZI or current mapping. The green arrows reflect the direction of the overflow flow. The narrow yellow ones show points of breakage or overflow. Red lines with break zones. Both the yellow stars and the red lines represent areas of breakage and overflow in the flood of October 1879. Current cartography corroborates the possibility of these points of breakage or overflow by the river. (**B**) shows the city of Murcia (Murcia). The image shows the flood danger mapping associated with a 500-year return period of the SNCZI or current mapping. The green arrows reflect the direction of the overflow flow. The narrow yellow ones show points of breakage or overflow. Red lines with break zones. Both the yellow stars and the red lines represent areas of breakage and overflow in the flood of October 1879. Current cartography corroborates the possibility of these points of breakage or overflow by the river. (**C**) shows the Vega Baja del Segura region (Alicante). The image shows the flood danger mapping associated with a 500-year return period of the SNCZI or current mapping. The green arrows reflect the direction of the overflow flow. The narrow yellow ones show points of breakage or overflow. Red lines with break zones.

It is worth remembering that these sensitive points of breaks or overflows on the map (stars) have been identified through historical information and historical cartography from 1881 with the surface represented as "sands". As a curious fact, in many of these points the Segura River continued to overflow until the 1987 flood and the execution of a Segura Basin Flood-Defence Plan. Even in the most recent flood (2019) it overflowed at several points in image C, a fact that confirms the importance of historical analysis of floods to prevent possible future floods.

The results reveal the following points:

(a) Sensitive/weak/ruptured and/or overflowing points throughout the course of the River Guadalentín and that of the River Segura in the flood episode of October 1879, which enables us to determine the weak points of both rivers in extraordinary situations of swelling. Points to monitor and reinforce to reduce or mitigate river flooding. Although there are several possible points of rupture or overflowing in Lorca and Murcia (Figure 7A,B), it is from the town of Orihuela to the river mouth in Guardamar del Segura where the river exhibits a greater number of weak points (Figure 7C), with the most conflictive points being identified from letter A to O.

(b) The area of the flood which, as previously mentioned, is highly similar to the flood of October 1879 and which, subsequently, has also been similar in other flooding episodes of the Rivers Segura and Guadalentín, such as those in 1946, 1948, 1973, 1987, and 2019.

(c) The behaviour of the flows enables us to understand the direction of the waters and zones of water retention as a result of anthropological actions in the territory (housing, infrastructures and railways, industrial estates, etc.) which will allow better planning and management to be carried out in the event of a flood and the elaboration and development of rational flood adaptation proposals in a floodable area. As we can see in Figure 7C the River Segura runs above its river valley or riverbed. This implies that all of the water that overflows in the lower section of the River Segura will do so on the left side, flooding a large part of the territory. At the height of the town of Dolores, the surface circulation experiences a twist towards the east in its search for the lowest point, flowing towards the River Segura and discharging into the sea in its old course.

The results obtained have enabled us to see how the floods in the area of study behaved and to identify weak points throughout the course of the Rivers Guadalentín and Segura. The SNCZI map allows us to observe where the highest accumulation levels are located and the current flood area. In this respect, as we can see in the orthophotos used, humans have implemented social and economic activities in the largest riverbed. This is why it is

necessary to identify how many constructions are located in the floodable area today and how many would be affected in an episode similar to the Santa Teresa flood (1879).

### *3.2. Analysis of the Data Referring to the Occupation of Floodable Areas*

The floodable area of the reconstructed map of the flood of October 1879 was calculated at a total of 60,391 ha. Given that the SNCZI map associated with the river hazard for a 500-year return period was a raster image and the existing shapefile generated errors when geoprocesses were carried out in a GIS program, we decided to conduct a polygon layer representing the floodable zone indicated in this map. The total floodable zone in the area of study amounted to 60 019.5 ha. There was a very small difference between the flood zone maps in the valley of the Rivers Guadalentín and Segura of just 371.5 ha.

Taking into account that the SNCZI map is updated in each cycle of the basin plan, this means that, despite the defence works constructed in the Segura basin, the potentially floodable area coincides, on the whole, with the impacted area of the Santa Teresa flood of October 1879. Therefore, if a similar event were to occur, it is possible that a large part of the territory that was flooded in 1879 would be flooded again.

As analysed in the description of the episode in Section 3.1, the social and economic effects were severe. However, the current situation is even more serious, given that from the second half of the 20th century, a mass occupation process began to take place in the floodable areas of the Guadalentín valley and that of the River Segura. In particular, there was a greater intensification of the occupation of floodable zones during the property "boom" period (1990–2007), when rain-fed land or that of the orchard area (river valley) was transformed into buildable plots on which buildings were constructed. The majority of the buildings are houses, industrial estates, road infrastructures, and railway lines as well as municipal facilities and services.

All of the data related to the consolidated or constructed area in the flood zone were extracted. To do this, the SIOSE was used and the following coverage uses were included: buildings, artificial green and urban tree areas, paved or sealed areas, swimming pools, sumps and ponds, other constructions, sports facilities, unbuilt land, open areas, extraction areas, discharge areas, unclassified land transport networks, motorways, highways, urban roads, tracks and paths, and railway lines (Figure 10).

Images A, B, and C show in red the built-up areas within the flood zones according to the historical cartographic reconstruction of the 1879 flood, showing an intense occupation in the foothills near the alluvial fan of the River Guadalentín and the massive anthropic construction in the alluvial fan of the River Guadalentín.

Image B shows a massive occupation corresponding to Murcia and all its huerta.

In image C there is also an intense presence of anthropic constructions in the flood zones, including the totality of some municipalities. Although the area is more extensive and may alter the perception of the occupation of the flood zone, the reality is that most of this area has some type of anthropic construction (municipalities, roads, hospitals, rural housing, and irrigation networks, among others).

As we can see in Figure 8, there is a large amount of land that has been artificially constructed. The series of urban constructions, buildings, transport networks, and other uses can lead to a greater or lesser impact in certain areas or to worse flooding in certain municipalities downstream. They would also cause permanence of the overflowed waters in a flooding event.

The greater cover of floodable zones with consolidated areas favours the sealing of the soil, the increase in runoff and the reduction in the time, and the increase in the speed of the waters, and even hinders the flow of the waters, worsening the floods in specific spaces.

It has been calculated that a total of 11,145.5 ha of consolidated or constructed land in the flood area of the Santa Teresa flood (1879) of around 60,667.7 corresponds to the Guadalentín valley and that of the River Segura (middle and lower section), which represents 18.4% of the floodable area (Table 3).

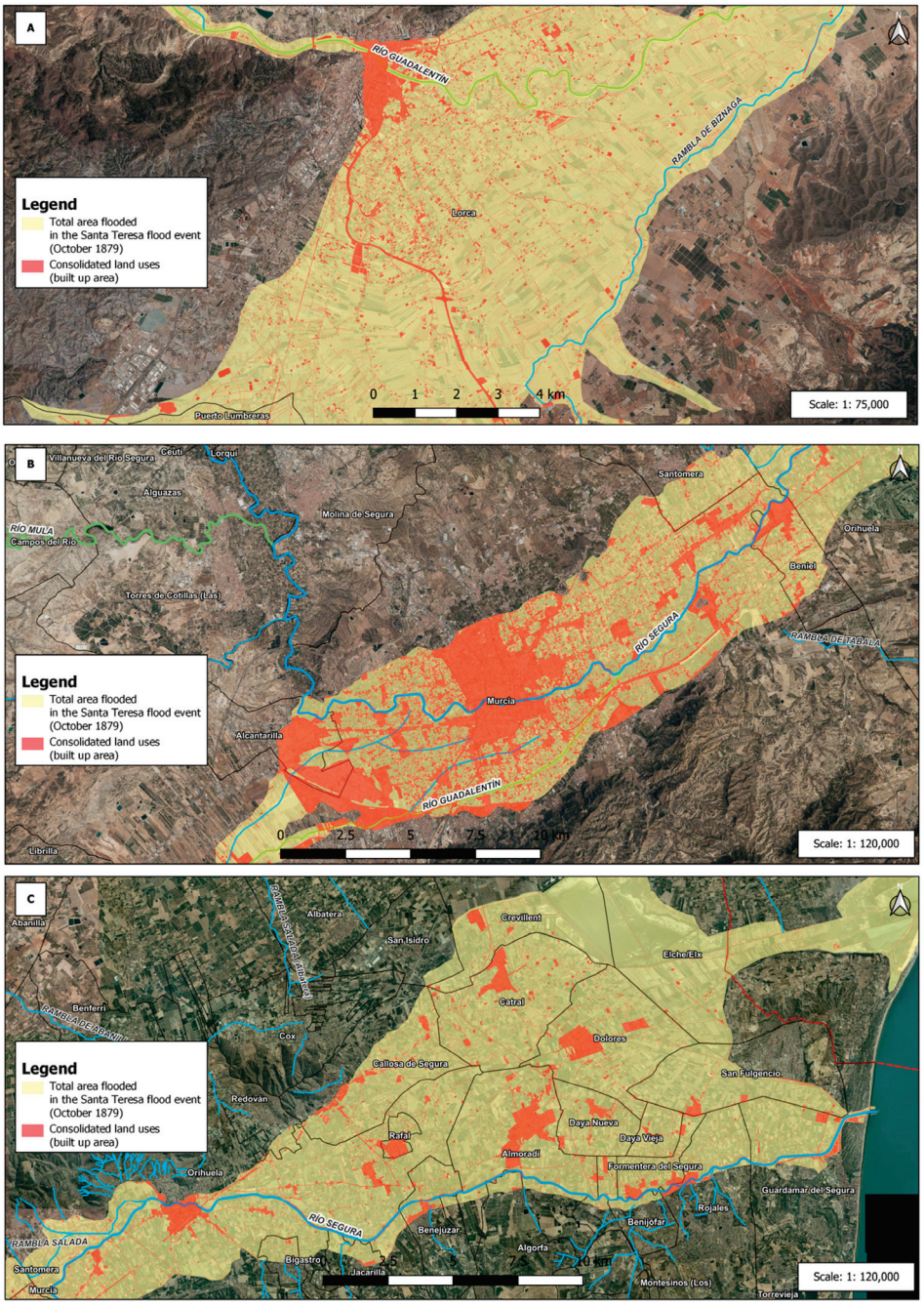



**Figure 10.** Consolidated surface area in the area flooded by the Santa Teresa flood of October 1879. Source: SIOSE. Own elaboration. (**A**) shows the extent of the flooded area in the flood of October 1879 and the existing buildings (housing, roads, equipment and services, road infrastructure, etc.) that are currently in the flooded area in 1879. Therefore, they are constructions installed in flood-prone areas in the town of Lorca (Murcia). (**B**) shows the extent of the flooded area in the flood of October 1879 and the existing buildings (housing, roads, equipment and services, road infrastructure, etc.) that are currently in the flooded area in 1879. Therefore, they are constructions installed in flood-prone areas in the town of Murcia (Murcia). (**C**) shows the extent of the flooded area in the flood of October 1879 and the existing buildings (housing, roads, equipment and services, road infrastructure, etc.) that are currently in the flooded area in 1879. Therefore, they are constructions installed in flood-prone areas in the Vega Baja del Segura region (Alicante).

**Table 3.** Surface area flooded in the Santa Teresa flood (1879) and the current built-up surface area.

| Study Area | Flooded Area (Ha) (2023) | Built-Up Area (Ha) (1879–2023) | Percentage (%) |
|---|---|---|---|
| Guadalentín and Segura River Valley (middle section) (Region of Murcia) | 36,094 | 8186 | 23 |
| Segura River Valley (Lower Section) (Alicante, Comunitat Valenciana) | 24,574 | 2960 | 12.05 |
| **TOTAL** | **60,668** | **11,145.5** | **18.4** |

Source: SIOSE. Own elaboration.

Although this figure is 18.4% of the total, it is a high percentage in terms of the exposure of human lives and economic material damage. In fact, in the last two floods occurring in the Segura basin (1987 and 2019), there was an exponential increase in the economic and material damage caused. This increasing trend is the consequence of the continued occupation of floodable areas in the area of study (Table 4).

**Table 4.** Comparison of fatalities and economic damage in the October 1897 flood and the last two major floods in the Segura basin (1987 and 2019).

| Flood Episodes | Deaths | Estimated Material Damage Approx. (in Euros in 2023) |
|---|---|---|
| October 1879 | 778 | 14,000,000 |
| November 1987 | 3 | 49,000,000 |
| September 2019 | 3 | 1,319,000,000 |

Source: Gil Olcina and Canales (2022) [34] and Olcina (1994) [31]. Own elaboration.

## 4. Discussion

The methodological process applied in this research can be used by any interested party who wants to reconstruct a historical mapping of a past flood, where georeferencing is not the best tool in order to avoid distortion of the historical map. This was the main problem encountered by the authors.

For this, it is necessary to have the historical description, sketches, plans, or historical maps, and to have a good knowledge of the analysis area to know which areas are prone to be flooded and which are not.

The use of historical maps and documents enabled us to reconstruct the map of the flood zone in the Santa Teresa flood, completing the initial sketch made in 1881. Furthermore, we obtained the maximum area of this flood event, allowing us to compare it with the current map elaborated by the SNCZI. The comparison of the two maps reveals a great similarity with respect to the flood zones, although there are certain differences in some sectors, which the SNCZI map does not currently contemplate as possible affected areas, therefore showing a small difference in very specific sectors. However, the rest of the flood zone (99.38% of the coinciding area) is practically identical, in spite of the regulation works existing in the basin today. It is worth noting that the comparison was made with the river flood hazard map associated with a 500-year return period.

Moreover, using the "sand" layer, the historical map has shown points of weakness, rupture, or overflow throughout the courses of the Rivers Guadalentín and Segura. In particular, there are several rupture points in the Vega Media section of the River Segura that coincide with the confluence of the Canal de El Reguerón (an artificial canal that collects the waters of the Guadalentín) with the River Segura, together with sharp meanders. However, the highest number of "Sand" layers is in the Vega Baja del Segura district, which enables us to identify the most sensitive points and those prone to the overflowing of the River Segura as it passes through the Vega Baja del Segura. In fact, some of these points have

been the cause of the subsequent floods in the Vega Baja del Segura district, with many playing a part in the flood of September 2019.

Therefore, superimposing the layer of weak points or points prone to overflowing or bank bursts with the SNCZI map and assuming a great similarity with the flood of October 1879, we are able to identify the current sensitive or affected areas. In fact many overflow areas of the Rivers Guadalentín or Segura shown by the SNCZI modelling for a 500-year return period coincide with the same rupture or overflow points of the Santa Teresa flood.

Furthermore, the results show a progressive mass occupation of the river valley of the Rivers Guadalentín and Segura in the Region of Murcia and in the south of the Region of Valencia, in the Alicante district of Vega Baja del Segura. This mass occupation occurred in parallel along the whole of the Mediterranean coastline, particularly in the period 1990–2007, which, as indicated by certain authors, gave rise to a completely enclosed space [52], as crop land had been converted into built-up spaces. This represented a greater exposure of the population to the flood risk existing in these two large river valleys.

The flood episode chosen for the study is the largest event in the Segura basin due to its impact on the population as a result of the enormous swelling of the River Guadalentín and the devastation caused with the confluence of this river with the River Segura downstream until its discharge into the sea. However, this major flood episode has not constituted an element to take into consideration in the territorial management and planning of the area, even though it is one of the most effective and cheapest measures for adapting to flood risk.

The flood of October 1879 led to the naming of the Commission responsible for designing a flood-defence plan in the Segura and Almanzora valley and the holding of the Congress against Floods in the Levante Region in Murcia in 1885. The conclusions obtained in the studies presented in this congress and the assessment of the Commission enabled priority flood-defence actions to be established in the Segura basin. They included the urgent need to focus the first actions in the Guadalentín basin and to protect the urban centres of Murcia and Orihuela [34].

All of this gave rise to the "Segura Valley Flood Defence Project" in the year 1886. In summary, the proposed actions can be divided into three large groups: (a) works that directly combat overflows with longitudinal dikes (walls, channels); (b) works that modify the water regime (dams, reservoirs, lakes, bypass channels, hydrological–forestry corrections); and (c) indirect measures, such as insurance, savings deposits, support, crop selection, and the regulation of floodable zones.

Therefore, the works proposed in the plan were: (1) the heightening and rehabilitation of the Valdeinfierno reservoir, (2) the construction of the Agua Amarga reservoir, which was subsequently replaced with the construction of the Puentes III reservoir, (3) the bypass channel of the River Guadalentín in Totana, diverting the waters to the Moreras watercourse and discharging them into the sea in the municipality of Mazarrón, (4) the widening and dredging of the El Reguerón canal, and (5) the construction of reservoirs at the headwaters of the River Segura and its tributaries on the right side. The only action undertaken was the widening of the El Reguerón canal, as the Puentes III dam (1881) was constructed two years after the Santa Teresa flood before including it in the cited defence plan. The rest of the actions were carried out throughout the 20th century after the approval of different plans.

Even though only one action of those proposed in the Plan was implemented, it is considered as a milestone in Spanish hydraulic history, with the majority of the others being included in subsequent flood-defence plans until the approval of the Segura Basin Flood-Defence Plan in the year 1987, after the floods of November 1987 and after other major historical floods such as the ones in April 1946, October 1948, and October 1973, among others.

However, the Segura Basin Flood-Defence Plan approved in 1987 does not class as a "model" flood the one occurring in October 1879, but uses the flood of 1973 as a model flood. It was smaller even than that of 1987, that of 1946, or that of 1879. The action proposals executed today can be classified into two large blocks: (1) actions in the Guadalentín basin and (2) actions in the Segura basin.

In the case of the former, the construction of the Puentes IV reservoir was proposed, together with the channelling of the River Guadalentín in Lorca, the conditioning of the watercourses, the widening of the Paretón canal of Totana, the construction of the Romeral or Engineer José Bautista Martín dam, and the widening, again, of the El Reguerón canal. For the second group, the construction of six dams was proposed to regulate the Segura tributaries on its left and right sides (Moro, Judío, Cárcabo, Pliego, Rodeos, and José Bautista), together with channelling and the widening of the canal of Paretón de Totana, the conditioning of the El Reguerón canal, the channelling of the River Segura from Contraparada (Murcia) to Guardamar del Segura (Alicante) through meander cut-offs, and a transfer channel from the River Argos to the River Quípar. Also contemplated were defence actions in towns, for example, the channelling of the watercourse of Hondón in Cartagena, the conditioning of the River Guadalentín and the Tiata watercourse in Lorca, or the design of a bypass in Orihuela (which was not executed). In addition to all of these actions was the hydrological–forestry correction based on the forest repopulation of the basins. Finally, we also have a list of the new works studied.

Therefore, the effect of the Santa Teresa flood on the subsequent territorial planning was more negative than positive. Territorial actions based on planning that avoids the occupation of floodable areas were not undertaken. Basically, hydraulic civil works were carried out that were proposed in the Segura Basin Flood-Defence Plan of 1885.

The figure below summarises the most important flood events occurring in the Segura basin between 1879 and 2023, indicating the measures for reducing the hazard and risk and the improvements made in terms of the emergency management and hydrological and meteorological warning carried out during this time period. As we can see, the measures related to hydraulic works were more prominent than those aimed at limiting the occupation of the floodable area through territorial planning (Figure 11).

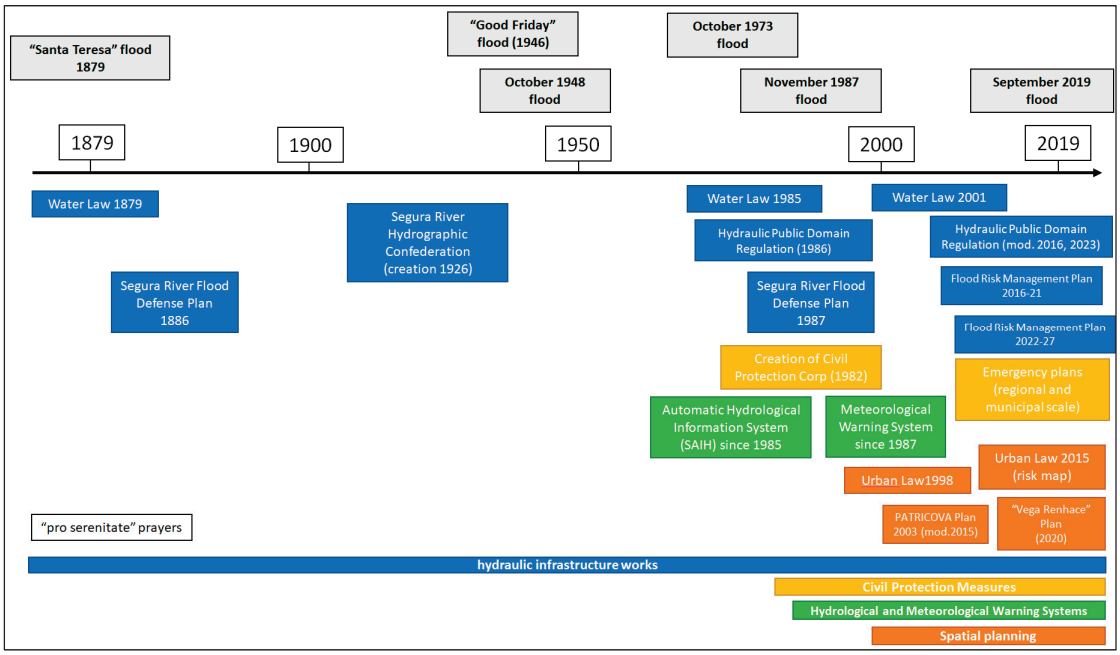



**Figure 11.** The most important floods in the Segura basin and measures carried out to reduce the risk of flooding (1879–2023). Source: Own elaboration. The lower bars represent two aspects: the application of these measures over time (1879–2023) and examples of measures applied by each group.

As a result, the construction of these works encouraged the occupation of floodable areas, due to the false sense of security generated among the population, who believed that the execution of all of these works would prevent more flood episodes. This coincided with the property boom period (1990–2007), which favoured the occupation of floodable zones.

However, since the construction of the works, the Segura basin has experienced episodes of significant river flooding (without overflow or flooding) (2000, 2001, 2007, 2007, 2009, 2012) and episodes with overflow and minor flooding (2016). After the 1987 flood, the next episode of overflowing of the Segura River occurred in 2016; however, it was a very localized flood. In September 2019, after record torrential rainfall (520 mm in two days; 300 mm on September 12 and 220 mm on September 14), the Segura River overflowed after several motes broke, causing one of the more serious floods in the final stretch of the Segura River. This latter flood also brought to light the fact that ruptures or failures could occur in structural works, which worsened the flood, and that certain overflow points coincided with those indicated in the sketch of the Santa Teresa flood of 1879.

The results are reflected in Section 3.2. This is where the importance of consulting historical maps, sources, and documents resides, as they teach us about the behaviour of the floods in the territory.

With respect to territorial planning, it should be pointed out that in Spain, the treatment of natural risks in territorial management and planning dates back to 1998, with the passing of Law 6/1998 on the land and valuation regime. In Article 9, it indicates that for land to be classified as "non-buildable land" it is necessary to accredit the natural risk that exists. However, some authors have highlighted that this regulation could not be applied as it does not indicate how the risk is accredited [53–57]. This situation prevailed until the passing of Law 8/2007 and, particularly until the subsequent passing of the Legislative Royal Decree 2/2008 approving the revised text of the Land Law in Article 12, indicating that in order to declare land as rural land, among other elements, it is necessary to protect those spaces with natural risks, including floods. In order to accredit the risk, Article 15 indicates that the urban development processes will be subject to sustainability assessment and monitoring. Therefore, it is necessary to elaborate an environmental sustainability report of the planning instruments of urbanisation actions, which should include a map of natural risks (in plural) for the area object of the planning. Furthermore, another report must be elaborated by the hydrological administration on water resources and the protection of the Public Water Domain, among other aspects. Since then, the successive state land regulations have maintained that it is necessary to accredit the natural risk of a territory in an urbanisation process. In summary, the way to accredit the existence of natural risks in Spain, including floods, is through the elaboration of a risk map or cartography.

It should be noted that until the existence of this regulation, the municipalities contemplated natural risks through the General Urban Development Plans (PGOU). Some municipalities, with a population of fewer than 10,000 inhabitants, were governed according to the so-called Subsidiary Regulations (SR), which only referred to urban regulations without contemplating all of the issues of the PGOUs. In both cases, authorisation or green light was required from the basin authority to carry out urban development based on the existence or not of flood risk. The majority of the reports indicated that the areas were flood risk zones and encouraged urbanisation measures that reduced the impact. Only in very specific spaces was the permission to construct refused. The regulations, on the whole, were fairly permissive, particularly in the PGOUs and SRs from the mid-1980s to 2007, when Directive 60/2007/EC was passed. This period coincided with the property boom. Despite the valuations and suggestions of the reports of the basin authority, no monitoring or assessment was made as to whether the municipalities adopted the measures recommended by the basin authority, and the municipalities constructed without implementing adaptation measures in floodable zones.

It should be pointed out that in the Region of Murcia, no importance was given to considering natural risks, specifically floods, in the territorial planning processes on either a regional or municipal level. Therefore, there are no flood risk plans such as the PATRICOVA in the Region of Valencia, although, after the flood in September 2019, an attempt was made to elaborate one, but it was never completed. The only planning documents attempting to prevent the occupation of floodable areas were the PGOUs. As reflected in the results of construction in floodable zones by the SNCZI for a 500-year return period, they were

highly permissive, increasing the exposure of human lives to the possible catastrophic effects of flooding. Furthermore, the PGOUs of the area of study were elaborated before the new Land Law of 2015. Therefore, risk maps would never have been used to approve new land uses.

In the Region of Valencia, from 2003, a sectoral territorial planning document has existed for floods called the Territorial Action Plan. It has a sectoral nature and addresses the Flood Risk in the Region of Valencia (PATRICOVA) and is accompanied by regulations for a flood risk plan and how it is related to territorial and urban planning. It is interesting to highlight Article 22, which indicates that on Non-Buildable Land affected by a flood hazard level 2 (T25-100 years and Q > 0.80 m), 3 (T < 25 years and Q < 0.80 m) and 4 (T25-100 years and Q < 0.80 m), the following uses and activities are prohibited: housing; stables, farms, and animal rearing facilities; fuel supply stations; chemical industries or those classified as having chemical hazard; hotel establishments or tourist camps; horse-riding centres and zoos; funeral services and cemeteries; waste storage tanks or landfills; strategic facilities such as emergency centres, fire stations, barracks, schools, and health centres, and covered sport pavilions; and specific strategic infrastructures, such as water treatment plants and energy production, and transformation and storage centres.

Furthermore, it should be noted that Article 27, which refers to the general conditions of adapting the buildings, indicates that: (a) buildings with one storey should have a roof that is accessible from the inside via a staircase; and (b) new buildings will be constructed in such a way that they are oriented in the direction of the overflow. Their transversal orientation should be avoided so as not to cause a barrier effect that would lead to a heightening of the depth of the water in the surrounding area.

Article 28 indicates a series of additional adaptations to those in Article 27, exclusively for areas that have a risk level 2 (T25-100 years and Q > 0.80 m), 3 (T < 25 years and Q < 0.80 m), and 4 (T25-100 years and Q < 0.80 m), which are the following:

Basements and semi-basements are not permitted, except for intensive residential use, provided that they fulfil the following conditions:

a. The access is watertight.
b. The drainage system is not connected to the sewage network and has an independent pumping system powered by a generator.
c. The use of these basements is exclusively for parking vehicles.
d. The access ramp is at a height that is 10 centimetres (10 cm) above the level of the pavement.
e. The sanitation pipes that run through or discharge into its interior should be watertight and resistant to the pressure arising in the case of a flood.

All of these elements were maintained in the revised version of the PATRICOVA in 2015, in which the geomorphological hazard layer was incorporated as zones prone to being affected by floods but which had not been taken into account in the elaboration of the flood risk maps. These regulations were applied in the district of Vega Baja del Segura (Alicante) in the area of study.

Despite all of these existing indications and regulations, the reality has been very different, given that there are many homes with basements and semi-basements, and homes that are not adapted to flood risk; furthermore, the number of homes existing in the floodable zone has risen. Along these lines, an important field of research has been opened for future studies related to the presence of basements or semi-basements in floodable areas, which is highly interesting to qualify a greater flood risk in a town or region.

Finally, the Santa Teresa flood of October 1879 represented a good opportunity to carry out correct planning and adaptation to flood risk in terms of management and territorial planning. However, it has not been taken into consideration, so it can be considered as learning and a failed action on the part of those responsible for making territorial decisions, generating a true panorama of flood risk.

In this line, the first failure is found in the basin organization that, despite the works it has been carrying out, has not been forceful in denying the construction of homes in

flood-prone areas. It has been very permissive despite being aware of the existing flood risk. The second failure is found in Spanish regulations. In Spain, at the end of the 1990s, land regulations were approved that mentioned for the first time taking into consideration the risk of flooding in any urban planning action, as long as the existence of this risk was proven. However, this regulation did not indicate how to accredit the risk until the approval of a new Land Law (2007) and its Royal Legislative Decree (RDL 2/2008), which states that to accredit the risk it is necessary to carry out a mapping of the risk, leaving this land protected from any urban planning action.

As can be seen, the approved regulations are very recent and are closely related to the approval of Directive 60/2007/EC on the evaluation and management of flood risk. Here lies the importance of researching cartography and historical documents: it allows us to analyse the past and take into consideration possible floods in the future.

## 5. Conclusions

Historical cartography and documentation are fundamental tools for assessing and managing flood risk, given that they enable us to determine the extension of the affected areas and the size of the impact on a geographical space.

Before the passing of the Flood Directive (60/2007/EC), many descriptive studies were conducted with a strong historical component, which has enabled us to learn about the functioning of the river swellings and floods and their effects, together with the personal and material damage caused. This information has been vital for taking decisions for defence actions and territorial planning. After the passing of the Directive 60/2007/EC, one of the most important elements when conducting flood risk assessment has been the consultation and inventory of historical floods with their causes and consequences, enabling us to understand how floods function in the basin.

The flood episode of 1879 has not had a great influence or repercussion on the decisions taken related to territorial management and planning. We could say that it has had some influence on the elaboration of flood defence projects and plans in the Segura valley, with ideas proposed in 1886 which subsequently prevailed until the approval and execution of the Segura Basin Flood-Defence Plan of 1987, although this did not consider the Santa Teresa flood as a model flood for the actions to implement. Rather, it used the 1973 flood and even ignored that of April 1946, that of 1948, or even the recent flood of 1987, occurring just before the approval of the plan of the same year.

However, with respect to territorial management and planning, the result has been dire. The river valleys and, therefore, the floodable zones of the Rivers Guadalentín and Segura have literally been invaded with buildings, increasing the flood risk in the area of study and exponentially increasing the economic losses that would be generated by a flood episode. This has been due to massive and uncontrolled urbanisation that was misaligned with the objectives of sustainable development in the property boom period (1990–2007) and to the false sense of security of the population who believe that the construction of many structural works will prevent any more floods from occurring.

In summary, consultation of the available historical information is vital for flood management, which, combined with the new GIS techniques and hydraulic modelling, together with structural defence measures and adaptation or non-structural measures, enables a greater adaptation to floods and the effects related to climate change.

**Author Contributions:** Conceptualization, A.O. and J.O.; methodology, A.O. and J.O.; software (QGIS 3.26.2), A.O.; Validation, J.O.; formal analysis, A.O. and J.O.; investigation, A.O. and J.O.; resources, A.O. and J.O.; writing—original draft preparation, A.O. and J.O.; writing—review and editing, A.O. and J.O.; supervision, J.O. All authors have read and agreed to the published version of the manuscript.

**Funding:** This research received no external funding.

**Institutional Review Board Statement:** Not applicable.

**Informed Consent Statement:** Not applicable.

**Data Availability Statement:** Data are contained within the article.

**Conflicts of Interest:** The authors declare no conflict of interest.

## References


1. Swiss Re. SIGMA Research 2/2019: Secondary Natural Catastrophe on the Front Line. Available online: https://www.swissre.com/institute/research/sigma-research/sigma-2019-02.html (accessed on 14 November 2023).
2. Swiss Re. SIGMA Research: A Natural Catastrophes and Inflation in 2022: A Perfect Storm. Available online: https://www.swissre.com/institute/research/sigma-research/sigma-2023-01.html (accessed on 14 November 2023).
3. EM-DAT: The International Disaster Database. Centre for Research on the Epidemiology of Disasters. Available online: https://www.emdat.be/publications/ (accessed on 14 November 2023).
4. Wadgure, K.S.; Kamble, R.K. *Zona de Inundaciones. Gestión de Catástrofes*; Science Scripts; Ediciones Nuestro Conocimiento: Chisnau, Moldavia, 2022; pp. 1–52.
5. Camarasa-Belmonte, A.M. El riesgo de inundación en ramblas y barrancos mediterráneos. In *Riesgo de Inundación en España: Análisis y Soluciones para la Generación de Territorios Resilientes*, 1st ed.; López Ortiz, M.I., Melgarejo Moreno, J., Eds.; Universidad de Alicante: San Vicente del Raspeig, Spain, 2020; Volume 1, pp. 239–255.
6. Estrela Monreal, T. Evolución de la Gestión de las Inundaciones en España: Retos futuros. In *Riesgo de Inundación en España: Análisis y Soluciones para la Generación de Territorios Resilientes*, 1st ed.; López Ortiz, M.I., Melgarejo Moreno, J., Eds.; Universidad de Alicante: San Vicente del Raspeig, Spain, 2020; Volume 1, pp. 517–529.
7. Llasat Botija, M.C. Floods evolution in the Mediterranean Region in a context of climate and environmental change. *Cuad. Investig. Geográfica* **2021**, *47*, 13–32. [CrossRef]
8. European Court of Auditors (ECA). *Special Report: The Spatial Effects and Management of Natural and Technological in Europe*; Publications Office of the European Union: Luxembourg, 2018; pp. 1–71.
9. European Commision (EC). Available online: https://www.boe.es/doue/2007/288/L00027-00034.pdf (accessed on 14 November 2023).
10. Joint Research Centre (JRC). PESETA III: River Floods Report. Available online: https://joint-research-centre.ec.europa.eu/peseta-projects/peseta-iii_en (accessed on 14 November 2023).
11. JRC. PESETA IV: Adaptating to Rising River Flood Risk in the EU under Climate Change. Available online: https://publications.jrc.ec.europa.eu/repository/handle/JRC118425 (accessed on 14 November 2023).
12. Ministerio para la Transición Ecológica y Reto Demográfico (MITERD). *Inundaciones y Cambio Climático*; Ministerio para la Transición Ecológica y Reto Demográfico: Madrid, Spain, 2018; pp. 1–106.
13. MITERD. *Impactos y Riesgos Derivados del Cambio Climático en España*; Ministerio para la Transición Ecológica y Reto Demográfico: Madrid, Spain, 2020; pp. 1–212.
14. Ministerio del Interior. *Anuario Estadístico del Ministerio del Interior*; Ministerio del Interior: Bilbao, España, 2022; pp. 1–708.
15. Consorcio de Compensación de Seguros (CCS). *Histórico de Informes Anuales*; Ministerio de Asuntos Económicos y Transformación Digital y Consorcio de Compensación de Seguros: Madrid, Spain, 2022; pp. 1–200.
16. Olcina Cantos, J.; Saurí Pujol, D.; Hernández-Hernández, M.; Ribas Palom, A. Flood policy in Spain: A review for the period 1983–2013. *Disaster Prev. Manag. Int. J.* **2016**, *25*, 41–58. [CrossRef]
17. Pérez-Morales, A.; Gil-Guirado, S.; Quesada García, A. ¿Somos todos iguales ante una inundación? Análisis de la vulnerabilidad social en el litoral mediterráneo español. *Boletín Asoc. Geogr. Española (BAGE)* **2021**, 1–39. [CrossRef]
18. Agencia Estatal de Meteorología (AEMET). Proyecciones Climáticas para el Siglo XXI en España. Available online: https://www.aemet.es/es/serviciosclimaticos/cambio_climat (accessed on 14 November 2023).
19. Intergovernmental Panel Climate Change. AR6 Climate Change 2021–2022. Available online: https://www.ipcc.ch/report/sixth-assessment-report-cycle/ (accessed on 14 November 2023).
20. Olcina Cantos, J.; Oliva Cañizares, A. Medidas estructurales vs cartografía de inundación en la valoración del riesgo en áreas urbanas: El caso del barranco de las Ovejas (Alicante, España). *Cuad. Geográficos* **2020**, *59*, 199–220. [CrossRef]
21. Ollero Ojeda, A. *El Curso Medio del Ebro: Geomorfología Fluvial, Ecogeografía y Riesgos*; Universidad de Zaragoza: Aragón, Spain, 1992; pp. 1–311.
22. Gil Olcina, A.; Olcina Cantos, J. *Tratado de Climatología*; Publicaciones Universidad de Alicante: San Vicente del Raspeig, Spain, 2017; pp. 1–949.
23. Kjeldsen, T.R.; Macdonald, N.; Lang, M.; Mediero, L.; Alburquerque, T.; Bogdanowicz, E.; Brazdil, R.; Castellarin, A.; David, V.; Fleig, A.; et al. Documentary evidence of past flood in Europe and their utility in flood frequency estimation. *J. Hydrol.* **2014**, *517*, 963–973. [CrossRef]
24. Mediero, L.; Kjeldsen, T.R.; Macdonald, N.; Kohnova, S.; Merz, B.; Vorogushyn, S.; Wilson, D.; Alburquerque, T.; Blöschl, G.; Bogdanowicz, E.; et al. Identification of coherent flood regions across Europe by using the longest streamflow records. *J. Hydrol.* **2015**, *528*, 341–360. [CrossRef]
25. Szczepanek, R.; Tos, C.; Bodziony, M. Temporary flood marks proposal: What we learned after losing the baroque artifact from Cracow, Poland. *Int. J. Disaster Risk Reduct.* **2022**, *74*, 102942. [CrossRef]

26. Barriendos Vallvé, M. La climatología histórica en el marco geográfico de la antigua monarquía Hispana. *Scripta Nova. Rev. Electrónica Geogr. Cienc. Soc.* **1999**, *53*, 1–34.
27. Barriendos Vallvé, M. Variabilidad climática y riesgos climáticos en perspectiva histórica. El caso de Catalunya en los siglos XVIII-XIX. *Rev. Hist. Mod.* **2005**, *23*, 11–34. [CrossRef]
28. Alberola Romá, A. *Los Cambios Climáticos: La Pequeña Edad del Hielo en España*; Cátedra: Madrid, Spain, 2014; pp. 1–341.
29. Arrioja Díaz Viruell, L.; Alberola Romá, A. *Clima, Desastre y Convulsiones Sociales en España e Hispanoamérica, siglos XVII-XX*; Universidad de Alicante y El Colegio de Muchoacán: San Vicente del Raspeig, Spain, 2016; pp. 1–399.
30. Barriendos, M.; Gil-Guirado, S.; Pino, D.; Tuset, D.; Pérez-Morales, A.; Alberola, A.; Costa, J.; Balasch, J.C.; Castelltort, X.; Mazón, J.; et al. Climatic and social factors behind the Spanish Mediterranean Flood event chronologies from documentary sources (14th–20th centuries). *Glob. Planet. Chang.* **2019**, *182*, 102997. [CrossRef]
31. Olcina Cantos, J. *Tormentas y Granizadas en las Tierras Alicantinas*; Universidad de Alicante e Instituto Universitario de Geografía: San Vicente del Raspeig, Spain, 1994; p. 317.
32. Gil-Guirado, S. *Reconstrucción Climática Histórica y Análisis Evolutivo de la Vulnerabilidad y Adaptación a las Sequías e Inundaciones en la Cuenca del Segura (España) y en la Cuenca del río Mendoza (Argentina)*; Universidad de Murcia: Murcia, Spain, 2013; pp. 1–769.
33. Galván Plaza, R. Cuatro grandes inundaciones históricas del Ebro en la ciudad de Zaragoza: 1643, 1775, 1871 y 1961. *Papeles Geogr.* **2018**, *1*, 7–25. [CrossRef]
34. Gil Olcina, A.; Canales Martínez, G. *Concausas y Tipos de Inundaciones en la Vega Baja del Segura*; Universidad de Alicante: San Vicente del Raspeig, Spain, 2022; pp. 1–472.
35. Gil Olcina, A.; Olcina Cantos, J.; Rico-Amorós, A.M. *Aguaceros, Aguaduchos e Inundaciones en Áreas Urbanas Alicantinas*; Publicaciones Universidad de Alicante: San Vicente del Raspeig, Spain, 2004; pp. 1–735.
36. Criado, M.; Martínez-Graña, A.; San Román, J.S.; Santos-Francés, F. Flood risk evaluation in urban spaces: The study case of Tormes River (Salamanca, Spain). *Int. J. Environ. Res. Public Health* **2019**, *16*, 5. [CrossRef] [PubMed]
37. Marco Molina, J.A.; Giménez Font, P.; Padilla Blanco, A.; García Botella, E.; Prieto Cerdán, A. La rambla de Abanilla-Benferri como paradigma para el estudio del conocimiento tradicional relativo al aprovechamiento de las aguas de avenida. In *Riesgo de Inundación en España: Análisis y Soluciones para la Generación de Territorios Resilientes*, 1st ed.; López Ortiz, M.I., Melgarejo Moreno, J., Eds.; Universidad de Alicante: San Vicente del Raspeig, Spain, 2020; Volume 1, pp. 881–896.
38. Benita, G.; Rico, M.; Sánchez-Moya, Y.; Sopeña, A.; Thorndycraft, V.R.; Barriendos, M. The impact of late Holocene climatic variability and land use change on the flood hydrology of the Guadalentin River, southeast Spain. *Glob. Planet. Chang.* **2010**, *70*, 53–63. [CrossRef]
39. Gardiol, M.R. Las fotografías antiguas como fuente de información en inundaciones históricas. *Contrib. Científicas GAEA* **2013**, *25*, 101–109.
40. Giménez Font, P. Cartografía histórica y alteración de cursos fluviales en la España mediterránea. In *Desastre Natural, Vida Cotidiana y Religiosidad Popular en la España Moderna y Contemporánea*; Alberola, A., Olcina, J., Eds.; Publicaciones de la Universidad de Alicante: San Vicente del Raspeig, Spain, 2009; pp. 391–432.
41. Olcina Cantos, J.; Díez-Herrero, A. Cartografía de inundaciones en España. *Estud. Geográficos* **2017**, *78*, 283–315. [CrossRef]
42. Oliva Cañizares, A.; Olcina Cantos, J. La importancia de la cartografía histórica en la elaboración de mapas de peligrosidad de inundación en el contexto del cambio climático: Propuestas para la rambla de Abanilla (Alicante). *Estud. Geográficos* **2021**, *82*, 283–315. [CrossRef]
43. Gil-Guirado, S.; Olcina Cantos, J.; Pérez-Morales, A. Grandes inundaciones en la ciudad de Murcia a través de la documentación histórica: Medidas de defensa y contexto socioeconómico. *Estud. D'història Agrària* **2021**, *1*, 33–62. [CrossRef]
44. González López, S. La Avenida de Santa Teresa, 14–15 de Octubre de1879, en la Ciudad y Término de Lorca. *Alberca* **2014**, 183–207. Available online: http://www.amigosdelmuseoarqueologicodelorca.com/alberca/pdf/alberca12/11_12.pdf (accessed on 20 October 2023).
45. Calvo García-Tornel, F.; Conesa García, C.; Álvarez Rogel, Y. La inundación de octubre de 1879 en el Bajo Segura. Magnitud y efectos inducidos. *Estud. Geográficos* **2001**, *62*, 7–27. [CrossRef]
46. Masachs Alavedra, V. *El Régimen de los ríos Peninsulares*; CSIC: Barcelona, Spain, 1948; pp. 1–511.
47. López Bermúdez, F.; Navarro Hervás, F.; Montaner Salas, M.E.; Blázquez Calvo, F.; Cebrián Egea, A.; Cerezuela Martínez, J.; Fernández Pérez, C.; Gómez López, L.; Olmos Alcaraz, T.; Pellicer Fernández, J.; et al. Inundaciones Catastróficas, Precipitaciones Torrenciales y Erosión en la Provincia de Murcia. *Papeles Dep. Geogr.* **1978**, 49–91. Available online: https://revistas.um.es/geografia/article/view/41791 (accessed on 25 October 2023).
48. Martínez Jódar, A. Fotografía y Catástrofes en la España del Siglo XIX: El Reportaje Sobre las Inundaciones en Octubre de 1879. II Jornadas Sobre Investigación en Historia de la Fotografía. pp. 47–57. Available online: https://ifc.dpz.es/recursos/publicaciones/37/13/04martinezjodar.pdf (accessed on 18 October 2023).
49. Biblioteca Nacional de España (BNE). Hemeroteca digital: Journal Publié au Profit des Victimes des Inundations d´Espagne, par le Comité de la Presse Française. Numéro Unique. Décembre 1879. Available online: https://hemerotecadigital.bne.es/hd/es/advanced (accessed on 14 November 2023).
50. Biblioteca Nacional de España (BNE). Hemeroteca Digital: A la Prensa de París, Testimonio de Admiración y Agradecimiento, la Prensa de Murcia. Tip. Del «Murcia-París». Available online: http://www.bne.es/es/catalogos/HemerotecaDigital/ (accessed on 14 November 2023).

51. Archivo General Región de Murcia (AGRM). Hemeroteca Digital: Riada Santa Teresa (1879). Available online: https://archivogeneral.carm.es/archivoGeneral/arg.inicio (accessed on 14 November 2023).
52. Conesa García, C.; Canales Martínez, G. *La Vega Baja del Segura, una Huerta Sitiada. La Transformación del Territorio*; Cátedra Arzobispo de Loazes y Universidad de Alicante: San Vicente del Raspeig, Spain, 2018; pp. 1–93.
53. Ayala-Carcedo, F.J. La Ordenación del Territorio en la Prevención de Catástrofes Naturales y Tecnológicas. Bases para un Procedimiento Técnico-administrativo de Evaluación de Riesgos para la Población. *Boletín Asoc. Geogr. Española BAGE* **2000**, 37–49. Available online: https://www.bage.age-geografia.es/ojs/index.php/bage/article/download/381/352/372 (accessed on 18 October 2023).
54. Ayala-Carcedo, F.J.; Olcina Cantos, J. *Riesgos Naturales*; Ariel: Barcelona, Spain, 2002; pp. 1–1304.
55. Ayala-Carcedo, F.J. La inundación torrencial catastrófica del camping "Las Nieves" del 7 de agosto de 1996 en el cono de deyección del Arás (Biescas, Pirineo Aragonés). In *Riesgos Naturales*; Ayala-Carcedo, F.J., Olcina Cantos, J., Eds.; Ariel: Barcelona, Spain, 2002; pp. 889–912.
56. Olcina Cantos, J. Cambios en la consideración territorial, conceptual y de método de los riesgos naturales. Diez años de cambios en el mundo, en la geografía y en las ciencias sociales, 1999–2008. *Geocrítica* **2008**, *12*, 1–13.
57. Olcina Cantos, J. De los mapas de zonas afectadas a las cartografías de riesgo de inundación en España. *An. Geogr.* **2012**, *32*, 91–131. [CrossRef]


**Disclaimer/Publisher's Note:** The statements, opinions and data contained in all publications are solely those of the individual author(s) and contributor(s) and not of MDPI and/or the editor(s). MDPI and/or the editor(s) disclaim responsibility for any injury to people or property resulting from any ideas, methods, instructions or products referred to in the content.

land

MDPI

*Article*

# MAGUS (Model for the Analysis of Geomorphological Urban Systems): From Conception to Validation on the Historic City Center of Turin (Italy)

**Asia Bernardi *, Michele Licata, Francesco Seitone and Giandomenico Fubelli ***

Department of Earth Sciences, University of Turin, Via Valperga Caluso, 35, 10125 Turin, Italy; michele.licata@unito.it (M.L.); francesco.seitone@unito.it (F.S.)
* Correspondence: asia.bernardi@unito.it (A.B.); giandomenico.fubelli@unito.it (G.F.)

**Abstract:** This study introduces and tests the MAGUS (Model for the Analysis of Geomorphological Urban Systems), a GIS-based methodological framework designed to analyze the complex interplay between urbanization and natural landscapes. Focusing on the historical evolution of Turin city center (Italy), the research employs an interdisciplinary approach to examine how urban expansion has interacted with pre-existing geomorphological features. The study leverages historical documents, digitized and georeferenced within a cartographic space, to reveal the relationships between natural and anthropogenic landforms from the Roman period through the 20th century. A key innovation of MAGUS is the integration of Multi-Temporal Markers (MTM) and Volumetric Unit of Building (VUB), which enhances the accuracy of historical data analysis. The results demonstrate that urbanization significantly alters the natural landscape in the historic city center of Turin, where the stratification of urban expansion phases partially obscures the original landform. By overlaying topographical data with historical urban expansion maps, the research highlights the concealed geomorphological elements beneath Turin's urban fabric. This interdisciplinary study not only contributes to the field of urban geomorphology but also provides a foundation for future research into the impacts of urbanization on natural landscapes, which is increasingly critical as urban populations continue to grow.

**Keywords:** urban geomorphology; anthropic landform; historical map; urban sprawl; Turin (Italy)

**Citation:** Bernardi, A.; Licata, M.; Seitone, F.; Fubelli, G. MAGUS (Model for the Analysis of Geomorphological Urban Systems): From Conception to Validation on the Historic City Center of Turin (Italy). *Land* **2024**, *13*, 1851. https://doi.org/10.3390/land13111851

Academic Editors: Mariano Barriendos Vallvé, Fabio Luino, Laura Turconi, Fabrizio Terenzio Gizzi, Ruediger Glaser, Christoph Gruetzner, Sabina Porfido, Walter Palmieri and Heather Sangster

Received: 5 September 2024
Revised: 31 October 2024
Accepted: 3 November 2024
Published: 6 November 2024



**Copyright:** © 2024 by the authors. Licensee MDPI, Basel, Switzerland. This article is an open access article distributed under the terms and conditions of the Creative Commons Attribution (CC BY) license (https://creativecommons.org/licenses/by/4.0/).

## 1. Introduction

Over the last century, socio-economic development, urban expansion, and the intensification of human activities have led to significant changes in landscapes. In many regions of the Earth, landforms are the result of complex interactions between human and natural processes [1].

Urban areas, where people interact with biotic and abiotic factors [2,3], have often been overlooked in geomorphological studies [4], with features typically estimated through spatial interpolation and geostatistical methods. However, the reliability and efficiency of these predictions are often undermined by the heterogeneous composition and management of urban environments [5]. For example, the amount of available borehole data is often inadequate for creating precise geomorphological models. In urban environments, the visibility of landforms, processes, and deposits is frequently obscured or modified by the presence of built structures. This complexity is particularly evident in territories that have been subjected to repeated transformation and layering as a result of the continuous expansion of the city over time [6–8].

Szabò et al. [9] suggest that one of the primary geomorphological consequences of urban development is its capacity to alter the natural processes of the area. Consequently, new forms emerge in the vicinity of urbanized areas due to the changes induced by construction and overbuilding. The principal categories of human-made structures that shape

settlement patterns and the urban landscape encompass earthworks designed for strategic defense, macro terraces and plateaus created for housing development, water management structures like dams and river channels, and transport surfaces, including roads, railways, and airports. However, identifying natural landforms in densely urbanized contexts is often challenging, as they have been progressively obliterated by urban expansion [10,11]. The identification of urbanization processes in the Mediterranean area and European cities is particularly complex due to the stratification of urban expansion phases [7,12] spanning centuries or millennia. In ancient times, the expansion of urban settlements was constrained by topographical obstacles such as watercourses, cliffs, rises, ravines, coastlines, and marshes. While these landscape features were once considered unfavorable for urban development and challenging to overcome in certain historical periods, technological advances eventually allowed for their urbanization. However, this often led to significant impacts on pre-existing natural environments and increased natural risk for human settlements due to the less harmonized construction techniques [6].

In recent decades, global population growth and the intensified occupation of high-hazard areas, such as floodplains and coastal zones, have escalated disaster risk. This trend is compounded by several factors: the vulnerability of built structures and infra-structures, limitations in mitigation efforts, and the potential impact of climate change [13,14]. As spatial and resource pressures increase, expanding populations are moving into areas previously avoided due to issues like poor accessibility or high-hazard exposure. The interaction between human settlements and natural hazards thus becomes increasingly complex, posing escalating challenges in a context of diminishing available land [15]. Research on natural hazards in urban geomorphology confronts two primary challenges. The first involves forecasting extreme events and developing predictive models, a task made uncertain by the unpredictable consequences of anthropogenic climate change. The second challenge centers on reconstructing past low-frequency events and rare occurrences whose sparse documentation, especially in the modern instrumental record, complicates understanding. Here, historical data are invaluable, offering insights into past events, patterns, and vulnerabilities that might otherwise remain obscured [15]. Advancements in technology have improved our ability to observe the Earth and monitor geomorphological processes. By combining historical datasets with these contemporary tools, we can deepen our understanding of vulnerable areas, providing the scientific community with a stronger basis for resilient land management and adaptive planning.

In urban settings, the necessity for a multidisciplinary approach becomes apparent, encompassing geomorphological, geographical, cultural, archaeological, geoarchaeological, and geohistorical research fields. The urban geomorphology proved to be a valuable multidisciplinary scientific approach to investigate the geomorphology of urban areas [16], especially in historic city centers where such data are typically abundant and readily available [17–21]. A multidisciplinary approach to urban geomorphology encompasses not only the analysis of natural phenomena and physical processes that shape the land, but also the study of historical archival documents and urban planning analysis. This allows for the identification of the most vulnerable urban areas [22], hereby facilitating a more nuanced comprehension of the impact of urban development on natural landforms and associated natural hazards [23–26]. Furthermore, the field of urban geomorphology promotes the preservation and enhancement of the geomorphological heritage of urban areas [6,12,27–30].

The study of urban geomorphology in European and Italian cities has made a significant contribution to the development of a methodological approach [11,27,31–42]. In this context, the Working Group on Urban Geomorphology of the Italian Association of Physical Geography and Geomorphology (AIGeo) has made a substantial impact on the discipline through its activities, emphasizing the importance of urban geomorphological analysis in Europe and, particularly, in Italy [16]. Geomorphological mapping studies, from which this work was inspired, focuses both on geomorphological features of natural origin and on the characterization of landforms related to anthropogenic activities on the territory [6,10,32,43].

The aim of this research is to present and test and validate MAGUS (Model for the Analysis of Geomorphological Urban Systems). The core of MAGUS consists of investigating the historical urban expansion phases, such as the conversion of land-use from natural to urban cover [44,45], to elucidate how urbanization and other anthropogenic activities are related to the pre-existing natural landscape. To achieve this, a Geographic Information System (GIS) approach was employed to spatially analyze historical documents and conduct morphometric analysis. By analyzing ancient iconographic documents, digitizing elements from historical maps, and overlaying these with current elevation data, our study aims to identify a significant correlation between natural morphological elements and urban expansions in the city from the Roman age until the 19th century.

To test the MAGUS framework, we selected the city of Turin (Figure 1). This research holds significant relevance for the scientific community as it addresses the challenges faced by modern metropolitan cities globally. Historically, Turin's development was closely tied to its natural fluvial systems, but rapid urbanization has since obscured the landscape's original landforms. With the increasing frequency of extreme natural events [46], it becomes crucial to accurately identify vulnerable areas and examine how human activities have altered these landscapes. This understanding not only enhances urban resilience but also contributes to preserving and enriching the cultural and environmental heritage of the city.



**Figure 1.** Panoramic view of the historic city center of Turin from the Turin Hill. Below, the Po River can be seen flowing through the Murazzi embankment complex, skirting the city center.

## 2. Materials and Methods

### *2.1. Study Area and Geomorphological Setting*

Turin is located in the northwest of Italy in the Po Plain, between the Western Alps to the west and Turin Hill to the east (Figure 2A). The city spans an area of 365 km$^2$, with elevations ranging from 200 to 300 meters above sea level. Over the past decade, the Turin Plain has seen significant commercial, industrial, and residential developments, while the western and northwestern slopes of the hillside have experienced limited urban expansion (see Figure 2A). The city center of Turin is the focus of this research (Figure 2B). Specifically, the Borgo Nuovo, the Quadrilatero, the Porta Nuova neighbors, the Murazzi complex, the Vittorio Veneto Square, and the Giardini Reali Park.

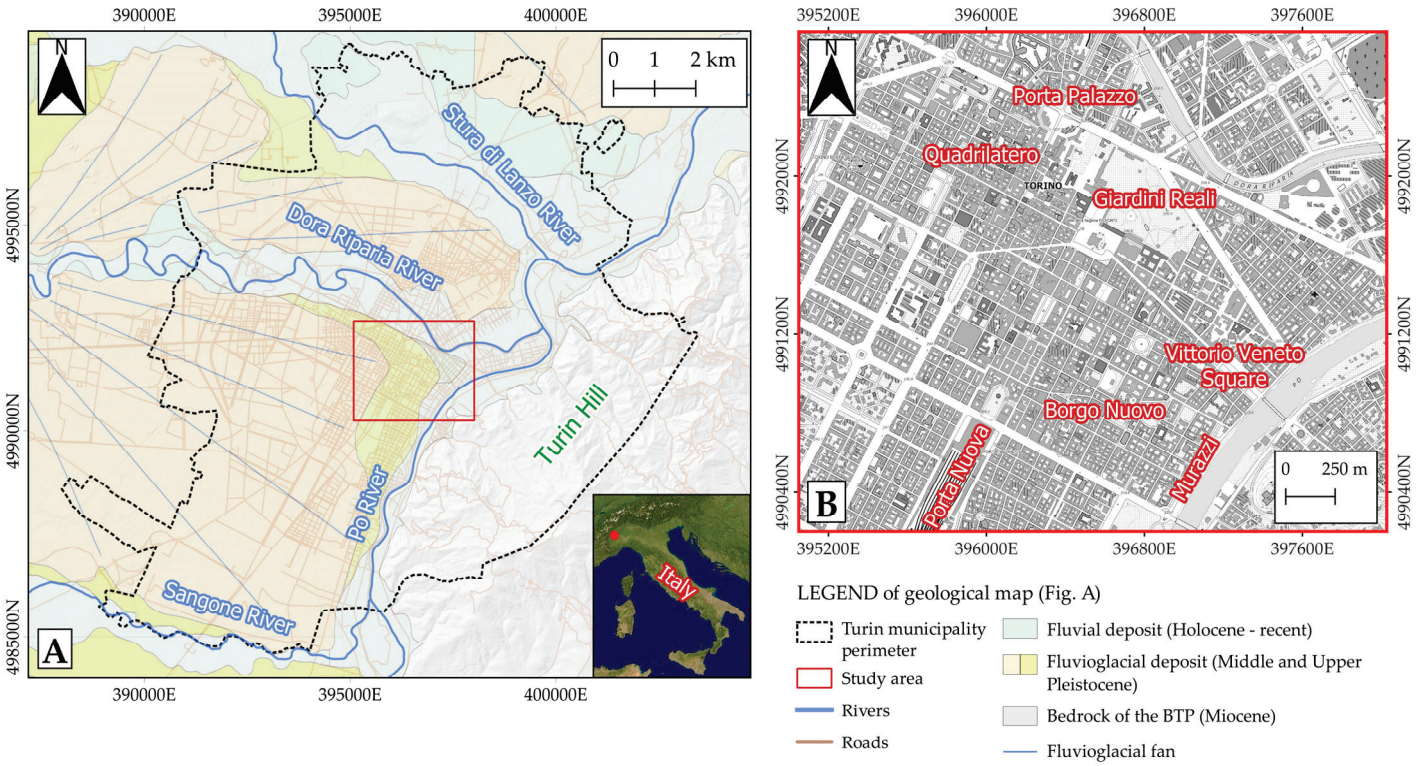



**Figure 2.** Geographical setting of Turin city's area: (**A**) Geological and geomorphological context (source: Lithological map of Piedmonts [47]); (**B**) Boundaries and neighborhoods toponymy of the study area (basemap: BDTRE 2023 1:10,000 [47]).

Turin's urban landscape is significantly characterized by four rivers: the Dora Riparia and the Stura di Lanzo rivers to the northeast, and the Sangone River to the southwest, all of which are tributaries of the Po River. The Po River, one of Italy's most important rivers, flows along the northwestern slope of Turin Hill.

The city and its suburbs are in the western section of the Po Plain, where it forms a narrow band between the Western Alps and the Turin Hill. This area features Upper Pleistocene outwash sediments that formed fluvioglacial fans connected to the Alpine tributaries of the Po River [48]. Turin's city center has developed on the fan-shaped deposit from the Dora Riparia River. This fan has a gentle steepness slope southeastward, extending from the outlet of the Susa Valley and tapering towards the Po River [48]. The deposits in this large fluvioglacial fan are primarily composed of coarse gravels and sands of fluvioglacial origin, while the alluvial plain areas of the Dora Riparia are characterized by fluvial deposits, mainly sands.

The Turin Hill is the surface expression of a northeast–southwest anticline formed during the Miocene [49] at the top of the main Padane Thrust Front [50]. The stratigraphic succession forming the bedrock of Turin Hill is part of the Tertiary Piemonte Basin (BTP) [51,52].

### *2.2. Methodological Framework*

Urban geomorphology has significant implications for territorial planning, integrating historical, cultural, and scientific dimensions to address the complexities of ongoing urban growth. In cities across the Mediterranean and Central Europe, with over 2000 years of historical soil stratification, historical documents offer essential resources for landscape evolution studies.

According to Pica et al. [16], the study of urban geomorphology requires multi-temporal data and multidisciplinary methods. The methodological framework employed in this study was designed to explore the interactions between anthropogenic urban expansion and natural landforms process [34,53,54].

Before presenting the data and methodological framework, it is essential to highlight some key methodological assumptions to apply MAGUS workflow:

1. The multi-temporal analysis of city's urban expansion is feasible due to the ancient origins of its historic center's core. The older the city's foundation, the further back in time the historical analysis can potentially extend.
2. The city's expansion must be gradual and relatively slow until the modern age. This slow rate of growth provides a wider range of historical data within the same timeframe, enabling a detailed examination of urban transformations across centuries.
3. The city's architectural heritage must be well preserved, with many historic buildings serving as temporal markers. This offers valuable georeferenced markers for studying urban morphometry and the dynamics of the city's growth.
4. Buildings act as indicators of the standardized process. Any extensions or renovations they may have undergone over time were not considered in this analysis.

Finally, it is important to acknowledge that while modern cartography benefits from standardized validation processes that ensure precision and accuracy, historical maps do not offer the same degree of certainty due to the evolving nature of cartographic techniques. This often results in distortions and inaccuracies in earlier maps [8,43,55].

### *2.3. Data*

The dataset employed in this research encompasses the statistical surfaces (elevation and slope steepness) and historical documents (maps, paintings, and iconographic records) related to the urban development of Turin.

The concept of "statistical surface" is defined as the distribution phenomenon's values across a defined space, where each coordinate pair is associated with a measured or calculated Z-value [56]. This serves as a fundamental data source for spatial analysis processes and is essential in applied quantitative geomorphology and geomorphometry. In the course of the analysis, the Digital Terrain Model (DTM) was employed as raster data obtained from LiDAR data of the 2009–2011 ICE flight for the topographical analysis of the study area. The DTM, which is available for download from the Piedmont Region's geoportal [47], represents the ground surface without elevation data for buildings and anthropogenic artefacts. As a result, it is a valuable resource for analyzing the shapes of the city's natural landscape. The DTM, which has been processed from LiDAR data in accordance with level 4 standards, offers comprehensive coverage of the regional territory with a grid resolution of 5 m and an altimetric accuracy of $\pm$0.30 m ($\pm$0.60 m in areas of lesser accuracy, corresponding to wooded and densely urbanized areas).

Thirteen maps and paintings were collected from the City Historical Archive, the Museo Torino website [57], and are focusing on city buildings, walls, and water channels. These provide a comprehensive overview of Turin's urban evolution from the Roman era to 1879, while the georeferenced topographic maps from 1880 to 1969 were acquired from the IGM (Military Geographic Institute) database [58]. Table 1 provides a summary of the historical data collected used for more details on the maps used in the current research see Appendix A.

**Table 1.** List of historical maps resources.

| Year | Title | Description |
|---|---|---|
| 1572 | Augusta Taurinorum | Military map |
| 1640 | Plan of the ring road made to the city of Turin (…) | Renaissance map |
| 1680 | Map of Turin | Renaissance map |
| 1751 | Map of the Royal City of Turin (…) | Renaissance city plan |
| 1839 | Map of the City of Turin | Modern city plan |
| 1852 | Map of the City and Suburbs of Turin | Thematic city plan |
| 1878 | Topographical map of the outskirts of Turin | Topographic map |
| 1896 | Map of Turin | Topographic map |
| 1911 | Map of Turin and its surroundings (IGM) | Topographic map |
| 1934 | Historical IGM map 1922–1934 | Topographic WMS |
| 1969 | Historical IGM map 1955–1969 | Topographic WMS |
| 1985 | Technical map (1980–1985) | Topographic WMS |

The latest topographic map and the building polygon shapefile were obtained from the WMS (Web Map Service) of the Regione Piemonte geodatabase [58] and the municipality of Turin geodatabase [59], respectively.

### *2.4. Methodological Workflow*

The methodological workflow adopted in our research is schematically shown in Figure 3. This integrates diverse disciplinary techniques, moving beyond a purely multidisciplinary approach, and it can be considered an interdisciplinary [60]. This approach was specifically developed to investigate the urban development of the cities by analyzing both anthropogenic and natural landscape features over time. We used the open-source software QGIS v3.34 to process historical maps alongside modern georeferenced data, enabling a comprehensive analysis of the geographical data obtained from diverse sources. It is important to note that the primary aim of this study is to test the MAGUS methodology on a real case study. In Figure 3, we propose an extended workflow to illustrate how MAGUS can contribute to the creation of an urban geomorphological map. However, this aspect is beyond the scope of the current research questions. The MAGUS steps are represented by color-filled elements, while the white-filled elements indicate the proposed methodological steps to achieve an effective urban geomorphological map. The use of historical documents, particularly ancient maps and paintings that depict the landscape, serves as a starting point for this research. These sources offer a glimpse into the past configurations of the urban environment and provide essential context for interpreting subsequent geomorphological changes. In particular, data from the Geoportale Piemonte [47], such as the volumetric units of buildings, enable dating of changes in land cover and ability to map them accurately. This integration of historical data with modern geospatial technologies allows for a multitemporal analysis of urban growth and its impact on the landscape. In addition, historical and cultural data are essential sources of information that can enhance the understanding of the relationship between human culture and the local landscape. For instance, toponymic studies—the analysis of place names—can reveal insights into the historical uses of land or the cultural significance of geographic features.

Geomorphological fieldwork and geological data are essential for analyzing terrain features and subsurface characteristics. When combined with anthropogenic, historical, and cultural data, they enable the comprehensive mapping of an urban geomorphological system. This integration is crucial for producing detailed urban geomorphological maps, which, while not the primary focus of this study, are valuable tools for future urban planning and development. Such maps offer critical insights into the interactions between natural landforms and human activities.

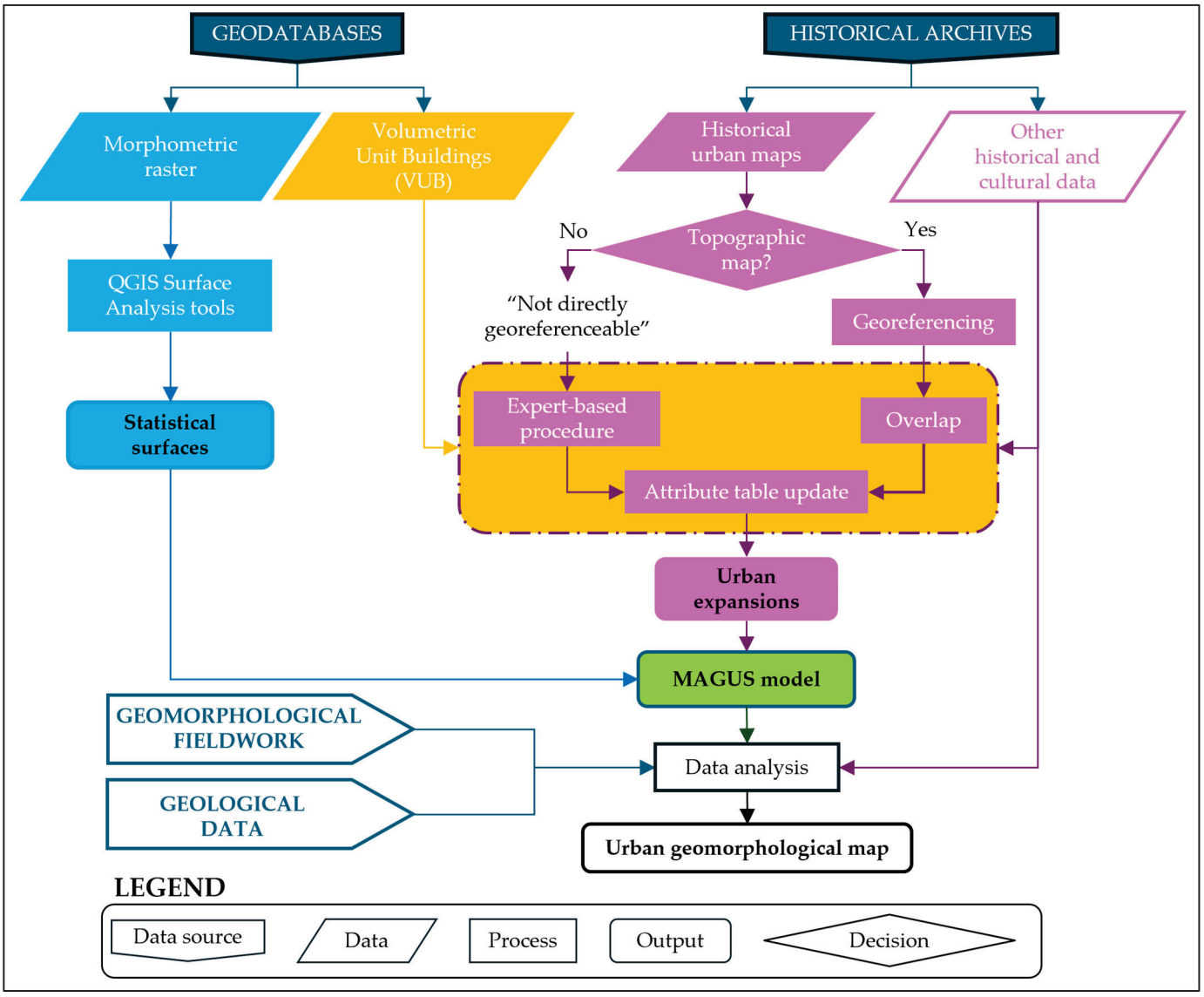



**Figure 3.** Methodological workflow proposed to create an urban geomorphological map.

#### 2.4.1. Surface Analysis

Due to the significant anthropogenic alterations in the study area, we chose to emphasize terrain morphometry by directly employing DTM 5 m-resolution elevation data rather than shaded relief representations. We applied a false-color visualization technique, using single bands with linear interpolation, equal elevation intervals, and a high-contrast color palette. This visualization method facilitated the classification of morphometrical elevation classes by fine-tuning the colormap's contrast and setting ranges specific to the local topography. The SAGA algorithm was employed to calculate slope steepness for morphometric analysis.

#### 2.4.2. Urban Expansion Analysis

Before proceeding to urban expansion mapping methodology, it is crucial to distinguish between "urban expansion" and "building development". Urban expansion examines how cities grow spatially, particularly the expansion of urban boundaries into rural areas, using tools like GIS and remote sensing to study land-use changes and urban sprawl. In contrast, building development focuses on the building's evolution, analyzing architectural style, density, and sustainability. This involves examining construction data and

urban design to understand vertical growth and regulatory influences. Our methodological framework focuses exclusively on urban expansion.

The georeferencing process involved the identification and placement of Ground Control Points (GCPs) corresponding to known spatial coordinates within the images. Since historical maps often do not include geographical or kilometric grids, GCPs were positioned by identifying specific objects and buildings depicted. The choice of transformation method plays a significant role in the georeferencing outcome. Terrone et al. [55] recommend the Helmert transformation for historical maps, as it applies a roto-translational adjustment without distorting the image, minimizing deviations between the source and georeferenced images. The georeferencing accuracy was qualitatively validated by spot-checking the georeferenced map against a modern basemap. We considered that only maps created according to topographical criteria are suitable for georeferencing. For maps produced with non-topographical criteria, we proposed an expert-based procedure to transpose the data into cartographic space, addressing spatial inaccuracies and perspective distortions.

After georeferencing the historical topographical maps, the Volumetric Unit of Buildings (VUB) shapefile from the Municipality of Turin was used to digitalize the city's expansion phases. A new field was added to the shapefile's attribute table to record the year each building footprint first appeared on historical maps.

For the historical non-topographical maps, the process involved a straightforward overlay of shapefile VUB polygons on historical IGM maps to identify the buildings. An expert-based method was applied for maps dated before 1880, summarized as follows:

1. Multi-Temporal Marker (MTM) identification: historical data were examined to identify architectural elements that are still recognizable, such as historical buildings, bridges, roads, churches, and squares.
2. Marker validation: when multiple historical documents confirmed a selected marker, it was considered reliable. Otherwise, the marker was treated with caution during urban expansion analysis due to historical data uncertainty.
3. GIS-based mapping: the validated multi-temporal markers were mapped within a georeferenced environment.
4. Dating of buildings: the VUB's shapefile attribute table was updated with the building dates. This procedure is based on the interpretation of MTMs on historical maps, with digitization resolutions typically of the order of the neighboring structures (aggregates of buildings) rather than of individual buildings.

This interdisciplinary method integrates historical, geographical, and urbanistic studies to produce a detailed georeferenced map of Turin's urban sprawl, highlighting different phases of growth and transformation over time. It is crucial to note that using the current VUB shapefile imposes a geographic constraint on the historical expansion phases, ensuring consistency in cartographical errors and enhancing spatial comparability.

## 3. Results and Discussion

### *3.1. Topographic and Morphometric Analysis*

To investigate the relationship between the geomorphological natural landscape and the urban environment, a comprehensive topographic and morphometric analysis was undertaken. The DTM (Digital Terrain Model) was categorized using a false-color elevation-interval technique, resulting in 17 distinct classes, each with a 2 m elevation range (Figure 4A). Comparing this classification with the geological map (see Figure 2) effectively highlights the fluvioglacial fan (located in the southwest in Figure 4A), as well as the lateral fluvial migration zones of the Po and Dora Riparia rivers (northeast in Figure 4A). Anthropogenic features, such as embankments, road modifications, and historical city ramparts, are distinctly recognizable due to their geometric patterns.

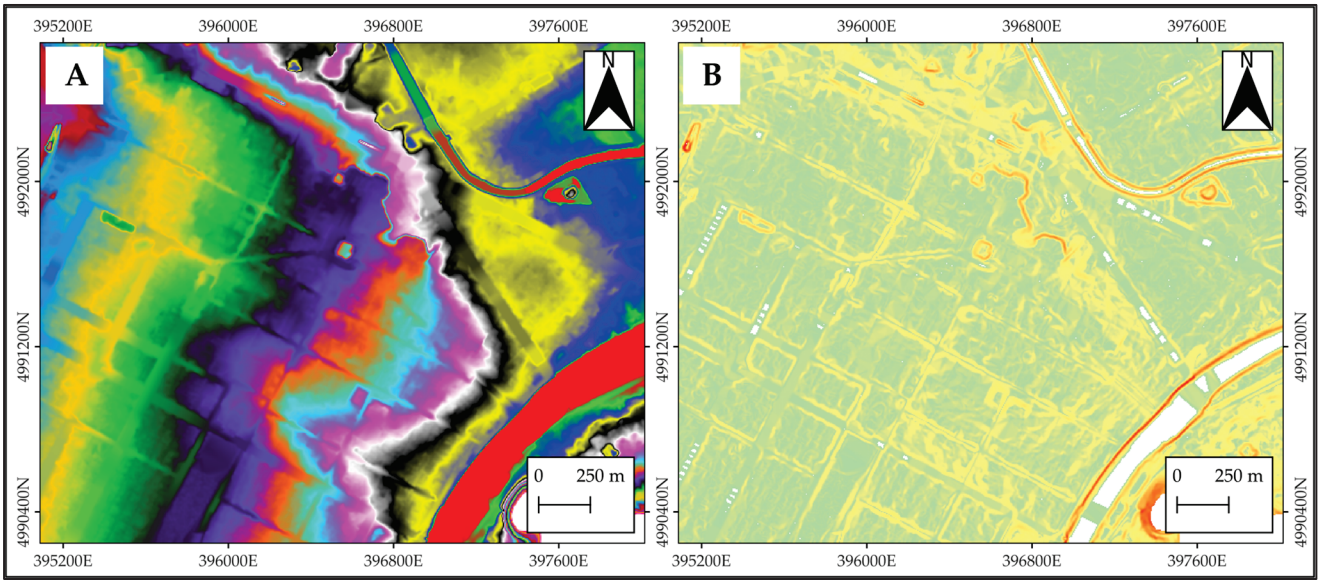



**Figure 4.** Morphometrical analysis results of the study area. (**A**) Elevation map categorized with false-color elevation-interval technique; (**B**) steepness slope map (green: 0–1.96°; yellow: 1.96–50.48°; red: >50.48°).

The slope-steepness analysis (Figure 4B) reveals that some areas exceed the study area's average slope angle. To enhance the visibility of gentle fluvial scarps that have been reshaped by human activity, we excluded slope angle values below the average (1.96°) and classified the raster pixels using the quantile method. Two distinct slope classes can be identified: the first (1.96° to 2.05°) emphasizes natural landforms, while the second (2.05° to 50.48°) highlights steeper slopes, particularly in areas modified by human intervention and near the Dora River. The first class effectively reveals fluvial features that are otherwise obscured by urban infrastructure.

### *3.2. Turin's Urban Expansion from Roman Age to the 20th Century*

The analysis of historical maps reveals five distinct phases in Turin's urban expansion, each characterized by significant shifts in spatial planning: the Roman age; the Renaissance and the Baroque periods; the 19th century; and the 20th century.

Turin's origins date back to Roman times, with the initial urban core originally delimited by defense walls and four gates of entrance to the city (Figure 5A). Now only evidences of two gates can be referred to the Porta Palatina and the Palazzo Madama. Despite changes in its form, architectural style, and function, the Palazzo Madama was built on the ancient Roman gate, as demonstrated by archeological research [61]. The ancient city was divided into four main districts by the Cardo and the Decumanus roads that connected the four gates of the city. The MTMs identified for this period are four related to the Roman age, and two for the late Middle Ages. Roman's MTMs are the Palazzo Madama, the Porta Palatina, the Cardo, and the Decumanus streets, which are still recognizable today in the urban pattern as Garibaldi Street, Porta Palatina Street, and San Tommaso Street. The MTMs related to the early Middle Ages are scarce. However, with documentation from the 14th century (Figure 5B) onwards, it was possible to identify the Santi Martiri and the Santa Maria di Piazza churches.

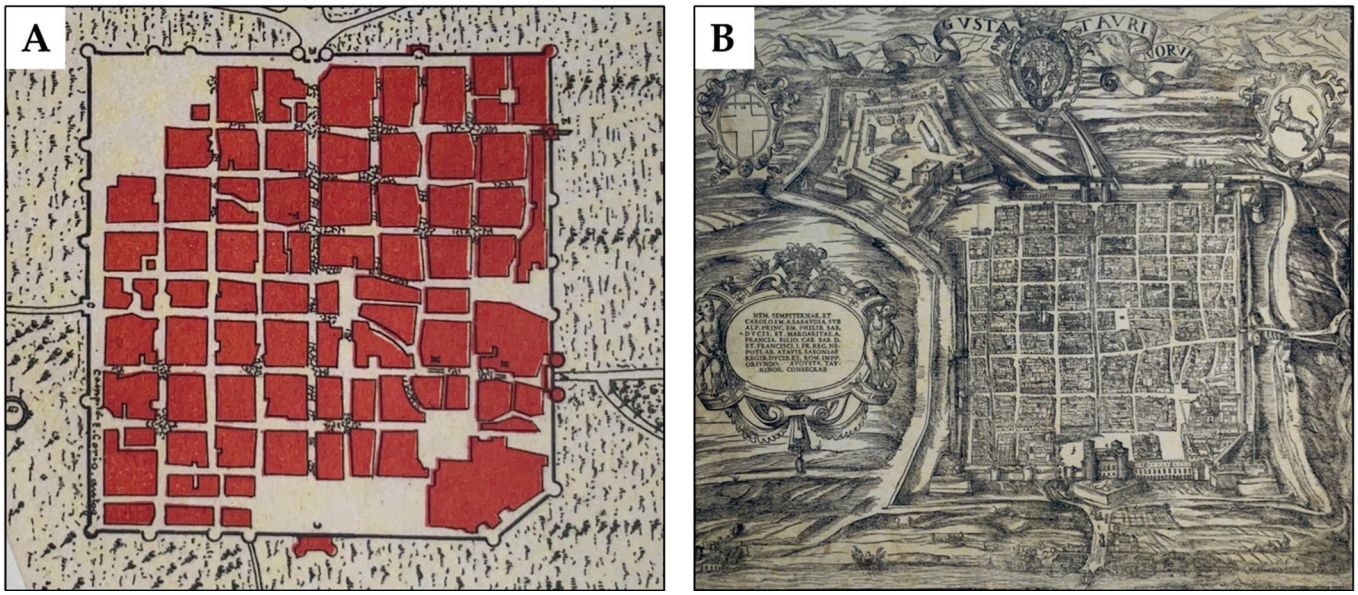



**Figure 5.** Historical maps of Turin in Roman and late Middle Ages periods. (**A**) The plan illustrates the configuration of the Augusta Taurinorum within the context of the medieval urban layout (source: ASCT, Tipi e Disegni 64.1.7, in [62] p. 18; (**B**) map of Turin in the early Renaissance (1577) with the new defense walls and the Cittadella fortress (source: Augusta Taurinorum, di Giovanni Caracha, incisione di Giovanni Criegher, 1572. Archivio Storico della Città di Torino, Collezione Simeom, D 1 in [62] p. 77).

Under the leadership of the Savoy dynasty during the Renaissance (14th century, Figure 6A) and Baroque (17th century, Figure 6B) periods, Turin was gradually transformed into the capital of their kingdom. This period was characterized by the construction of numerous palaces, churches, and monuments, which significantly enhanced the city's cultural heritage. Many of these historic structures can be used as MTMs. For the Renaissance period, the Mastio della Cittadella, the ramparts near the Palazzo Reale (Bastion Verde), and the Santa Cristina church have been identified. As for the Baroque period, the Palazzo del Pozzo, the Palazzo Campana, the Palazzo Barolo, the Santuario della Consolata church, the Jewish ghetto, and the Military district have been identified.

In the 19th and 20th centuries, Turin experienced significant industrial growth, largely fueled by the rise of the automobile industry, which catalyzed accelerated urban expansion and the extension of the city's boundaries beyond its medieval confines. This period was characterized by the construction of extensive residential neighborhoods, industrial facilities, and infrastructure, which coincided with a substantial population increase (Figure 7).

The urban expansion mapping of Turin facilitated the digitization of historical data. As described in the methodological workflow in Section 2.2 (see Figure 3), the digitization of historical maps predating 1880 involved the identification of MTMs as an initial step. Following this, the expert-based methodology was used to classify the building shapefile in alignment with historical urban expansion phases. For the period after the 1880s, IGM's topographical maps were employed to trace Turin's urban growth, using overlay criteria between the WMS of the Piedmont Region and the building shapefile. The final mapping results are illustrated in Figure 8.

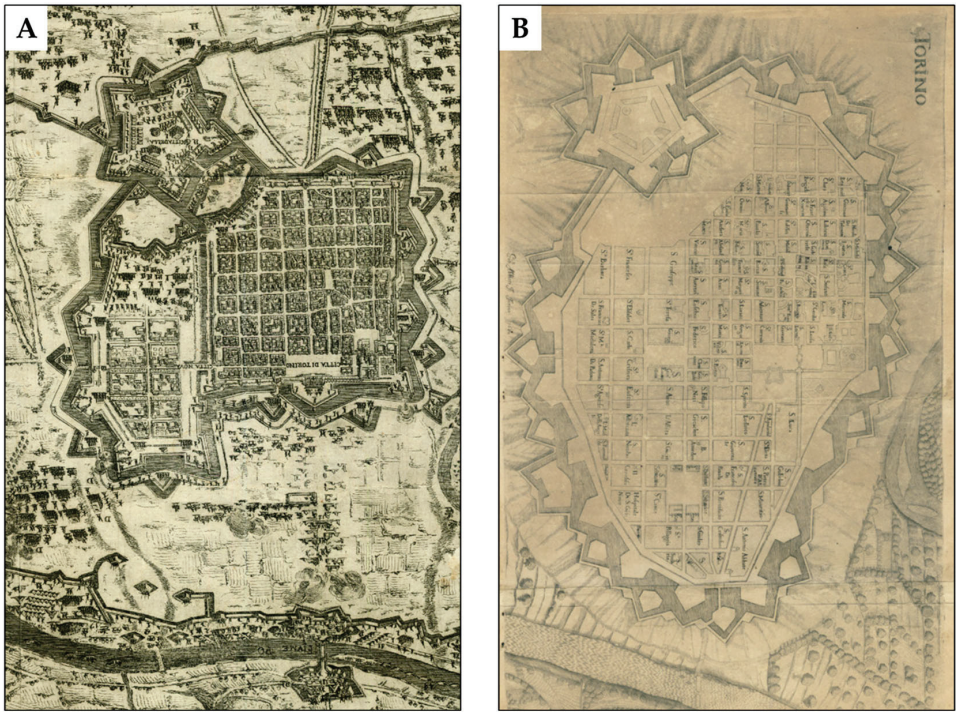



**Figure 6.** Details of historical maps from the Renaissance and Baroque periods (see Appendix A), focusing on the area of interest and oriented to show the Po River at the bottom of the images. (**A**) Piano della circonvallazione fatta alla città di Torino dall'Armate di S. Maestà... (assedio del 1640), di Michele Antonio Raynero, incisione di Giovenale Boetto, 1643. ASCT, Collezione Simeom, D 11. In [57]. (**B**) Giovanni Abbiati, Pianta di Torino, 1680. Archivio Storico della Città di Torino, Collezione Simeom, D 13. In [57].

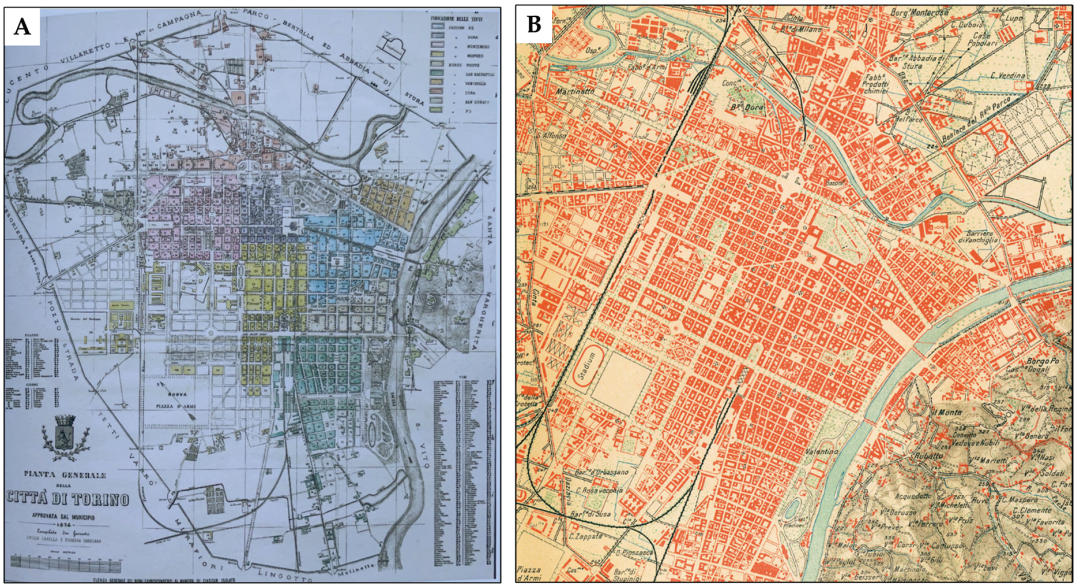



**Figure 7.** Historical Turin's city development maps: (**A**) 19th century, Pianta Topografica disegnata dei geometri Emilio Cabellla e Firmino Caneparo con l'elenco generale dei nomi corrispondenti al numero di ciascun isolato. Litografia a colori, anno 1874 (ASCT, Collezione Simeom, D113, in [62], p. 231), and (**B**) 20th century (Pianta di Torino e dintorni, 1911. ASCT, Collezione Simeom, D135 in [57]).

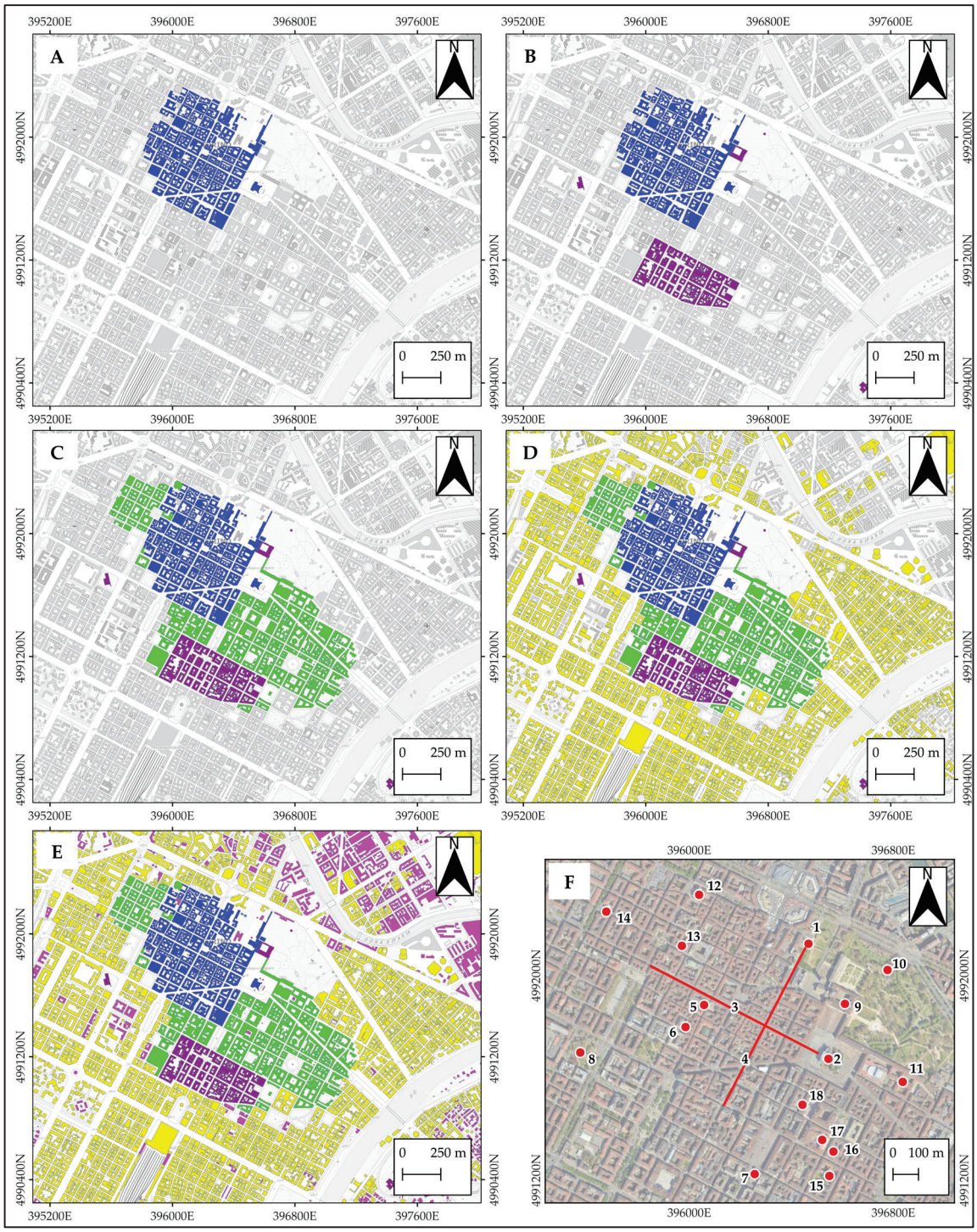



**Figure 8.** Urban expansion phase results obtained with the MAGUS methodological framework. The five expansion phases are: (**A**) the Roman period and the Middle Ages (blue), (**B**) the Renaissance period (deep purple), (**C**) the Baroque period (green), (**D**) the 19th century (yellow), and (**E**) the 20th century (purple). (**F**) Shows the Multi-Temporal Markers used for the MAGUS expert-based procedure (1: Porta Palatina; 2: Palazzo Madama; 3: Cardo; 4: Decumano; 5: Santi Martiri church; 6: Santa Maria di Piazza church; 7: Santa Cristina church; 8: Mastio della Cittadella; 9: Palazzo Reale; 10: Bastion Verde; 11: Cavallerizza buildings; 12: Santuario della Consolata; 13: Palazzo Barolo; 14: Military districts; 15: Palazzo del Pozzo; 16: Jewish ghetto; 17: Palazzo Campana; 18: Palazzo Carignano). Basemaps: (**A**–**E**) BDTRE 2023 1:10,000 [47]; (**F**) Google® Satellite.

### *3.3. Anthropogenic Landform*

The anthropogenic landforms in Turin's historic city center include the ancient city walls, the extensive water channels, and reclaimed land used for residential development. Mapping the temporal progression of these ancient city walls and river channels was fundamental to this research, providing essential insights into Turin's spatial and infrastructural history.

#### 3.3.1. The City Walls

In the georeferencing process, over 40 GCPs were selected throughout the city center, many of which matched the previously identified MTMs. Helmert's transformation was applied, and the digitalized outcome is shown in Figure 9.

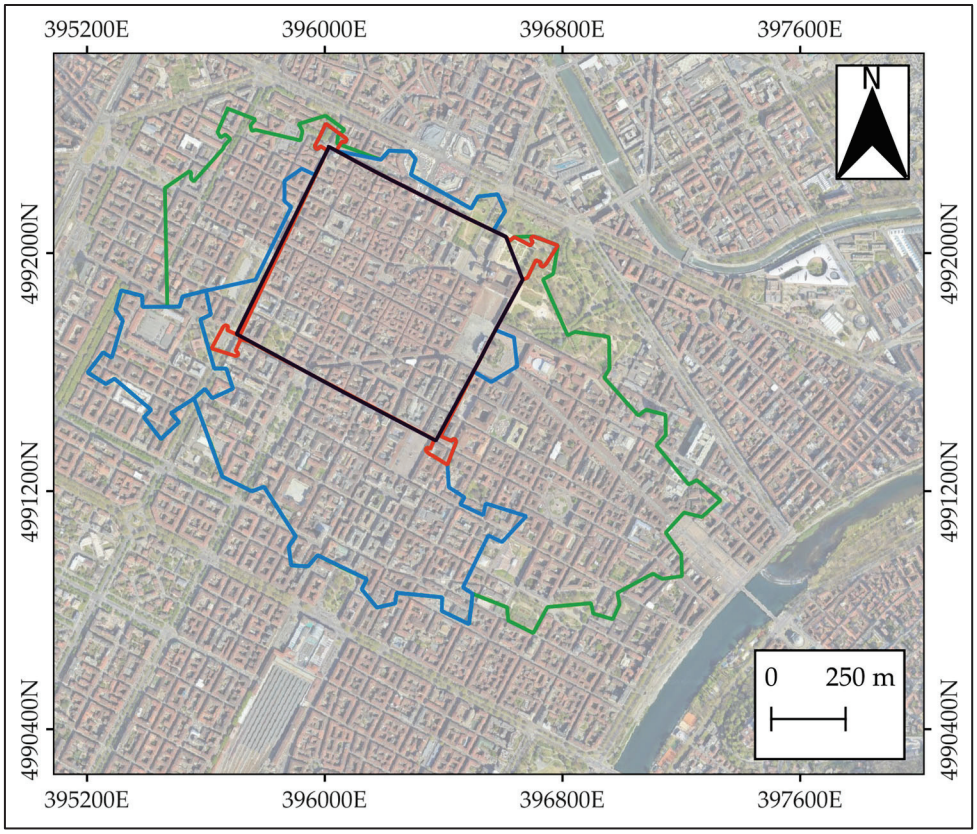



**Figure 9.** Turin's defense city walls mapped the Roman Age (black), the late Middle Ages (red), the Baroque period (blue), and the Renaissance period (green). Basemaps: Google® Satellite.

The ancient city walls of Turin are robust MTMs in both temporal and geographical terms, having defined the boundaries of urban expansion over the centuries. These defensive structures, including lines of defense and fortifications, embody the strategic military concepts and technical standards of their time. However, identifying these military structures within the modern urban fabric was challenging due to their integration with other engineering infrastructures.

Few remnants of the Roman defensive walls of the city have survived to the present day. As discussed in Section 3.2, two of the four gates still exist, and evidence of wall sections has been uncovered during archaeological excavations [61]. Additionally, some defensive bastions remain visible along the original wall lines. Furthermore, it is important to note that Roman cities typically had a square shape in the plan. Archaeological studies [61,63] have revealed that Turin's Roman walls had one corner chamfered (see Figure 9).

During the Middle Ages, ramparts and earthen walls were constructed using earth-filled piling techniques, while rock fortifications required the substantial transport of

materials. Supported by stone and brickwork, these fortifications involved extensive earthworks, such as steep slopes, tank traps, and concrete-lined moats [9].

Turin's fortifications underwent significant transformations during the 16th and 17th centuries. The construction of the Cittadella district necessitated a complete redesign of the city's defense system to support urban expansion. Trenches and bastions were strategically constructed and closely associated with urban settlements. Some of these structures were integrated into the broader fortification system, while others were built along the urban periphery. By the 21st century, most of these structures had been abandoned due to urban development, leading to their classification as sites of anthropogenic surface formation.

#### 3.3.2. Channels in Turin Between the 19th and 20th Centuries

A document from 1882 (Figure 10A) provides valuable insights into the layout of the channels within the city during the 19th and 20th centuries, especially in relation to the urban landscape evolution (Figure 10B). In fact, these channels were chiefly used for agricultural irrigation and as a source of energy for mills and industrial operations, playing a vital role in the city's economic and social development.




**Figure 10.** Anthropogenic channels (bealere) in Turin's historical city center. (**A**) Historical 1882 topographical map of "bealere" (ASCT Tipi e Disegni 12.1.90) and (**B**) digitalized results using MAGUS workflow (orange: Borghesi channel; light blue: Valentino; dark pink: Valentino extension; purple: Arsenale; dark green: Vanchiglia; blue: Torino; yellow: Torino extension; green: Giardino Reale channel; pink: Fontane; light green: Molassi). Basemaps: Google® Satellite.

The term "bealera" (or bealere at plural) in Piedmontese dialect usually refers to a long, narrow, artificial watercourse. The Turin's bealere were predominantly fed by branches of the Dora Riparia River, extending for kilometers from their source and ending in the Po River. Although no longer visible on the surface, the artificial channels still function underground.

### *3.4. MAGUS Model Results*

The morphometrical and urban expansion analysis results were compared in a GIS environment. As shown in Figure 8, it can be clearly demonstrated that the most extensive urban expansion of Turin's city center occurred after the second part of the 19th century. Before this significant growth, the city largely remained within its historic fortifications.

Focusing on these ancients' urban expansions, we analyzed the data obtained with the MAGUS framework to make a first qualitative interpretation of the urban geomorphology

of the Turin city center. It is important to note that this is a preliminary analysis. In fact, it cannot return a complete urban geomorphological map (Figure 3) but only a first overview of the pre-existing natural landscape of Turin city center. Further analysis will be conducted to obtain a detailed model.

The overlapping of urban growth of Turin up to 1735 with the reclassified DTM (Figure 11) highlights interesting features. The natural morphologies seem to have influenced the expansion of the city, as evidenced by the development of the city which was located exclusively on the fluvioglacial fan of the Dora Riparia. In addition, the southern and northeastern perimeters of the city correspond to the upper edges of two significant scarps, which are well highlighted by the DTM (Figure 12).

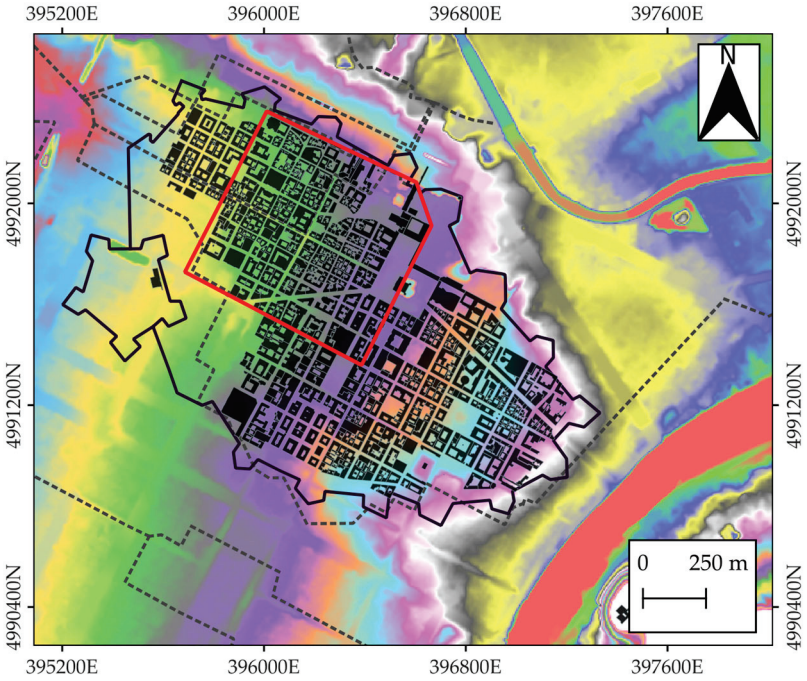



**Figure 11.** MAGUS model result. Roman and Baroque urban expansions with defensive walls, artificial water channels on reclassified DTM.

The northeastern scarp corresponds to the fluvial scarp of the Dora Riparia River (Figure 12). This morphological feature marks the boundary between the fluvioglacial fan and the alluvial plain of the Dora Riparia River, which extends to the northeast. Additionally, as shown in Figure 5A, which depicts Turin's Roman city plan, the southeastern corner of the walls was chamfered. This anomaly is closely related to the Romans' adaptation to the terrain's morphology of the fluvial scarp. It is also evident that this boundary was extended in later centuries with the construction of the walls in the Wars of Italy period, which compensated for that section along the Dora Riparia River scarp. As shown in Figures 4B and 11, the walls built in the 14th century were constructed in accordance with natural morphologies while also adding anthropic material to create the typical arrow shape of the defensive walls (i.e., Bastion Verde).

This intricate context reveals a clear correlation between the development of the city walls relating to pre-existing Dora Riparia and Po rivers scarps. These natural obstacles were overcome through new construction techniques in the following decades.

A closer examination of the correlation between morphometric data and the presence of channels and derivations from the 18th and 19th centuries reveals a notable overlap between the historical Arsenale Channel and a morphometric elongated depression located south of the city center (see Figure 12), oriented northwest to southeast.

In the first hypothesis, the depression observable on the actual DTM should be interpreted as an ancient natural channel. Construction work on the man-made Arsenale

Channel may have utilized the pre-existing natural waterway in this section. A second hypothesis can be explained by the ancient presence of defensive wall infills and/or related defensive moats, subsequently filled and smoothed to allow urban expansion in the 19th century. Both hypotheses must be verified with geological, geomorphological, and other historical data, and other options should be considered, too.

Furthermore, the elevation data show how the road embankment has altered the contours of this depression. While the nature of this feature remains unclear, it nonetheless offers valuable insights into how the urban landscape may have interacted with the natural terrain.

All these geomorphological features played a crucial role in shaping the boundaries of the City of Turin from Roman times until the end of the 18th century, highlighting the impact of the natural landscape on the historical development of the city. The ancient Roman city was likely constructed upon a fluvioglacial fan, providing a naturally elevated and stable foundation. This strategic location, combined with the natural fluvial scarp to the east, played a borderline role that limited the city's expansion for centuries. However, by the end of the 18th century, urban development began to extend beyond these natural limits. The construction moved to the alluvial plain of the Dora Riparia and Po rivers, requiring significant modifications to the terrain. To accommodate the city's growth, large amounts of terrain may have been added to raise the topographical surface and to modify the course of both rivers. Today, the Po River is heavily constrained between urban developments and the foothills, while the Dora Riparia is channelized throughout its course within the city, reflecting the long-term geomorphological transformations driven by anthropic activity. To map the urban geomorphology of Turin more effectively, it will be necessary to investigate the locations of these fill materials and determine their thickness. Understanding where these imported fills were placed and how much they altered the natural surface is crucial for reconstructing the city's geomorphological history.

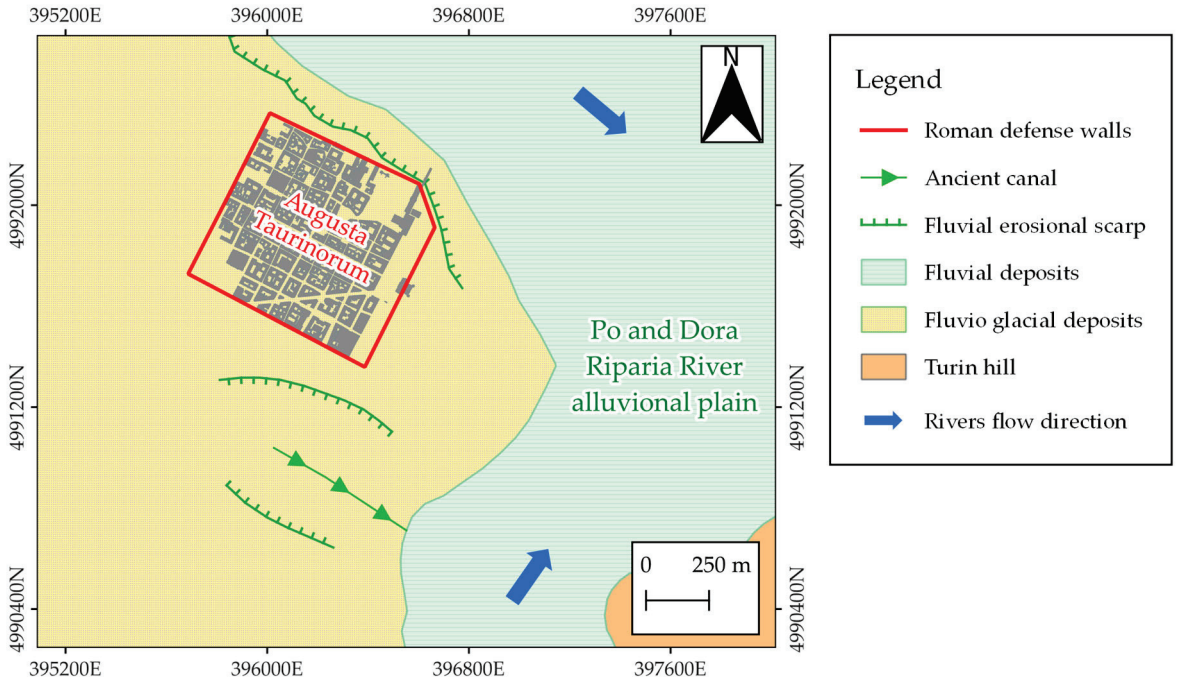



**Figure 12.** Preliminary geomorphological model reconstruction of Augusta Taurinorum's ancient natural surroundings landscape.

## 4. Conclusions

This research presents the development and testing of the MAGUS (Model for the Analysis of Geomorphological Urban Systems) methodological workflow, specifically designed to map urban geomorphological evolution through morphometric and historical

urban expansion analyses. Using a GIS-based approach, we successfully imported and analyzed both topographical and non-topographical historical documents. These were digitized and georeferenced, allowing for the direct comparison of quantitative morphometric data, such as DTM and slope steepness, with qualitative historical data in an interdisciplinary framework.

As outlined in Section 2.2, the MAGUS framework has some limitations, based on its underlying methodological assumptions. The ability to conduct a multi-temporal analysis of urban expansion hinges on the ancient origins of the city's historic core. Furthermore, the framework assumes that the city's growth occurred gradually and at a relatively slow rate until the modern era. Another key assumption is the preservation of the city's architectural heritage, with many historic buildings serving as essential temporal markers for studying urban morphometry and growth dynamics. Finally, buildings are treated as indicators of the standardized urban development process, with any extensions or renovations they may have undergone excluded from the analysis to maintain data consistency.

Despite these limitations, the MAGUS framework proves to be a robust and effective tool, utilizing Multi-Temporal Markers (MTM) and georeferenced Volumetric Unit of Building (VUB) shapefiles to enhance the accuracy of historical data digitization, an approach that surpasses the reliability of relying solely on GCPs.

Turin is a city with a well-documented historical evolution dating back to Roman times, and it was selected as the case study for testing MAGUS. The goal was to explore how urbanization and other anthropogenic activities have interacted with the pre-existing natural landscape. Historical documents from the City's Historical Archive were collected and analyzed. This archival research enabled a detailed reconstruction of Turin's urban expansion, distinguishing anthropogenic landforms (such as construction recesses for buildings, streets, and squares) from fluvial landforms (such as scarps, terraces, and river alluvial plains). Overlaying layers of anthropogenic features (urban expansion, artificial channels, and city walls) with topographic data revealed natural geomorphological elements concealed by urbanization.

MAGUS enabled the integration and analysis of diverse data types—historical, social, and geo-environmental—within a georeferenced cartographic space. This research aims to thoroughly examine the anthropo-geomorphological characteristics of the study area, serving as a foundation for more detailed future investigations. The methodological framework we developed enabled the georeferencing of historical non-cartographic data by relying on existing historical buildings rather than on Ground Control Points-based transformations, which can introduce spatial inconsistencies. This approach established a formal method for merging data from diverse disciplines, underscoring the importance of high-precision digitization techniques for accurate urban geomorphological analysis.

In conclusion, urban geomorphology has proven to be a rich interdisciplinary field that offers new perspectives on the future of territories where much of the world's population resides. According to a United Nations study [64], by 2030, more than two-thirds of the world's population will live in large urban centers and metropolis. Understanding urban expansion, its impact on natural processes, and how these processes are influenced by urbanization will be, therefore, crucial.

**Author Contributions:** Conceptualization, A.B., M.L. and F.S.; methodology, A.B.; validation, A.B., M.L. and F.S.; formal analysis, A.B.; investigation, A.B.; resources, A.B.; data curation, A.B.; writing—original draft preparation, A.B., M.L. and F.S.; writing—review and editing, A.B., M.L., F.S. and G.F.; visualization, A.B., M.L. and F.S.; supervision, G.F.; project administration, G.F.; funding acquisition, G.F. All authors have read and agreed to the published version of the manuscript.

**Funding:** This research received no external funding.

**Data Availability Statement:** The original contributions presented in the study are included in the article, further inquiries can be directed to the corresponding authors.

**Acknowledgments:** We would like to express our gratitude to the staff of the Archivio Storico della città di Torino for their assistance and availability during the consultation process for the historical research.

**Conflicts of Interest:** The authors declare no conflicts of interest.

## Appendix A. Sources of Historical Maps with Title, Authors, and Archival Index

| Years | Source |
|---|---|
| 1572 | Augusta Taurinorum, di Giovanni Caracha, incisione di Giovanni Criegher, 1572. Archivio Storico della Città di Torino, Collezione Simeom, D 1. © Archivio Storico della Città di Torino; |
| 1640 | Piano della circonvallazione fatta alla città di Torino dall'Armate di S. Maestà. . . (assedio del 1640), di Michele Antonio Raynero, incisione di Giovenale Boetto, 1643. ASCT, Collezione Simeom, D 11. © Archivio Storico della Città di Torino; |
| 1680 | Giovanni Abbiati, Pianta di Torino, 1680. Archivio Storico della Città di Torino, Collezione Simeom, D 13. © Archivio Storico della Città; |
| 1751 | Nova Pianta della Reale Città di Torino con i nomi di ciascheduna Isola con la Tavola per Ritrovare le Chiese, è luoghi Pii co' numeri segnati. . . di Beltramo Antonio Re, 1751. ASCT, Collezione Simeom, D 56. © Archivio Storico della Città di Torino; |
| 1839 | Pianta della Città di Torino, 1839. Archivio Storico della Città di Torino, Collezione Simeom, D 93. © Archivio Storico della Città; |
| 1852 | Pianta della Città e Borghi di Torino, 1852. ASCT, Collezione Simeom, D 104. © Archivio Storico della Città di Torino; Carta degli Stati Sardi 1852 Provincia di Torino |
| 1878 | Carta topografica dei contorni di Torino, di Antonio Rabbini, incisione di Vittorio Angeli, 1878. Archivio Storico della Città di Torino, Collezione Simeom, D 116. © Archivio Storico della Città di Torino; |
| 1896 | Pianta di Torino, 1896. Archivio Storico della Città di Torino, Collezione Simeom, D 126. © Archivio Storico della Città di Torino; |
| 1911 | Pianta di Torino e dintorni, 1911. Archivio Storico della Città di Torino, Collezione Simeom, D 135. © Archivio Storico della Città di Torino; |
| 1934 | Carta IGM impianto storico 1922–1934 Provincia di Torino |
| 1969 | Carta IGM impianto storico 1955–1969 Provincia di Torino |
| 1985 | Carta Tecnica (1980–1985) Comune di Torino—Fogli alla scala 1:1000 in b/n |

## References

1. Crutzen, P.J. The "Anthropocene". In *Earth System Science in the Anthropocene, Emerging Issues and Problems*; Springer: Berlin/Heidelberg, Germany, 2006; p. 267. ISBN 978-3-540-26588-7.
2. Rebele, F. Urban Ecology and Special Features of Urban Ecosystems. *Glob. Ecol. Biogeogr. Lett.* **1994**, *4*, 173. [CrossRef]
3. Bai, X. Eight Energy and Material Flow Characteristics of Urban Ecosystems. *Ambio* **2016**, *45*, 819–830. [CrossRef] [PubMed]
4. Meersmans, J.; Van Wesemael, B.; De Ridder, F.; Fallas Dotti, M.; De Baets, S.; Van Molle, M. Changes in Organic Carbon Distribution with Depth in Agricultural Soils in Northern Belgium, 1960–2006. *Glob. Change Biol.* **2009**, *15*, 2739–2750. [CrossRef]
5. Van Delm, A.; Gulinck, H. Classification and Quantification of Green in the Expanding Urban and Semi-Urban Complex: Application of Detailed Field Data and IKONOS-Imagery. *Ecol. Indic.* **2011**, *11*, 52–60. [CrossRef]
6. Brandolini, P.; Cappadonia, C.; Luberti, G.M.; Donadio, C.; Stamatopoulos, L.; Di Maggio, C.; Faccini, F.; Stanislao, C.; Vergari, F.; Paliaga, G.; et al. Geomorphology of the Anthropocene in Mediterranean Urban Areas. *Prog. Phys. Geogr. Earth Environ.* **2020**, *44*, 461–494. [CrossRef]
7. Bathrellos, G.D.; Skilodimou, H.D.; Kelepertsis, A.; Alexakis, D.; Chrisanthaki, I.; Archonti, D. Environmental Research of Groundwater in the Urban and Suburban Areas of Attica Region, Greece. *Environ. Geol.* **2008**, *56*, 11–18. [CrossRef]
8. Luberti, G.M.; Vergari, F.; Pica, A.; Del Monte, M. Estimation of the Thickness of Anthropogenic Deposits in Historical Urban Centres: An Interdisciplinary Methodology Applied to Rome (Italy). *Holocene* **2019**, *29*, 158–172. [CrossRef]
9. Szabó, J. Anthropogenic Geomorphology: Subject and System. In *Anthropogenic Geomorphology*; Szabó, J., Dávid, L., Lóczy, D., Eds.; Springer: Dordrecht, The Netherlands, 2010; pp. 3–10. ISBN 978-90-481-3057-3.
10. Del Monte, M.; D'Orefice, M.; Luberti, G.M.; Marini, R.; Pica, A.; Vergari, F. Geomorphological Classification of Urban Landscapes: The Case Study of Rome (Italy). *J. Maps* **2016**, *12*, 178–189. [CrossRef]
11. Vergari, F.; Marco Luberti, G.; Pica, A.; Del Monte, M. Geomorphology of the Historic Centre of the *Urbs* (Rome, Italy). *J. Maps* **2021**, *17*, 6–17. [CrossRef]

12. Zwoliński, Z.; Hildebrandt-Radke, I.; Mazurek, M.; Makohonienko, M. Anthropogeomorphological Metamorphosis of an Urban Area in the Postglacial Landscape: A Case Study of Poznań City. In *Urban Geomorphology*; Elsevier: Amsterdam, The Netherlands, 2018; pp. 55–77. ISBN 978-0-12-811951-8.
13. Barredo, J.I. Major Flood Disasters in Europe: 1950–2005. *Nat. Hazards* **2007**, *42*, 125–148. [CrossRef]
14. Neumayer, E.; Barthel, F. Normalizing Economic Loss from Natural Disasters: A Global Analysis. *Glob. Environ. Change* **2011**, *21*, 13–24. [CrossRef]
15. Luino, F.; Barriendos, M.; Gizzi, F.T.; Glaser, R.; Gruetzner, C.; Palmieri, W.; Porfido, S.; Sangster, H.; Turconi, L. Historical Data for Natural Hazard Risk Mitigation and Land Use Planning. *Land* **2023**, *12*, 1777. [CrossRef]
16. Pica, A.; Lämmle, L.; Burnelli, M.; Del Monte, M.; Donadio, C.; Faccini, F.; Lazzari, M.; Mandarino, A.; Melelli, L.; Perez Filho, A.; et al. Urban Geomorphology Methods and Applications as a Guideline for Understanding the City Environment. *Land* **2024**, *13*, 907. [CrossRef]
17. Brown, A.G.; Tooth, S.; Bullard, J.E.; Thomas, D.S.G.; Chiverrell, R.C.; Plater, A.J.; Murton, J.; Thorndycraft, V.R.; Tarolli, P.; Rose, J.; et al. The Geomorphology of the Anthropocene: Emergence, Status and Implications. *Earth Surf. Process. Landf.* **2017**, *42*, 71–90. [CrossRef]
18. Cooke, R.U. Urban Geomorphology. *Geogr. J.* **1976**, *142*, 59. [CrossRef]
19. Cooke, R.U. *Urban Geomorphology in Drylands*; Nationen, V., Ed.; Oxford University Press: Oxford, UK, 1982; ISBN 978-0-19-823239-1.
20. Rosenbaum, M.S.; McMillan, A.A.; Powell, J.H.; Cooper, A.H.; Culshaw, M.G.; Northmore, K.J. Classification of Artificial (Man-Made) Ground. *Eng. Geol.* **2003**, *69*, 399–409. [CrossRef]
21. Tarolli, P.; Cao, W.; Sofia, G.; Evans, D.; Ellis, E.C. From Features to Fingerprints: A General Diagnostic Framework for Anthropogenic Geomorphology. *Prog. Phys. Geogr. Earth Environ.* **2019**, *43*, 95–128. [CrossRef]
22. Giulietto, W.; Luino, F. Utilizzo di un'analisi multidisciplinare per la delimitazione delle aree potenzialmente inondabili: Il caso del Torrente Sangone presso la confluenza con il Fiume Po (provincia di Torino). *G. Geol. Appl.* **2006**, *4*, 57–64. [CrossRef]
23. Slaymaker, O. The Future of Geomorphology. *Geogr. Compass* **2009**, *3*, 329–349. [CrossRef]
24. Cafiso, F.; Cappadonia, C. Landslide Inventory and Rockfall Risk Assessment of a Strategic Urban Area (Palermo, Sicily). *Rend. Online Soc. Geol. Ital.* **2019**, *48*, 96–105. [CrossRef]
25. Galve, J.P.; Cevasco, A.; Brandolini, P.; Piacentini, D.; Azañón, J.M.; Notti, D.; Soldati, M. Cost-Based Analysis of Mitigation Measures for Shallow-Landslide Risk Reduction Strategies. *Eng. Geol.* **2016**, *213*, 142–157. [CrossRef]
26. Loczy, D.; Süto, L. Human Activity and Geomorphology. In *The SAGE Handbook of Geomorphology*; Sage Publications: London, UK, 2011; pp. 267–285.
27. Cappadonia, C.; Di Maggio, C.; Agate, M.; Agnesi, V. Geomorphology of the Urban Area of Palermo (Italy). *J. Maps* **2020**, *16*, 274–284. [CrossRef]
28. Pica, A.; Vergari, F.; Fredi, P.; Del Monte, M. The Aeterna Urbs Geomorphological Heritage (Rome, Italy). *Geoheritage* **2016**, *8*, 31–42. [CrossRef]
29. Reynard, E.; Pica, A.; Coratza, P. Urban Geomorphological Heritage. An Overview. *Quaest. Geogr.* **2017**, *36*, 7–20. [CrossRef]
30. Rodrigues, M.L.; Machado, C.R.; Freire, E. Geotourism Routes in Urban Areas: A Preliminary Approach to the Lisbon Geoheritage Survey. *Geoj. Tour. Geosites* **2011**, *8*, 281–294.
31. Ascione, A.; Aucelli, P.P.C.; Cinque, A.; Di Paola, G.; Mattei, G.; Ruello, M.; Russo Ermolli, E.; Santangelo, N.; Valente, E. Geomorphology of Naples and the Campi Flegrei: Human and Natural Landscapes in a Restless Land. *J. Maps* **2021**, *17*, 18–28. [CrossRef]
32. Mandarino, A.; Luino, F.; Turconi, L.; Faccini, F. Urban Geomorphology of a Historical City Straddling the Tanaro River (Alessandria, NW Italy). *J. Maps* **2021**, *17*, 29–41. [CrossRef]
33. Pelfini, M.; Brandolini, F.; D'Archi, S.; Pellegrini, L.; Bollati, I. *Papia Civitas Gloriosa:* Urban Geomorphology for a Thematic Itinerary on Geocultural Heritage in Pavia (Central Po Plain, N Italy). *J. Maps* **2021**, *17*, 42–50. [CrossRef]
34. Faccini, F.; Giardino, M.; Paliaga, G.; Perotti, L.; Brandolini, P. Urban Geomorphology of Genoa Old City (Italy). *J. Maps* **2021**, *17*, 51–64. [CrossRef]
35. Porta, M.; Buosi, C.; Trogu, D.; Ibba, A.; De Muro, S. An Integrated Sea-Land Approach for Analyzing Forms, Processes, Deposits and the Evolution of the Urban Coastal Belt of Cagliari. *J. Maps* **2021**, *17*, 65–74. [CrossRef]
36. Brandolini, P.; Mandarino, A.; Paliaga, G.; Faccini, F. Anthropogenic Landforms in an Urbanized Alluvial-Coastal Plain (Rapallo City, Italy). *J. Maps* **2021**, *17*, 86–97. [CrossRef]
37. Roccati, A.; Mandarino, A.; Perasso, L.; Robbiano, A.; Luino, F.; Faccini, F. Large-Scale Geomorphology of the Entella River Floodplain (Italy) for Coastal Urban Areas Management. *J. Maps* **2021**, *17*, 98–112. [CrossRef]
38. Guerra, V.; Guerra, C.; Nesci, O. Geomorphology of the Town of Rimini and Surrounding Areas (Emilia-Romagna, Italy). *J. Maps* **2021**, *17*, 113–123. [CrossRef]
39. Santangelo, M.; Marchesini, I.; Bucci, F.; Cardinali, M.; Cavalli, M.; Crema, S.; Marchi, L.; Alvioli, M.; Guzzetti, F. Exposure to Landslides in Rural Areas in Central Italy. *J. Maps* **2021**, *17*, 124–132. [CrossRef]
40. Zumpano, V.; Ardizzone, F.; Bucci, F.; Cardinali, M.; Fiorucci, F.; Parise, M.; Pisano, L.; Reichenbach, P.; Santaloia, F.; Santangelo, M.; et al. The Relation of Spatio-Temporal Distribution of Landslides to Urban Development (a Case Study from the Apulia Region, Southern Italy). *J. Maps* **2021**, *17*, 133–140. [CrossRef]

41. Aucelli, P.P.C.; Valente, E.; Di Paola, G.; Amato, V.; Cesarano, M.; Cozzolino, M.; Pappone, G.; Scorpio, V.; Rosskopf, C.M. The Influence of the Geological–Geomorphological Setting on Human Settlements and Historical Urban Development: The Case Study of Isernia (Southern Italy). *J. Maps* **2021**, *17*, 141–150. [CrossRef]
42. Forno, M.G.; Gianotti, F.; Sartori, G. Anthropogenic Morphological Modifications in Turin along the Po, Sangone and Dora Riparia Rivers (NW Italy). *Alp. Mediterr. Quat.* **2024**, *37*, 5–27. [CrossRef]
43. Luberti, G.M.; Vergari, F.; Marini, R.; Pica, A.; Del Monte, M. Anthropogenic Modifications to the Drainage Network of Rome (Italy): The Case Study of the Aqua Mariana. *Alp. Mediterr. Quat.* **2018**, *31*, 119–132. [CrossRef]
44. Sheppard, S. Chapter 7. Measuring and Modeling Global Urban Expansion. In *Global Urbanization*; Birch, E.L., Wachter, S.M., Eds.; University of Pennsylvania Press: Philadelphia, PA, USA, 2011; pp. 107–125. ISBN 978-0-8122-4284-3.
45. De Bellefon, M.-P.; Combes, P.-P.; Duranton, G.; Gobillon, L.; Gorin, C. Delineating Urban Areas Using Building Density. *J. Urban Econ.* **2021**, *125*, 103226. [CrossRef]
46. Acquaotta, F.; Faccini, F.; Fratianni, S.; Paliaga, G.; Sacchini, A. Rainfall Intensity in the Genoa Metropolitan Area: Secular Variations and Consequences. *Weather* **2018**, *73*, 356–362. [CrossRef]
47. Geoportale Regione Piemonte. Available online: https://geoportale.igr.piemonte.it/cms/ (accessed on 2 November 2024).
48. Festa, A.; Boano, P.; Irace, A.; Lucchesi, S.; Forno, M.G.; Dela Pierre, F.; TrenkWalder, S. *Foglio 156 "Torino Est" Della Carta Geologica d'Italia*; CINECA: Casalecchio di Reno, Italy, 2009.
49. Festa, A.; Boano, P.; Irace, A.; Lucchesi, S.; Forno, M.G.; Dela Pierre, F.; TrenkWalder, S. *Note Illustrative del Foglio 156 "Torino Est" della Carta Geologica d'Italia*; APAT—Agenzia per la Protezione dell'Ambiente e per i Servizi Tecnici—Dipartimento Difesa del Suolo: Roma, Italy, 2009; pp. 1–143.
50. Pieri, M.; Groppi, G. *Subsurface Geological Structure of the Po Plain, Italy*; Consiglio Nazionale delle Ricerche: Piazzale Aldo Moro, Roma, 1981; Volume 13.
51. Gelati, R.; Gnaccolini, M. Evoluzione Tettonico-Sedimentaria Della Zona Limite Tra Alpi Ed Ap-Pennino Tra l'inizio Dell'Oligocene Ed Il Miocene Medio. *Mem. Soc. Geol. Ital.* **1982**, *24*, 183–191.
52. Biella, G.C.; Polino, R.; De Franco, R.; Rossi, P.M.; Clari, P.A.; Corsi, A.; Gelati, R. The Crustal Structure of the Western Po Plain: Reconstruction from the Integrated Geological and Seismic Data. *Terra Nova* **1997**, *9*, 28–31. [CrossRef]
53. Ellison, R.A.; Booth, S.J.; Strange, P.J. Geological Mapping in Urban Areas—The BGS Experience in London. *Episodes* **1993**, *16*, 383–388. [CrossRef] [PubMed]
54. Perotti, L.; Lasagna, M.; Clemente, P.; Dino, G.A.; De Luca, D.A. Remote Sensing and Hydrogeological Methodologies for Irrigation Canal Water Losses Detection: The Naviglio di Bra Test Site (NW-Italy). In *Engineering Geology for Society and Territory—Volume 3*; Lollino, G., Arattano, M., Rinaldi, M., Giustolisi, O., Marechal, J.-C., Grant, G.E., Eds.; Springer International Publishing: Cham, Switzerland, 2015; pp. 19–22. ISBN 978-3-319-09053-5.
55. Terrone, M.; Piana, P.; Paliaga, G.; D'Orazi, M.; Faccini, F. Coupling Historical Maps and LiDAR Data to Identify Man-Made Landforms in Urban Areas. *ISPRS Int. J. Geo-Inf.* **2021**, *10*, 349. [CrossRef]
56. Noti, V. *GIS Open Source per Geologia e Ambiente Analisi Gestione di Dati Territoriali e Ambientali Con QGIS—II*; Editore, D.F., Ed.; Forme e tempi dell'urbanizzazione nella Cisalpina (II sec.a.C.-I sec.d.C.); Dario Flaccovio Editore: Palermo, Italy, 2021; ISBN 978-88-579-1377-3.
57. Museo Torino. Available online: https://www.museotorino.it/ (accessed on 1 September 2024).
58. Geodatabase Regione Piemonte. Available online: https://geomap.reteunitaria.piemonte.it/mapproxy/service?version=1.3.0 (accessed on 1 September 2024).
59. Geodatabase Città Metropolitana di Torino. Available online: https://www.geoportale.cittametropolitana.torino.it/geonetwork/cmto/ita/catalog.search#/home (accessed on 2 November 2024).
60. Gerbaudo, A.; Lozar, F.; Lasagna, M.; Tonon, M.D.; Egidio, E. For a Sustainable Future: A Survey about the 2030 Agenda among the Italian Geosciences Community. *Sustainability* **2023**, *15*, 11397. [CrossRef]
61. Brecciaroli Taborelli, L.; Gabucci, A. *Le Mura e Il Teatro di Augusta Taurinorum: Sequenze Stratigrafiche e Dati Cronologici*; Brecciaroli Taborelli, L., Ed.; Forme e tempi dell'urbanizzazione nella Cisalpina (II sec.a.C.-I sec.d.C.); Borgo S. Lorenzo: Florence, Italy, 2007; pp. 243–259.
62. Manzo, L.; Peirone, F. *La Città in Archivio: Storie di Torino dalle Origini alla Vigilia della Grande Guerra*; Archivio Storico: Torino, Italy, 2014; ISBN 978-88-908898-2-0.
63. Cavaglià, G. *Progetti Integrati D'Ambito a Torino: Complesso dei Murazzi del Po, via Giuseppe Garibaldi, Piazza Vittorio Veneto*; CELID: Torino, Italy, 2009; ISBN 978-88-7661-837-6.
64. UN-Habitat. *Urbanization and Development: Emerging Futures*; World Cities Report; UN-Habitat: Nairobi, Kenya, 2016; ISBN 978-92-1-132708-3.


**Disclaimer/Publisher's Note:** The statements, opinions and data contained in all publications are solely those of the individual author(s) and contributor(s) and not of MDPI and/or the editor(s). MDPI and/or the editor(s) disclaim responsibility for any injury to people or property resulting from any ideas, methods, instructions or products referred to in the content.

land

MDPI

*Article*

# Historicizing Natural Hazards and Human-Induced Landscape Transformation in a Tropical Mountainous Environment in Africa: Narratives from Elderly Citizens

**Violet Kanyiginya [1,2,3,*], Ronald Twongyirwe [3,4], David Mubiru [5], Caroline Michellier [1,6], Mercy Gloria Ashepet [1,7,8], Grace Kagoro-Rugunda [5], Matthieu Kervyn [2] and Olivier Dewitte [1,*]**

1 Department of Earth Sciences, Royal Museum for Central Africa, 3080 Tervuren, Belgium; caroline.michellier@africamuseum.be (C.M.); mercy.ashepet@africamuseum.be (M.G.A.)
2 Department of Geography, Vrije Universiteit Brussel, 1050 Brussels, Belgium; makervyn@vub.be
3 Department of Environment and Livelihoods Support Systems, Mbarara University of Science and Technology, Mbarara P.O. Box 1410, Uganda; rtwongyirwe@must.ac.ug
4 School of Agriculture, Policy and Development, University of Reading, Reading RG6 6BZ, UK
5 Department of Biology, Mbarara University of Science and Technology, Mbarara P.O. Box 1410, Uganda; davidmubiru26@gmail.com (D.M.); kgraceug2002@must.ac.ug (G.K.-R.)
6 Environmental Sciences, Earth and Life Institute, Université Catholique de Louvain, 1348 Ottignies-Louvain-la-Neuve, Belgium
7 Department of Biology, Royal Museum for Central Africa, 3080 Tervuren, Belgium
8 Division of Bioeconomics, Department of Earth and Environmental Sciences, Katholieke Universiteit Leuven, 3001 Leuven, Belgium
* Correspondence: kanyiga@gmail.com (V.K.); olivier.dewitte@africamuseum.be (O.D.); Tel.: +256-783-09-24-87 (V.K.)

Academic Editors: Fabio Luino, Mariano Barriendos Vallvé, Fabrizio Terenzio Gizzi, Ruediger Glaser, Christoph Gruetzner, Walter Palmieri, Sabina Porfido, Heather Sangster and Laura Turconi

Received: 3 December 2024
Revised: 22 January 2025
Accepted: 31 January 2025
Published: 8 February 2025

**Citation:** Kanyiginya, V.; Twongyirwe, R.; Mubiru, D.; Michellier, C.; Ashepet, M.G.; Kagoro-Rugunda, G.; Kervyn, M.; Dewitte, O. Historicizing Natural Hazards and Human-Induced Landscape Transformation in a Tropical Mountainous Environment in Africa: Narratives from Elderly Citizens. *Land* **2025**, *14*, 346. https://doi.org/10.3390/land14020346

**Copyright:** © 2025 by the authors. Licensee MDPI, Basel, Switzerland. This article is an open access article distributed under the terms and conditions of the Creative Commons Attribution (CC BY) license (https://creativecommons.org/licenses/by/4.0/).

**Abstract:** Studying natural hazards in the context of human-induced landscape transformation is complex, especially in regions with limited information. The narratives of the elderly can play a role in filling these knowledge gaps at the multi-decadal timescale. Here, we build upon a citizen-based elderly approach to understanding natural hazard patterns and landscape transformation in a tropical mountainous environment, the Kigezi Highlands (SW Uganda). We engaged 98 elderly citizens (>70 years old) living in eight small watersheds with different characteristics. Through interviews and focus group discussions, we reconstructed historical timelines and used participatory mapping to facilitate the interview process. We cross-checked the information of the elderly citizens with historical aerial photographs, archives, and field visits. Our results show that major land use/cover changes are associated with a high population increase over the last 80 years. We also evidence an increase in reported natural hazard events such as landslides and flash floods from the 1940s until the 1980s. Then, we notice a stabilization in the number of hazard events per decade, although the two most impacted decades (1980s and 2000s) stand out. Despite this new information, an increase in natural hazard frequency due to land use/cover change cannot yet be quantitatively validated, especially when the probable modulator effect of climate variability is considered. Nevertheless, the increase in the exposure of a vulnerable population to natural hazards is clear, and population growth together with poor landscape management practices are the key culprits that explain this evolution. This study demonstrates the added value of historical narratives in terms of understanding natural hazards in the context of environmental changes. This insight is essential for governments and non-governmental organizations for the development of policies and measures for disaster risk reduction that are grounded in the path dependence of local realities.

**Keywords:** geo-hydrological hazards; land use and land cover change; citizen science; historical narratives; participatory mapping; disaster risk; population growth; climate variability; Uganda

## 1. Introduction

The use of historical (multi-decadal) records of natural hazard events, including their types, mechanisms, causal factors, and incidence, is important for constraining the driving factors behind the evolution of risk in a region and devising appropriate disaster risk reduction measures [1–5]. For example, the scars of hazards, such as flash floods and landslides, are not permanent in a landscape, disappearing sometimes over short, month-to-year periods of time [6,7]. In other words, that a landscape currently does not show any recent evidence of a hazard does not mean that it cannot pose dangerous problems.

Although climate change is deemed to play a role in natural hazard occurrence [8], human-induced landscape transformations have been linked to an increase in the incidence of natural hazards [9–11]. For example, deforestation, urbanization, and road construction change the spatiotemporal distribution patterns of the occurrence of landslide and flood events [5,12–15]. These human disturbances of the landscape are particularly pronounced in the tropics, and are frequently associated with population growth, land needs, and agricultural expansion, e.g., [12,16,17]. In addition, an increase in settlements frequently pushes populations into hazard-prone areas, thereby increasing their exposure to natural hazards [18–20]. This exposure is expected to rise, especially in the tropical regions of the Global South, due to the projected population increases and weak management policies [14,21].

Understanding multi-decadal natural hazard patterns and landscape transformation is challenging, especially in data-scarce environments [22,23]. In such regions, data collection is impeded by inadequate resources, insufficient monitoring systems, and a lack of technical expertise for effective collection and analysis, often combined with difficult-to-access terrain [24,25]. Such hindrances preclude the proper trend analysis of natural hazards and understanding the environmental processes driving them [23,26]. Addressing the challenge of data collection requires multi-facetted approaches, involving participatory processes and remote sensing products to gain information on the historical patterns of natural hazard occurrences and the evolution of the landscape, e.g., [27–30].

Most studies of multi-decadal natural hazard occurrences and landscape transformation have been based on the analysis of historical aerial photographs, e.g., [31,32]. Historical aerial photographs are valuable sources of information as they provide some of the earliest records of land use/cover at a high spatial resolution of around 1 m [33]. For example, Luino et al. [34] analyzed historical maps to understand the impact of past natural hazards on various features, whereas Requelme et al. [33] analyzed historical archived photographs to understand past landforms. However, due to the limited number of photograph acquisition periods in many regions, historical aerial photographs often miss subtle details about the dynamics of the landscape [1]. Additionally, for the inventory of natural hazards, only relatively large-scale features such as large landslides can be identified in a reliable manner with these photographs [35].

Historical narratives about the evolution of the local environment reported by elderly citizens provide an opportunity to mitigate these historical data gaps in environments with limited information [36,37]. Because of their long interactions with the environment, elderly citizens have a rich knowledge of past hazards, and their understanding of historical landscape transformation is recognized as highly valuable. As Richardson et al. [38]

and Moezzi et al. [39] argue, narratives constructed from reliable participants such as elderly citizens are based on non-fictional events and thus provide credible insights in research. For instance, Nyssen et al. [27] applied the elderly citizen approach to reconstruct gully evolution in northern Ethiopia over several decades. Despite their importance in contributing to knowledge, the added value of the elderly citizens in understanding landscapes and past natural hazards has hitherto been overlooked [29].

Engaging elderly citizens through participatory approaches, such as participatory mapping, facilitates the structured narration of historical events, ensuring that their knowledge is shared in a coherent and systematic manner [40,41]. Participatory mapping is a collaborative process where community members actively engage in creating maps that reflect their local knowledge, experiences, and perceptions of their environment [28,41]. Researchers have used this approach to facilitate the understanding of environmental changes through the integration of local knowledge with scientific methods [42,43]. These methods allow for the visualization and spatial contextualization of historical events, enhancing the accuracy and depth of the narratives. Moreover, timelines have been shown to effectively aid in the reconstruction of historical events, particularly in overcoming the challenges associated with memory decay when recalling past occurrences [44]. Timelines, defined as visual representations of chronological events, have been successfully applied to reconstruct historical information across various domains. For instance, Hoffman et al. [45] applied timelines to examine historical environmental changes in the river systems of South Africa, while Bwambale et al. [46] used them to analyze the processes that shape indigenous knowledge regarding understanding flood risk in the Rwenzori region in Uganda. Moreover, Ben-Malek et al. [44] demonstrated that the temporal recall of past events heavily relies on reconstructive and inferential processes, where individuals draw upon their general knowledge of notable periods in their lives to place events in time.

The aim of our research is to document historical natural hazard patterns in relation to the human-induced transformation of the landscape in a data-scarce environment of Africa through the narratives of elderly citizens. More specifically, we focus on the Kigezi Highlands (southwestern Uganda), a mountainous region where problems associated with the occurrence of natural hazards are a growing concern [22,47,48]. This research also aims to assess the relevance of the elderly citizens' knowledge and experiences in terms of enriching the understanding of natural hazards and landscape characteristics. First, we focus on the implementation of the elderly citizen approach that is at the heart of this research. Then, we compile data on natural hazards and land transformation from the narratives of the elderly, complemented by secondary data sources and the interpretation of aerial photographs. We then analyze these patterns and discuss results with respect to disaster risk reduction, land management, and population dynamics.

## 2. Study Area

The Kigezi Highlands are part of the southwestern highlands of Uganda, bordering Rwanda to the south and the Democratic Republic of Congo to the west. More specifically, the study was conducted in eight relatively small watersheds (see Section 4) distributed throughout the three districts of Kabale, Rubanda, and Kisoro (Figure 1). The Kigezi Highlands experience rainfall during two wet seasons, March to May and September to November. The region received an average annual rainfall of 2500 mm between 2014 and 2020, as measured by the Kabale weather station [49]. The study area is one of the most densely populated regions in Uganda, with an average of 370 to 600 inhabitants per $km^2$ [50]. For many decades, the Kigezi Highlands have had an 'overpopulated' status, which is frequently cited as a primary cause of environmental degradation in the region [51]. The population consists mainly of smallholder

farmers, dependent on subsistence agriculture and livestock production. The vegetation cover, which was largely composed of montane forests many years ago [52], has been greatly modified due to human activities arising from an increasing population [52–54]. According to Nseka et al. [48], subsistence agricultural land has been increasing, at the expense of forests and woodlands. Recent research in the region shows an increase in reported impactful landslide and flood hazard occurrences [47,55] that have caused the loss of lives, displacement of people, and severe damage to property [56]. Anthropogenic processes most likely play preparatory roles in the occurrence of landslides and floods [12,47,57]. According to OPM [56], Kigezi is the most exposed region to natural hazards in Uganda, highlighting the urgent need for disaster risk reduction interventions. The study area consists of eight small watersheds (Figure 1) of rather similar sizes (3–8 $m^2$). The watersheds, however, possess different natural and human-related characteristics (Figure 2) such as land use/cover (e.g., the proportion of forest vs. agricultural land), lithology, topography, land management practices, and population density (see Section 4, Results).

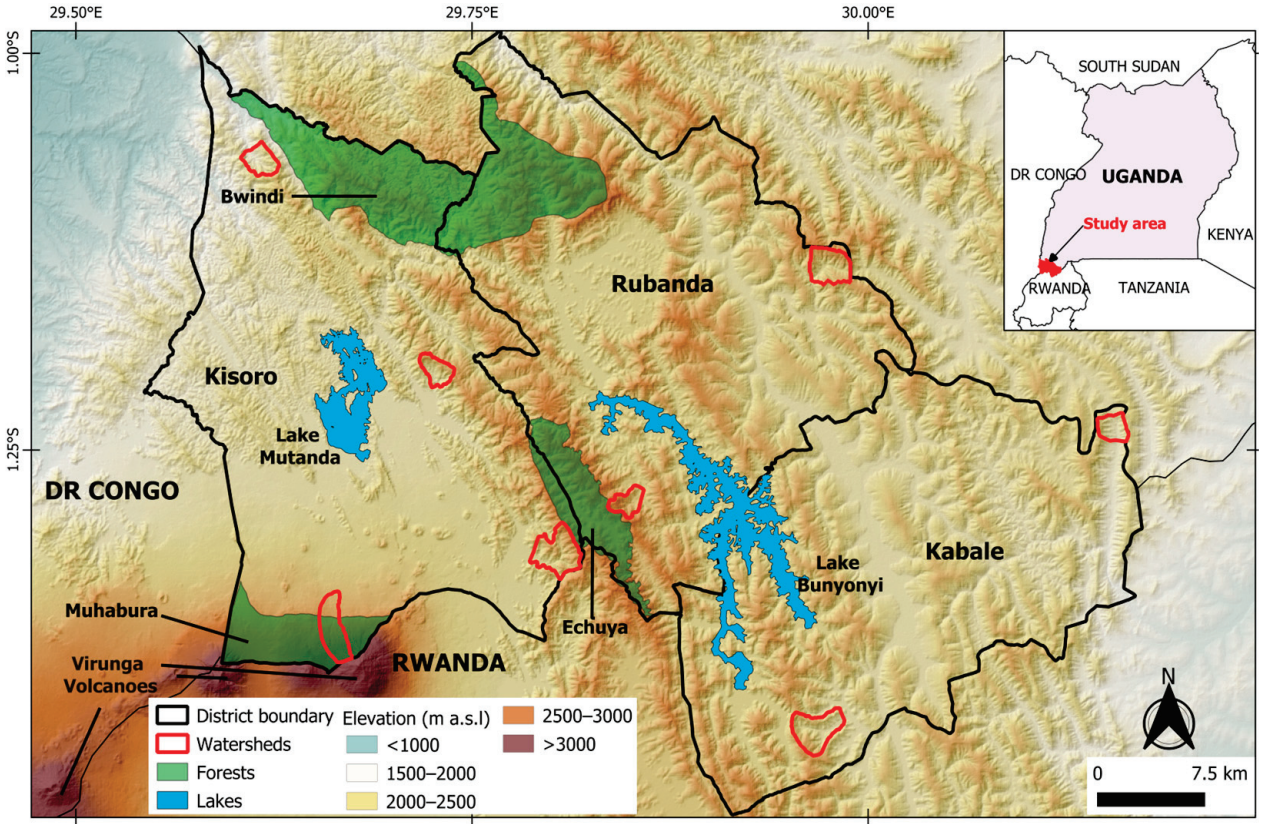



**Figure 1.** The location of the Kigezi Highlands comprising the Kabale, Rubanda, and Kisoro districts and the eight studied watersheds (W1 to W8). The forest cover data are from Google Earth imagery 2021. The map background is a shaded relief with elevation in color extracted from 1 arc sec SRTM DEM (https//lpdaac.usgs.gov/products/astgtmv003/, last access: 22 January 2022).




**Figure 2.** Field pictures of the eight watersheds (W1 to W8) illustrating dissimilar topographic and land use/cover characteristics. Photos taken by Violet Kanyiginya during fieldwork in September and October 2021.

## 3. Materials and Methods

### *3.1. Data Collection*

#### 3.1.1. Selection of the Study Participants

In this study, we engaged elderly citizens to gather their insightful narratives about past natural hazard events and landscape changes (Figure 3). This approach addresses the challenge of historical data scarcity, as elderly individuals often possess extensive knowledge and insights about historical landscape transformation due to their long-term interaction with the environment [36–38]. The elderly approach enables combining local knowledge with scientific knowledge, which is essential for the reliable and accurate monitoring of the environment [58].

To ensure the narratives provided a sufficient historical scope, participants were required to be at least 70 years old in order to enable coverage of periods corresponding to the acquisition of historical aerial photographs (see Section 4.3). Additional eligibility criteria included being a native of the watershed and possessing the ability to provide clear and detailed historical accounts of landscape events. We worked with community leaders who knew the community members well and were therefore our mobilisers and field guides. These included local chiefs, community-based officers, and geo-observers; the latter being a network of citizens trained in reporting natural hazard events and the associated impacts occurring in their communities [47]. To identify suitable elderly citizens, we integrated a snowball approach—a sampling technique suited for hard-to-reach or hidden populations [58]. The snowball sampling process begins with identifying a few participants who are part of the target population. These participants are then asked to refer other individuals they know who meet the study's criteria [58]. This approach was advantageous

in finding the targeted population given the difficulty of finding eloquent elderly citizens who could recall and ably narrate the historical aspects of their environment.

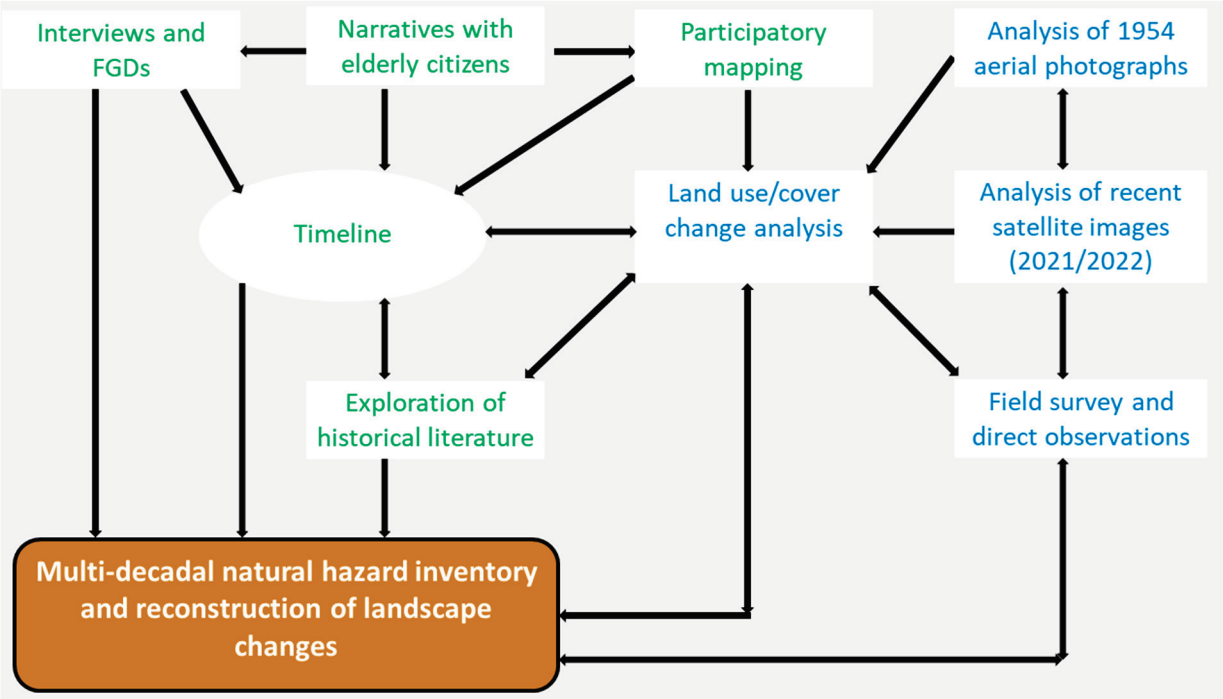



**Figure 3.** The methodological framework of the study illustrating how the multi-decadal inventory of natural hazards and landscape changes was achieved through a combination of historical narratives/approaches (in green text) and empirical methods (in blue text).

#### 3.1.2. Historical Narratives with the Elderly Citizens

We conducted interviews and focus group discussions (FGDs) with a total of 98 elderly citizens, of which 37% were women. Guiding questions (see Appendix A) were prepared and administered during the interviews and FGDs. We interviewed 24 elderly citizens in their homes, while 74 participants were engaged through FGDs. The house-to-house interviews allowed us to reach elderly citizens (mostly >80 years old) who were unable to move to the designated centers for FGDs. In addition to enabling triangulation [59], the FGDs allowed for the validation of information provided in individual interviews, thereby enhancing the reliability of the findings. As compared to individual interviews, FGDs offer the advantage that respondents complemented one another to remember and clearly describe past events. Further validation of the narratives of the elderly was carried out during field visits, where we observed features related to past hazard events. For example, boulders associated with flash flood or landslide events were examined in the field, and their age and time of appearance were confirmed with residents. All the interviews and FGDs were carried out in November 2021.

#### 3.1.3. Reconstructing of Key Events with a Timeline

To complement the interviews and FGDs, we constructed historical timelines and incorporated them into these discussions. This approach helped establish the actual years when natural hazards and key landscape changes took place, as narrated by elderly citizens (Appendix A.1). Using key political and social events as references in the timeline (e.g., presidential regimes: Elizabeth II (British colonial rule), Edward Mutesa II (first Ugandan president), Obote I, Obote II, Idi Amin, and Museveni), we asked the elderly what the landscape looked like in different past periods, i.e., the type of vegetation/tree cover,

housing characteristics, roads, the types of crops grown, land management practices, and the associated policies that existed as well as any natural hazards that occurred. The narratives provided by the elderly highlighted key changes occurring between the colonial (pre-1962) and post-colonial (post-1962, i.e., 1962–2021) eras. Therefore, the timing of key events was analyzed in relation to these two distinct periods to better contextualize the transformations. The interview and FGD sessions were recorded and transcribed with the consent of the participants, and key thematic areas were extracted for further exploration and analysis.

#### 3.1.4. Participatory Mapping and Spatial Reference of Events

For the eight FGDs, we applied the participatory mapping technique, where the elderly drew on manila papers the past (i.e., from the 1940s) and current (2021) land use/cover of their land (Figure 4). The mapping was guided by providing the exact delineation of the watershed boundaries as background information. The elderly citizens indicated (1) the locations and numbers of buildings and roads, and (2) the extent of croplands, tree cover, wetlands, and water bodies. Colored markers were used to distinguish between past and present land use/cover (Figure 4).




**Figure 4.** Interviews and participatory mapping with the elderly citizens. (**a**) One of the maps drawn by the elderly citizens during an FGD in W6, showing past (blue marker) and current (red marker) land use and cover. (**b**,**c**) Participatory mapping during FGDs with elderly citizens in W2 and W5, respectively. (**d**) An individual interview session with an elderly citizen in W8. Photos taken by David Mubiru in September 2022.

#### 3.1.5. Field Assessment of the Extent of Human Activities

To better understand the extent of land transformation by human activities, we conducted a rapid assessment of the level of human disturbance in each watershed through direct observations in the field. Based on the methodology by [60], we assessed parameters including:

- Vegetation characteristics: the density and type of vegetation, such as native species versus invasive plants;
- Land use: the size and distribution of agricultural fields, settlements, commercial areas, and road infrastructure;
- Signs of soil erosion: evidence of erosion along riverbanks or hillsides and sediment deposits in lower areas;
- Water quality: water clarity and the presence of debris or foam in rivers.

We employed a scoring system ranging from 0 to 5 to evaluate the parameters of human disturbance, where 0 = no disturbance; 1 = very low disturbance; 2 = low disturbance; 3 = moderate disturbance; 4 = high disturbance, and 5 = very high disturbance. This systematic approach enabled us to classify the overall level of human disturbance within each watershed into three categories: low, moderate, or high (see Section 4).

### *3.2. Secondary Data Sources*

Historical data sources include documentary archives and literature with information of considerable value in terms of establishing the characteristics of landscape processes [61]. These historical records also played a crucial role in validating the narratives provided by elderly citizens. We used keywords such as 'history', 'land use', 'colonial policies', and 'disasters', which we combined with 'Kigezi' to search the scientific literature in the Web of Science and Google Scholar. We also explored historical books and the other past literature and archives such as 'Old Maps online'. Some of this literature was obtained during our interactions with the elderly interview participants. Of relevance was the 'Kigezi n'Abantu Baamwo' (Kigezi and its people) book by [62], which details the historical evolution of the people of Kigezi, including land use and management practices, economic activities, population trends, and migration dynamics. Additionally, other historical research publications about Kigezi, such as [51,63,64], provided valuable insights.

### *3.3. Land Use/Cover Change Analysis with Historical Panchromatic Aerial Photographs and Satellite Images*

To examine historical changes in land use/cover, we analyzed panchromatic aerial photographs from 1954 at a scale of ~1/40,000 and recent (2021/2022) satellite imagery available on Google Earth for a comparative understanding of landscape transformations over time. The historical aerial photos were acquired from the Department of survey and mapping of Uganda in Entebbe in digital format, scanned by a Ricoh MP500 at a 600 dpi resolution. The photographs were empirically analyzed in stereoscopy, then the georeferenced images were used to manually digitize land use/cover classes including forest/tree cover, settlements, agricultural terraces, wetlands, and roads. We focused on mapping agricultural terraces, as this represents an important land use practice that is easily identifiable in aerial photographs. In contrast, cropland and grassland often lack distinct visual markers, making them challenging to differentiate with certainty. The same classes were digitized from Google Earth satellite imagery. This analysis not only highlighted land use/cover changes over time but also served to validate the narratives provided by the elderly citizens. The general methodological framework is shown in Figure 3.

## 4. Results

From the elderly citizens' narratives, we generated a record of natural hazards that occurred since the 1940s. We recorded 73 natural hazard occurrences (landslides and flash floods) for the period between 1940 and 2021. We also analyzed landscape change dynamics for the same period using historical narratives from the elderly citizens, aerial photographs from 1954, and the available historical literature about the Kigezi region.

### *4.1. Watershed Characteristics*

The eight watersheds exhibit diverse characteristics that highlight the distinct variations in their environmental profiles (Table 1). The variations include differences in size, reflecting the spatial extent of each watershed; land use/cover, which provide insights into the dominant vegetation, agricultural activities, and urban development within the watersheds; and topography. Additionally, the watersheds differ in terms of lithology, the level of human disturbance, and the type of frequent natural hazards experienced in each watershed.

**Table 1.** The characteristics of the eight watersheds. Lithology information is from the geological map of Uganda [65]. Information on frequent natural hazards is from the elderly citizens.

| Watershed | Size ($km^2$) | Land Use/Cover | Average Slope (%) | Lithology | Level of Human Disturbance | Frequent Natural Hazards |
|---|---|---|---|---|---|---|
| W1 | 3.5 | Forest, shrubs, crops (millet, tea, sweet potatoes, beans). Settlements on hilltops and upper slopes | 48 | Mudstone, shale, slate, phyllite | Low | Landslides |
| W2 | 4.5 | Eucalyptus, crops (maize, potatoes, beans), agricultural terraces, drained wetland | 42 | Mudstone, shale, slate, phyllite, sandstone, quartzite, grit | Moderate | Landslides, flash floods |
| W3 | 7.2 | Eucalyptus, crops (beans, maize, sweet potatoes), agricultural terraces, drained wetland | 49 | Mudstone, shale, slate, phyllite | Moderate | Landslides, flash floods |
| W4 | 6.7 | Forest, eucalyptus, crops (potatoes, climbing beans, maize), ridges | 34 | Leucite, basanite | Moderate | Flash floods |
| W5 | 8.2 | Eucalyptus, crops (potatoes, climbing beans), rock outcrops on upper slopes, wetland under cultivation | 47 | Mudstone, shale, slate, phyllite, sandstone, quartzite, grit | High | Flash floods |
| W6 | 3.2 | Eucalyptus, crops (climbing beans, potatoes, maize), agricultural terraces, gullies | 40 | Mudstone, shale, slate, phyllite, sandstone, quartzite, grit | High | Floods |
| W7 | 3.5 | Eucalyptus, pine, grassland on hilltops. Settlements mainly in the valley, crops (banana, sorghum, peas) | 39 | Mudstone, shale, slate, phyllite, sandstone, quartzite, grit | Low | Landslides, flash floods |
| W8 | 7.2 | Eucalyptus, crops (sorghum, beans, maize), agricultural terraces, gullies, numerous gravel roads, drained wetland | 39 | Mudstone, shale, slate, phyllite | High | Landslides, flash floods |

### *4.2. The Characterization of Watersheds During the Colonial Era (1940–1962)*

From the narrations of the elderly citizens, we obtained historical information from as early as 1940. In a few cases, the elderly narrated events that they were told by their parents, thus delving into the 1930s. However, such narrations from before the 1940s were considered to be less reliable and were therefore not considered in our analysis. The information obtained since the 1940s comprised themes on land use/cover; management practices; land management laws and policies enforced; population and housing characteristics; road development; degradation activities, such as deforestation and wetland drainage; restoration programs; and natural hazard occurrences. Examples of quotes from the elderly narratives are provided in Appendix A.2.

#### 4.2.1. Land Use/Cover

When referring to their childhood (1940–1950s), the elderly citizens described the landscape as hills covered with different natural tree species such as Ficus, shrubs, and short grass, especially Hyperemia ruffa (emburara in the Runyankole–Rukiga dialect), which were inhabited by wild animals such as wild pigs, foxes, and leopards. In watersheds adjacent to national parks, elephants and buffaloes were also regularly present. Our analysis of the 1954 aerial photographs and participatory mapping with the elderly citizens shows that settlements were in the mid-lower slopes of the hills since most valleys were covered with large papyrus swamps and the hill tops were forested. In some watersheds, such as W5, W6, W7, the upper slopes and hilltops were used for cultivation and grazing, and much livestock was kept since grazing land was widely available.

#### 4.2.2. Land Use and Management Practices

Reports from the elderly show that, during the colonial period, land was freely acquired and the boundaries for land ownership were dependent on the family labor force and strength, i.e., as far as one could cultivate determined the boundary of their land. The elderly citizens reported that the main crops grown in the area included sorghum, maize, beans, millet, peas, sweet potatoes, and indigenous potatoes. These crops were notably resilient and could therefore be cultivated throughout the year. The elderly citizens also shared that farming was minimal due to the abundance of land, with cultivation primarily focused on subsistence food production. At that time, money was not a concept familiar to the community, and there were no markets for buying or selling food involving money. The elderly vividly recalled that barter trade was the sole method of exchange, where people traded food for other goods or services, as required.

Despite the low-intensity farming practices, the elderly indicated that food was abundant for the relatively small population, and there were established regulations regarding food storage. Regarding land management, the elderly recounted that the colonial administrators enforced strict fallowing practices, known locally as Hinga raza, along with the use of contours or strip cropping stabilized by elephant grass (locally known as katikankingo in the Runyankole–Rukiga dialect). Fallowing required farmers to divide their land into three plots, with one plot always left under fallow in rotation each season. The elderly citizens also emphasized that colonial administrators, through local chiefs, enforced laws to protect the vegetation cover. For instance, bush burning and tree cutting were strictly prohibited and punishable by law. It was also mandatory for every household to plant 18 black wattle trees on hilltops. Other tree species such as eucalyptus and pine were not allowed on the land. According to the elderly respondents, the black wattle tree species helped to prevent soil erosion, landslides, and flash floods. The elderly citizens believe that these regulations played a crucial role in protecting the land from soil erosion, preventing natural hazards, and enhancing soil fertility.

#### 4.2.3. Hydrology

According to the elderly citizens, the lowlands in some watersheds, such as W3, W7 and W8, were covered by wetlands, and no permanent river existed. In W3 and W8, the wetlands in the valley were drained through a channel to create the river during road construction in 1971 (post-colonial period). The river in W7 was formed in 1959 but the elderly residents have different beliefs on how it happened. Some believe that an aquifer was compromised during borehole construction which produced the river, others believe it emerged from the drainage of a wetland in the valley. In all aspects, the residents are happy with the river today as it helps to provide water for animals and domestic use. According to the elderly in W6, a narrow river existed in the 1950s and traversed through the watershed, but it has recently widened and silted because of flash floods.

#### 4.2.4. Natural Hazards

According to the elderly citizens, natural hazards were experienced in some watersheds as early as 1945 (Figure 5). However, they noted that these events did not cause severe damage, and their frequency was low at the time. For example, in W8 a large event involving the co-occurrence of landslides and flash floods happened in April 1945, but it did not cause human or property losses since it affected locations that were not inhabited. Despite the low population in the past, the elderly citizens reported that landslides frequently occurred in W8 during the colonial period. One village in W8, for instance, was named after landslides: Nyamutenguzi (literally meaning 'the sliding land' in the Runyankole–Rukiga dialect) a name that has remained to date. According to the elderly citizens, residents always relocated from Nyamutenguzi during the rainy season for fear of landslides. Similarly, the elderly in W5 reported the occurrence of landslides in the 1950s, which led people to avoid living on steep slopes for fear of these hazards. However, the elderly confirmed that flooding never existed before 1962, when the wetland was still in existence in W5. In addition, the elderly in W5 indicated that there were natural waterways which effectively drained the watershed during periods of excess water. They asserted that a desilting schedule existed in the community to maintain the channels, which prevented floods. The desilting practice was, however, abandoned after colonial rule in 1962, leading to the channels becoming silted and flooding starting to occur, as reported by the elderly citizens. The elderly acknowledged that the frequency of flooding worsened in the 1980s when the wetland was completely drained for cultivation and settlements. Today, the watershed experiences severe flooding every rainy season. In contrast, other watersheds like W1, W2, and W3 did not experience natural hazards during the colonial period (Figure 5).

As reported by the elderly, watersheds did not have gullies, which are associated with flash floods, until the 1980s when the first gully formed in W6. Gullies that were large enough to create a hazard began to appear in other watersheds during the 1990s and early 2000s.

#### 4.2.5. The Temporal Trend in Reported Natural Hazards in Relation to the Ages of the Elderly

According to the elderly citizens, the number of natural hazards increased significantly from the 1940s to the 1980s, and quite high frequencies continued to be observed in the following decades (Figure 6). The elderly citizens attribute the increase in the natural hazard occurrences to various factors. For instance, W4 suffered from severe flash floods, including fatalities, which the elderly believe were caused by the deforestation of the Muhabura forest before the 1960s. Similarly, they attribute the landslides experienced in W1 after the colonial period to the deforestation that took place between 1960 and 1980. During our field observations, we noted large boulders scattered throughout the watershed, reportedly carried by flash floods more than 20 years ago (as recounted by the elderly).

These boulders vividly demonstrate the intensity of the past flash floods. As attested by the elderly residents, protecting the forest from further human activities not only saved it from extinction but also reduced the frequency of severe fatal disasters.

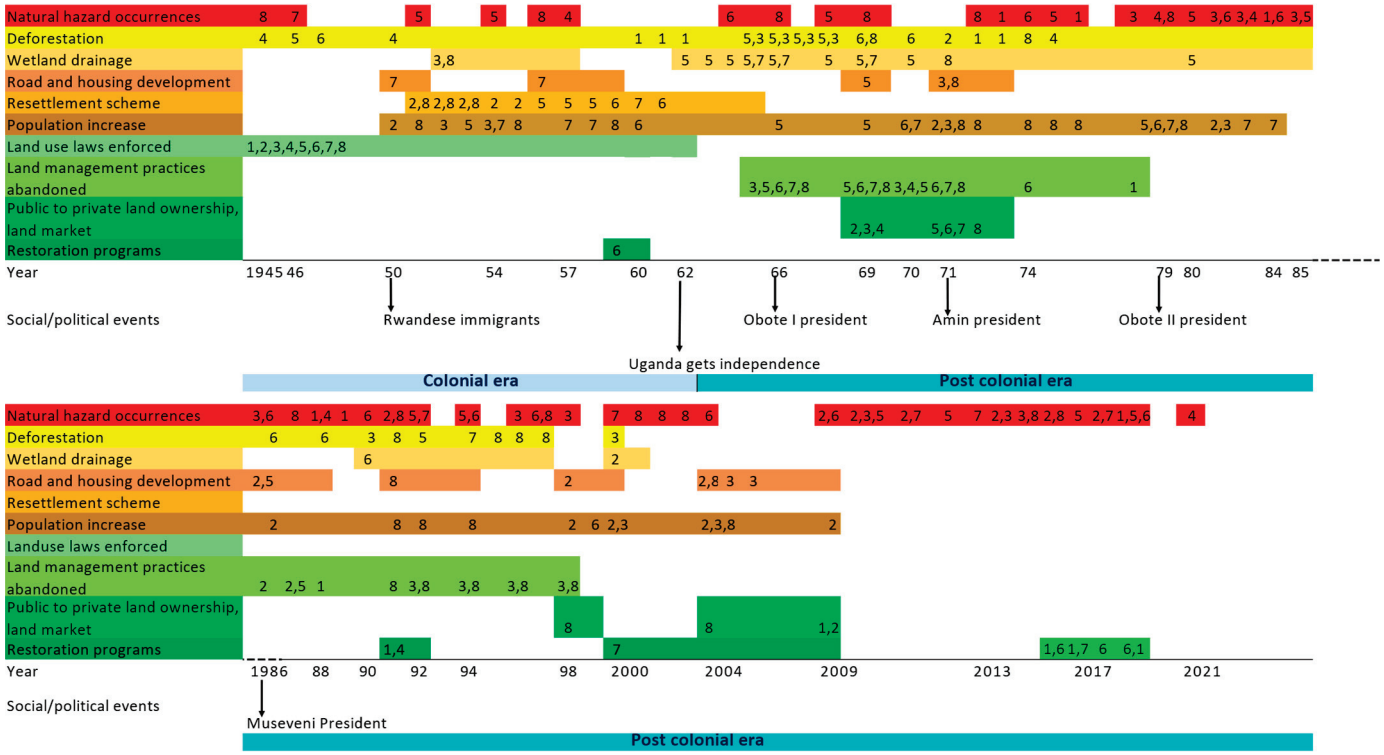



**Figure 5.** Timeline of events constructed from elderly interviews. The numbers represent watersheds where a particular event happened. "Natural hazard occurrences" includes landslides, floods, and gullies associated with flash flood events. "Deforestation" includes natural tree species that were cut down. "Wetland drainage" refers to the reclamation of wetlands for agricultural and construction purposes. "Road and housing development" includes the roads that were constructed and a change from grass-thatched to iron-roofed houses. "Resettlement schemes" are the measures implemented to depopulate the region. "Population increase" includes the increase in the numbers of both people and livestock, land shortages, and overcultivation. "Land laws enforced" includes the land management regulations that were followed during the colonial period. "Land management practices abandoned" includes the end of practices such as fallowing, the planting of native tree species, contour strip cropping, the avoidance of bush burning, and stabilizing contours with elephant grass. "Public land to private land ownership" refers to the time when land titling began to be given to individual owners and the rights of buying and selling land were established. "Restoration programmes" includes initiatives that have been implemented to rehabilitate the degraded landscapes like afforestation, diversion channels, and the creation of forest buffer zones.

Our analysis of the trend in reported hazards in relation to participant ages (Figure 6), shows that few or no hazards were reported for periods when the participants were younger (e.g., the 1940s). In contrast, more hazard reports concentrate in periods when the participants were middle-aged or older (typically 30 years and above). Notably, the 1980s show a high number of events and this coincides with a period when the median age of the elderly participants was 39, an age where they likely recall significant environmental changes [66].

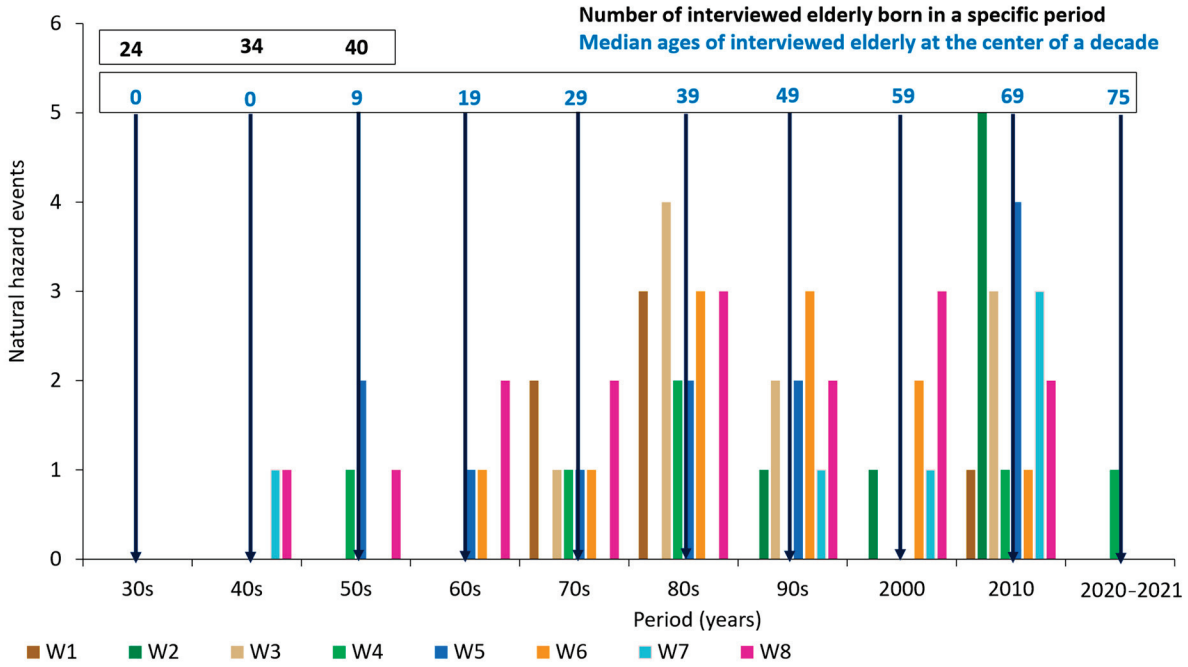



**Figure 6.** The temporal trend in natural hazard events recorded for each decade as per the elderly citizens between 1940 and 2010 and the corresponding median ages of the participants calculated for the middle of each decade. Note that the column for 2020 corresponds to only 2020 and 2021.

### *4.3. Catchment Characteristics in the Post-Colonial Era (1962–2021)*

Narrations from the elderly citizens indicate that major changes took place in policies, land management, and farming systems after independence in 1962 (Figure 5 and Appendix A.3). For instance, land ownership changed from public to private ownership and people were free to use their land in the way they wished. This period also saw a rise in the buying and selling of land, a practice that was uncommon before independence. The elderly reported that the land management practices and laws, which had been strictly enforced by the colonial government, were gradually abandoned, as shown in the timeline (Figure 5). These changes led to poor management practices on the land, according to the elderly citizens. For instance, there was an increase in the removal of vegetation cover through tree cutting and bush burning, including the cutting of natural tree species and black wattle for charcoal and timber. This deforestation intensified in 1971 during Idi Amin's regime. According to the elderly, this is the period when markets were opened and the trading of different commodities such as food, livestock, construction materials, and charcoal increased. Moreover, the population had increased and therefore the demand for construction materials and fuel energy was high. The elderly also reported that, after 1980, eucalyptus trees increasingly replaced native tree species, and by 2000, most landscapes had been planted with eucalyptus, leaving no traces of black wattle or other native species. The elderly further narrate that after independence, traditional practices such as fallowing and contour plowing were abandoned (Figure 5). Instead, people began cultivating land up and down the hills without contouring, and this was carried out year round. They also observed that, starting from the 1970s, both the human population and livestock numbers increased significantly (Figure 5). This led to overcultivation, characterized by excessive tillage, a reduction in grazing areas, and the draining of wetlands for farming and settlements. Additionally, the elderly pointed out that after the 1970s, with the emergence of a growing market economy, people began to recognize the value of money and began growing food for sale. This practice further contributed to overcultivation.

The elderly citizens also recall that after independence, new crop varieties were introduced to increase productivity. For example, a potato variety more suitable for growing in lowlands was introduced, which led to the further drainage of wetlands to accommodate its cultivation. Unlike the indigenous potato, this new variety required the extensive use of chemicals. From the 1980s through the 1990s, the construction of new roads accelerated, often cutting through hills and draining wetlands to improve access for the growing population. The elderly also noted changes in housing during this period, with traditional grass-thatched houses gradually being replaced by iron-roofed structures in the 1980s.

### *4.4. Land Use/Cover Change Analysis with the 1954 Aerial Panchromatic Photographs*

Major changes in land use/cover occurred between 1954 and 2021 (Figures 7c, 8 and 9). As explained by the elderly, forests existed on hilltops and the upper slopes of most watersheds in 1954. However, this is no longer the case for most of the watersheds in 2021. For W3, W7, and W8, forests existed in 1954 mainly along steep ridges on slopes, whereas the hilltops were covered with short grass. Generally, watersheds adjacent to large, forested areas like W1, W4, W5, and W6 experienced extensive deforestation before 1990. This occurred because there were no boundaries separating the forest from the community, and these areas had not yet been designated as National Parks with restricted access (Figures 7c and 8) [53]. The analysis further shows that W2 and W3 experienced deforestation as well. However, W8 did not show major changes in forest cover (Figures 7c and 8). Whereas deforestation in W1 commenced from 1954, the results suggest that the deforestation in W4, W5, and W6 was conducted well before 1954 (Appendix B). This is confirmed by [67] who showed that the heavy exploitation of Muhabura forest (adjacent to W4) for cultivation and grazing took place in the 1940s. The exploitation of the forest in W4 is also confirmed in the analysis of the 1954 landcover map, where terraces and cultivated fields are shown extending into the forest (Figure 9).

The land use and cover change analysis reveals a significant increase in the area covered by settlements across all watersheds (Figures 8 and 9). The most notable increase occurred in W5, where the area covered by settlements grew from 0.5% in 1954 to 22% in 2021. The analysis also shows that, with the exception of W7, settlements in most watersheds have extended to upper slopes, a shift from 1954 when settlements were primarily located on lower slopes or in valleys. The elderly citizens recall that in the past housing consisted of scattered grass-thatched huts locally known as kateteyi (dress-shaped). These huts were progressively replaced by iron-sheet roofs during the 1970s and 1980s as the population expanded.

The total road length increased from 29 km in 1954 to 66 km in 2021 (Figures 8 and 9). Increases in areas covered by agricultural terraces are noted in W2 and W5, by 75% and 61%, respectively, while a reduction was experienced in W4 and W8 (Figures 8 and 9). The other watersheds did not show major changes in terraced land coverage (Figures 8 and 9). Our field observations also revealed that many of the existing terraces were established during the colonial period and have not been maintained since then, leading to their collapse over time.

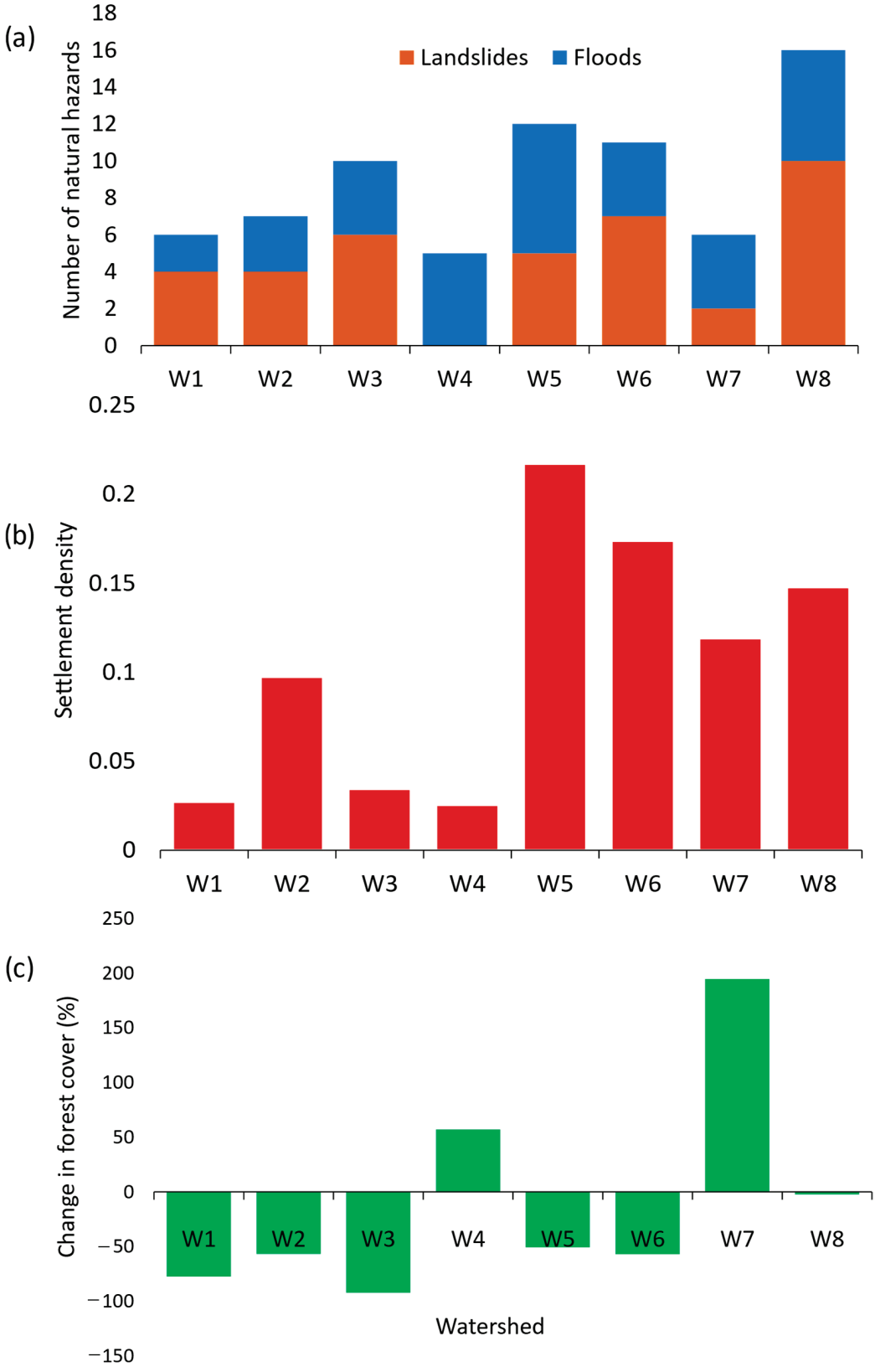



**Figure 7.** (**a**) Landslide and flash flood events recorded as per the elderly respondents from 1940 to 2021. (**b**) The watershed settlement density for 2021 expressed as a ratio of the total area covered by settlements and the total area of the watershed (the settlement area was manually extracted from Google Earth imagery 2021). (**c**) The percentage forest cover change between 1954 (historical aerial photographs) and 2021 (Google Earth). Positive values indicate an increase in forest cover since 1954, while negative values represent a decline in forest cover between 1954 and 2021.

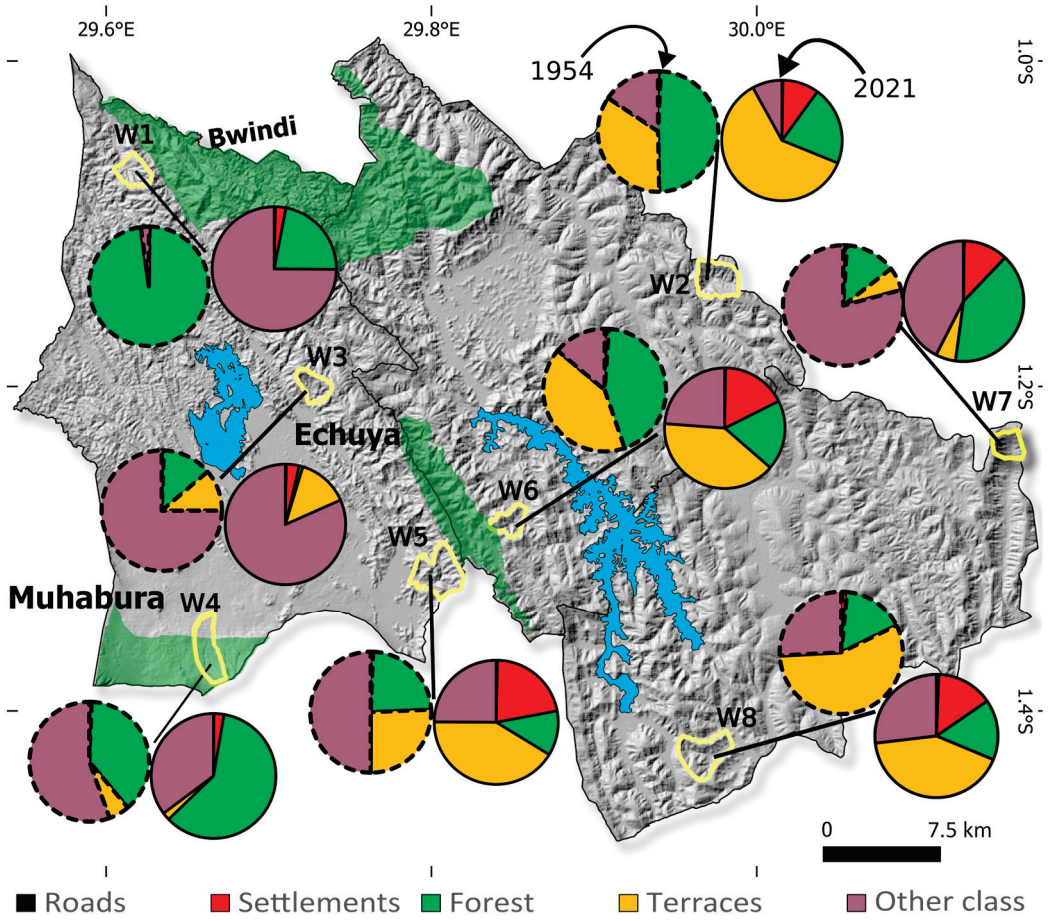



**Figure 8.** The proportions of different land use/cover classes for 1954 (circles with a black stippled line) and 2021 (circles with a black contour) in each watershed (yellow polygons) as mapped manually on the 1954 aerial photographs and 2021 Google Earth imagery. The 'other' class represents unterraced croplands, wetlands, and other mixed land uses. The map background is a shaded relief with elevations in color extracted from 1 arc sec SRTM DEM (USGS, 2021).

### *4.5. Population Dynamics*

The overall national population of Uganda has grown from two million people in 1911 to 46 million people in 2024, with an average population density of 224 people per square kilometer [50]. For the Kigezi region, based on the delineation of the areas covered by settlements on Google Earth imagery, we see that the highest settlement density is in W5, followed by W6 and W8, with settlement proportions of 22%, 17%, and 15%, respectively (Figure 7b). According to the elderly citizens, the population in all the watersheds was low and sparsely distributed in the 40s, ranging between 6 and 15 households in each watershed. This is confirmed from the 1954 historical land use/cover analysis (Figures 8 and 9). Early researchers reported a rapidly increasing population density in the 50s which put pressure on the land. In his book, 'Kigezi and its people' [62], Ngologoza describes the dilemma of the increasing population density in Kigezi with associated effects of conflicts and competition over land, which necessitated the colonial administrators to establish a resettlement scheme to relocate people to other regions in Uganda. The first resettlement was executed in 1957 where people were resettled from Kigezi to other districts in Uganda. According to the elderly, the resettlement scheme continued in Kigezi in the 60s and after the colonial period.

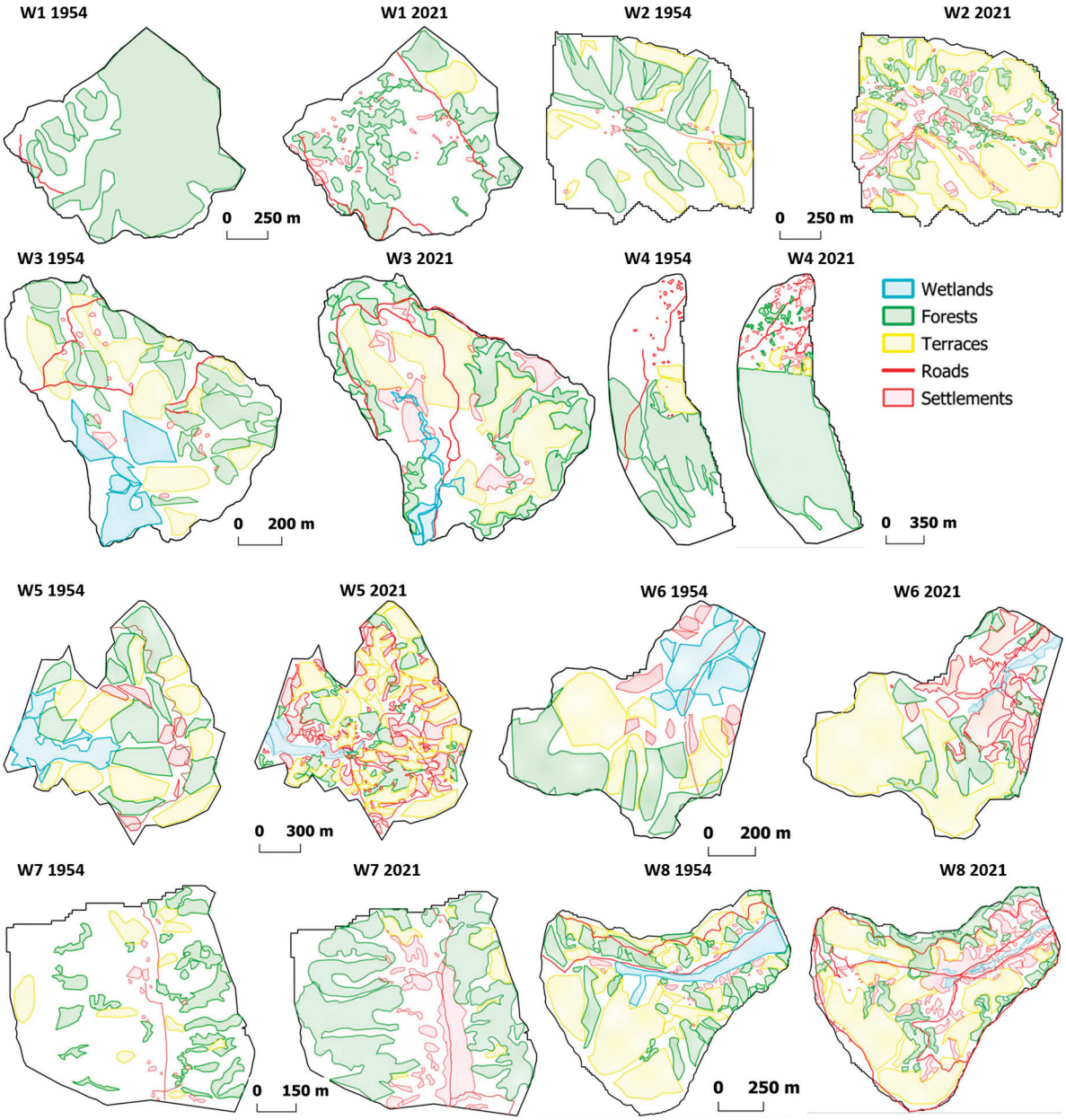



**Figure 9.** Land use/cover maps of the eight watersheds for 1954 and 2021. The empty spaces encompass other unmapped land uses such as unterraced croplands, grasslands, and all mixed land uses.

### *4.6. Restoration Programs and Natural Hazards*

We note that there is a forest cover increase in some watersheds such as W4 and W7. According to the elderly narratives in W4, Muhabura forest was inhabited by the community residents who carried out their farming activities in the forest until 1991 when they were evicted by the government, and the forest designated as a protected area. The demarcation and establishment of buffer zones for the forests significantly restored the lost forest cover in W4, which is noted in our results, i.e., from 38% in 1954 to 60% in 2021 (Figures 7c and 8). This forest increase was noted within the forest park and surrounding communities (Appendix A). A forest cover increase was also shown in W7 from 14% in 1954 to 40% in 2021 (Figures 7c and 8). According to the elderly in W7, this increase is attributed to restoration programs introduced in the watershed by NGO programs from 2000, which is confirmed in the Google Earth imagery. The elderly reported that afforestation programs

in W7 were carried out from 2000 on one side of the watershed where eucalyptus and pine trees were grown and resulted in increased tree cover. The elderly testimonies suggest that natural hazards have been controlled by the increased tree cover in this watershed. Our field observations indicate that restoration programs have been implemented in some watersheds, and they include afforestation and soil and water conservation programs. For instance, during our interactions with the elderly, we learnt that in W1 there are initiatives to plant indigenous tree species to replace those that were cut down long ago. In W6 and W7, NGOs and government programs installed soil and water conservation programs including water diversions; the planting of pine, eucalyptus, and grevilia trees; the implementation of mulching; and fanya chini trenches (trenches and earthen ridges facing downslope). According to the elderly, these practices, if adopted by all residents, could help in reducing incidences of natural hazards.

## 5. Discussion

### *5.1. The Added Value and Limitations of the Elderly Approach—Can the Information Be Trusted?*

Analysis of the aerial photographs from 1954 for the region and the historical literature validate the elderly citizens' narratives, confirming the reliability of the information collected on the region's landscape dynamics. This shows that elderly citizen-based approaches relying on their lived experience can be a reliable way to retrieve historical information. A detailed inventory of natural hazards in the Kigezi region was compiled from global databases and archives by [47]. When comparing this inventory with the data we gathered from the elderly citizens for the same period and locations, i.e., the eight watersheds, we found only 12 events recorded in the existing global databases. This inconsistency clearly highlights the added value of using the elderly approach in documenting natural hazards. While other researchers have recognized the importance of documentary historical records and archives in recording natural hazards and reconstructing the historical landscapes [1], such records are often lacking in both quantity and quality, particularly in data-scarce regions [68,69].

Obtaining historical narratives of environmental changes offers several advantages, including increasing the understanding of the dynamic nature of landscapes [68]. Records of past natural hazards not mentioned in other inventories might also contribute to improved risk assessments and a better understanding of potential future hazard events [70]. However, most current databases do not provide records for events that occurred many decades ago. For instance, the DesInventar database, which has the largest quantity of data for the Kigezi region, contains records from 1989 at the earliest [71]. In addition, historical trends in land use and land cover were not easily available before the start of satellite missions [34,72]. These efforts become even more difficult when historical aerial photography is required because such records are not always easy to find [1,73]. Consequently, elderly citizens could help to fill in this information gap. Natural hazard records from the elderly are often accurate at a spatial scale, as they typically provide the exact locations where events occurred. This positive attribute has been recognized in various studies using the citizen science approach; e.g., [74–76]. When reconstructing past land use/cover, the elderly articulate much landscape-related information that cannot be found in satellite images or aerial photographs. For instance, we gathered information on the farming systems, land management practices, types of vegetation that existed, and the regulations that governed land use. As demonstrated by [46], this comprehensive information offers a deeper understanding of natural hazard processes and mechanisms, which is crucial for effective disaster risk reduction.

While the elderly approach was valuable in creating an account of natural hazards and the historical landscape, there are limitations associated with the approach. First, the

recollections of the elderly are incomplete in terms of the exact timing of events. Even if the timeline assisted in memory recall, there were still challenges in obtaining the exact date of an event. In some cases, statements like 'the event happened during that regime' were experienced, leading to inaccuracy regarding the time of occurrence. In comparison, Jack et al. [77] demonstrated that children and adolescents tend to be less accurate in recalling past events compared to adults. In Friedman et al. [78], it was revealed that memory accuracy for past events improves with age, indicating that older adults often provide more precise accounts of historical events due to their broader life experience and more developed cognitive recall abilities. This suggests that elderly participants have clearer memories of hazards from the periods when they were most actively engaged with their environment or when their memory capacities were active, than when they were younger with limited early memories. However, research has also shown that information from the elderly is often limited by memory decay, as memories can fade or become distorted over time, leading to inaccuracies in recalled events [79]. The apparent trend of reported hazard events shown in Figure 6 may therefore be influenced by the age and memory capacity of elderly participants. Spatial biases also exist in the data collected because the elderly primarily recall events that occurred in their areas of residence [80]. Consequently, the information provided is highly context- and place-specific, necessitating caution when extrapolating these insights to broader scales. Such biases can lead to the underreporting of events in less populated or uninhabited areas, potentially skewing the data. As a result, it may seem that natural hazards are more frequent in densely populated areas, when in fact this could simply be due to higher rates of recollection and reporting in these regions. Regarding documenting natural hazards, biases exist in recording only large and impactful events [55,81,82]. The elderly tend to recall events that caused severe impacts or fatalities, while less impactful events are often overlooked. As noted by Flicker et al. [36], it is natural for people to remember events with a significant impact, while omitting or forgetting those of lower magnitude, which can result in incomplete historical records. The inventorying of low magnitude and frequent events is important in building a reliable hazard susceptibility assessment [83]. Similar biases in citizen science data have been reported by other authors, including Sekajugo et al. [76], Arazy et al. [81] and Foody et al. [84]. Another limitation is that the information provided by the elderly citizens is often limited in terms of the process understanding of the events, hence causal relationships are inferred from personal perceptions, cultural beliefs, and social contexts [36,85].

With such discrepancies and biases in mind, the information provided by the elderly, although valuable, must be carefully analyzed and complemented with other methods to ensure reliability. This complementarity between the narratives of the elderly and empirical methods has been effectively applied by researchers such as Nyssen et al. [27] and Solecka et al. [29]. In our study, apart from analyzing historical aerial photographs, field surveys were conducted to validate the reported land transformations in the landscape. Additionally, exploring the historical literature, including books and research publications, provided further insights and confirmed the plausibility of the accounts of the elderly. Some researchers, such as Kanyiginya et al. [47] and Sekajugo et al. [76], have utilized multiple methods for natural hazard inventorying to address spatial biases and the tendency to report only significant events. To mitigate inaccuracies arising from memory decay, our study employed a triangulation approach to cross-verify accounts from different elderly participants to ensure accuracy and reliability. This strategy, used by Bwambale et al. [46], for example, enhances the validity of findings from qualitative research.

### *5.2. Natural Hazards and Forest Cover Changes*

Accounts from the elderly attribute the increase in the reports of natural hazards to land use changes, especially vegetation removal and changes in land management practices. According to Kizza et al. [86], the most significant and predominant land use change that took place in the Kigezi region from 1987 to 2014 was the conversion of tropical high forests to small-scale farmland and woodlots, and the decline in the wetland areas. Similar findings were reported by Twongyirwe et al. [53] and Barasa et al. [87], which highlighted important deforestation in the Bwindi Impenetrable Forest Reserve. This included the largescale clearance of forest cover from 1960 to the 80s before restrictions and boundaries separating the forest and community land were established. It is possible that landslides were favored by this deforestation. Forest conversion, especially to agricultural land, has been associated with increased landslide activity in similar regions just south of our study area [12,22,88], demonstrating that when deforestation occurs, an increase in landslides is experienced over a span of approximately 10–15 years.

Our results further indicate that the natural vegetation as well as cultivable lands were or are quickly being converted to eucalyptus plantations. As mentioned by the elderly, black wattle trees which were enforced by the colonial government protected the land against soil degradation. This observation aligns with findings by De wit et al. [89] and Babur et al. [90] who highlighted that black wattle trees enhance soil aggregate stability and reduce soil erodibility, thereby preventing the risk of landslides and flash floods. According to the elderly citizens, the rising demand for wood products, their high economic value, and the fast maturing of eucalyptus are causing the rapid conversion of native tree species. Other countries in the region have recorded a rapid rate at which eucalyptus is replacing native tree species as well as crop land. In Ethiopia, for example, eucalyptus is perceived positively for its economic benefits and many small-holder farmers have engaged in the conversion of croplands to eucalyptus stands [91]. However, there is controversy from the elderly citizens surrounding the effectiveness of eucalyptus trees in controlling natural hazards. Some elderly citizens and local residents believe that eucalyptus has inflicted more harm than good regarding land management. Other elderly citizens have attached a positive role to eucalyptus in controlling natural hazards. For instance, the section of W7 where afforestation programs were implemented with eucalyptus has registered a reduction in landslides and flash floods according to the residents. In a recent fatal disaster that occurred in one of the watersheds (W4), a cascading event comprising landslides and flashfloods killed nine people and displaced about 300 households [92]. From our interactions with survivors, homes that had eucalyptus plantations around them were saved from being swept away by the flashfloods. Other controversies of eucalyptus in land management have been highlighted by some researchers such as Wang et al. [93] who noted that the successive planting of eucalyptus reduces soil aggregate stability and exposes the land to soil erosion and landslides. Moreover, eucalyptus landscapes were found with soil compaction problems, as well as poor aeration and water-holding capacity, which could be linked to flash flood occurrences. Another study in Ethiopia by Nyssen et al. [27] highlighted the role played by eucalyptus plantations in initiating gully formation and flash floods. Eucalyptus woodlots do not encourage undergrowth and limit water retention which in turn increases surface runoff and therefore contributes to flash flood occurrence [94].

### *5.3. Influence of Land Management Practices and Farming Systems on Natural Hazards*

Historical researchers in the region such as Purseglove et al. [63] had previously warned of the disasters that the Kigezi region might face due to the increasing population pressure that was noted as early as the colonial era. According to the elderly and confirmed by Purseglove et al. [63], the increase in population was attributed to immigration from Rwanda that started in 1932 and continued to the 1950s. The elderly

reported that the increase in population prompted the colonial administrators to set up laws and policies governing the use and management of land. These findings align with Turyahabwe et al. [40] and Purseglove et al. [63] who established that, in response to the increased population and shortage of land, the colonial administrators passed several policies including the planting of black wattle trees for every household, restrictions on the cutting down of trees and bush burning, fallowing, and terracing. These policies and practices to conserve the land, transformed and made Kigezi a model region as far as terracing is concerned [51,95]. The terraces still existing today are a heritage of the policies that were put in place to reduce the increasing land degradation. In W2 and W5, terraces increased at the expense of forest cover as forested land was converted into cropland land (Figures 8 and 9). On the other hand, the terraces in W8 reduced as the cropland land was turned into settlements as confirmed by the increase in the area covered by houses. The reduction in terraces in W4 can be explained by the restriction of cultivation in Muhabura forest. The terraces which were in the forest were concealed as the forest rejuvenated. With the abandonment of land management practices, the terraces have not been maintained and are therefore dilapidated.

According to the elderly, terracing and consistent fallowing practices prevented natural hazards from occurring; however, as the population grew and these practices were no longer practiced, the land became more susceptible to natural hazards. However, there is controversy on the effectiveness of terraces in terms of controlling natural hazards. For instance, Cornelis et al. [96] argues that terraces control floods by reducing the velocity of runoff. On the other hand, terraces create favorable conditions for landslides because of their capacity to increase water infiltration [97,98]. The problem is exacerbated by the unmaintained terraces which are a source of shallow landslides. Most shallow landslides we observed recently in the field have their scarp/head originating from an old terrace ridge. The role of terraces in initiating shallow landslides was demonstrated in a study by Schilirò et al. [99] in Italy. The same was also demonstrated in Eastern Uganda [100], and in a region of Rwanda close to our study area [101]. Furthermore, Rogger et al. [98] highlighted the risks associated with abandoned terraces in terms of causing gully initiation and flash floods. According to the elderly, the terraces in the past were stabilized with elephant grass, which prevented the terrace from collapsing and causing shallow landslides. The issue of terracing and landslides could therefore be linked to land management practices and the nature of the terraces, but we lack data from the current study to ascertain this. More studies are therefore required.

Another land management practice that has been abandoned was fallowing. Apart from keeping the soil covered, fallowing allows the soil to regenerate and therefore increase water infiltration, thereby reducing runoff and flash floods [102]. Previous research has shown the role played by fallows and elephant grass along contours in positively improving the soil's physical properties and preventing runoff and flash floods [103]. Our field observations discovered that W1 is making efforts to maintain the traditional crops; for instance, millet is still grown in this watershed, a crop which other watersheds abandoned after the colonial period. Millet promotes conservation agriculture by acting as a cover crop but also by improving the soil structure [104,105], which can be associated with reduced frequencies of natural hazards in W1.

### *5.4. Population Growth and Infrastructure Development in Relation to Natural Hazard Risks*

Our analysis shows that the population in the watersheds has grown rapidly, increasing exposure to natural hazards. For example, in contrast to the 1940s and 1950s, many settlements are currently located on hillslopes, which exposes people and their property to landslides (Figure 9). Similarly, other new settlements were mapped in the

drained wetlands, which puts the population at risk of floods. This trend is also highlighted by various authors who have reported the increasing impacts of natural hazards, exacerbated by population growth, which pushes people to live in more hazardous terrain [5,14,19,20,106]. Infrastructure has developed in the watersheds with more roads constructed, especially starting from 1980. With the hilly terrain of the region, roads had to be dissected through the hills, which probably reduced the stability of the slopes and increased the susceptibility of the landscape to landslides. The role played by road construction in causing landslides in mountainous environments is clearly demonstrated [107]. Furthermore, the type of roads constructed were of the sand and gravel type without embankments for the side cuts, which led to more slope instability. In our previous landslide inventory by Kanyiginya et al. [47], several landslides were mapped along newly constructed roads in W3 and W8. Moreover, in most cases the roads were crossing wetlands which necessitated drainage, a management action that can influence the occurrence of floods.

### *5.5. Natural Hazards and Climate Variability*

Despite the potential role of human activities in the occurrence of natural hazards as highlighted in the preceding sections, and the evident increase in the population's exposure, the trends observed in the reported hazards must also be analyzed in the context of climatic variability. El Niño and the Southern Oscillation (ENSO) are examples of such a variability that has influenced rainfall patterns in the region [108]. For instance, the 1982-83 El Niño event was particularly intense and was linked to a noticeable rise in rainfall and hazard occurrences [109]. Beyond ENSO variability, anomalous periods of rainfall not only lead to more frequent hazard events but may also potentially result in more impactful events [110]. Such impactful events are more likely to be vividly recalled by the elderly participants [80]. Future studies could consider a deeper investigation of the interaction between climate variability, land use change, and natural hazards in this region. However, much more data and knowledge would be needed, not only on natural hazards and land use [12,16], but also on climate [111].

## 6. Conclusions

Our findings reveal that major land use/cover changes associated with a high population increase have occurred over the last 80 years. The changes, which include vegetation removal, conversion from natural to exotic tree species, the increased cultivation of hillslopes, road construction, wetland drainage, the abandonment of agricultural terraces, and fallowing practices, are all associated with an increase in population pressure, laxity in the land management laws and policies, and change from public to private land ownership. These changes are commonly reported to be associated with an increase in natural hazard frequency. However, despite an unprecedented amount of new information for the region, this association between natural hazard frequency and land use change cannot yet be quantitatively validated. Nevertheless, the increasing exposure of vulnerable populations to the dangers of natural hazards is evident, with population growth and poorly designed landscape management practices as the key drivers. Integrating the knowledge of elderly citizens into the analysis of natural hazards and land transformation has proven to be highly valuable. The rich knowledge of the past narrated by the elderly citizens underscores the effectiveness of this approach in generating unique and otherwise inaccessible knowledge that would be hard to obtain with other scientific or social research methods. This contribution enhances a comprehensive understanding of landscape transformation and natural hazard dynamics. The elderly approach can also be useful to pass on historical memory about natural hazards from older to younger generations by leveraging

their lived experiences and long-term observations. Such information could be used in policy- and decision-making, for disaster risk reduction, and to bolster the resilience of local communities.

**Author Contributions:** Conceptualization, V.K., R.T., M.K. and O.D.; methodology, V.K., R.T., M.K. and O.D.; software, V.K.; validation, R.T., M.K. and O.D.; formal analysis, V.K., R.T., M.K. and O.D.; investigation, V.K., R.T., M.K. and O.D.; resources, V.K., R.T., M.K. and O.D.; data curation, V.K., D.M., R.T. and G.K.-R., writing—original draft preparation, V.K., R.T., M.K. and O.D.; writing—review and editing, V.K., R.T., M.K., O.D., M.G.A. and C.M., visualization, V.K., R.T., M.K. and O.D.; supervision, R.T., M.K. and O.D.; project administration, R.T. and O.D. All authors have read and agreed to the published version of the manuscript.

**Funding:** This research was funded by the Development Cooperation programme of the Royal Museum for Central Africa with the support of the Directorate-General Development Cooperation and Humanitarian Aid of Belgium (RMCA-DGD) through the HARISSA project (RMCA-DGD 2019–2024; https://georiska.africamuseum.be/en/activities/harissa (accessed on 30 January 2025)).

**Institutional Review Board Statement:** This research in its entirety was approved by the Research Ethics Committee of Mbarara University of Science and Technology and the Uganda National Council of Science and Technology.

**Data Availability Statement:** Data are available on request from the corresponding author.

**Acknowledgments:** We extend our gratitude to all the institutions and individuals whose invaluable contributions made this study possible. Special thanks go to the elderly citizens who generously shared their time and knowledge for this study. We are also grateful to François Kervyn for his exceptional coordination and unwavering moral support throughout this research.

**Conflicts of Interest:** The authors declare no conflicts of interest.

## Appendix A

Questionnaire A1: Questionnaire guide for the elderly interviews

Introduction

Hello. I am Violet Kanyiginya a PhD researcher attached to Mbarara University of Science and Technology. I will be having a discussion with you about how the landscape in your area has evolved and identify any natural hazards that have occurred in the past.

The purpose of the interview/discussions is to understand landscape change dynamics and how it is linked to natural hazard occurrences over the past decades. The information you provide is very important for this study to enable the understanding of the natural hazard processes, with a hope of contributing to disaster risk reduction

I will keep your name and your answers confidential. Your responses will be used only for the purpose of this research.

Name: _____

Sex: _____

Age (when were you born?) _____

Village: _____

Parish: _____

Sub-county: _____

District: _____

1. How long have you lived in this area?
2. From the time you started understanding, what do you remember about your village? How many were you in this village (household)? Show on the map where your houses were located.

3. How did your village look like generally? Or what was in the environment when you were young (structure of houses, roads, budlings, wetlands, forest, etc.) for FGDs use the map to show how the landscape looked like in the past and What it looks like currently.
4. What changes on the landscape do you remember happened? what has changed, what has not changed in your environment when did the change happen and where did it happen?—Use the timeline to re-member and the map to show where the changes occurred.
5. What about the river in your area, can you tell me about its history/evolution through time?
6. How were the land managed, what crops did you grow?
7. Any policies that existed?
8. Have you experienced landslides and floods in the past?
9. If yes, when did they happen—which years/months/seasons—use the timeline of historical political or social events to remember.

*Appendix A.1*

**Table A1.** Historical timeline guide used during interviews.

| **Year** | **Historical Event/Change** | | | **Visualization of Landscape Change** |
|---|---|---|---|---|
| | Political and cultural changes (new laws, policies and practices, immigrants) | Socio-economic changes (livelihoods, farming practices, promotion of certain crops, population, infrastructure, building architecture) | Environmental/landscape changes (deforestation, afforestation, what natural hazards occurred) | Using the available map, show how the landscape looked like in this period? (forested, terraced or not, bare, bushy, uncultivated, wetland, grazing land, uninhabited, etc.) |

*Appendix A.2*

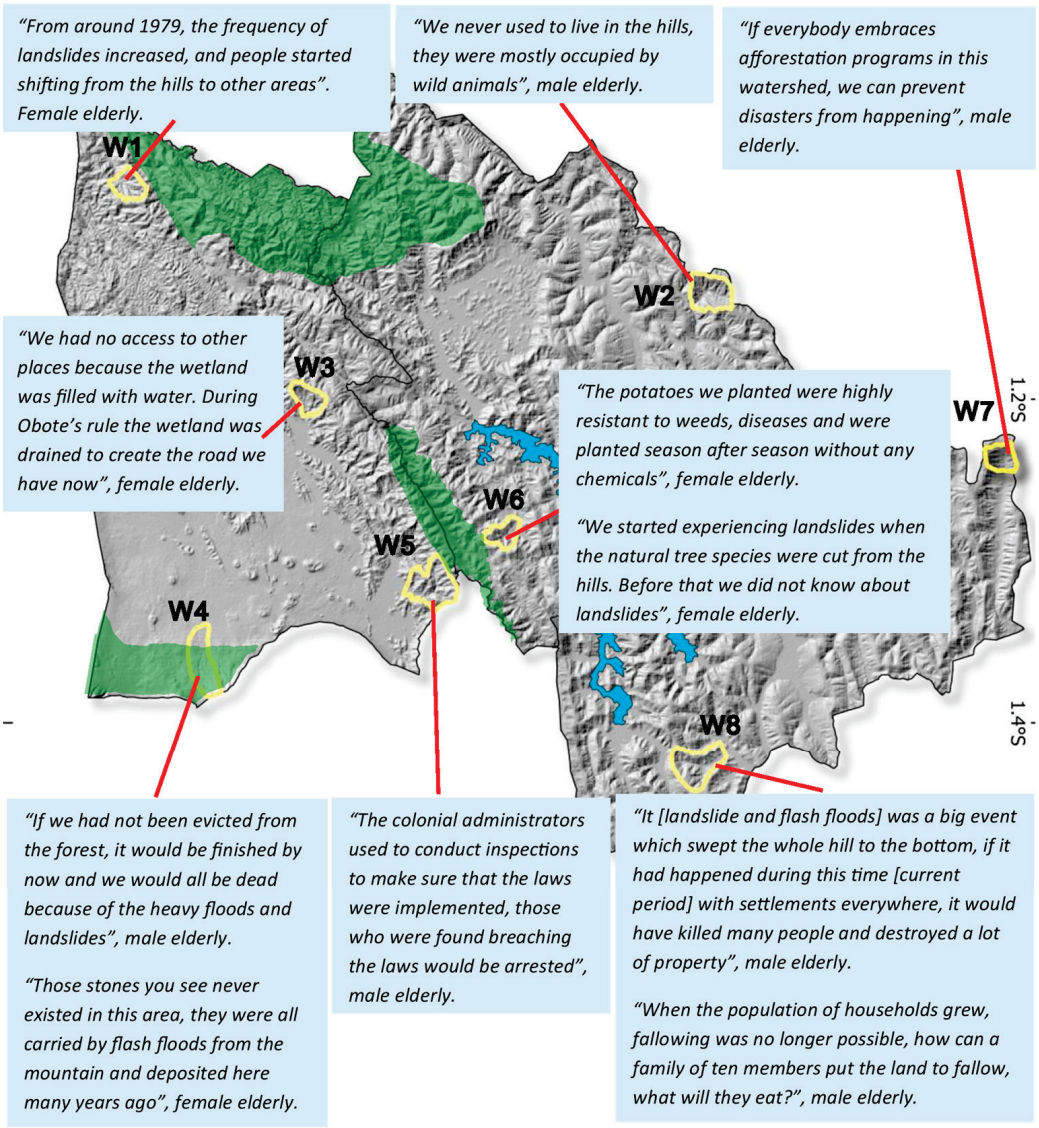



**Figure A1.** Examples of quotes from interactions with the elderly citizens.

*Appendix A.3*

**Table A2.** Detailed watershed timelines.

| W1—Nteko | | |
|---|---|---|
| **Dates** | **National/Regional Context** | **Local Events** |
| 1932 | Pre-colonial period | Park boundary was established separating Bwindi forest and communities |
| 1960 | Colonial period | Heavy deforestation in the catchment started |
| 1979 | Obote I president | Landslides experienced and people started shifting due to landslides |
| 1991 | Museveni's rule | Bwindi forest was designated a national park |
| 2016 | Museveni's rule | Restoration program by NGOs to plant indigenous trees |
| 2019 | Museveni's rule | Heavy landslides occurred |

**Table A2.** *Cont.*

| W2—Kyokezo | | |
|---|---|---|
| **Dates** | **National/regional context** | **Local events** |
| 1950–60 | Colonial period | Resettlement scheme took place as a depopulation strategy |
| 1971 | Obote I president | The natural forest started to decline, replaced with eucalyptus |
| 1980 | Obote II rule | Population grew, land fragmentation |
| 1986 | Museveni became president | Many iron sheet-roofed houses; fallowing competently ended |
| 1998 | Museveni's rule | The first road was constructed |
| 2000 | Museveni's rule | Swamp drainage |
| 2009 | Museveni's rule | The first serious landslides occurred killing 6 people and destroying several properties. Many large gulleys were formed |
| | Museveni's rule | Buying and selling of land increased; land fragmentation |
| April 2017 | Museveni's rule | Deadly landslides |
| 2004 | Museveni's rule | Road constructed began |
| 1980 | Obote II rule | Over-population and cultivation |
| W3—Nyundo | | |
| **Dates** | **National/regional context** | **Local events** |
| 1952 | Colonial period | Mass wetland drainage for cultivation and road access |
| 1966–70s | Obote I rule | Land management practices abandoned |
| 1971 | Obote I president | Construction of many roads cutting through the mountains |
| 1980 | Obote II rule | Population increase, over-cultivation overgrazing; disasters increased, happening in April and September every year |
| 1990–98 | Museveni's rule | Fallowing was no more |
| 2000 | Museveni's rule | Eucalyptus dominated the landscape, natural tree species cut down |
| 2004 | Museveni's rule | Road constructed began |
| W4—Rukonji | | |
| **Dates** | **National/regional context** | **Local events** |
| 1950 | Colonial period | Muhabura forest heavily cut down for cultivation |
| 1957 | Colonial period | Flash floods |
| April 1974 | President Amin rule | Heavy flashfloods involving deaths occurred |
| March 1982 | Obote II rule | Heavy flashfloods involving deaths occurred |
| April 1988 | President Museveni's rule | Heavy flashfloods involving deaths occurred |
| 1991 | Museveni's rule | Forest designated a national park and the regrowth of the forest |
| W5—Chibumba | | |
| **Dates** | **National/regional context** | **Local events** |
| 1950 | Colonial period | Landslides occurred in the hills, people relocated to lowlands |
| 1954 | Colonial period | Fallowing, planting elephant grass along contours, black wattle trees enforced |
| 1957 | Colonial period | Depopulation plan, people were resettled |

**Table A2.** *Cont.*

| W5—Chibumba | | |
|---|---|---|
| **Dates** | **National/regional context** | **Local events** |
| 1959 | Colonial period | Rwandese war, immigrants |
| 1960 | Colonial period | Mining of tin |
| 1966–70s | Obote I rule | Land management practices abandoned, natural trees cut down, cultivating in the swamp |
| 1969 | Obote I president | Iron-sheet houses |
| 1980 | Obote II rule | Wetland in the valley was reclaimed and finished |
| 1981 | Obote II rule | Natural hazards, especially floods increased in the catchment |
| 1986 | Museveni's rule | Road construction |
| W6—Kacereere | | |
| **Dates** | **National/regional context** | **Local events** |
| 1936 | Pre-colonial period | Echuya forest separated from community land |
| 1959 | Colonial period | Echuya forest gazetted a forest reserve |
| 1955–66 | Colonial period | Resettlement plan for depopulation happened |
| 1960 | Colonial period | Sinkholes experienced |
| 1970 | Obote I rule | Land management practices abandoned; natural trees cut down replaced with exotic ones |
| 1974 | President Amin rule | Elephants left the catchment |
| 1979 | President Amin rule | Over cultivation and shortage of land |
| 1980–90 | Obote II rule | Landslides and floods were experienced, and gulleys started to form |
| Apr-84 | Obote II rule | Serious flashfloods happened and swept crops and houses |
| 1990–98 | Museveni's rule | Wetland lost completely because of siltation |
| Sep-94 | Museveni's rule | Landslides occurred and destroyed 3 houses, bridges, animals, and crops |
| 2016 | Museveni's rule | Soil and water conservation programs introduced |
| W7—Kahondo | | |
| **Dates** | **National/regional context** | **Local events** |
| 1946 | Colonial period | Landslides occurred and killed livestock, destroyed crops |
| 1950 | Colonial period | First main road constructed |
| 1954 | Colonial period | Fallowing, planting elephant grass along contours, black wattle trees enforced |
| 1956–1959 | Colonial period | The first iron-sheet houses were built |
| 1966–70s | Obote I rule | Land management practices abandoned, natural trees cut down, cultivating in the swamp |
| 1971 | Obote I president | Public land became private land with land titles. There was no source of water, the first borehole was constructed. A river was formed and continues to flow |
| 1980 | Obote II rule | Overpopulation of people and livestock, overgrazing and cattle trails all over the landscape, over cultivation |
| 1984 | Obote II rule | Buying and selling of food, food scarcity |
| 1990–98 | Museveni's rule | Gullies started forming in the catchment |

**Table A2.** *Cont.*

| W7—Kahondo | | |
|---|---|---|
| **Dates** | **National/regional context** | **Local events** |
| 1992 | Museveni's rule | Severe famine happened in 1992 due to drought, and pests and diseases |
| 2000 | Museveni's rule | Afforestation programs introduced, with Eucalyptus and pine dominating |
| 2005–2009 | Museveni's rule | Soil and water conservation programs introduced |
| April 2013 | | Serious landslides and floods occurred |
| W8—Kibuga | | |
| **Dates** | **National/regional context** | **Local events** |
| 1945 | Colonial period | Deadly landslides occurred |
| 1952 | Colonial period | Mass wetland drainage |
| 1966–70s | Obote I rule | Land management practices abandoned |
| 1971 | Obote I president | Construction of many roads cutting through the mountains |
| 1972 | Immigration started | Population increase |
| 1980 | Obote II rule | Over-cultivation and overgrazing set in; landslides and floods increased |
| 1990–98 | Museveni's rule | The natural vegetation began to shrink, Eucalyptus dominated the land cover, iron-sheet houses replaced grass-thatched houses; fallowing was no more |
| | Museveni's rule | Buying and selling of land increased; land fragmentation |
| April 2017 | Museveni's rule | Deadly landslides |
| 2004 | Museveni's rule | Road construction began, more landsides occurred |
| 1980 | Obote II rule | Over-population and -cultivation; landslides and flash floods |

## Appendix B

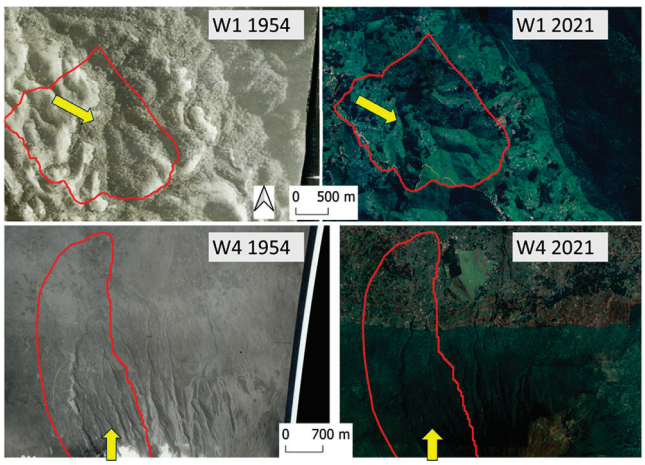



**Figure A2.** Examples of land use and land cover changes in the watersheds. W1 shows a reduction in forest cover, showing that deforestation took place after 1954, and W4 shows an increase in forest cover. The red polygons are the watershed boundaries. The yellow arrows indicate where forest cover change took place.

## References


1. Luino, F.; Barriendos, M.; Gizzi, F.T.; Glaser, R.; Gruetzner, C.; Palmieri, W.; Porfido, S.; Sangster, H.; Turconi, L. Historical data for natural hazard risk Mitigation and land use planning. *Land* **2023**, *12*, 1777. [CrossRef]
2. Sidle, R.C.; Taylor, D.; Lu, X.X.; Adger, W.N.; Lowe, D.J.; de Lange, W.P.; Newnham, R.M.; Dodson, J.R. Interactions of Natural Hazards and Society in Austral-Asia: Evidence in Past and Recent Records. *Quat. Int.* **2004**, *118–119*, 181–203. [CrossRef]
3. Napolitano, E.; Marchesini, I.; Salvati, P.; Donnini, M.; Bianchi, C.; Guzzetti, F. LAND-DeFeND—An Innovative Database Structure for Landslides and Floods and Their Consequences. *J. Environ. Manag.* **2018**, *207*, 203–218. [CrossRef]
4. Hill, E.M.; McCaughey, J.W.; Switzer, A.D.; Lallemant, D.; Wang, Y.; Sathiakumar, S. Human Amplification of Secondary Earthquake Hazards through Environmental Modifications. *Nat. Rev. Earth Environ.* **2024**, *5*, 463–476. [CrossRef]
5. Dille, A.; Dewitte, O.; Handwerger, A.L.; d'Oreye, N.; Derauw, D.; Ganza Bamulezi, G.; Ilombe Mawe, G.; Michellier, C.; Moeyersons, J.; Monsieurs, E.; et al. Acceleration of a Large Deep-Seated Tropical Landslide Due to Urbanization Feedback. *Nat. Geosci.* **2022**, *15*, 1048–1055. [CrossRef]
6. Deijns, A.A.J.; Michéa, D.; Déprez, A.; Malet, J.-P.; Kervyn, F.; Thiery, W.; Dewitte, O. A Semi-Supervised Multi-Temporal Landslide and Flash Flood Event Detection Methodology for Unexplored Regions Using Massive Satellite Image Time Series. *ISPRS J. Photogramm. Remote Sens.* **2024**, *215*, 400–418. [CrossRef]
7. Wang, X.; Fan, X.; Fang, C.; Dai, L.; Zhang, W.; Zheng, H.; Xu, Q. Long-Term Landslide Evolution and Restoration After the Wenchuan Earthquake Revealed by Time-Series Remote Sensing Images. *Geophys. Res. Lett.* **2024**, *51*, e2023GL106422. [CrossRef]
8. IPCC. *Climate Change 2022: Impacts, Adaptation, and Vulnerability. Contribution of Working Group II to the Sixth Assessment Report of the Intergovernmental Panel on Climate Change*; Cambridge University Press: Cambridge, UK; New York, NY, USA, 2022. [CrossRef]
9. Froude, M.J.; Petley, D.N. Global Fatal Landslide Occurrence 2004 to 2016. *Nat. Hazards Earth Syst. Sci.* **2018**, *18*, 2161–2181. [CrossRef]
10. Cendrero, A.; Forte, L.M.; Remondo, J.; Cuesta-Albertos, J.A. Anthropocene Geomorphic Change Climate or Human Activities? *Earth's Future* **2020**, *8*, e2019EF001305. [CrossRef]
11. Cendrero, A.; Remondo, J.; Beylich, A.A.; Cienciala, P.; Forte, L.M.; Golosov, V.N.; Gusarov, A.V.; Kijowska-Strugała, M.; Laute, K.; Li, D.; et al. Denudation and Geomorphic Change in the Anthropocene; a Global Overview. *Earth-Sci. Rev.* **2022**, *233*, 104186. [CrossRef]
12. Depicker, A.; Govers, G.; Jacobs, L.; Campforts, B.; Uwihirwe, J.; Dewitte, O. Interactions between Deforestation, Landscape Rejuvenation, and Shallow Landslides in the North Tanganyika–Kivu Rift Region, Africa. *Earth Surf. Dyn.* **2021**, *9*, 445–462. [CrossRef]
13. Rengers, F.K.; McGuire, L.A.; Kean, J.W.; Staley, D.M.; Hobley, D.E.J. Model Simulations of Flood and Debris Flow Timing in Steep Catchments after Wildfire. *Water Resour. Res.* **2016**, *52*, 6041–6061. [CrossRef]
14. Ozturk, U.; Bozzolan, E.; Holcombe, E.A.; Shukla, R.; Pianosi, F.; Wagener, T. How Climate Change and Unplanned Urban Sprawl Bring More Landslides. *Nature* **2022**, *608*, 262–265. [CrossRef] [PubMed]
15. McAdoo, B.G.; Quak, M.; Gnyawali, K.R.; Adhikari, B.R.; Devkota, S.; Rajbhandari, P.L.; Sudmeier-Rieux, K. Roads and Landslides in Nepal: How Development Affects Environmental Risk. *Nat. Hazards Earth Syst. Sci.* **2018**, *18*, 3203–3210. [CrossRef]
16. Depicker, A.; Jacobs, L.; Mboga, N.; Smets, B.; Van Rompaey, A.; Lennert, M.; Wolff, E.; Kervyn, F.; Michellier, C.; Dewitte, O.; et al. Historical Dynamics of Landslide Risk from Population and Forest-Cover Changes in the Kivu Rift. *Nat. Sustain.* **2021**, *4*, 965–974. [CrossRef]
17. Rentschler, J.; Salhab, M.; Jafino, B.A. Flood Exposure and Poverty in 188 Countries. *Nat. Commun.* **2022**, *13*, 3527. [CrossRef]
18. CRED-UNDRR. *Human Cost of Disasters: An Overview of the Last 20 Years (2000–2019)*; UCLouvain: Ottignies-Louvain-la-Neuve, Belgium, 2020. [CrossRef]
19. Otto, F.E.L.; Raju, E. Harbingers of Decades of Unnatural Disasters. *Commun. Earth Environ.* **2023**, *4*, 280. [CrossRef]
20. Raju, E.; Boyd, E.; Otto, F. Stop Blaming the Climate for Disasters. *Commun. Earth Environ.* **2022**, *3*, 1. [CrossRef]
21. Ferrer, J.V.; Samprogna Mohor, G.; Dewitte, O.; Pánek, T.; Reyes-Carmona, C.; Handwerger, A.L.; Hürlimann, M.; Köhler, L.; Teshebaeva, K.; Thieken, A.H.; et al. Human Settlement Pressure Drives Slow-Moving Landslide Exposure. *Earth's Future* **2024**, *12*, e2024EF004830. [CrossRef]
22. Merz, B.; Blöschl, G.; Vorogushyn, S.; Dottori, F.; Aerts, J.C.J.H.; Bates, P.; Bertola, M.; Kemter, M.; Kreibich, H.; Upmanu, L.; et al. Causes, Impacts and Patterns of Disastrous River Floods. *Nat. Rev. Earth Environ.* **2021**, *2*, 592–609. [CrossRef]
23. Muñoz-Torrero Manchado, A.; Allen, S.; Ballesteros-Cánovas, J.A.; Dhakal, A.; Dhital, M.R.; Stoffel, M. Three Decades of Landslide Activity in Western Nepal: New Insights into Trends and Climate Drivers. *Landslides* **2021**, *18*, 2001–2015. [CrossRef]
24. Monsieurs, E.; Kirschbaum, D.B.; Thiery, W.; van Lipzig, N.; Kervyn, M.; Demoulin, A.; Jacobs, L.; Kervyn, F.; Dewitte, O. Constraints on Landslide-Climate Research Imposed by the Reality of Fieldwork in Central Africa. In Proceedings of the 3rd North American Symposium on Landslides, Roanake, Virginia, 4–8 June 2017.
25. Juang, C.S.; Stanley, T.A.; Kirschbaum, D.B. Using Citizen Science to Expand the Global Map of Landslides: Introducing the Cooperative Open Online Landslide Repository (COOLR). *PLoS ONE* **2019**, *14*, e0218657. [CrossRef] [PubMed]

26. Schlögl, M.; Fuchs, S.; Scheidl, C.; Heiser, M. Trends in Torrential Flooding in the Austrian Alps: A Combination of Climate Change, Exposure Dynamics, and Mitigation Measures. *Clim. Risk Manag.* **2021**, *32*, 100294. [CrossRef]
27. Nyssen, J.; Poesen, J.; Veyret-Picot, M.; Moeyersons, J.; Haile, M.; Deckers, J.; Dewit, J.; Naudts, J.; Teka, K.; Govers, G. Assessment of Gully Erosion Rates through Interviews and Measurements: A Case Study from Northern Ethiopia. *Earth Surf. Process. Landf.* **2006**, *31*, 167–185. [CrossRef]
28. McCall, M.K. *Participatory Mapping and Participatory GIS (PGIS) for CRA, Community DRR and Hazard Assessment*; Participation Resources: Geneva, Switzerland, 2008. [CrossRef]
29. Solecka, I.; Krajewski, P.; Krzyżanek, A.; Garczyńska, A. Citizens' Perceptions of Landscape Changes and Their Driving Forces: Evidence from Poland. *Int. J. Environ. Res. Public Health* **2022**, *19*, 1688. [CrossRef]
30. Barclay, J.; Robertson, R.; Armijos, M.T. Scientists as Storytellers: The Explanatory Power of Stories Told about Environmental Crises. *Nat. Hazards Earth Syst. Sci.* **2023**, *23*, 3603–3615. [CrossRef]
31. Young, N.E.; Evangelista, P.H.; Mengitsu, T.; Leisz, S. Twenty-Three Years of Forest Cover Change in Protected Areas under Different Governance Strategies: A Case Study from Ethiopia's Southern Highlands. *Land Use Policy* **2020**, *91*, 104426. [CrossRef]
32. Kubwimana, D.; Ait Brahim, L.; Nkurunziza, P.; Dille, A.; Depicker, A.; Nahimana, L.; Abdelouafi, A.; Dewitte, O. Characteristics and Distribution of Landslides in the Populated Hillslopes of Bujumbura, Burundi. *Geosciences* **2021**, *11*, 259. [CrossRef]
33. Riquelme, A.; Del Soldato, M.; Tomás, R.; Cano, M.; Jordá Bordehore, L.; Moretti, S. Digital Landform Reconstruction Using Old and Recent Open Access Digital Aerial Photos. *Geomorphology* **2019**, *329*, 206–223. [CrossRef]
34. Luino, F.; Gizzi, F.T.; Palmieri, W.; Porfido, S.; Turconi, L. Historical Memory as an Effective and Useful Tool for Proper Land Use Planning: Lessons Learnt from Some Italian Cases. *Land* **2023**, *12*, 1751. [CrossRef]
35. Depicker, A.; Govers, G.; Jacobs, L.; Vanmaercke, M.; Uwihirwe, J.; Campforts, B.; Kubwimana, D.; Maki Mateso, J.-C.; Mugaruka Bibentyo, T.; Nahimana, L.; et al. Mobilization Rates of Landslides in a Changing Tropical Environment: 60-Year Record over a Large Region of the East African Rift. *Geomorphology* **2024**, *454*, 109156. [CrossRef]
36. Flicker, S.; Campo, P.O.; Monchalin, R.; Thistle, J.; Worthington, C.; Masching, R.; Guta, A.; Pooyak, S.; Whitebird, W.; Thomas, C. Research Done in "A Good Way": The Importance of Indigenous Elder Involvement in HIV Community-Based. *Am. J. Public Health* **2015**, *105*, 1149–1154. [CrossRef] [PubMed]
37. Lawrence, M.G.; Williams, S.; Nanz, P.; Renn, O. Characteristics, Potentials, and Challenges of Transdisciplinary Research. *One Earth* **2022**, *5*, 44–61. [CrossRef]
38. Richardson, D. Reconstructing a Community with Oral History. *Oral Hist. Rev.* **2002**, *29*, 97–102. [CrossRef]
39. Moezzi, M.; Janda, K.B.; Rotmann, S. Using Stories, Narratives, and Storytelling in Energy and Climate Change Research. Energy Res. *Soc. Sci.* **2017**, *31*, 1–10. [CrossRef]
40. Turyahabwe, N.; Banana, A.Y. An Overview of History and Development of Forest Policy and Legislation in Uganda. *Int. For. Rev.* **2008**, *10*, 641–656. [CrossRef]
41. Capitani, C.; Mukama, K.; Mbilinyi, B.; Malugu, I.O.; Munishi, P.K.T.; Burgess, N.D.; Platts, P.J.; Sallu, S.M.; Marchant, R. From Local Scenarios to National Maps: A Participatory Framework for Envisioning the Future of Tanzania. *Ecol. Soc.* **2016**, *21*, 4. [CrossRef]
42. Gregory, K. Mapping the Landscape of Identity. In *Yearbook (Conference of Latin Americanist Geographers)*; University of Texas Press: Austin, TX, USA, 2002; Volume 28, pp. 51–71.
43. Hordijk, M.; Baud, I. The Role of Research and Knowledge Generation in Collective Action and Urban Governance: How Can Researchers Act as Catalysts? *Habitat Int.* **2006**, *30*, 668–689. [CrossRef]
44. Ben Malek, H.; Berna, F.; D'Argembeau, A. Reconstructing the Times of Past and Future Personal Events. *Memory* **2017**, *25*, 1402–1411. [CrossRef]
45. Hoffman, M.T.; Rohde, R.F. Rivers Through Time: Historical Changes in the Riparian Vegetation of the Semi-Arid, Winter Rainfall Region of South Africa in Response to Climate and Land Use. *J. Hist. Biol.* **2011**, *44*, 59–80. [CrossRef] [PubMed]
46. Bwambale, B.; Nyeko, M.; Sekajugo, J.; Kervyn, M. The Essential Contribution of Indigenous Knowledge to Understanding Natural Hazards and Disaster Risk: Historical Evidence from the Rwenzori (Uganda). *Nat. Hazards* **2021**, *110*, 1847–1867. [CrossRef]
47. Kanyiginya, V.; Twongyirwe, R.; Kagoro-Rugunda, G.; Sekajugo, J.; Mutyebere, R.; Deijns, A.A.J.; Kervyn, M.; Dewitte, O. Inventories of Natural Hazards in Under-Reported Regions: A Multi-Method Insight from a Tropical Mountainous Landscape. *Afr. Geogr. Rev.* **2024**, *43*, 827–846. [CrossRef]
48. Nseka, D.; Mugagga, F.; Opedes, H.; Ayesiga, P.; Wasswa, H.; Mugume, I.; Nimusiima, A.; Nalwanga, F. The Damage Caused by Landslides in Socio-Economic Spheres within the Kigezi Highlands of southwestern Uganda. *Environ. Socio-Econ. Stud.* **2021**, *9*, 23–34. [CrossRef]
49. UBOS. *Statistical Abstract 2022*; UBOS: Kampala, Uganda, 2022; pp. 1–336.
50. UBOS. *National Population and Housing Census*; Main Report; UBOS: Kampala, Uganda, 2024; p. 73.
51. Carswell, G. Farmers and Fallowing: Agricultural Change in Kigezi District, Uganda. *Geogr. J.* **2002**, *168*, 130–140. [CrossRef]

52. Bagoora, F.D.K. Soil Erosion and Mass Wasting Risk in the Highland Area of Uganda. *Mt. Res. Dev.* **1988**, *8*, 173–182. [CrossRef]
53. Twongyirwe, R.; Majaliwa, J.; Ebanyat, P.; Tenywa, M.; Sheil, D.; Heist, M.; Oluka, M.; Kumar, L. Dynamics of Forest Cover Conversion in and around Bwindi Impenetrable Forest, Southwestern Uganda. *J. Appl. Sci. Environ. Manag.* **2011**, *15*, 189–195. [CrossRef]
54. Mwanjalolo, M.G.J.; Bernard, B.; Paul, M.I.; Joshua, W.; Sophie, K.; Cotilda, N.; Bob, N.; John, D.; Edward, S.; Barbara, N. Assessing the Extent of Historical, Current, and Future Land Use Systems in Uganda. *Land* **2018**, *7*, 132. [CrossRef]
55. Monsieurs, E.; Jacobs, L.; Michellier, C.; Basimike Tchangaboba, J.; Bamulezi Ganza, G.; Kervyn, F.; Maki Mateso, J.-C.; Mugaruka Bibentyo, T.; Kalikone Buzera, C.; Nahimana, L.; et al. Landslide Inventory for Hazard Assessment in a Data-Poor Context: A Regional-Scale Approach in a Tropical African Environment. *Landslides* **2018**, *15*, 2195–2209. [CrossRef]
56. OPM (Ed.) *National Vulnerability and Risk Atlas of Uganda*; OPM: Washington, DC, USA, 2019; Volume 1.
57. Nseka, D.; Kakembo, V.; Bamutaze, Y.; Mugagga, F. Analysis of Topographic Parameters Underpinning Landslide Occurrence in Kigezi Highlands of Southwestern Uganda. *Nat. Hazards* **2019**, *99*, 973–989. [CrossRef]
58. Atkinson, R.; Flint, J. Accessing Hidden and Hard-to-Reach Populations: Snowball Research Strategies. *Soc. Res. Updat.* **2001**, *33*, 1.
59. Carter, N.; Bryant-Lukosius, D.; DiCenso, A.; Blythe, J.; Neville, A.J. The Use of Triangulation in Qualitative Research. *Oncol. Nurs. Forum* **2014**, *41*, 545–547. [CrossRef] [PubMed]
60. Rocchio, F.J. *Assessing Ecological Condition of Headwater Wetlands in the Southern Rocky Mountains Using a Vegetation Index of Biotic Integrity*; Colorado State University: Fort Collins, CO, USA, 2007. [CrossRef]
61. Ibsen, M.-L.; Denys, B. The Nature, Use and Problems of Historical Archives for the Temporal Occurrence of Landslides, with Specific Reference to the South Coast of Britain, Ventnor, Isle of Wight. *Geomorphology* **1996**, *15*, 241–258. [CrossRef]
62. Ngologoza, P. *Kigezi and Its People*; Translation of Kigezi n'abantu Baamwo; East African Literature Bureau: Dar es Salaam, Tanzania, 1969.
63. Purseglove, J.W. Land Use in the Over-Populated Areas of Kabale, Kigezi District, Uganda. *East Afr. Agric. J.* **1946**, *12*, 3–10. [CrossRef]
64. Denoon, D. *A History of Kigezi in South-West Uganda*; The National Trust—Adult Education Centre: Kampala, Uganda, 1972; pp. 694–695.
65. Department of Geology. *Geological Map of Uganda*; Geological Survey and Mines Department: Entebbe, Uganda, 2012.
66. Teitelbaum, L.; Ginsburg, M.L.; Hopkins, R.W. Cognitive and Behavioural Impairment among Elderly People in Institutions Providing Different Levels of Care. *Cmaj* **1991**, *144*, 169–173.
67. Bill, A.; Mark, I. *Community Conservation Research in Africa: Principles and Comparative Practice*; Working Papers; Community Conservation at Mgahinga Gorilla National Park in Uganda; University of Manchester: Manchester, UK, 1998; ISBN 190251814.
68. Swetnam, T.W.; Allen, C.D.; Betancourt, J.L. Applied Historical Ecology: Using the Past to Manage for the Future. *Ecol. Appl.* **1999**, *9*, 1189–1206. [CrossRef]
69. Oliva, A.; Olcina, J. Historical Floods and Territorial Planning: Lessons Learned and Opportunities Lost after the Santa Teresa Flood (1879) in the Segura Basin (Spain). *Land* **2024**, *13*, 28. [CrossRef]
70. Blahut, J.; van Westen, C.J.; Sterlacchini, S. Analysis of Landslide Inventories for Accurate Prediction of Debris-Flow Source Areas. *Geomorphology* **2010**, *119*, 36–51. [CrossRef]
71. UNDRR. Uganda Profile of Landslide and Flood Events in the Kigezi Region. *DesInventar Database. DesInventar Sendai.* Available online: https://www.desinventar.net (accessed on 3 March 2021).
72. Hong, Y.; Alder, R.; Huffman, G. Evaluation of the Potential of NASA Multi-Satellite Precipitation Analysis in Global Landslide Hazard Assessment. *Geophys. Res. Lett.* **2006**, *33*, L22402. [CrossRef]
73. Lathouwers, E.; Segers, Y.; Verstraeten, G. Reconstructing Valley Landscapes. GIS-Analyses of Past Land Use Changes in Three Flemish River Valleys since the Late 18th Century. *Land Use Policy* **2023**, *135*, 106960. [CrossRef]
74. Bonney, R.; Phillips, T.B.; Ballard, H.L.; Enck, J.W. Can Citizen Science Enhance Public Understanding of Science? *Public Underst. Sci.* **2016**, *25*, 2–16. [CrossRef] [PubMed]
75. Jacobs, L.; Kabaseke, C.; Bwambale, B.; Katutu, R.; Dewitte, O.; Mertens, K.; Maes, J.; Kervyn, M. The Geo-Observer Network: A Proof of Concept on Participatory Sensing of Disasters in a Remote Setting. *Sci. Total Environ.* **2019**, *670*, 245–261. [CrossRef]
76. Sekajugo, J.; Kagoro-Rugunda, G.; Mutyebere, R.; Kabaseke, C.; Namara, E.; Dewitte, O.; Kervyn, M.; Jacobs, L. Can Citizen Scientists Provide a Reliable Geo- Hydrological Hazard Inventory? An Analysis of Biases, Sensitivity and Precision for the Rwenzori. *Environ. Res. Lett.* **2022**, *17*, 045011. [CrossRef]
77. Jack, F.; Friedman, W.; Reese, E.; Zajac, R. Age-Related Differences in Memory for Time, Temporal Reconstruction, and the Availability and Use of Temporal Landmarks. *Cogn. Dev.* **2016**, *37*, 53–66. [CrossRef]
78. Friedman, W.J.; Wilkins, A.J. Scale Effects in Memory for the Timeof Events. *Mem. Cognit.* **1985**, *13*, 168–175. [CrossRef]
79. Baydala, L.; Worrell, S.; Fletcher, F.; Letendre, S.; Letendre, L.; Ruttan, L. "Making a Place of Respect": Lessons Learned in Carrying out Consent Protocol with First Nations Elders. Prog Community Heal. *Partnersh* **2013**, *7*, 135–143.

80. Andrews, G.J.; Kearns, R.A.; Kontos, P.; Wilson, V. "Their Finest Hour": Older People, Oral Histories, and the Historical Geography of Social Life. *Soc. Cult. Geogr.* **2006**, *7*, 153–177. [CrossRef]
81. Arazy, O.; Malkinson, D. A Framework of Observer-Based Biases in Citizen Science Biodiversity Monitoring: Semi-Structuring Unstructured Biodiversity Monitoring Protocols. *Front. Ecol. Evol.* **2021**, *9*, 693602. [CrossRef]
82. Nsabimana, J.; Henry, S.; Ndayisenga, A.; Kubwimana, D.; Dewitte, O.; Kervyn, F.; Michellier, C. Geo-Hydrological Hazard Impacts, Vulnerability and Perception in Bujumbura (Burundi): A High-Resolution Field-Based Assessment in a Sprawling City. *Land* **2023**, *12*, 1876. [CrossRef]
83. Corominas, J.; Van Westen, C.; Frattini, P.; Cascini, L.; Fotopoulou, S.; Catani, F.; Van Den Eeckhaut, M.; Mavrouli, O.; Agliardi, F.; Pitilakis, K.; et al. Recommendations for the Quantitative Analysis of Landslide Risk. *Bull. Eng. Geol. Environ.* **2014**, *73*, 209–263. [CrossRef]
84. Foody, G.M.; See, L.; Fritz, S.; Van der Velde, M.; Perger, C.; Schill, C.; Boyd, D.S. Assessing the Accuracy of Volunteered Geographic Information Arising from Multiple Contributors to an Internet Based Collaborative Project. *Trans. GIS* **2013**, *17*, 847–860. [CrossRef]
85. Mahlangu, M.; Garutsa, T.C. Application of Indigenous Knowledge Systems in Water Conservation and Management: The Case of Khambashe, Eastern Cape South Africa. *Acad. J. Interdiscip. Stud.* **2014**, *3*, 151–160. [CrossRef]
86. Kizza, C.L.; Tenywa, M.M.; Majaliwa, J.G.M.; Kansiime, F.; Magunda, M.; Nakileza, B.; Barasa, B.; Gabiri, G.; Sebuliba, E.; Nampijja, J. Land Use/Cover Change Patterns in Highland Ecosystems of Lake Bunyonyi Catchment in Western Uganda. *Afr. Crop Sci. J.* **2017**, *25*, 43. [CrossRef]
87. Barasa, B.; Egeru, A.; Patrick, O.; Fridah, M. Dynamics of Land Use/Cover Trends in Kanungu District, South-Western Uganda. *J. Appl. Sci. Environ. Manag.* **2011**, *14*, 67–70. [CrossRef]
88. Maki Mateso, J.-C.; Bielders, C.L.; Monsieurs, E.; Depicker, A.; Smets, B.; Tambala, T.; Bagalwa Mateso, L.; Dewitte, O. Characteristics and Causes of Natural and Human-Induced Landslides in a Tropical Mountainous Region: The Rift Flank West of Lake Kivu (Democratic Republic of the Congo). *Nat. Hazards Earth Syst. Sci.* **2023**, *23*, 643–666. [CrossRef]
89. De Wit, M.P.; Crookes, D.J.; Van Wilgen, B.W. Conflicts of Interest in Environmental Management: Estimating. *Biol. Invations* **2001**, *3*, 167–178. [CrossRef]
90. Babur, E.; Kara, O.; Fathi, R.A.; Susam, Y.E.; Riaz, M.; Arif, M.; Akhtar, K. Wattle Fencing Improved Soil Aggregate Stability, Organic Carbon Stocks and Biochemical Quality by Restoring Highly Eroded Mountain Region Soil. *J. Environ. Manag.* **2021**, *288*, 112489. [CrossRef] [PubMed]
91. Tesfaw, A.; Alemu, D.; Feyera, S.; Teferi, E. Eucalyptus Succession on Croplands in the Highlands of Northwestern Ethiopia: Economic Impact Analysis Using Farm Household Model. *Resources* **2022**, *11*, 71. [CrossRef]
92. Floodlist. At Least 9 Killed in Western Region Flash Floods. Available online: https://floodlist.com/africa/uganda-floods-kisoro-january-2022 (accessed on 22 December 2022).
93. Wang, J.; Deng, Y.; Li, D.; Liu, Z.; Wen, L.; Huang, Z.; Jiang, D.; Lu, Y. Soil Aggregate Stability and Its Response to Overland Flow in Successive Eucalyptus Plantations in Subtropical China. *Sci. Total Environ.* **2022**, *807*, 151000. [CrossRef] [PubMed]
94. Du, W.; Zhang, J.; Chen, H.; Wang, T. Do Ecological Evidences Support Biodiversity Optimizing Roles of Eucalyptus Plantation 4 Forests? *SSRN Electron. J.* **2022**. *Preprint*.
95. Hartter, J.; Ryan, S.J.; Mackenzie, C.A.; Goldman, A.; Diem, J.E.; Chapman, C.A. Now There Is No Land: A Story of Ethnic Migration in a Protected Area Landscape in Western Uganda. *Popul. Environ.* **2015**, *36*, 452–479. [CrossRef]
96. Cornelis, W.; Waweru, G.; Araya, T. Building Resilience Against Drought and Floods: The Soil-Water Management Perspective. *Sustain. Agric. Rev.* **2019**, *29*, 125–142. [CrossRef]
97. Sidle, R.C.; Bogaard, T.A. Dynamic Earth System and Ecological Controls of Rainfall-Initiated Landslides. *Earth-Sci. Rev.* **2016**, *159*, 275–291. [CrossRef]
98. Rogger, M.; Agnoletti, M.; Alaoui, A.; Bathurst, J.C.; Bodner, G.; Borga, M.; Chaplot, V.; Gallart, F.; Glatzel, G.; Hall, J.; et al. Land Use Change Impacts on Floods at the Catchment Scale: Challenges and Opportunities for Future Research. *Water Resour. Res.* **2016**, *2013*, 5209–5219. [CrossRef] [PubMed]
99. Schilirò, L.; Cevasco, A.; Esposito, C.; Mugnozza, G.S. Shallow Landslide Initiation on Terraced Slopes: Inferences from a Physically Based Approach. *Geomat. Nat. Hazards Risk* **2018**, *9*, 295–324. [CrossRef]
100. Kitutu, M.G.; Muwanga, A.; Poesen, J.; Deckers, J.A. Farmer's Perception on Landslide Occurrences in Bududa District, Eastern Uganda. *Afr. J. Agric. Res.* **2011**, *6*, 7–18.
101. Sibomana, P.; Vanmaercke, M.; Nahayo, D.; Depicker, A.; Tychon, B.; Hubert, A.; Rukundo, E.; Dewitte, O. Potential effect of agricultural terraces on landslide occurrence: The tropical mountains of Rwanda. In Proceedings of the EGU General Assembly 2023, Vienna, Austria, 23–28 April 2023. EGU23-9126. [CrossRef]
102. Srivastava, S.; Basche, A.; Traylor, E.; Roy, T. The Efficacy of Conservation Practices in Reducing Floods and Improving Water Quality. *Front. Environ. Sci.* **2023**, *11*, 1136989. [CrossRef]

103. Sinore, T.; Kissi, E.; Aticho, A. The Effects of Biological Soil Conservation Practices and Community Perception toward These Practices in the Lemo District of Southern Ethiopia. *Int. Soil Water Conserv. Res.* **2018**, *6*, 123–130. [CrossRef]
104. Mason, S.C.; Ouattara, K.; Taonda, S.J.B.; Palé, S.; Sohoro, A.; Kaboré, D. Soil and Cropping System Research in Semi-Arid West Africa as Related to the Potential for Conservation Agriculture. *Int. J. Agric. Sustain.* **2015**, *13*, 120–134. [CrossRef]
105. Raj, S.; Chaudhary, S.; Ghule, N.S.; Baral, K.; Padhan, S.R.; Gawande, K.N.; Singh, V. Sustainable Farming and Soil Health Enhancement through Millet Cultivation: A Review. *Int. J. Plant Soil Sci.* **2024**, *36*, 222–233. [CrossRef]
106. Tellman, B.; Sullivan, J.A.; Kuhn, C.; Kettner, A.J.; Doyle, C.S.; Brakenridge, G.R.; Erickson, T.A.; Slayback, D.A. Satellite Imaging Reveals Increased Proportion of Population Exposed to Floods. *Nature* **2021**, *596*, 80–86. [CrossRef] [PubMed]
107. Tanyaş, H.; Görüm, T.; Kirschbaum, D.; Lombardo, L. Could Road Constructions Be More Hazardous than an Earthquake in Terms of Mass Movement? *Nat. Hazards* **2022**, *112*, 639–663. [CrossRef]
108. Emberson, R.; Kirschbaum, D.; Stanley, T. Global Connections between El Nino and Landslide Impacts. *Nat. Commun.* **2021**, *12*, 2262. [CrossRef] [PubMed]
109. Nicholson, S.E.; Kim, J. The relationship of the el nino–southern oscillation to african rainfall. *Int. J. Climatol.* **1997**, *17*, 117–135. [CrossRef]
110. Marc, O.; Gosset, M.; Saito, H.; Uchida, T.; Malet, J.P. Spatial Patterns of Storm-Induced Landslides and Their Relation to Rainfall Anomaly Maps. *Geophys. Res. Lett.* **2019**, *46*, 11167–11177. [CrossRef]
111. IPCC. *Climate Change 2021: The Physical Science Basis. Contribution of Working Group I to the Sixth Assessment Report of the Intergovernmental Panel on Climate Change*; Masson-Delmotte, V., Zhai, P., Pirani, A., Connors, S.L., Péan, C., Berger, S., Caud, N., Chen, Y., Goldfarb, L., Gomis, M.I., et al., Eds.; Cambridge University Press: Cambridge, UK; New York, NY, USA, 2021. [CrossRef]


**Disclaimer/Publisher's Note:** The statements, opinions and data contained in all publications are solely those of the individual author(s) and contributor(s) and not of MDPI and/or the editor(s). MDPI and/or the editor(s) disclaim responsibility for any injury to people or property resulting from any ideas, methods, instructions or products referred to in the content.

MDPI AG
Grosspeteranlage 5
4052 Basel
Switzerland
Tel.: +41 61 683 77 34

*Land* Editorial Office
E-mail: land@mdpi.com
www.mdpi.com/journal/land




Disclaimer/Publisher's Note: The title and front matter of this reprint are at the discretion of the Guest Editors. The publisher is not responsible for their content or any associated concerns. The statements, opinions and data contained in all individual articles are solely those of the individual Editors and contributors and not of MDPI. MDPI disclaims responsibility for any injury to people or property resulting from any ideas, methods, instructions or products referred to in the content.





Academic Open
Access Publishing

mdpi.com

ISBN 978-3-7258-3986-5